

AD-A062 606

GENERAL ELECTRIC CORPORATE RESEARCH AND DEVELOPMENT --ETC F/G 1/3
ANALYSIS AND CALCULATIONS OF LIGHTNING INTERACTIONS WITH AIRCRAFT--ETC(U)
AUG 78 F A FISHER

F33615-76-C-3122

UNCLASSIFIED

SRD-78-044

AFFDL-TR-78-106

NL

1 OF 5
ADA
062606



AD A062606

DDC FILE COPY

(18) (19)
AFFDL TR-78-106

LEVEL II

(20)

(6) ANALYSIS AND CALCULATIONS OF
LIGHTNING INTERACTIONS
WITH AIRCRAFT ELECTRICAL CIRCUITS

(13) F. A. FISHER

GENERAL ELECTRIC COMPANY
CORPORATE RESEARCH & DEVELOPMENT
SCHENECTADY, NEW YORK 12301



(11) AUG 1978

(12) 399 P.

(14) SRD-78-Φ44

TECHNICAL REPORT AFFDL-TR-78-106

Final Report, May 1976 - Feb 1978

(15) (16) (21) F33615-76-Q-3122

(16) (17) 24Φ2 02

Approved for public release; distribution unlimited.

AIR FORCE FLIGHT DYNAMICS LABORATORY
AIR FORCE WRIGHT AERONAUTICAL LABORATORIES
AIR FORCE SYSTEMS COMMAND
WRIGHT-PATTERSON AIR FORCE BASE, OHIO 45433

406 617

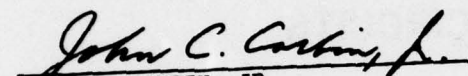
48 14 26 002

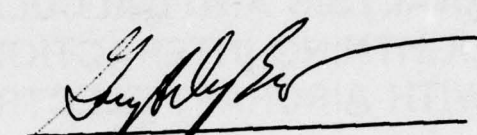
mt

NOTICE

When Government drawings, specifications, or other data are used for any purpose other than in connection with a definitely related Government procurement operation, the United States Government thereby incurs no responsibility nor any obligation whatsoever, and the fact that the government may have formulated, furnished, or in any way supplied the said drawings, specifications, or other data, is not to be regarded by implication or otherwise as in any manner licensing the holder or any other person or corporation, or conveying any rights or permission to manufacture, use, or sell any patented invention that may in any way be related thereto.

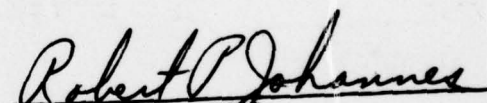
This report has been reviewed and is approved for publication.


JOHN C. CORBIN, JR.
Project Engineer
Vehicle Equipment Division


GARY A. DUBRO
Aerospace Engineer
Flight Controls Division

FOR THE COMMANDER


AMBROSE B. NUTT
Director, Vehicle Equipment Division
AF Flight Dynamics Laboratory


ROBERT P. JOHANNES
Assistant Chief, Flight Controls Division
AF Flight Dynamics Laboratory

"If your address has changed, if you wish to be removed from our mailing list, or if the addressee is no longer employed by your organization please notify AFFDL/FES, W-P AFB, OH 45433 to help us maintain a current mailing list".

Copies of this report should not be returned unless return is required by security considerations, contractual obligations, or notice on a specific document.

UNCLASSIFIED

SECURITY CLASSIFICATION OF THIS PAGE (When Data Entered)

REPORT DOCUMENTATION PAGE		READ INSTRUCTIONS BEFORE COMPLETING FORM
1. REPORT NUMBER AFFDL-TR-78-106	2. GOVT ACCESSION NO.	3. RECIPIENT'S CATALOG NUMBER
4. TITLE (and Subtitle) ANALYSIS AND CALCULATIONS OF LIGHTNING INTERACTIONS WITH AIRCRAFT ELECTRICAL CIRCUITS		5. TYPE OF REPORT & PERIOD COVERED FINAL TECHNICAL REPORT 76 May 16 - 78 Feb 21
7. AUTHOR(s) F.A. Fisher		6. PERFORMING ORG. REPORT NUMBER SRD-78-044
9. PERFORMING ORGANIZATION NAME AND ADDRESS General Electric Company Corporate Research and Development P.O. Box 8 - Schenectady, NY 12301		10. PROGRAM ELEMENT, PROJECT, TASK AREA & WORK UNIT NUMBERS 2402-02-23
11. CONTROLLING OFFICE NAME AND ADDRESS Air Force Flight Dynamics Laboratory (FES) Wright-Patterson AFB, OH 45433		12. REPORT DATE August 1978
14. MONITORING AGENCY NAME & ADDRESS (if different from Controlling Office)		13. NUMBER OF PAGES 379
		15. SECURITY CLASS. (of this report) Unclassified
		15a. DECLASSIFICATION/DOWNGRADING SCHEDULE
16. DISTRIBUTION STATEMENT (of this Report) Approved for public release; distribution unlimited		
17. DISTRIBUTION STATEMENT (of the abstract entered in Block 20, if different from Report)		
18. SUPPLEMENTARY NOTES		
19. KEY WORDS (Continue on reverse side if necessary and identify by block number) Lightning, Aircraft, Induced Voltages, Noise Immunity, Interference Protection; Electromagnetic Compatibility		
20. ABSTRACT (Continue on reverse side if necessary and identify by block number) This report documents the results of a study performed to evaluate the indirect effects of lightning strikes - specifically, induced voltages - on the electrical systems of aircraft. Numerical methods for evaluating the fields produced by lightning currents flowing in the skin of the aircraft are presented as a first analytical step. Additional numerical methods, for computing the voltages induced in wiring systems by the fields evaluated in the first step, are also presented, as are recommendations on the direction of further study.		

DD FORM 1473 EDITION OF 1 NOV 65 IS OBSOLETE

UNCLASSIFIED
SECURITY CLASSIFICATION OF THIS PAGE (When Data Entered)

FOREWORD

This Final Report documents the results of work conducted by the General Electrical Company, Pittsfield, Massachusetts, on Lightning Interactions with Aircraft Electrical Circuits. The work was sponsored by the Air Force Flight Dynamics Laboratory, Wright-Patterson AFB, OH, under Contract F33615-76-C-3122 and covers the period May 1976 to February 1978. Mr. Gary DuBro (AFFDL/FGL) and Dr. John Corbin (AFFDL/FES) were the AFFDL Project Engineers.

The report includes an assessment of the state-of-the-art by Mr. Frank A. Fisher, the Principal Author, and does not necessarily represent the viewpoint of the Air Force Flight Dynamics Laboratory.

ERRATA

TIME 1 is incorrectly called TIME 2 on Line 5320 of Figure 6.9. The maximum values of the responses in Figures 6.15 and 6.18 should be doubled as a result.

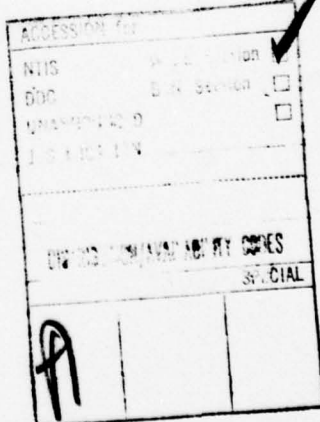


TABLE OF CONTENTS

<u>Section</u>	<u>Page</u>
I INTRODUCTION.	1
II ASSESSMENT OF THE ART OF CALCULATING LIGHTNING INTERACTIONS.	5
2.1 Purpose of this Section	5
2.2 Approaches to Lightning Compatibility	5
2.2.1 Discussion of Approaches in General	5
2.2.2 Approach Used in this Study	8
2.2.3 Understanding Phenomena Through Experimentation	10
2.2.4 Zonal Approach for Internal Induced Electromagnetic Effects	10
2.3 Lightning Flash Phenomena	17
2.3.1 General Observations.	17
2.3.2 General Characteristics of the Lightning Flash	17
2.3.3 The Return Stroke	18
2.3.4 Nearby Flashes.	22
2.4 Interaction of the Lightning Flash with the Aircraft	23
2.5 Applicability of EMP Knowledge and Technology.	25
2.5.1 Aperture Analysis	28
2.5.2 Cable Analysis Programs	37
2.5.3 Test Techniques	37
III THE LUMPED PARAMETER METHOD (LPM) OF MODELING	43
3.1 Basic Considerations in LPM Modeling.	43
3.2 Determining Inductance, Capacitance, and Resistance.	45
3.2.1 Concentric Geometry	45
3.2.2 Physical Significance of Inductance and Capacitance	48
3.2.2.1 Self-Inductance	48
3.2.2.2 Mutual Inductance	50
3.2.2.3 Self-Capacitance.	53
3.2.2.4 Mutual Capacitance.	53
3.2.2.5 Multiple Dielectrics.	54
3.2.2.6 Relation Between Inductance and Capacitance	55
3.2.3 Isolated Conductors and Conductor Pairs	55
3.2.4 Conductor Over a Ground Plane	59
3.2.4.1 Self- and Mutual Inductance	59
3.2.4.2 Second Order Effects.	60
3.2.4.3 Capacitance	60
3.2.5 Practical Calculation of Inductance and Capacitance	62
3.2.6 Effects of Line Losses.	66

TABLE OF CONTENTS (CONT'D)

<u>Section</u>	<u>Page</u>
III THE LUMPED PARAMETER METHOD (LPM) OF MODELING (Cont'd)	
3.3 Lumped Constant Representation of Conductors	67
3.3.1 Single Conductors.	67
3.3.2 How Many Sections To Use?.	67
3.3.3 Coupled Conductors	68
3.3.3.1 Capacitance.	69
3.3.3.2 Inductance	77
3.3.3.3 Aids to Calculation.	79
3.3.3.4 Formulation of an Equivalent Circuit.	79
3.4 Driving Sources.	80
3.4.1 Response to Magnetic Fields.	81
3.4.2 Response to Electric Fields.	84
3.4.3 Connecting the Sources to the LPM Model.	90
3.5 An Illustrated Example of an Equivalent Circuit.	94
3.5.1 Inductance and Capacitance	94
3.5.2 Driving Sources.	97
3.5.3 Problems Regarding Mutual Inductance	105
3.6 ECAP Analysis of the Circuit	106
3.6.1 The ECAP Data File	106
3.6.2 Output Data from ECAP.	110
3.7 Treatment of Shielded Conductors	118
IV DETERMINING THE ELECTROMAGNETIC FIELD ENVIRONMENT.	135
4.1 Introduction	135
4.2 The External Magnetic Field.	135
4.2.1 Elementary Concepts.	136
4.2.2 Calculation of External Magnetic Field Intensity.	140
4.3 The External Electric Field.	141
4.4 The Aperture Coupling Mechanism.	142
4.4.1 Magnetic Fields.	142
4.4.2 Electric Fields.	154
4.4.3 Use of APERTURE Program.	156
4.4.4 Aperture Theory - A Summary and Assessment	160
4.5 The Diffusion Coupling Mechanism	164
4.5.1 Theoretical Considerations	164
4.5.1.1 Circular Cylinders	164
4.5.1.2 Structures of Other Than Circular Shape	171
4.5.2 Experimental Verification.	179
4.5.3 Fields Within Cavities	183
4.5.4 Diffusion Theory - A Summary	188

TABLE OF CONTENTS (CONT'D)

<u>Section</u>			<u>Page</u>
VI DETERMINING THE ELECTROMAGNETIC FIELD ENVIRONMENT (Cont'd)			
4.6 The Computer Program DIFFMAG.			190
4.6.1 Introduction.			190
4.6.2 MAIN.			191
4.6.2.1 Theory Behind MAIN.			191
4.6.2.2 Calculation of Mutual Inductance. .			196
4.6.2.3 Calculation of Self-Inductance. . .			200
4.6.2.4 Program Description - MAIN.			201
4.6.2.5 Subroutine MATRIX			235
4.6.3 Subroutine FILSUM			235
4.6.4 Subroutine VSUM			244
4.6.5 Subroutines PLANI and INCEPT.			244
4.6.5.1 PLANI			251
4.6.5.2 INCEPT.			252
4.6.6 Subroutine LOOP			256
4.7 Usage of DIFFMAG.			270
4.7.1 Geometry Chosen for Analysis.			270
4.7.2 Example of DIFFMAG Output			270
4.7.3 How to Use the Data			292
4.7.3.1 Magnetic Field Within the Structure			292
4.7.3.2 Voltage to Ground on Conductors . .			293
4.7.3.3 Voltage Waveshape			295
4.7.4 Waveshape of Magnetic Field			296
V THE INFLUENCE OF COMPOSITE MATERIALS ON DIFFUSION EFFECTS.			299
5.1 Introduction.			299
5.2 Experimental Studies on Composite Materials .			299
5.3 Significance of Transfer Impedance.			302
5.4 Miscellaneous Observations About Composite Structures.			303
VI ADDITIONAL TOOLS USEFUL FOR ANALYSIS.			307
6.1 Introduction.			307
6.2 Program CONVOLUT.			307
6.2.1 Purpose of CONVOLUT			307
6.2.2 Method of Operation			308
6.2.3 Notes on Input Data			322
6.2.4 Example of Usage of CONVOLUT.			323
6.3 Program TIFREQ.			324
6.3.1 Purpose of TIFREQ			324
6.3.2 Method of Operation			329
6.3.3 Example of Usage of TIFREQ.			338

TABLE OF CONTENTS (CONT'D)

<u>Section</u>		<u>Page</u>
VI	ADDITIONAL TOOLS USEFUL FOR ANALYSIS (Cont'd)	
6.4	Program FREQTI	338
6.4.1	Purpose of FREQTI.	338
6.4.2	Method of Operation.	344
6.4.3	Example of Usage of FREQTI	350
6.5	Internal Impedance	351
6.6	Resonance Modes of Cavities.	356
VII	INTERACTION WITH OTHER EMC ANALYSIS TECHNIQUES . . .	361
VIII	CONCLUSIONS AND RECOMMENDATIONS.	377

LIST OF ILLUSTRATIONS

<u>Figure</u>		<u>Page</u>
2.1	Topological Shielding	8
2.2	Shielded Zones Within the Orbiter Structure . . .	11
2.3	Waveforms of Aperture- and Diffusion-Coupled Magnetic Fields (a) Lightning Current (b) Aperture-Coupled Field, A-component (c) Diffusion-Coupled Field, B-component	12
2.4	The Transient Coordination Philosophy	15
2.5	Short Circuit Current (I_{SC}) Resulting from a Transient Source with VOC Open Circuit Voltage and $50 \Omega/50 \mu\text{H}$ Source Impedance	17
2.6	Front Waveshapes of Lightning Currents as Measured by Berger	19
2.7	Lightning Flashes Near and to an Aircraft (a) Near Miss (b) Direct Hit	21
2.8	Charge on Branches That Affects Current Waveshape	22
2.9	A Postulated Worst Case External Electric Field Intensity	24
2.10	Aircraft Illuminated by EMP-Created Plane Electromagnetic Wave	27
2.11	Aircraft Struck by Lightning	27
2.12	Apertures (a) An Aperture in a Plane (b) An Equivalent Dipole (c) Multiple Dipoles (d) Field Strengths	29
2.13	Available Data on Polarizabilities	31
2.14	Available Data on Polarizabilities	32
2.15	Available Data on Polarizabilities	33
2.16	Traveling Waves Incident upon a Surface (a) The Traveling Wave (b) Resolution into Components . .	34
2.17	Moment Method of Determining Aperture Effects (a) A Single Dipole (b) Multiple Dipoles (c) and (d) Field Strength in the Aperture . . .	35
2.18	Some Surfaces Are too Large or Complex to Model as an Array of Dipoles	36
3.1	Geometry of a Cable with Concentric Return . . .	45
3.2	Self-Impedance	46
3.3	Mutual Impedances	47

LIST OF ILLUSTRATIONS (CONT'D)

<u>Figure</u>		<u>Page</u>
3.4	Magnetic Field Around an Infinite Conductor	49
3.5	Current Return on a Concentric Cylinder	51
3.6	Magnetically Coupled Conductors	52
3.7	Self-Impedance - Two-Media Case	54
3.8	Elementary Conductors (a) An Isolated Conductor Possessing Self-Inductance (b) Adjacent Conductors Possessing Mutual Inductance	56
3.9	Connected Conductors.	57
3.10	Conductor Over a Ground Plane	59
3.11	Second Order Effects	61
3.12	Line to Ground Impedances — Summary	63
3.13	Self-Inductance of Typical Conductors	65
3.14	Self-Capacitance of Typical Conductors	66
3.15	Lumped Constant Approximations	68
3.16	Coupled Conductors (a) Physical (b) Pi Section Equivalent.	70
3.17	Images of the Conductors	71
3.18	Charges Relating to Self-and Mutual Capacitance .	75
3.19	Currents Relating to Self-and Mutual Inductance .	78
3.20	Zones and Ruling Fields in an Aircraft	81
3.21	Cable in Zone A (a) Lengths (b) Position for Run A (c) Position for Run B	82
3.22	Cable in Zone B	83
3.23	Conductors in Zone C (a) Lengths (b) Orientation of Coupled Conductors	84
3.24	Response to Magnetic Fields (a) Geometry (b) Elementary Voltage Source (c) Voltage Source Embedded in the Model	85
3.25	A Surface Exposed to an Electric Field (a) Isometric View (b) End View.	86
3.26	Elevated Surfaces (a) Flat Surface (b) Embedded Hemisphere - Isometric (c) Embedded Hemisphere - End View.	87
3.27	A Conductor Over a Ground Plane (a) Geometry (b) Elementary Voltage Source (c) Elementary Circuit Source.	88

LIST OF ILLUSTRATIONS (CONT'D)

<u>Figure</u>		<u>Page</u>
3.28	Conductor Height Factor	90
3.29	A Current Source Connected to the LPM Model . . .	91
3.30	Specifying the Waveform (a) Basic Waveform (b) Coarsely Sampled (c) Finer Sampling	91
3.31	The Use of Auxiliary Circuits (a) A Way of Re- presenting Magnetic Field Effects (b) An Aux- iliary Circuit to Control T1 (c) An Alternate Way of Representing Magnetic Field Effects (d) A Way of Representing Electric Field Effects (e) An Auxiliary Circuit to Control T2	92
3.32	Equivalent Concentric Geometry	96
3.33	Total Impedances in the Various Sections	98
3.34	Larger Impedances Divided Into Two Lumps	98
3.35	Capacitances at Ends of Lumps Combined	99
3.36	Electric Field Effects in Zone A (a) Electric Field (b) Injected Current	100
3.37	Magnetic Field Effects in Zone A (a) Magnetic Field (b) Injected Voltage.	101
3.38	Magnetic Field Effects in Zone B (a) Magnetic Field (b) Injected Voltage.	102
3.39	Magnetic Field Effects in Zone C (a) Magnetic Field (b) Injected Voltage - Conductor 1	103
3.40	Component Values of Equivalent Circuit	103
3.41	Component Values of Equivalent Circuit (Aux- iliary Circuits) (a) Circuit Used to Excite T1 (b) Circuit Used to Excite T2 (c) Circuit Used to Excite T3 (d) Circuit Used to Excite T4 . . .	104
3.42	Representation of Mutual Inductance with De- pendent Current Generators (a) One-Way Coupling (Generally Stable) (b) Two-Way Coupling (Po- tentially Unstable)	105
3.43	Nodes and Branches Numbered for ECAP Analysis (Main Circuit).	106
3.44	Nodes and Branches Numbered for ECAP Analysis (Auxiliary Circuits)	107
3.45	ECAP Data File	108
3.46	1000 Ω Terminations - Current at Center of Conductor 1	111

LIST OF ILLUSTRATIONS (CONT'D)

<u>Figure</u>			<u>Page</u>
3.47 1000 Ω Terminations — Voltage at Ends of Main Conductor	113		
3.48 1000 Ω Termination — Voltages at Ends of Coupled Conductor	114		
3.49 A Simplified Equivalent Circuit	115		
3.50 Conductors Shorted — Current in Main Conductor	116		
3.51 Conductors Shorted — Current in Coupled Conductor	117		
3.52 Conductor Open at One End — Current in Main Conductor	119		
3.53 Conductor Open at One End — Voltages on Main Conductor	120		
3.54 Conductor Open at One End — Voltages on Coupled Conductor	121		
3.55 Treatment of a Shielded Cable (a) The Total Cable (b) Factors Governing Propagation Internal to the Sheath (c) Factors Governing Propagation External to the Sheath	122		
3.56 A Shielded Cable (a) Elementary (b) More Detailed	124		
3.57 Component Values of Equivalent Circuit	125		
3.58 Nodes and Branches Numbered for ECAP Analysis	126		
3.59 Shield Open at One End — Voltage from Shield to Ground	127		
3.60 Shield Open at One End — Voltage at Open End of Cable	128		
3.61 Shield Open at One End — Voltage at Terminated End of Cable.	129		
3.62 Effect of Capacitance — Voltage at Termination	131		
3.63 Effect of Capacitance — Current Through Capacitor	132		
3.64 Shield Grounded at Both Ends — Voltage at Termination	133		
3.65 Shield Grounded at Both Ends — Current Through Capacitor	134		

LIST OF ILLUSTRATIONS (CONT'D)

<u>Figure</u>	<u>Page</u>
4.1 Magnetic Fields Around Current-Carrying Conductors (a) Current-Carrying Filament (b) Tubular Conductor (c) Irregular Conductor	137
4.2 Field Intensity Vs. Radius of Curvature	138
4.3 Magnetic Field Intensity at the Surface of an Elliptical Conductor	139
4.4 A Structure Defined as an Array of Wires (a) The Array (b) Coordinates Defining Location (c) Definition of the Return Path for Current	140
4.5 Wire Grid Approximation of the Elliptical Fuselage	141
4.6 Aperture-Type Magnetic Field Coupling (a) External Field Patterns (b) Internal Field Patterns . .	143
4.7 The Aperture-Coupling Problem (a) A Field Across an Aperture (b) Equivalent Dipole Producing the Same Internal Field	144
4.8 An Elliptical Aperture (a) Geometry and the Components of the External Magnetic Field Vector (b) The Equivalent Magnetic Dipoles	145
4.9 Shape Factor for Elliptical Apertures	146
4.10 Field Patterns Produced by a Dipole Lying Along the X-Axis.	147
4.11 An Illustrated Example of Aperture-Coupled Fields.	150
4.12 Dipole Approximation (a) Elementary Dipole (b) Dipole of Finite Size	151
4.13 Reflecting Surface	151
4.14 Multiple Reflecting Surfaces	152
4.15 Determination of the Voltage Produced by Aperture Coupling	153
4.16 Aperture-Type Electric Field Coupling (a) External Field Patterns (b) Internal Field Patterns . .	154
4.17 Geometry Appropriate to Electric Coupling	155
4.18 A Sample Problem That Can Be Solved by APERTURE (a) The Aperture and the Sheet in Which it Is Related (b) Loops Behind the Aperture	157
4.19 Data File Used to Describe an Aperture Problem. .	158
4.20 Input Data for Program APERTURE — Long Form . .	159

LIST OF ILLUSTRATIONS (CONT'D)

<u>Figure</u>		<u>Page</u>
4.21	APERTURE Output Resulting from Input Data of Figure 4.20.	161
4.22	Fields Coupled Through an Aperture-Major Axis Oriented Vertically (0.2×0.1 m Aperture) . . .	162
4.23	APERTURE Sample (Flux Produced in Loops).	163
4.24	Magnetic Fields Around A Circular Cylinder (a) Geometry (b) Field Intensity vs. Radius (For $I = 116$ A)	164
4.25	External Voltage (Not to scale)	166
4.26	Factors Governing the Internal Voltage (a) Geo- metry and Decaying Eddy Currents (b) Current Density at Different Times.	167
4.27	Diffusion-Type Response to a Step Function . . .	168
4.28	Skin Thickness vs. Penetration Time Constant . .	169
4.29	Magnetic Fields Around an Elliptical Cylinder (a) Penetrating Lines of Flux (b) Detail Showing Resolution into Components (c) Circulating Cur- rents Induced by Penetrating Lines of Flux . . .	171
4.30	Variation of Current-Density with Time (a) Cur- rent Components Defined (b) Edge and Center Cur- rents (c) Circulating Currents	173
4.31	The Internal Magnetic Field that Arises as a Result of Flux Penetration	174
4.32	Factors Governing the Early Time Build-up of the Internal Magnetic Field (a) Physical Factors (b) Equivalent Circuit.	176
4.33	Final Equivalent Circuit Governing Increase of Internal Circulating Circuit.	177
4.34	Factors Governing the Internal Voltage (a) The Geometry (b) Internal Flux Linkages	177
4.35	The Internal Voltages (a) Detail of the Edge Surface (b) Paths of Integration (c) Components of V_1 (d) Components of V_2	178
4.36	Arrangement of Conductors Inside Elliptical Cy- linder (a) Detail (b) End View Showing Locations of Conductors (c) Electrical Termination of In- ternal Conductors (Typical)	180
4.37	Variation of Conductor Voltage with Time (Leading edges of waveforms retouched for photographic clarity)	181

LIST OF ILLUSTRATIONS (CONT'D)

<u>Figure</u>		<u>Page</u>
4.38	Difference Voltages and Total Flux (Leading edges of waveforms retouched for photographic clarity)	182
4.39	Voltages as a Function of Position.	183
4.40	A Cavity Exposed to a Field on Only One Side (a) Cavity and External Field Orientations (b) Internal Magnetic Field and the Current Loop Defining the Internal Inductance.	184
4.41	Generalized Behavior of Current and Magnetic Field (a) Total Current (step function) (b) Current on Inner Surface of Outer Sheet (c) Current on Inner Sheet (Also Shape of Magnetic Field) . .	185
4.42	Typical Current Paths and Characteristic Impedance (a) Long Sheets (b) Rectangular Box (c) Circular Cylinder	186
4.43	Correction Factors for Inductance (a) Parallel Strips (b) Rectangular Boxes (c) Circular Cylinders	187
4.44	Effects of Covers and Fasteners	188
4.45	Possible Equivalent Circuit Governing Build-up of Magnetic Field Inside a Cavity	189
4.46	A Surface Defined by Filaments.	192
4.47	Mutually Coupled Inductances	192
4.48	A General Conductor in Space	195
4.49	Layout of Matrix D(i,j)	196
4.50	Two Filaments Placed in any Arbitrary Locations .	196
4.51	Two Filaments in the Same Plane but not Parallel.	199
4.52	Parallel Filaments	199
4.53	Input Data for Program DIFFMAG	202
4.54	Listing of Program DIFFMAG	206
4.55	Program DIFFMAG - MAIN.	220
4.56	Calculation of Self and Mutual Inductance . . .	231
4.57	Program Listing of Subroutine MATRIX Concluded	236
4.58	A Current Carrying Filament	238
4.59	Program Listing of Subroutine FILSUM	241
4.60	Flow Chart of Subroutine FILSUM	242

LIST OF ILLUSTRATIONS (CONT'D)

<u>Figure</u>	<u>Page</u>
4.61 Conventions Regarding Angles: (a) Latitude and Longitude Angles Defined; (b) Quadrant Designations for Longitude; (c) Quadrant Desig- nations for Latitude	245
4.62 Program Listing of Subroutine VSUM.	246
4.63 Flow Chart of Subroutine VSUM	247
4.64 A Surface Defined by Filaments.	249
4.65 A Plane Intersecting the Filaments.	249
4.66 The Tangential Magnetic Field	249
4.67 A Source of Error	250
4.68 Program Listing of Subroutine PLANI	256
4.69 Program Listing of Subroutine INCEPT.	257
4.70 Flow Chart of Subroutine INCEPT	259
4.71 Flux Linking an Arbitrary Four Sided Loop	262
4.72 Integration Techniques for Flux in a Plane.	263
4.73 Program Listing of Subroutine LOOP.	264
4.74 Flow Chart of Subroutine LOOP	266
4.75 Illustrative Geometry	270
4.76 Conductor Locations	271
4.77 Loops Contained Within Structure.	272
4.78 Input Data for Illustrative Example	273
4.79 Input Data for Illustrative Example (Conclusion).	274
4.80 First Lines of Output Data.	274
4.81 Conductor Locations	275
4.82 Conductor Locations (Conclusion).	276
4.83 Length and Diameter of Conductors	277
4.84 Distances Between Ends of Conductors.	278
4.85 Total Current and How It Divides.	279
4.86 Intercept Calculations for Z = 2 m.	281
4.87 Intercept Calculations for Z = 4 m.	282
4.88 Field Intensities Over a Volume	283
4.89 Field Intensities Over a Volume (Conclusion).	284
4.90 Field Intensities at Discrete Points.	285

LIST OF ILLUSTRATIONS (CONT'D)

<u>Figure</u>		<u>Page</u>
4.91	Field Patterns as Determined by Magnetic Distribution of Current	286
4.92	Field Patterns as Determined by Resistive Distribution of Current	286
4.93	Loop Calculations.	287
4.94	Data Format When Field Intensity is Resolved into Polar Coordinates	288
4.95	Data Format When Field Intensity is Resolved into Polar Coordinates (Conclusion).	289
4.96	Data Format When Only Initial and Final Magnitudes of Field Intensity are Presented	290
4.97	Data Format When Only Initial and Final Magnitudes of Field Intensity are Presented	291
4.98	Structure with Parallel Geometry (a) Isometric View (b) End View	294
4.99	Waveshapes of Voltages to Ground	296
4.100	Waveshape of Voltage Between Conductors.	297
4.101	Integral of Voltage Between Conductors (Hence waveshape of magnetic field)	297
5.1	Schematic of Quadraxial Test Fixture	300
5.2	Measured Surface Transfer Impedance of 12-Ply HTS and 24-Ply T300 Graphite (6 in. diameter cylinder, 36 in. long)	301
5.3	Transfer Impedance of Graphite Compared to Aluminum	302
5.4	Predicted Waveshapes in Structures of Different Materials.	304
6.1	Analysis of a General Function as the Superposition of Elementary Functions (a) Superposition of step functions (b) Superposition of impulse functions.	308
6.2	Original Input Functions (unequal time intervals). .	309
6.3	Derived Input Functions (equal time intervals) . .	310
6.4	Function E When Option 1 is Selected (E = derivative of C)	310
6.5	Function E When Option 2 is Selected	311
6.6	Multiplication Steps at t1	311
6.7	Multiplication Steps at t2	312

LIST OF ILLUSTRATIONS (CONT'D)

<u>Figure</u>		<u>Page</u>
6.8	Multiplication Steps at t5	313
6.9	Program CONVOLUT	314
6.10	Functions with Discontinuities (a) Discontinuity of slope (b) Discontinuity of amplitude.	322
6.11	Response of an Elliptical Cylinder to a Step Function of Current ($I = 1000$ Amperes = 1 kA)	323
6.12	Arbitrary Input Current ($I = 41$ kA)	324
6.13	Listing of Data File INCOFIL.	325
6.14	First Part of Tabular Output.	326
6.15	Second Part of Tabular Output	327
6.16	Step Response of Elliptical Cylinder as Plotted by Program.	328
6.17	Arbitrary Input Function as Plotted by Program.	328
6.18	Response of Cylinder to Arbitrary Input Shown on Figure 6.17.	329
6.19	Generalized Time Function $A(t)$	330
6.20	Program TIFREQ.	333
6.21	Time-Domain Test Wave	338
6.22	Input Data for TIFREQ	339
6.23	First Part of TIFREQ Output Data.	340
6.24	Second Part of TIFREQ Output Data	341
6.25	Real and Imaginary Parts of Fourier Transform	343
6.26	Total Part of Fourier Transform	343
6.27	Generalized Frequency Domain Function $R(\omega)$	344
6.28	Program FREQTI.	347
6.29	Input Data for FREQTI	351
6.30	First Part of Output Data	352
6.31	Second Part of Output Data.	353
6.32	Reconstructed Time Domain Wave.	354
6.33	An Open-Ended Cylinder.	355
6.34	An Elementary Mode of Cavity Resonance.	356
6.35	Some Resonance Modes in a Rectangular Enclosure	357
7.1	Program CHANGER	363

LIST OF ILLUSTRATIONS (CONT'D)

LIST OF TABLES

<u>Table</u>		<u>Page</u>
2.1	Magnetic Fields in Different Zones of the <u>Space Shuttle</u>	12
2.2	Proposed Transient Control Levels.	16
2.3	Alternative Transient Control Levels	16
3.1	Impedance Parameters for the Coupled Lines	95
4.1	Calculations Related to Figure 4.11.	149
4.2	Resistivities of Typical Metals.	170
4.3	Correspondence Between Terms Used in Equations and Terms Used in the Program.	232
5.1	A Comparison of Pulse Penetration and Redistribution Time Constants	303
6.1	Some Resonance Modes in a Rectangular Enclosure.	358

SECTION I

INTRODUCTION

The work covered in this report is an attempt to improve upon a method of calculating lightning induced voltages that was reported in an earlier work (Reference 1.1). That earlier work discussed how the voltages upon an electrical circuit within an aircraft are related to the magnetic field produced within the aircraft as a result of lightning current passing through the aircraft. Basically, there are two ways that magnetic fields are produced within an aircraft as a result of lightning current: (1) by coupling through apertures and (2) by coupling through the walls of metal skin that form the structure of the aircraft. This latter type of coupling is called diffusion coupling. In that earlier work, the aircraft was modeled as a group of filaments, the filaments making up an outline of the aircraft. Given a total lightning current entering the aircraft, the manner in which the current divided among the various filaments was calculated and the total magnetic field produced by those currents was calculated; then the voltage upon a conductor exposed to that field was calculated.

At the time that work was undertaken the phenomenon of diffusion coupling of magnetic fields was imperfectly understood; consequently, some of the concepts upon which the work was based were incorrect. As a result, the waveshapes of voltages predicted to be produced by the calculated magnetic field were incorrect. However, during the period the work was being performed, other studies were improving our understanding of how voltages were developed by the internal magnetic fields. The first set of studies was undertaken by Burrows (Reference 1.2); a second set, of shorter duration, was under undertaken by Fisher (Reference 1.3). These latter studies were particularly effective in clarifying the mechanism of diffusion coupling.

On the basis of the earlier work together with the studies of the diffusion mechanism, it seemed worthwhile to try to improve upon the earlier computer routines for calculating lightning-induced voltages. In addition to incorporating new routines to take into account better the diffusion mechanism, it appeared worthwhile to add additional objectives to the program. Individually those additional objectives were worthy, but their accumulation made the programming highly complex, and ultimately impractical. A critical reappraisal of the goals focused attention on a more realistic scope, which could be brought to a valid conclusion. Also, a change in the principal investigator (during this reappraisal process) provided a different perspective--one that called upon previous successful experience in related fields.

The central task that was undertaken was to develop a lightning computer program with which the average engineer familiar

with lightning, or the electrical effects produced by lightning, could do the following:

- 1) Describe an aircraft to the computer
- 2) Describe the wires within that aircraft
- 3) Describe the structural members and electrical apertures on the aircraft and then direct the computer to calculate the voltages upon those circuits, preferably in a manner that was directly compatible with other computer programs used to treat other electromagnetic compatibility (EMC) problems.

Indeed, the ultimate desire had been to have the Lightning Computer Program be made into a subroutine of an EMC program such as IEMCAP. This was a worthy goal, but, with hindsight, it appears to have been too ambitious a project for resources allocated to the contract.

Recognizing that the program undertaken could not result in a complete computer analysis of lightning interactions, the researchers focused on achieving as many useful results from the study as possible. Their aim was to provide those working in the field of lightning interactions both guidance and tools for undertaking calculations of lightning interactions. This report, in summarizing the work accomplished, presents a program that combines several computer routines with human intervention at the intermediate steps in the calculation of lightning interactions with aircraft electrical circuits.

This report also discusses the author's viewpoints on how lightning compatibility might be achieved and on what direction research into the nature of lightning and lightning interactions should take in order to achieve that compatibility.

In summarized form, the conclusions are that lightning compatibility will be achieved through wider dissemination of recommended practices, different specifications placed upon manufacturers of electronic equipment for aircraft, and better test procedures to verify that the aims of those specifications are achieved. Those practices, specifications, and tests should be drawn up by people with considerable experience in lightning phenomena and lightning interactions. Lightning compatibility is not likely to be achieved through analyses, however sophisticated or however well supported by computer routines they may be, unless the routines and results of computer programs follow a path anchored in reality and incorporate the experience of engineers well-versed in the field of lightning interactions.

REFERENCES

- 1.1 K.J. Maxwell, F.A. Fisher, J.A. Plumer, and P.R. Rogers, Computer Programs for Prediction of Lightning Induced Voltages in Aircraft Electrical Circuits, Air Force Flight Dynamics Laboratory, Air Force Systems Command, Wright-Patterson Air Force Base, Ohio, AFFDL-TR-75-36 (April 1975).
- 1.2 B.J.C. Burrows, "Induced Voltages, Measurement Techniques and Typical Values," Proceedings of the 1975 Conference on Lightning and Static Electricity, (Culham Laboratory, England, 14-17 April 1975), Session IV: Aircraft Applications, the Royal Aeronautical Society of London, 1975.
- 1.3 F.A. Fisher and J.A. Plumer, Lightning Protection of Aircraft, NASA Reference Publication 1008, October 1977, pp. 293-327.

SECTION II

ASSESSMENT OF THE ART OF CALCULATING LIGHTNING INTERACTIONS

2.1 PURPOSE OF THIS SECTION

In this section, an assessment is given of the present state of the art of determining how electronic equipment in aircraft responds to the electromagnetic effects produced by lightning and of ways to assure that electronic equipment continues to work in the presence of lightning. This assessment will be concerned largely with the approaches taken toward analysis in this program and with the directions it might have taken.

The dividing lines between assessment, conclusion, and recommendations are seldom clear. By its very nature, an assessment is a subjective process, subject to acceptance or criticism by others. In this section, the author's views are more directly stated than in the sections treating computations or physical facts. This subjective assessment is offered in a constructive spirit; whenever appropriate, other views of the subject are also mentioned.

2.2 APPROACHES TO LIGHTNING COMPATIBILITY

2.2.1 Discussion of Approaches in General

Broadly speaking, there seem to be three approaches to achieving compatibility between electronic systems in aircraft and the electromagnetic fields produced by lightning. They are:

1. Understanding phenomena through analysis
2. Understanding phenomena through experimentation
3. Forcing compatibility through standards and recommended practices

We will discuss further these approaches later in the section. This particular report is concerned with understanding phenomena by analysis. This analytical approach may not turn out to be the best method to achieve lightning transient compatibility, but it was explored in order to define its possibilities and limitations.

A line of demarcation exists between those who feel that lightning analyses are fundamentally simple and can be undertaken by the working engineer or other nonspecialists, and those who feel that lightning interactions are complex and so feel that specialists in the field will be able to provide the only satisfactory leadership. This study was undertaken on the premise that interactions in an aircraft system were sufficiently simple to allow development of a lightning transient analysis program and eventually have that program used by nonspecialists. Although

this author had some misgivings on the validity of the premise, the effort was directed initially toward that goal. In this respect a quotation (Reference 2.1) from Dr. Carl Baum of the Air Force Weapons Laboratory (AFWL) seem appropriate. For the words "EMP" one can equally well substitute the word "lightning."

EMP is a formidable problem in two ways. First, a system, such as a ballistic missile, a communications terminal, an aircraft, a satellite, a ship, etc., is generally an electromagnetic mess. The electromagnetic existence and uniqueness theorem, properly utilized, guarantees that there is a unique solution to a given complicated distribution of conductors, dielectrics, and magnetic materials in space (including even nonlinear and active devices, within restrictions) excited by a distribution of sources consistent with Maxwell's equations. However, existence and uniqueness do not, in general, tell one how to calculate the voltage here or current there in some complicated problem.

A general approach to solving complicated geometries is to formulate an integral equation (say, involving both electric and magnetic current densities) and having the "computer" solve the problem in some way. This is an appealing idea but somewhat naive. It is practical to solve pieces of the EMP interaction problem this way (such as for simplified external shapes of the system of concern), but gridding up an entire system, including pieces of the external skin, zones on apertures, every wire and cable shield, etc., is a formidable problem indeed for the largest computers existing or seriously contemplated.

Even if one could do a moment method of gridding of the entire system, it is not clear that it would be the best thing to do. Questions of accuracy become extremely difficult. The variation of the response to various parameters of the problem becomes much more complicated because of the very large number of parameters involved. A more clever approach is called for so that at least approximately the rational processes of human minds can comprehend what the important features are, how they depend on the important variable, and what can be done to correct the situation if required. Computer techniques are an invaluable aid in understanding EMP interaction, and such techniques will need to be refined and extended. However, by themselves such techniques are not adequate. I [Carl Baum] suppose that at some point there may be some blurring between analytical computer techniques (some of which may be already beginning), but this is likely a healthy thing which can lead to yet further progress.

One of Baum's comments in the first of the previous extracts needs to be emphasized--real systems "are a mess," at least from the point of view of electromagnetic interaction problems. They always were a mess, probably always will be a mess, and it is

unrealistic and wasteful not to recognize it. This leads to a dilemma--what to do about it. There are two ways to go (perhaps more than two) and each of them has advantages and disadvantages.

The first path involves giving up on the attempt to calculate the voltages or currents to which electronic equipment in aircraft would be subjected in the event of a lightning flash and, rather, defining construction practices appropriate to different zones in the aircraft. A start on such a formulation of electromagnetic zones has been made (Reference 2.2) in the Space Shuttle Lightning Protection Criteria Document. Coupled with those definitions of zones would be better standards relating to what transient voltages and currents electronic equipment should be required to withstand. Reduced to its simplest form, this implies that the way to solve lightning interaction problems is for the working circuit designer or engineer to follow the practices that have been laid down for him by experts in the field.

The concept of electromagnetic field zones for aircraft has not yet been applied on programs other than the Space Shuttle.

Baum, in his note at the FULMEN Meeting, presents an approach to looking at interaction problems that seems to parallel in some ways the concept of electromagnetic field zones with wiring and circuit practices graded for those zones. The concept is called Topological Shielding. Wiring and equipment practices, and engineering analysis or concern would be graded according to the shielding order involved (Figure 2.1). The shielding order, even though expressed numerically in values ranging from zero, for systems with little or no shielding, to high values, for systems with lots of shielding, is a philosophical concept. No one should confuse it with the concept of shielding effectiveness used to describe materials, structures, or cables.

The second way is to attempt to calculate the voltages, currents, and power levels on electrical circuits, in spite of the difficulties presented by problem formulation and electromagnetic complexity, on the principle that the induced voltages calculated are valuable for comparison and design purposes even if the actual magnitudes obtained are not always correct. This latter approach is the one that was taken in this contract.

A problem that one has with numerical answers to a complex or poorly formulated problem is to ensure that people do not read excessive precision into numerical results. Group A making a series of calculations may have an understanding of the assumptions used in the calculations and whether the results of the calculations are satisfactory or not, but their task has been only partially fulfilled if they do not communicate those assumptions and assessments of errors to Group B, the group making use of or expanding upon these numerical results.

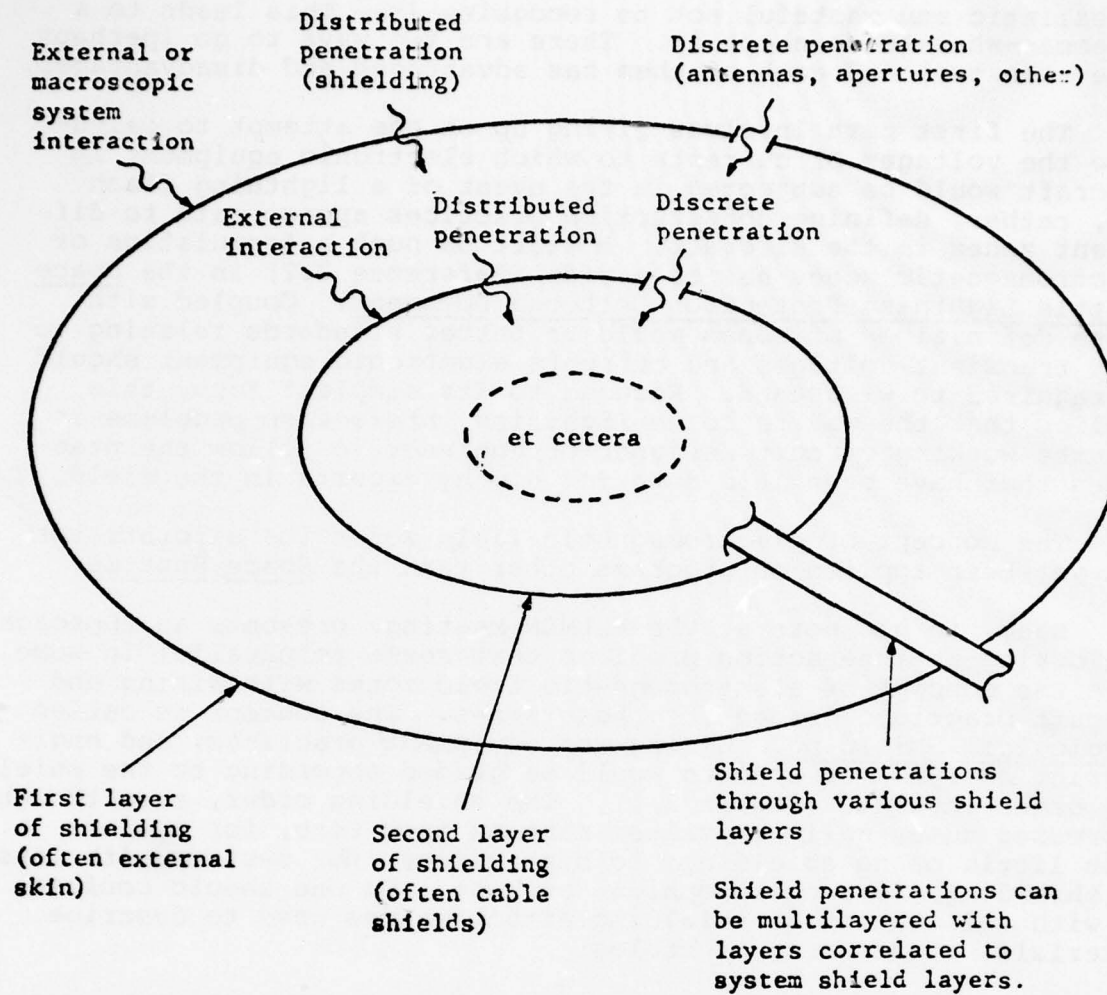


Figure 2.1 Topological Shielding

2.2.2 Approach Used in This Study

The approach to analysis used in this study is based on the following basic steps:

1. Determine the magnitudes of the electric and magnetic fields on the exterior of the aircraft.
2. Determine the magnitudes and governing time constants that define the magnetic fields penetrating the conducting skin (diffusion fields).
3. Determine the magnitudes of the electric and magnetic fields that penetrate apertures (aperture fields).
4. Determine how these fields interact with the aircraft wiring.

Some additional tasks are sometimes necessary, but these are appendages to the tasks outlined above.

These appendages include being able--

1. To define the waveshape of the lightning current in a variety of ways.
2. To convert time domain data to frequency domain data or vice versa through use of the direct and reverse Fourier transforms.
3. To convert step function response into the response to arbitrary waveshapes through use of the convolution integral.
4. To chain programs together with a minimum amount of human intervention.

The last point deserves special consideration because it touches a central theme of much computer work. This work was undertaken with the expectation that it would be possible to generate a computer program with which the nonspecialist could describe an aircraft by a limited number of data points and from which "the computer" would be able to determine the internal electromagnetic fields and the voltages upon conductors, all with a bare minimum of human intervention. Our present understanding of the physics of the lightning interaction problem is too limited to allow us to write such a lightning interaction computer program even if we were sophisticated enough to do all the computer book-keeping required to write and validate such a program. Attempts to force-fit complex physical phenomena into an overly simplified form that fits our available computer skills and practical software capabilities seems likely to generate only invalid numbers. Speed of computation is desirable, as is ease of data input and output, and reduction of data transcription and key punch operations, but unless the end result is numbers that have physical significance, the task is all for naught.

Given the premise that we wished to attempt to calculate voltages and currents, there are no alternatives to the task of mapping the internal electromagnetic fields and making (or at least attempting to make) calculations of voltages and currents from those fields. Two factors provide us with some relief in that task. The problem of calculating voltages or currents on conductors from knowledge of the electromagnetic fields is harder at higher frequencies, where the cavity resonances and conductor resonances are important. These resonances would seem most important in the EMP frequency spectrum. They may (and the stress on the word "may" is deliberate) be less important for lightning. The second is that even if the numerical complexity of calculating electromagnetic field distributions inside an aircraft were to be so difficult that the task could not be carried to successful completion, it is still possible to measure these electromagnetic fields, at least during tests using simulations of lightning.

In the past, the electromagnetic field problem has been treated as having two major aspects, the problems of electromagnetic penetration by diffusion through materials and the problem of electromagnetic penetration through apertures. In Figure 2.1, from Baum, these are referred to as distributed penetration and discrete penetration. Baum's discrete penetration includes the effects of antennas and elements exposed to the exterior of the aircraft, as well as coupling through apertures. These latter have not been dealt with in analyses such as those for the Shuttle. The concept of dividing the problem into diffusion and aperture coupling modes still seems to be the best way to go. In particular, this holds true when one considers the effects of composite structural materials--with their inherently poor shielding capabilities--on the design of the aircraft. Diffusion effects, while frequently overshadowed by aperture effects in metal aircraft, should be much more important in aircraft employing large amounts of composite materials. The concepts that have been developed lately to treat the electromagnetic field mapping of metal aircraft seem to offer a powerful tool for the analysis of the effects of composite structures.

2.2.3 Understanding Phenomena Through Experimentation

Analysis is only one of the ways that one can determine the voltages and currents to which a piece of electronic equipment might be subjected. Experimentation in which an aircraft is subjected to currents or voltages representative of those produced by lightning is another, and, for a specific aircraft, probably more useful. One variant of the experimental philosophy is embodied in the Lightning Transient Analysis (LTA) (References 2.3 and 2.4) technique in which the response of aircraft circuits is measured when the aircraft is subjected to relatively low-level currents and voltages of the same shape as those postulated to be produced by lightning. Measurements made at low levels are then extrapolated to predict what would be produced by the postulated worst case lightning threat.

The LTA technique has been criticized on numerous grounds, usually because of the necessary assumption about linear response. Measurements with some sort of LTA technique, however, seem to be the only way of validating any sort of analytical approach to determine voltages and currents.

2.2.4 Zonal Approach for Internal Induced Electromagnetic Effects

Calculating the voltages and currents on an actual circuit can be a formidable task, even if one assumes that it is possible to separate out one circuit from the interactions that it will inevitably have with other circuits. Calculating the electromagnetic fields to be found within different portions of an aircraft is also a formidable job, but not as formidable as calculating voltages and currents.

A possible solution to the problem lies in recognizing that aircraft, or at least aircraft within a particular category, tend to possess characteristic zones. On a fighter aircraft, for example, the cockpit can be regarded as a magnetically open zone exposed primarily to aperture-coupled magnetic fields. Within reasonable limits, all fighter aircraft have approximately the same magnetic field in the cockpit. Another type of equipment zone characteristic of fighters would be equipment bays located in the forward section and behind the radome. All such equipment bays tend to be alike, the differences relating mostly to the type of fasteners used to hold the covers in place. The structure within a wing is a type of magnetic field structure fundamentally different from either the cockpit or the forward equipment bays. Accordingly, it would seem possible to divide an aircraft into a small number of typical zones, to assign a ruling or characteristic magnetic field intensity to those zones, and to provide simplified tables of nomograms listing the characteristic transient to be induced in wiring of a given length.

This concept of dividing an aircraft into shielding zones was first used on the Space Shuttle (Reference 2.5). The zones so defined are shown in Figure 2.2 (Reference 2.6). The electromagnetic fields assigned to each of these zones were initially determined by engineering judgment. They were then refined during the course of an extensive analytical investigation. The magnetic field amplitudes assigned to each of these zones, based on the analytical study, are given in Table 2.1 (Reference 2.7). These fields were divided into two components--an A-component, referring to the fields coupled through apertures, and a B-component, referring to fields coupled by diffusion through metal surfaces. The A-component of the field would tend to have the same rapidly changing waveshape as the external magnetic field, while the B-component would have a much slower waveshape. In the Space Shuttle study the waveforms of the different components were taken to be as shown on Figure 2.3 (Reference 2.8). In each case the field intensity was based on a worst case 200 kA lightning current

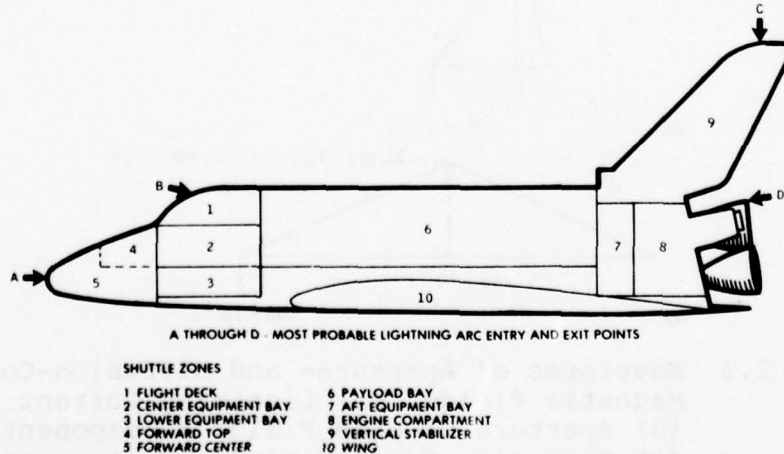


Figure 2.2 Shielded Zones Within the Orbiter Structure

TABLE 2.1
MAGNETIC FIELDS IN DIFFERENT ZONES
OF THE SPACE SHUTTLE

Zone	Aperture Fields A-component (A/m)	Diffusion Fields B-component (A/m)
1	1200	800
2	60	200
3	0	200
4	50	150
5	50	100
6	280	300*
		150**
7	50	570
8	200	680
9	200	3700
10	65	300

*Payload

**No payload

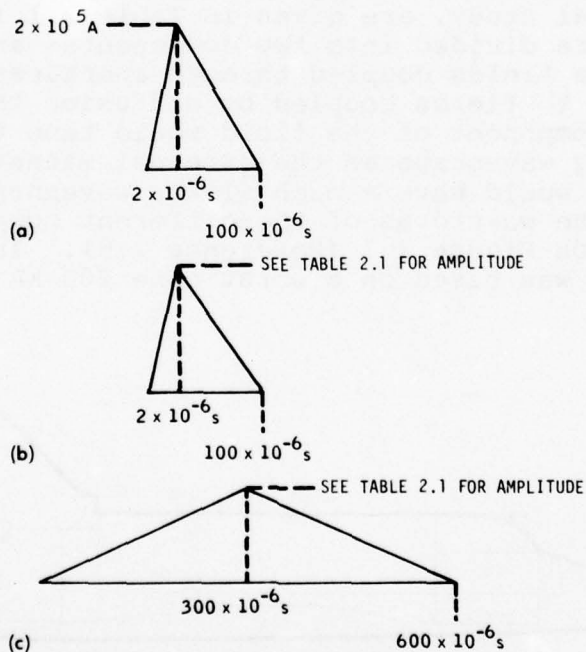


Figure 2.3 Waveforms of Aperture- and Diffusion-Coupled Magnetic Fields
(a) Lightning Current
(b) Aperture-Coupled Field, A-component
(c) Diffusion-Coupled Field, B-component

passing through the Orbiter vehicle. The field amplitudes of Table 1 were the maximum amplitudes calculated for any of the possible lightning current entry or exit points. While no particular claim for accuracy can be made about any individual point within the Orbiter, the aperture field amplitudes seem reasonable.

The concept of dividing an aircraft structure into different magnetic field zones and assigning a ruling magnetic field strength to each zone, while imperfectly formulated at present, is fundamentally no different from the civil engineering practice of designing a structure to withstand a standard (generally worst case) wind loading. While the wind loading may differ widely at different points on the structure, the task of calculating the wind loading on each and every structural member would probably be sufficiently expensive that it would offset the savings that one might realize by tailoring each structural member to its own specific wind loading.

The task of dividing aircraft into typical magnetic field zones and of calculating and assigning the appropriate field strength to each of the zones is probably of sufficient complexity that it should be done by specialists in the field. It should be done only once, and then the results communicated to all those performing analyses on that particular aircraft without unnecessary repetition of that first step in dealing with the problem.

Analytical studies of field intensity could well be supplemented by experimental studies in which currents were circulated through an aircraft and the magnetic fields inside measured.

It may also be that the most straightforward method of achieving lightning transient compatibility is by straightforward specification of the levels of voltage and current that any piece of electronic equipment should be expected to withstand. An approach to the setting of such levels was first presented to the industry through the concept of Transient Control Levels (TCL) (References 2.9, 2.10, and 2.11).

Transient coordination is a concept which, when reduced to its simplest terms, implies that targets relative to transients will be assigned both to those that design electronic equipment ("black boxes") and those that design wiring to interconnect those black boxes. The task that is to be assigned the designers of black boxes is to produce equipment which will be able to withstand transients on all of the input and output wiring. The targets that form a part of the task will be specifications describing the type of transients that the equipment must withstand and to which it will be subjected as part of an acceptance or proof test. The task that is to be assigned to the groups designing interconnecting wiring is that no external threat, such as lightning or switching of inductive devices, shall produce on the wiring transients larger than those which the black box was designed to withstand. The target numbers to which the wiring designer must work will be maximum amplitudes of current, voltage, and surge energy.

The assignment of such tasks implies that there must be a systems engineer, a "referee," who assigns the appropriate target numbers and oversees the work to ensure that both parties fulfill the tasks assigned. This referee may be called the system coordinator. The transient coordination philosophy is illustrated in Figure 2.4. The aims of transient coordination are the following:

1. Ensure that the actual transient level produced by lightning (or any other source of transient) will be less than that associated with the transient control level number assigned to the cable designer. The cable designer's job is then to analyze the electromagnetic threat that lightning would present and to use whatever techniques of circuit routing or shielding are necessary to ensure that the actual transients produced by lightning will not exceed the values specified for that particular type of circuit.
2. The transient design level controlling the type of circuit or circuit protection techniques used, and assigned to the avionics designer, must be higher than the transient control level by a margin reflecting how important it is that lightning will not in fact interfere with the piece of equipment under design. A margin is necessary because any single lightning flash might produce an actual transient level higher than the assigned transient control level, which would have been derived for a predicted average in spite of the cable designer's good intentions, for the prediction of actual transient levels is an imperfect art.
3. The job of the avionics designer is then to ensure that the vulnerability and susceptibility levels of the equipment that he is to supply are higher than the assigned transient design levels. The vulnerability level is that level of transient which, if applied to the input or output circuit under question, would cause the equipment to be permanently damaged. The susceptibility level is defined as that level of transient that would result in interference with or malfunction of the equipment. The vulnerability level by definition, then, must be at least as high as the susceptibility level.

There are several ways in which the levels might be set. First, the system integrator would set the desired transient level, then set the required margin, which in turn would set the transient control level. Whatever the rationale by which the system integrator sets the transient design level, that level would become a part of the purchase specifications and would, presumably, not be subject to variation by the vendor of the avionics. As an alternative, the avionics designer might determine by suitable testing the vulnerability and susceptibility levels of his equipment and provide a guarantee as to the level of transients that his

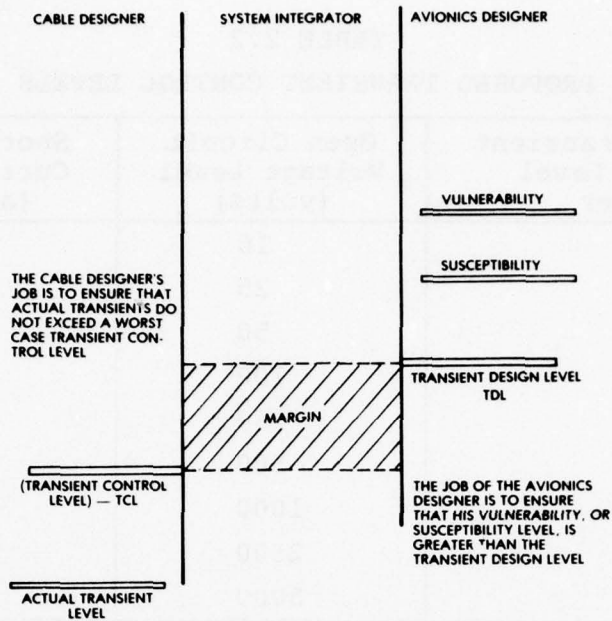


Figure 2.4 The Transient Coordination Philosophy

equipment could withstand. That level would then be the transient design level. After the system integrator has set the desired safety margin, the appropriate transient control level for the cable designer would have been established. One approach to the setting of margins appears in the Space Shuttle Lightning Criteria Document (Reference 2.12).

The numbers that would be assigned to the transient design level probably should be expressed in terms of the maximum voltage appropriate to a high-impedance circuit (open circuit voltage) or the maximum current appropriate to a low-impedance circuit (short circuit current). In order for the transient coordination philosophy to have most impact, there should be a limited number of levels. Two sets of levels that have been proposed (Reference 2.13) are shown in Tables 2.2 and 2.3. With each level there is associated an open circuit voltage and a short circuit current; the two are related by a standard transient-source impedance, shown in Figure 2.5 (Reference 2.14).

TABLE 2.2
PROPOSED TRANSIENT CONTROL LEVELS

Proposed Transient Control Level Number	Open Circuit Voltage Level (volts)	Short Circuit Current Level (amperes)
1	10	0.68
2	25	1.7
3	50	3.4
4	100	6.8
5	250	17.0
6	500	34.0
7	1000	68.0
8	2500	170.0
9	5000	340.0

An alternative set of levels for which some voltages are numerically equal to the voltages in existing specifications is presented in Table 2.3.

TABLE 2.3
ALTERNATIVE TRANSIENT CONTROL LEVELS

Proposed Transient Control Level Number	Open Circuit Voltage Level (volts)	Short Circuit Current Level (amperes)
1	15	1
2	30	2
3	60	4
4	150	10
5	300	20
6	600	40
7	1500	100
8	3000	200
9	6000	400

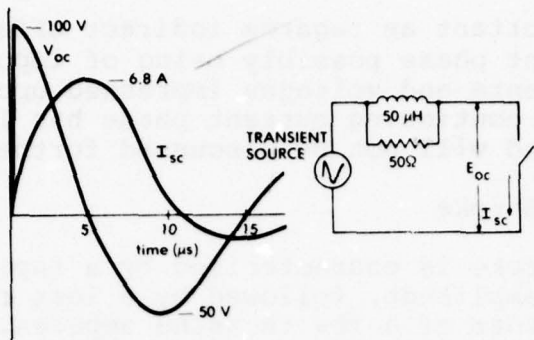


Figure 2.5 Short Circuit Current (I_{SC}) Resulting From a Transient Source with V_{OC} Open Circuit Voltage and $50 \Omega/50 \mu H$ Source Impedance

2.3 LIGHTNING FLASH PHENOMENA

2.3.1 General Observations

Historically, research into the characteristics of lightning has been concerned with protection against the direct effects (burning and blasting) and with considerations of the safety of people and animals. Not nearly as much research has been concerned with protection against the indirect effects with which this program deals. Much of the work has been sponsored by the electric utility industry and has dealt with effects at ground level. The electric utility industry was not concerned with lightning effects at altitudes where aircraft operate. The problems that lightning posed to the electric utility industry, by and large, have been solved, and little work of a fundamental nature is now being sponsored by the electric utility industry. Work that bears upon the indirect effects of lightning is being sponsored by other organizations, but the knowledge that has been accumulated by that work is not yet as comprehensive or as well assimilated by workers dealing with indirect effects as is the knowledge that deals with direct effects.

In the following sections we will address some specific characteristics of the lightning flash to try to separate out those areas where our knowledge is full from those where it is scanty. In those areas where our knowledge is full, it is here worthy to note that the work by Cianos and Pierce (Reference 2.15) has become almost a classic reference.

2.3.2 General Characteristics of the Lightning Flash

Once a lightning flash occurrence has been established, there are three broad regimes that characterize the flash: the return stroke phase (including restrikes), the intermediate current phase, and the long continuing current phase. The return stroke phase

seems the most important as regards indirect effects, with the intermediate current phase possibly being of importance as regards long duration currents and voltages impressed upon electronic apparatus. The long continuing current phase has little effect upon indirect effects and will not be discussed further.

2.3.3 The Return Stroke

The return stroke is characterized by a rapid build-up of current to a high amplitude, followed by a less rapid decay to a current on the order of a few thousand amperes, the intermediate current phase. The peak amplitude of current is well known, at least at ground level. A peak current of 200 kA is often cited as a realistic worst case, a figure that seems to have achieved ready acceptance in the lightning community.

The rate at which the current decays is on the order of 25 to 100 μ s--figures generally accepted. The rate of decay does not greatly affect the voltages or currents induced in the electrical circuits of aircraft, and, as a consequence, there seems little reason to try to refine the rate of decay.

The situation regarding the rate of build-up of current is considerably different. One of the most important aspects of the lightning environment for aircraft is the high-frequency content of the lightning flash. The fact that the words "high-frequency characteristics of the lightning flash" are vague is merely a reflection of our state of knowledge of the lightning flash. One of the aspects that are probably of most importance with respect to interacting with aircraft electrical systems is the nature of the front of the return stroke as it passes through a lightning flash that has gone to ground. Whether there is a clearly defined stroke in a flash going between charge centers in the clouds (intracloud flash) is a point that is not clearly understood. It is, however, clearly understood that there is a return flash associated with cloud-ground strokes and that aircraft are indeed involved with cloud-ground strokes. Our knowledge of the characteristics of this return stroke is biased by the fact that virtually all of the measurements of lightning that have been made were made at ground level. All of the modern measurements of lightning waveforms, as for instance those obtained by Berger (References 2.16 and 2.17), have shown the return stroke to rise in a concave manner, initially rising at a slow rate and then rising at faster rates until the fastest rate of change occurs just before the peak of the lightning current. Examples of such measurements are shown on Figure 2.6. In an unpublished memo, Fisher has speculated that this rapid transition of current is representative of the rate of change of current to which an aircraft in flight might be subjected (Reference 2.18).

Frequently in specifications the build-up of current is assumed to be linear and to require two microseconds for the current

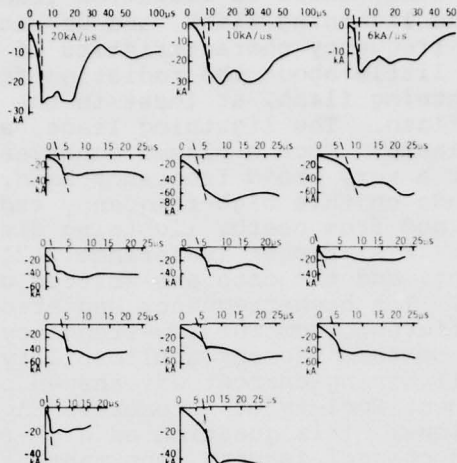


Figure 2.6 Front Waveshapes of Lightning Currents as Measured by Berger

to build from zero to its ultimate value. The assumption of a linear rate of build-up is purely for the sake of convenience in specifications. The figure of two microseconds is generally accepted, but only with reservations.

The question of the front time of the lightning return stroke is being investigated in one way by Martin Uman in Florida (References 2.19 and 2.20). He is measuring the electrical radiation from distant return strokes and using those measurements to calculate the initial rise time of the lightning current. His preliminary measurements indicate that the rise time of the return stroke at altitude might be much faster than the rise time of the return stroke as measured at ground level.

One of the conclusions, then, would be that the lightning community needs to sponsor research as to how fast the return stroke may change as it passes through an aircraft.

Regarding the measurements upon which our knowledge is based, there have been doubts expressed that the bandwidth of the oscilloscopes used in past measurements may have been so limited as to distort the front times of the currents measured. This is a distinct possibility, particularly for those measurements made prior to World War II. The most important measurements, however, are those made after World War II, particularly those of Berger. This author has talked to Berger about this subject, and it is Berger's opinion that the bandwidth was indeed sufficient for the measurements that he has presented.

On the other hand, there is radiation from the hot plasma associated with the lightning flash, and we know practically nothing about the frequency characteristics of that radiation. We also know very little about the radiation from the developing leader of the lightning flash, at least in the immediate vicinity of the lightning flash. The lightning leader and the return stroke represent a hot plasma. Such a plasma doubtless radiates electrical energy over a very broad frequency band. Some investigations have been made on this high-frequency radiation from nearby lightning flashes and from nearby lightning discharges simulating lightning flashes. F.A. Fisher (Reference 2.21) has done some work on the subject, and the data are written up in the reports for the Air Force. The high-frequency radiation characteristics are distinctly different from the low-frequency radiation characteristics; none of them has any applicability to the Fourier transform of the lightning current waveshapes postulated in Mil-B-5087B or the recent Society of Automotive Engineers (SAE) Task Force recommendations. This question of high-frequency radiation from the lightning channel is very important, since one can speculate that there would be considerable radiation at the frequencies to which digital processing equipment is most susceptible--roughly 1 to 30 MHz. These high-frequency radiations are those that couple most readily through apertures in aircraft. One can speculate that a near miss of lightning flash (Figure 2.7a) is less severe than a direct hit on the aircraft (Figure 2.7b), but such speculation should not blind one to the fact that no one has conclusively proven this to be true. If no one has ever truly measured the high-frequency radiation characteristic from nearby lightning flashes of any kind, it is axiomatic that no one has investigated the differences between cloud-ground and cloud-cloud flashes in the high-frequency regions.

Some recent work done under the sponsorship of the Air Force (Reference 2.22) has touched upon this high-frequency radiation. The work done to date only scratches the surface of the subject and should be continued.

Some work (Reference 2.23) has been done in which the lightning channel was modeled as a lumped constant transmission line and an attempt made to study the propagation of the return stroke along such a line by means of analog measurement. It was claimed that these measurements indicated that the front time of a lightning return stroke would lengthen with distance away from the point at which the downward coming leader makes contact with the upward induced leader. The suggestion was also made that the wiggles and wobbles seen on measurements of lightning current might be explained as the result of impedance discontinuities along the leader channel of the lightning flash. It is this author's belief that neither of these premises is likely to be correct. The wiggles and wobbles can be explained more readily as being due to the charge stored on branches of the lightning flash, as shown on Figure 2.8. The build-up of current is more apt to be controlled by the physics

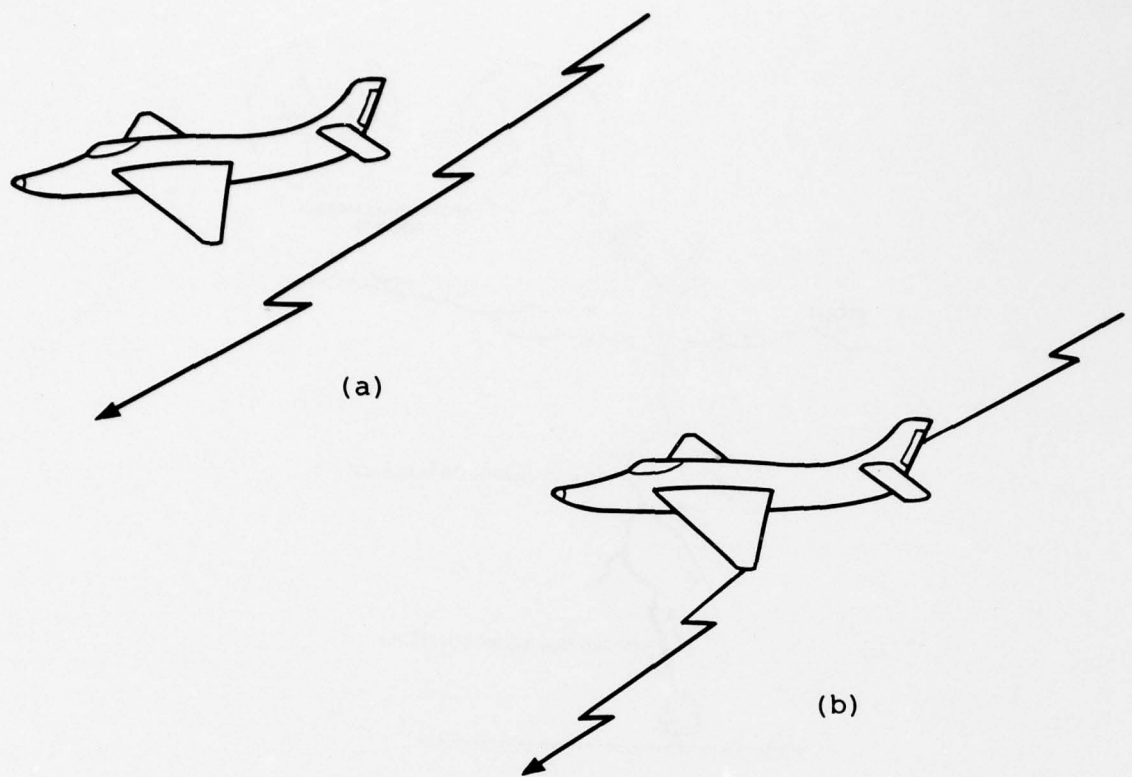


Figure 2.7 Lightning Flashes Near and To an Aircraft

- (a) Near Miss
- (b) Direct Hit

of the transition between the low current and high impedance of the leader channel and the high current and low impedance of the channel when it is carrying a return stroke of current. This transition region could be investigated in the laboratory.

Work on long arc discharges has been conducted by the Renardières Group. Les Renardières is the name of a high voltage laboratory operated by Electricité de France (EDF). Workers from the various universities of Europe, principally those in Great Britain, France, Italy, and Germany, have been funded by the members' respective universities and have used laboratory facilities donated by EDF. The group's subject of endeavor has been the mechanism of the development and propagation of long arcs such as might be produced by switching overvoltages on high-voltage transmission lines. This group and other workers dealing with long arcs have published extensively (References 2.24, 2.25, and 2.26).

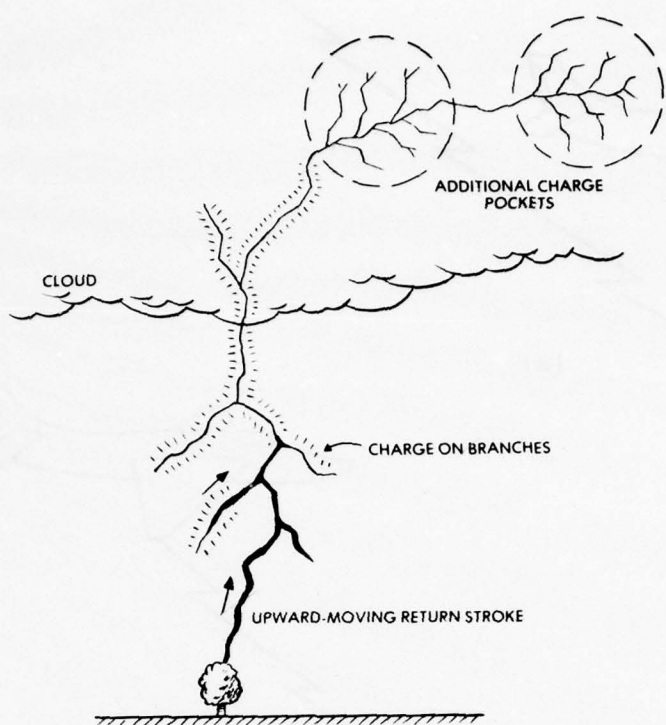


Figure 2.8 Charge on Branches That Affects Current Waveshape

2.3.4 Nearby Flashes

It is axiomatic that aircraft are going to be involved with more near misses of lightning flashes than they are going to be involved with direct hits of lightning flashes. All studies to date have gone on the premise that a direct hit of a flash will be more hazardous than a near miss and that, if aircraft could be designed to withstand the effects produced by a direct hit, they would then be able equally well to withstand the effects of a near miss. The supposition seems reasonable, but it is by no means a certainty. The electromagnetic fields produced by a near miss of a lightning flash may produce a relatively long-duration oscillation in the aircraft of a type that might not be excited by a direct hit. The aircraft would tend to ring as an antenna at its characteristic resonance frequency and, in so doing, couple more severe fields into its interior.

Whether this supposition is true or not has not been studied one way or the other. The best that can be said about nearby flashes is that they have not yet been studied to the degree that they should be.

2.4 INTERACTION OF THE LIGHTNING FLASH WITH THE AIRCRAFT

The EMP community has studied extensively the interaction of aircraft or missile systems with the transient electromagnetic field propagating past the aircraft or missile. The work has been directed at determining the axial and transverse currents induced on the aircraft or, perhaps more importantly, determining the current density on the surface. Because of the high-frequency characteristics of the EMP phenomena, the work is concerned with both the electric and magnetic fields. Phrased another way, this means that the EMP community must determine both the current on the aircraft and the electrical charge on the aircraft. This work has led to a large body of literature on methods of calculating the interaction of bodies with an electromagnetic field. A number of computer codes governing this interaction have been prepared. Many of the computer codes are available; however, their applicability to lightning is uncertain. For NEMP analyses, the interaction has been studied through the use of geometric models and wire grid models, both experimentally and analytically. A variety of tools is available to the EMP community for experimental measurements. While they will not be discussed here, those same tools would be useful for evaluating the interaction of an aircraft with the electric fields radiated by a nearby lightning flash or for determining the interaction of an aircraft with a lightning leader.

The interaction of an aircraft with a lightning flash would seem to be more complicated than the interaction of an aircraft with an EMP field, at least one originating from a distant detonation. The lightning current will set up a magnetic field around the aircraft and also set up an electric field radial away from the aircraft. In the low-frequency region, the magnetic field is fairly easy to understand. The low-frequency electric field is less easy to understand, since it involves nonlinear behavior. There is also a high-frequency region, where conditions are more complex yet.

Passage of the lightning return stroke through the aircraft probably will excite high-frequency oscillations of the structure, and these oscillations will be superimposed upon the basic waveform of the lightning current. These oscillations would be more pronounced for large aircraft than for small aircraft. The frequencies that would be excited would depend upon the physical size of the aircraft. Internally, resonant frequencies of wire bundles would tend to be proportional to the lengths of the wire bundles. It is these lengths, both of the wire bundles and of the aircraft, that govern the dominant resonant frequencies of the wire and of the aircraft.

The only one of these interactions that has been studied in detail is how the low-frequency component of current sets up magnetic fields around the aircraft. The manner in which the current divides can be determined by methods well known to specialists in the field of lightning interactions or in the field of electromagnetics. The methods may not be well understood by nonspecialists and they may be time-consuming, but they are basically easy.

The electric field is a different story. The nature of the electric field at the surface of an aircraft is strongly influenced by the nonlinear behavior of corona and of partial or developing electrical breakdown in gases. Only the most rudimentary attempts have been made to study this interaction. Fisher (Reference 2.27) has done some work related to the magnitude and shape of this electric field which develops as the lightning leader approaches the aircraft. The work has been described in Air Force contracts reports and in one of the EMC papers. His conclusions are that the electric field at the surface of the aircraft will be limited to less than 500 kV/m and probably in most parts of the aircraft will be limited to less than 100 kV/m. These numbers are much lower than numbers other workers in the EMP field may have calculated. Their judgments, however, may be influenced by the fact that the voltage waves that they deal with are of very short duration. The lightning leader will, in fact, expose the aircraft to electric fields having much longer durations. When the electric field around an electrode reaches about 500 kV/m, the electrode is in a developing breakdown state, and the corona or prebreakdown discharges from the electrode will reduce the field strength at the surface. This phenomenon has been studied in detail in connection with the work on breakdown processes on large air gaps. The work on the large air gaps should be written up in format more appropriate to the study of lightning effects on aircraft. There is practically no knowledge of the aircraft lightning community of the things that have been learned by the groups dealing with breakdown of large air gaps.

In the absence of any better description of the external electric field intensity, the electric field waveshape shown on Figure 2.9 may be taken for design purposes as a reasonable worst case threat.

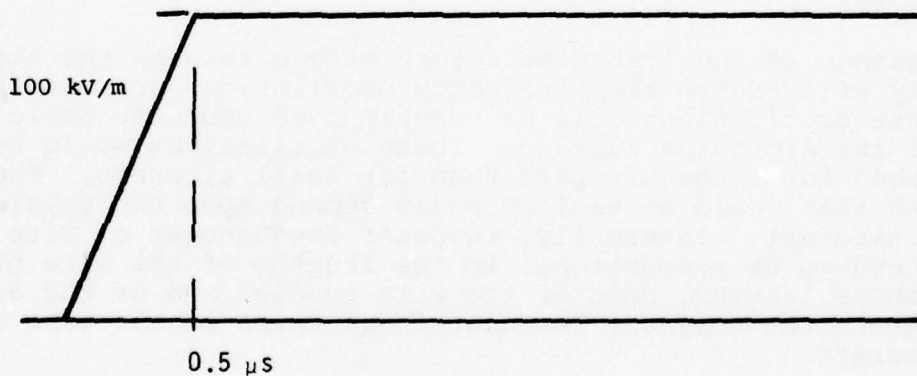


Figure 2.9 A Postulated Worst Case External Electric Field Intensity

The degree to which a lightning flash excites an oscillatory current along the aircraft has also been studied in only the most rudimentary way. It is quite feasible to measure this interaction through the use of models, just as models have been used to study the interaction of an aircraft with an EMP field. One crude example of such modeling analysis is discussed by Fisher (References 2.28 and 2.29). One of the tools with which one could measure these effects would be the skin current probes that have been developed by AFWL. These are a semicommercially available piece of hardware now and are available from the firm EG&G. The use of these probes has been described in connection with the work on the one-fifth scale model of the B-1 aircraft. Another of the tools that could well be used for such studies is the high-frequency data link that is described in the notes regarding those model studies.

One of the factors governing such interaction is the surge impedance of the lightning channel, a quantity to which reference has already been made. Little is known about the impedance of the lightning channel.

Surge impedance has been discussed most notably by the group of workers dealing with the effects of lightning on power transmission lines. Two of the major workers (usually working as a team) have been Wagner and Hileman. Their work has been extensively reported in the literature, usually in IEEE publications (References 2.30 and 2.31). Fisher has extracted some of these observations and discussed them in a memorandum dealing with an analysis of lightning current waveforms through the Space Shuttle (Reference 2.32). The impedance of the lightning flash would be strongly dependent upon the amount of current involved and, almost certainly, a strong function of the frequency or time at which one observed the impedance. Since the impedance strongly affects the interaction of the lightning flash with the aircraft, it follows that this represents a field in which additional analytic or experimental work would be helpful to the aircraft community. In sum, it can be said that there is a very large and unexplored field of endeavor in which future research could profitably be undertaken.

2.5 APPLICABILITY OF EMP KNOWLEDGE AND TECHNOLOGY

For some time there has been an extensive and well-supported group of workers concerned with the effects of the nuclear electromagnetic pulse (EMP) upon aircraft and missiles. That community of workers has developed a very large body of literature, sponsored extensive studies of the ability of semiconductors to withstand voltages and currents, conducted numerous experiments to determine how aircraft and missiles respond to electromagnetic fields, and strongly influenced the evolving standards that relate to transient compatibility of electronic systems. No comparable study effort has ever been undertaken for lightning effects. One of the aims of this program was to help determine how much of this body of knowledge related to EMP effects is directly related to the problems of aircraft compatibility and how much of it could guide the development of work in lightning compatibility.

One of the first considerations of this program was to determine which, if any, of the analytical techniques developed to solve EMP coupling problems on aircraft might be used for analysis of lightning indirect effects. The discussions at AFWL developed several differences between lightning and EMP characteristics which render available EMP techniques somewhat less applicable than had been first expected for solution of the basic lightning problem. Two areas where differences between EMP and lightning are of major technical importance are--

1. Differences in the origins of the electric and magnetic fields at the surface of the aircraft
2. Differences in the frequencies/wavelengths of these fields

One of the differences between EMP and lightning is that, in the EMP situation, the aircraft is considered to be illuminated by a traveling electromagnetic wave, as shown in Figure 2.10, whereas lightning involves direct conduction of current into and out of the aircraft structure as shown in Figure 2.11. This difference between EMP and lightning engenders different viewpoints, particularly regarding the flow of current in the airframe. In most EMP formulations reviewed at AFWL, the aircraft is treated as an assembly of cylindrical dipole antennas with respect to this electromagnetic wave. From these formulas the induced skin currents, both longitudinal and circumferential, are calculated as is the surface charge density. On the other hand, the total lightning current flowing in the skin can usually be specified as an a priori condition in which all of the current enters the aircraft at one point and, eventually, leaves it from another point. Only the initial (inductive) and final (resistive) current distributions need to be computed. As a result, the basic analyses of EMP-excited currents on airframes are inapplicable for determination of first-order (at least) distributions of lightning currents on airframes.

The second major difference between EMP and lightning is that of the frequencies (or wavelengths) involved. The EMP electromagnetic field has characteristically faster times to crest than the electromagnetic field from lightning; the factor may possibly be 100:1. The wavelengths involved for EMP can be comparable to, but are generally shorter than, the important dimensions of the aircraft system under consideration. Lightning electromagnetic fields, at least those produced by stroke currents injected into the airframe, are thought to be slower than EMP, and thus the wavelengths involved are often greater than the equivalent length of the aircraft. Summarized, these are as follows:

$$\begin{array}{ll} \text{EMP:} & \lambda < a \\ \text{Lightning:} & \lambda > a \end{array}$$

where "a" represents the characteristic dimensions of the structure under consideration.

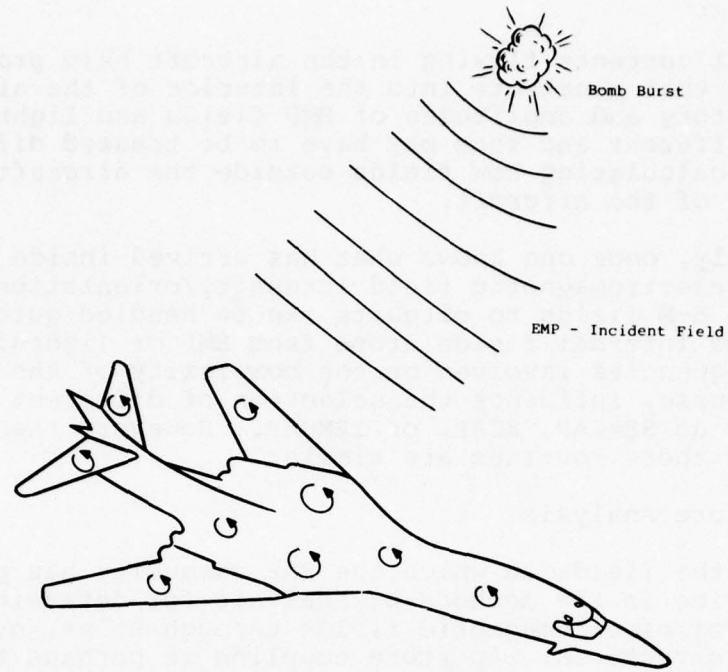


Figure 2.10 Aircraft Illuminated by EMP-Created Plane Electromagnetic Wave

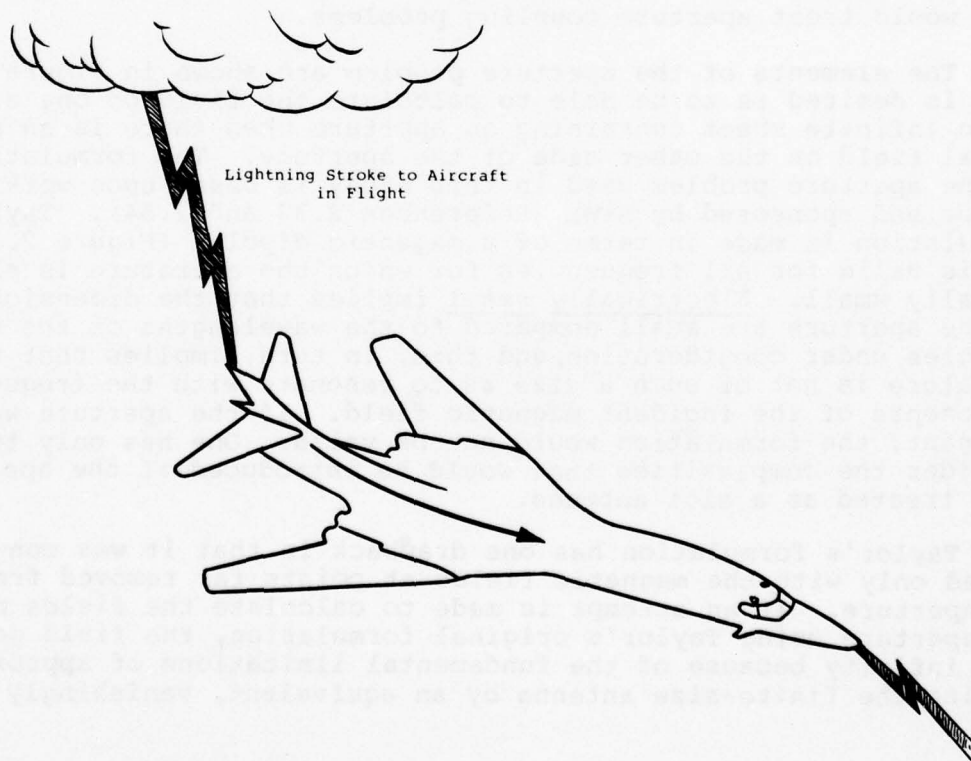


Figure 2.11 Aircraft Struck by Lightning

External currents flowing in the aircraft skin produce magnetic fields that penetrate into the interior of the aircraft. The time history and amplitudes of EMP fields and lightning fields are quite different and thus may have to be treated differently when one is calculating how fields outside the aircraft get into the interior of the aircraft.

Obviously, once one knows what has arrived inside the aircraft in terms of electromagnetic field intensity/orientation, then coupling of the E-M fields to circuits can be handled quite similarly, whether those internal fields arose from EMP or lightning. The range of frequencies involved or the complexity of the cable system could, of course, influence the selection of different computational schemes such as SEMCAP, ECAP, or IEMCAP. However, the basic elements of all these routines are similar.

2.5.1 Aperture Analysis

One of the fields in which the EMP community has performed a great service is the methods of analysis for determining the penetration of electromagnetic fields through holes, or apertures, in metallic structures. Aperture coupling is perhaps the most important mechanism by which fields penetrate into aircraft and, in so penetrating, produce currents and voltages on aircraft wiring. Indeed, the researcher is likely to be overwhelmed by the variety and analytical sophistication of the methods that are available to him. Still, there remain problems as to how the working engineer would treat aperture coupling problems.

The elements of the aperture problem are shown in Figure 2.12. What is desired is to be able to calculate the field on one side of an infinite sheet containing an aperture when there is an external field on the other side of the aperture. The formulation of the aperture problem used in this study is based upon work by Taylor and sponsored by AFWL (References 2.33 and 2.34). Taylor's formulation is made in terms of a magnetic dipole, (Figure 2.12b) and is valid for all frequencies for which the aperture is electrically small. Electrically small implies that the dimensions of the aperture are small compared to the wavelengths of the frequencies under consideration, and this, in turn, implies that the aperture is not of such a size as to resonate with the frequency components of the incident magnetic field. If the aperture were resonant, the formulation would not be valid. One has only to consider the complexities that would be introduced if the aperture were treated as a slot antenna.

Taylor's formulation has one drawback in that it was concerned only with the magnetic fields at points far removed from the aperture. If an attempt is made to calculate the fields near the aperture using Taylor's original formulation, the field goes into infinity because of the fundamental limitations of approximating the finite-size antenna by an equivalent, vanishingly

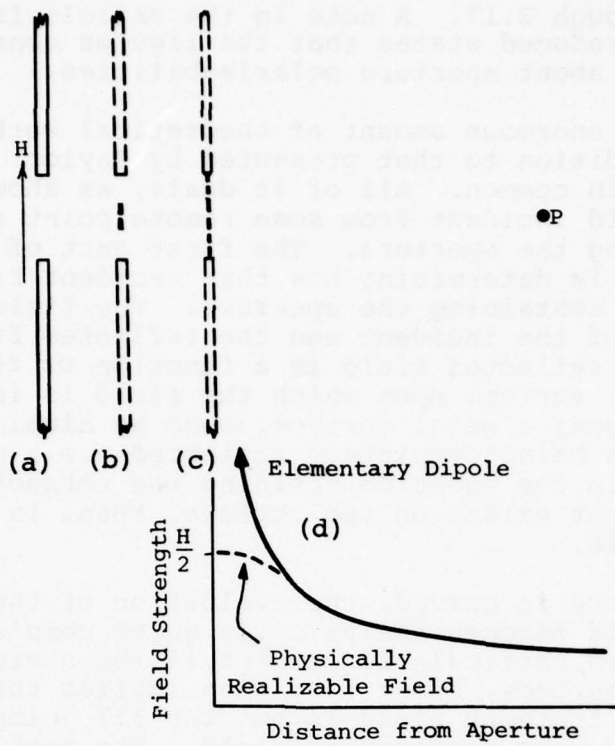


Figure 2.12 Apertures

- (a) An Aperture in a Plane
- (b) An Equivalent Dipole
- (c) Multiple Dipoles
- (d) Field Strengths

small, dipole. Fisher (References 2.35 and 2.36) uses a brute force expansion of the dipole equations to give a formulation that is more mathematically tractable in the region close to the aperture. This can be done, since, again for electrically small apertures, one knows the limiting value of the field in the plane of the aperture. In the plane of the aperture the field intensity would be one-half the external intensity were the aperture not there.

Taylor's formulations, and hence Fisher's expansion thereof, treat the equivalent dipole in terms of polarizabilities. The present formulation of the APERTURE program calculates these polarizability constants in terms of the major and minor axes of an ellipse and hence, strictly speaking, is able only to deal with elliptical apertures. A circle, of course, is a limiting case of an elliptical aperture.

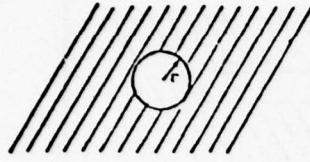
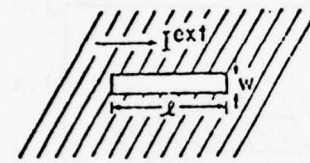
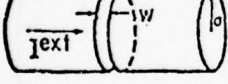
The program APERTURE, to which we refer in Section 4, is able to derive an equivalent elliptical aperture. The program would be in better form if it included routines or data on the polarizability of other kinds of apertures. AFWL data on the polarizability of other types of apertures are shown reproduced on

Figures 2.13 through 2.17. A note in the article from which the figures were reproduced states that the figures constitute the state of the art about aperture polarizabilities.

There is an enormous amount of theoretical work dealing with apertures in addition to that presented by Taylor. All of it has one element in common. All of it deals, as shown in Figure 2.16, with a field incident from some remote point upon the metal surface containing the aperture. The first part of all of the solutions, then, is determining how that incident field interacts with the surface containing the aperture. The field at the surface is the sum of the incident and the reflected fields. The magnitude of the reflected field is a function of the electrical properties of the surface upon which the field is incident, but for highly conductive metal surface, such as aluminum, the field can be treated as being completely reflected-i.e., no frequency-dependent terms in the equation defining the reflected wave. The magnetic field that exists on the surface, then, is equal to twice the incident field.

If the surface is curved, the evaluation of the reflected component of field becomes analytically quite complex, and the evaluation becomes particularly complex if the source of the field is close to the surface, since this then implies that the source impedance of the incident field is not the 377Ω impedance associated with a TEM wave propagating field. The task of determining these reflected fields (also called the task of determining the scattering properties of the surface under investigation) is quite complex and has led to the development of a great many sophisticated analytical procedures. Much (though obviously not all) of this analytical procedure is superfluous to the problem of evaluating the interaction of lightning current with aircraft, since the surface magnetic field is given directly by the current density on the exterior of the aircraft, and this can be found relatively easily, either by numerical techniques such as DIFFMAG (Section 4), by computer solution of Laplace's equation, by handplotting of the fields, or by experimental measurement. Actual measurement of the surface field intensity is perhaps the most powerful tool that could be used for any actual program.

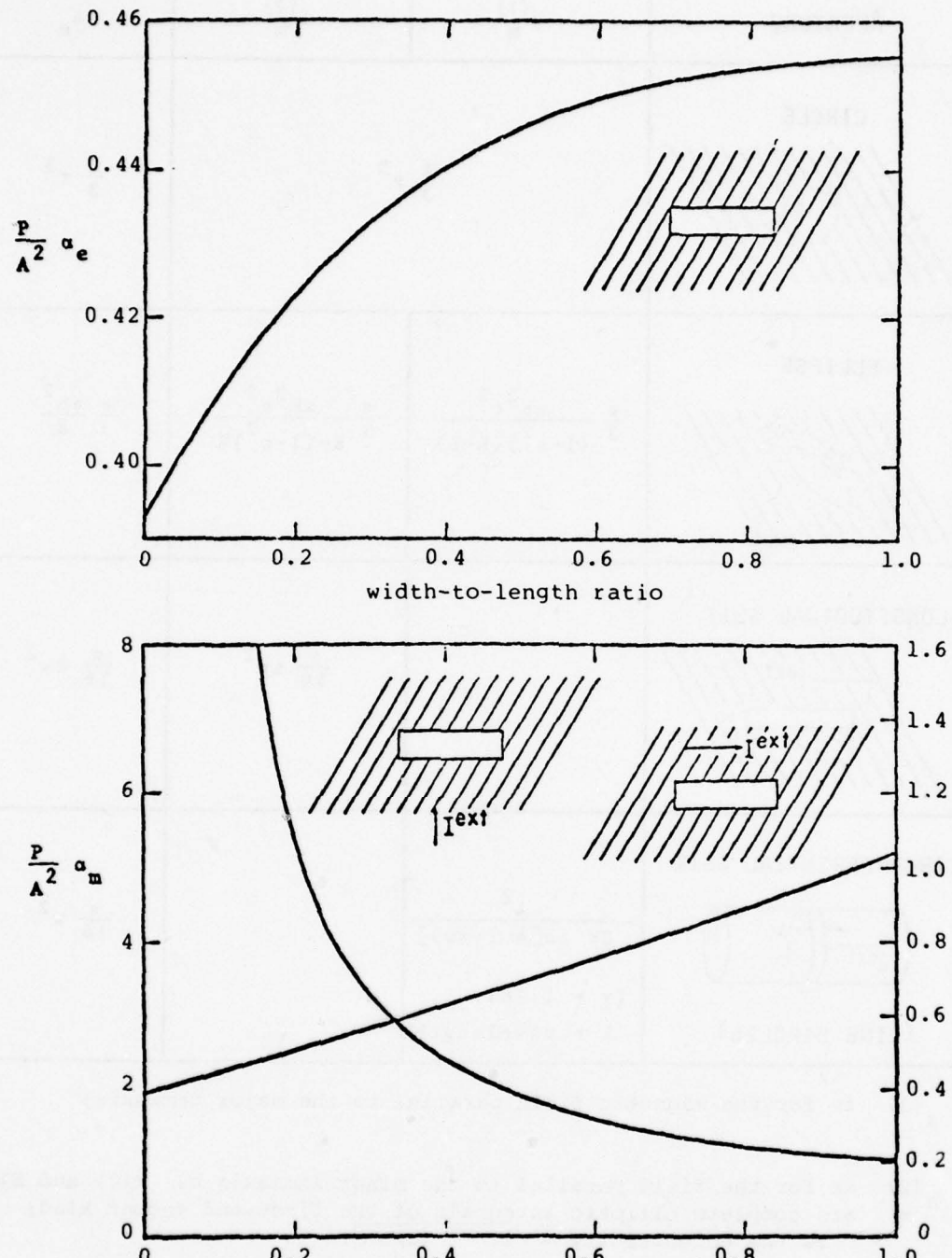
Another important class of analyses that have been supported by AFWL deals with better methods of evaluating the fields coupled through the aperture, particularly for the fields close to the aperture. Some of the differences between the more elaborate analyses and the analysis presently used in the APERTURE program are shown in Figure 2.17. In the present APERTURE program, based on the work of Taylor, it will be remembered that the aperture is replaced by an elementary dipole and that the field on the interior region is calculated in terms of the field produced by that one dipole. It is also possible to break the aperture into a number of parts and to put one dipole at each point on the grid. The formulation may be in terms of magnetic dipoles or electrical charges;

APERTURE	$a_m^{(1)}$	$a_m^{(2)}$	a_e
CIRCLE 		$\frac{4}{3} \pi r^3$	$\frac{2}{3} \pi r^3$
ELLIPSE * 	$\frac{\pi}{3} \frac{ab^2 \epsilon^2}{(1-\epsilon^2)(K-E)}$	$\frac{\pi}{3} \frac{ab^2 \epsilon^2}{E - (1-\epsilon^2)K}$	$\frac{\pi}{3} \frac{ab^2}{E}$
LONGITUDINAL SLIT 		$\frac{\pi}{16} \ell w^2$	$\frac{\pi}{16} \ell w^2$
CIRCUMFERENTIAL SLIT (LINE DIPOLES) 	$-\frac{\lambda^2}{8\pi \ln[4\lambda/(\gamma\pi w)]}$ ($\gamma = 1.781\dots$, $\lambda = \text{wavelength}$)		$\frac{\pi}{16} w^2$

* $a_m^{(1)}$ is for the magnetic field parallel to the major semiaxis;

$a_m^{(2)}$ is for the field parallel to the minor semiaxis b . $K(\epsilon)$ and $E(\epsilon)$ are complete elliptic integrals of the first and second kind; ϵ is the eccentricity = $\sqrt{1 - (b/a)^2}$.

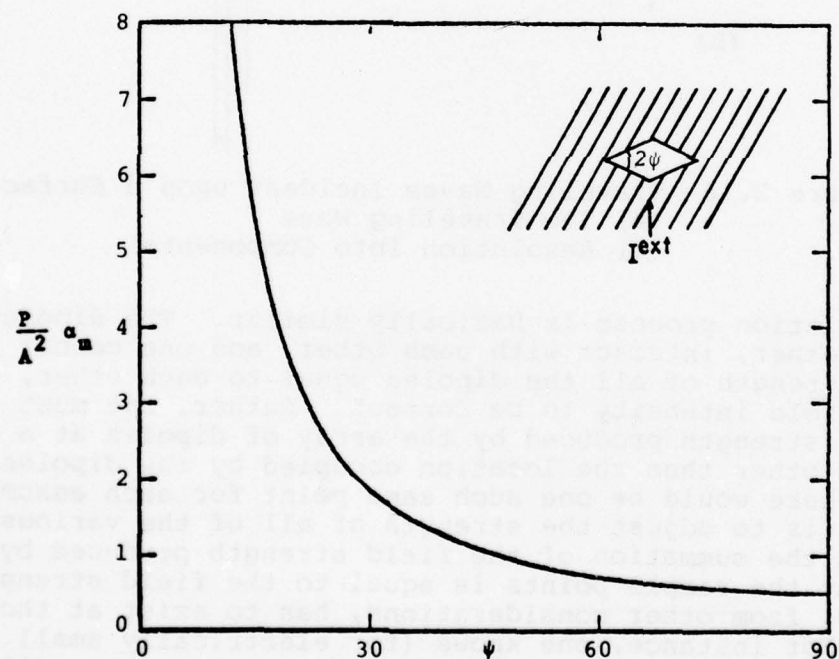
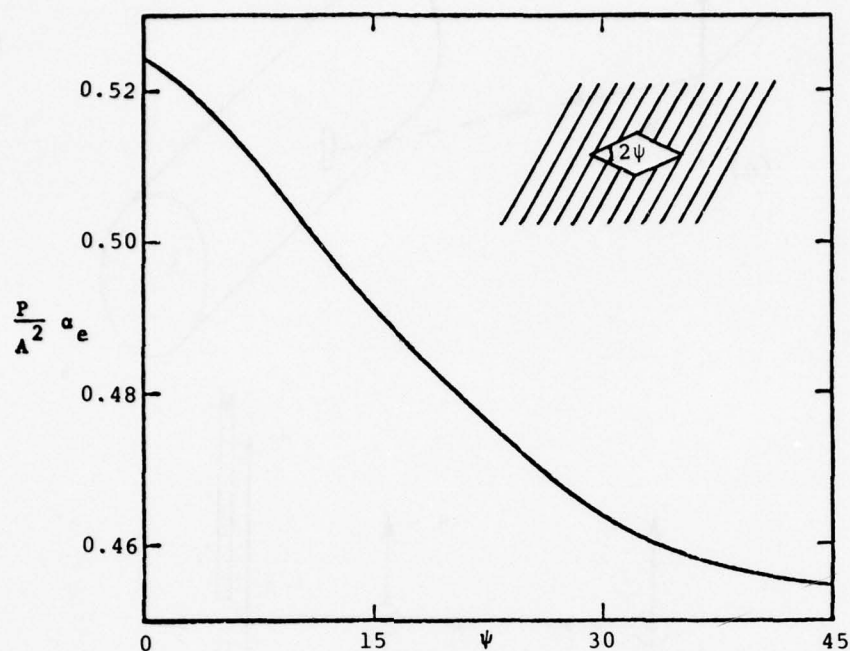
Figure 2.13 Available Data on Polarizabilities



α_e and α_m for Rectangles

P = perimeter, A = area

Figure 2.14 Available Data on Polarizabilities



α_e and α_m for diamonds

P = perimeter, A = area

Figure 2.15 Available Data on Polarizabilities

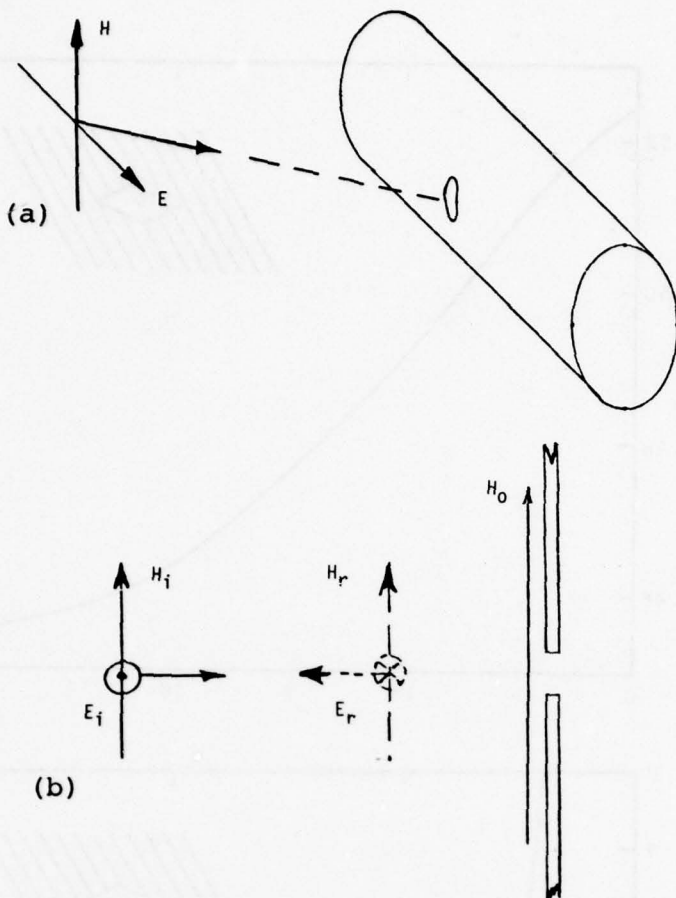


Figure 2.16 Traveling Waves Incident upon a Surface
(a) The Traveling Wave
(b) Resolution into Components

the formulation process is basically similar. The dipoles, being close together, interact with each other, and one cannot simply set the strength of all the dipoles equal to each other, expecting the field intensity to be correct. Rather, one must evaluate the field strength produced by the array of dipoles at a number of points other than the location occupied by the dipoles. Typically, there would be one such same point for each assumed dipole. The trick is to adjust the strength of all of the various dipoles such that the summation of the field strength produced by those dipoles at the sample points is equal to the field strength that one knows, from other considerations, has to exist at those sample points. For instance, one knows (for electrically small apertures) that the field strength in the center of the aperture will be one-half the field strength that would exist at that point were the aperture not there. One likewise knows that the field strength at the edge of the aperture has to go to zero. What the field

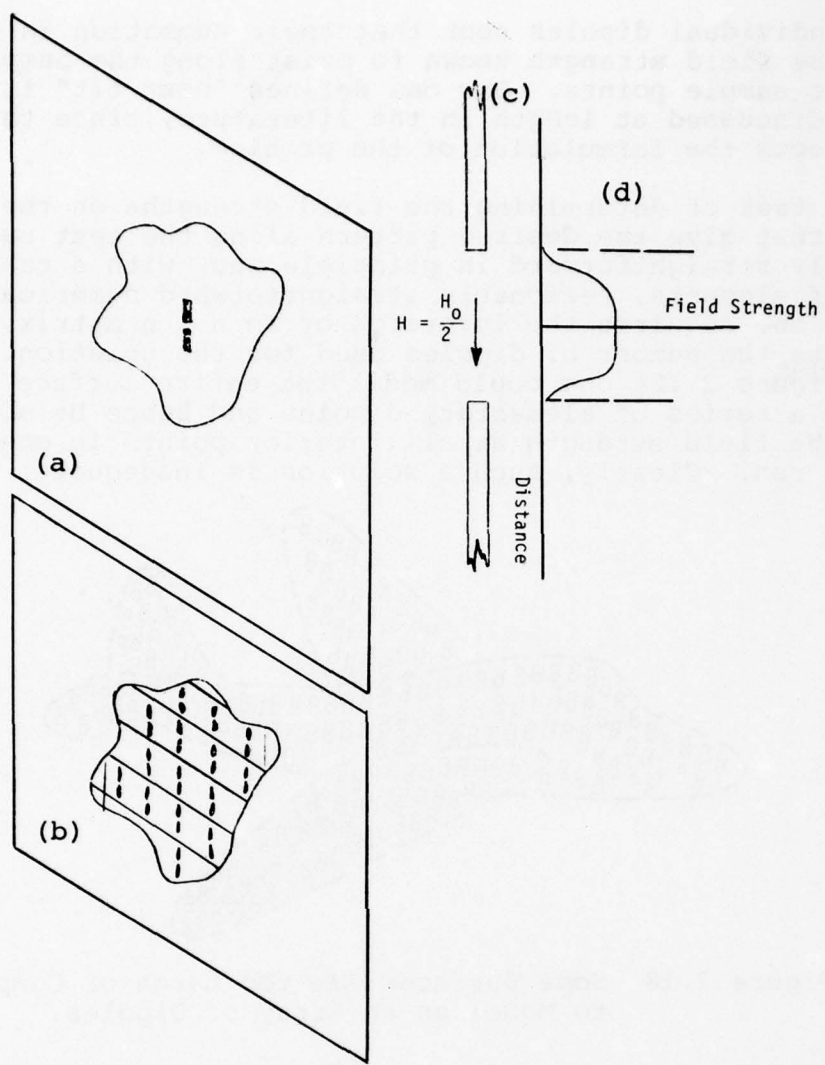


Figure 2.17 Moment Method of Determining Aperture Effects
 (a) A Single Dipole
 (b) Multiple Dipoles
 (c) and (d) Field Strength in the Aperture

strength is at intermediate points is another matter that has received extensive analytical investigations. Analytically, it is a far from trivial problem, though possibly one skilled in the art of making aperture calculations could guess the shape of the field strength pattern closely enough for all practical purposes. Be that as it may, the problem is to manipulate the field strength

of the individual dipoles such that their summation is the best fit to the field strength known to exist along the sample surface or at the sample points. How one defines "best fit" is another subject discussed at length in the literature, since the definition used affects the formulation of the problem.

The task of determining the field strengths on the individual dipoles that give the desired pattern along the test surface is relatively straightforward in principle and, with a reasonable number of elements, reasonably straightforward numerically. Basically, one requires the inversion of an $n \times n$ matrix, where n represents the number of dipoles used for the solution. In principle (Figure 2.18) one could model the entire surface of an aircraft by a series of elementary dipoles and hence be able to calculate the field strength at all interior points in one complete computer run. Clearly, such a solution is inadequate.

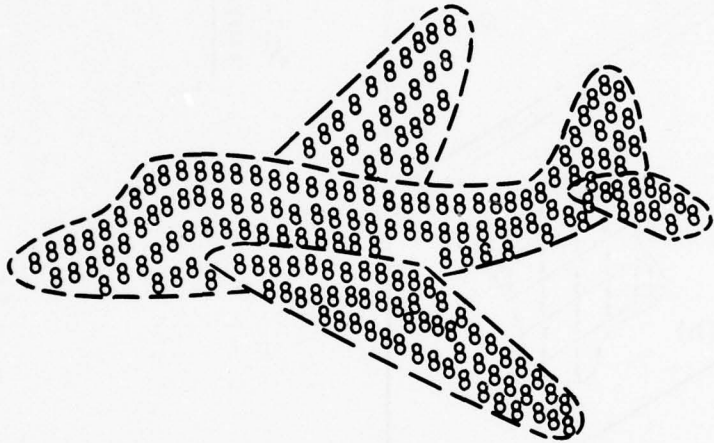


Figure 2.18 Some Surfaces Are too Large or Complex to Model as an Array of Dipoles.

The question arises: How necessary is it to be well grounded analytically in the analysis of apertures and what degree of complexity of aperture formulations is necessary to give satisfactory answers? Frankly, we do not know. More elaborate formulations than those of the APERTURE program are likely to be an improvement on those formulations at some point and at some frequency and eventually to supersede them. On this program however, we did not attempt to improve the low-frequency, brute force formulations of the APERTURE program.

Another area where improvements are needed is in knowing the effective dipole strength for poorly defined apertures. The most important of these poorly defined apertures is that existing around access covers where there is an electrical aperture, even if a direct-line-of-sight aperture cannot be seen. Little Air Force work seems to bear as yet on this problem of poorly defined apertures. It is suspected that only experimental programs can allow the definition of such aperture strengths.

2.5.2 Cable Analysis Programs

The EMP community has sponsored nearly all of the work that has led to the variety of computer programs now available for the solution of complex electrical networks. Examples of programs include ECAP, CIRCUS, and SCEPTRE. In Section 3 of this report the use of ECAP, to solve for the currents and voltages in a lumped parameter model of an aircraft electrical harness, is discussed.

In addition to the circuit solution programs sponsored by the EMP community, there are others, such as the Dommel program diffused through the electrical industry by the Bonneville Power Administration (BPA), that are available for use by those wishing to make numerical analyses of electrical circuits. This report will not go into the strengths and weaknesses of the various programs. Clearly, the task of making a computer-aided analysis of an equivalent circuit of an actual aircraft wiring harness is much easier than is the task of formulating the equivalent circuit in the first place.

2.5.3 Test Techniques

The EMP community has sponsored the development of a variety of techniques for making tests on electronic equipment to determine their resistance to electromagnetic fields. This report cannot cover all of them. Several threads might be traced, though, to show how knowledge obtained in the EMP community has led to methods of injecting specified currents in interconnecting cables through use of pulse-injection transformers. In the book by Fisher and Plumer (Reference 2.37) and in the article by Fisher and Martzloff (Reference 2.38) are presented some test techniques. Such equipment, and the method of making the tests, was directly influenced by similar test equipment developed for EMP analyses.

Strip line simulators of the type used by AFWL would be well adapted to the study of how aircraft respond to the electromagnetic field produced by a nearby lightning flash. Such simulators could accommodate a full-sized aircraft or at least a large scale model.

Those additional model techniques currently used for studying the response of small models of aircraft and missiles to EMP fields could also be used to study the response of aircraft to the fields produced by lightning. Such studies would be easier to make than studies on full-sized craft, since the pulses used to represent the lightning fields would be easier to generate and measure than would the pulses used to represent EMP fields.

REFERENCES

- 2.1 Carl E. Baum, "How to Think About EMP Interaction," 1974 Spring FULMEN Meeting, Air Force Weapons Laboratory, 16 and 17 April 1974, pp. 12-23.
- 2.2 Space Shuttle Program Lightning Protection Criteria Document, JSC-07636, Revision A, National Aeronautics and Space Administration, Lyndon B. Johnson Space Center, Houston, Texas, November 4, 1975.
- 2.3 K.J. Lloyd, J.A. Plumer, and L.C. Walko, Measurements and Analysis of Lightning-Induced Voltages in Aircraft Electrical Circuits, National Aeronautics and Space Administration, Lyndon B. Johnson Space Center, Houston, Texas, NASA CR-1744, February 1971.
- 2.4 J.A. Plumer, F.A. Fisher, and L.C. Walko, Lightning Effects on the NASA F-8 Digital-Fly-By-Wire Airplane, prepared by the High Voltage Laboratory, Environmental Electromagnetics Unit, Corporate Research and Development, General Electric Company, Pittsfield, Massachusetts, for the National Aeronautics and Space Administration, Lewis Research Center, Cleveland, Ohio, NASA Cr-2524, March 1975.
- 2.5 Space Shuttle Lightning Protection Criteria Document, JSC-07636, National Aeronautics and Space Administration, Lyndon B. Johnson Space Center, Houston, Texas, September 11, 1973.
- 2.6 Space Shuttle Program Lightning Protection Criteria Document, JSC-07636, Revision A, National Aeronautics and Space Administration, Lyndon B. Johnson Space Center, Houston, Texas, November 4, 1975, p. F-7.
- 2.7 Space Shuttle Program Lightning Protection Criteria Document, Revision A, p. F-6.
- 2.8 Space Shuttle Program Lightning Protection Criteria Document, Revision A, p. F-8.
- 2.9 F.A. Fisher and F.D. Martzloff, "Transient Control Levels: A Proposal for Insulation Coordination in Low-Voltage Systems," IEEE Transactions on Power Apparatus and Systems, Institute of Electronic and Electrical Engineers, New York, New York, PAS-95, 1, January/February 1976, pp. 120-29.
- 2.10 F.A. Fisher and F.D. Martzloff, Transient Control Levels --Philosophy and Implementation, prepared by the High Power Electronics Unit, Corporate Research and Development, General Electric Company, Schenectady, New York, 77CRD086, April 1977. (Also presented at the 1977 EMC Symposium, Montreux).

- 2.11 F.D. Martzloff, "Transient Control Levels," Telephone Engineer and Management, September 15, 1977, pp. 55-57.
- 2.12 Space Shuttle Program Lightning Protection Criteria Document, Revision A, p. D-2 to D-5.
- 2.13 Fisher and Martzloff, "Transient Control Levels."
- 2.14 Fisher and Martzloff, "Transient Control Levels," p. 128.
- 2.15 N. Cianos and E.T. Pierce, A Ground-Lightning Environment for Engineering Use, Technical Report 1, prepared by the Stanford Research Institute for the McDonnell Douglas Astro-nautics Company, Huntington Beach, California, August 1972.
- 2.16 K. Berger and E. Vogelsanger, "Photographische Blitzuntersuchungen der Jahre 1955...1965 auf dem Monte San Salvatore," Bulletin des Schweizerischen Elektrotechnischen Vereins, 14, July 9, 1966, pp. 599-620:608.
- 2.17 K. Berger, "Novel Observations on Lightning Discharges: Results of Research on Mount San Salvatore," Journal of The Franklin Institute 283, 6, June 1967, pp. 478-525:514.
- 2.18 F.A. Fisher, Some Observations Regarding Amplitude, Aircraft Lightning Protection Note 74-1, June 14, 1974, unpublished memo.
- 2.19 D.K. McLain and M.A. Uman, Lightning Criteria Relative to Space Shuttles: Currents and Electric Field Intensities in Florida Lightning, NAS8-28168 (NASA), June 30, 1972, and also NASA CR-2161, November 1972.
- 2.20 J.A. Tiller, M.A. Uman, Y.T. Lin, R.D. Brantley, and E.P. Frider, "Electric Field Statistics for Close Lightning Return Strokes Near Gainsville, Florida," Journal of Geophysical Research, August 20, 1976, pp. 4430-4434.
- 2.21 F.A. Fisher, D.L. Jones, and B. MacCiaroli, Lightning Effects Relating to Aircraft Part II -- Characteristics of Simulated Lightning Flashes and Their Effects on Lightning Arresters and Avionic Equipment, AFAL-TR-72-5, January 1972.
- 2.22 R.C. Adams, R.T. Bly, Jr., and J.E. Nanewicz, "Airborne Measurement of the Electromagnetic Environment Near Thunder-storm Cells," 1977 IEEE International Symposium on Electromagnetic Compatibility, (Seattle, WAshington, August 2-4, 1977), pp. 232-236.
- 2.23 R.L. Boggess, G.A. DuBro, D.G. Kim, and L.P. Tessler, "Transmission Line Theory Applied to Aircraft Lightning Interactions," 1977 IEEE International Symposium on Electromagnetic Compatibility, (Seattle, Washington, August 2-4, 1977), pp. 215-222.

2.24 "Research on Long Air Gap Discharges at Les Renardières," Electra, Vol. 23, pp. 53-157.

2.25 "Research on Long Air Gap Discharges at Les Renardières - 1973 Results," Electra, Vol. 35, pp. 49-156.

2.26 "Positive Discharges in Long Air Gaps at Les Renardières - 1975 Results and Conclusions," Electra, Vol. 53, pp. 31-153.

2.27 Fisher, Jones, and Macciaroli, Lightning Effects Relating to Aircraft Part II, AFAL-TR-72-5.

2.28 F.A. Fisher, Analysis of Lightning Current Waveforms Through the Space Shuttle, Aircraft Lightning Protection Note 75-1, unpublished memo, 17 January 1975.

2.29 Fisher, Analysis of Lightning Current Waveforms.

2.30 C.F. Wagner, "Lightning and Transmission Lines," Journal of the Franklin Institute 283, 6, June 1967, pp. 558-594:560, and C.F. Wagner, "The Relation Between Stroke Current and the Velocity of the Return Stroke," IEEE Transactions on Power Apparatus and Systems 82, American Institute of Electrical Engineers, New York, New York, October 1963, pp. 609-17:609.

2.31 C.F. Wagner and A.R. Hileman, "The Lightning Stroke - II," AIEE Transactions 80, Part III, American Institute of Electrical Engineers, New York, New York, October 1961, pp. 622-42:623.

2.32 Fisher, Analysis of Lightning Current Waveforms.

2.33 C.D. Taylor, "Electromagnetic Pulse Penetration Through Small Apertures," IEEE Transactions on Electromagnetic Compatibility, EMC-15, 1, Institute of Electronic and Electrical Engineers, New York, New York, February 1973, pp. 17-26.

2.34 C.D. Taylor, "Electromagnetic Pulse Penetration Through Small Apertures," Electromagnetic Pulse Interaction Notes, 5, Air Force Weapons Laboratory, Kirtland Air Force Base, Albuquerque, New Mexico, Interaction Note 74, March 1973.

2.35 K.J. Maxwell, F.A. Fisher, J.A. Plumer, and P.R. Rogers, Computer Programs for Prediction of Lightning Induced Voltages in Aircraft Electrical Circuits, Air Force Flight Dynamics Laboratory, Air Force Systems Command, Wright-Patterson Air Force Base, Ohio, AFFDL-TR-75-36, April 1975.

2.36 Fisher and Plumer, Lightning Protection of Aircraft, pp. 329-348.

2.37 Fisher and Plumer, Lightning Protection of Aircraft, pp. 495-530.

2.38 F.A. Fisher and F.D. Martzloff, "Transient Control Levels: A Proposal for Insulation Coordination in Low-Voltage Systems," IEEE Transactions on Power Apparatus and Systems, PAS-95, 1 Institute of Electronic and Electrical Engineers, New York, New York, January/February 1976, pp. 120-29.

SECTION III

THE LUMPED PARAMETER METHOD (LPM) OF MODELING

3.1 BASIC CONSIDERATIONS IN LPM MODELING

LPM modeling is a procedure whereby a distributed conductor excited by an electromagnetic field, usually of different character at different points along the conductor, is modeled as an equivalent circuit composed of a number of elementary lumped constant circuits. Generally the modeling is done in such a manner that the equivalent circuits can be solved with the aid of one of the standard circuit solution computer programs. Sometimes the distributed circuit is physically modeled by an appropriate selection of lumped inductors, capacitors, and resistors. In such a case physical voltage and current generators can be connected to the model, the voltages, and currents at different points in the model measured with oscilloscopes or other measuring instruments. Physical models of distributed networks have been used for many years to study the transient response of electrical power transmission and distribution systems, but such models seem to have been used very little to study the problems of lightning interaction with aircraft. In the material to be presented here, it will be assumed that the equivalent circuits will be solved with the aid of the Electronic Circuit Analysis Program (ECAP) computer code.

The degree to which the model approximates the real circuit under study will depend partly on the skill with which the investigator is able to visualize all the parameters that need to be modeled. The degree of model approximation will also depend on the complexity of the model that is made; generally speaking, the more complex the model, the greater the accuracy, but the expense of making the calculations with which the solution is developed is also greater.

There are a number of steps involved in making an LPM type of model solution. Those steps will be covered in more detail momentarily, but they will now be introduced. First of all, the physical circuit to be modeled must be identified and in some way separated from the rest of the circuits to which it is in proximity. The wiring harnesses in an aircraft are very complex, consisting of large numbers of individual wires all in close proximity to each other. It would be desirable to be able to determine the voltage and current upon each of the conductors within the aircraft. As a practical matter this determination can never be done; the wiring system is of complexity far beyond what the state-of-the-art can truly handle. What is more practical is to determine the voltage or current acting upon a bundle of conductors, perhaps better described as the average voltage and current upon conductors comprising a bundle of conductors.

Another practical step is to make an estimate of the currents and voltages induced upon a bundle of cables by the voltages and currents on an adjacent bundle of conductors.

It is highly doubtful that anyone will ever develop an easy way to tell what kind of circuit can be modeled with what kind of accuracy when that circuit is in the presence of a large number of other conductors. Since any such prediction would seem to be purely speculative, this report will not make any such predictions nor will it offer much guidance as to how to select the degree of complexity of a circuit to be modeled. It is better to regard modeling as an art and to recognize that the skill of the artisan depends upon his experience in his trade. There is no substitute for experience, and the only way that experience is likely to be obtained is through considerable interaction between analytic calculations of currents and voltages and actual measurements upon physical hardware.

Naturally, the problem of developing an equivalent circuit is simplified if the conductor or group of conductors are well isolated from other conductors or groups of conductors. In the material presented here, it is assumed that the conductors or groups of conductors are well isolated from all other conductors or groups of conductors.

The next step in the process of modeling solution is to determine the total inductance, capacitance, and resistance of the conductor or group of conductors. Since any actual circuit will probably follow a circuitous physical path in an aircraft, it will probably be necessary to determine the inductance, capacitance, and resistance of individual segments of that conductor or group of conductors.

The following step in the process is to divide the total inductance, capacitance, and resistance into an equivalent circuit composed of an appropriate number of elementary sections, Pi, Tee, Gamma, etc.

Another step in the process is to determine how the electromagnetic fields impinging upon the conductor can be described in terms of elementary voltage and current generators which can be integrated into the equivalent circuit being developed.

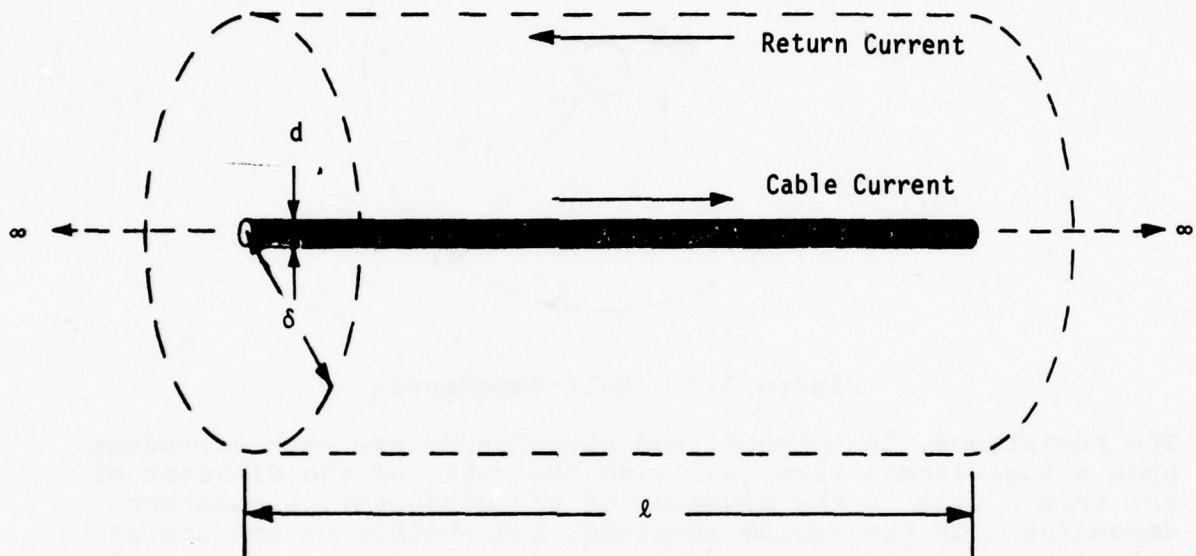
Once the circuit has been developed, it must be programmed in some manner for solution upon a computer. Fortunately, there are well-developed circuit solution programs that are able to handle quite complex electrical circuits. This report will deal with how the ECAP program can be used. There are other types of programs (CIRCUS, SCEPTRE, etc.) which can be used also. The choice of programs to be used depends largely upon the experimenter's preferences, his experience, and the degree of availability of the various programs.

Finally, after making the solutions of the equivalent circuit with the aid of the computer, the degree of validity of the resulting solutions must be evaluated in some way.

3.2 DETERMINING INDUCTANCE, CAPACITANCE, AND RESISTANCE

3.2.1 Concentric Geometry

The simplest type of geometry to consider is one in which a conductor is surrounded by some type of ground plane or current-carrying conductor, as in Figure 3.1. Later sections will extend the analysis to isolated conductors, conductor pairs, and conductors over a ground plane.



Conductivity = σ mhos per meter ($\Omega^{-1} \cdot \text{m}$)

Resistivity = $\frac{1}{\sigma} = \rho$ ohm · meters ($\Omega \cdot \text{m}$)

Permeability $\approx \mu_0 = 4\pi \times 10^{-7}$ henries per meter (H/m)

Permittivity = $\epsilon_R \epsilon_0 \approx \frac{\epsilon_R}{36\pi \times 10^9}$ farads per meter (F/m)

Figure 3.1 Geometry of a Cable with Concentric Return

The conductor of Figure 3.1 is located in a medium having resistivity ρ , permeability μ , and permittivity $\epsilon = \epsilon_R \epsilon_0$. Under these conditions the shunt resistance, the series inductance, and the shunt capacitance, as shown in Figure 3.2, may all be determined from the classic field pattern existing in coaxial cylinders.

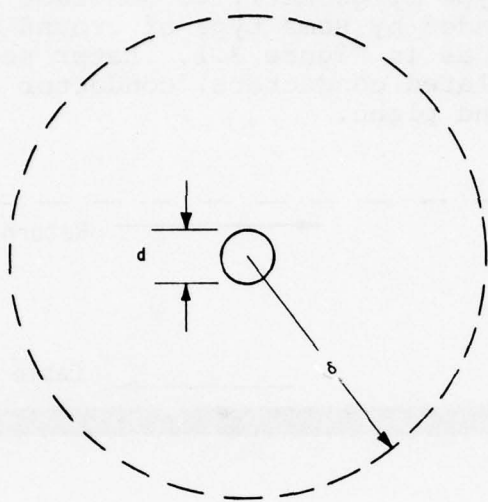


Figure 3.2 Self-Impedances

The resistance, inductance, and capacitance are each dependent upon a logarithmic term involving the ratio of the diameter of the return path to the diameter of the conductor, a constant depending upon the medium involved, and whether or not one is calculating resistance, inductance or capacitance. These calculations are shown in Equations 3.1, 3.2, and 3.3. Equation 3.3 gives the reciprocal of the shunt capacitance in order that the essential similarity of the equations may be shown more clearly.

$$R = \frac{1}{\ell} \cdot \frac{\rho}{2\pi} \cdot \ln \frac{2\delta}{d} \quad (3.1)$$

$$L = \frac{1}{\ell} \cdot \frac{\mu_0}{2\pi} \cdot \ln \frac{2\delta}{d} \quad (3.2)$$

$$\frac{1}{C} = \frac{1}{\ell} \cdot \frac{1}{2\pi\epsilon} \cdot \ln \frac{2\delta}{d} \quad (3.3)$$

While in many lightning interaction problems the shunt resistance of the conductor can be neglected, that resistance is shown in order to preserve the symmetry of the equations.

The impedances presented above are the self-impedances: basically, the voltage produced on a conductor by the flow of current along that conductor. One may also define mutual impedances as the voltage induced on a conductor by the flow of current along another conductor. The magnitudes of these impedances again depend upon a constant proportional to the medium involved and upon a common logarithmic term involving the geometry of the conductors and the return path. The geometry is shown in Figure 3.3, and the mutual resistance, inductance, and capacitance are given by Equations 3.4, 3.5, and 3.6.

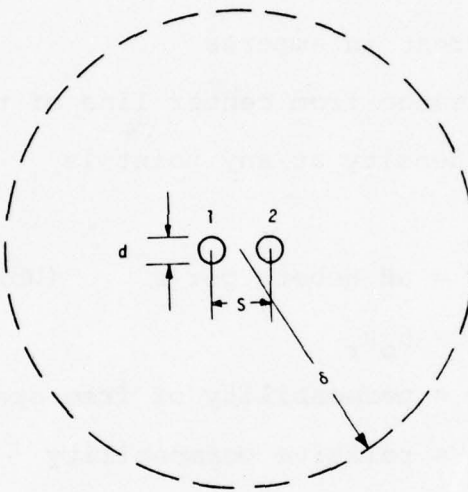


Figure 3.3 Mutual Impedances

$$R_{12} = \frac{e_2}{i_1} = \frac{1}{\ell} \cdot \frac{\rho}{2\pi} \cdot \ln \frac{\delta}{s} \quad (3.4)$$

$$L_{12} = \frac{\phi_2}{i_1} = \frac{1}{\ell} \cdot \frac{\mu}{2\pi} \cdot \ln \frac{\delta}{s} \quad (3.5)$$

$$\frac{1}{C_{12}} = \frac{V_2}{Q_1} = \frac{1}{\ell} \cdot \frac{1}{2\pi\epsilon} \cdot \ln \frac{\delta}{s} \quad (3.6)$$

3.2.2 Physical Significance of Inductance and Capacitance

A bit of digression into the origin of these equations, or into the physical significance of self-and mutual impedances is helpful as an aid to understanding lightning interaction problems.

3.2.2.1 Self-Inductance. If an isolated conductor of infinite length carries a current i , as in Figure 3.4, the magnetic field intensity external to that conductor is

$$H = \frac{i}{2\pi r} \quad A/m \quad (3.7)$$

where

i = current in amperes

r = distance from center line of the conductor in meters

The magnetic flux density at any point is

$$B = \mu H \text{ Webers per m}^2 \quad (\text{Wb/m}^2) \quad (3.8)$$

$$\text{where } \mu = \mu_0 \mu_r \quad (3.9)$$

μ_0 = permeability of free space

μ_r = relative permeability

$$\mu = 4\pi \times 10^{-7} \text{ H/m}$$

For virtually all cases in which one wishes to consider lightning interactions, the relative permeability is unity. In most future discussions in this presentation, the symbol μ_r will be considered as unity and suppressed.

The total flux between any two points p_s and p_2 is

$$\phi = \mu_0 H \int_s^{r_2} \frac{i}{2\pi r} dr \quad (3.10)$$

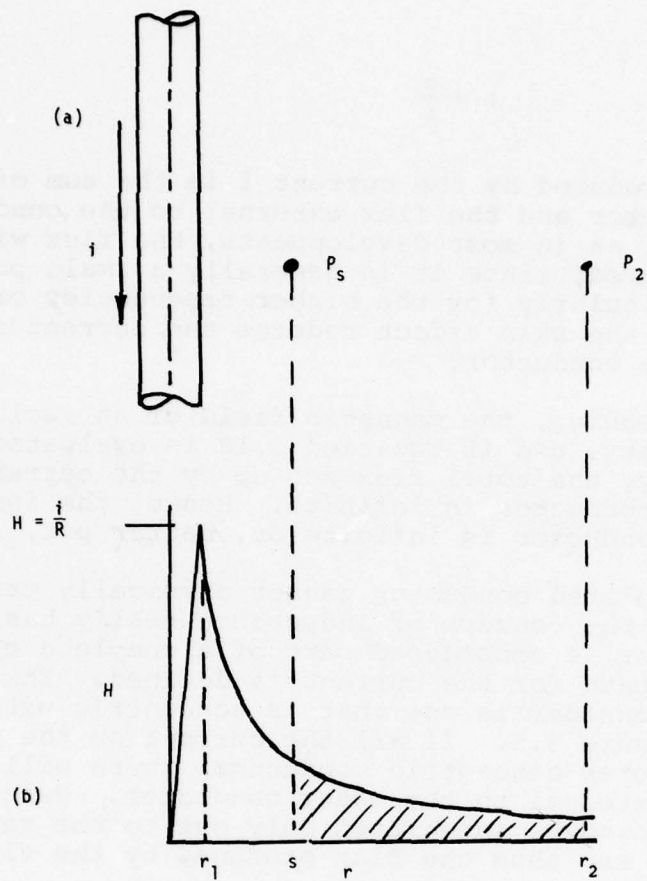


Figure 3.4 Magnetic Field Around an Infinite Conductor

(a) Geometry

(b) Field

$$= \frac{\mu_0 i}{2\pi} \ln \left(\frac{r_2}{r_1} \right) \quad (3.11)$$

The inductance of a conductor is defined as

$$L = \frac{d\Phi}{di} \quad (3.12)$$

and if the flux is always proportional to i , as it is for air,

$$L = \frac{\phi}{i} \quad (3.13)$$

The total flux produced by the current i is the sum of the flux within the conductor and the flux external to the conductor. In this development, as in most developments, the flux within the conductor is ignored, since it is generally a small part of the total flux, particularly for the higher frequencies or faster transients where the skin effect reduces the current density on the inside of the conductor.

Strictly speaking, the magnetic field of an isolated conductor extends to infinity, and if Equation 3.10 is evaluated and r_2 equal to infinity, the total flux set up by the current i in an infinitely long conductor is infinite. Hence, the inductance of an isolated conductor is infinite or, better put, indeterminate.

Since an isolated conductor cannot physically carry a continuous current, the concept of inductance really has meaning only when the conductor is considered part of a complete circuit: i.e., when the return path for the current is defined. The simplest return path to consider is one that is concentric with the conductor, as in Figure 3.5. If all the current on the conductor returns on the outer concentric conductor, there will be no magnetic field external to the outer conductor. Hence the field intensity need be integrated only out to the radius of the outer conductor, and thus the flux produced by the flow of current would be

$$\phi_1 = \frac{\mu_0 i_1}{2\pi} \ln \left(\frac{r_2}{r_1} \right) \quad (3.14)$$

$$L = \frac{\phi_1}{i_1} = \frac{\mu_0}{2\pi} \ln \left(\frac{r_2}{r_1} \right) \quad (3.15)$$

3.2.2.2 Mutual Inductance. If there is a second conductor, one is frequently interested in the amount of flux produced in the region beyond the second conductor by the current in the first conductor. If the geometry is as shown in Figure 3.6, that flux is

$$\phi_2 = \frac{\mu i_1}{2\pi} \left(\frac{r_2}{s} \right) \quad (3.16)$$

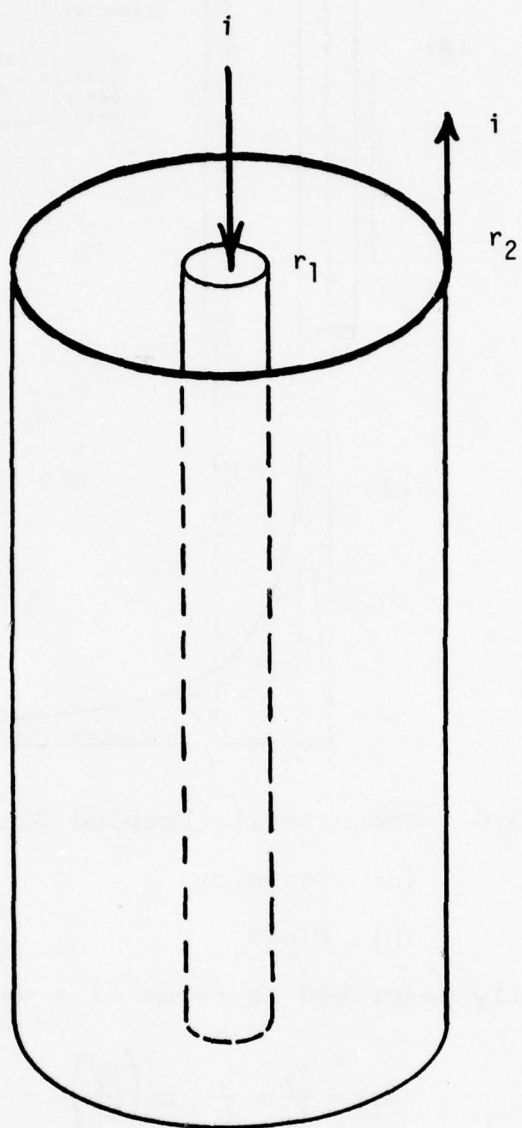


Figure 3.5 Current Return on a Concentric Cylinder

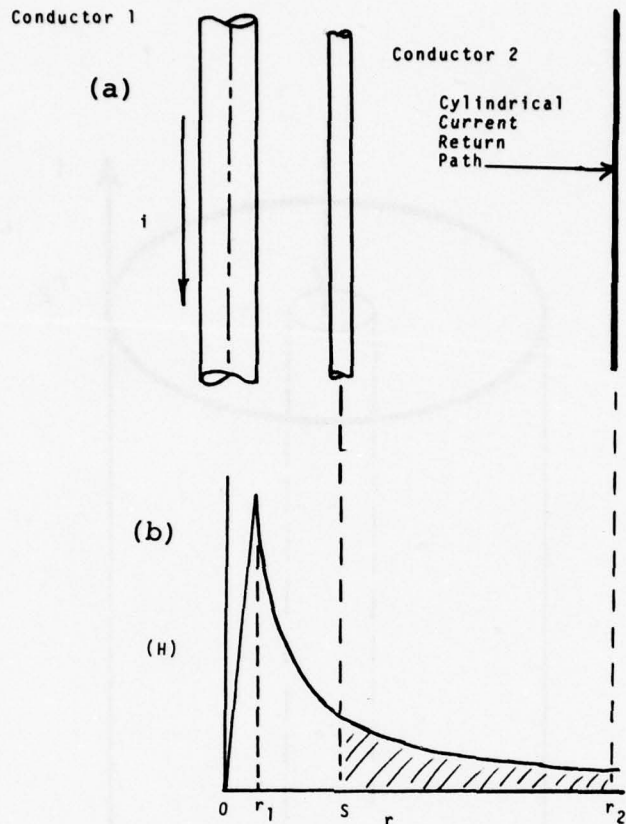


Figure 3.6 Magnetically Coupled Conductors

(a) Geometry

(b) Field

This flux is usually described in terms of a mutual inductance.

$$M_{12} = \frac{\phi_2}{i_1} = \frac{\mu_0}{2\pi} \ln \left(\frac{r_2}{s} \right) \quad (3.17)$$

Since

$$v = \frac{d\phi}{dt} \quad (3.18)$$

it follows that self-and mutual inductance can also be expressed as

$$L = \frac{d\phi_1}{dt} = \frac{v_1}{di/dt} \quad (3.19)$$

$$M = \frac{d\phi_2}{dt} = \frac{V_2}{di_1/dt} \quad (3.20)$$

3.2.2.3 Self-Capacitance. If the conductor of Figure 3.4 (or Figure 3.5) instead of carrying a current, has upon it a charge q per unit length, the electric field at any point P_s external to the conductor is

$$e = \frac{2q}{\epsilon_0 \epsilon_r r} \quad \text{volts per meter (V/m)} \quad (3.21)$$

where q = charge per unit length - coulombs per meter (C/m)
 $\epsilon_0 \approx \frac{10^9}{36\pi}$ F/m.

In a manner similar to that in which magnetic flux was evaluated as the integral of the flux density, the voltage between two points is defined as the integral of the electric field or

$$V = \int_{r_1}^{r_2} e dr = \frac{2q}{\epsilon_0 \epsilon_r} \ln\left(\frac{r_2}{r_1}\right) \quad (3.22)$$

Capacitance is defined as

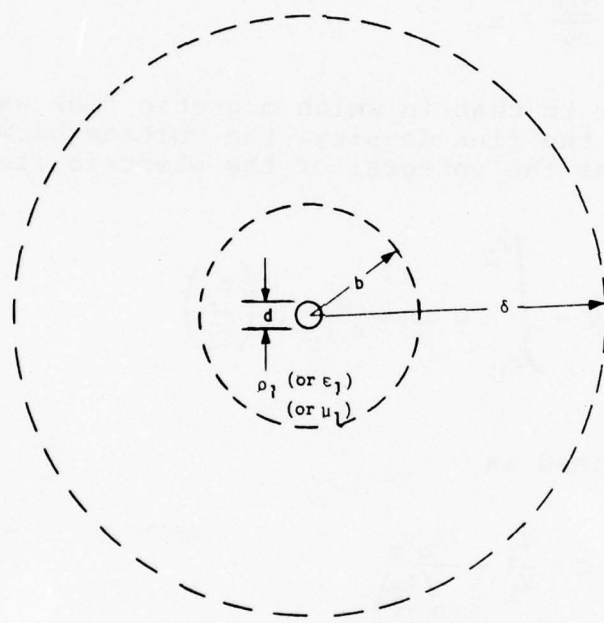
$$C = \frac{q_1}{V_1} = \frac{2\epsilon_0 \epsilon_r}{\ln\left(\frac{r_2}{s}\right)} \quad (3.23)$$

3.2.2.4 Mutual Capacitance. If the integral is evaluated over the entire distance r_1 to r_2 , the capacitance so defined is the self-capacitance of the conductor. If the integral is evaluated over the distance s to r_2 , (Figure 3.3), the capacitance so defined is what amounts to a mutual capacitance, or the ratio of the voltage induced on one conductor to the charge on another conductor.

$$C_{12} = \frac{2q}{\epsilon_r \epsilon_0} \ln\left(\frac{r_2}{s}\right) \quad (3.24)$$

3.2.2.5 Multiple Dielectrics. It frequently happens that a conductor is surrounded by two dielectric media, the natural example being a wire with insulation, but placed in the air. In a concentric geometry it is easy to evaluate the effects of the second medium. The geometry is shown in Figure 3.7. The governing equations are

$$R = \frac{1}{\lambda} \cdot \frac{1}{2\pi} \cdot \left[\rho_1 \ln \left(\frac{\delta}{b} \right) + \rho_2 \ln \left(\frac{2b}{d} \right) \right] \quad (3.25)$$



$$R = \frac{1}{\lambda} \cdot \frac{1}{2\pi} \left[\rho_1 \log \frac{\delta}{b} + \rho_2 \log \frac{2b}{d} \right]$$

$$\frac{1}{C} = \frac{1}{\lambda} \cdot \frac{1}{2\pi\epsilon_0} \left[\frac{1}{\epsilon_{r1}} \cdot \log \frac{\delta}{b} + \frac{1}{\epsilon_{r2}} \cdot \log \frac{2b}{d} \right]$$

$$L = \lambda \cdot \frac{\mu_0}{2\pi} \left[\mu_{r1} \log \frac{\delta}{b} + \mu_{r2} \log \frac{2b}{d} \right]$$

Figure 3.7 Self-Impedance – Two-Media Case

$$L = \ell \cdot \frac{\mu_0}{2\pi} \cdot \left[\mu_{rl} \ln\left(\frac{\delta}{b}\right) + \frac{1}{\epsilon_{r2}} \ln\left(\frac{2b}{d}\right) \right] \quad (3.26)$$

$$\frac{1}{C} = \frac{1}{\ell} \cdot \frac{1}{2\pi\epsilon_0} \cdot \left[\frac{1}{\epsilon_{rl}} \ln\left(\frac{\delta}{b}\right) + \frac{1}{\epsilon_{r2}} \ln\left(\frac{2b}{d}\right) \right] \quad (3.27)$$

3.2.2.6 Relation Between Inductance and Capacitance. Formulas for inductance and capacitance are seen to include similar logarithmic terms. In fact, it can be shown that

$$LC = \mu\epsilon \quad (3.28)$$

and that, if one knows one of the quantities (inductance or capacitance) of a structure, one can determine the other quantity. In fact, one can determine the inductance of a structure by measurement of the capacitance, or vice versa, subject to the important proviso that the effective dielectric constant of the medium is known. Particularly with insulated wires placed in the air this is easier said than done.

3.2.3 Isolated Conductors and Conductor Pairs

While it must be remembered that an isolated conductor cannot carry a continuous current, it is instructive to consider what the magnetic field would be if one postulates an isolated conductor or conductor pair. Figure 3.8 shows such a conductor or conductor pair. If the conductor is of finite length, the total flux set up by the postulated current sums up to a finite value, and hence an isolated conductor has associated with it a certain inductance

$$L_s = \frac{\phi_1}{i_1} \quad (3.29)$$

If the flux is again neglected within the conductor, that inductance can be shown to be

$$L_s = \frac{\mu_0}{2\pi} \cdot \ell \cdot \left[\ln\left(\frac{4\ell}{d}\right) - 1 \right]_H \quad (3.30)$$

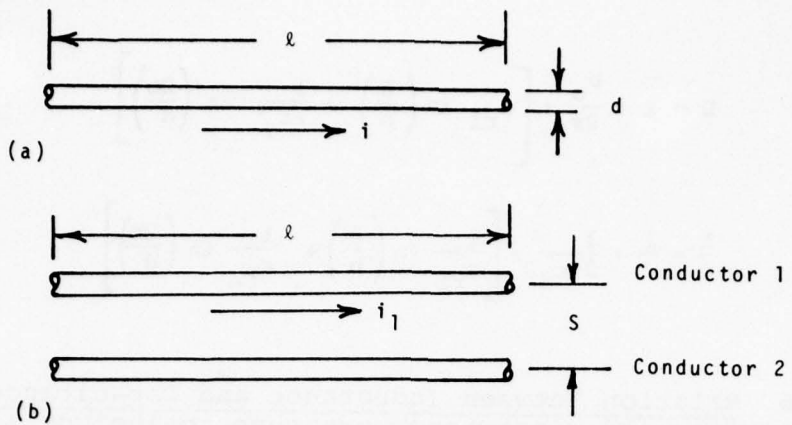


Figure 3.8 Elementary Conductors

(a) An Isolated Conductor Possessing Self-Inductance

(b) Adjacent Conductors Possessing Mutual Inductance

$$L_s = 0.2 l \left[\ln \left(\frac{4l}{d} \right) - 1 \right] \text{ H} \quad (3.31)$$

where

d = diameter of conductor — m

l = length of conductor — m

Note that the inductance is not directly proportional to the conductor length unless the conductor is very long compared to its diameter. L_s , as defined in Equation 3.30, relates only to the self-inductance of the conductor and has only mathematical significance, since it is not a measurable quantity. In order for the indicated current to flow, there must be other conductors making up that complete circuit; and in order for inductance to have a physical significance, the magnetic fields produced by the flow of current on the other conductors must be taken into account. This is done through the use of mutual inductance. For the parallel conductors shown in Figure 3.8b the mutual inductance, defined as

$$M = \frac{\phi_{12}}{i_1} \quad (3.32)$$

is

$$M = \ell \cdot \frac{\mu_0}{2\pi} \left[\ln\left(\frac{2\ell}{s}\right) - 1 + \frac{s}{\ell} \right]_H \quad (3.33)$$

$$M = 0.2 \ell \left[\ln\left(\frac{2\ell}{s}\right) - 1 + \frac{s}{\ell} \right]_H \quad (3.34)$$

The total inductance of the circuit is the sum of the self-inductance and the mutual inductance to the return path. The mutual inductance may be either positive or negative, depending upon whether the field produced by the current in the return path adds to or subtracts from the flux set up by the first conductor. Figure 3.9 shows two possible ways of interconnecting the two conductors shown in Figure 3.8. In Figure 3.9a, which is easily realized in a physical sense, the current goes down Conductor 1 and returns through Conductor 2. The total inductance of the circuit is

$$L_T = (L_{s1} - M_{12}) + (L_{s2} - M_{21}) \quad (3.35)$$

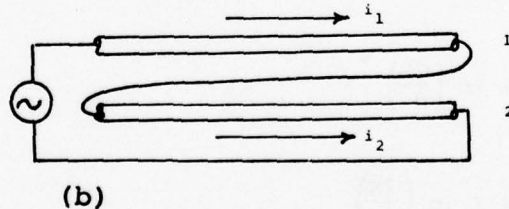
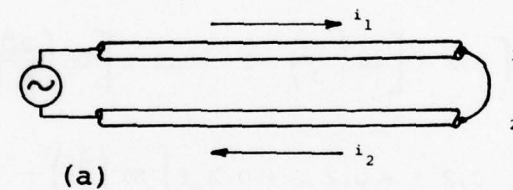


Figure 3.9 Connected Conductors

(a) Currents in Reverse Directions

(b) Currents in Same Direction

If the conductors are about the same diameter, M_{12} and M_{21} are nearly equal, even if the conductors are fairly close together. L_{s1} and L_{s2} will also be equal if the diameters are the same. Hence

$$L_T = 2 (L_s - M) \quad (3.36)$$

In Figure 3.9b the two conductors are interconnected so that the current goes the same way in each one, and is interconnected by conductors in which the current produces no magnetic field, a situation not physically realizable for straight conductors but perfectly feasible for loops. In such a case the fields add, and hence

$$L_T = (L_{s1} + M_{12}) + (L_{s2} + M_{21}) \quad (3.37)$$

If the conductors are long compared to their spacing, so that the D/l term in Equation 3.33 can be disregarded, then the inductance of the conductor pair, as connected and shown in Figure 3.9 a becomes

$$L_T = 2 \left\{ 0.2 l \left[\ln \left(\frac{4l}{d} \right) - 1 \right] - 0.2 l \left[\ln \left(\frac{2l}{s} \right) - 1 \right] \right\} \quad (3.38)$$

$$L_T = 2 \left\{ -0.2 l + 0.2 l + 0.2 l \left[\ln \left(\frac{4l}{d} \right) - \ln \left(\frac{2l}{s} \right) \right] \right\} \quad (3.39)$$

$$L_T = \frac{\mu}{\pi} l \ln \left(\frac{2s}{d} \right) \quad (3.40)$$

$$L_T = 0.4 l \ln \left(\frac{2s}{d} \right) \quad (3.41)$$

Thus, the inductance of the wire pair is directly proportional to its length, provided only that the length of the pair is large compared to the spacing between the conductors.

3.2.4 Conductor Over a Ground Plane

3.2.4.1 Self- and Mutual Inductance. Frequently a conductor is over a ground plane, as in Figure 3.10. The self-inductance of the conductor would again be as given by Equation 3.30. The mutual inductance would be that between the conductor and its image (the spacing to that image being twice the height of the conductor over the ground plane) and can again be calculated by Equation 3.33. Since the concept of a perfect ground plane implies that it has no inductance of its own, the inductance of the circuit in which the return is through the ground plane becomes

$$L_T = L_s - M \quad (3.42)$$

$$L_T = 0.2 \ell \left[\ln \left(\frac{4\ell}{d} \right) - 1 \right] - 0.2 \ell \left[\ln \left(\frac{2h}{2\ell} \right) - 1 \right] \quad (3.43)$$

$$L_T = 0.2 \ell \ln \left(\frac{4h}{d} \right) \quad (3.44)$$

Equation 3.44 again assumes that the length of the conductor is long compared to its height above the ground plane.

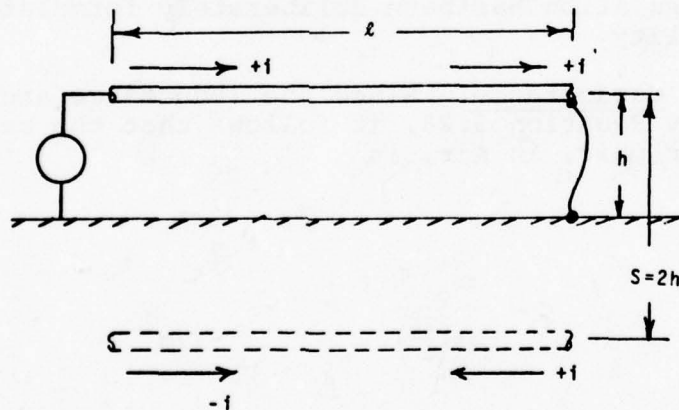


Figure 3.10 Conductor Over a Ground Plane

3.2.4.2 Second Order Effects. All the equations presented up to this point have assumed that the conductor is sufficiently far from the other conductor or ground plane that the current density is uniform over the surface of the conductor, which it will be if $h \gg d$. If this is not the case, (Figure 3.11a), the current will not be uniformly distributed. An exact formulation of the above equations is made possible by using a different argument for the logarithmic terms. If, for example, Equation 3.44 is written as

$$L_T = 0.2 \ell \ln \left[\left(\frac{2h}{d} \right) - \sqrt{\left(\frac{2h}{d} \right)^2 - 1} \right] \quad (3.45)$$

it is an exact expression for inductance. Generally the error involved in ignoring proximity effects is so small, at least in relation to the other uncertainties inherent in calculations relating to lightning response, it need not be cause for serious concern. Even when $h = d$, the simplified formula of Equation 3.44 predicts an inductance only 5% higher than the exact expression of Equation 3.45.

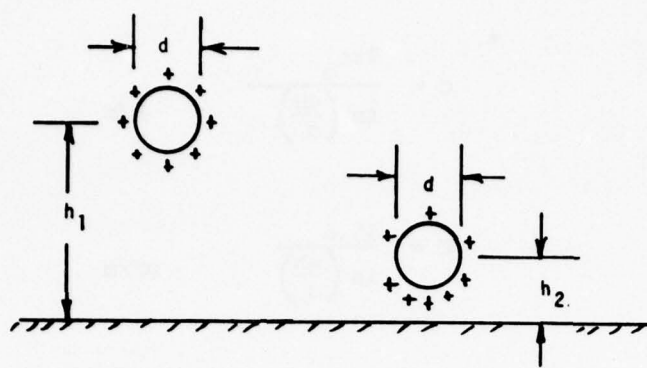
Finally, it might be noted that the presence of insulation over the conductors, (Figure 3.11b), does not affect the inductance unless the insulation has been deliberately formulated to have high permeability.

3.2.4.3 Capacitance. Since the inductance and capacitance are related by Equation 3.28, it follows that the capacitance of a conductor pair, in air, is

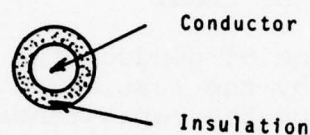
$$C = \frac{\pi \epsilon_0}{\ln \left(\frac{2s}{d} \right)} \quad F/m \quad (3.46)$$

or

$$C = \frac{27.8}{\ln \left(\frac{2s}{d} \right)} \quad pF/m \quad (3.47)$$



(a)



(b)

Figure 3.11 Second Order Effects

(a) Proximity Effects

(b) Conductor Insulation

and for a conductor over a ground plane

$$C = \frac{2\pi\epsilon_0}{\ln\left(\frac{4h}{d}\right)} \quad F/m \quad (3.48)$$

or

$$C = \frac{55.6}{\ln\left(\frac{4h}{d}\right)} \quad pF/m \quad (3.49)$$

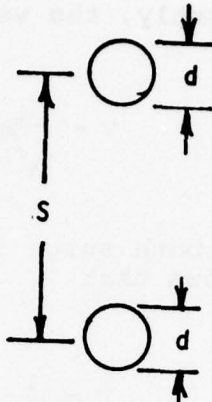
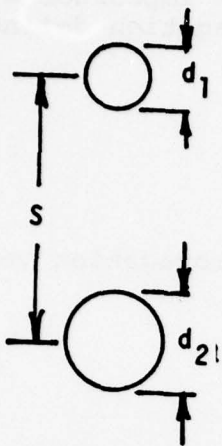
If the conductors are close together or close to a ground plane, the more exact formulation for the argument of the logarithmic term should be used.

The capacitance of conductors, unlike inductance, can be strongly affected by the insulation over the conductors. Accurate equations predicting the capacitance of insulated conductors seem not to exist, except for concentric conductors, as described in the preceding section. The effect of insulation can be approximated, however. Since the dielectric constant of the insulation is substantially higher than that of air, it follows that the greater fraction of the voltage between the conductor and ground will appear across the air and only a small portion appear across the insulation. Hence, a limiting value of the capacitance can be obtained by using the diameter over the insulation in the capacitance formulas rather than the actual wire diameter.

3.2.5 Practical Calculation of Inductance and Capacitance

A collection of working formulas for line-to-ground impedances of some common conductor geometries is shown in Figure 3.12. The figures also show the expression for surge impedance, defined as

$$Z = \sqrt{\frac{L}{C}} \quad \Omega \quad (3.50)$$



$$L = 0.2 \ln \frac{4S^2}{d_1 d_2} \mu\text{H/m}$$

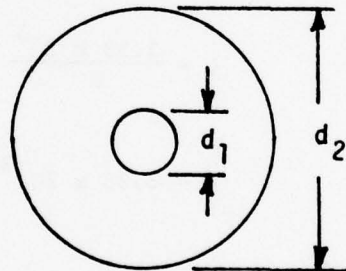
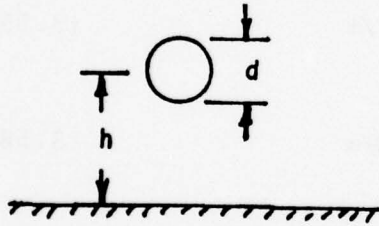
$$L = 0.4 \ln \frac{2S}{d} \mu\text{H/m}$$

$$C = \frac{55.6}{\ln \frac{4S^2}{d_1 d_2}} \text{ pF/m}$$

$$C = \frac{27.8}{\ln \frac{2S}{d}} \text{ pF/m}$$

$$Z = 60 \ln \frac{4S^2}{d_1 d_2} \Omega$$

$$Z = 60 \ln \frac{2S}{d} \Omega$$



$$L = 0.2 \ln \frac{4h}{d} \mu\text{H/m}$$

$$L = 0.2 \ln \frac{d_2}{d_1} \mu\text{H/m}$$

$$C = \frac{55.6}{\ln \frac{4h}{d}} \text{ pF/m}$$

$$C = \frac{55.6}{\ln \frac{d_2}{d_1}} \text{ pF/m}$$

$$Z = 60 \ln \frac{4h}{d} \Omega$$

$$Z = 60 \ln \frac{d_2}{d_1} \Omega$$

Figure 3.12 Line to Ground Impedances — Summary

Frequently, for a set of conductors, the surge impedance will be known. Less frequently, the velocity of propagation defined as

$$v = \frac{1}{\sqrt{LC}} \quad (3.51)$$

will be given. If both surge impedance and propagation velocity are known, it follows that

$$C = \frac{1}{VZ} \quad F/m \quad (3.52)$$

$$L = \frac{Z}{V} \quad H/m \quad (3.53)$$

If we assume $\epsilon_r = \mu_r = 1$, then

$$V \approx 3 \times 10^3 \text{ m/s} \quad (3.54)$$

$$C = \frac{3.33 \times 10^3}{Z} \quad pF/m \quad (3.55)$$

$$L = 3.33 \times 10^{-3} Z \quad \mu H/m \quad (3.56)$$

The permeability of the medium in which the conductors are placed is practically never different from μ_r , but the relative dielectric constant can be substantially greater than unity. If ϵ_r is other than unity

$$C = \frac{3.33 \times 10^3 \sqrt{\epsilon_r}}{Z} \quad pF/m \quad (3.57)$$

$$L = 3.33 \times 10^{-3} \sqrt{\epsilon_r} Z \quad \mu H/m \quad (3.58)$$

A type of conductor frequently found is the common 50Ω coaxial cable, in which the dielectric is most typically polyethylene of $\epsilon_r = 2.3$. The inductance and capacitance of such a cable is $0.253 \mu\text{H/m}$ and 101 pF/m respectively.

Figures 3.13 and 3.14 show plots of the inductance and capacitance of typical sizes of wires, or of wire bundles. It can be seen that rather reasonable rules of thumb for values of inductance and capacitance are $0.8 \mu\text{H/m}$ and 2.0 pF/m . For insulated conductors, the capacitance might be increased about 20%. In interaction problems, more accurately calculated or measured values are preferable to the use of rules of thumb.

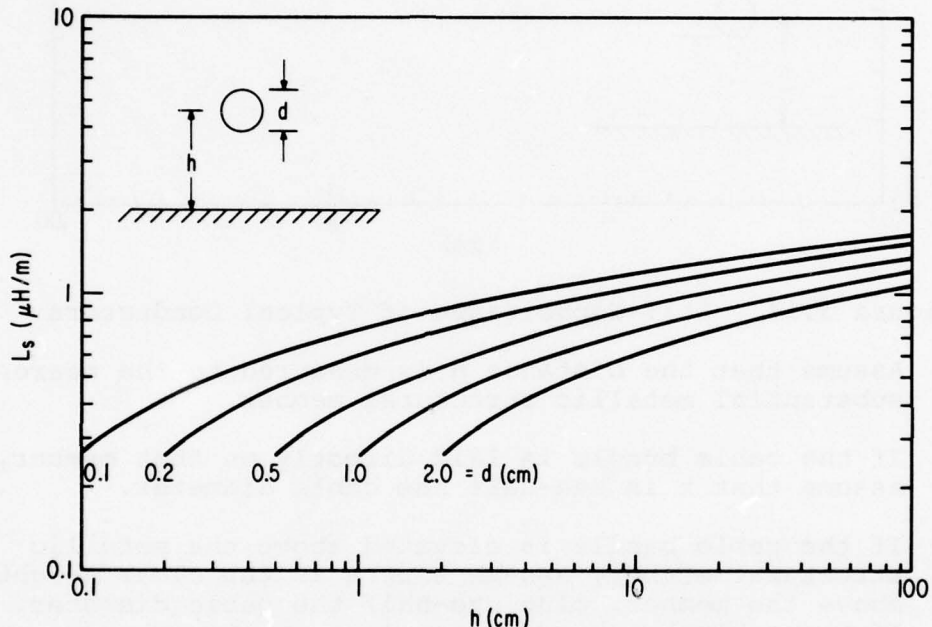


Figure 3.13 Self-Inductance of Typical Conductors

One of the major difficulties in determining the inductance and capacitance of a cable bundle is that the height, h , of the wire or cable bundle above a ground plane is difficult to specify, partly because the ground plane is seldom purely a plane surface and because cable bundles are frequently strapped directly to a supporting structure. In the absence of any better definition of height, the following rules might be used:

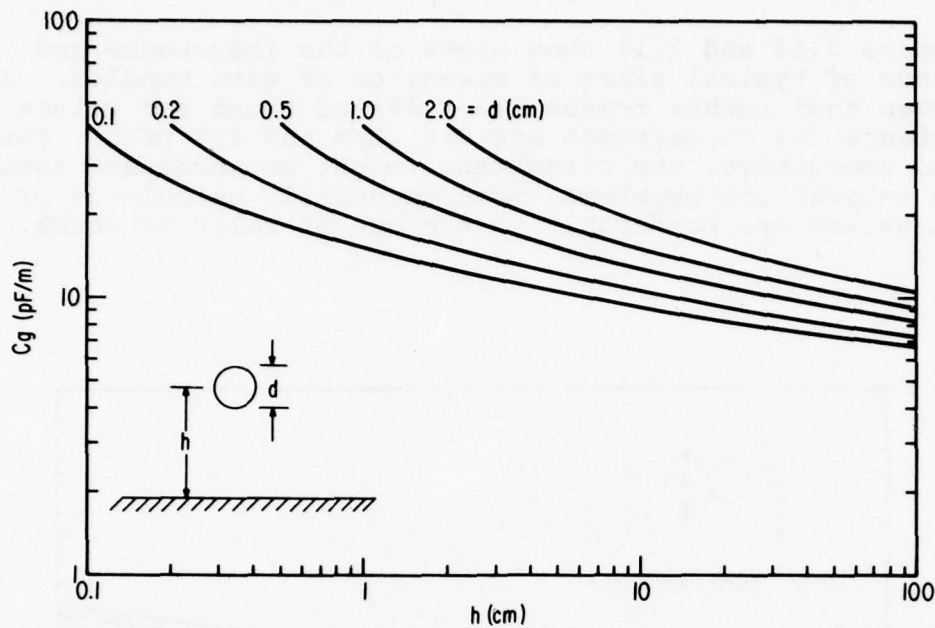


Figure 3.14 Self-Capacitance of Typical Conductors

1. Assume that the distance h is measured to the nearest substantial metallic structural member.
2. If the cable bundle is laid directly on that member, assume that h is one-half the cable diameter.
3. If the cable bundle is elevated above the metallic structural member, assume that h is the clear height above the member, plus one-half the cable diameter. If the cable height differs along its length, use an average height.

The fact that the height is difficult to specify is one of the reasons that it is frequently preferable to use measured values of inductance and capacitance for analysis of the response of a cable system to the electromagnetic fields produced by lightning.

3.2.6 Effects of Line Losses

None of the preceding work has touched on the subject of line losses or line resistance. While it is a considerable oversimplification of the matter, conductor resistance does not affect the response very much as long as the frequency is well below the resonance points of the conductor system. At frequen-

cies well above the first response point, circuit loss does significantly affect the response. Some of the circuit losses at these frequencies are accounted for by the intrinsic resistance of the conductors involved, but part is accounted for by radiation loss or by the effects of eddy currents in nearby surfaces of less than perfect conductivity. While such effects can be discussed in great detail, in the final analysis their effects are usually described in terms of empirical measurements or educated judgment.

Skin effect also plays a role in the losses, but probably that role is significant only at frequencies sufficiently high enough that the analysis procedure is of dubious validity, or at frequencies sufficiently high that little is really known about the electromagnetic fields exciting the response under study. Skin effect is most noticeable on large conductors, but the large conductors for which calculations are probably to be made are most likely to be bundles of smaller conductors. The Litz wire effect helps minimize skin effects.

As a result of the above factors, it is recommended that the resistance of conductors be taken as the dc resistance of the conductors for purposes of lightning interaction calculations.

3.3 LUMPED CONSTANT REPRESENTATION OF CONDUCTORS

3.3.1 Single Conductors

Figure 3.15 shows a distributed conductor of length l ; it has a total inductance and capacitance of L_t and C_t , those values having been determined with the preceding equations. This distributed conductor must then be divided into N elementary sections, of which the simplest and most generally usable is a Pi section as shown in Figure 3.15b. A virtue of a Pi representation is that it provides a capacitance at the end of each section. This leads generally to better numerical stability than does a representation having inductance at the ends. The capacitance at the ends of the adjacent elementary sections can, of course, be combined as shown in Figure 3.15c.

3.3.2 How Many Sections To Use?

It should be recognized that the lumped constant representation of the distributed conductor forms a low pass filter. One should not expect the response of the lumped constant representation to be an accurate representation of the distributed system at frequencies higher than the cutoff frequency of the filter. The maximum frequency for which one should place any reliance in the results calculated with this representation is

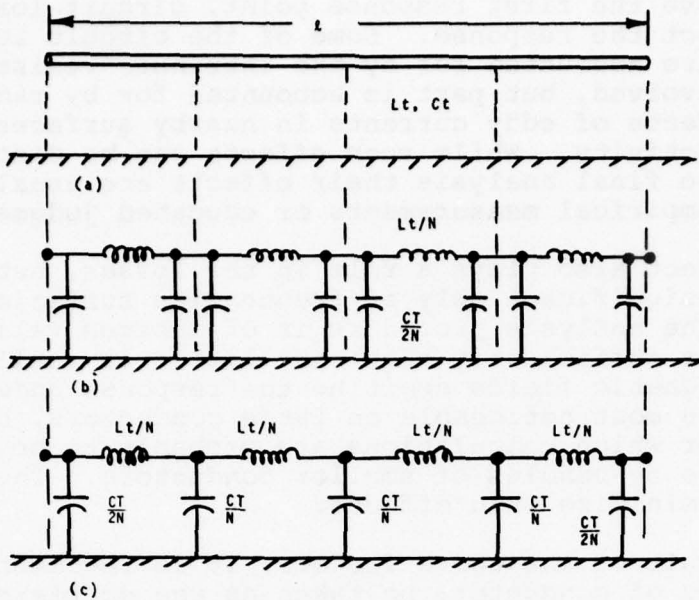


Figure 3.15 Lumped Constant Approximations

(a) Distributed Conductor

(b) Elementary Pi Sections

(c) Capacitances Combined

$$f_m = \frac{100}{\ell} N \quad \text{MHz} \quad (3.59)$$

where N = number of sections

ℓ = line length — m

It would be particularly well not to trust results above half this frequency.

3.3.3 Coupled Conductors

Finding equivalent circuits for the propagation along one conductor, or group of conductors treated as a cable bundle, is only part of the analysis problem. Another important part of the analysis problem is to determine the interactions between two

conductors or two bundles of conductors. Figure 3.16a shows two conductors. The object of the analysis to follow is to derive the quantities of the double Pi section shown on Figure 3.16b. The indicated quantities are not those that one would calculate for a conductor by itself. The analysis will treat only two conductors. To extend the analysis to more conductors, is straightforward in principle, but the complexity of the equivalent circuits increases so rapidly that one should be dubious about the results predicted by a circuit representing more than two conductors.

In general, both the height and the diameter of the two conductors can be unequal, but the analysis is simplified if the diameters d_1 and d_2 are the same. The conductors will be assumed to be parallel to each other and to the ground plane.

3.3.3.1 Capacitance. If, as in Figure 3.16, there are two isolated conductors and upon Conductor 1 a charge Q_1 is placed, there will be induced upon Conductor 2 a charge Q_2 . These charges will give rise to voltages, V_1 and V_2 , to ground from each of the conductors, the relationship between the voltages and charges being

$$C_x = \frac{Q_x}{V_x} \quad (3.60)$$

The task is to define the quantities C_x that satisfy Equation 3.60, and from these quantities, to determine the physical capacitances from which one could construct for the two conductors the lumped constant representation shown in Figure 3.16 b.

The first step in the analysis is to formulate the equations

$$V_1 = B_{11} Q_1 + B_{12} Q_2 \quad (3.61)$$

$$V_2 = B_{21} Q_1 + B_{22} Q_2 \quad (3.62)$$

These may be written in matrix form as

$$\begin{bmatrix} V_1 \\ V_2 \end{bmatrix} = \begin{bmatrix} B_{11} & B_{12} \\ B_{21} & B_{22} \end{bmatrix} \begin{bmatrix} Q_1 \\ Q_2 \end{bmatrix} \quad (3.63)$$

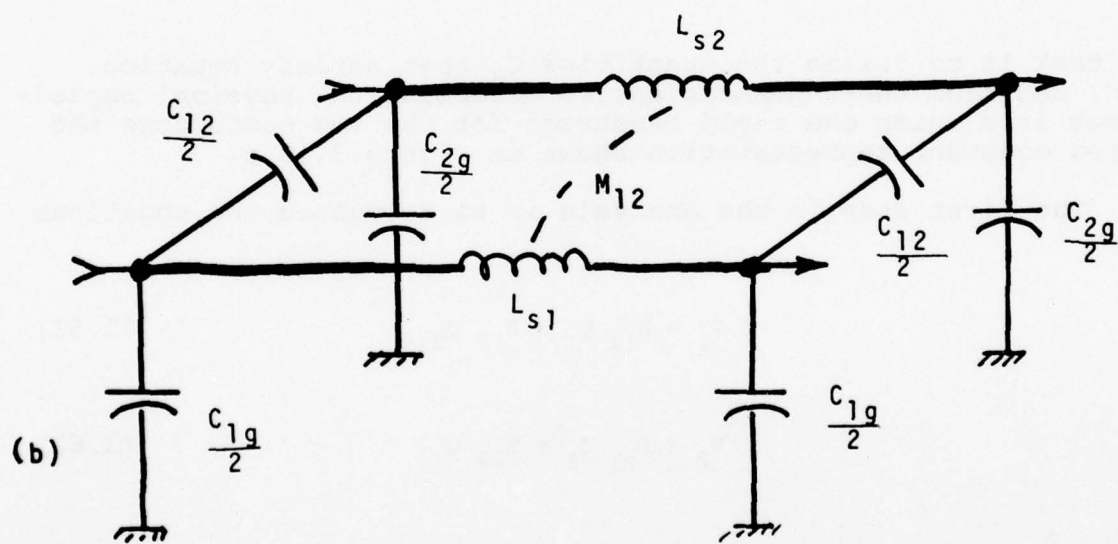
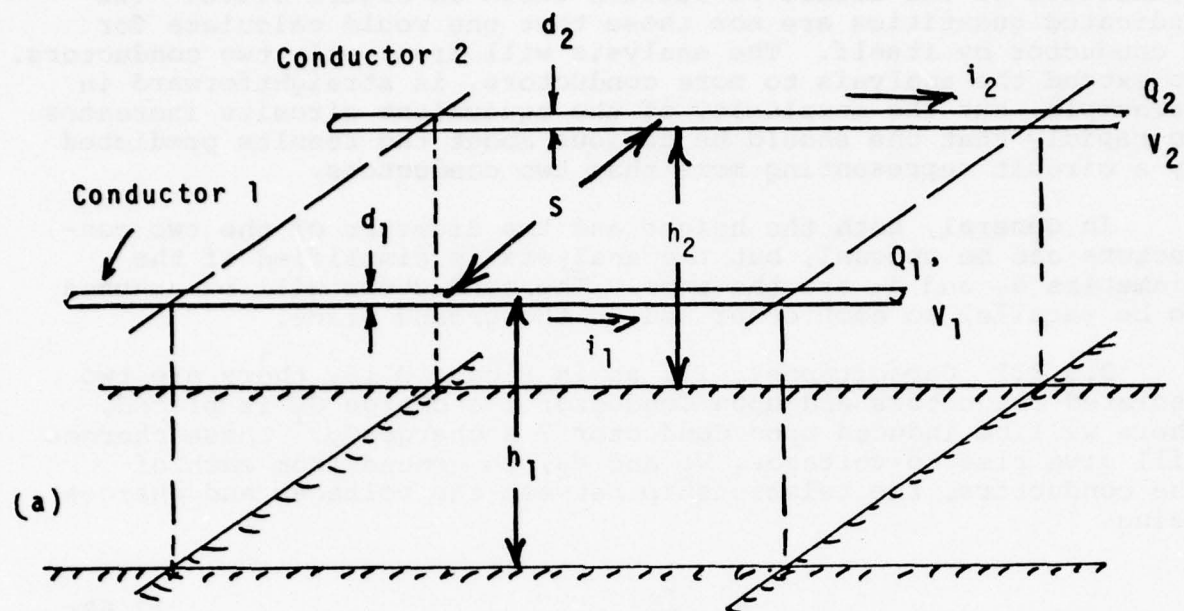


Figure 3.16 Coupled Conductors

(a) Physical

(b) Pi Section Equivalent

or more compactly as

$$\underline{V} = \underline{B} \underline{\Omega} \quad (3.64)$$

The bar under the quantities in Equation 3.64 indicates that these should be regarded as matrix quantities. Since the conductors are over a perfectly conducting ground plane, the method of images may be applied, as shown in Figure 3.17 and from electrostatics

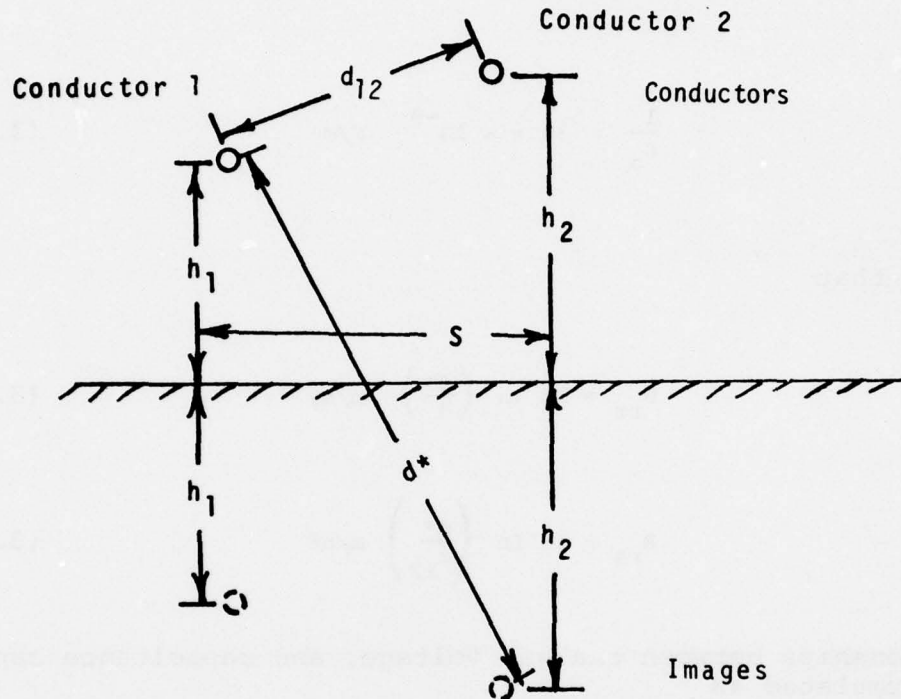


Figure 3.17 Images of the Conductors

$$B_{rr} = \frac{1}{2\pi\epsilon_0} \ln \left(\frac{4h}{d} \right) \quad (3.65)$$

$$B_{rs} = \frac{1}{2\pi\epsilon_0} \ln \left(\frac{d^*}{d_{12}} \right) \quad (3.66)$$

where

d = diameter of the conductors

h = height of the conductor over the ground plane

d^* = distance between Conductor 1 and the image of Conductor 2

d_{12} = distance between Conductor 1 and Conductor 2

Since

$$\frac{1}{\epsilon_0} \approx 36 \pi \times 10^{-9} \text{ F/m} \quad (3.67)$$

it follows that

$$B_{rr} = 18 \ln \left(\frac{4h}{d} \right) \text{ m/nF} \quad (3.68)$$

$$B_{rs} = 18 \ln \left(\frac{d^*}{d_{12}} \right) \text{ m/nF} \quad (3.69)$$

The relationships between charge, voltage, and capacitance can also be formulated as

$$Q_1 = K_{11} V_1 + K_{12} V_2 \quad (3.70)$$

$$Q_2 = K_{21} V_1 + K_{22} V_2 \quad (3.71)$$

or in matrix notation

$$\begin{bmatrix} Q_1 \\ Q_2 \end{bmatrix} = \begin{bmatrix} K_{11} & K_{12} \\ K_{21} & K_{22} \end{bmatrix} \begin{bmatrix} V_1 \\ V_2 \end{bmatrix} \quad (3.72)$$

or

$$Q = K V \quad (3.73)$$

If we multiply each side of Equation 3.64 by the inverse of the B matrix, then

$$\underline{B}^{-1} \underline{V} = \underline{B}^{-1} \underline{B} Q \quad (3.74)$$

$$\underline{B}^{-1} \underline{V} = Q \quad (3.75)$$

which is of the same form as Equation 3.73. Hence there must be one-to-one correspondence between the elements of the B⁻¹ and the K matrices.

The elements of the inverse of the B matrix, in terms of elements of the K matrix, are

$$K_{11} = \frac{B_{22}}{D} \quad (3.76)$$

$$K_{12} = \frac{B_{21}}{D} \quad (3.77)$$

$$K_{21} = K_{12} \quad (3.78)$$

$$K_{22} = \frac{B_{11}}{D} \quad (3.79)$$

$$D = B_{11} B_{22} - B_{21} B_{12} \quad (3.80)$$

The quantities K_{11} , K_{12} , and K_{22} of Equations 3.76 - 3.79 are related to the physical capacitors that would make up a lumped constant representation of the two conductors. Those capacitors can be related to the elements of the K matrix as follows: On the network of capacitors shown in Figure 3.18, if the voltages V_1 and V_2 are held on Points 1 and 2, respectively, the charges on the various capacitors will be the net charge seen at Points 1 and 2, and will be

$$Q_1 = q_1 + q_3 \quad (3.84)$$

$$Q_2 = q_2 - q_3 \quad (3.85)$$

$$Q_1 = C_{1g} V_1 + C_{12} V_1 - C_{12} V_2 \quad (3.86)$$

$$Q_2 = -C_{12} V_1 + C_{12} V_2 - C_{2q} V_2 \quad (3.87)$$

or $Q_1 = (C_{1g} + C_{12}) V_1 - C_{12} V_2 \quad (3.88)$

$$Q_2 = -C_{12} V_1 + (C_{12} + C_{2q}) V_2 \quad (3.89)$$

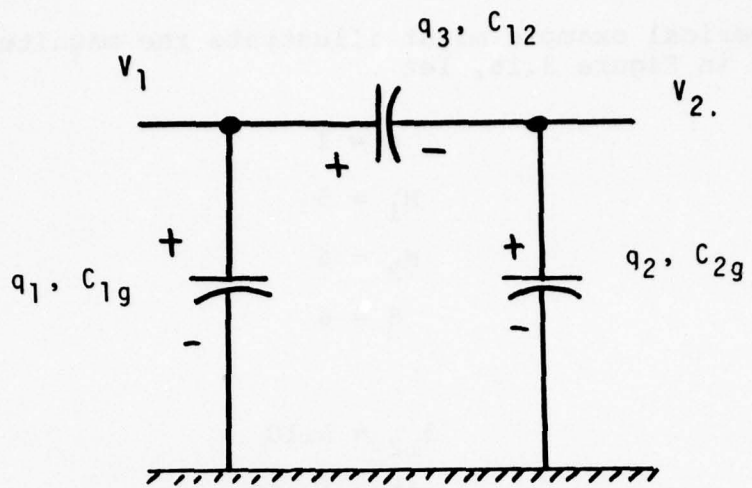


Figure 3.18 Charges Relating to Self-and Mutual Capacitance

and in matrix notation

$$\begin{bmatrix} Q_1 \\ Q_2 \end{bmatrix} = \begin{bmatrix} (C_{1g} + C_{12}) - C_{12} \\ -C_{12} \quad (C_{12} + C_{2g}) \end{bmatrix} \begin{bmatrix} V_1 \\ V_2 \end{bmatrix} \quad (3.90)$$

or

$$Q = C V \quad (3.91)$$

This corresponds to the same form as Equation 3.73 and hence there must be a one-to-one correspondence between the elements of the C matrix and the K matrix. It therefore follows that

$$C_{1g} = K_{11} + K_{12} \quad (3.92)$$

$$C_{2g} = K_{22} + K_{12} \quad (3.93)$$

$$C_{12} = C_{21} = -K_{12} \quad (3.94)$$

A numerical example might illustrate the magnitude of the terms. As in Figure 3.16, let

$$d = 1$$

$$H_1 = 5$$

$$H_2 = 6$$

$$S = 6$$

and thus

$$d_{12} = 5.10$$

$$d^* = 12.08$$

From Equations 3.68 and 3.69

$$B_{11} = 5.392 \times 10^{10} \text{ m/F}$$

$$B_{22} = 5.720 \times 10^{10} \text{ m/F}$$

$$B_{12} = B_{21} = 1.552 \times 10^{10} \text{ m/F}$$

By either inverting the B matrix numerically or, more easily in this simple case, working directly from Equations 3.76 - 3.80,

$$K_{11} = 20.12 \text{ pF/m}$$

$$K_{12} = 5.46 \text{ pF/m}$$

$$K_{22} = 18.96 \text{ pF/m}$$

and thus

$$C_{1G} = 14.66 \text{ pF/m}$$

$$C_{2G} = 13.50 \text{ pF/m}$$

$$C_{12} = 5.46 \text{ pF/m}$$

3.3.3.2 Inductance. In a similar manner, if a current i_1 is passed through Conductor 1, there will be induced in Conductor 2 a current i_2 , assuming the conductors are of infinite length so that the current in the second conductor is not influenced by end effects. These currents will set up magnetic flux in the surrounding area, the relationship between flux and current being

$$L_x = \frac{\phi_x}{i_x} \quad (3.95)$$

The relationships between flux and current may be formulated as

$$\phi_1 = F_{11} i_1 + F_{12} i_2 \quad (3.96)$$

$$\phi_2 = F_{21} i_1 + F_{22} i_2 \quad (3.97)$$

$$\begin{bmatrix} \phi_1 \\ \phi_2 \end{bmatrix} = \begin{bmatrix} F_{11} & F_{12} \\ F_{21} & F_{22} \end{bmatrix} \begin{bmatrix} i_1 \\ i_2 \end{bmatrix} \quad (3.98)$$

$$\underline{\phi} = \underline{F} \underline{i} \quad (3.99)$$

The elements of the F matrix may be evaluated as

$$F_{rr} = \frac{\mu}{2\pi} \ln \left(\frac{4h}{d} \right) \text{ H/m} \quad (3.100)$$

$$F_{rs} = \frac{\mu}{2\pi} \ln \left(\frac{D^*}{D_{12}} \right) \mu\text{H/m} \quad (3.101)$$

or $F_{rr} = 0.2 \ln \left(\frac{4h}{d} \right) \mu\text{H/m}$ (3.102)

$$F_{rs} = 0.2 \ln \left(\frac{4h}{d} \right) \text{ } \mu\text{H/m} \quad (3.103)$$

In the lumped constant representation shown in Figure 3.19

$$\int v_1 = \phi_1 = (L_{s1} - M)i_1 - Mi_2 \quad (3.104)$$

$$\int v_2 = \phi_2 = -Mi_1 + (L_{s2} - M)i_2 \quad (3.105)$$

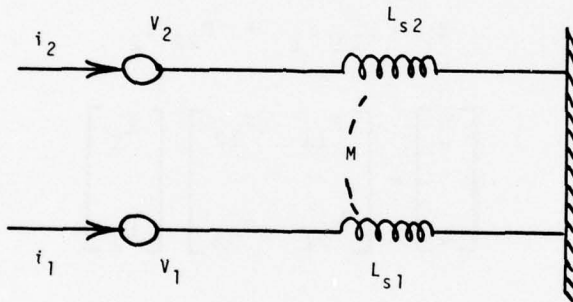


Figure 3.19. Currents Relating to Self-and Mutual Inductance

or in matrix form

$$\begin{bmatrix} \phi_1 \\ \phi_2 \end{bmatrix} = \begin{bmatrix} (L_{s1} - M) & \\ -M & + (L_{s2} - M) \end{bmatrix} \begin{bmatrix} i_1 \\ i_2 \end{bmatrix}. \quad (3.106)$$

$$\underline{\phi} = \underline{L} \underline{i} \quad (3.107)$$

AD-A062 606

GENERAL ELECTRIC CORPORATE RESEARCH AND DEVELOPMENT --ETC F/G 1/3
ANALYSIS AND CALCULATIONS OF LIGHTNING INTERACTIONS WITH AIRCRA--ETC(U)

AUG 78 F A FISHER

F33615-76-C-3122

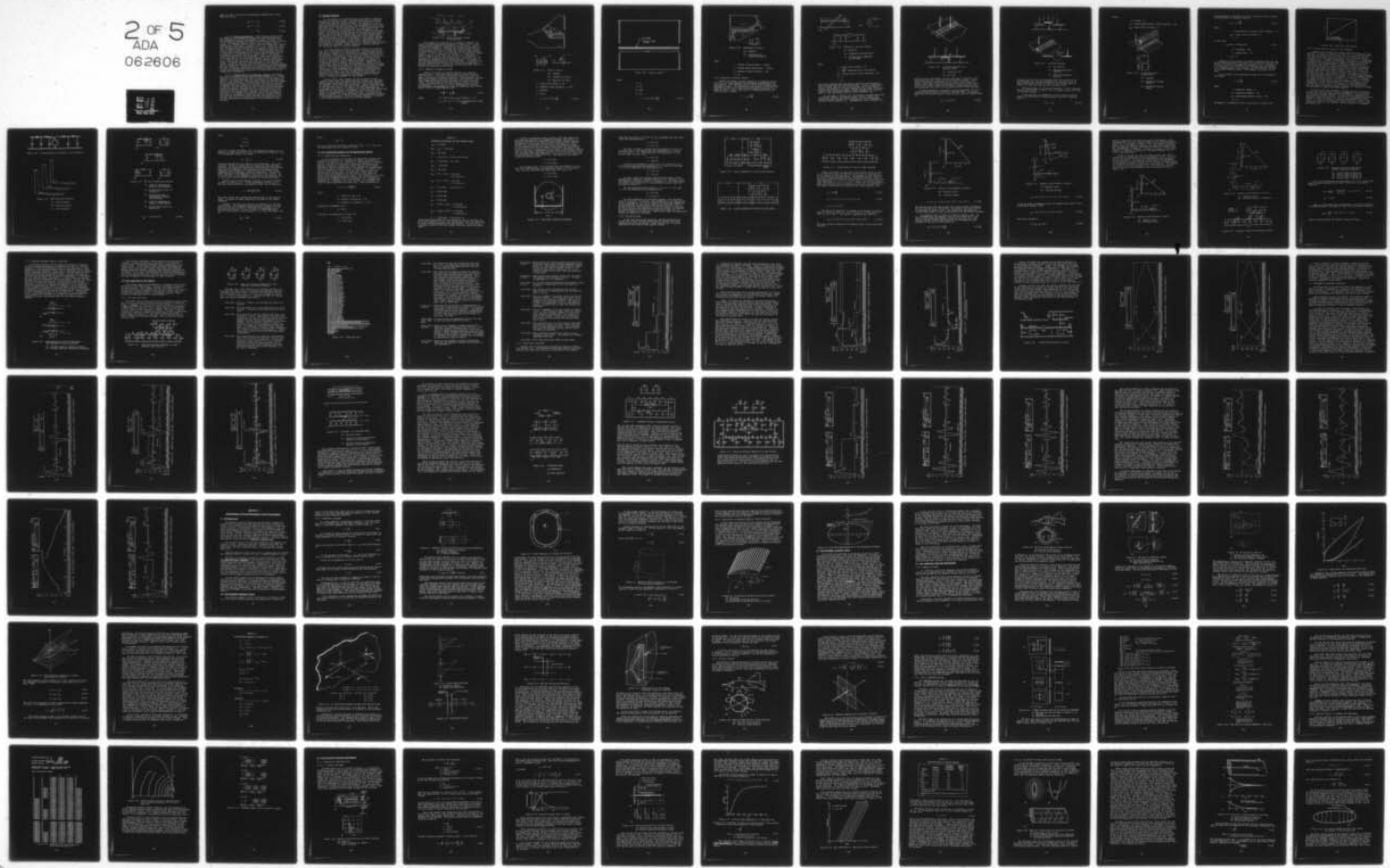
UNCLASSIFIED

SRD-78-044

AFFDL-TR-78-106

NL

2 OF 5
ADA
062606



There is thus a one-to-one correspondence between the L and F matrices, and so

$$L_{s1} - M = F_{11} \quad (3.108)$$

$$L_{s2} - M = F_{22} \quad (3.109)$$

$$M = F_{12} \quad (3.110)$$

3.3.3.3 Aids to Calculation. There does not appear to be any simple way to present on a graph the relationship between the component values of the equivalent circuit of Figure 3.15b and the physical geometry of typical conductors as given in Figure 3.15a. The simplest approach seems to be to present several examples of calculations for typical conductor geometries. Several such examples are given in Figures 3.19 - 3.22. They will indicate the approximate magnitude of the component values with which one is likely to work. In general, it should be noted that the line-to-ground capacitance C_{1g} and C_{2g} of the equivalent circuit is less than that calculated for the line-ground capacitance of a conductor by itself, less by an amount equal to the mutual capacitance between the two conductors. That mutual capacitance is not the same as the capacitance between the two conductors of a conductor pair; it is of the order of one-half that capacitance. The series inductance for each side of the equivalent circuit is greater than the self-inductance of the conductor by itself, greater by an amount equal to the mutual inductance between the two. Naturally, the greater the spacing between the conductors, the less the mutual capacitance and the mutual inductance, and the closer the inductance and capacitance values become to those of conductors by themselves.

3.3.3.4 Formulation of an Equivalent Circuit. The formulation of an equivalent circuit for multiple conductors is a simple extension of the formulation shown in Figure 3.14 for single conductors. One would calculate the capacitance and inductance per meter of the conductors, multiply those values by the total length of the conductor involved, and then split the line into as many elementary sections necessary to achieve the desired accuracy. In general, one can say that the more sections of the equivalent circuit the better, recognizing that, as the complexity of the equivalent circuit increases, the time required to solve that circuit on the computer will increase. It is best to keep in mind that in a lightning interaction problem the magnitudes of the electric and magnetic fields internal and external to the aircraft are likely to be known with much less precision than are the inductances and capacitances of the conductors under analysis.

3.4 DRIVING SOURCES

In an aircraft, the conductors will be exposed to changing electric and magnetic fields. The amplitudes will be different in different portions of the aircraft. The fields will be of complex waveshape and generally unlike the waveshape of the current passing through the aircraft. The waveshape, as well as the amplitude, will in general be different in the different portions of the aircraft. In all probability, the waveshapes of the electric and magnetic fields will be greatly different from each other. The fact that the waveshapes of the electric and magnetic fields will be different, implies that the fields impinging upon the conductor will not be simple plane wave fields whose amplitudes are related by the 377Ω impedance of free space; and also implies that the directions of the electric and magnetic fields will not be at right angles to each other. Those fields will be different, too, depending upon where the lightning flash contacts and leaves the aircraft. Those fields will also be different for different types of lightning flashes.

It is this author's belief that those fields will never be able to be calculated with any precision. The best that one is ever able to achieve is a calculation giving the average electric and magnetic fields likely to be found in different portions of the aircraft - for each an average over the volume of the portion of the aircraft under study. The magnitudes of those average electric and magnetic fields might be expressed in terms of a severe or worst-case type of lightning flash. Accordingly, it is suggested that an aircraft be divided into a number of different zones, each zone being distinguished by the type of shielding that the physical structure of the aircraft provides in those zones. It is also suggested that a series of ruling electric and magnetic field amplitudes and waveshapes be determined for each of those zones. The task of describing those zones, or determining the amplitudes and waveshapes of the electric and magnetic fields to be considered as representative in those zones, is discussed elsewhere in this report.

At this point, then, assume that the aircraft in which a conductor under study is located has been divided into the appropriate types of zones and that in each zone the ruling electric and magnetic fields have been determined. Figure 3.20 shows such an aircraft with the ruling electric and magnetic fields for each of the particular zones. In Figure 3.20, the waveshapes and amplitudes of the electric and magnetic fields have been arbitrarily chosen for the purposes of illustration, but the values are at least not unrealistic for an actual aircraft. The figure also shows a conductor, or conductor bundle, running between two pieces of electronic apparatus. In Zone C another conductor is coupled to the conductor running fore to aft in the aircraft.

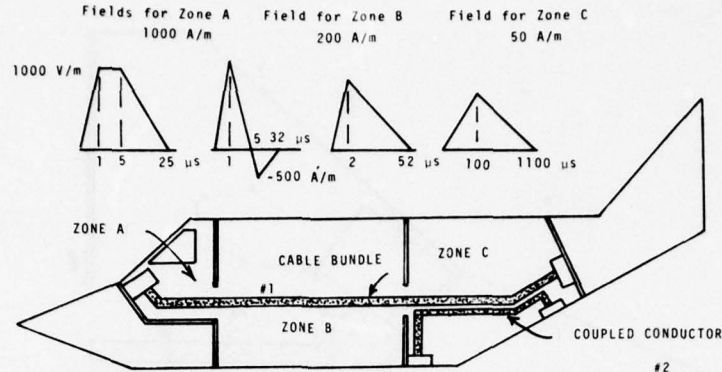


Figure 3.20 Zones and Ruling Fields in an Aircraft

For purposes of illustration, the length, diameter, and height of these conductors are shown in Figures 3.21 - 3.23. This conductor might be considered to be the overall shield on a bundle of conductors. Although the figures do not show it, later on this report will consider how the equivalent circuit is represented if there is a conductor inside of this overall shield. In Figure 3.21, the first part of the conductor, designated as Run A, is assumed to be located in a cable tray, as shown in Figure 3.21b. The rest of the run is assumed to be 4 cm over a well-defined ground plane. In Figure 3.22, the conductor is assumed to be an average height of 6 cm above a well-defined ground plane for the entire zone. In Figure 3.23c, the two conductors are shown to be 4 cm and 5 cm above well-defined ground planes, at least for those places where the conductors run parallel to each other.

3.4.1 Response to Magnetic Fields

Figure 3.24a shows a conductor exposed to a changing magnetic field. That field will produce a voltage across an open circuit, or a current through the conductor if the conductor is shorted to ground at each end. The elementary voltage and current sources that this conductor would present to the other portions of the circuit are shown in Figure 3.24b and 3.24c. The magnitudes of the open circuit voltage are given on Equations 3.111, 3.112, or 3.113, depending upon whether the expression is presented in terms of elementary units, mixed metric units, or mixed English units.

$$e = \frac{d\phi}{dt} = \mu_0 A \frac{dH}{dt} \quad (3.111)$$

where

A = area of the loop involved — m^2

$$\mu_0 = 4\pi \times 10^{-7} \text{ — H/m (permeability of free space)}$$

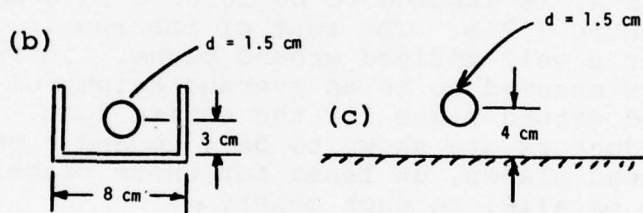
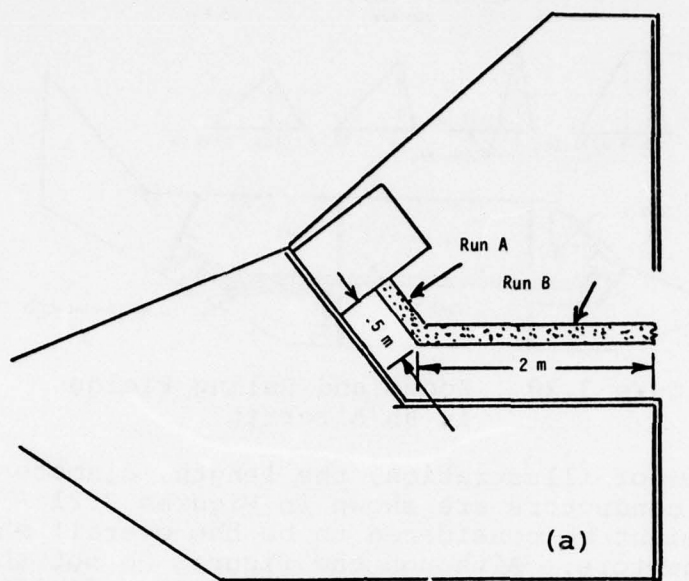


Figure 3.21 Cable in Zone A

(a) Lengths

(b) Position for Run A

(c) Position for Run B

ϕ = total flux linked — Wb

H = magnetic field intensity — A/m

t = seconds

e = volts

$$e = 1.26 \times 10^{-2} \ \ell h \frac{dH}{dt} \quad (3.112)$$

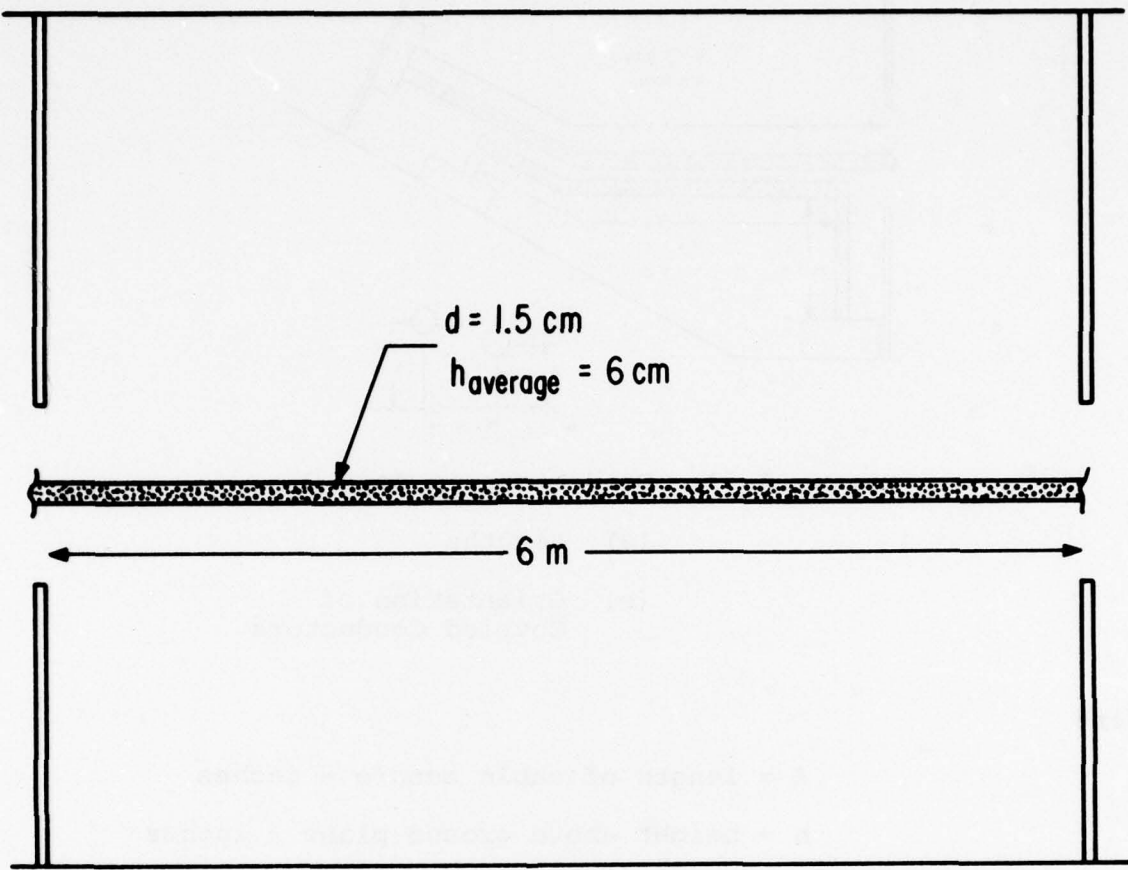


Figure 3.22 Cable in Zone B

where

$$l = \text{m}$$

$$h = \text{cm}$$

$$H = \text{A/m}$$

$$t = \mu\text{s}$$

$$e = 8.11 \times 10^{-4} l h \frac{dH}{dt} \quad (3.113)$$

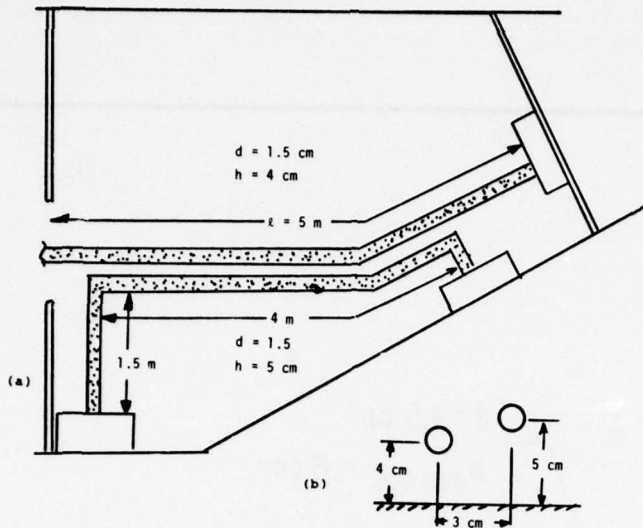


Figure 3.23 Conductors in Zone C

(a) Lengths

(b) Orientation of
Coupled Conductors

where

ℓ = length of cable bundle - inches

h = height above ground plane - inches

H = magnetic field intensity - A/m

t = μ s

3.4.2 Response to Electric Fields

Figure 3.25 shows a surface exposed to a changing electric field E_u , the field assumed to be oriented perpendicularly to this surface. That changing electric field will produce a displacement current. If a portion of that surface is isolated and connected to the rest of the surface through a conductor, as shown in Figure 3.35b, there will be intercepted by that isolated portion a current

$$i = \epsilon_0 A \frac{dE}{dt} \quad (3.114)$$

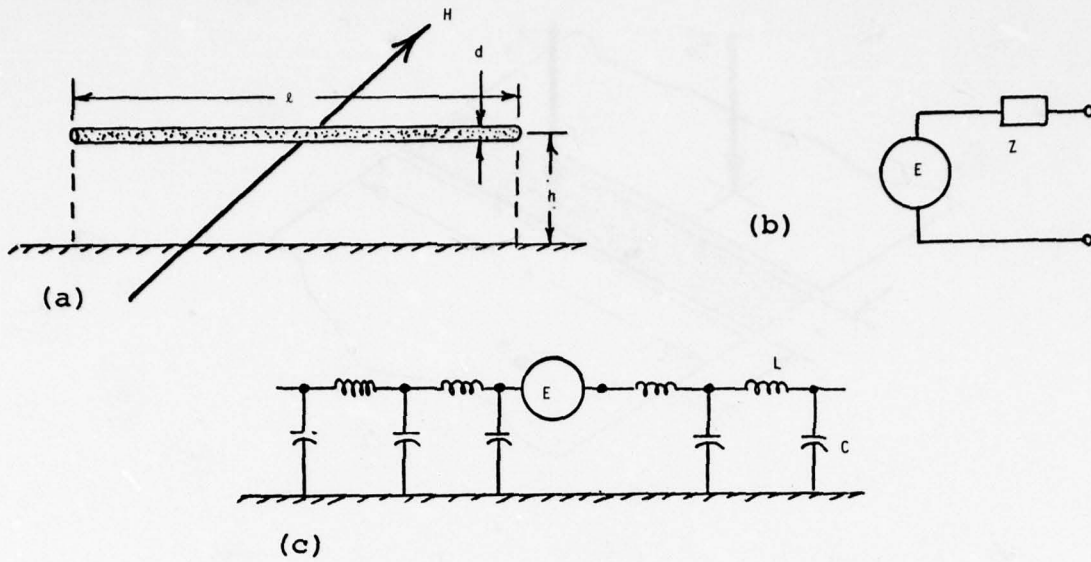


Figure 3.24 Response to Magnetic Fields

(a) Geometry

(b) Elementary Voltage Source

(c) Voltage Source Embedded
in the Model

where

$A = \text{area of the surface} - \text{m}^2$

$\epsilon_0 \approx \frac{10^{-9}}{36\pi} (\text{Permittivity of free space})$

$E_a = \text{actual electric field intensity} - \text{V/m}$

$t = \text{s}$

$i = A$

The current depends upon the actual intensity of the electric field incident upon the isolated section. If that isolated section is flush with the rest of the surface and if the spacing between the surfaces w is small compared to the width of the surfaces d , then the actual electric field intensity, E_a , will be equal to the undisturbed electric field intensity, E_u .

If, as shown in Figure 3.26, the surface is raised above the surrounding surface, the actual electric field intensity E_a acting upon that surface will be higher than the undisturbed electric field intensity, E_u . Consequently, such a surface will

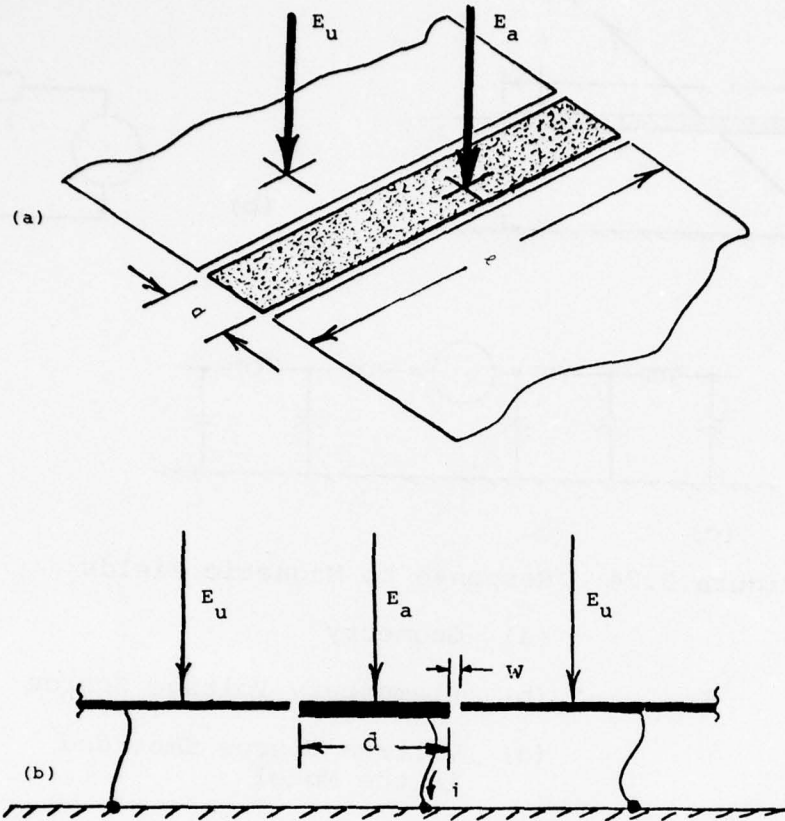


Figure 3.25 A Surface Exposed to an Electric Field

(a) Isometric View

(b) End View

intercept more displacement current than would a surface of the same projected area flush with the surrounding surface. Calculating the current intercepted by the raised flat surface of Figure 3.26a would require evaluating the electric field intensity at all points, either by cut-and-try field plotting or by field plotting with one of the available electric field programs.

A simple geometry to calculate is the hemicylinder (or half-exposed cylinder) shown in Figures 3.26b and 3.26c. It can be shown that the actual electric field incident upon the hemicylinder is

$$E_a = 2E_u \cos \phi \quad (3.115)$$

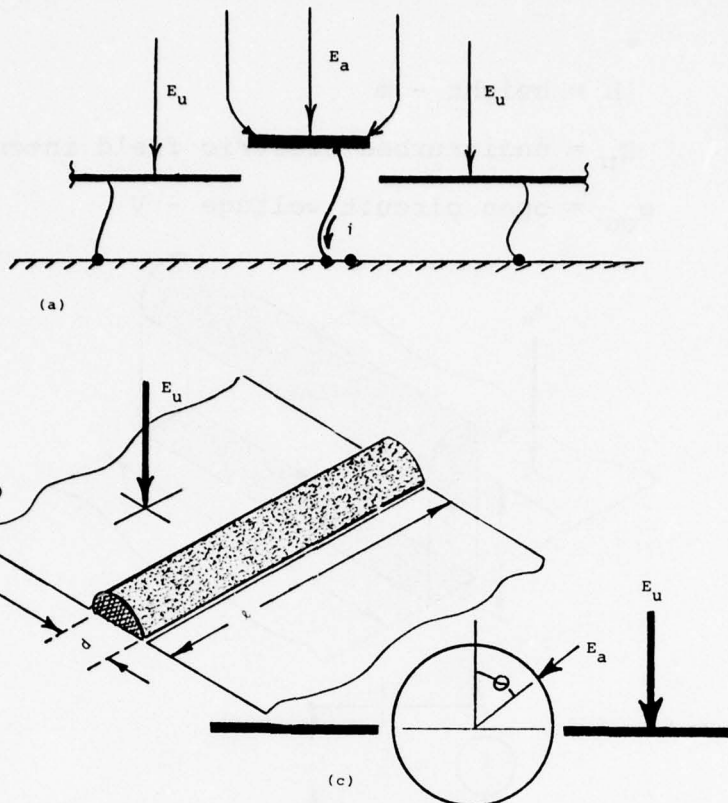


Figure 3.26 Elevated Surfaces

(a) Flat Surface

(b) Embedded Hemisphere -
Isometric

(c) Embedded Hemisphere -
End View

If this electric field is integrated over the surface of the hemicylinder, then the hemicylinder will intercept twice as much displacement current as does the flat surface shown in Figure 3.25 and will have the same projected area.

The hemicylinder is of interest because it is the limiting case as the cylinder in Figure 3.27 is brought closer and closer to the ground plane.

If the cylinder (or conductor) is well above the ground plane, the open circuit voltage produced upon that conductor will be

$$e_{oc} = hE_u \quad (3.116)$$

where

$$h = \text{height} - \text{m}$$

$$E_u = \text{undisturbed electric field intensity} - \text{V/m}$$

$$e_{oc} = \text{open circuit voltage} - \text{V}$$

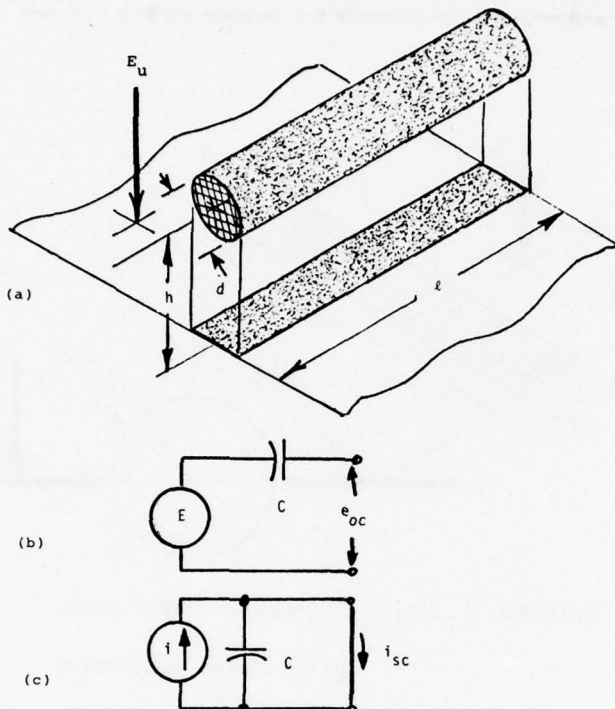


Figure 3.27 A Conductor Over a Ground Plane

(a) Geometry

(b) Elementary Voltage Source

(c) Elementary Current Source

If the conductor is shorted to ground, the short circuit current intercepted by the conductor will be

$$i_{sc} = hC \frac{dE_u}{dt} \quad (3.117)$$

where

C = capacitance to ground of the conductor - μF

i_{sc} = short circuit current - A

t = μs

In rms terms

$$i_{sc\text{-rms}} = 2\pi f h C E_{u\text{-rms}} \quad (3.118)$$

f = frequency - MHz

C = capacitance - μF

i_{sc} = A

Equations 3.116 through 3.118 seem to indicate that the conductor would intercept no current if its height were brought down to zero, a result at variance with Equation 3.114. Equations 3.116 through 3.118 are based on the premise that the conductor is an infinitesimally thin cylinder, one that does not disturb the incident electric field. This premise, of course, is not true.

For cylinders, the intercepted current can be expressed in the format

$$i = K l d \frac{dE_u}{dt} \quad (3.119)$$

where

l = conductor length - m

d = conductor diameter - cm

E_u = undisturbed electric field - V/m

t = μs

and where K, a function of h/d , is as given in Figure 3.28.

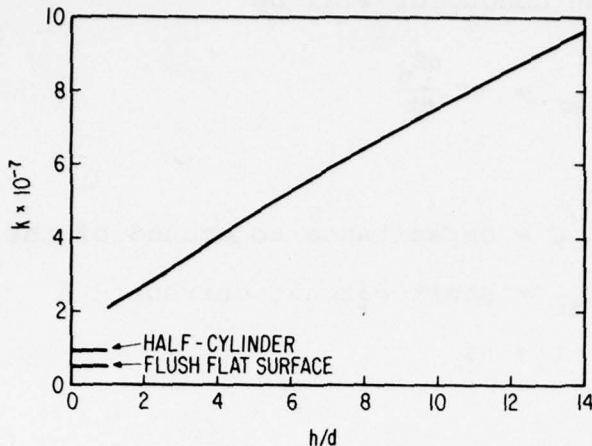


Figure 3.28 Conductor Height Factor

3.4.3 Connecting the Sources to the LPM Model

Inserting the voltage and current sources directly into the LPM model as shown in Figures 3.24 and 3.29 is a perfectly acceptable way of treating those sources, but this insertion suffers from one defect that is more a limitation of the ECAP computer program than of the models themselves. The problem is illustrated in Figure 3.30. In ECAP, time-dependent sources can be described by specifying the amplitude at a number of equally spaced time intervals. The maximum number of intervals permitted is 40. The voltage and current sources described so far use the derivatives of the internal electric and magnetic fields, waveshapes that are inherently more complex than is the field itself. To specify those waveforms with an equally spaced set of intervals becomes difficult. For example, Figure 3.30a shows a typical derivative of an assumed electric field. The ECAP program assumes the time-dependent source to be composed of linear segments between the times at which the wave is sampled. If the wave is sampled at widely separated points, (Figure 3.30b), in order to minimize the amount of input data needed, the sampled waveform is a poor construction of the original waveform. If it is sampled more frequently, (Figure 3.30c), the waveform is described better, but the number of sampling points increases and frequently exceeds the available 40 points that ECAP provides.

A way to avoid that problem is through the use of auxiliary circuits and the provision in ECAP for dependent current sources, current sources where amplitude and waveshape are controlled by the current in another branch. In place of the independent voltage generator shown in Figure 3.24, one can use a dependent current source, T , connected across a resistor, as shown in Figure 3.31a. If E_a , in volts, in the auxiliary circuit of Figure 3.31b is made numerically equal to the magnetic field intensity H , in amperes per meter, and

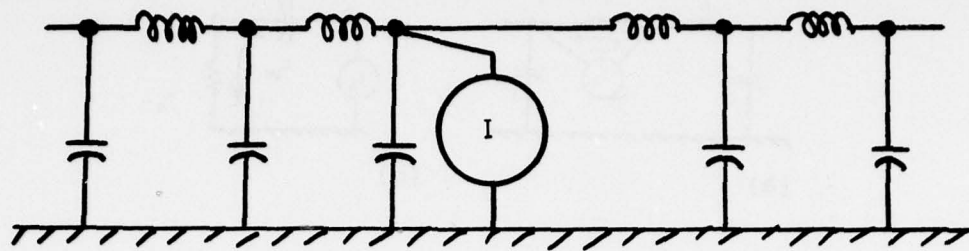


Figure 3.29 A Current Source Connected to the LPM Model

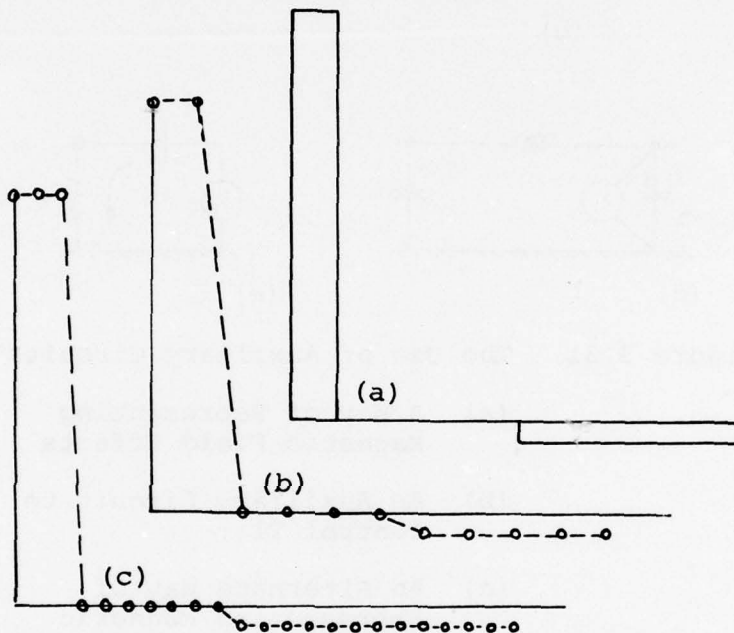


Figure 3.30 Specifying the Waveform

- (a) Basic Waveform
- (b) Coarsely Sampled
- (c) Finer Sampling

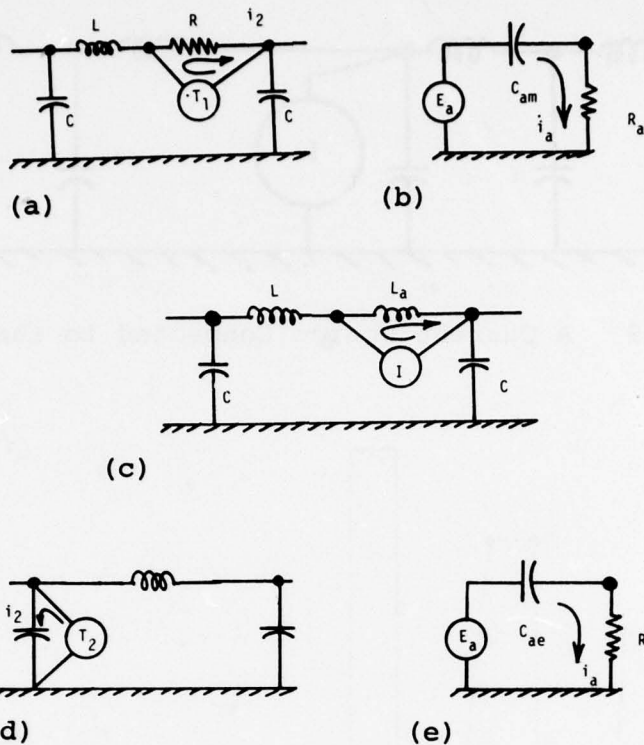


Figure 3.31 The Use of Auxiliary Circuits

- (a) A Way of Representing Magnetic Field Effects
- (b) An Auxiliary Circuit to Control T1
- (c) An Alternate Way of Representing Magnetic Field Effects
- (d) A Way of Representing Electric Field Effects
- (e) An Auxiliary Circuit to Control T2

$$C_{am} = 1.26 \times 10^{-2} \text{ } \mu\text{H} \quad (3.120)$$

where

$$l = m$$

$$h = cm$$

$$C_{am} = \mu F$$

and if R_a is made very small, then the auxiliary current, i_a , in amperes, is numerically equal to e , as predicted by Equation 3.112. If the dependent current i_2 is made

$$i_2 = \frac{1}{R_a} i_a \quad (3.121)$$

then that voltage will be inserted in the LPM Model. R_a in the auxiliary circuit is needed only to satisfy the required ECAP topology. R_a should be sufficiently small that the time constant $R_a C_a$ is small compared to the duration of the magnetic field. Frequently, the resistor R in the LPM model can be one of the resistors used to represent conductor resistance. R should be small compared to the impedance of the rest of the circuit. If it is not, part of the dependent current will flow into the rest of the circuit and the correct voltage will not be developed.

Another way that the problem in Figure 3.30 can be avoided is shown in Figure 3.31c. If the independent current, I , is made the same waveshape as the magnetic field, and of amplitude

$$I = \frac{1.26 \times 10^{-2} l h H}{L} \quad (3.122)$$

then that current will produce the same voltage as the magnetic field. L_a should be small compared to the rest of the circuit impedance.

Figures 3.31d and 3.31e show how to represent the electric field effects. The dependent current source T injects into the circuit a current i_2 equal in amplitude and waveshape to i_a in the auxiliary circuit. If E_a , in volts, is made numerically equal to the electric field intensity, E , in volts per meter, and if

$$C_{ae} = k l d \quad (3.123)$$

where

$$C_{ae} = \mu F$$

the i_2 will be as called for in Equation 3.119. K , ℓ , and d are the same quantities as in Equation 3.119.

3.5 AN ILLUSTRATED EXAMPLE OF AN EQUIVALENT CIRCUIT

3.5.1 Inductance and Capacitance

It is now possible to evaluate the equivalent circuits and equivalent sources for the illustrative sample illustrated in Figures 3.20 through 3.23. Normally, in an analysis of lightning effects, one must, of necessity, assume that the electric and magnetic fields are uniform over large sections of the cable. Sometimes a physical examination of the system will indicate that this is too gross a simplification to tolerate. In Figure 3.21 there is shown such a case. Run A of the cable in Zone A is assumed to be in some sort of a cable tray. That cable tray will provide some shielding for the cable and will have an effect upon the impedance of the cable. The conductor in the tray will have an impedance somewhere between that of a concentric geometry and a conductor over a flat plane. As it happens, the impedance of a conductor in a tray like this is a geometry for which an exact expression has been given. That expression is

$$Z = 60 \ln \frac{4 W \tanh \pi h}{\pi d} \quad (3.124)$$

where

W = width of tray, 8 cm

h = height of conductor, 3 cm

d = diameter of conductor, 1.5 cm

predicts the impedance to be

$$Z = 103 \Omega$$

from which, by Equations 3.53 and 3.56

$$C = 32.2 \text{ pF/m}$$

$$L = 0.345 \mu H/m$$

TABLE 3.1
IMPEDANCE PARAMETERS FOR THE COUPLED LINES

$$B_{11} = 42.6 \text{ m/nF}$$

$$B_{12} = B_{21} = 19.78 \text{ m/nF}$$

$$B_{22} = 46.6 \text{ m/nF}$$

$$D = 42.6 \times 46.6 - 19.78 \times 19.78 = 1593.9$$

$$K_{11} = 0.0292 \text{ nF/m} = 29.2 \text{ pF/m}$$

$$K_{12} = -12.41 \text{ pF/m}$$

$$K_{22} = 26.7 \text{ pF/m}$$

$$C_{1g} = 29.2 - 12.41 = 16.8 \text{ pF/m}$$

$$= 67.2 \text{ pF for 4 m}$$

$$C_{2g} = 26.7 - 12.41 = 14.3 \text{ pF/m}$$

$$= 57.2 \text{ pF for 4 m}$$

$$C_{12} = 12.41 \text{ pF/m} = 49.6 \text{ pF for 4 m}$$

$$F_{11} = 0.4734 \mu\text{H/m}$$

$$F_{12} = 0.2197 \mu\text{H/m}$$

$$F_{22} = 0.5181 \mu\text{H/m}$$

$$L_{S1} = 0.4737 + 0.2197 = 0.693 \mu\text{H/m}$$

$$= 2.77 \mu\text{H for 4 m}$$

$$L_{S2} = 0.5181 + 0.2197 = 0.783 \mu\text{H/m}$$

$$= 2.95 \mu\text{H for 4 m}$$

$$M = 0.2197 \mu\text{H/m} = 0.879 \mu\text{H for 4 m}$$

(Calculations were made with the values K_{11} and K_{22} reversed, an error that resulted in $C_{1g} = 14.3 \text{ pF}$ and $C_{2g} = 16.8 \text{ pF}$. This type of error carried through all the calculations. Its effects on calculated results is not very large, since the values are nearly equal.)

If such an expression were not known, one could reason that the conductor should have an impedance somewhat like that of a conductor enclosed in a concentric return path, coaxial geometry. The spacing to the return path could be evaluated with a bit of insight into the patterns of the electric and magnetic fields. One can reason that the relatively close spacing of the conductor to the bottom of the tray is offset by the fact that there is no cover on the tray. Accordingly, if one makes a calculation assuming that the equivalent concentric geometry is as shown in Figure 3.32, one calculates the surge impedance Z as 100.5Ω , a value very close to that predicted by Equation 3.123. The inductance and capacitance then turn out to be

$$C = 33.2 \text{ pF/m}$$

$$L = 0.335 \mu\text{H/m}$$

On the other hand, if one assumes that the geometry is like that of a conductor over a ground plane, where $d = 1.5 \text{ cm}$ and $h = 3 \text{ cm}$, then the inductance and capacitance turn out to be

$$C = 26.9 \text{ pF/m}$$

$$L = 0.413 \mu\text{H/m}$$

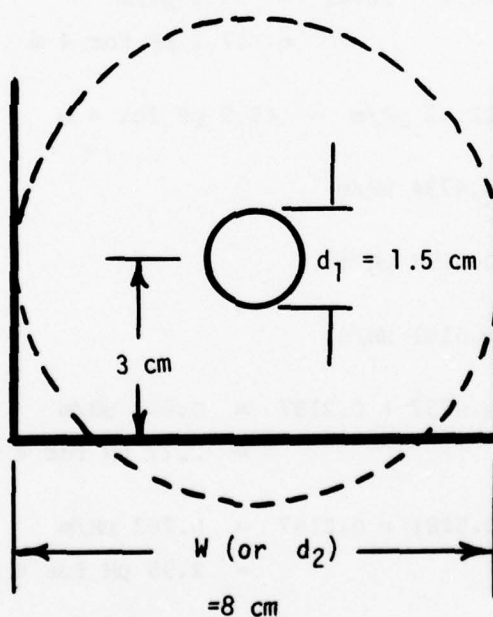


Figure 3.32 Equivalent Concentric Geometry

Since Run A is only 0.5 m long, it can be assumed that the inductance and capacitance are

$$C = 16.8 \text{ pF}$$

$$L = 0.17 \mu\text{H}$$

For Run B in Zone A, assume that the geometry is that of a conductor over a flat ground plan with dimensions $d = 1.5 \text{ cm}$, $h = 4 \text{ cm}$ and $l = 2 \text{ m}$. The inductance and capacitance of this section then turn out to be

$$C = 47.2 \text{ pF}$$

$$L = 0.49 \mu\text{H}$$

In Zone B the geometry is again that of a conductor over a flat ground plane and with dimensions $d = 1.5 \text{ cm}$, $h = 6 \text{ cm}$, and $l = 6 \text{ m}$, the inductance and capacitance are

$$C = 120.5 \text{ pF}$$

$$L = 3.32 \mu\text{H}$$

In Zone C there are coupled conductors with which to deal. Designate the conductor extending fore to aft as Conductor 1 and the conductor entirely in Zone C as Conductor 2. The calculations that define the parameters of the equivalent circuit, then, are as shown on Table 3.1.

For the uncoupled section where $d = 1.5 \text{ cm}$, $l = 4 \text{ cm}$, and $l = 1 \text{ m}$, the capacitance and inductance are

$$C = 23.6 \text{ pF}$$

$$L = 0.472 \mu\text{H}$$

If those impedances are connected together, the equivalent circuit of Figure 3.33 results. The impedances at the ends of the line, Z_1 through Z_4 , are for the moment just arbitrary impedances. If the impedances of the larger lumps are divided into two Pi sections and the capacitances of all sections placed at the ends of the Pi section, the equivalent circuit of Figure 3.34 develops. The capacitances at the ends of the individual lumps can, of course, be connected in parallel. When this is done, the equivalent circuit of Figure 3.35 develops.

3.5.2 Driving Sources

In the next step of the analysis, one must determine the voltage and current sources acting upon the network and place those sources into the network. These sources are, of course, functions of the electric and magnetic fields.

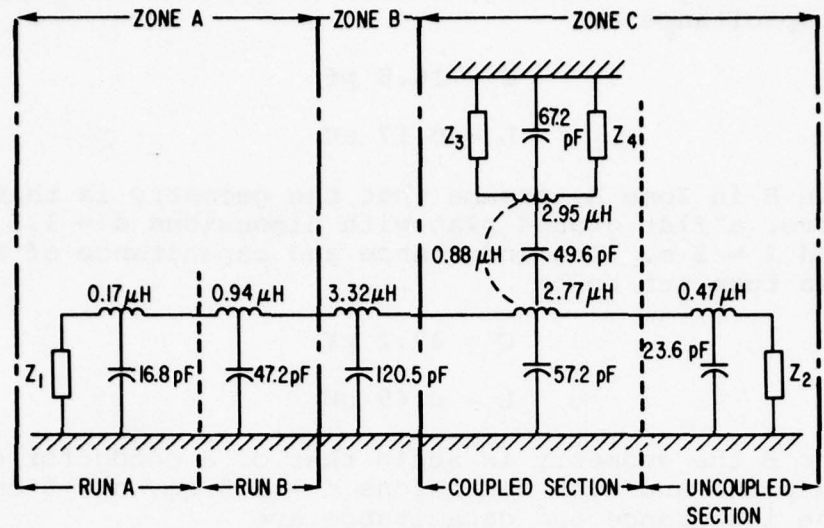


Figure 3.33 Total Impedances in the Various Sections

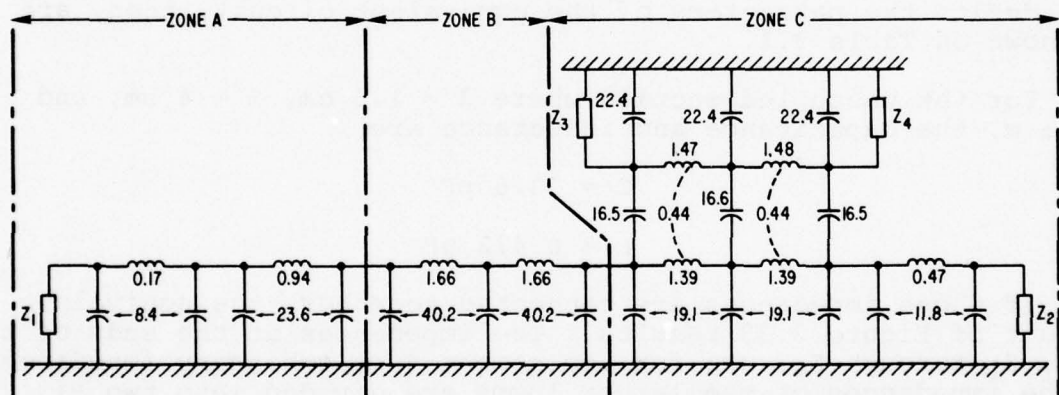


Figure 3.34 Larger Impedances Divided Into Two Lumps

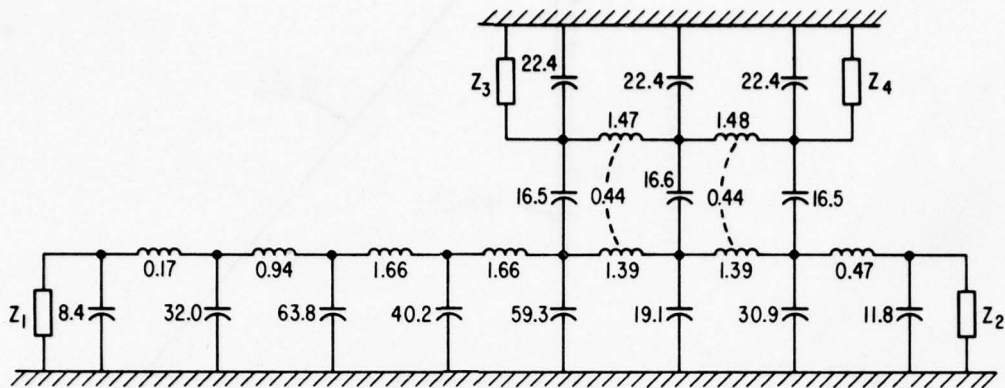


Figure 3.35 Capacitances at Ends of Lumps Combined

Figure 3.36 shows in more detail the electric field in Zone A. In the cable tray, the electric field will be less than the ruling electric field for Zone A. For purposes of this analysis, it is arbitrarily assumed that the undisturbed electric field in the tray is one-half of the electric field in the rest of the zone, with dimensions $\ell = 0.5 \text{ m}$, $d = 1.5 \text{ cm}$, and $h = 3 \text{ cm}$ from Figure 3.28, where $h/d = 2$, $K = 2.7 \times 10^{-7}$. During the first microsecond, where the electric field is changing at the rate of $1000 \text{ V/m} \cdot \mu\text{s}$, the current induced by this field will be, from Equation 3.119

$$i_A = Kld \frac{dE_u}{dt} \quad (3.125)$$

$$i_A = 2.7 \times 10^{-7} \times 0.5 \times 1.5 \times 1/2 \times 10^3 \quad (3.126)$$

$$i_A = 1.013 \times 10^{-4} \text{ A}$$

For Run B the conductor is assumed to be exposed to the full electric field E_u , with $\ell = 2 \text{ m}$, $d = 1.5 \text{ cm}$, $h = 4 \text{ cm}$ and $h/d = 2.67$, $K = 3.1 \times 10^{-7}$. The current induced by the field is

$$i_B = 3.1 \times 10^{-7} \times 2 \times 1.5 \times 10^3 = 9.30 \times 10^{-4} \text{ A} \quad (3.127)$$

The total current induced by the electric field is the sum of the currents:

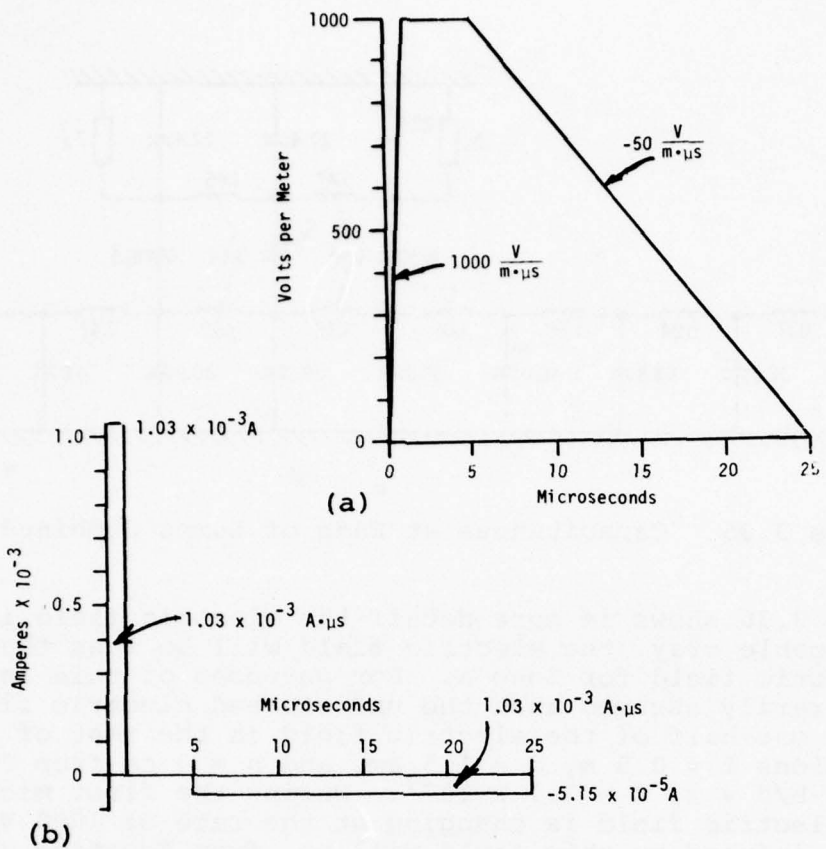


Figure 3.36 Electric Field Effects in Zone A

(a) Electric Field

(b) Injected Current

$$i = i_A + i_B = (1.013 \times 9.30) \times 10^{-4} = 1.03 \times 10^{-3} \text{ A} \quad (3.128)$$

The current during the period when the electric field is decaying will be less but will last longer. The shape of the total current is indicated in Figure 3.36b. The figure also indicates the current-time product of the various portions of the current waveform.

The magnetic field in Zone A is shown in Figure 3.37a. If it is assumed that the magnetic field in the cable tray is one-half of the undisturbed magnetic field for the zone, then the voltage induced in Run A by the portion of the magnetic field changing at the rate of $1000 \text{ A}/\mu\text{s}$ is

$$e_A = 1.26 \times 10^{-2} \text{ } \text{m} \frac{dH}{dt} \quad (3.129)$$

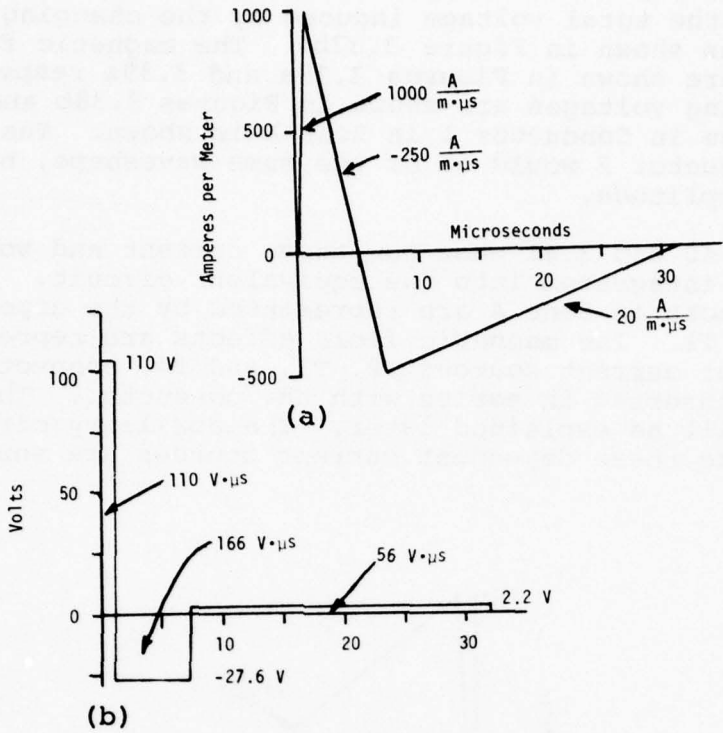


Figure 3.37 Magnetic Field Effects in Zone A

(a) Magnetic Field

(b) Injected Voltage

$$e_A = 1.26 \times 10^{-2} \times 0.5 \times 3 \times 1/2 \times 10^3 = 9.45 \text{ V} \quad (3.130)$$

In Run B, where the magnetic field is assumed to be equal to the undisturbed magnetic field

$$e_B = 1.26 \times 10^{-2} \times 2 \times 4 \times 10^3 = 100.8 \text{ V} \quad (3.131)$$

The total voltage is

$$e = e_A + e_B = 110 \text{ V} \quad (3.132)$$

Similar analysis for the other portions of the magnetic field indicates that the total voltage induced by the changing magnetic field will be as shown in Figure 3.37b. The magnetic fields in Zones B and C are shown in Figures 3.38a and 3.39a respectively. The corresponding voltages are shown in Figures 3.38b and 3.39b. Only the voltage in Conductor 1 in Zone A is shown. The voltage induced in Conductor 2 would be of the same waveshape, but of 0.101 V peak amplitude.

Figures 3.40 and 3.41 show how these current and voltage sources can be integrated into the equivalent circuit. The electric field effects in Zone A are represented by the dependent current source T1. The magnetic field effects are represented by the dependent current sources T2, T3, and T4, connected across 1Ω resistors inserted in series with the conductor. The purpose of T5 and T6 will be explained later. The auxiliary circuits used to energize these dependent current sources are shown in Figure 3.41.

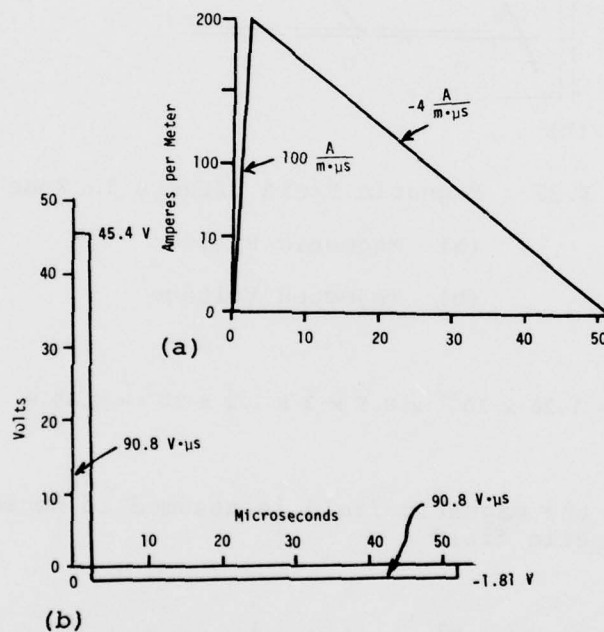


Figure 3.38 Magnetic Field Effects in Zone B

- (a) Magnetic Field
- (b) Injected Voltage

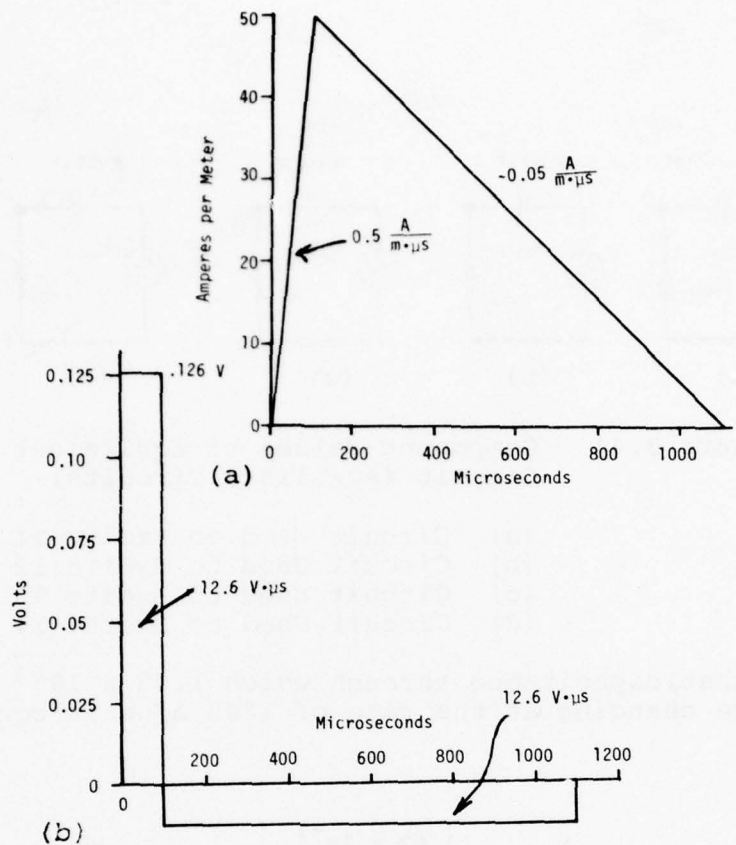


Figure 3.39 Magnetic Field Effects in Zone C

(a) Magnetic Field
 (b) Injected Voltage - Conductor 1

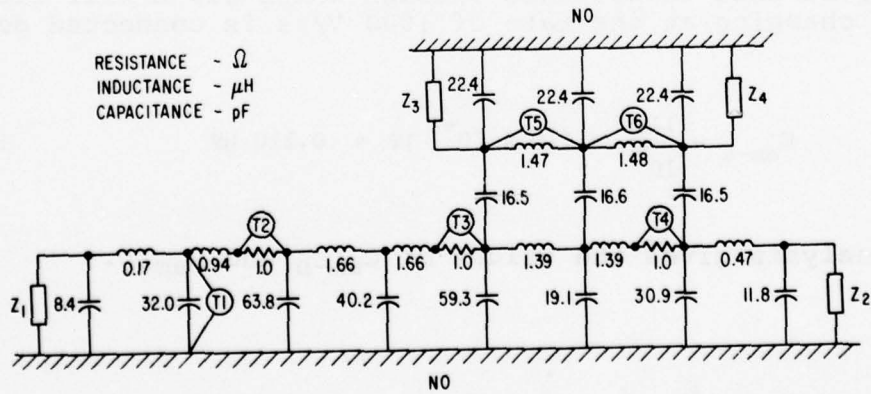


Figure 3.40 Component Values of Equivalent Circuit

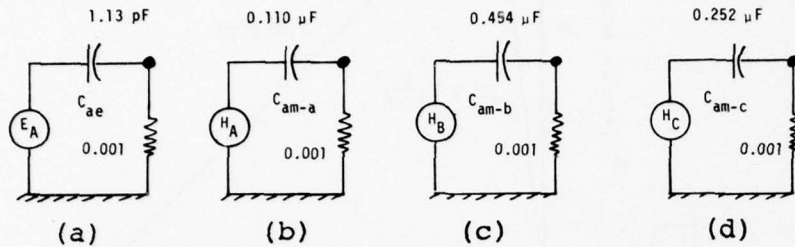


Figure 3.41 Component Values of Equivalent Circuit (Auxiliary Circuits)

- (a) Circuit Used to Excite T1
- (b) Circuit Used to Excite T2
- (c) Circuit Used to Excite T3
- (d) Circuit Used to Excite T4

C_{ae} is that capacitance through which 1.03×10^{-3} A will flow when a voltage changing at the rate of $1000 \text{ A}/\mu\text{s}$ is connected across it.

$$C_{ae} = \frac{i}{dE/dt} = \frac{1.03 \times 10^{-3}}{10^3 \text{ V}/\mu\text{s}} = 1.03 \times 10^{-6} \mu\text{F} \quad (3.133)$$

$$C_{ae} = 1.03 \text{ pF} \quad (3.134)$$

C_{am-a} is that capacitance through which 110 A will flow when a voltage changing at the rate of $1000 \text{ V}/\mu\text{s}$ is connected across it.

$$C_{am-a} = \frac{110}{10^3} = 110 \times 10^{-3} \mu\text{F} = 0.110 \mu\text{F} \quad (3.135)$$

Similar analysis gives the values of C_{am-b} and C_{am-c} .

3.5.3 Problems Regarding Mutual Inductance

T5 and T6 in Figure 3.40 are used to represent the effects of mutual inductance between the conductors in Zone C. ECAP can operate in either the frequency domain or the time domain. When operating in the frequency domain, mutual inductance can be represented; but when operating in the time or transient analysis domain, mutual inductance cannot be represented. The limitation on the simulation of mutual inductance is rather serious, and some artifice for getting around the limitation is necessary. In principle, one can simulate mutual inductance in a network solution program through the use of dependent current generators. Figure 3.42 shows how such generators may be used. Figure 3.42a shows one-way coupling, in this case coupling from Conductor 1 into Conductor 2. This form of coupling is generally adequate if the circuits are loosely coupled with the current in Conductor 2 being dependent on the current in Conductor 1; whereas, the current in Conductor 1 is primarily controlled by outside elements and not really capable of being influenced by the current in Conductor 2. Frequently, this is a realistic assumption. Simulation of one-way coupling in this manner has the major virtue that it seems to yield numerically stable results when used in this circuit solution program.

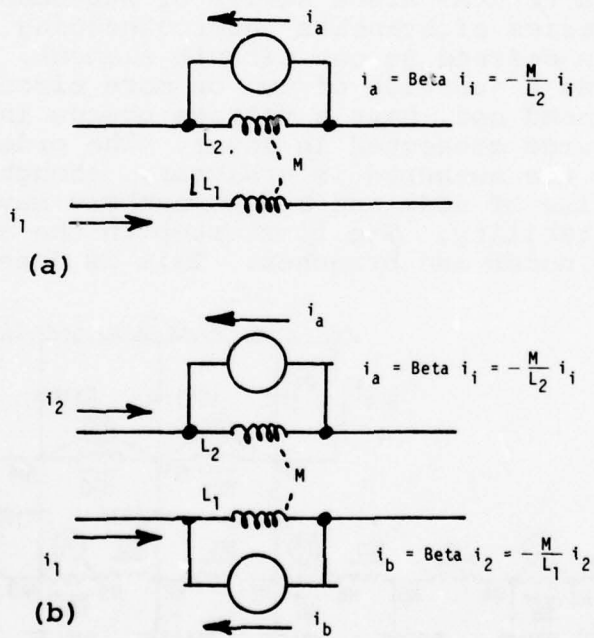


Figure 3.42 Representation of Mutual Inductance with Dependent Current Generators

- (a) One-Way Coupling (Generally Stable)
- (b) Two-Way Coupling (Potentially Unstable)

Since mutual inductance causes coupling both ways between circuits, it would be better, in principle, to use two-way coupling with two separate dependent current generators, as in Figure 3.42b. In the cases to date where this procedure has been tried in circuit calculations using ECAP, only unstable answers have been yielded. Whether these unstable solutions are characteristic of cross-coupled dependent current generators is not known. At any rate, the numerical instabilities encountered so far have been sufficiently serious that only one-way coupling has been attempted in the analysis of these circuits.

3.6 ECAP ANALYSIS OF THE CIRCUIT

This report cannot be considered as a complete course in the operation of the ECAP Program. For that the reader is referred to the literature. This report, however, will show how this particular circuit was analyzed with the aid of ECAP. The version of ECAP used is that resident in the General Electric Mark III Information Processing System, a time-sharing system. Other versions of ECAP may differ in some respects.

3.6.1 The ECAP Data File

The input data to ECAP are a series of statements which define the circuit as a series of branches interconnecting a series of nodes. A branch is defined as one circuit element, R, L, C, or M. A node is defined as a junction of two or more circuit elements. A branch may, but need not, have a voltage source in series with it or a current source connected in shunt. The order in which branches and nodes are numbered is arbitrary, though in some cases a particular ordering of node and branch numbers may result in better numerical stability. The first step in the analysis is thus to number the nodes and branches. This is done in Figures 3.43 and 3.44.

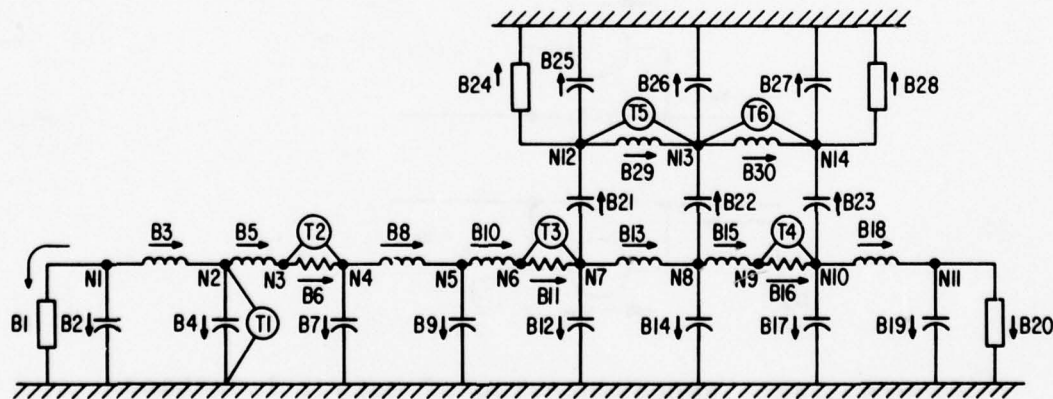


Figure 3.43 Nodes and Branches Numbered for ECAP Analysis (Main Circuit)

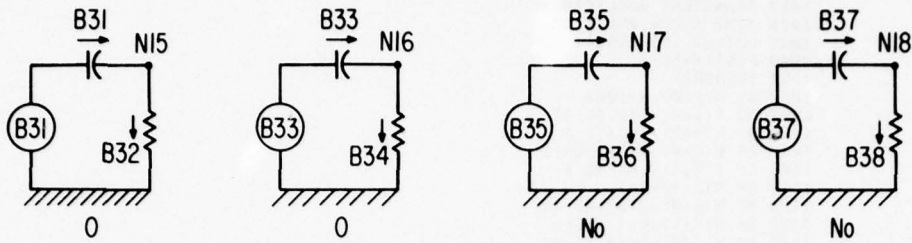


Figure 3.44 Nodes and Branches Numbered for ECAP Analysis (Auxiliary Circuits)

The next step in the analysis is to prepare the data file that describes the circuit and supplies the commands necessary to operate the ECAP Program. The data file describing the circuit in Figures 3.40, 3.41, 3.42, and 3.44 is shown in Figure 3.45. It will be described on a line-by-line basis to indicate what the various statements mean and do.

Line 1000 - This is a comment line and does not affect the program.

Line 1010 - This specifies that a time domain solution is to be made. Frequency and dc solutions can also be done.

Line 1020 - This specifies that the transient solution is to be done in a step-by-step manner with each time step being 0.05 μ s. The time step should be small compared to the natural time constants of the system. Barring previous knowledge of the system response, one is forced to make an arbitrary guess as to what is a satisfactorily small time step. If subsequent calculations with smaller time steps give similar results, then, presumably, the original time step was satisfactory. Experience with circuits and circuit solutions helps considerably.

Line 1030 - This specifies that the results of calculations are to be printed after each time step calculation, i.e., at 0.05 μ s intervals. If the line had read "output interval = 5", then the data would still have been calculated at 0.05 μ s intervals, but the circuit response would have been printed after every fifth interval, i.e., at 0.25 μ s intervals.

READY
LIST

AFFILE 13:11EDT 10/18/77

1000 C CABLE RUNNING BETWEEN ZONES A AND C
1010 TRANSIENT ANALYSIS
1020 TIME STEP=.05E-6
1030 OUTPUT INTERVAL=1
1040 FINISH=5E-6
1050 IERROR=1
1060 B1 N(1,0),R=1000
1070 B2 N(1,0),C=8.4E-12
1080 B3 N(1,2),L=.17E-6
1090 B4 N(2,0),C=32.0E-12
1100 B5 N(2,3),L=.94E-6
1110 B6 N(3,4),R=1
1120 B7 N(4,0),C=63.8E-12
1130 B8 N(4,5),L=1.66E-6
1140 B9 N(5,0),C=40.2E-12
1150 B10 N(5,6),L=1.66E-6
1160 B11 N(6,7),R=1
1170 B12 N(7,0),C=59.3E-12
1180 B13 N(7,8),L=1.39E-6
1190 B14 N(8,0),C=19.1E-12
1200 B15 N(8,9),L=1.39E-6
1210 B16 N(9,10),R=1
1220 B17 N(10,0),C=30.9E-12
1230 B18 N(10,11),L=.47E-6
1240 B19 N(11,0),C=11.8E-12
1250 B20 N(11,0),R=1000
1260 B21 N(7,12),C=16.5E-12
1270 B22 N(8,13),C=16.4E-12
1280 B23 N(10,14),C=16.5E-12
1290 B24 N(12,0),R=1000
1300 B25 N(12,0),C=22.4E-12
1310 B26 N(13,0),C=22.4E-12
1320 B27 N(14,0),C=22.4E-12
1330 B28 N(14,0),R=1000
1340 B29 N(12,13),L=1.47E-6
1350 B30 N(13,14),L=1.48E-6
1360 B31 N(0,15),C=1.13E-12
1370 B32 N(15,0),R=.001
1380 B33 N(0,16),C=.110E-6
1390 B34 N(16,0),R=.001
1400 B35 N(0,17),C=.454E-6
1410 B36 N(17,0),R=.001
1420 B37 N(0,18),C=.252E-6
1430 B38 N(18,0),R=.001
1440 T1 B(32,4),BETA=1.0
1450 T2 B(34,6),BETA=1.0
1460 T3 B(36,11),BETA=1.0
1470 T4 B(38,16),BETA=1.0
1480 T5 B(13,29),BETA=.299
1490 T6 B(16,30),BETA=.299
1500 E31(20),0,1000,1000,1000,1000,950,900,850,800,750,700,650,
1510 +600,550,500,450,400,350,300,250,200,150,100,50,0
1530 E33(20),0,1000,750,500,250,0,-250,-500,-400,-460,-440,-420,-400,
1540 -380,-360,-340,-320,-300,-280,-260,-240,-220,-200,-180,-160,-140,
1550 -120,-100,-80,-60,-40,-20,0
1560 E35(40),0,200,192,184,176,168,160,152,144,136,128,120,112,104,
1570 +96,88,80,72,64,56,48,40,32,24,16,8,0
1590 E37(2000),0,0.5,0.45,.40,.35,.30,.25,.20,.15,.10,.05,0
1610 TAB,NV(1)
1620 PLOT,NV(1,11)
1630 BINARY,NV,CA
1640 +TYPE
1650 EXECUTE

Figure 3.45 ECAP Data File

Line 1040 - This specifies that the calculations will end at 5.0 μ s. In connection with lines 1020 and 1030, it implies that there will be 100 lines of output data printed.

Line 1050 - This controls the degree to which the network solutions must converge before the calculations for each time step have been completed. For each time step, ECAP makes a prediction of the new voltage at each node and the current in each branch, and then performs an analysis to see if such predictions satisfy Kirchoff's laws, at least to the desired tolerance. That analysis consists of taking the sum over all the nodes of the absolute value of the current unbalance at each of the nodes. A command "l error = 1" specifies that this unbalance must not exceed 1.0 A. If the unbalance exceeds 1.0 A, calculations are repeated until the required convergence is reached. The smaller the allowable error, the more accurate will be (presumably) the results, but the longer will be the running time. Again, about the best guide to the allowable error is experience.

Lines 1060 to 1430 - These specify the method of interconnection of the various branches and the values of the circuit components in the various branches. For example, Line 1100 specifies that Branch 5 is composed of an inductance of 0.94 μ H connected between Nodes 2 and 3. The positive sense of the branch is from Node 2 to Node 3.

Lines 1060, - 1250, 1290, 1330 - In these lines, the impedance Z1-Z4 at the ends of the lines were taken to be 1000 Ω .

Lines 1440 to 1470 - These are the dependent current sources that represent the voltage and current sources. Line 1440, for example, specifies that T1 is a dependent current source connected in parallel with Branch 4, whose waveshape and amplitude are equal to those of the current in Branch 36. T1 happens to represent the current injected into the system by the electric field in Zone A.

Lines 1480 to 1490 - These are the dependent current sources that represent the magnetic coupling from Conductor 1 into Conductor 2.

Lines 1500 - These specify the voltage source that excites the auxiliary circuit that controls dependent current source T1. The voltage is made numerically equal to the electric field strength in Zone A. The voltage is specified at intervals of 1 μ s 20 times the width of the basic time step specified in Line 1020.

Lines 1530 - These specify the voltage source that represents the magnetic field effects in Zone A. It also is specified at 1 μ s intervals.

Lines 1560 - The voltage source representing the magnetic field in Zone B is specified at 2 μ s intervals 40 x 0.05 μ s.

Line 1590 - The voltage source representing the magnetic field in Zone C is specified at 100 μ s intervals, 2000 x 0.05 μ s.

Line 1610 - This is a command to tabulate on the printer the voltage at Node 1. One could also cause a tabulation of the current in Branches X and Y by a command of the form TAB, CA(X,Y). The operation of ECAP, as implemented on the GE time-sharing service, requires that at least one quantity be tabulated.

Line 1620 - This is a command to plot the voltages at Nodes 1 and 2. The plotting is done under the control of an auxiliary program, TRPLOT, to which GE's ECAP transfers automatically. The plotting is done on the printer. Other users of ECAP may have other plotting devices and routines which may be used.

Line 1630 - This specifies that all node voltages and branch currents are written, for each output interval, into a binary sequential file. It is from this file that the plotting routine, TRPLOT, reads the data to be plotted.

Line 1640 - This instruction ensures that output data is printed on the printer. An instruction "NOPRINT" suppresses printing.

Line 1650 - This instruction tells ECAP to begin work.

3.6.2 Output Data from ECAP

Several sets of output data from ECAP are shown in Figures 3.46 through 3.54. The conditions under which the data are calculated and the quantities plotted are indicated on the figures.

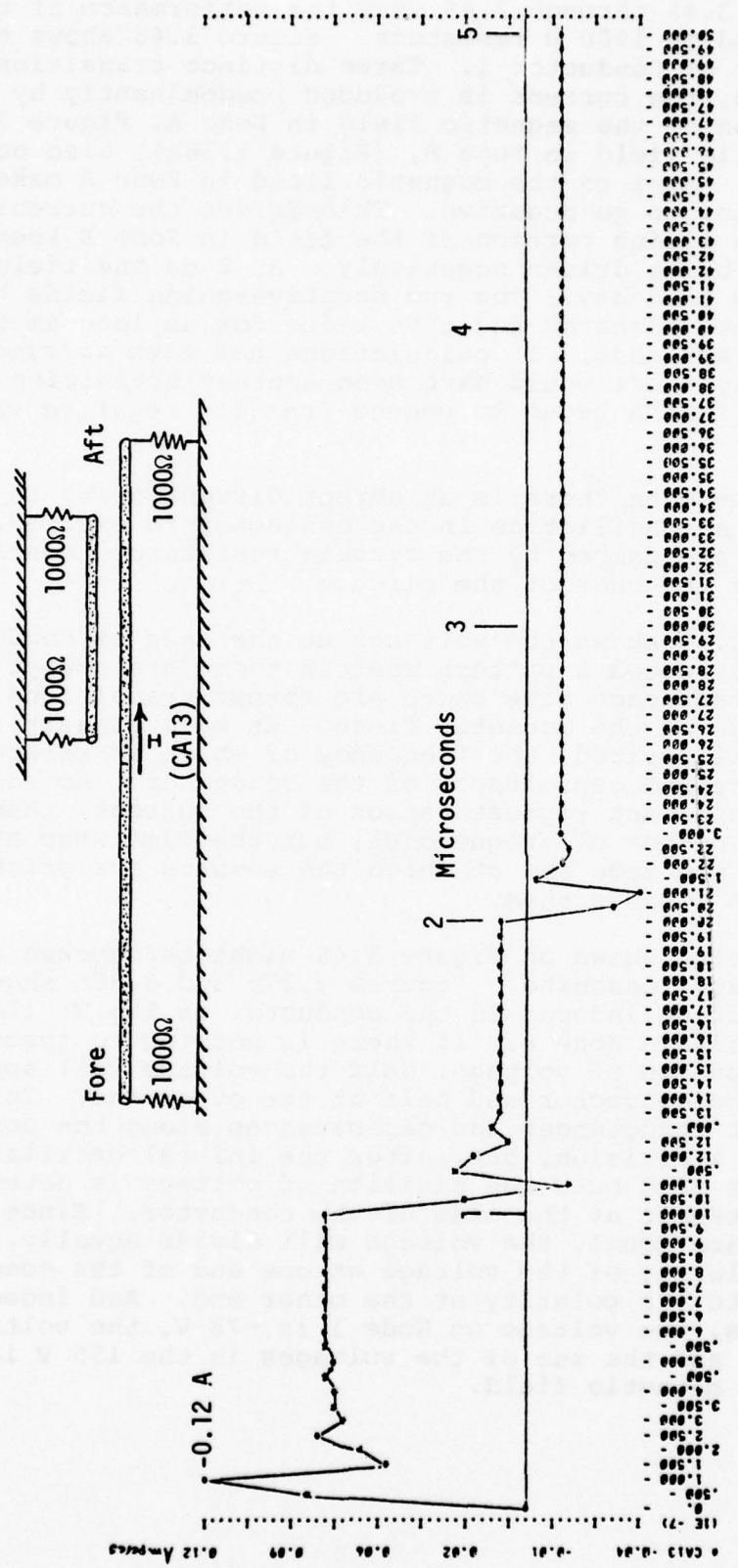


Figure 3.46 1000 Ω Terminations - Current at Center of Conductor 1

Figures 3.46 through 3.48 show the performance if the lines are terminated in 1000Ω resistors. Figure 3.46 shows the current at the center of Conductor 1. Three distinct transitions are shown. From 0 - 1 μs , the current is produced predominantly by the initial rising portion of the magnetic field in Zone A, Figure 3.38a. The rising magnetic field in Zone B, (Figure 3.38a), also contributes some current. At 1 μs the magnetic field in Zone A makes a transition and begins to go negative. This drives the current towards zero, but the rising portion of the field in Zone B keeps the current from being driven negatively. At 2 μs the field in Zone B also begins to decay. The two negative-going fields hold the current at the indicated negative value for as long as the calculations are made. If calculations had been carried past 7 μs , presumably there would have been another transition at 7 μs as the field in Zone A began to change from its negative value back to zero.

Each time when there is an abrupt discontinuity in the magnetic field, an oscillation in the conductor is excited. These oscillations are damped by the circuit resistance, mostly the resistance at the ends of the circuit.

Figure 3.47 shows the voltages at the ends of Conductor 1. Again there is noted a pattern wherein there are abrupt transitions of voltage each time there are abrupt transitions in the rate of change of the magnetic field. At each transition an oscillation is excited, the frequency of which is related to the inductance and capacitance of the conductor. Actually, in this lumped constant representation of the current, there will be excited a number of frequencies, but the time step at which calculations are made and at which the results are printed is too coarse to resolve them.

The results shown on Figure 3.48 might be checked against some elementary reasoning. Figures 3.37b and 3.38b show that the total voltage induced in the conductor is 155 V; 110 V in Zone A and 45 V in Zone B. If there is nothing to force an unequal distribution of voltage, half the voltage will appear at one end of the conductor and half at the other end. Initially, the different inductances and capacitances along the conductor prevent such a division, but, after the initial oscillations in the line have died out, the division of voltage is determined by the resistances at the ends of the conductor. Since those resistances are equal, the voltage will divide equally. Furthermore, the polarity of the voltage at one end of the conductor will be opposite to the polarity at the other end. And indeed, after about 0.75 μs , the voltage on Node 1 is -78 V, the voltage on Node 11 is +77 V, and the sum of the voltages is the 155 V induced by the changing magnetic field.

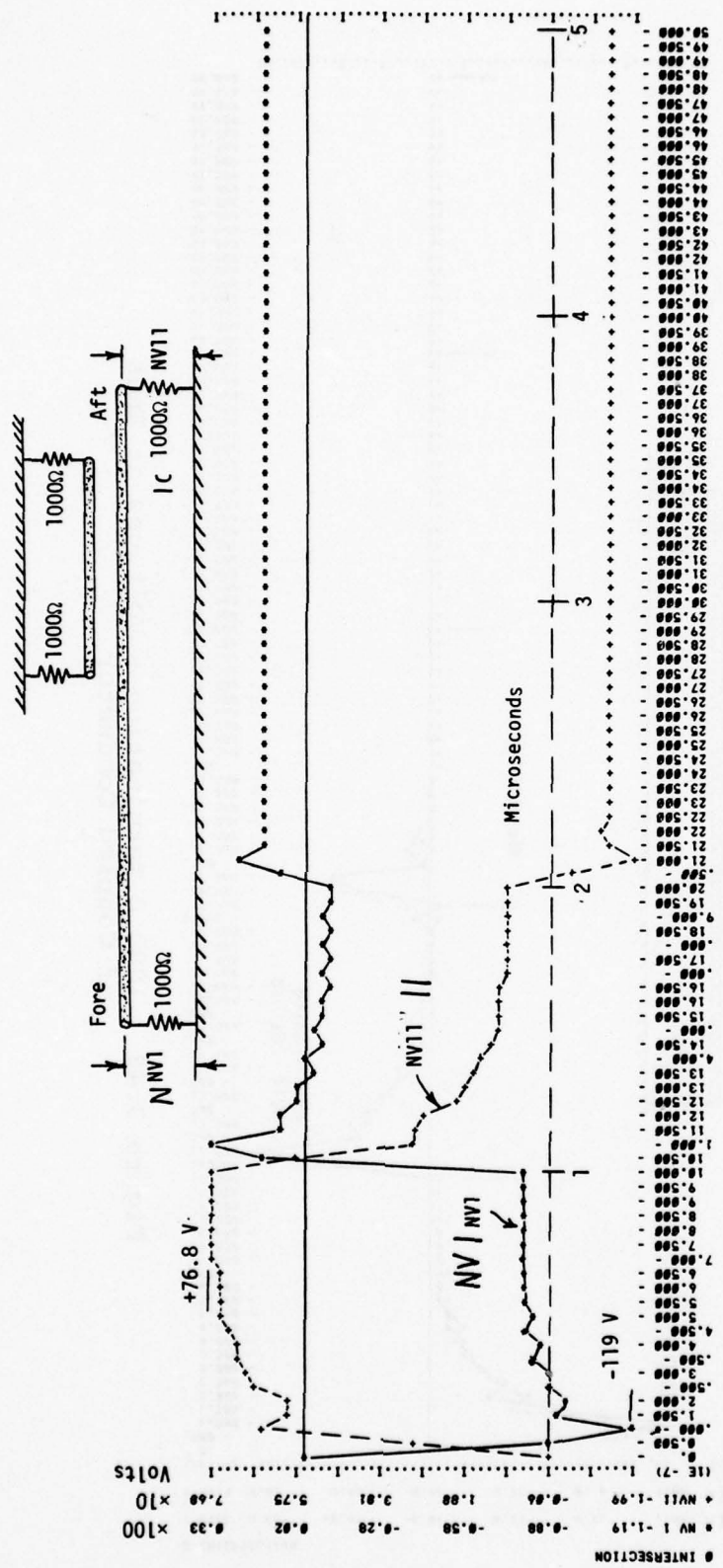


Figure 3.47 1000 Ω Terminations - Voltages at Ends of Main Conductor

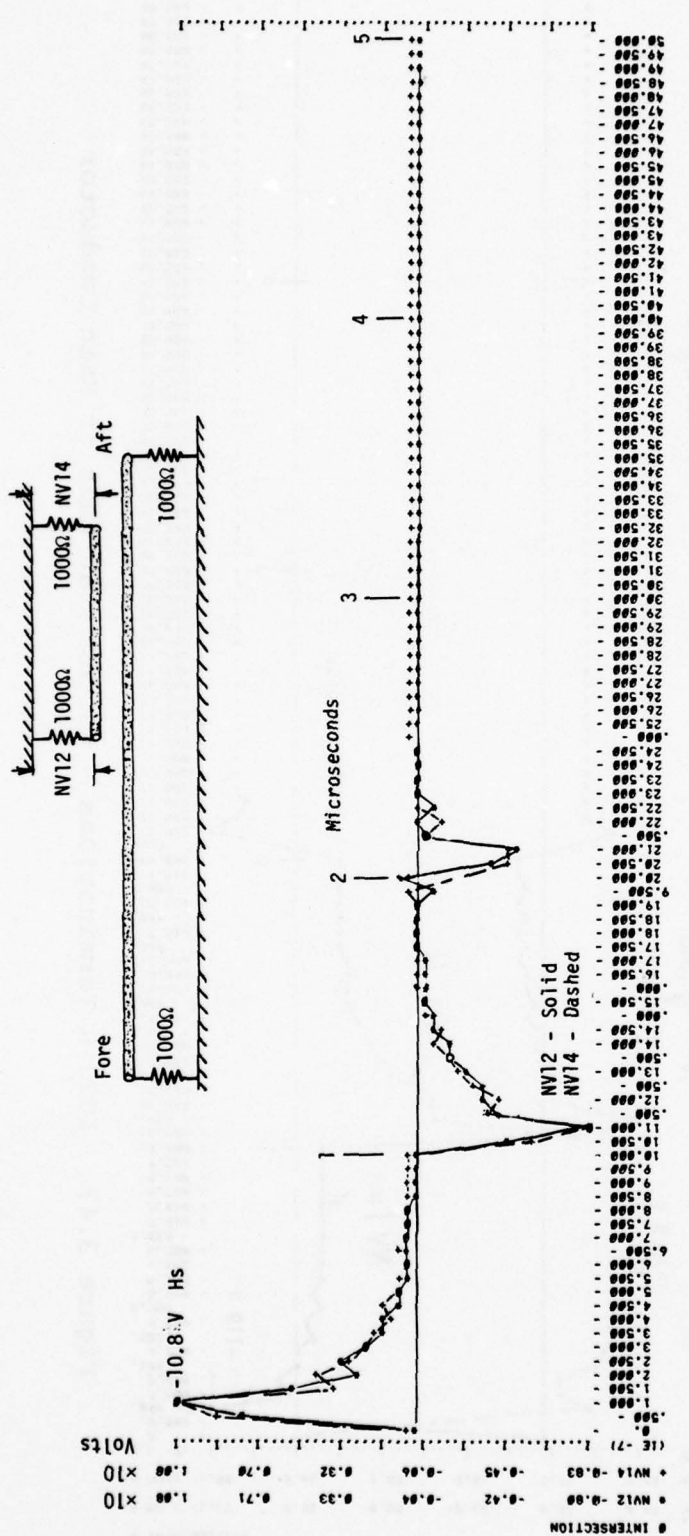


Figure 3.48 1000 Ω Termination - Voltages at Ends
of Coupled Conductor

Figure 3.48 shows the voltages at the ends of Conductor 2. The character of these voltages is entirely different from that of the voltage on Conductor 1. First, the voltages are of equal amplitude and equal polarity. Second, the voltages are different in waveshape from the voltages on Conductor 1. The shape is characteristic of the voltage produced across a resistor coupled through a small capacitor to a square wave generator. This is exactly the case here. The coupling from Conductor 1 to Conductor 2 is almost entirely capacitive. A simplified diagram that explains the behavior of the circuit is shown in Figure 3.49. If the voltage at (NV 11) were a square wave, NV 12 or NV 14 would have a peak voltage of 33 V and would decay with a 0.06 μ s time constant. Since NV 11 has a rounded front, NV 12 and NV 14 are less than 33 V.

Figures 3.50 and 3.51 show the circuit response when the ends of the conductors are shorted to ground through 0.01Ω resistors. To make this circuit change, the resistances in lines 1060, 1250, 1290, and 1330, were changed from 1000Ω to 0.01Ω . The calculation was also made using time steps of $0.025 \mu s$. The current was seen to be proportional to the integral of the driving voltage, and since that voltage was proportional to the derivative of the magnetic field, the current had basically the same waveshape as the magnetic field.

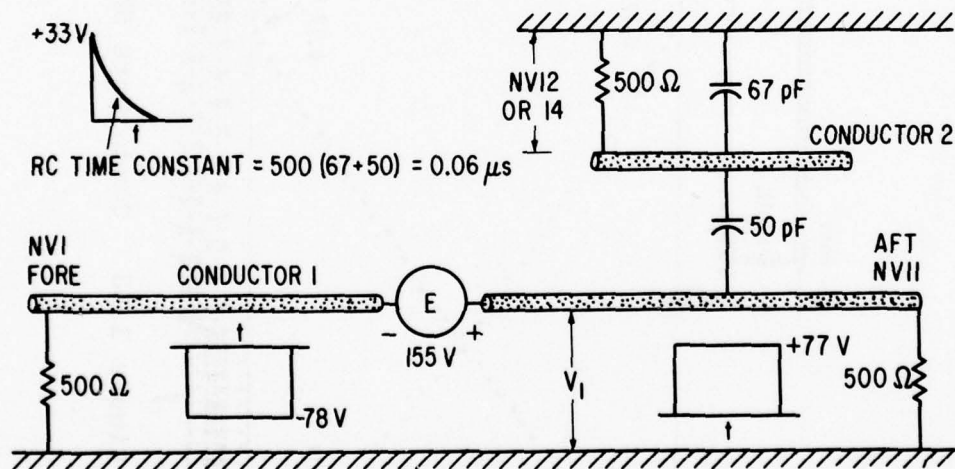
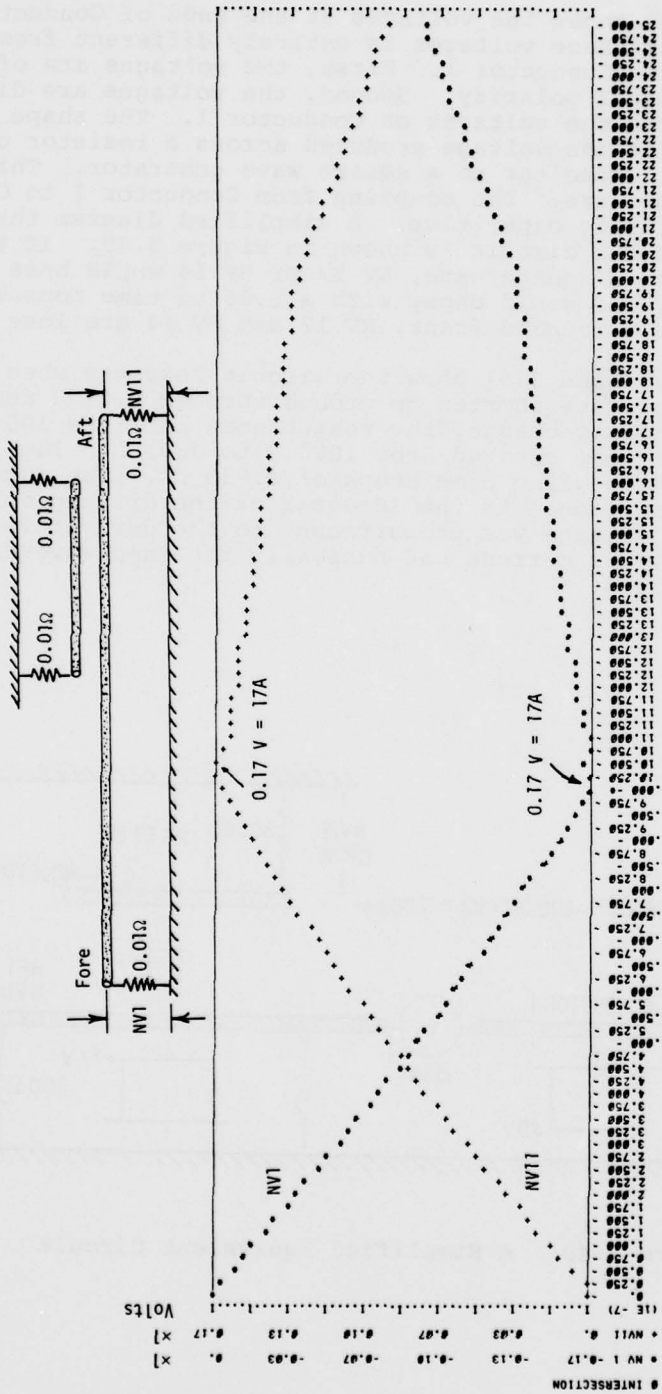


Figure 3.49 A Simplified Equivalent Circuit

Figure 3.50 Conductors Shorted — Current in Main Conductor



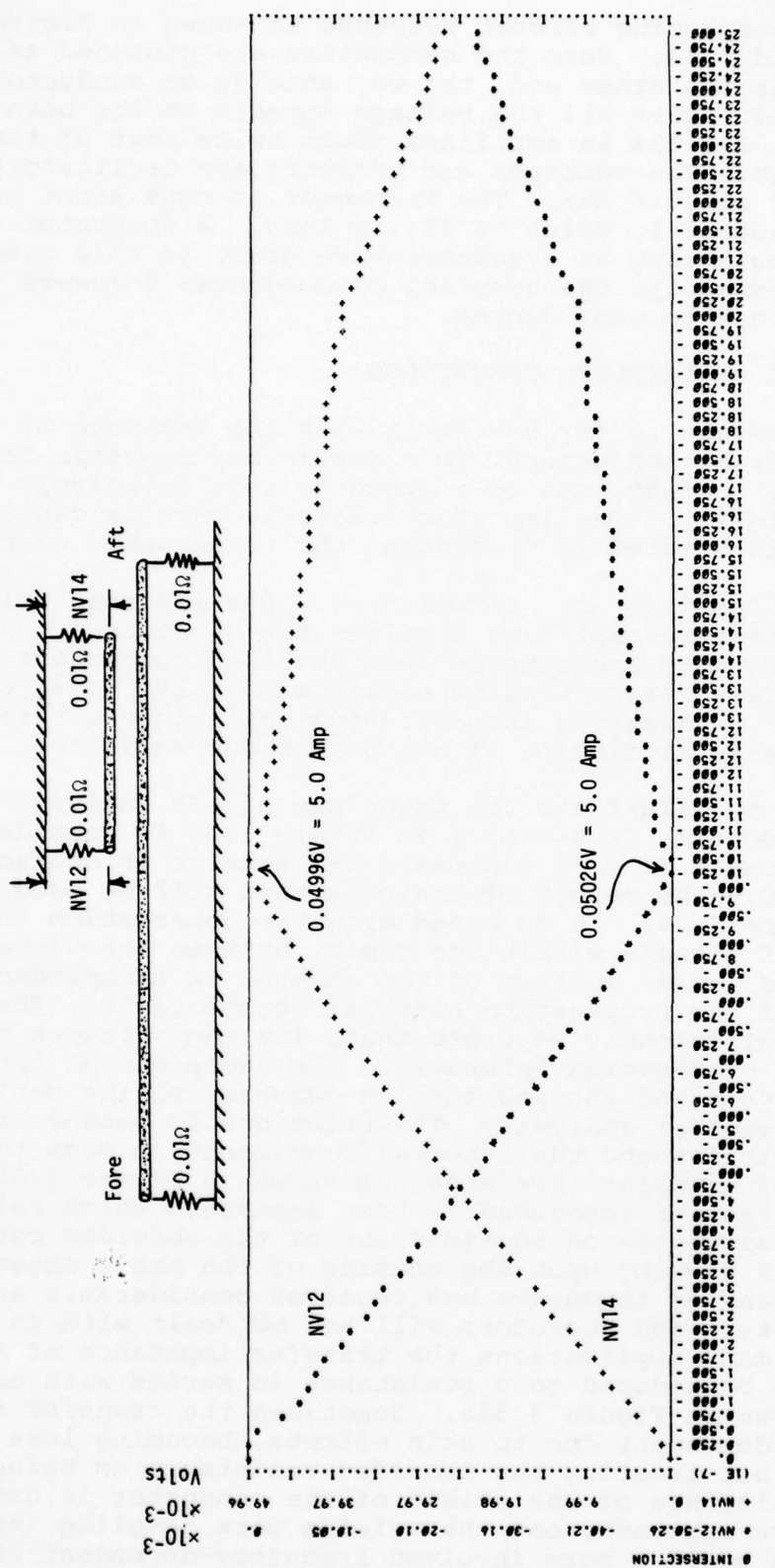


Figure 3.51 Conductors Shorted — Current in Coupled Conductor

A more interesting circuit response is shown in Figures 3.52, 3.53, and 3.54. Here the conductors are grounded at one end and open at the other end, the way shields on conductors are usually treated. Here all the voltage appears at the open end of Conductor 1 and has an amplitude about twice that of the driving voltage. The voltages and currents are oscillatory with a frequency of about 5 MHz. The frequency is consistent with the length of Conductor 1, which is 13.5 m long. A conductor grounded at one end should ring as a quarter-wave stub, in this case at 5.56 MHz. Presumably, the coupling of Conductor 2 lowers the ringing frequency to some degree.

3.7 TREATMENT OF SHIELDED CONDUCTORS

The discussion so far has dealt with the response of a conductor, or pair of conductors, to electric and magnetic fields. Some problems, in fact, can be reduced to this relatively low level of complexity. One important class is that of cable bundles where one is interested in predicting the total cable current.

Most problems are more complicated. One important class of problems of greater complexity involves the question of what voltages or currents are coupled into shielded conductors. Some of these problems can be treated easily with a LPM model analysis; others require an analysis incorporating sufficient artifice to make the analysis difficult, if not of dubious validity.

In order to illustrate the technique of LPM analysis of shielded conductors, Conductor 1 in Figure 3.20 is considered to be a coaxial cable of 50Ω impedance and similar in characteristics to RG 8/U. The method of analysis that will be used is shown in Figure 3.54. It is based upon the observation that the propagation of signals within the cable, between the signal conductor and the inside surface of the sheath, is independent (virtually) of the propagation external to the cable. These signals are sufficiently separate that, for many classes of problems, the propagation internal to the cable can be treated with one analysis and the propagation external to the cable treated with another analysis. The relationship between the external conditions and the internal conditions is made through the concept of transfer impedance, as shown in Figure 3.55b and 3.55c. The transfer impedance is that impedance which relates the voltages developed on the interior of the shielded conductor to the current flowing upon the outside of the cable sheath. The subject of transfer impedance has received considerable attention in the literature and therefore will not be dealt with in this report. For many applications the transfer impedance of a shielded conductor can be reduced to a resistance in series with an inductance, as shown in Figure 3.55b. Sometimes the transfer resistance is frequency-dependent due to skin effects, becoming less at higher frequencies, but treating the transfer resistance as being equal to the dc resistance of the shield of the conductor is usually a conservative approach, one that yields more coupling into the interior than would a more involved frequency-dependent resistance.

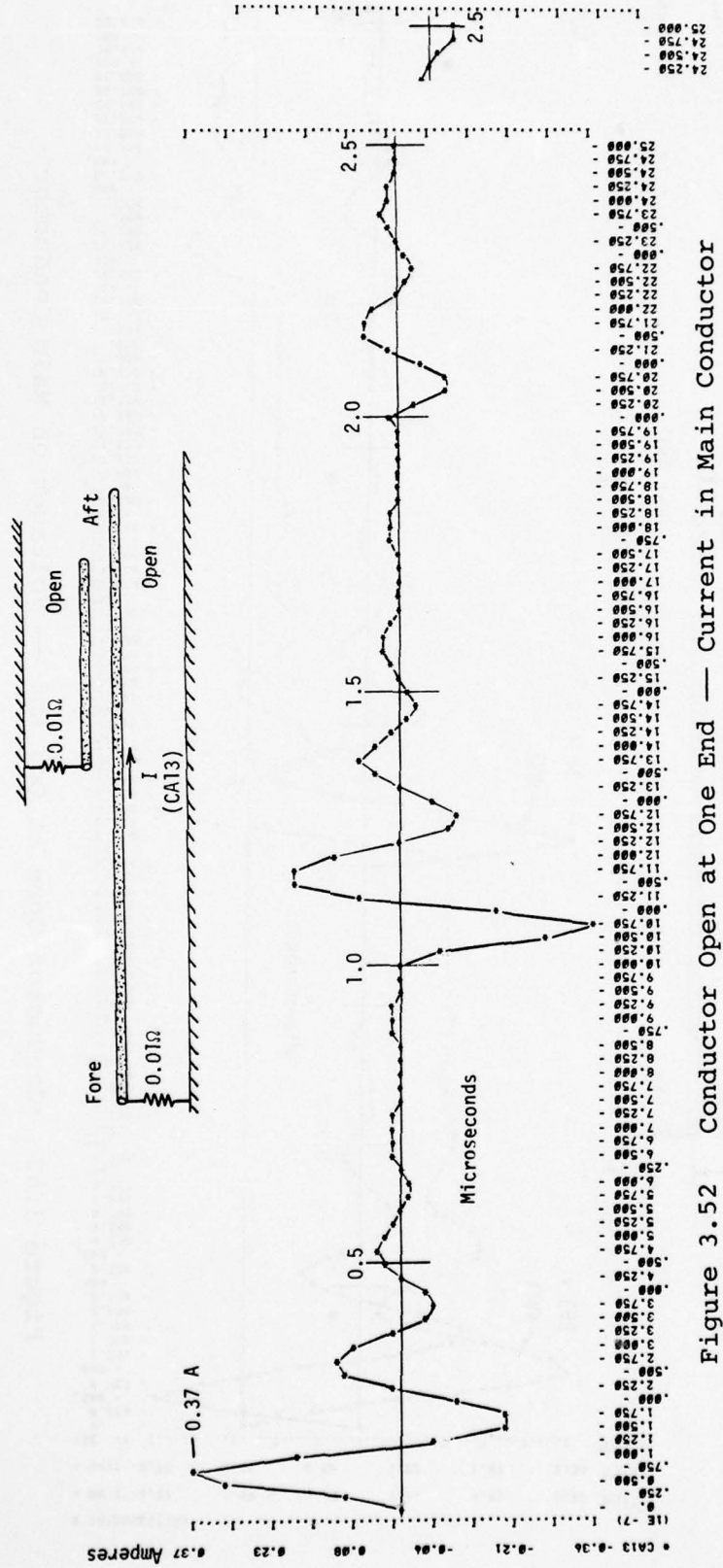


Figure 3.52 Conductor Open at One End — Current in Main Conductor

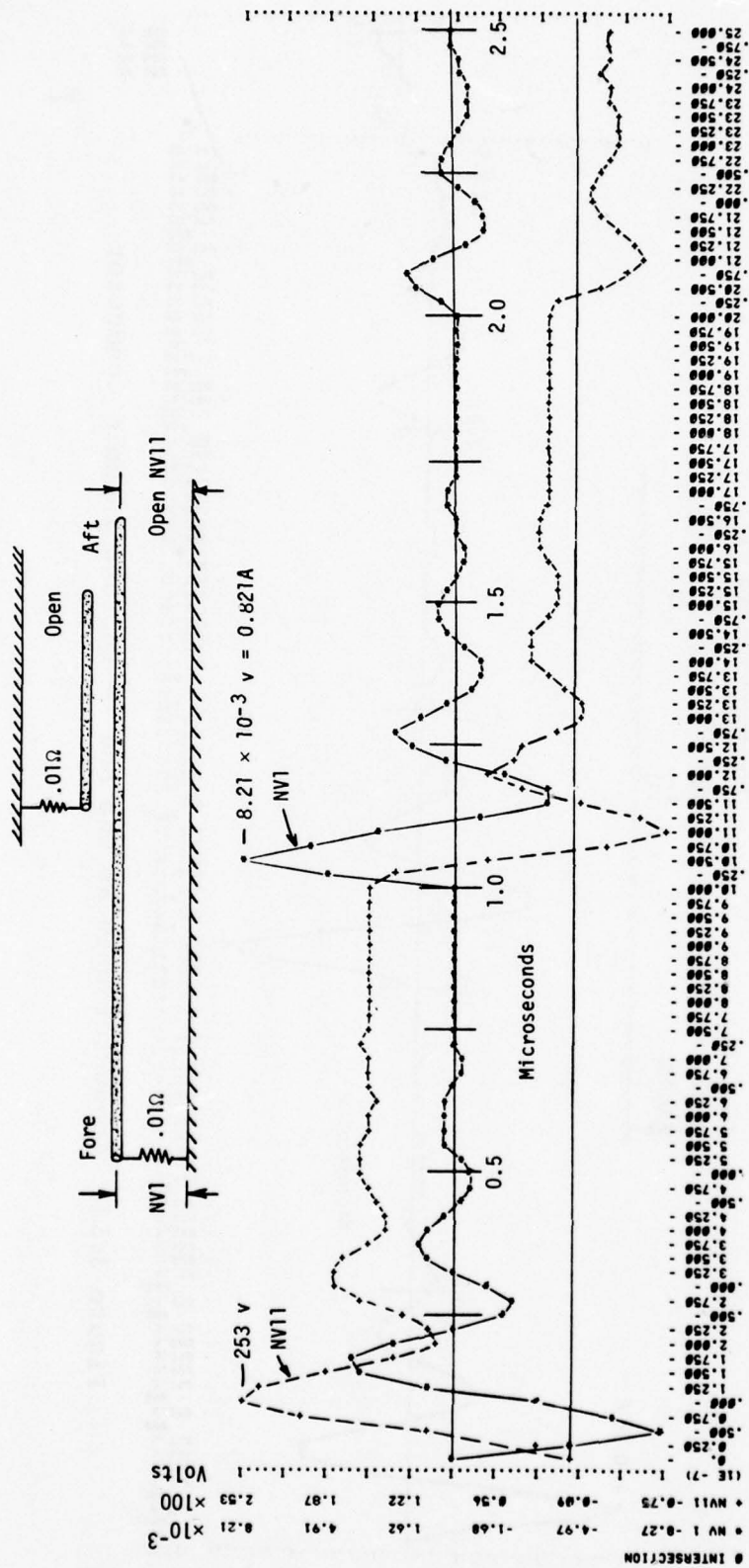


Figure 3.53 Conductor Open at One End — Voltages on Main Conductor

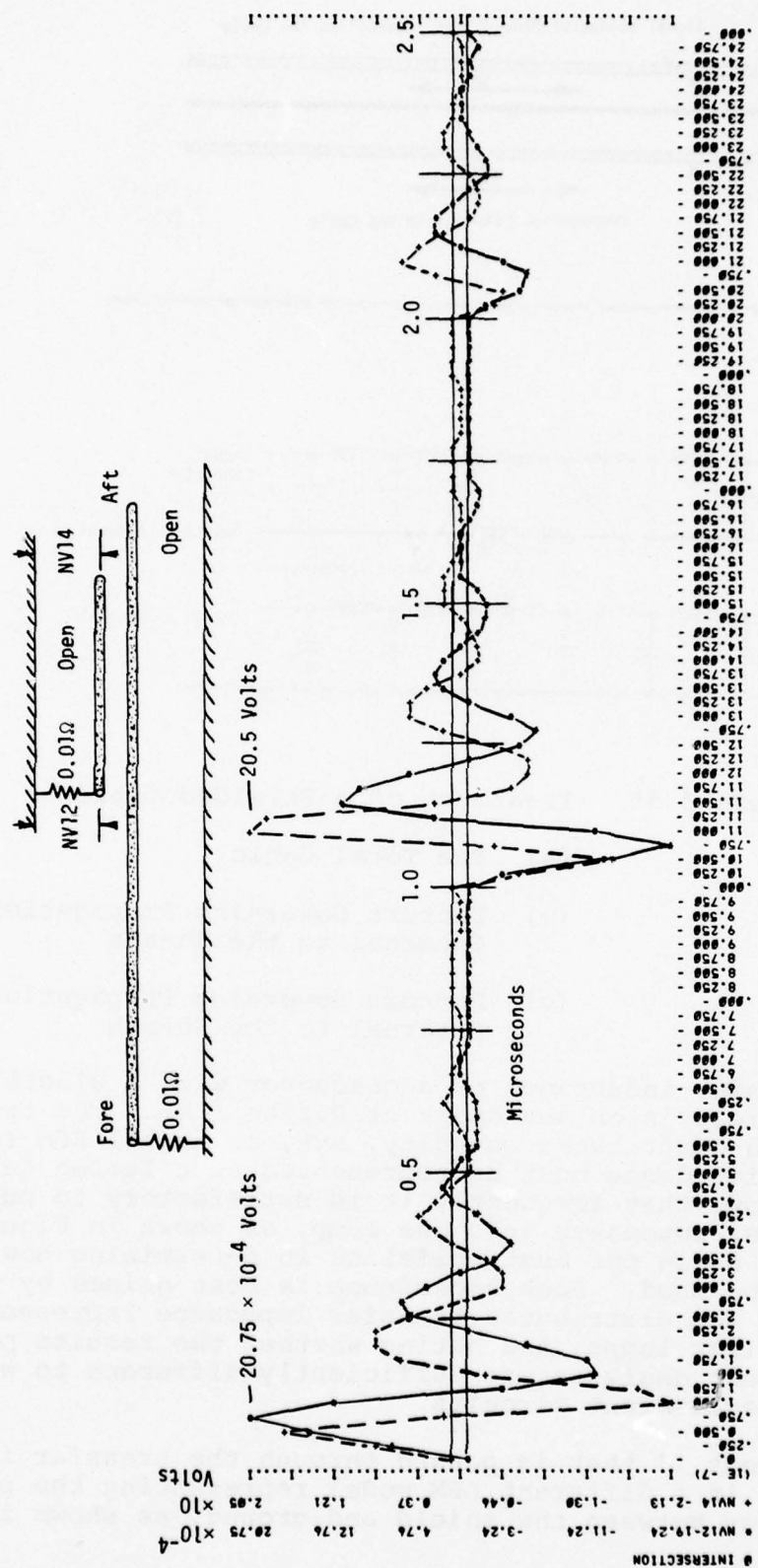


Figure 3.54 Conductor Open at One End — Voltages on Coupled Conductor

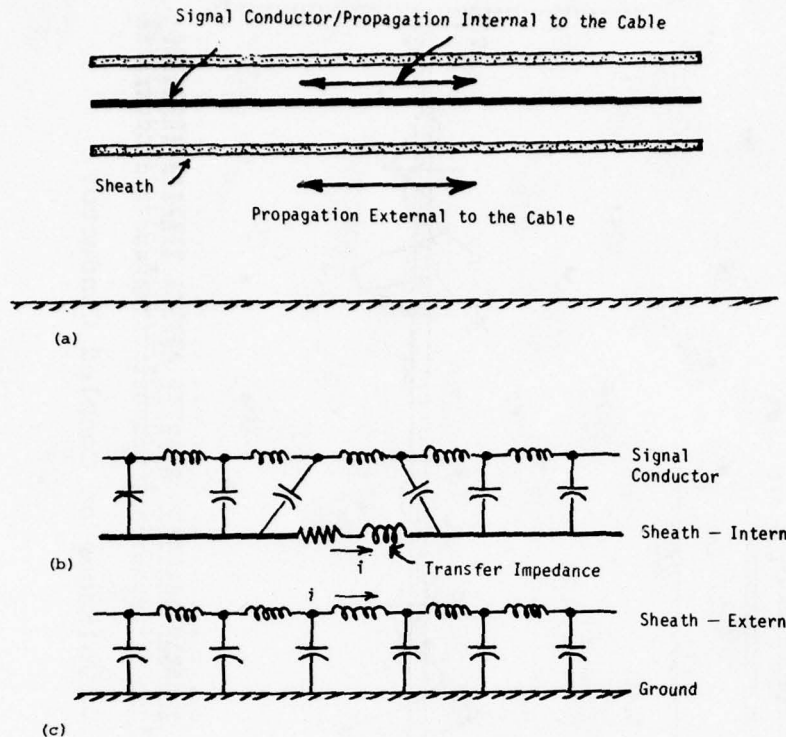


Figure 3.55 Treatment of a Shielded Cable

- (a) The Total Cable
- (b) Factors Governing Propagation Internal to the Sheath
- (c) Factors Governing Propagation External to the Sheath

The transfer inductance of a conductor with a single layer of braided shield is on the order of 0.1 to 1 nH. The transfer impedance is a distributed quantity, but, as in all LPM solutions, the transfer impedance must be represented as a lumped quantity. Experience shows that frequently it is satisfactory to put all of the transfer impedance into one lump, as shown in Figure 3.55b. Experience is again the best guideline in determining how many lumps should be used. Such experience is best gained by making analyses with the distributed transfer impedance represented as bigger or smaller lumps, and noting whether the results predicted by the different analyses are sufficiently different to warrant more complex equivalent circuits.

The current i' that is passed through the transfer impedance is determined in a different LPM model representing the propagation characteristics between the shield and ground, as shown in Figure 3.55c.

For purposes of this analysis we will assume the transfer resistance and inductance of the cable shield to be $4 \text{ m}\Omega$ and 0.25 nH/m , figures that are quoted in the literature. For the 13.5 m length of cable, this gives a transfer impedance of $0.054 \text{ }\Omega$ and 3.88 nH .

If it is assumed that the shielded conductor is of $50 \text{ }\Omega$ impedance and insulated with polyethylene of relative dielectric constant 2.3, the total internal inductance and capacitance of the cable is, from Equations 3.57 and 3.58, $3.41 \mu\text{H}$, and 1364 pF . The propagation characteristics external to the cable will be taken to be the same as in the previous analysis, allowing for the fact that one is not considering the coupled Conductor 2 to be present. The total set of impedances defining the cable system is then as shown in Figure 3.56a. These impedances must then be broken into smaller lumps. The degree of lumping chosen for this analysis is shown in Figure 3.56b.

The final equivalent circuit chosen for this analysis is shown in Figures 3.57 and 3.58. Some observations about this circuit are in order. First, the analysis will not include the effects of the electric field in Zone A or of the magnetic field in Zone C. Those effects seemed to have little effect on the total cable current. The dependent current sources that represent these magnetic fields are shown as T_1 and T_2 . Those dependent current sources are driven by the auxiliary circuits shown at the top of the figure. Second, the LC network that represents the propagation external to the cable shield is shown at the bottom of the figure. Third, the LC network that represents the propagation internal to the cable is shown in the center of the figures. T_3 is the dependent current source that energizes the transfer impedance of the cable shield. T_3 is controlled by the current in Branch 9. Branch 28, the $1 \text{ M}\Omega$ resistor connected between Nodes 9 and 11, is a dummy branch required to satisfy the ECAP topology. A dependent current source cannot be connected across a single branch. The $1 \text{ M}\Omega$ resistor represents that branch. Fourth, the $100 \text{ M}\Omega$ resistors, Branches 19 and 34, connected across the ends of the cable, serve as a means of measuring the voltage at the ends of the cable. The plotting routine supplied with the GE time-sharing version of the ECAP does not allow one to plot the difference in voltage between two nodes, but it does allow one to plot the current through a resistor of sufficiently high resistance so that it does not affect the voltage. Fifth, the impedances Z_1 through Z_4 are impedances, the values of which may be changed as appropriate during the analysis.

While in many respects the interior of the cable shield can be treated completely separated from the exterior of the cable shield, the facts of the matter are that the interior and exterior are joined at the ends of the cable. With regard to the physics of the situation, then, Nodes 1 and 9 represent the same physical point and Nodes 8 and 11 represent the same point. In the analysis it is not possible to directly interconnect these pairs of nodes,

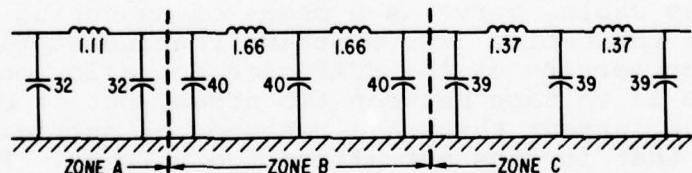
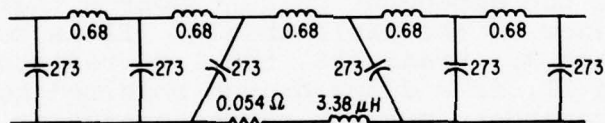
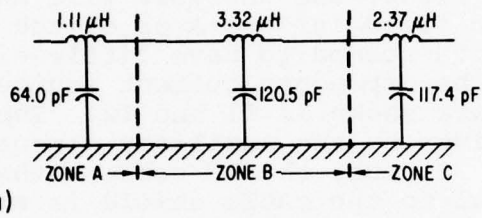
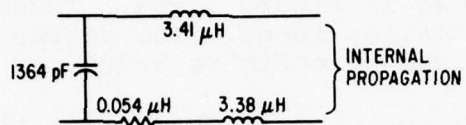


Figure 3.56 A Shielded Cable

(a) Elementary

(b) More Detailed

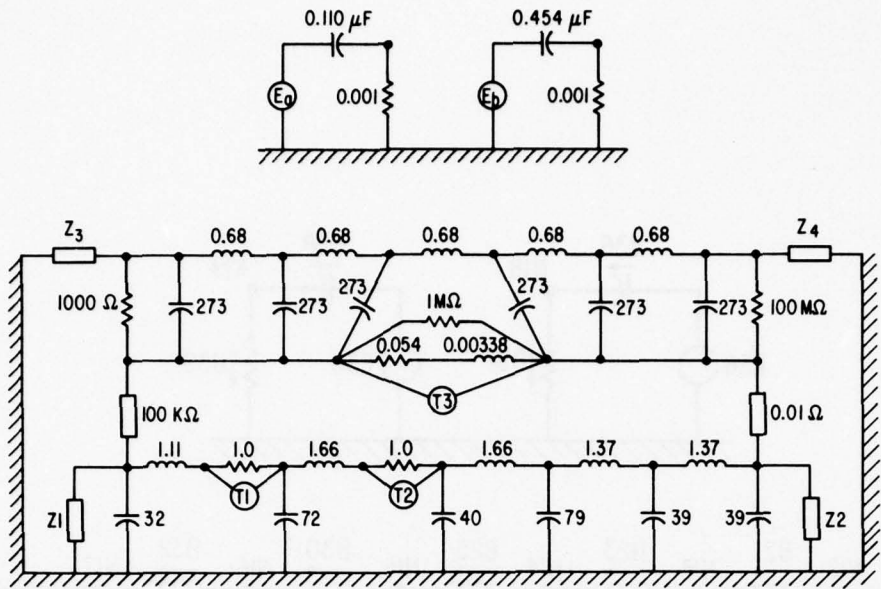


Figure 3.57 Component Values of Equivalent Circuit

for, if they were connected, Node 1 would be shorted to Node 8 through the very low impedance of the cable shield. Such a connection would prevent calculation of the propagation of current along the exterior of the cable. The nodes can be connected through appropriate resistances, however, to satisfy many of the conditions that must be modeled. Branches 16 and 17 provide for such interconnections. For the analysis to be presented here, Branch 16 will be treated as a high impedance resistor having no practical effect on the circuit, while Branch 17 will be treated as a 0.01Ω resistor, a short circuit.

With $Z2$ and $Z4$ treated as open circuits, the response of the circuit becomes as shown in Figure 3.59, 3.60, and 3.61. Both the physical condition of the circuit and the way that the circuit was modeled are shown on the figures. The current on the outside of the sheath was calculated, but is not shown, since it is virtually identical to that shown in Figure 3.52. The voltage at the open end of the sheath, V_{35} , is shown in Figure 3.59. This voltage is, of course, very similar to that calculated at the open end of the conductor when the conductor was not treated explicitly as a shield. That voltage is shown in Figure 3.53. The voltage shown in Figure 3.59 is slightly less because the electric field effects were not modeled for the circuit of Figure 3.59.

The voltage between the signal conductor and the shield at the open end, V_{34} , is shown in Figure 3.60. That voltage is much smaller than the voltage to ground, as it otherwise would be, since both the signal conductor and the shield are exposed to virtually the same magnetic field. The amount of leakage through the shield,

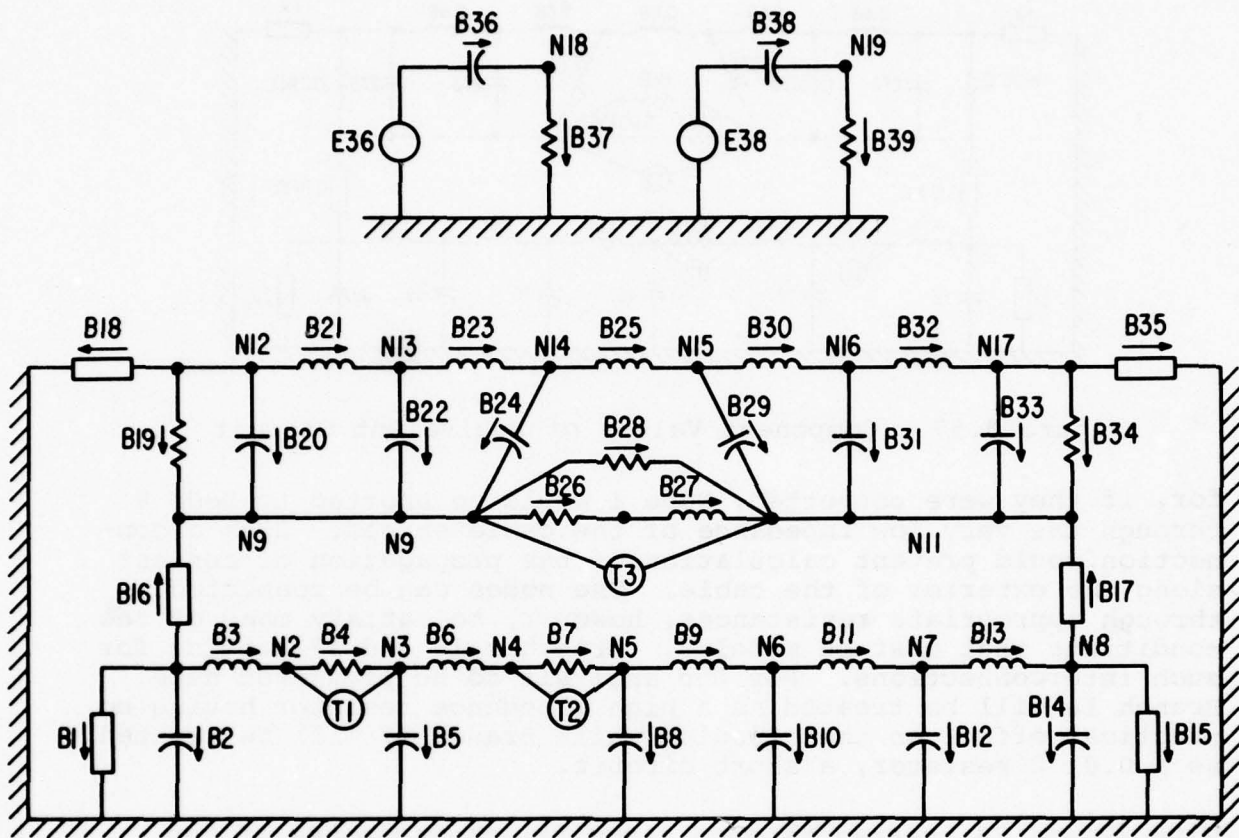


Figure 3.58 Nodes and Branches Numbered for ECAP Analysis

represented by Branches 26 and 27 of Figure 3.58, excite the internal oscillation of the cable, and hence the voltage of Figure 3.60 is much more oscillatory than is the voltage of Figure 3.59. The voltage across the load resistor of the conductor, V19, is shown on Figure 3.61. It also is oscillatory and of about the same magnitude as the voltage at the open end of the cable.

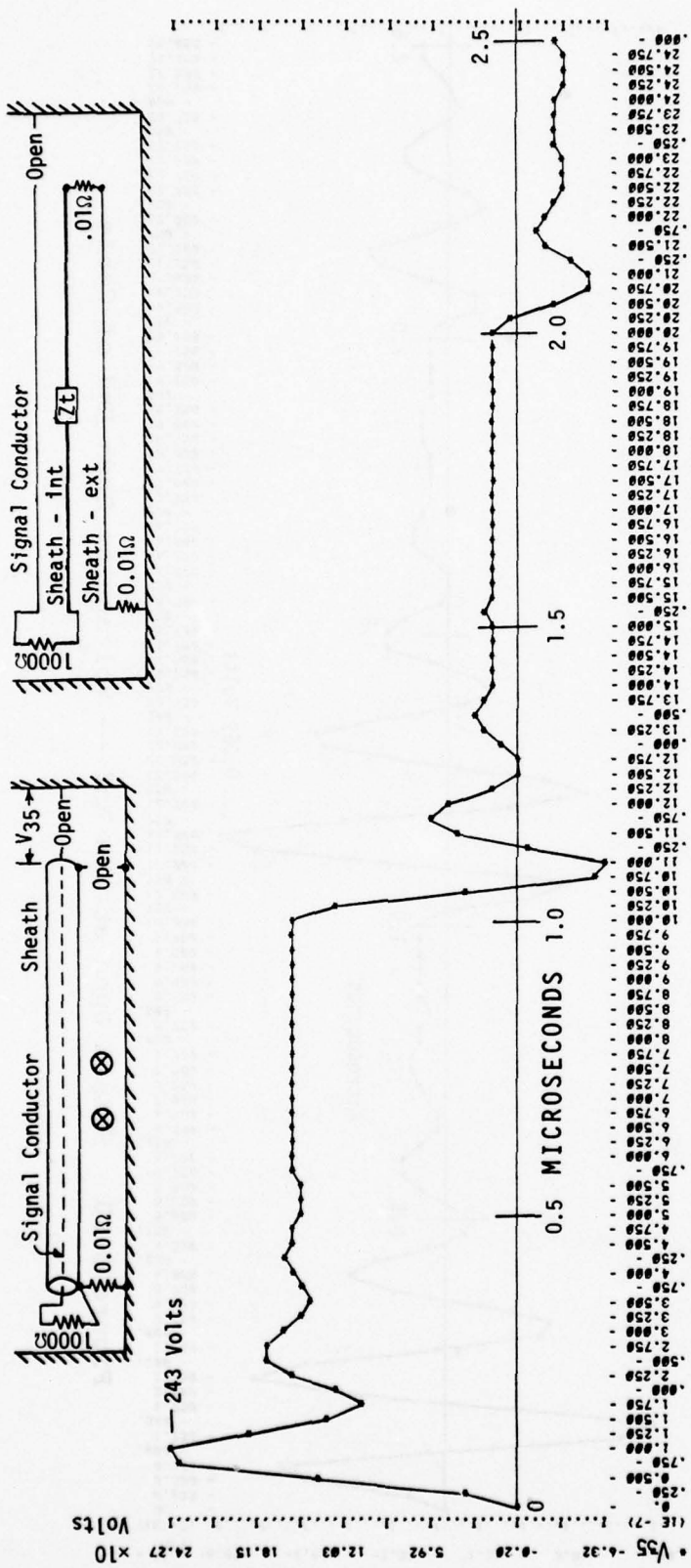


Figure 3.59 Shield Open at One End — Voltage from Shield to Ground

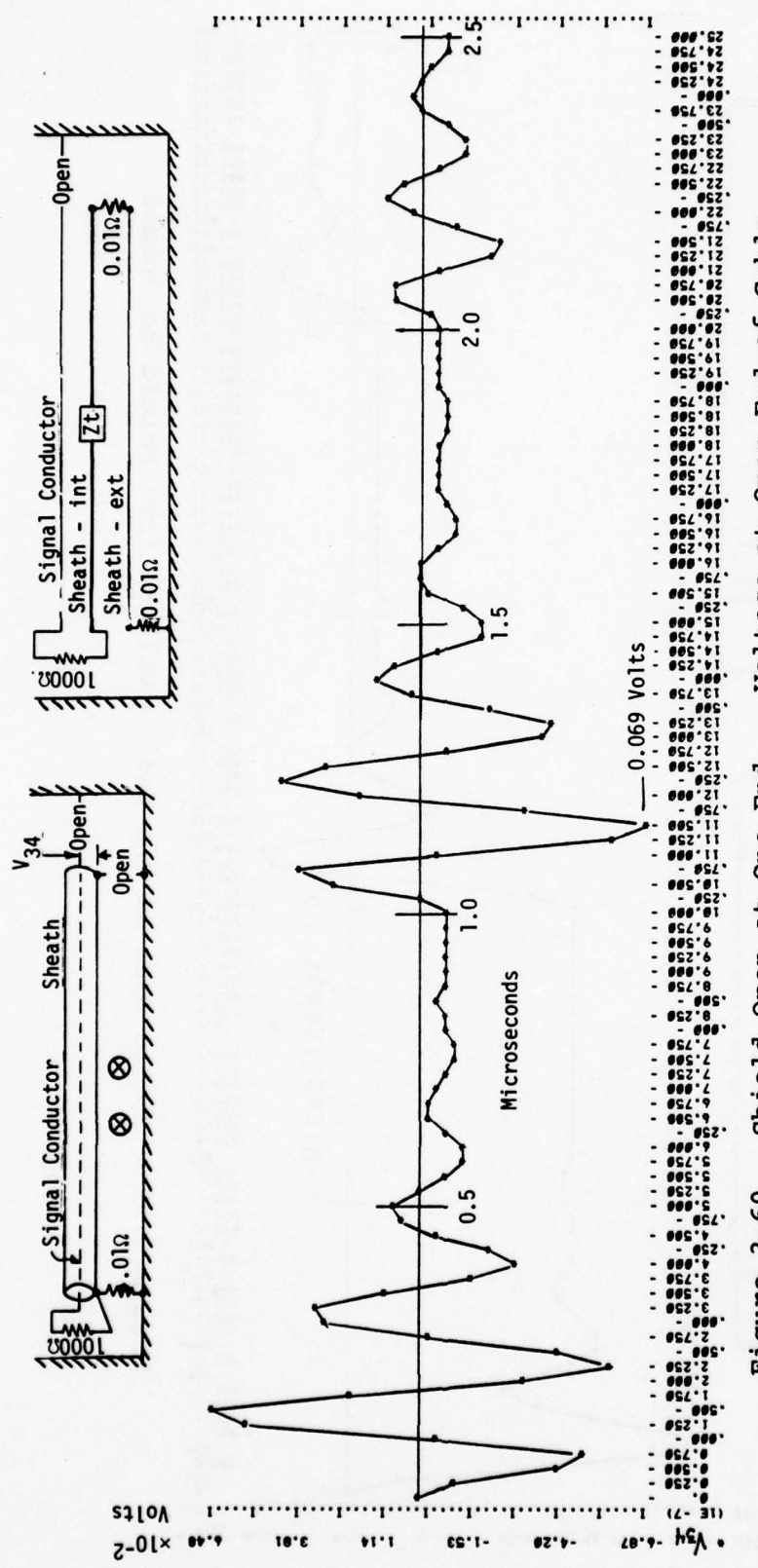


Figure 3.60 Shield Open at One End — Voltage at Open End of Cable

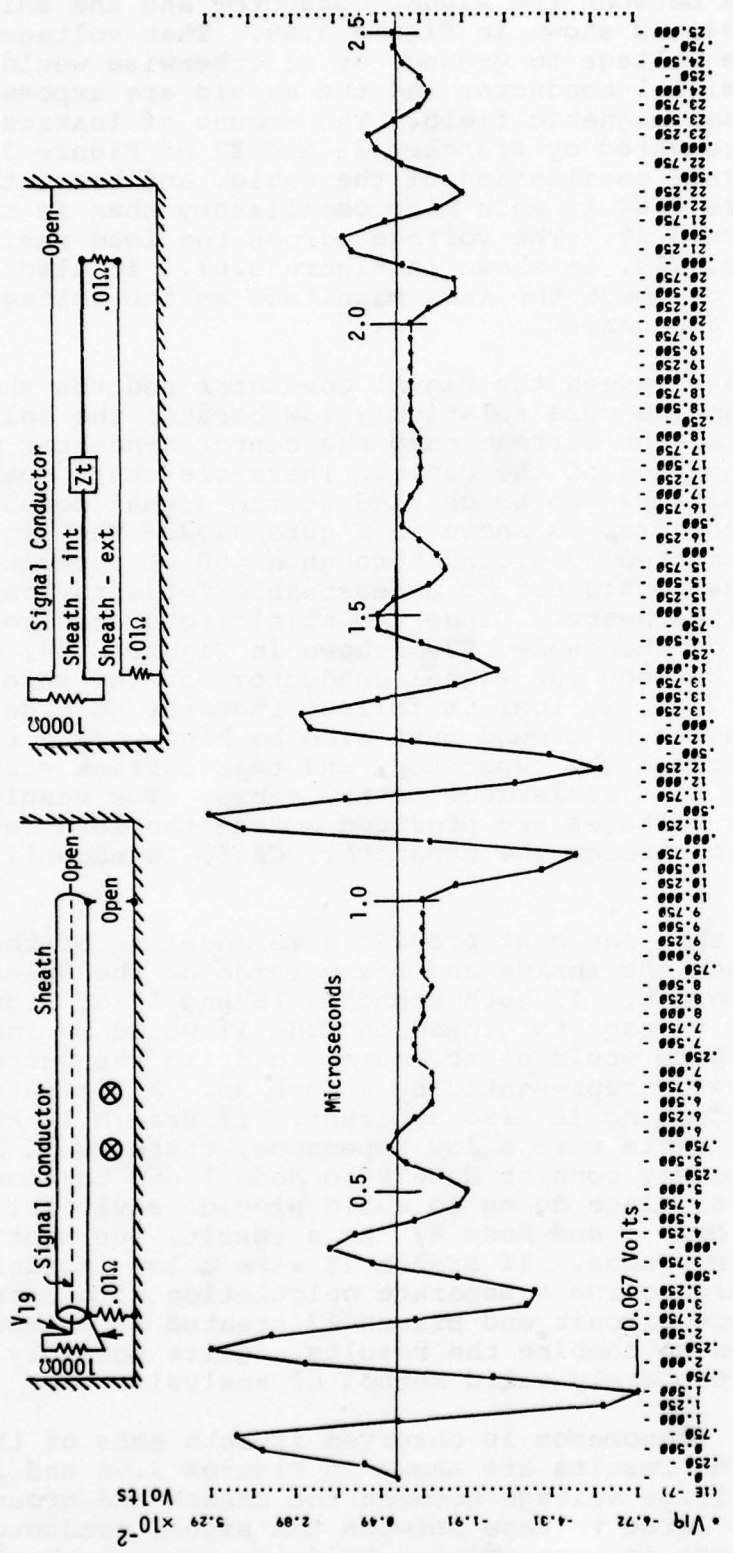


Figure 3.61 Shield Open at One End — Voltage at Terminated End of Cable

The voltage between the signal conductor and the shield at the open end, V34, is shown in Figure 3.60. That voltage is much smaller than the voltage to ground, as it otherwise would be, since both the signal conductor and the shield are exposed to virtually the same magnetic field. The amount of leakage through the shield, represented by Branches 26 and 27 of Figure 3.58, excite the internal oscillation of the cable, and hence the voltage of Figure 3.60 is much more oscillatory than is the voltage of Figure 3.59. The voltage across the load resistor of the conductor, V19, is shown in Figure 3.61. It also is oscillatory and of about the same magnitude as the voltage at the open end of the cable.

The voltages between the signal conductor and the sheath in the previous examples were relatively low because the only means of coupling voltage or current onto the center conductor was through the transfer impedance of the cable. There are other means, however, whereby voltages can be coupled to the signal conductor. One of these procedures is shown in Figure 3.62. The signal conductor is connected to ground through a 400 pF capacitance, a capacitance that would not be unreasonable for stray capacitance in some kinds of hardware. Since the shield to ground voltage at the open end of the cable, V35, shown in Figure 3.59, is high, and the voltage between the signal conductor and the shield, V35, shown in Figure 3.60, is low, it follows that the voltage from the signal conductor to ground must also be high. As a result, current flows through the capacitor, and that current must then pass through the load resistance of the cable. The result is that much higher voltages are produced across the load resistor, V19. The current through the capacitor, CA35, is shown in Figure 3.63.

The reason that one must provide some modeling of the physical connection between the inside and the outside of the shield now becomes more apparent. If both Branches 16 and 17 of Figure 3.58 were absent, the voltage to ground on Node 11 would be indeterminate, and hence there would be no source to drive the current through the 500 pF capacitor represented by Branch 35. A limitation of this method of modeling is also apparent. If Branch 18 at the other end of the cable were a low impedance, there would be no way to simultaneously connect Node 9 to Node 1 and to connect Node 11 to Node 8, since doing so would provide a virtual short circuit between Node 1 and Node 8. As a result, one must then treat problems in stages. If Branch 18 were a low impedance, it would be necessary to run a separate calculation with Branch 16 treated as a short circuit and Branch 17 treated as an open circuit, and then to combine the results. Quite possibly this would not be a completely valid method of analysis.

A different phenomenon is observed if both ends of the sheath are grounded. The results are shown in Figures 3.64 and 3.65. By removing the large voltage between the sheath and ground, one also removes the large voltage between the signal conductor and ground; hence there is less voltage to drive current through the capacitor.

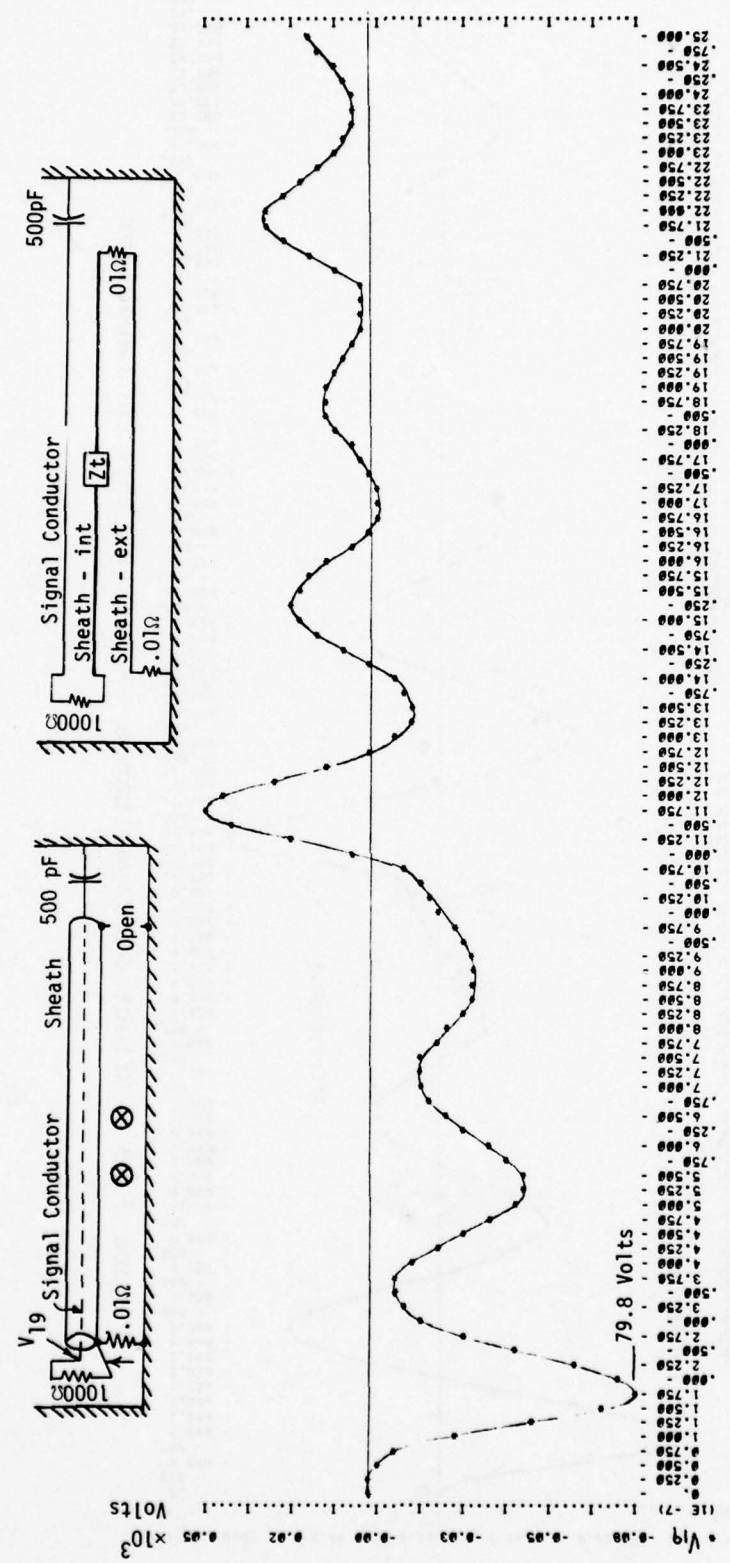


Figure 3.62 Effect of Capacitance — Voltage at Termination

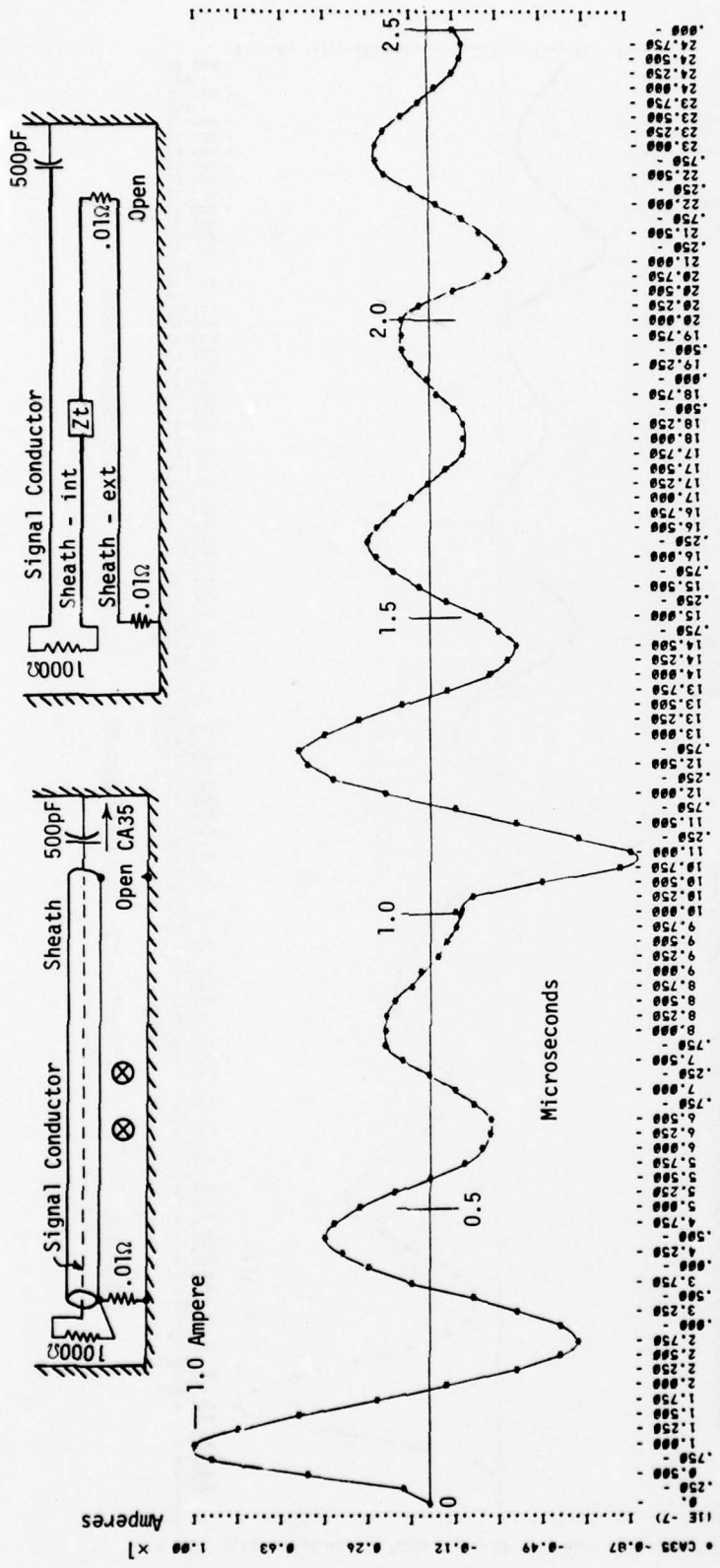


Figure 3.63 Effect of Capacitance — Current Through Capacitor

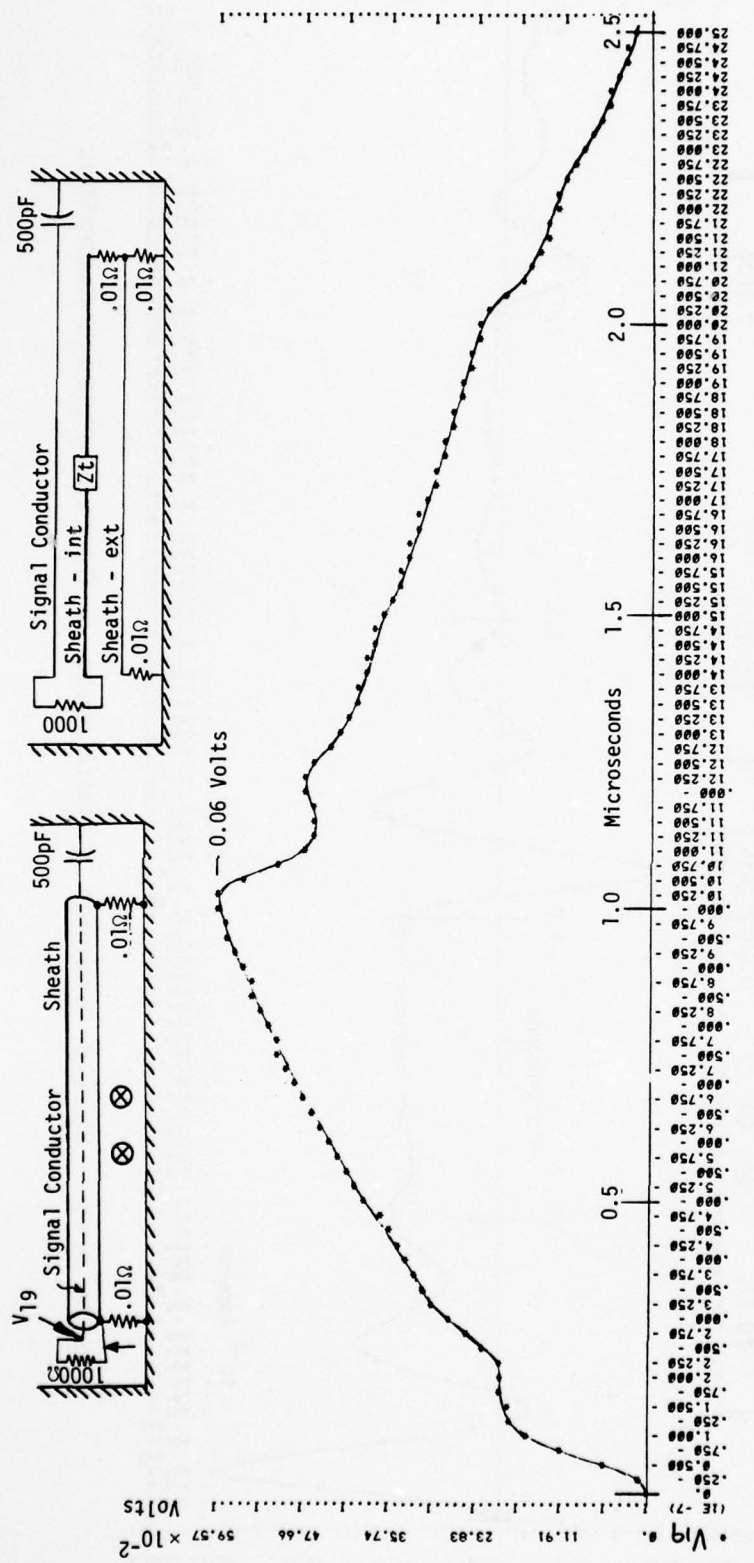


Figure 3.64 Shield Grounded at Both Ends — Voltage at Termination

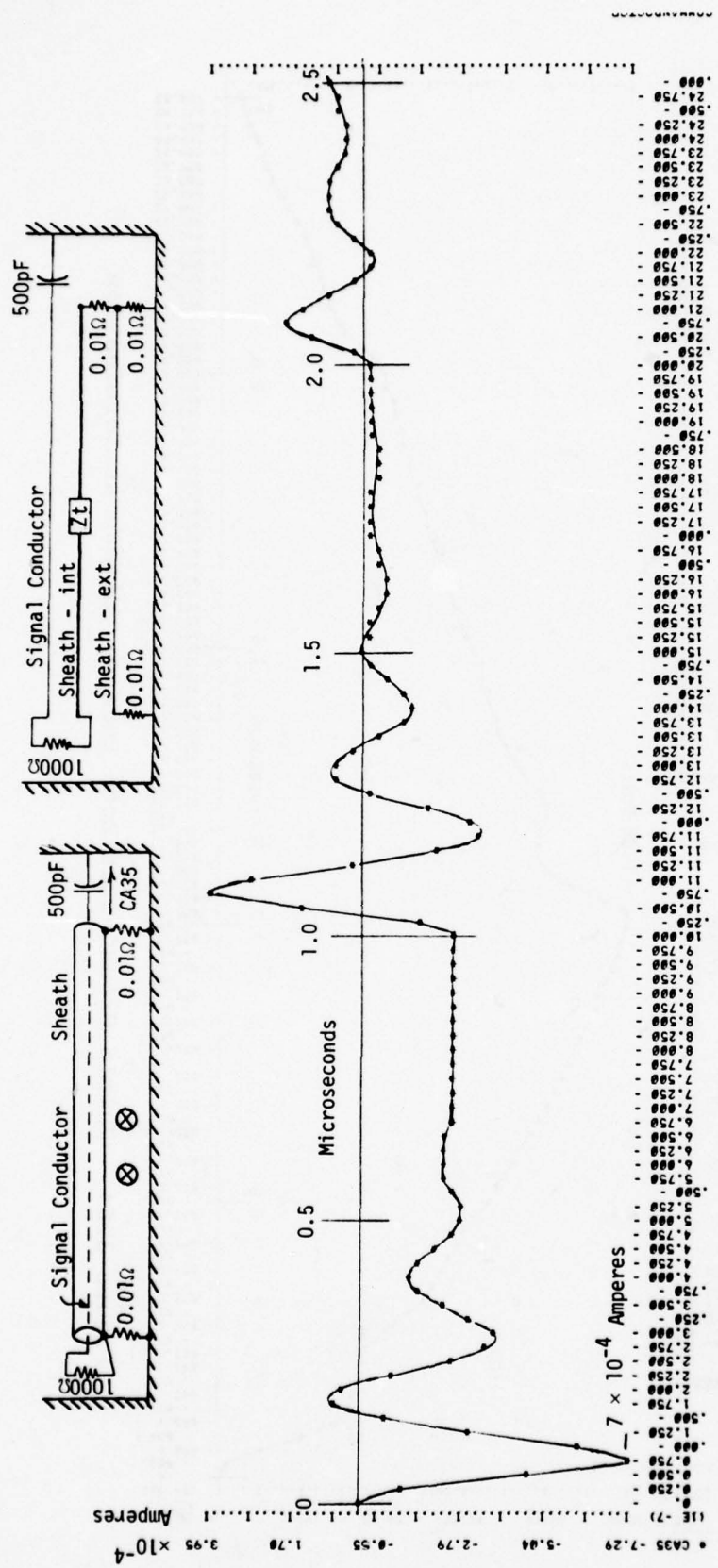


Figure 3.65 Shield Grounded at Both Ends — Current Through Capacitor

SECTION IV

DETERMINING THE ELECTROMAGNETIC FIELD ENVIRONMENT

4.1 INTRODUCTION

The previous section showed how the equivalent voltage and current sources acting upon the equivalent circuits could be related to the intensities of the magnetic and electric fields within the aircraft. This section will give some guidance as to how those fields may be determined. There are two dominate modes by which electromagnetic energy can be coupled into the interior of the aircraft: through apertures and through the metallic (usually) walls of the aircraft. Loosely speaking, coupling through apertures governs the high-frequency behavior of the fields and coupling through the walls, the low-frequency behavior. Coupling through the walls is often called the diffusion coupling mode.

The circuits within the aircraft respond to both magnetic and electric fields. Magnetic fields may be produced by either the aperture or diffusion coupling modes. Electric fields, on the other hand, can, as a practical matter, be coupled only through apertures.

Changing magnetic fields gives rise to changing electric fields, and changing electric fields give rise to changing magnetic fields.

The ratio of electric to magnetic field intensity is called the characteristic impedance of the structure or enclosure. That impedance is highly dependent upon location within a structure and highly dependent upon the equipment located within that structure. In principle, one can calculate that impedance for structures of elementary shapes, at least as long as they are empty. While the interdependence of electric and magnetic fields has an important bearing upon the response of electric circuits, it is rather doubtful that available tools are of sufficient power to predict what that interdependence will actually be in an aircraft where the enclosures are of complex geometry and full of equipment.

In this section there will be discussed four major themes: the external electromagnetic field environment, the mechanism of coupling through apertures, the diffusion coupling phenomena, and the use of two of the tools available for study of the electromagnetic field environment. One of the tools, a computer program APERTURE, was developed under a previous contract (Reference 4.1) and will only be reviewed here. The other tool, a computer program called DIFFMAG, is new and will be described in considerable detail.

4.2 THE EXTERNAL MAGNETIC FIELD

The external magnetic field is primarily of interest in that it is the field to which apertures are exposed and is hence the

source of the field that leaks into the interior through the apertures. It also has a bearing upon the character of the voltages produced by the diffusion mechanism.

4.2.1 Elementary Concepts

If a long conductor is carrying a current, I , and the return path is far removed, the average field intensity, H_{av} , at a distance, r , from the conductor, as shown in Figure 4.1a, is

$$H = \frac{I}{2\pi r} \quad (4.1)$$

If, instead of being carried on a solid wire, the current is carried on a hollow tube of radius r , as shown in Figure 4.1b, the field intensity, H , at radius r is again

$$H = \frac{I}{2\pi r} \quad (4.2)$$

and at the surface of the tube, where $r = r_o$, the field intensity is

$$H = \frac{I}{2\pi r_o} \quad (4.3)$$

In the interior of the tube, $r < r_o$, the field intensity is zero, a concept that will be treated in more detail later.

Since the circumference, P , of the tube is

$$P = 2\pi r_o \quad (4.4)$$

it follows that the field intensity at the surface of the tube is also equal to the total current divided by the circumference.

$$H = \frac{I}{P} \quad (4.5)$$

The unit of field intensity is amperes per meter if the radius or circumference is measured in meters.

From Equation 4.5, it can be seen that the numerical value of the average magnetic field intensity is the same as the numerical value of the average current density. This holds true on any level; the magnetic field intensity is equal to the current density at that surface, at least as long as the surface is composed of a good conductor. The reason for qualifying the statement to include only good conductors will be elaborated upon later.

If the conductor is not cylindrical, as shown in Figure 4.2, the field intensity will be different at different points on the structure.

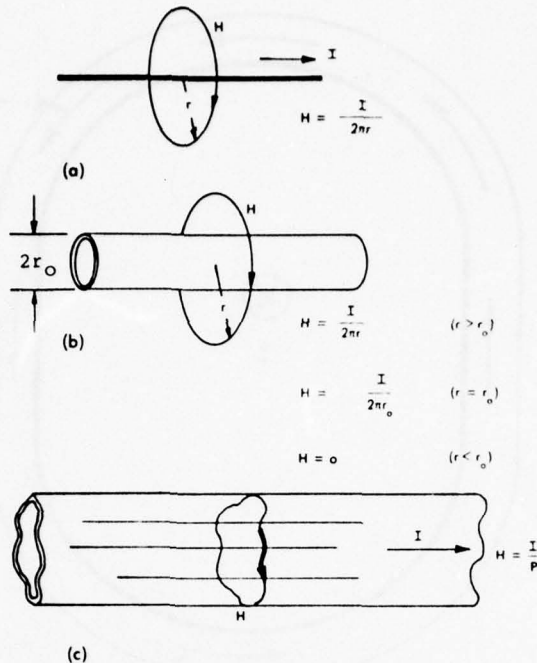


Figure 4.1 Magnetic Fields Around Current-Carrying Conductors

- (a) Current-Carrying Filament
- (b) Tubular Conductor
- (c) Irregular Conductor

The actual field intensity will be greater than average at points where the radius of curvature is less than average; it will be less than average at points where the radius of curvature is greater than average, as shown in Figure 4.2. For example, the circumference of the fuselage of a typical fighter aircraft just forward of its wing is about 5.5 m. Assuming a lightning stroke current of 30,000 A to flow through the fuselage, the average field intensity at the surface would be

$$H = \frac{I}{2\pi r} = \frac{I}{P} = \frac{30,000}{5.5} = 5455 \text{ A/m} \quad (4.6)$$

Since there are no points of very sharp radius, the field intensity around the fuselage would probably not vary greatly from the average value.

The situation along a wing carrying lightning current is considerably different in that the leading and trailing edges have radii of curvature much smaller than the average. Field intensity along the leading and trailing edges would be quite high compared to the field intensity along the top and bottom surfaces, for example. The field intensity would, at any rate, be equal to the current density at that point.

The current density at the surface of a conductor is determined by both magnetic effects and by resistive effects. At high

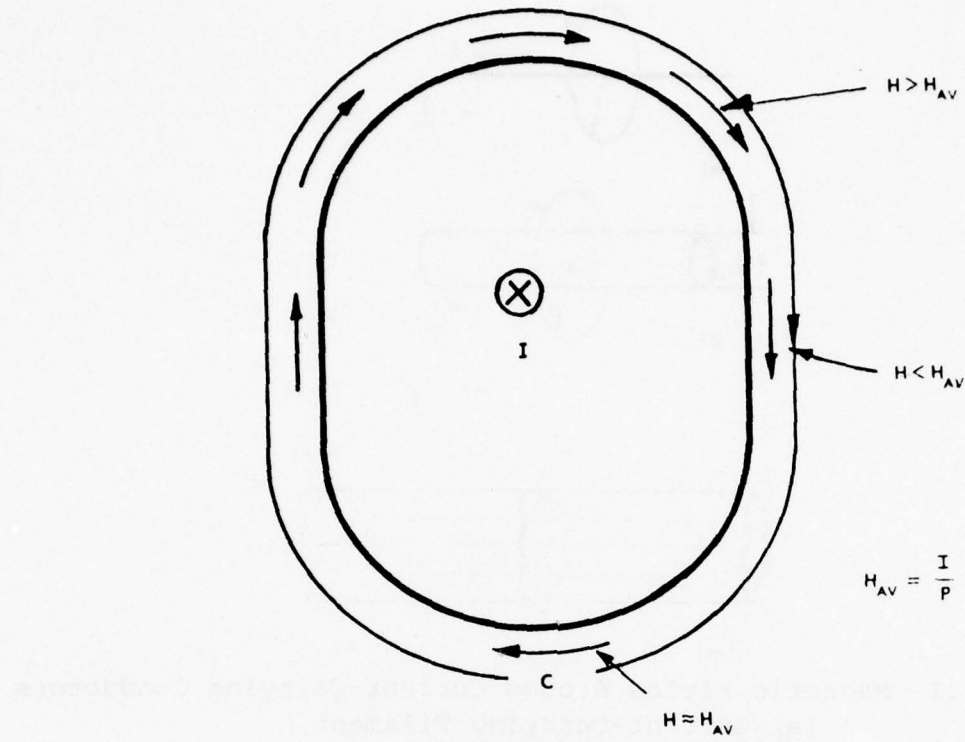


Figure 4.2 Field Intensity Vs. Radius of Curvature

frequencies, the distribution of current is controlled by the magnetic effects. At low frequencies, it is determined by resistance effects. The question of what is "high" and what is "low" depends upon the physical size of the structure and the resistivity of the material from which the structure is made. In many cases the "high" frequency is surprisingly low in absolute terms. Since the distribution of current is frequency-dependent, it follows that it is also time-dependent. If a step function of current is injected into a structure, the current will initially distribute in accordance with the magnetic effects. As time progresses, the current distribution will shift until at dc the current density will be determined by resistance effects. The manner in which the current is distributed upon a surface and the manner in which the distribution changes with time or with frequency has some important bearing upon the magnetic fields around and inside the aircraft structures and upon the voltages or currents that may be induced upon wires within those structures. The phenomena have been discussed in detail in other works, but since it is central to an understanding of lightning interaction phenomena and to an understanding of what the computer routine DIFFMAG (to be presented shortly) is intended to do, we will discuss the phenomena in considerable detail in the section on diffusion coupling phenomena. For the moment, it is sufficient to say that a study of lightning interaction phenomena requires a knowledge of both the initial and final distributions of current and of the way in which the distribution changes from the initial to the final value.

In some simple geometries, the distribution of current can be calculated rather easily. Around the periphery of a cylinder, for example, the current density is uniform, assuming the return path for the current is far removed from the cylinder—i.e., greater than ten times the diameter of the cylinder. The density of current as determined by magnetic effects is the same as that determined by resistance effects, assuming that the wall of the cylinder is of uniform thickness.

Another geometry of considerable practical importance is the ellipse, shown in Figure 4.3. At the center ($X = 0$), the magnetic field intensity is given by

$$H = \frac{I}{\pi b} \quad (4.7)$$

and at the edge ($Y = 0$)

$$H = \frac{I}{\pi d} \quad (4.8)$$

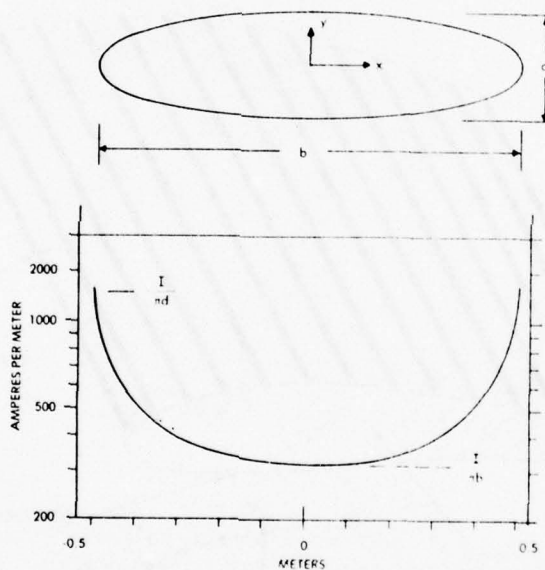


Figure 4.3 Magnetic Field Intensity at the Surface of an Elliptical Conductor

At intermediate points, the magnetic field intensity or current density is given by the expression (References 4.2 and 4.3)

$$H_{\text{surface}} = \frac{I}{\pi} \frac{1}{\sqrt{b^2 - (2x)^2} \left[1 - \frac{d^2}{b^2} \right]} \quad (4.9)$$

This current distribution does not hold for dc currents where the current density over the surface is determined by the dc resistance. If the conductor were an elliptical cylinder of uniform thickness, the current density would be uniform.

4.2.2 Calculation of External Magnetic Field Intensity

In many cases the external current density may be determined with accuracy sufficient for practical purposes by approximating the surface under consideration by an ellipse or ellipses. If such an approximation does not give sufficient accuracy, there are other techniques that may be used. These techniques are discussed in considerable detail in other works. One of those techniques is shown on Figure 4.4. It involves approximating the surface by a grid of wires, determining how the current divides among those wires, and then determining the magnetic field produced by the wires. The computer routine DIFFMAG provides a means of evaluating how the current divides among the conductors and of determining the magnetic fields produced by the current. Figure 4.5 gives an example of how a wire grid model predicts the tangential magnetic field around such an ellipse.

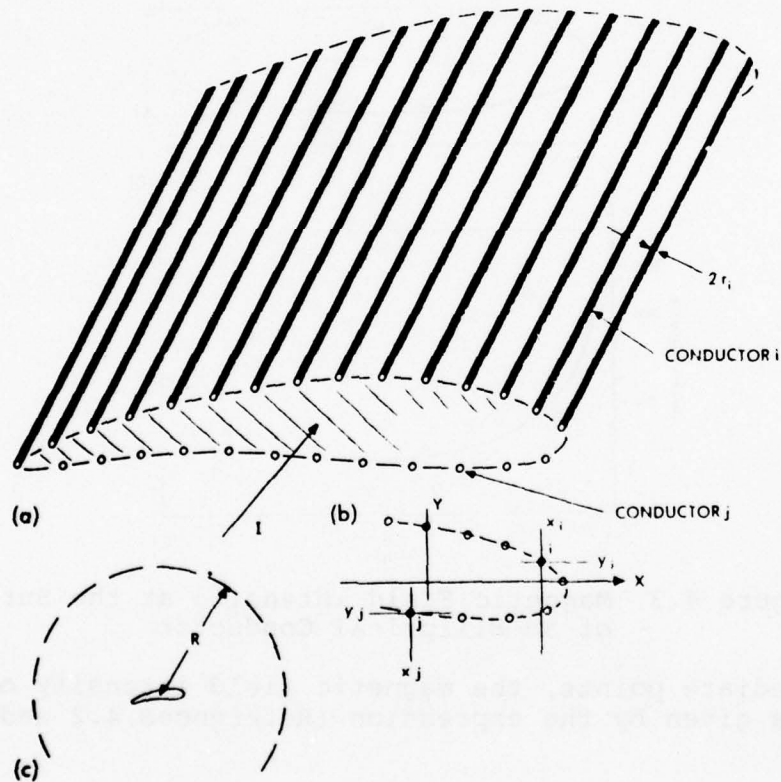


Figure 4.4 A Structure Defined as an Array of Wires
 (a) The Array
 (b) Coordinates Defining Location
 (c) Definition of the Return Path for Current

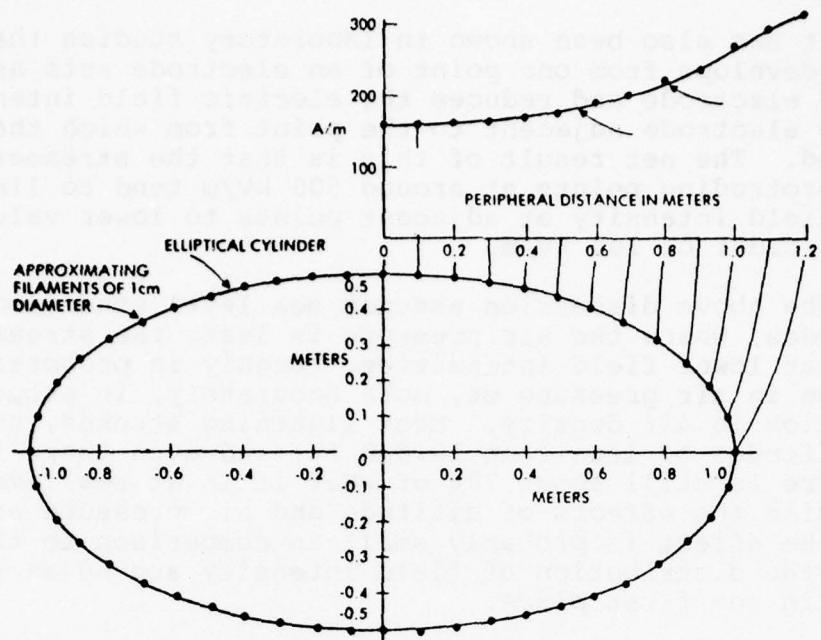


Figure 4.5 Wire Grid Approximation of the Elliptical Fuselage

4.3 THE EXTERNAL ELECTRIC FIELD

Little work has been done to determine the electric field around an aircraft when it is struck by lightning. In theory, if one knows the charge deposited upon the aircraft during the passage of the lightning stroke, one can calculate how that charge will distribute upon the surface of the aircraft and determine what the electric field strength would be. In practice this is difficult for two reasons: first, the total charge, which is related to the total potential on the aircraft is not known, at least to the degree to which the total current passing through the aircraft is known, and, second, because of the nonlinear behavior of the field intensity when the aircraft is raised to very high potentials. The nonlinear effects are due to the influence of electrical streamers on the electric field at points adjacent to the streamer. Tests in laboratories have shown that, when the electric field intensity around an electrode reaches about 500 kV/m , ($5 \times 10^5 \text{ V/m}$), electrical discharges take place from the electrode. These discharges are called streamers. If the field is maintained long enough, a few microseconds or a few tens of microseconds, the streamers can develop into full-fledged electrical arcs between electrodes. The electrical discharges are initiated at points where the electric field intensity is highest. On an aircraft, the electric field intensity will be highest around leading and trailing edges and around the tips of wings and stabilizers. It follows that the electric field intensity around more gently curved surfaces will be less. Possibly, though it is mostly speculation, the electric field intensity around gently curved surfaces would be no more than 100 kV/m when the field intensity around protruding points reaches 500 kV/m .

It has also been shown in laboratory studies that a streamer which develops from one point of an electrode acts as an extension of the electrode and reduces the electric field intensity at points on the electrode adjacent to the point from which the streamer developed. The net result of this is that the streamers which develop from protruding points at around 500 kV/m tend to limit the electric field intensity at adjacent points to lower values, possibly on the order of 100 kV/m.

The above discussion assumes sea level conditions. At higher altitudes, where the air pressure is less, the streamers will develop at lower field intensities, roughly in proportion to the reduction in air pressure or, more accurately, in proportion to the reduction in air density. Most lightning strokes, however, occur at altitudes of less than 10,000 ft, and even there the atmospheric pressure is still about 70% of what it is at sea level. Accordingly, while the effects of altitude and air pressure are significant, the effect is probably small in comparison to the degree to which the distribution of field intensity around an aircraft is known in the first place.

From this discussion it is obvious that little is known about the electric field around the surface of an aircraft during the time a lightning stroke is approaching or passing through the aircraft. An educated guess about the magnitude of the electric field is perhaps as accurate as a more involved analytical calculation. Accordingly, it is this author's recommendation that, in the absence of better information, a value of 100 kV/m be used as the worst case value of electric field intensity at the surface of an aircraft when that aircraft is struck by lightning.

4.4 THE APERTURE COUPLING MECHANISM

4.4.1 Magnetic Fields

In lightning interaction problems, the external magnetic fields are of importance only inasmuch as they are the starting point for determining the magnetic fields within a structure.

The most important mode by which magnetic fields are coupled from the exterior of the aircraft to the interior is coupling through apertures. There are two major reasons for the importance of aperture-coupled fields. The first is that some apertures may be quite large, windows being a prime example. The second reason is that, unlike fields coupled by diffusion through metal surfaces, the waveshape of the interior field is not retarded, but tends to be the same for small apertures as that of the external magnetic field. The most important consequence of the coupled magnetic fields relates to the voltages induced by such fields. A field of given peak intensity is more apt to cause trouble if it rises to its peak quickly than if it is delayed and distorted.

Physically, the basic problem is as shown on Figure 4.6. An external magnetic field tangential to a metal surface passes across

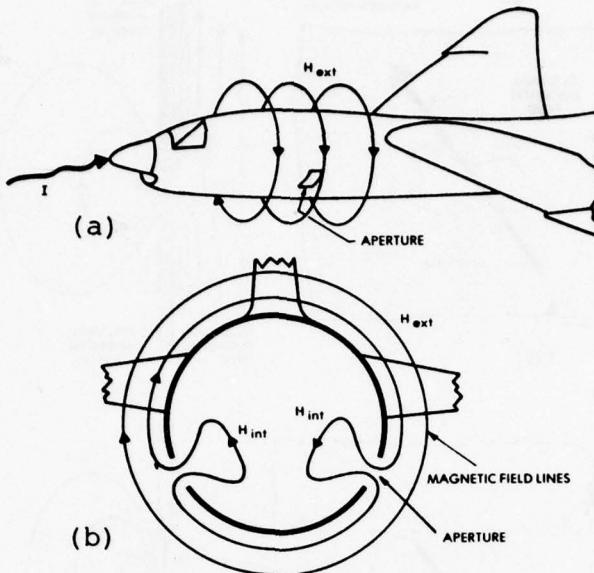


Figure 4.6 Aperture-Type Magnetic Field Coupling

- (a) External Field Patterns
- (b) Internal Field Patterns

an aperture. At the aperture some of the lines of magnetic force leak into the interior region. Analytically, the problem is to be able to determine the field strength at any point in the interior volume, preferably to be able to determine both the magnitude and the direction of the magnetic field.

Often the analytical problem is best solved by placing an equivalent magnetic dipole in the plane of the aperture. The fields may then be determined from dipole theory. Such an equivalent dipole is shown on Figure 4.7. The strength of the equivalent dipole is determined by the strength of the external magnetic field and by the size, shape, and orientation of the aperture. A geometry amenable to mathematical analysis (Figure 4.8) is that of an elliptical aperture in a conductive sheet of a size large enough to separate completely the interior volume in which the fields are to be calculated from the exterior volume in which the basic magnetic field exists. In the following analysis we will treat only fields tangential to the conductive surface, since, as explained in the previous sections, a magnetic field with components perpendicular to the conductive surface induces circulating currents that initially cancel the penetrating component.

Mathematically the problem is most directly solved if the external magnetic field is resolved into two components, H_x and H_y , lying along an axis directed through the major and minor axes of the elliptical aperture. These field components give rise to two equivalent magnetic dipoles, M_x and M_y , again oriented along the major and the minor axes of the aperture. The strength of these

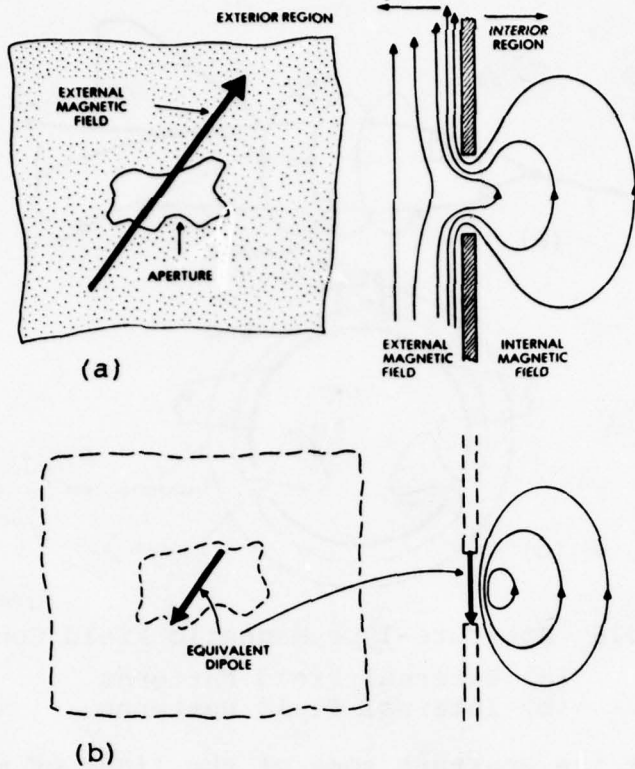


Figure 4.7 The Aperture-Coupling Problem

- (a) A Field Across an Aperture
- (b) Equivalent Dipole Producing the Same Internal Field

dipoles is a function of the strength of the external magnetic field that would exist in the plane of the aperture if the aperture were absent. The governing expressions (Reference 4.4) are

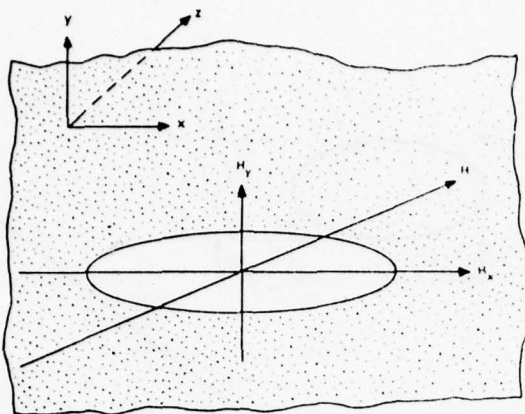
$$M_x = \alpha_{11} H_x \quad (4.10)$$

$$M_y = \alpha_{22} H_y \quad (4.11)$$

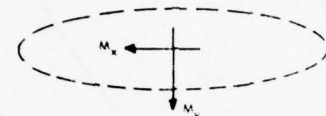
$$\alpha_{11} = -\frac{2\pi}{3} \left[\frac{l_1}{2} \right]^3 \frac{e^2}{K(e^2) - E(e^2)} = -\left[\frac{l_1}{2} \right]^3 \alpha'_{11} \quad (4.12)$$

$$\alpha_{22} = -\frac{2\pi}{3} \left[\frac{l_1}{2} \right]^3 \frac{e^2(1-e^2)}{E(e^2) - (1-e^2)K(e^2)} = -\left[\frac{l_1}{2} \right]^3 \alpha'_{22} \quad (4.13)$$

$$e^2 = 1 - \left[\frac{l_2}{l_1} \right]^2 \quad (l_2 < l_1) \quad (4.14)$$



(a)



(b)

Figure 4.8 An Elliptical Aperture

(a) Geometry and the Components of
the External Magnetic Field Vector
(b) The Equivalent Magnetic Dipoles

The expressions K_e and E_e are elliptical integrals of the first and second kinds, respectively. The quantities α'_{11} and α'_{22} are shown in Figure 4.9. Since the dipole strength is proportional to the cube of the major axis length of the aperture, it follows that large apertures will couple much more field into an inner volume than will small apertures, the strength of the dipole increasing faster than the area of the aperture increases.

The pattern of magnetic fields in the interior volume produced by a dipole lying along the X axis would appear as on Figure 4.10. Assuming the dipole to lie in the XY plane, the field patterns will be concentric closed loops lying in planes passed through the X axis. At any point, P, the total magnetic field will be tangential to the corresponding closed loop. The components of the magnetic field at point P-- H_x , H_y , and H_z --(Reference 4.5) will be

$$H_x = \frac{M_x}{4\pi} \frac{3x^2 - r^2}{r^5} \quad (4.15)$$

$$H_y = \frac{M_x}{4\pi} \frac{3xy}{r^5} \quad (4.16)$$

$$H_z = \frac{M_x}{4\pi} \frac{3xz}{r^5} \quad (4.17)$$

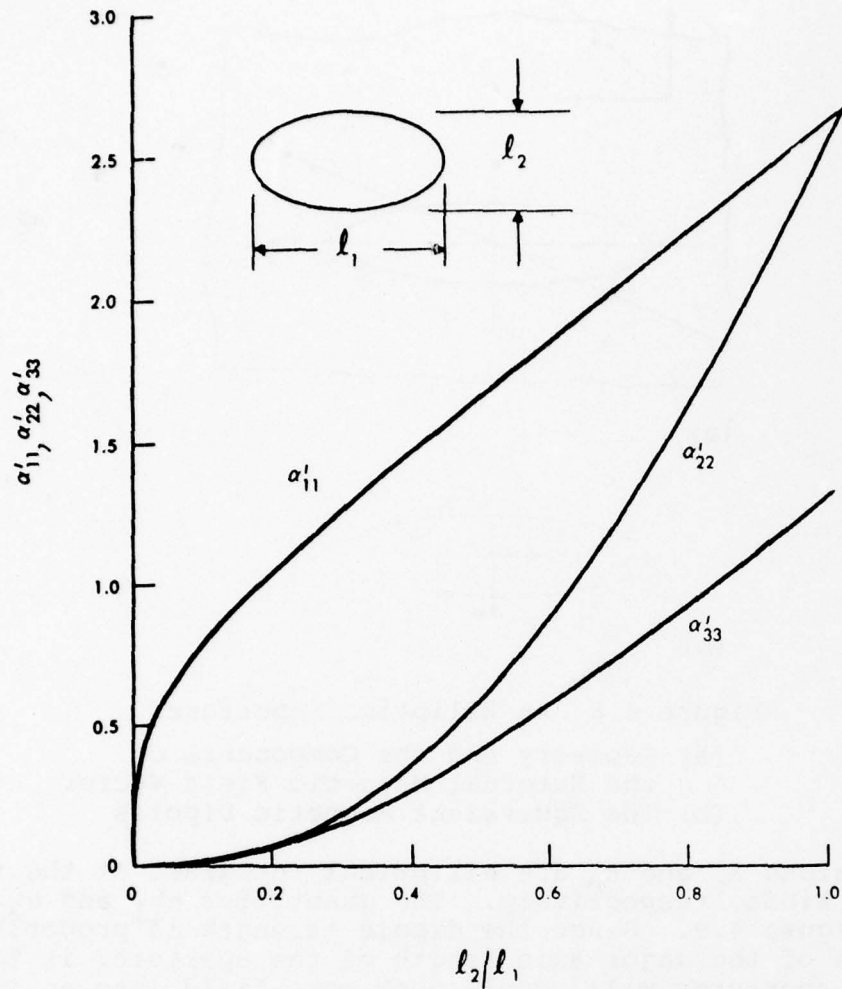


Figure 4.9 Shape Factor for Elliptical Apertures

Typically, the external magnetic field would include an equivalent dipole oriented along the Y axis as well. This dipole would likewise produce a magnetic field at the point P, the components of which would be

$$H_x = \frac{M_y}{4\pi} \frac{3xy}{r^5} \quad (4.18)$$

$$H_y = \frac{M_y}{4\pi} \frac{3y^2 - r^2}{r^5} \quad (4.19)$$

$$H_z = \frac{M_y}{4\pi} \frac{3yz}{r^5} \quad (4.20)$$

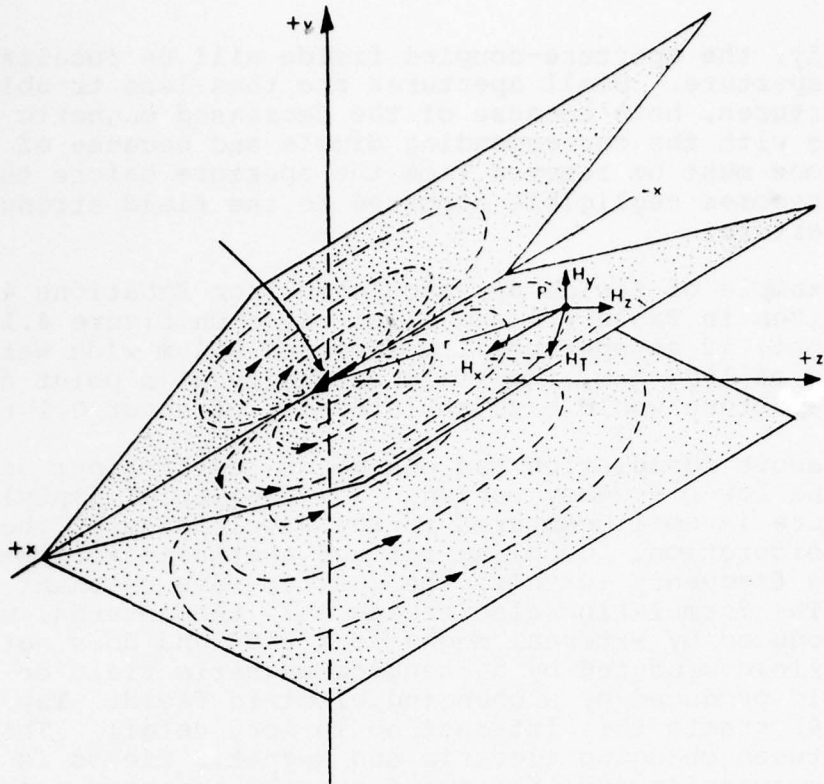


Figure 4.10 Field Patterns Produced by a Dipole Lying Along the X-Axis

The total magnetic field strength at P , then, would be the sum of the components produced by the dipoles lying along the X and Y axes. Thus,

$$H_x = H_{xx} + H_{xy} \quad (4.21)$$

$$H_y = H_{yx} + H_{yy} \quad (4.22)$$

$$H_z = H_{zx} + H_{zy} \quad (4.23)$$

The total field strength at point P would be the vector summation of the X , Y , Z components of the field.

$$H_T = \sqrt{H_x^2 + H_y^2 + H_z^2} \quad (4.24)$$

The field strength is seen to be inversely proportional to the cube of the distance from the aperture to the point in question.

Accordingly, the aperture-coupled fields will be localized in space near the aperture. Small apertures are thus less troublesome than large apertures, both because of the decreased magnetic field strength associated with the corresponding dipole and because of the lesser distance one must be removed from the aperture before the field strength becomes negligible compared to the field strength closer to the aperture.

An example of fields as calculated from Equations 4.15 through 4.17 is given in Table 4.1 and illustrated on Figure 4.11. It indicates that, if an aperture 1 m long and 0.4 m wide were exposed to a field of 1000 A/m, the field intensity at a point about 5 m from the aperture would have an intensity of about 0.1 to 0.2 A/m.

The above formulation has one major restriction: it is valid only in the low-frequency region, "low-frequency" implying that the aperture is small compared to the wavelengths of the field under consideration. Coupling through apertures increases with increasing frequency (witness the quarter-wave resonant slot antenna). The formulation also treats only the internal magnetic fields produced by external magnetic fields and does not treat the electric field produced by a changing magnetic field or the magnetic field produced by a changing electric field. Taylor (Reference 4.4) treats this interaction in more detail. This interaction between changing electric and magnetic fields is greater at high frequencies and, for the frequency spectrum associated with lightning, is possibly of importance only at those frequencies for which the aperture is not electrically small.

The above formulation is also valid only when the point at which the field is to be calculated is at a distance from the aperture that is large compared to the dimensions of the aperture. If an attempt is made to calculate the fields close to the aperture, the results are inaccurate. If the distance from the point to the aperture goes to zero, the calculated magnitude of fields becomes infinite, whereas the field itself can never in fact become larger (barring reflections) than the external field. It can be shown, in fact, that the actual field strength in the plane of the aperture, as distinct from the strength of the equivalent dipole, will be half the field strength that would exist if the aperture were not there. This intractable behavior of the calculated magnitude of the field near the aperture arises as a result of a simplifying assumption commonly used in dipole analysis. This assumption, illustrated in Figure 4.12a, is that point P is sufficiently far from the center of the dipole that each of the radial distances r_1 and r_2 , from the ends of the dipole to the point P may be represented by the average radial distance, r , and that each of the angles θ_1 and θ_2 may be represented by the angle θ .

With a great increase in numerical complexity, it is possible to develop a formulation for the fields at point P that, as shown in Figure 4.12b, allows the dipole to have a finite length. Such a formulation allows one to determine with better, though not

TABLE 4.1
CALCULATIONS RELATED TO FIGURE 4.11

$$l_1 = 1 \text{ m}$$

$$l_2 = 0.4 \text{ m}$$

$$l_{2/l_1} = 0.4 \text{ m}, \alpha'_{11} = 1.5 \text{ m}, \alpha'_{22} = 0.4$$

$$\alpha_{11} = - \left[\frac{l_1}{2} \right]^3 \quad \alpha'_{11} = -0.188$$

$$\alpha_{22} = - \left[\frac{l_1}{2} \right]^2 \quad \alpha'_{22} = -0.050$$

$$H_x \text{ ext} = 1000 \text{ A/m}$$

$$H_y \text{ ext} = 0$$

$$M_x = \alpha_{11} H_x \text{ ext} = -188$$

$$M_y = \alpha_{11} H_y \text{ ext} = 0$$

At Point 1

$$X = 0, Y = 0, Z = 5 \text{ m}, r = 5 \text{ m}$$

$$H_x = + 0.120 \text{ A/m}$$

At Point 2

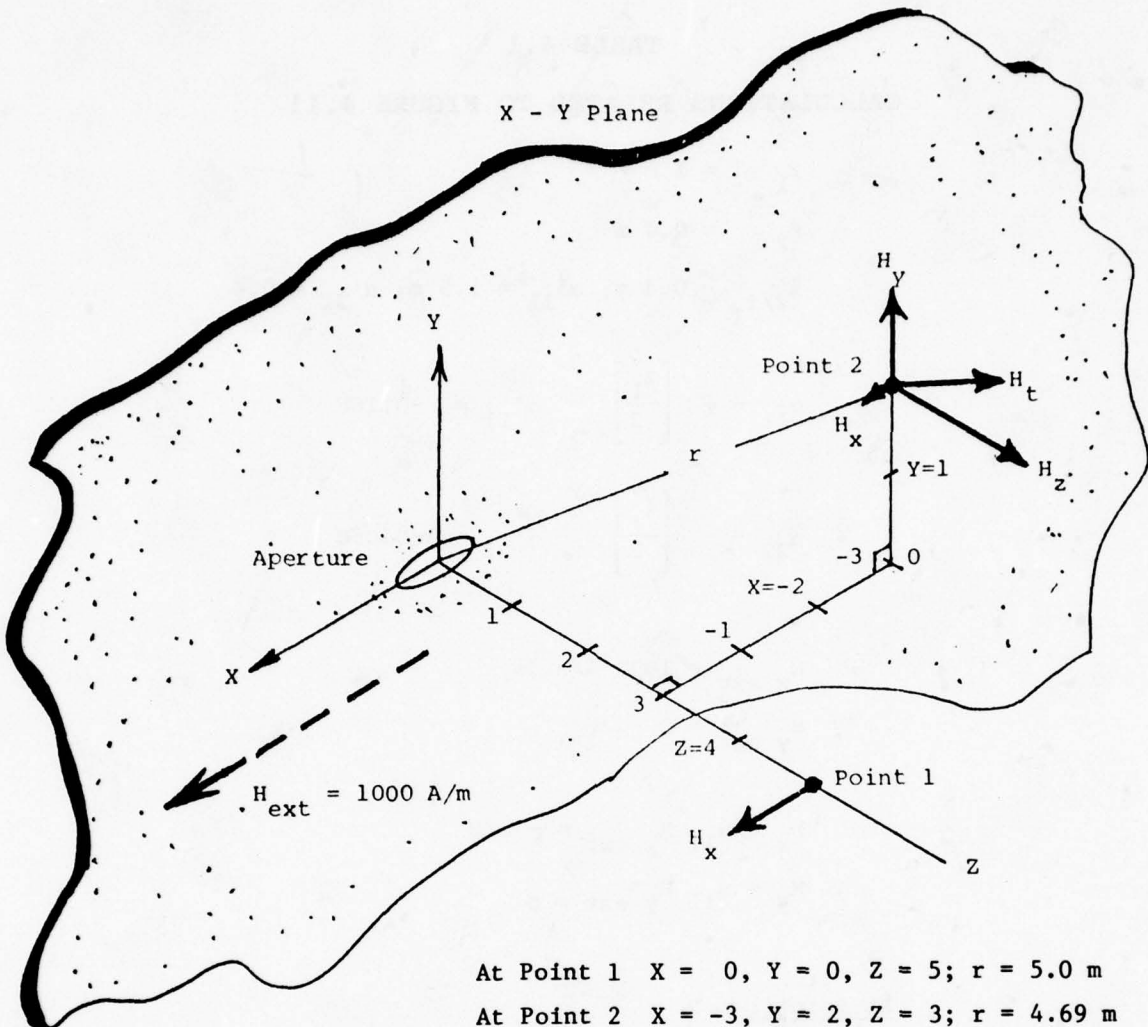
$$X = -3, Y = 2, Z = 3, r = 4.69 \text{ m}$$

$$H_x = + 0.033 \text{ A/m}$$

$$H_y = + 0.119$$

$$H_z = + 0.178$$

$$H_t = 0.217$$



At Point 1 $X = 0, Y = 0, Z = 5; r = 5.0 \text{ m}$

At Point 2 $X = -3, Y = 2, Z = 3; r = 4.69 \text{ m}$

At Point 1 $H_x = 0.120 \text{ A/m}$

$H_y = 0$

$H_z = 0$

At Point 2 $H_x = 0.033 \text{ A/m}$

$H_y = 0.119$

$H_z = 0.178$

$H_t = 0.217$

Figure 4.11 An Illustrated Example of Aperture-Coupled Fields

perfect, accuracy the field close to the aperture. While that formulation will not be given here, it is given in the literature (Reference 4.6).

Frequently, a calculation made to determine the effects of coupling through apertures needs to take into account the presence of reflecting surfaces. The simplest case, shown in Figure 4.13, treats one reflecting surface of infinite dimensions and parallel to the surface containing the aperture. The total field at any

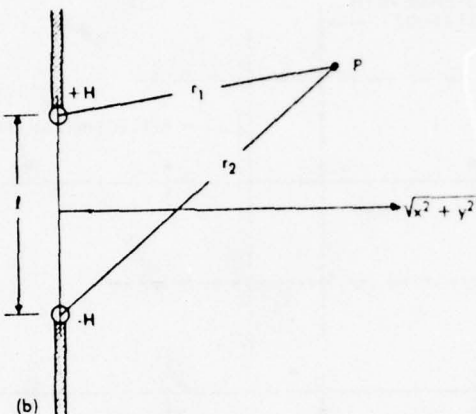
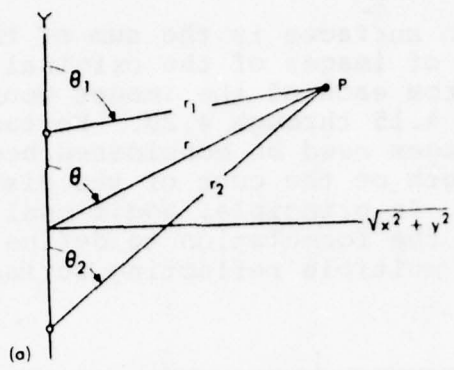


Figure 4.12 Dipole Approximations

- (a) Elementary Dipole
- (b) Dipole of Finite Size

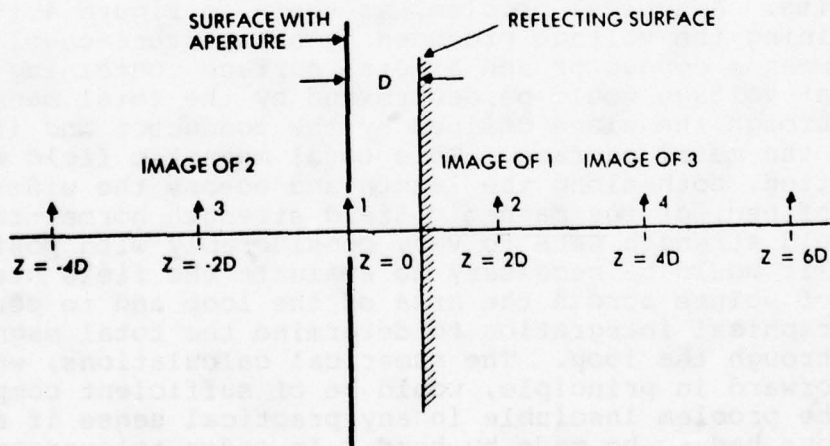


Figure 4.13 Reflecting Surface

point between the two surfaces is the sum of the fields produced by an infinite array of images of the original magnetic dipole. The field strength from each of the images would again be determined from Equations 4.15 through 4.20. Fortunately, in most cases only a few of the images need be considered because of the dependence of field strength on the cube of the distance to the point under consideration. In principle, additional reflecting surfaces could be included in the formulation to define completely an interior volume. Such multiple reflecting surfaces are shown on Figure 4.14.

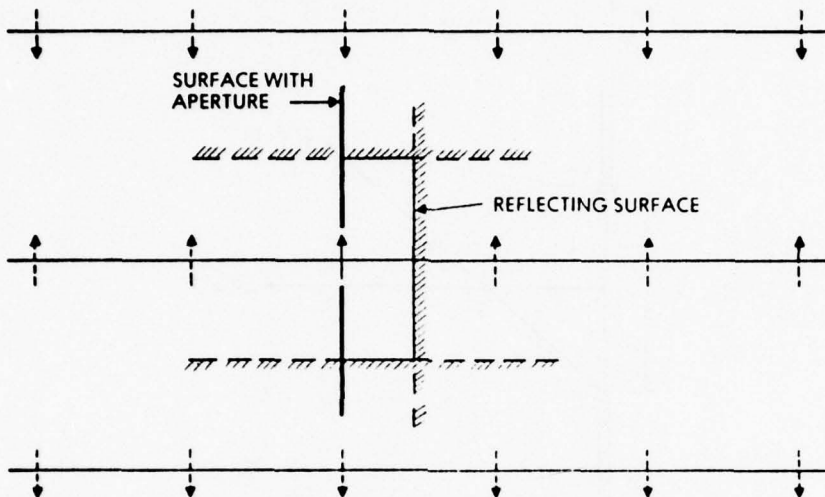


Figure 4.14 Multiple Reflecting Surfaces

Typically, one is concerned, not with the magnitude of the fields themselves, but with the effects of the fields on electrical circuits. A typical problem, as shown in Figure 4.15, might be determining the voltage produced by an aperture-coupled magnetic field between a conductor and a metal surface containing the aperture. That voltage would be determined by the total magnetic flux passing through the plane defined by the conductor and its projection onto the metal surface. This total magnetic field would be the summation, both along the length and across the width of the loop so defined, of the magnetic field strength normal to the loop. If the field strength were to vary considerably with position along the loop, it would be necessary to evaluate the field strength at a number of points across the area of the loop and to perform some sort of graphical integration to determine the total magnetic flux passing through the loop. The numerical calculations, while straightforward in principle, would be of sufficient complexity to make the problem insoluble in any practical sense if all the calculations had to be made by hand. In order to overcome the numerical problems, a computer program, APERTURE, has been written and is described in the literature (Reference 4.7). This program allows one to define an arbitrary elliptical aperture in an X-Y plane. The orientation of the aperture and the orientation and

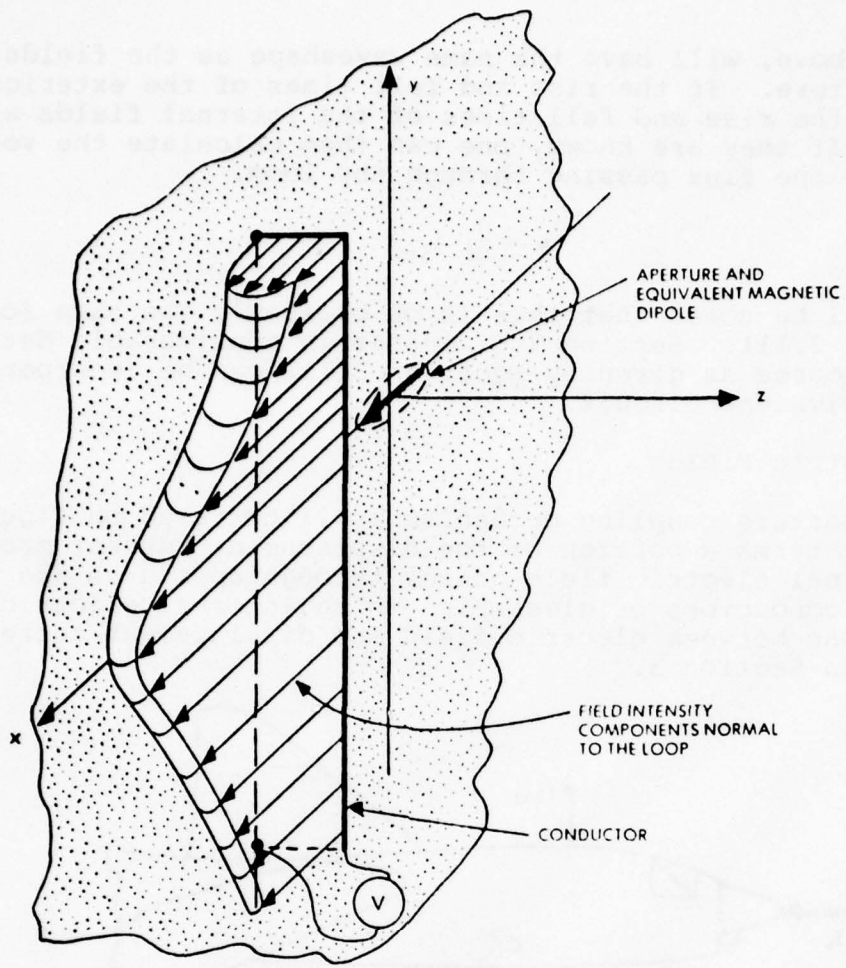


Figure 4.15 Determination of the Voltage Produced by Aperture Coupling

strength of the external field are defined as input quantities and do not necessarily have to be oriented along the X and Y reference axes. The program allows one to tabulate the interior field strength at whatever points are desired, in either rectangular or polar coordinates. The program also allows one to determine the total magnetic flux passing through any arbitrary four-sided plane surface. The program calculates the field strength normal to that surface and performs the graphical integration suggested in Figure 4.15 and necessary to determine the total magnetic flux passing through the plane of the loop.

If the total flux is known, the voltage may be calculated if one knows the waveshape of the flux external to the aperture.

Since the formulation of the aperture coupling equations presented above treats only the low-frequency approximation to the coupling mechanism and neglects any frequency-dependent properties of the mechanism, it follows that the fields on the interior, as

predicted above, will have the same waveshape as the fields external to the aperture. If the rise and fall times of the exterior fields are known, the rise and fall times of the internal fields will also be known. If they are known, one can then calculate the voltage produced by the flux passing through the loop.

$$e = \frac{d}{dt} \phi_{int} \quad (4.25)$$

It will be noted that this is of basically the same format as Equation 3.111. Section 3 discusses in considerable detail how a voltage source as given by Equation 3.111 can be incorporated into an equivalent circuit.

4.4.2 Electric Fields

The aperture coupling mechanism is illustrated on Figure 4.16. In simplest terms a portion of the displacement current produced by an external electric field passes through apertures and either flows upon conductors or gives rise to an internal electric field. The relations between electric field and displacement current were discussed in Section 3.

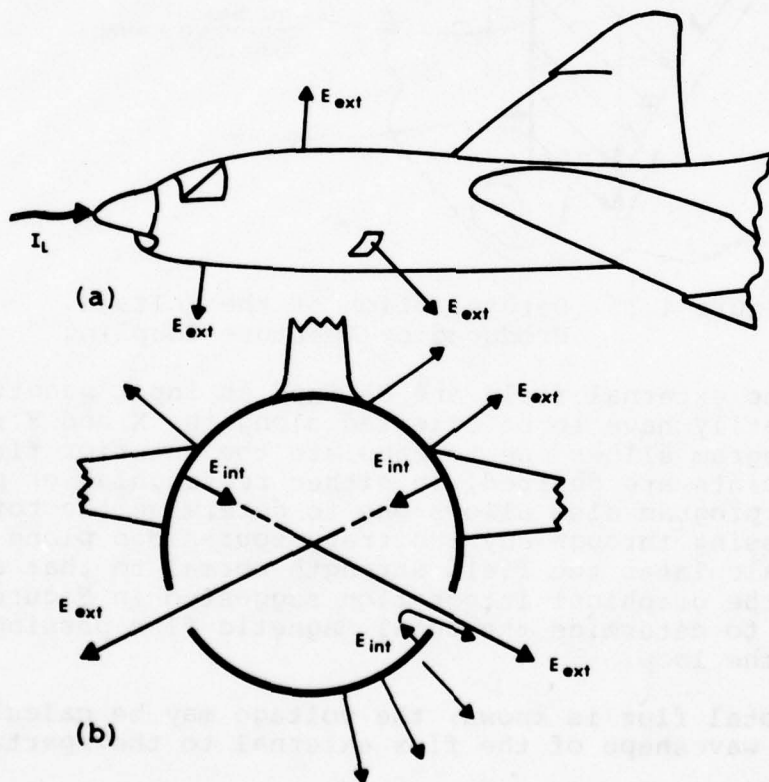


Figure 4.16 Aperture-Type Electric Field Coupling

- (a) External Field Patterns
- (b) Internal Field Patterns

Unlike magnetic fields, which may penetrate into an interior region either through apertures or by diffusion through continuous walls, electric fields, as a practical matter, can couple only through apertures. Any metallic surface provides sufficient shielding against electric fields that considerations of direct penetrations of the field through a metal surface can be neglected. Electric fields of practical consequence can exist only perpendicular to a metallic surface, since, in a manner analogous to penetrating magnetic fields, electric fields of oblique incidence have all but the perpendicular component of the field shorted out by the low impedance of the metallic surface. The appropriate geometry for electric field coupling, then is as shown in Figure 4.17. The electric fields of the interior region may be calculated as though they were produced by an electric dipole of strength (Reference 4.8):

$$D = \alpha_{33} E_z \quad (4.26)$$

$$\alpha_{33} = -\frac{2\pi}{3} \left[\frac{\ell_1}{2} \right]^3 \frac{(1 - e^2)}{E(e^2)} = \left[\frac{\ell_1}{2} \right]^3 \alpha'_{33} \quad (4.27)$$

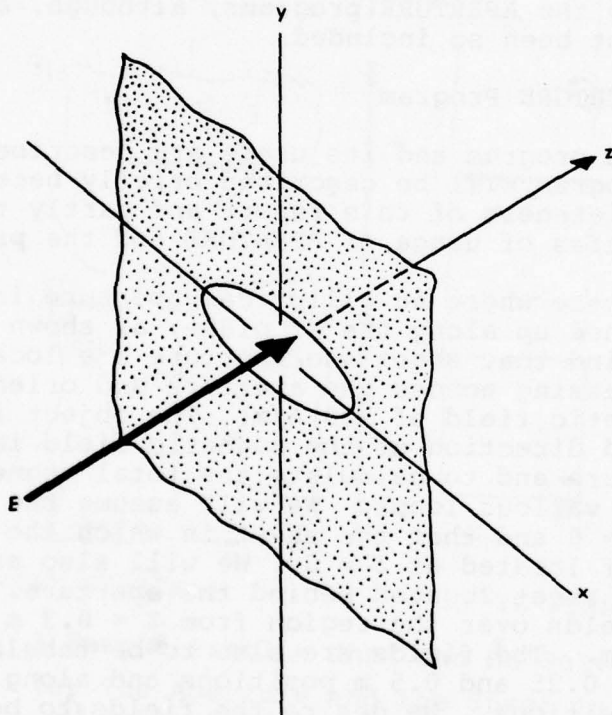


Figure 4.17 Geometry Appropriate to Electric Coupling

The quantity α'_{33} has previously been presented in Figure 4.9. Subject to the provisions that the dimensions of the aperture be small compared to the wavelengths of the highest frequency component in the external electric field and that electric fields produced by changing magnetic fields can be neglected, the electric field in the interior region becomes

$$E_x = \frac{D_o}{4\pi} \left[\frac{3xz}{r^5} \right] \quad (4.28)$$

$$E_y = \frac{D_o}{4\pi} \left[\frac{3yz}{r^5} \right] \quad (4.29)$$

$$E_z = \frac{D_o}{4\pi} \left[\frac{3z^2 - r^2}{r^5} \right] \quad (4.30)$$

These expressions are based upon the further assumption of a pure dipole and, as with Equations 4.15 through 4.20 for the magnetic field formulation, would indicate infinite field strengths as one approached the plane of the aperture, whereas in fact the field in the plane of the aperture would be one-half the field strength that would exist at that point if the aperture were absent. A power series expansion of the field from a dipole of finite size could be prepared but, as of this writing, has not been. The bookkeeping routines necessary to handle electric fields are virtually identical with those used for magnetic fields and could be incorporated into the APERTURE programs, although, as of this writing, they have not been so included.

4.4.3 Use of APERTURE Program

The APERTURE program and its usage are described in the literature. The program will be described briefly here, partly for the sake of completeness of this report and partly to illustrate certain similarities of usage of APERTURE and the program DIFFMAG.

Consider a case where an elliptical aperture is located in a metal sheet lined up along the XY plane, as shown in Figure 4.18a. In the space behind that sheet and aperture are located four loops, Figure 4.18b. Passing across the aperture and oriented along the Y axis is a magnetic field of 100 A/m. The object is to calculate the magnitude and direction of the magnetic field in the space behind the aperture and to calculate the total magnetic flux passing through the various loops. We will assume the loop to be located at X = Y = 0 and that the sheet in which the aperture is located is itself located at Z = 0. We will also assume that there is no reflecting sheet located behind the aperture. We wish to calculate the fields over the region from Z = 0.3 m to Z = 1.9 m in steps of 0.2 m. The fields are also to be tabulated along the X axis at the 0, 0.25 and 0.5 m positions and along the Y axis at the 0 and 1 m positions. We desire the fields to be tabulated in rectangular coordinates, though they could be tabulated in polar coordinates.

The four loops to be treated are all 1 meter deep and extend from Z = 0.5 m behind the aperture to A = 1.5 m behind the aperture. Loops 1, 2, and 3 are oriented along the XZ plane. Loop 4 is oriented along the YZ plane, and is therefore parallel to the internal field produced by the coupling through the aperture.

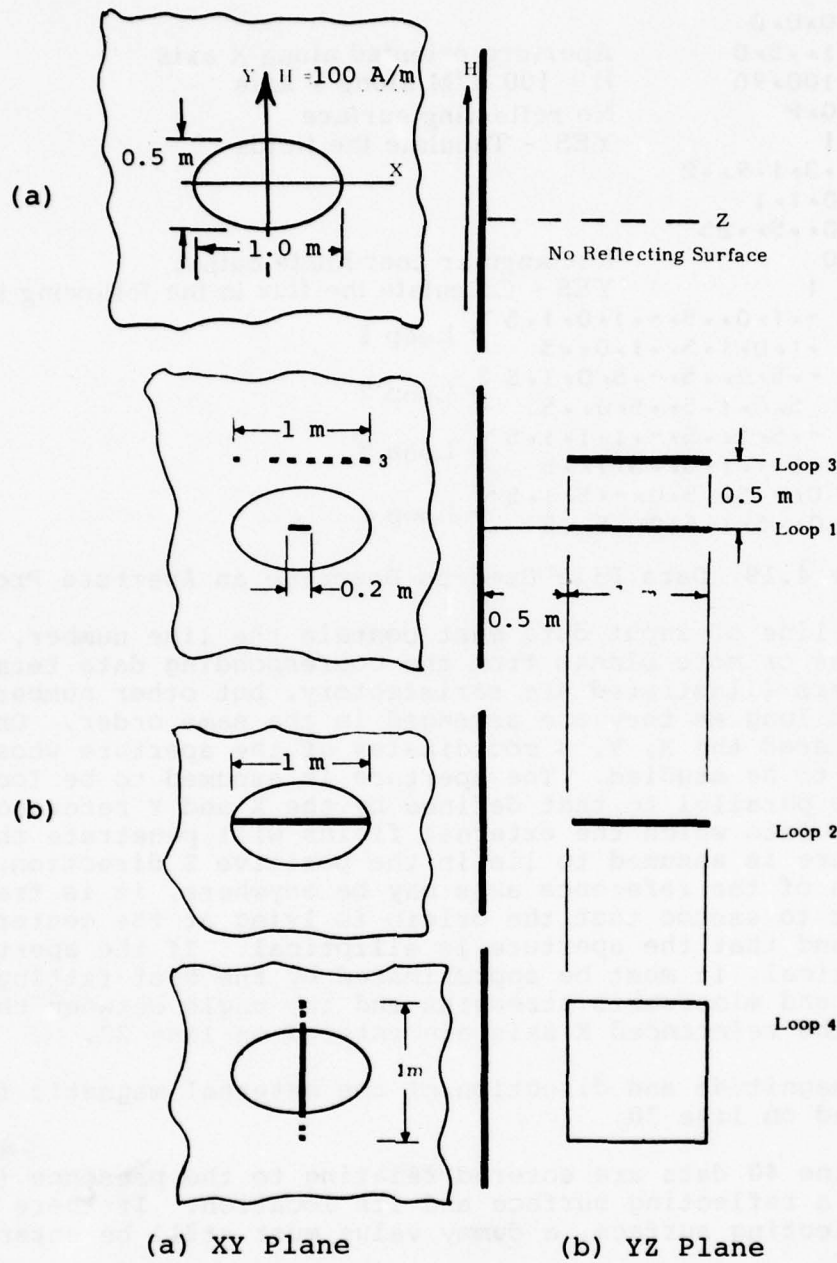


Figure 4.18 A Sample Problem That Can Be Solved by APERTURE

- (a) The Aperture and the Sheet in Which it Is Related
- (b) Loops Behind the Aperture

The data file that initiates the calculations is shown on Figure 4.19. The characteristics of the required data file are shown in more detail on Figure 4.20.

```

10 0,0,0
20 1,.5,0 Aperture oriented along X axis
30 100,90 H = 100 A/M along Y axis
40 0,2 No reflecting surface
50 1 YES - Tabulate the fields
60 .3,.1,.9,.2
70 0,1,1
80 0,.5,.25
90 0 Rectangular coordinate output
100 1 YES - Calculate the flux in the following loops
110 -.1,0,.5,-.1,0,1.5 } Loop 1
120 .1,0,1.5,.1,0,.5
130 -.5,0,.5,-.5,0,1.5 } Loop 2
140 .5,0,1.5,.5,0,.5
150 -.5,1,.5,-.1,1,1.5 } Loop 3
160 .5,1,1.5,.5,1,.5
170 0,-.5,.5,0,-.5,1.5 } Loop 4
180 0,.5,1.5,0,.5,.5

```

Figure 4.19 Data File Used to Describe an Aperture Problem

Each line of input data must contain the line number, separated by one or more blanks from the corresponding data terms. The line numbers illustrated are satisfactory, but other numbers may be used as long as they are arranged in the same order. On line 10 are entered the X, Y, Z coordinates of the aperture whose effects are to be studied. The aperture is assumed to be located in a plane parallel to that defined by the X and Y reference axes. The region into which the external fields will penetrate through the aperture is assumed to lie in the positive Z direction. While the origin of the reference axis may be anywhere, it is frequently convenient to assume that the origin is lying at the center of the aperture and that the aperture is elliptical. If the aperture is not elliptical, it must be approximated by the best fitting ellipse. The major and minor axis strengths and the angle between the major axis and the referenced X axis are entered on line 20.

The magnitude and direction of the external magnetic field are entered on line 30.

On line 40 data are entered relating to the presence (or absence) of a reflecting surface and its location. If there is to be no reflecting surface, a dummy value must still be entered for D2.

On line 50 a term is entered signifying whether or not the magnetic fields are to be tabulated over an interior volume. Lines 60, 70, and 80 define the X, Y, Z coordinates of the volume over which the fields are to be tabulated. If a tabulation is not desired, dummy values must be entered here. ZPA is the distance along the Z axis at which the tabulation should start, XPB is the location at which the tabulation should stop, and XPC is the increment between the start and stop values. YPA, YPB, and XPC are the corresponding quantities for the Y and X directions.

<u>Coordinates of the Aperture</u>			
10b	X Coordinate, (XA)	Y Coordinate (YA)	
	Z Coordinate (ZA)		
<u>Dimensions and Orientation of the Aperture</u>			
20b	Major Axis Length _____ (L1)	Minor Axis Length _____ (L2)	Orientation of Major Axis with Respect to the X-Axis _____ (ANAH)
		_____ (ANAH)	
<u>Magnitude and Direction of the External Magnetic Field</u>			
30b	Field Strength, (HEXT)	Orientation with Respect to X-Axis _____ (ANGH)	
<u>Reflecting Surface</u>			
40b	Is there a reflecting surface? For Yes enter 1 (one) and for No enter 0 (zero) _____ (D1)	How far from the aperture is the reflecting surface? If there is no reflecting surface enter the dummy number 1000 _____ (D2)	
<u>Tabulation of Field Strength</u>			
50b	Do you want a table of the field strengths over the interior region? For Yes enter 1 (one) and for No enter 0 (zero) _____ (D3)		
<u>Volume Over Which Fields are to be Calculated</u>			
<u>Z Dimension</u>			
60b	a) Start at, (ZPA)	b) End at, (ZPB)	c) And Increment in Steps of (ZPC)
<u>Y Dimension</u>			
70b	a) Start at, (YPA)	b) End at, (YPB)	c) And Increment in Steps of, (YPC)
<u>X Dimension</u>			
80b	a) Start at, (XPA)	b) End at, (XPB)	c) And Increment in Steps of, (XPC)
On lines 60, 70, and 80 enter the dummy numbers 0 (zero) in each of the locations if you don't want the fields tabulated			
<u>Output Format</u>			
90b	Do you want the tabulation in rectangular or spherical coordinates? Enter 1 (one) for spherical or 0 (zero) for rectangular. Enter a dummy value if no tabulation is desired. _____ (DY)		
<u>Total Flux in a Loop</u>			
100b	Do you want to determine the total flux linking a loop? Enter 1 (one) for Yes and 0 (zero) for No. _____ (D5)		
Enter the X, Y, Z coordinates of the four points defining the loop. They should go in sequence around the loop. All four points must lie in the same plane. If a loop calculation is not desired the following lines may be left blank, in which case the program makes an automatic stop.			
110b	Point 1 $\frac{X}{(PX1)}'$, $\frac{Y}{(PY1)}'$, $\frac{Z}{(PZ1)}'$	Point 2 $\frac{X}{(PX2)}'$, $\frac{Y}{(PY2)}'$, $\frac{Z}{(PZ2)}'$	
	Point 3 $\frac{X}{(PX3)}'$, $\frac{Y}{(PY3)}'$, $\frac{Z}{(PZ3)}'$	Point 4 $\frac{X}{(PX4)}'$, $\frac{Y}{(PY4)}'$, $\frac{Z}{(PZ4)}'$	
120b	Successive lines following the format of 110 and 120 may be used to enter the defining points for other loops. The program will automatically stop when it runs out of data.		

Figure 4.20 Input Data for Program APERTURE — Long Form

Line 90 determines whether the tabulated values should be in spherical or rectangular coordinates. Again, a dummy value should be entered if no tabulation is desired.

On line 100 the user enters the value corresponding to whether or not calculation of the total magnetic flux passing through a loop is desired. If such a calculation is desired, the X, Y, Z coordinates of the four points defining the corners of that loop should be entered on lines 110 and 120. Additional lines in the same format may be used to identify additional loops.

The output data that results from this data file are shown in Figure 4.21. Figure 4.21 shows the format of the manner in which the magnitude and direction of the fields are tabulated when they are printed in rectangular coordinates.

Another example of an aperture-coupled field is shown in Figure 4.22. An elliptical fuselage, shown dotted, has been approximated by two sheets of infinite size, one containing the aperture and another serving as the reflecting surface. This elliptical fuselage is the same that discussed in Section 4.2.2. The figure shows only the top half of the field pattern, the field in the bottom half being symmetrical. The aperture considered was 0.2 m high by 0.1 m wide, the long axis of the ellipse being oriented at right angles to the plane of the figure. The field strength at the surface of the aperture, assuming the aperture not to be there, was 167 A. That field strength would be produced by a current of 1000 A flowing axially along the fuselage.

Figure 4.22 was mapped by hand interpolation of the field strength calculated at discrete points by APERTURE. Presumably an interpolation and plotting routine could be incorporated into APERTURE, but, at present, the program does not incorporate such routines. The incorporation of such routines might be a valuable addition to APERTURE, since a map of fields, such as that on Figure 4.22, provides a much more graphic display of field intensities than does the tabular display of field intensities shown on Figure 4.21.

Perhaps the most valuable type of data that one can derive from APERTURE, and the most easily usable in the analysis of response of circuits to the fields coupled through apertures, is the calculation of total flux passing through a loop. Figure 4.23 shows the type of data provided by APERTURE for the four loops shown on Figure 4.18. The way in which such data can be used was discussed in Section 4.4.1.

4.4.4 Aperture Theory - A Summary and Assessment

Aperture coupling is the dominant mode by which high-frequency energy is coupled into the interior of an aircraft. Both magnetic and electric fields may be coupled through apertures, and, as a practical matter, electric fields can only be coupled through apertures. Magnetic fields by contrast can also be coupled through the mechanism of diffusion.

APERTURE COORDINATES--X= 0. METERS
 Y= 0. METERS
 Z= 0. METERS
 APERTURE DIMENSIONS--MAJOR AXIS= 0.100E+01 METERS
 MINOR AXIS= 0.500E+00 METERS
 APERTURE INCLINED 0. DEGREES FROM X AXIS

EXTERNAL MAGNETIC FIELD= 0.100E+03 AMPERES PER METER
 AND INCLINED 0.900E+02 DEGREES FROM THE X AXIS

THERE IS NO REFLECTING SURFACE

X	Y	Z	H-X	H-Y	H-Z
0.	0.	0.300E+00	0.831E-08	0.976E+01	0.
0.	0.	0.500E+00	0.466E-08	0.333E+01	0.
0.	0.	0.700E+00	0.259E-08	0.142E+01	0.
0.	0.	0.900E+00	0.151E-08	0.713E+00	0.
0.	0.	0.110E+01	0.934E-09	0.405E+00	0.
0.	0.	0.130E+01	0.610E-09	0.251E+00	0.
0.	0.	0.150E+01	0.417E-09	0.165E+00	0.
0.	0.	0.170E+01	0.296E-09	0.115E+00	0.
0.	0.	0.190E+01	0.217E-09	0.826E-01	0.
0.	0.100E+01	0.300E+00	0.106E-08	-0.751E+00	-0.496E+00
0.	0.100E+01	0.500E+00	0.897E-09	-0.367E+00	-0.555E+00
0.	0.100E+01	0.700E+00	0.718E-09	-0.104E+00	-0.477E+00
0.	0.100E+01	0.900E+00	0.557E-09	0.311E-01	-0.364E+00
0.	0.100E+01	0.110E+01	0.427E-09	0.853E-01	-0.265E+00
0.	0.100E+01	0.130E+01	0.327E-09	0.990E-01	-0.189E+00
0.	0.100E+01	0.150E+01	0.252E-09	0.950E-01	-0.135E+00
0.	0.100E+01	0.170E+01	0.196E-09	0.847E-01	-0.977E-01
0.	0.100E+01	0.190E+01	0.154E-09	0.730E-01	-0.714E-01
0.250E+00	0.	0.300E+00	0.153E-08	0.583E+01	-0.704E-08
0.250E+00	0.	0.500E+00	0.269E-08	0.253E+01	-0.358E-08
0.250E+00	0.	0.700E+00	0.201E-08	0.121E+01	-0.174E-08
0.250E+00	0.	0.900E+00	0.134E-08	0.643E+00	-0.897E-09
0.250E+00	0.	0.110E+01	0.893E-09	0.377E+00	-0.495E-09
0.250E+00	0.	0.130E+01	0.611E-09	0.238E+00	-0.290E-09
0.250E+00	0.	0.150E+01	0.431E-09	0.159E+00	-0.179E-09
0.250E+00	0.	0.170E+01	0.313E-09	0.111E+00	-0.116E-09
0.250E+00	0.	0.190E+01	0.233E-09	0.805E-01	-0.775E-10
0.250E+00	0.100E+01	0.300E+00	-0.351E+00	-0.569E+00	-0.421E+00
0.250E+00	0.100E+01	0.500E+00	-0.247E+00	-0.274E+00	-0.484E+00
0.250E+00	0.100E+01	0.700E+00	-0.152E+00	-0.650E-01	-0.427E+00
0.250E+00	0.100E+01	0.900E+00	-0.926E-01	0.447E-01	-0.333E+00
0.250E+00	0.100E+01	0.110E+01	-0.560E-01	0.890E-01	-0.247E+00
0.250E+00	0.100E+01	0.130E+01	-0.344E-01	0.991E-01	-0.179E+00
0.250E+00	0.100E+01	0.150E+01	-0.215E-01	0.941E-01	-0.129E+00
0.250E+00	0.100E+01	0.170E+01	-0.138E-01	0.836E-01	-0.939E-01
0.250E+00	0.100E+01	0.190E+01	-0.908E-02	0.721E-01	-0.690E-01
0.500E+00	0.	0.300E+00	-0.104E-07	0.228E+01	-0.104E-07
0.500E+00	0.	0.500E+00	-0.677E-09	0.138E+01	-0.555E-08
0.500E+00	0.	0.700E+00	0.128E-08	0.809E+00	-0.270E-08
0.500E+00	0.	0.900E+00	0.132E-08	0.489E+00	-0.142E-08
0.500E+00	0.	0.110E+01	0.105E-08	0.309E+00	-0.810E-09
0.500E+00	0.	0.130E+01	0.789E-09	0.205E+00	-0.490E-09
0.500E+00	0.	0.150E+01	0.591E-09	0.142E+00	-0.311E-09
0.500E+00	0.	0.170E+01	0.447E-09	0.101E+00	-0.205E-09
0.500E+00	0.	0.190E+01	0.343E-09	0.748E-01	-0.140E-09
0.500E+00	0.100E+01	0.300E+00	-0.456E+00	-0.240E+00	-0.274E+00
0.500E+00	0.100E+01	0.500E+00	-0.334E+00	-0.969E-01	-0.334E+00
0.500E+00	0.100E+01	0.700E+00	-0.225E+00	0.123E-01	-0.315E+00
0.500E+00	0.100E+01	0.900E+00	-0.144E+00	0.725E-01	-0.260E+00
0.500E+00	0.100E+01	0.110E+01	-0.915E-01	0.959E-01	-0.201E+00
0.500E+00	0.100E+01	0.130E+01	-0.582E-01	0.984E-01	-0.151E+00
0.500E+00	0.100E+01	0.150E+01	-0.375E-01	0.912E-01	-0.112E+00
0.500E+00	0.100E+01	0.170E+01	-0.246E-01	0.805E-01	-0.836E-01
0.500E+00	0.100E+01	0.190E+01	-0.165E-01	0.694E-01	-0.626E-01

Figure 4.21 APERTURE Output Resulting from Input Data of Figure 4.20

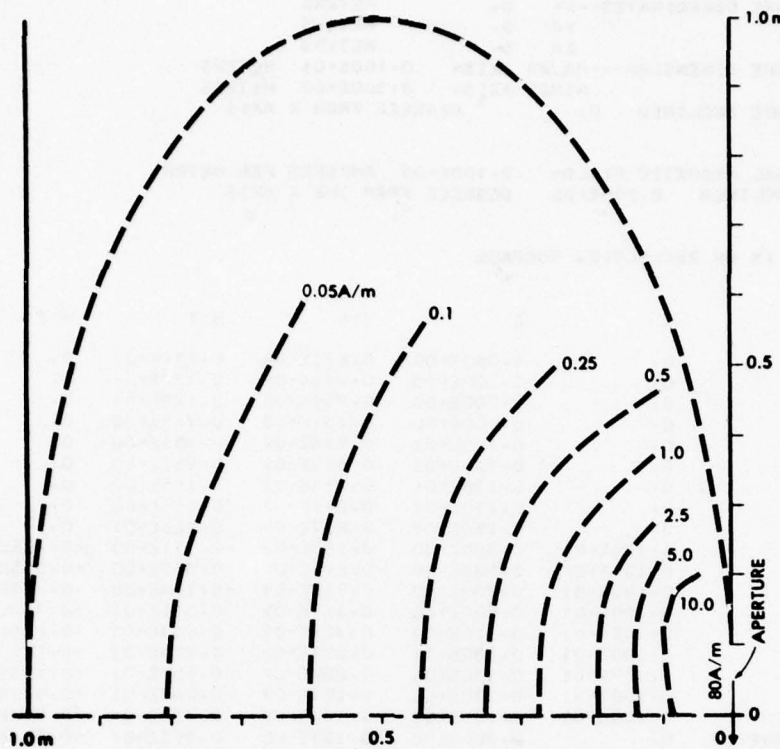


Figure 4.22 Fields Coupled Through an Aperture-Major Axis Oriented Vertically (0.2×0.1 m Aperture)

Elementary aperture theory indicates that the waveshapes of fields coupled through apertures would be the same as the waveshapes of the external fields. More advanced theory indicates that the efficiency of an aperture as a coupling mechanism rises with frequency. As a consequence, the aperture acts as a high pass filter.

Aperture theory is well developed for well-defined apertures, such as elliptical or circular holes in infinite sheets. The development is frequently done in terms of equivalent dipole sources having moments that are given in terms of the physical size and shape of the aperture. A limitation on aperture theory is that there is little information with which to determine the dipole moments of poorly defined apertures, such as a hatch cover that is only loosely fastened around the edges. Such information could presumably be determined by measurements on actual structures, but to date there seems to have been little work of this nature done.

```

LOOP NUMBER      1
  1 -0.100E+00  0.        0.500E+00
  2 -0.100E+00  0.        0.150E+01
  3  0.100E+00  0.        0.150E+01
  4  0.100E+00  0.        0.500E+00

LOOP AREA= 0.200E+00  SQUARE METERS
TOTAL FLUX= 0.213E-06  WEBERS

LOOP NUMBER      2
  1 -0.500E+00  0.        0.500E+00
  2 -0.500E+00  0.        0.150E+01
  3  0.500E+00  0.        0.150E+01
  4  0.500E+00  0.        0.500E+00

LOOP AREA= 0.100E+01  SQUARE METERS
TOTAL FLUX= 0.896E-06  WEBERS

LOOP NUMBER      3
  1 -0.500E+00  0.100E+01  0.500E+00
  2 -0.100E+00  0.100E+01  0.150E+01
  3  0.500E+00  0.100E+01  0.150E+01
  4  0.500E+00  0.100E+01  0.500E+00

LOOP AREA= 0.800E+00  SQUARE METERS
TOTAL FLUX= 0.218E-07  WEBERS

LOOP NUMBER      4
  1  0.        -0.500E+00  0.500E+00
  2  0.        -0.500E+00  0.150E+01
  3  0.        0.500E+00  0.150E+01
  4  0.        0.500E+00  0.500E+00

LOOP AREA= 0.100E+01  SQUARE METERS
TOTAL FLUX= -0.175E-14  WEBERS

```

Figure 4.23. APERTURE Sample (Flux Produced in Loops)

4.5 THE DIFFUSION COUPLING MECHANISM

4.5.1 Theoretical Considerations

4.5.1.1 Circular Cylinders

Consider Figure 4.24, in which a current, I , is entering a circular cylinder. The cylinder is considered long compared to other dimensions, so that there are no end effects, but short compared to the electrical wavelength of any of the frequency components of the current I . The return path for the current is not shown, but it is assumed to be sufficiently far away from the cylinder that there are no proximity effects. Also shown are two conductors, one external (1) and one internal (2) to the cylinder. These are connected to an end cap considered sufficiently massive that no electromagnetic fields penetrate the cap. At the other end of the cylinder are shown two voltages: V_1 , measured from Conductor 1 to the external surface of the cylinder, and V_2 , measured from Conductor 2 to the inner surface of the cylinder.

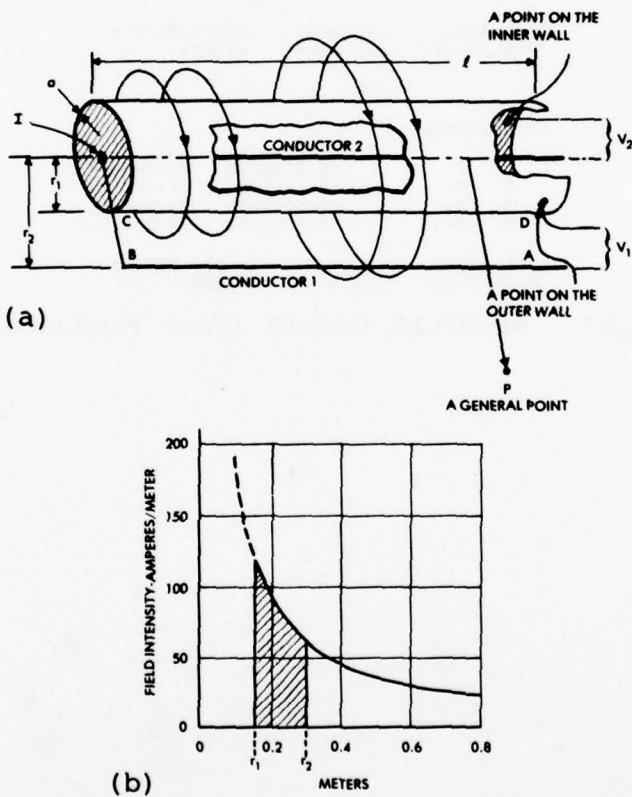


Figure 4.24 Magnetic Fields Around A Circular Cylinder

- (a) Geometry
- (b) Field Intensity vs. Radius
(For $I = 116$ A)

The cylinder will have a dc resistance

$$R = \frac{\rho l}{A} = \frac{\rho l}{2\pi r_1 a}$$

where ρ = resistivity
 l = length
 A = cross-sectional area
 r_1 = radius of cylinder
 a = thickness ($a \ll r$)

If the cylinder has the following dimensions and is made of aluminum of the indicated resistivity

$$\begin{aligned}l &= 2m \\r_1 &= 15.7 \text{ cm} \\a &= 0.281 \text{ mm (0.015 in.)} \\\rho &= 2.69 \times 10^{-8} \Omega \cdot \text{m}\end{aligned}$$

then the dc resistance, R , will be $1.43 \times 10^{-4} \Omega$. If we consider that the input current is 116 A, there will then be developed a voltage

$$e = IR = 116 \times 1.43 \times 10^{-4} = 0.0166 \text{ V} \quad (4.32)$$

If the current of 116 A is established and allowed to flow for a time sufficiently long that steady state conditions are reached, the voltage developed along the cylinder will then be 16.6 mV. This same voltage drop would be measured by a conductor external to the cylinder or by one internal to the cylinder.

Until such steady state conditions have been established, V_1 will not be equal to V_2 , and neither of them will be equal to the steady state resistance voltage drop. Consider first voltage V_1 . External to the cylinder, the flow of current sets up a magnetic field of intensity

$$\begin{aligned}H &= \frac{1}{2\pi r} \\I &= \text{current} \\r &= \text{radius} \\H &= \text{field strength}\end{aligned} \quad (4.33)$$

having a pattern as shown in Figure 4.24b. V_1 will then be

$$V_1 = \frac{d\phi}{dt} = \left[\mu_0 H l \log_e \left(\frac{r_2}{r_1} \right) \right] \frac{dI}{dt} \quad (4.34)$$

and ϕ , the flux passing through the loop ABCD, is represented by the shaded area of Figure 4.24. The flux ϕ would be measured in webers. Remembering that

$$\mu_0 = 4\pi 10^{-7} \text{ A/m}$$

V_1 becomes

$$V_1 = \left[2 \times 10^{-7} l \log_e \left(\frac{r_2}{r_1} \right) \right] \frac{di}{dt} \quad (4.35)$$

If r_2 is 31.4 cm and the indicated current of 116 A rises to crest in an equivalent time of 0.25 μ s (Figure 4.25), V_1 will then rise to an initial voltage of 129 V. As steady state conditions are reached and the external magnetic field ceases to change with time, V_1 will decay to its steady state value of 0.0166 V.

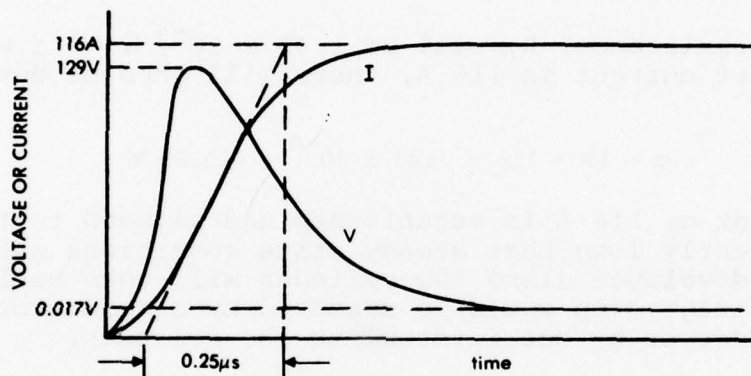


Figure 4.25 External Voltage (Not to scale)

This analysis ignores the skin effect, a phenomenon that causes the effective resistance to be higher under transient conditions than under steady state conditions. For conductors external to the cylinder, the increased resistance resulting from skin effect will be of little consequence compared to the much larger voltage induced by the changing magnetic field.

While conductors external to a current-carrying cylinder, such as an aircraft fuselage, are not common, they are not unknown. An example might be the cables on a missile or rocket that run between a control assembly in the nose and the engine controls at the tail. Of necessity, such cables must run external to the fuel and oxidizer tanks. If the cables are not in a shielded cable tunnel, they will be exposed to the external magnetic field.

Let us now consider the very different conditions internal to the cylinder. First, it can be shown (Reference 4.9) that the magnetic field within the cylinder is zero, at least as long as the current is uniformly distributed over the circumference of the cylinder.

The second important factor is that the phenomenon of skin effect delays the buildup of current on the inner surface of the cylinder. The origin of the skin effect phenomenon is shown in Figure 4.26. If a magnetic field line is assumed to be suddenly established internal to the wall of the conducting cylinder, there will be induced eddy currents circulating around that field line. These eddy currents will induce a magnetic field of their own of polarity opposite to that set up by the external magnetic field. Only as the eddy currents decay will the magnetic field penetrate the wall of the cylinder.

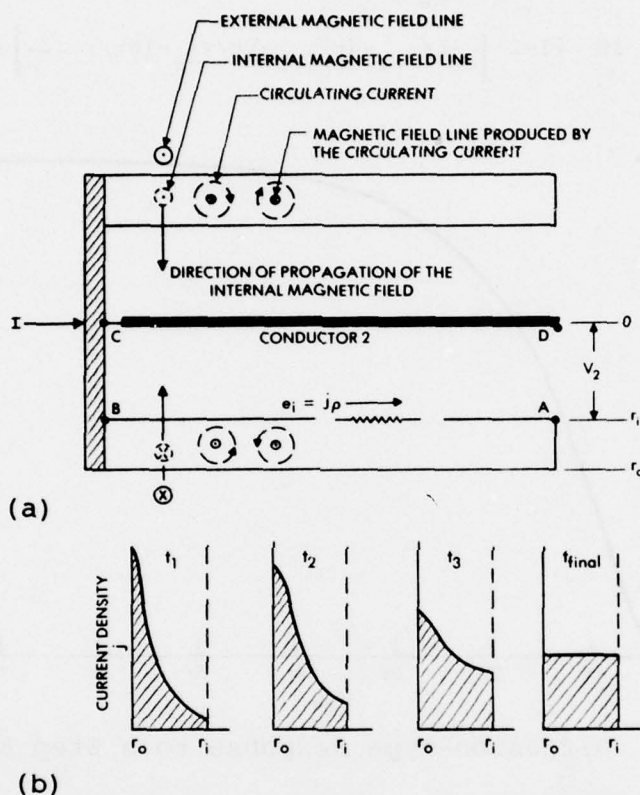


Figure 4.26 Factors Governing the Internal Voltage

- (a) Geometry and Decaying Eddy Currents
- (b) Current Density at Different Times

The current density across the wall thickness at several times is shown in Figure 4.26b. Initially, the current density for a step-function input current is entirely confined to the outer surface. At a slightly later time, t_1 , the current density will still be high near the outer surface, but a small amount of current will have penetrated to the inner surface. As time increases, the current density on the outer surface will fall, and the current density on the inner surface will increase, until at t_{final} the current density will be uniform across the surface of the wall. At

any time, the area under the current density curve multiplied by the peripheral distance around the cylinder will equal the input current. The resistive voltage drop along any surface (including any line internal to the wall of the cylinder) will be equal to the product of the current density at that point times the resistivity of the material. Accordingly, the voltage drop along the inner surface must follow the curve defining the buildup of current density on the inner surface.

The nature of this response is shown in Figure 4.27 and is governed by the following equation:

$$V = IR \left\{ 1 - 2 \left[e^{-t/\tau} - e^{-4t/\tau} + e^{-9t/\tau} - e^{-16t/\tau} \dots \right] \right\} \quad (4.36)$$

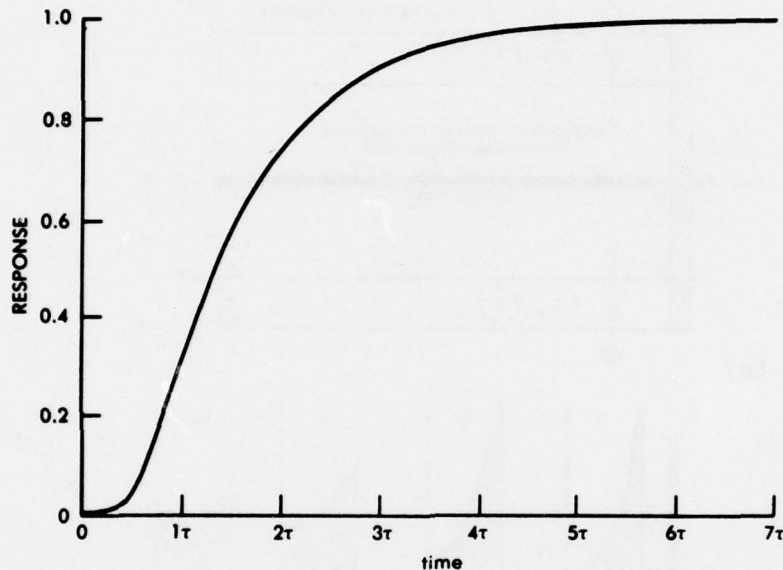


Figure 4.27 Diffusion-Type Response to a Step Function

Figure 4.27 is plotted in terms of a characteristic time constant, τ , sometimes called the penetration time constant.

$$\tau = \frac{\mu a^2}{\pi^2 \rho} \quad (4.37)$$

where ρ = resistivity of the material

a = thickness of the wall

μ = relative permeability of the material

The response curve, shown in Figure 4.27, is called a diffusion-type response and is characteristic of many types of situations involving the transmission of energy through a distributed medium.

Several important observations might be made about the shape of the response curve shown in Figure 4.27. The first is that the response initially changes only slowly and thus has a zero first derivative, unlike a simple exponential response, which has a finite first derivative. The second is that the response approaches its final value much more slowly than does a simple exponential response. The third is that in three time constants the response has reached a large fraction of its final value. In three time constants the diffusion-type response reaches 90%, while the exponential response reaches 95% of its final value.

With respect to Equation 4.37, it should be noted that the penetration time constant is directly proportional to the permeability of the material, inversely proportional to the resistivity of the material, and directly proportional to the square of thickness of the material. The relative permeability of structural material used in aircraft is almost always very nearly unity. Thickness and resistivity can vary over wide ranges.

For reference, Equation 4.37 is shown plotted in Figure 4.28 as a function of material thickness and the resistivity of the material. The resistivities of some typical metals are shown in Table 4.2. For example, if we assume an aluminum alloy of resistivity twice that of copper and a skin thickness of 0.040 in., the

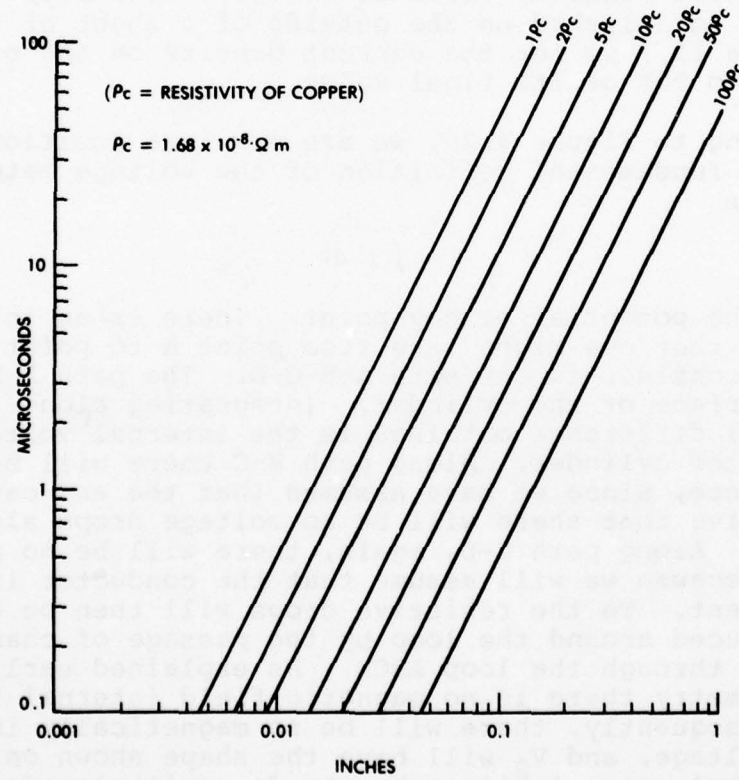


Figure 4.28 Skin Thickness vs. Penetration Time Constant

TABLE 4.2
RESISTIVITIES OF TYPICAL METALS

Material	Resistivity ohm-meters	Conductivity as a fraction of that of copper	Resistivity relative to copper
copper	1.68×10^{-8}	1.0	1.0
aluminum*	2.69×10^{-8}	0.62	1.6
magnesium**	4.46×10^{-8}	0.38	2.65
nickel	10×10^{-8}	0.17	6
Monel	42×10^{-8}	0.04	25
stainless steel	70×10^{-8}	0.024	42
Inconel	100×10^{-8}	0.017	60
titanium	180×10^{-8}	0.009	107

*Aluminum alloys range from 2.8 to $5.6 \times 10^{-8} \Omega \cdot \text{m}$; harder alloys generally have higher resistivities.

**Magnesium alloys containing aluminum and zinc range from 10 to $17 \times 10^{-8} \Omega \cdot \text{m}$.

penetration time constant would be $3.9 \mu\text{s}$. If a step-function current were established on the outside of a sheet of such metal, it would take $11.7 \mu\text{s}$ for the current density on the other side to build up to 90% of its final value.

Returning to Figure 4.26, we are now in a position to evaluate V_2 . The fundamental definition of the voltage between any two points is

$$V = \int P \, d\ell \quad (4.38)$$

where P is the potential at any point. There is an infinite variety of paths that one might take from point A to point D, but the simplest to consider is the path A-B-C-D. The path A-B is along the inner surface of the cylinder. Integrating along this path, the potential difference obtained is the internal voltage drop on the wall of the cylinder. Along path B-C there will be no potential difference, since we have assumed that the end cap is sufficiently massive that there will be no voltage drops along its inner surface. Along path C-D, again, there will be no potential difference because we will assume that the conductor is not carrying any current. To the resistive drops will then be added the voltage produced around the loop by the passage of changing magnetic fields through the loop ABCD. As explained earlier, in a circular geometry there is no magnetic field internal to the cylinder. Consequently, there will be no magnetically induced component of voltage, and V_2 will have the shape shown on Figure 4.27, where the final value is given by the dc resistance drop along the cylinder.

4.5.1.2 Structures of Other Than Circular Shape

If we consider a structure of other than circular shape, conditions may be considerably different. Figure 4.29 shows an elliptical cylinder into which a step-function current is injected. As previously, we will assume that the cylinder is long enough that all end effects may be neglected, that it is short compared to the wavelengths of any frequency components of the injected current, and that the return path for the current is far enough removed that no proximity effects need be considered.

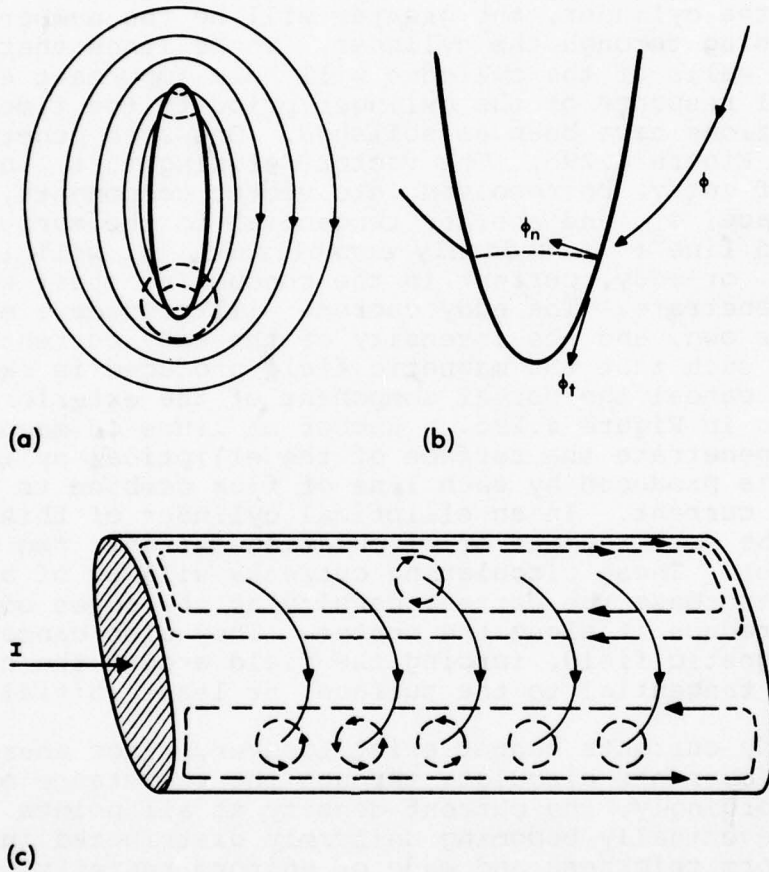


Figure 4.29 Magnetic Fields Around an Elliptical Cylinder

- (a) Penetrating Lines of Flux
- (b) Detail Showing Resolution into Components
- (c) Circulating Currents Induced by Penetrating Lines of Flux

We will also treat the instantaneous current in the cylinder as being composed of the sum of a steady state and a transient component of current. The transient component takes the form of a circulating eddy current. For the following section it should

be kept in mind that the eddy currents described represent only the transient component of current and that the total current at any point or time is the sum of the two components.

Under steady state conditions the current density along the wall of the cylinder will be governed by the dc resistance and, if we assume uniform wall thickness, will have a uniform current density. The current in the cylinder will produce a magnetic field. Most of the field lines will completely encircle the cylinder, as shown in Figure 4.29a, but some, because of the uniform current density, will pass through the cylinder. The greater the eccentricity of the cylinder, the greater will be the number of lines of flux passing through the cylinder. Those lines that do pass through the walls of the cylinder will have important effects on the internal response of the cylinder prior to the time that steady state conditions have been established. One such penetrating line is shown in Figure 4.29b. The vector defining that line may, at the point of entry, be resolved into vector components, one normal to the surface, ϕ_n , and another tangential to the surface, ϕ_t . If the field line ϕ is suddenly established, it will induce a circulating, or eddy, current in the conducting sheet which it attempts to penetrate. The eddy current will produce a magnetic field of its own, and the intensity of the eddy current will be of a nature such that the magnetic field produced is exactly that required to cancel the normal component of the exterior field. If, as shown in Figure 4.29c, a number of lines of magnetic flux attempt to penetrate the surface of the elliptical cylinder, the eddy currents produced by each line of flux combine to produce a circulating current. In an elliptical cylinder of this nature, there will be four regions of circulating current, two on each of the two sides. These circulating currents will be of a nature such as to increase the current density at the edges of the cylinder and to reduce it along the center. They also cancel any penetrating magnetic field, forcing the field around the cylinder to be entirely tangential to the surface, at least initially.

The eddy currents cannot exist forever, since energy will be lost as the currents circulate through the resistance of the metal sheet. Accordingly, the current density at all points will vary with time, eventually becoming uniformly distributed in structures having uniform thickness and made of uniform resistivity materials. Figure 4.30 shows the manner in which the current density will vary. As the circulating current shown in Figure 4.30c decays to zero, the current at the edge will decay from its initial high value to the final resistively determined value, and the current at the center will increase from its initially low value. The current densities will change according to an essentially exponential pattern, though the transient increase in surface resistance produced by skin effects will prevent the circulating current from following a true exponential decay.

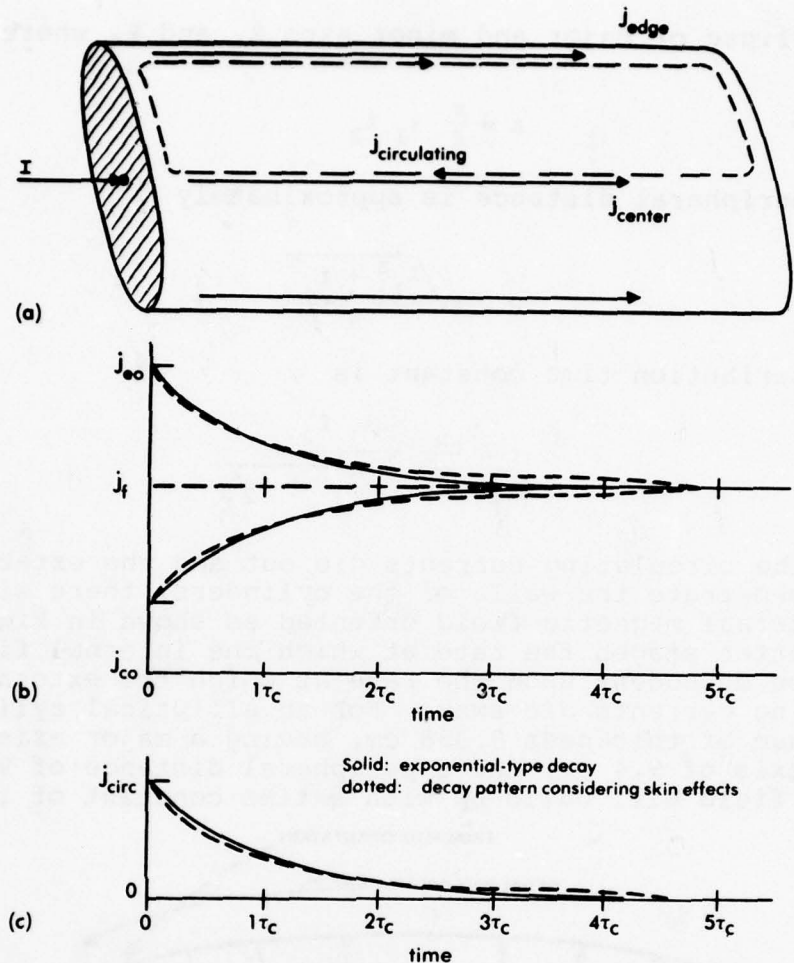


Figure 4.30 Variation of Current-Density with Time

- (a) Current Components Defined
- (b) Edge and Center Currents
- (c) Circulating Currents

One expression giving the magnitude of this redistribution time constant that has appeared in the literature (Reference 4.10) is —

$$\tau = \frac{\mu A a}{\rho P} \quad (4.39)$$

where A = enclosed area of structure
 P = peripheral distance around the structure

The thickness of the wall, a , is assumed to be very small compared to other dimensions. For a rectangular box of sides height h and width d , Equation 4.39 becomes

$$\tau = \frac{\mu h d a}{2\rho (h+d)} \quad (4.40)$$

For an ellipse of major and minor axes ℓ_1 and ℓ_2 where the enclosed area is

$$A = \frac{\pi}{4} \ell_1 \ell_2 \quad (4.41)$$

and the peripheral distance is approximately

$$P = \pi \sqrt{\frac{\ell_1^2 + \ell_2^2}{4}} \quad (4.42)$$

the redistribution time constant is

$$\tau = \frac{\mu a}{\rho \sqrt{2}} \cdot \frac{\ell_1 \ell_2}{\sqrt{\ell_1^2 + \ell_2^2}} \quad (4.43)$$

As the circulating currents die out and the external lines of flux penetrate the walls of the cylinders, there will be set up an internal magnetic field oriented as shown in Figure 4.31. In its latter stages the rate at which the internal field builds up will be dependent upon the rate at which the externally induced circulating currents die away. For an elliptical cylinder made of aluminum of thickness 0.038 cm, having a major axis of 47 cm, a minor axis of 9.4 cm, and a peripheral distance of 98.7 cm, the internal field will build up with a time constant of the 1.16 ms.

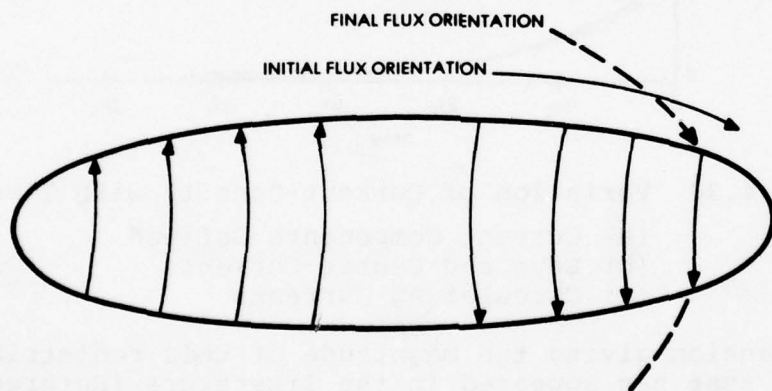


Figure 4.31 The Internal Magnetic Field that Arises as a Result of Flux Penetration

The early time build-up of the magnetic field will be strongly influenced by the phenomenon of skin effect, and the initial rate of build-up of magnetic field will now be seen to have an important effect on the voltages induced on circuits contained within such an elliptical cylinder. Figures 4.26 and 4.27 showed how an electric field will be built up along the inner surface of a circular cylinder. In a similar manner, an electric field will be built up along the inner surface of the elliptical cylinder, but, unlike

AD-A062 606

GENERAL ELECTRIC CORPORATE RESEARCH AND DEVELOPMENT --ETC F/G 1/3
ANALYSIS AND CALCULATIONS OF LIGHTNING INTERACTIONS WITH AIRCRA--ETC(U)
AUG 78 F A FISHER

F33615-76-C-3122

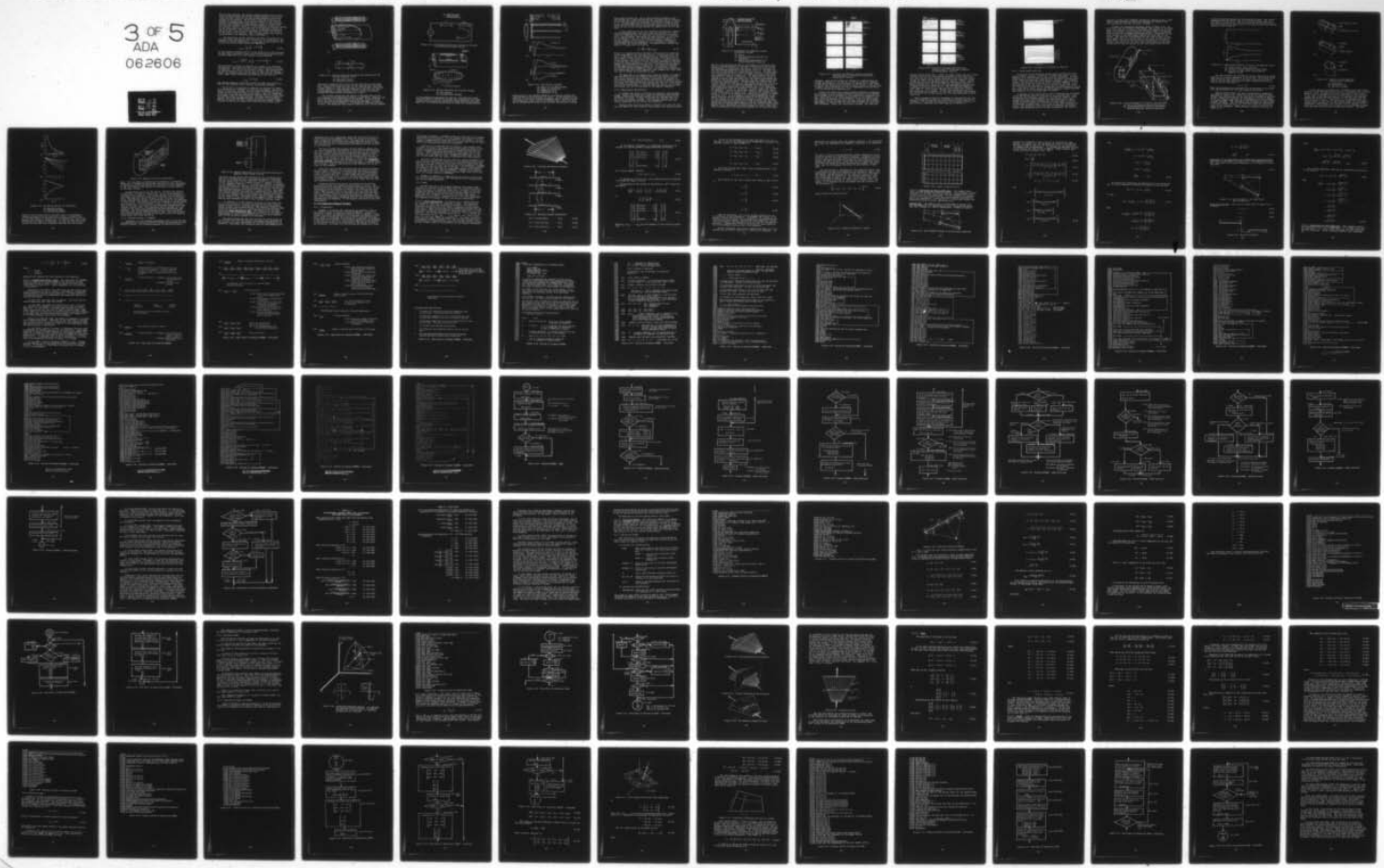
UNCLASSIFIED

SRD-78-044

AFFDL-TR-78-106

NL

3 OF 5
ADA
062608



the circular cylinder, the electric field intensity will be different at different points on the internal surface of the elliptical cylinder, since the initial current density on the outer surface is not uniform. The internal electrical field will be essentially proportional to the current density on the exterior surface, but delayed and distorted as a result of the pulse penetration time produced by eddy currents (shown in Figure 4.27). The internal electric field, E_i , being different at different points on the inner surface, will give rise to circulating currents on the inner surface. The currents may be visualized as flowing on paired strips. There will be four pairs of strips, two on each of the sides of the cylinder. Each of these strips will have associated with it an inductance and a resistance.

The equivalent circuit governing the rate of build-up of internal current then becomes that of Figure 4.32, which may be simplified to that of Figure 4.33. If e_{ie} were a step function, the build-up of current would follow the expression

$$i_{circ} = \frac{e_{ie}}{R} \left[1 - e^{-t/(L/R)} \right] \quad (4.44)$$

If the internal voltage were not a step function but were governed by some other function of time, such as the pulse penetration predicted by Equation 4.36, the internal current would be

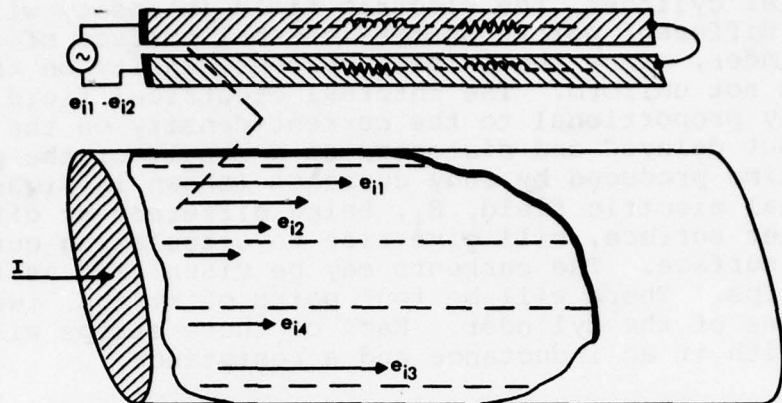
$$i_{circ} = \int \frac{e_{ie} f(t)}{R} \frac{dt}{dt} \left[1 - e^{-(t-\tau)/(L/R)} \right] d\tau \quad (4.45)$$

The convolution integral of Equation 4.45 need not be evaluated analytically, since only the early time rate of change of current is important. So long as the current is small, the voltage across the resistive part of the circuit will be small and the voltage across the inductive part will be equal to the internal resistance drop. Under these conditions the internal current will be

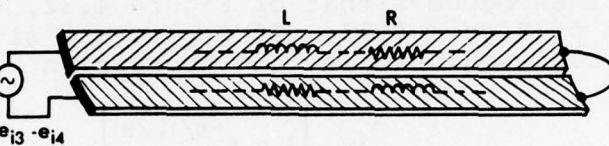
$$I_{i_{circ}} = \frac{1}{L} \int e_{ie} dt \quad (4.46)$$

The internal magnetic field will follow the same time pattern as that of the build-up of the internal circulating currents.

We are now in a position to evaluate the voltages on conductors contained in a cylinder of noncircular geometry. Figure 4.34 shows an elliptical cylinder with two internal conductors, one adjacent to the surface and one in the center. Both are connected at one end to an end cap sufficiently massive that no voltage drops will appear along its inner surface. The other ends are open circuited. The usual assumptions about the length of the cylinder and the return path for the injected current are assumed to apply. Voltages V_1 and V_2 are shown, both being measured between their



(a)



(b)

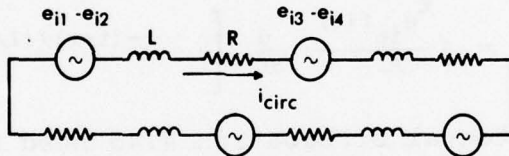


Figure 4.32 Factors Governing the Early Time Build-up of the Internal Magnetic Field

- (a) Physical Factors
- (b) Equivalent Circuit

respective conductors and a point on the inner wall of the cylinder. Figure 4.34b shows that all of the internal flux will pass between Conductor 2 and the inner wall of the cylinder, while only a small amount will pass between Conductor 1 and the inner wall. Correspondingly, a large fraction of the internal flux passes through the plane defined by Conductors 1 and 2.

The voltage between any two points is defined again as the line integral of the potentials around a closed path. Figures 4.35a and 4.35b show the simplest paths to consider. V_1 would be the sum of the potentials developed around the loop ABCD. If there is no current along Conductor 1, the potential along path A-B will be zero. The potential drop along the path B-C will be zero because

e_{ie} = an effective driving voltage
related to the initial non-uniformity of external current

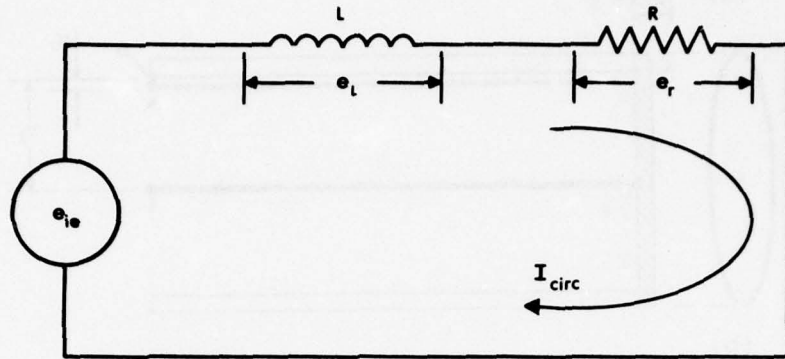


Figure 4.33 Final Equivalent Circuit Governing Increase of Internal Circulating Circuit

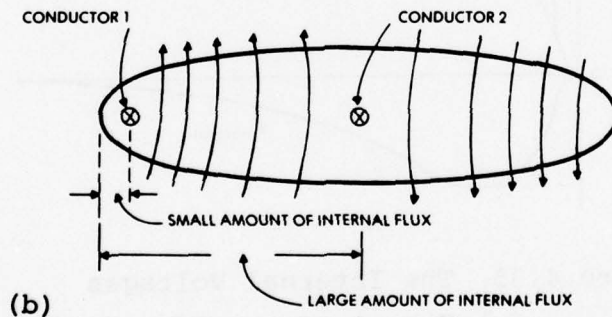
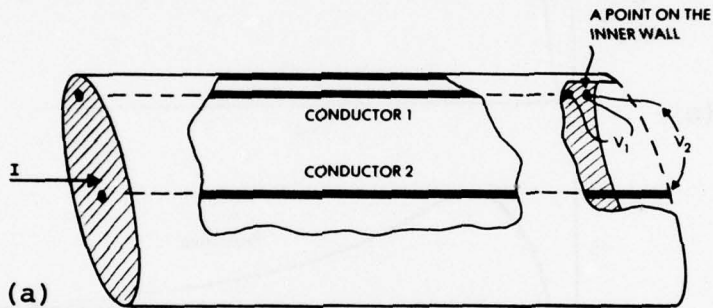


Figure 4.34 Factors Governing the Internal Voltage

- (a) The Geometry
- (b) Internal Flux Linkages

of the assumptions regarding the end cap. The potential along the path C-D will then be the voltage drop produced by the inner current density times the resistivity of the material along the path C-D. To these potentials must be added the voltage induced

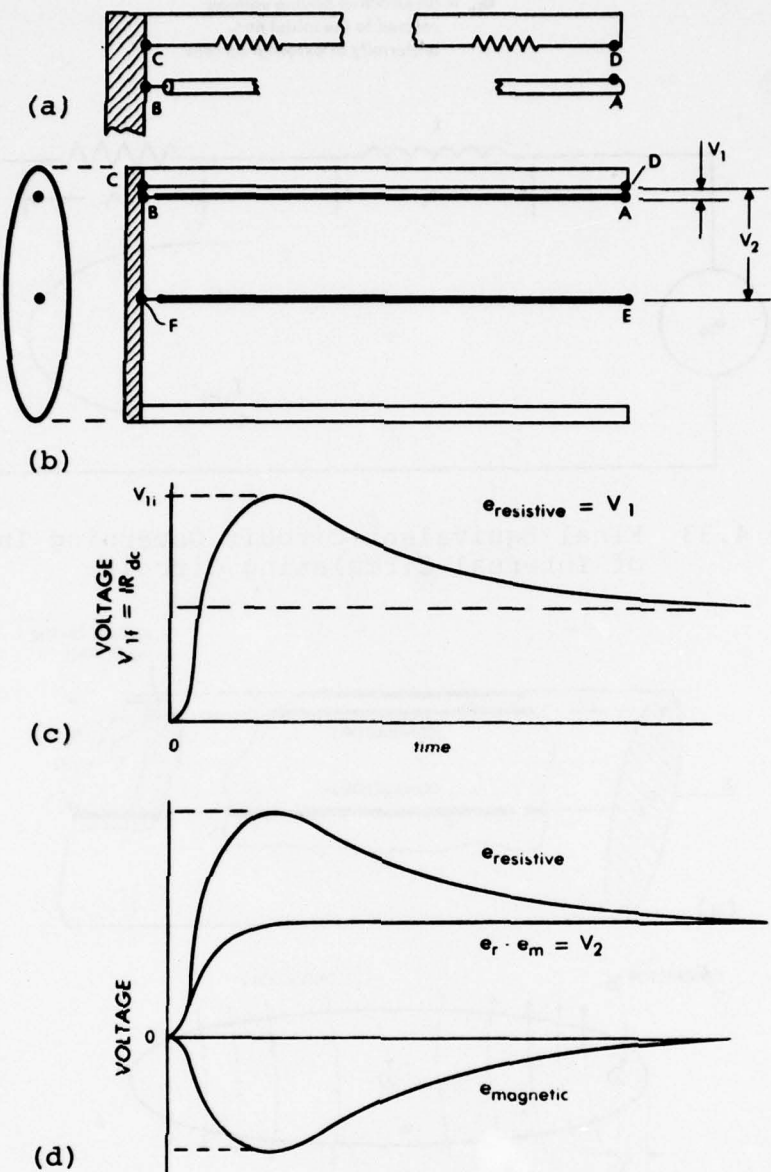


Figure 4.35 The Internal Voltages

- (a) Detail of the Edge Surface
- (b) Paths of Integration
- (c) Components of V_1
- (d) Components of V_2

magnetically by the changing magnetic flux passing through the loop defined by the points A, B, C, and D. If the spacing of the conductor to the wall is made vanishingly small, so that C-B and D-A become zero, there will be no magnetic flux; hence the voltage V_1 between points A and D will be only the resistive voltage

drop along the path C-D. As in the cylindrical geometry case, the voltage for a step-function current injected into the exterior of the tube will build up according to the pattern shown in Figure 4.27. Its magnitude will be greater than the dc resistance drop by the ratio to which the initial current density on the exterior along the end of the ellipse exceeds the steady state current density.

V_2 will again be the sum of a resistive voltage and a magnetically induced voltage, this time along the path E-F-C-D. The resistive component will be identical to the resistive component of V_1 , the resistance drop along the path identical to the resistive component of V_1 , the resistance drop along the path C-D. For V_2 , however, there will be a nonzero magnetic component of voltage produced by the passage of a finite amount of magnetic flux through the finite loop EFCD. The magnetically induced component of voltage will be given by

$$e_m = \frac{d\phi}{dt} = K \frac{d}{dt} (I_{circ}) \quad (4.47)$$

where K is a proportionality constant relating the flux produced in the loop EFCD to the internal current. In Equation 4.46, however, it was shown that the internal current was proportional to the integral of the internal resistance drop. This leads to the rather unusual observation that the magnetically induced component of voltage has, initially at least, the same waveshape as the component of voltage produced by the flow of internal current density through the resistance of the material. The long-term response of the magnetically induced voltage will be different from the resistively generated component, since, as steady state conditions are reached and the internal magnetic field reaches its final value, its rate of change will decrease to zero.

The magnitude of the magnetically induced voltage will depend upon the location of the conductor and upon the degree to which the initial distribution of magnetic flux around the outside of the cylinder differs from the final distribution of magnetic flux. Since the difference between the initial and the final flux patterns is greater for cylinders of high eccentricity than it is for cylinders of low eccentricity, it follows that the flatter the cylinder, the greater will be the influence of the magnetic component.

4.5.2 Experimental Verification

An example may better illustrate the diffusion coupling mechanism. Figure 4.36 shows how a group of conductors were located inside an elliptical cylinder formed from an aluminum sheet 0.38 mm (0.015 in.) thick. A pulse of current was injected into one end of the elliptical cylinder. The voltages induced upon the various conductors by the current were measured.

Typical tests results are shown in Figures 4.37 and 4.38; Figure 4.37 shows, on four different time scales, the injected current

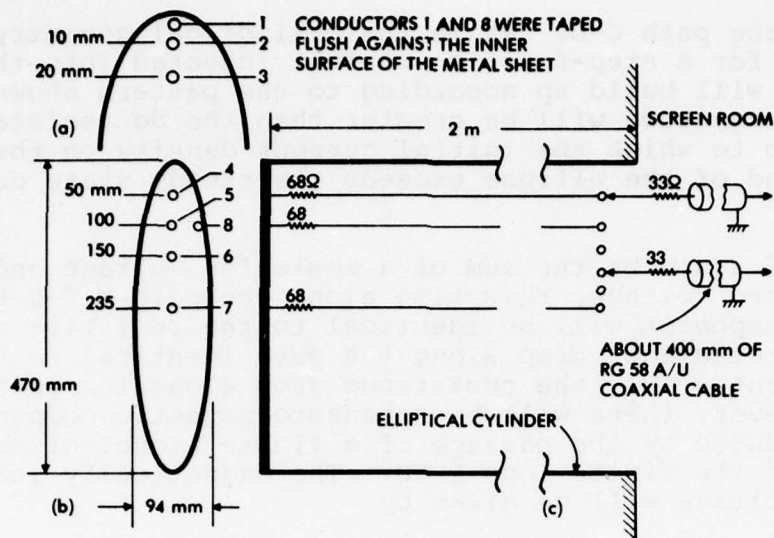


Figure 4.36 Arrangement of Conductors Inside Elliptical Cylinder

- (a) Detail
- (b) End View Showing Locations of Conductors
- (c) Electrical Termination of Internal Conductors (Typical)

and the line-to-ground voltage on two different conductors, Conductor 1 located adjacent to the small radius end of the ellipse and Conductor 7 located near the center. With the exception of the oscillograms displayed at 500 ms per division, the input current can be considered as a step-function current. In both cases the line-ground voltage is seen to display the pulse penetration-type response shown in Figure 4.27. The small bump at the leading end of the voltage on Conductor 1 is primarily the result of leakage from the surge generator into the screen room housing the measuring instruments and to coupling from the trigger pulse used to fire the surge generator. In both cases the initial rise of voltage follows the same pattern and reaches essentially its final value in about 3 μ s, a time in accordance with three times the calculated pulse penetration time constant of 1.2 μ s calculated for aluminum of 0.015 in. thickness. At later times, the voltage on Conductor 1 is seen to decay back toward a lower final value in the manner shown in Figure 4.35. Likewise, the voltage on Conductor 7 is seen to be nearly flat, rising only slightly, as shown in Figure 4.37. It is probably a fortuitous combination of conductor location and the characteristics of the elliptical cylinder that result in the voltage on Conductor 7 being nearly flat. If the injected current were truly a step function, the two voltages would eventually become equal to the dc resistance drop. The bottom set of oscillograms indicates that the current significantly departs from a step-function current pattern at later times, and this is reflected in the long-time response of the two line-ground

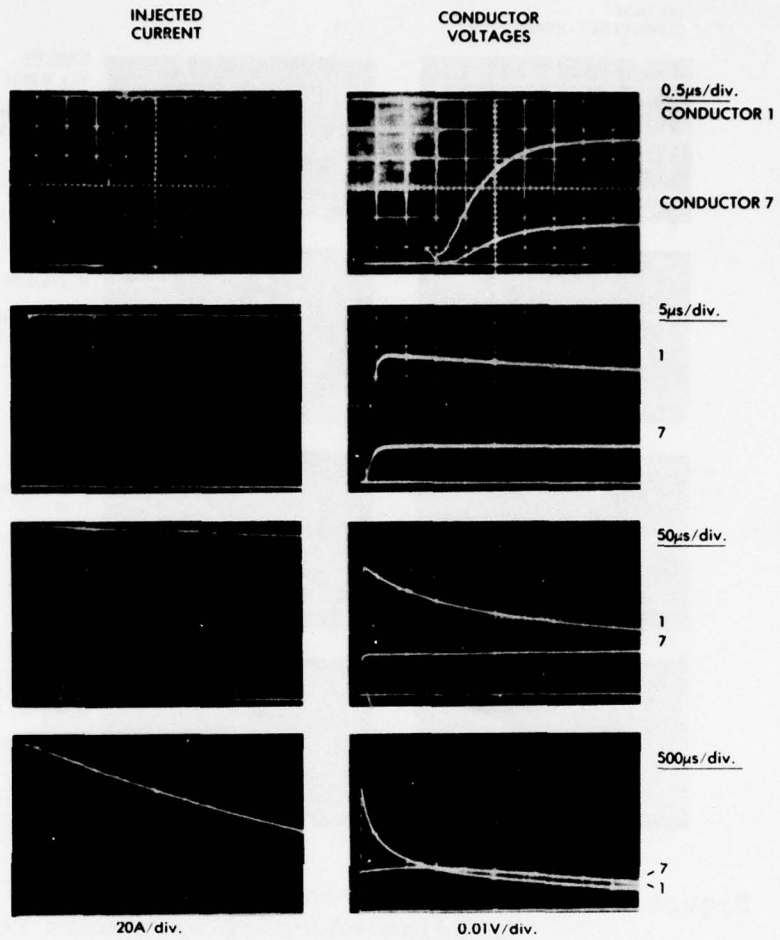


Figure 4.37 Variation of Conductor Voltage with Time
(Leading edges of waveforms retouched for photographic clarity)

voltages. Just as the voltage on Conductor 7 lagged behind the voltage on Conductor 1 during the initial phase of the response, it lags behind during the final decay of the current. The redistribution time constant with which V_1 decays toward its final value is seen to be of the order of 1 ms, in accordance with the value (1.16 ms) predicted by Equation 4.43.

Figure 4.38 shows the voltages between conductors (displayed on two separate oscilloscopes and hence displayed on two separate oscilloscopes) and the integral of the conductor-to-conductor voltage. This latter is of course proportional to the magnetic flux that builds up internal to the cylinder. Since, at early times, the line-to-ground voltages have the same waveshape but different amplitudes, it follows that the line-line voltage will also have that waveshape. Unlike the line-ground voltages, the line-line

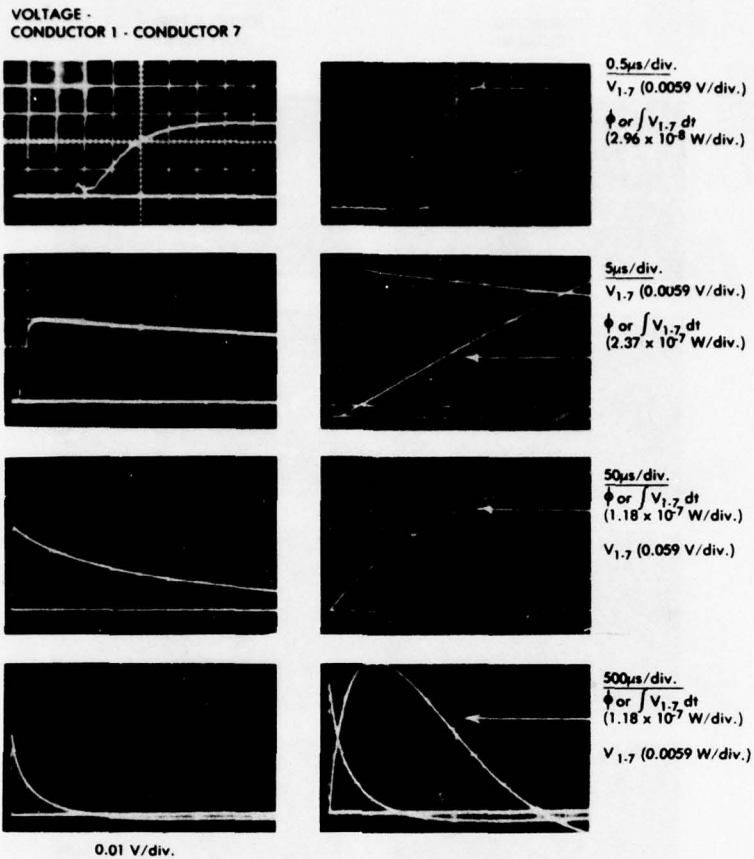


Figure 4.38 Difference Voltages and Total Flux
(Leading edges of waveforms retouched
for photographic clarity)

voltage decays toward zero. Since the input current was not a step-function current, the oscilloscopes displayed at 500 μ s per division show the line-line voltage decaying to zero and then reversing as the input current decays and the internal magnetic fields attempt to follow the decaying external magnetic fields. The input current did not last long enough for the magnetic field to reach a steady state value, but the oscilloscopes do indicate that it seems to crest at about 850 μ s. Why the indicated magnetic field does not crest at the time the line voltage goes through zero, 1300 μ s, is not known. Perhaps instrumentation errors in the integrator are to blame. At any rate, the decay time constant for the line-line voltage agrees with the value predicted by Equation 4.43.

With a somewhat different waveshape of injected current, Figure 4.39 shows the voltages as a function of the position of the conductor. The voltage on Conductor 8 was not shown; however, it was virtually identical with that shown for Conductor 5.

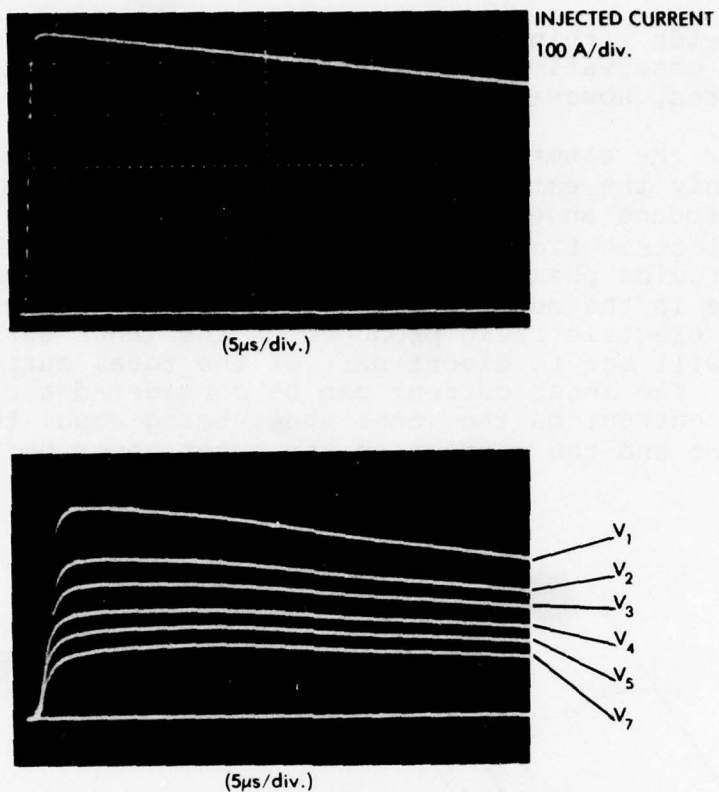


Figure 4.39 Voltages as a Function of Position

4.5.3 Fields Within Cavities

The nature of the diffusion fields within cylindrical structures, whether circular, elliptical, or some other shape, is fundamental to an understanding of the diffusion phenomena. In some cases those structures are representative of actual aircraft structures, wings and fuselages being obvious examples. Most commonly, however, the structure is not as simple as these examples. A simple calculation of the field within a cylindrical fuselage is not of much use if that fuselage is filled with an engine, for example. The engine itself is not susceptible to electromagnetic fields but would, in any case, change the electromagnetic fields from what they would be in an otherwise empty structure.

A problem of more importance is that of determining the fields within enclosures, such as a gun bay or an electronic bay. Such enclosures are frequently exposed to the external magnetic field on only one side, either because the interior walls are thick enough to provide more shielding from the other parts of the external field or because the enclosure is much closer to one of the external surfaces than it is to any of the other external surfaces. The analytical tools available to calculate the fields within such enclosures are not as well developed as the tools to

calculate fields within complete structures, such as wings or fuselages. Some observations about the character of fields within such enclosures, however, are still in order.

Consider the elementary enclosure shown in Figure 4.40. We will treat only the external field shown. The current in the outer sheet will produce an electric field along the inner face of that sheet, the electric field rising to its final value in accordance with the diffusion phenomena discussed earlier. Connected to that inner surface is the metal sheet forming the inner wall of the cavity. The electric field produced on the inner surface of the outer sheet will act to divert part of the total current onto the inner sheet. The inner current can be considered a circulating current, the current on the inner sheet being equal to the circulating current and the current on the outer sheet being the sum

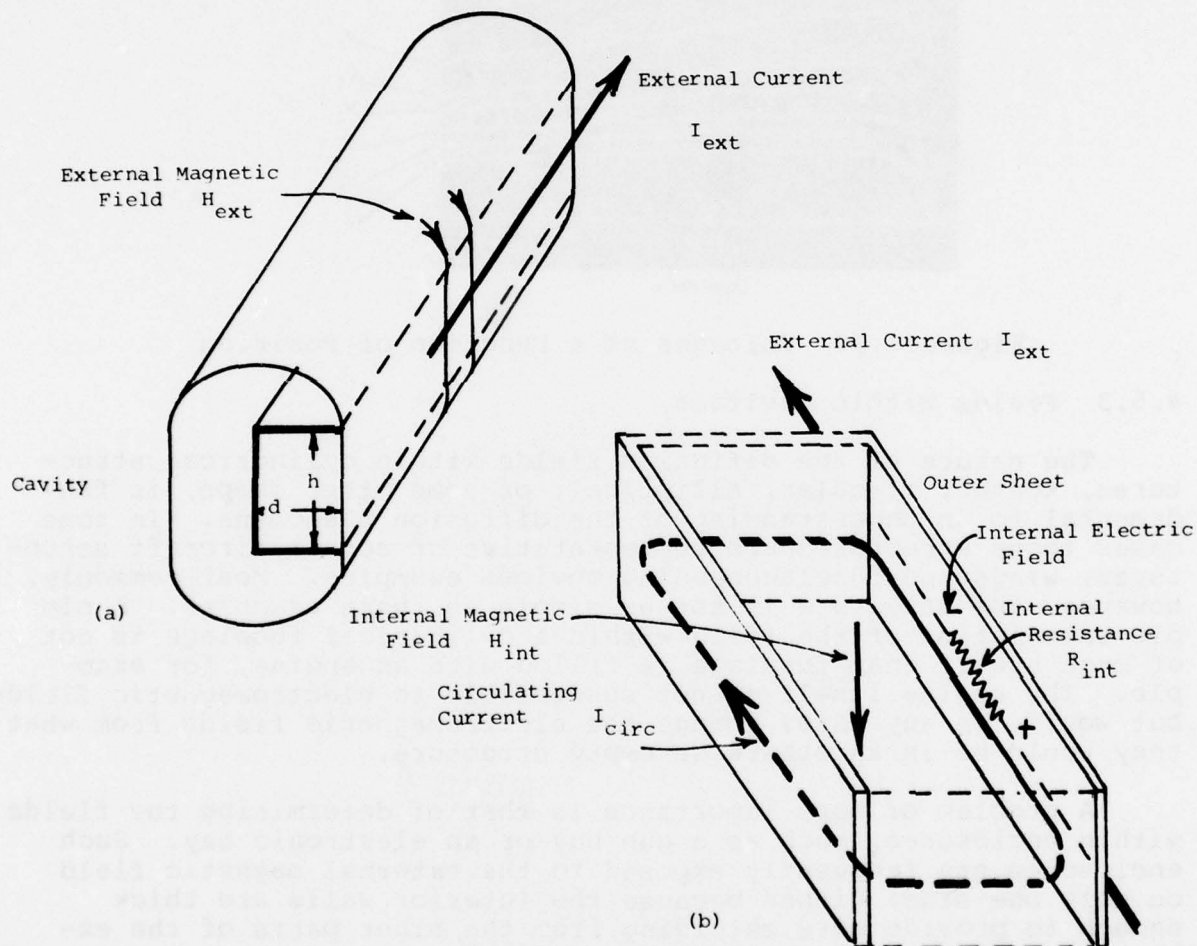


Figure 4.40 A Cavity Exposed to a Field on Only One Side

- (a) Cavity and External Field Orientations
- (b) Internal Magnetic Field and the Current Loop Defining the Internal Inductance

of the circulating current and the external current. The current components and the general nature of how they change with time are shown on Figure 4.41. The rate at which the circulating current builds up to its final value is the rate at which the internal magnetic field builds up.

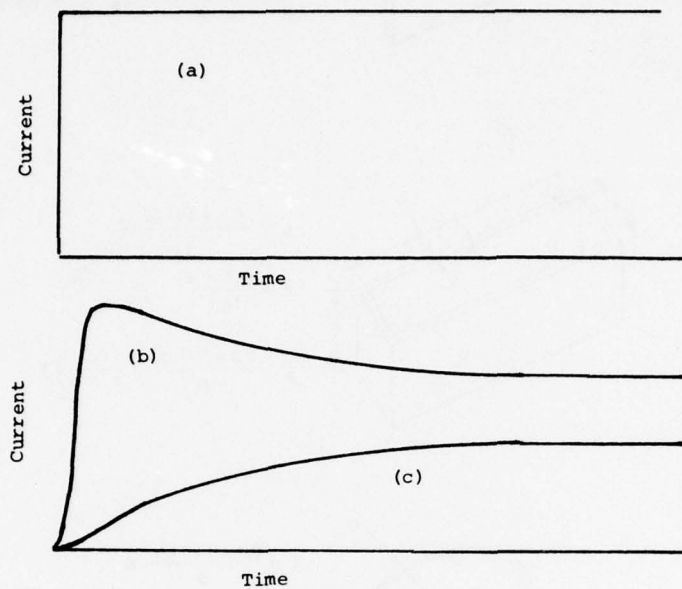


Figure 4.41 Generalized Behavior of Current and Magnetic Field

- (a) Total Current (step function)
- (b) Current on Inner Surface of Outer Sheet
- (c) Current on Inner Sheet (Also Shape of Magnetic Field)

The rate at which the circulating current builds up is determined by the internal impedance of the cavity. The voltage developed along the inner surface of the outer sheet by the flow of current through that sheet may be viewed as impressed across a loop or cavity inductance, Z

$$Z = R + j\omega L \quad (4.48)$$

Both the resistance and inductance will be governed by the effective characteristics of the loop defining the cavity.

Typical current paths and their characteristic impedances are shown in Figure 4.42. Some cavities may be viewed as being sufficiently long and narrow that they may be defined by parallel strips. Others are basically of rectangular or circular shape, or of some simple shape that may be approximated by an equivalent circular cylinder. The inductance and resistance of each configuration are shown. Each of the inductance equations (Reference 4.11) has a correction factor $\log_e k$, F' , K that relates to the shape of the enclosure. These correction factors are shown in Figure 4.43.

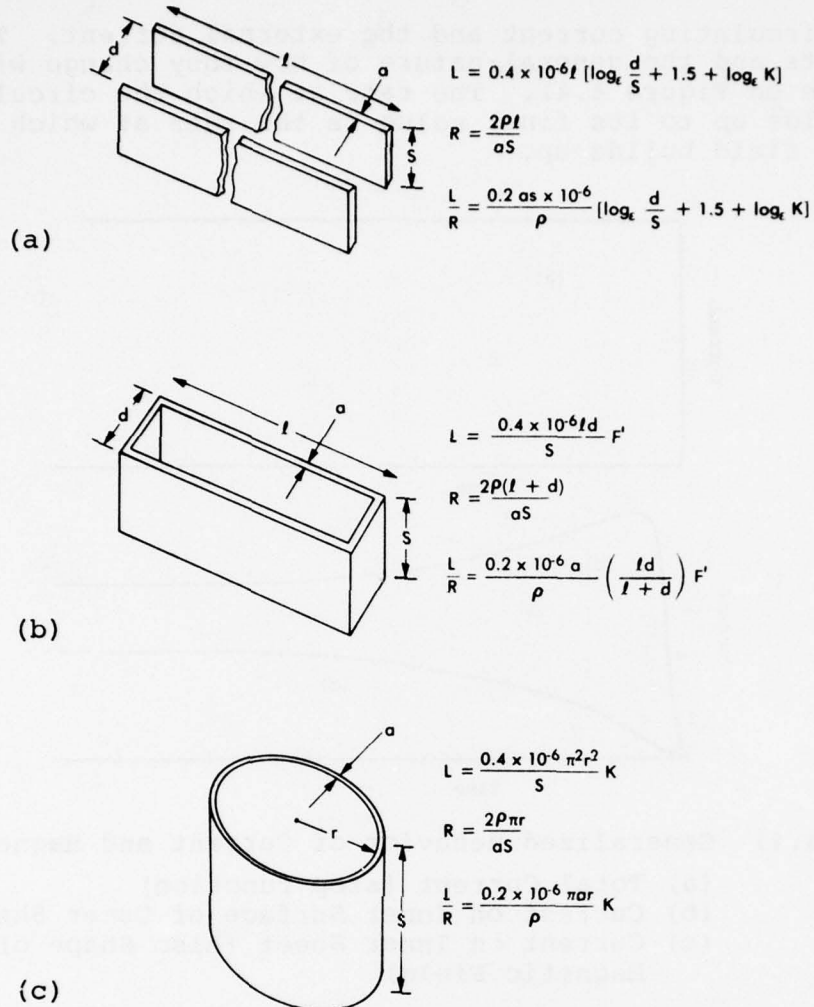


Figure 4.42 Typical Current Paths and Characteristic Impedance

- (a) Long Sheets
- (b) Rectangular Box
- (c) Circular Cylinder

If the cavity is provided with a removable cover and if this cover is in the external current flow or is exposed to the external magnetic field, the effects are as illustrated in Figure 4.44. If the cover is assumed to be of the same material and thickness as the rest of the face upon which it is mounted, the principal effects are related to the resistance of the fasteners used to hold the cover in place. The covers will seldom make good electrical contact to the rest of the surface except at the fasteners themselves. Accordingly, the external currents flowing in the face will be constricted in the vicinity of the fastener and pass from that face onto the cover through the fastener. The major

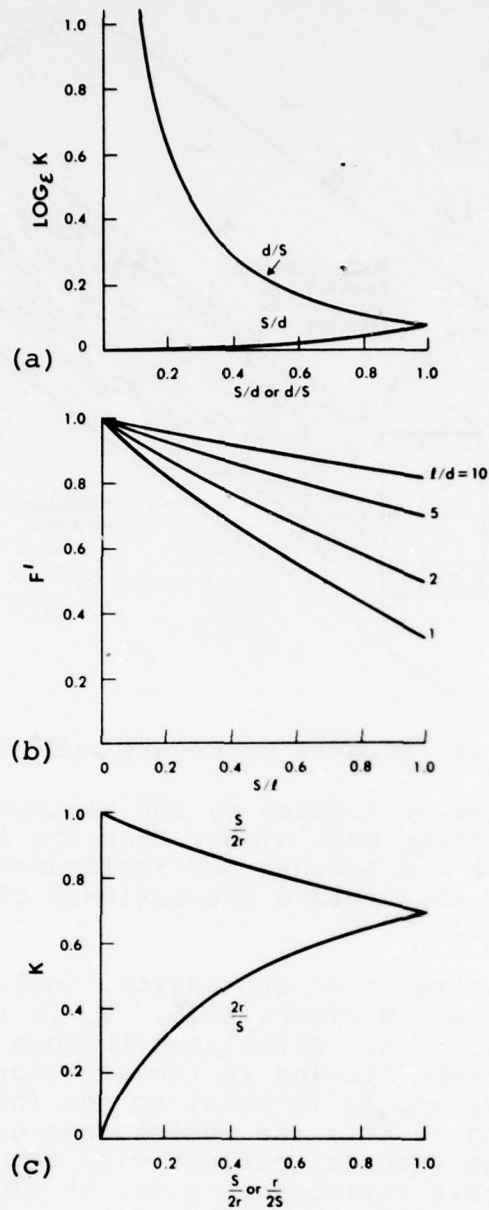


Figure 4.43 Correction Factors for Inductance

- (a) Parallel Strips
- (b) Rectangular Boxes
- (c) Circular Cylinders

effect of this constriction of current flow is to introduce a lumped resistance into the electrical circuit, although there is a certain amount of influence on the inductance of the circuit whenever the current is constricted. It will be seen, then, that the greater the number of fasteners, the less the restriction of current flow and the less resistance inserted into the current

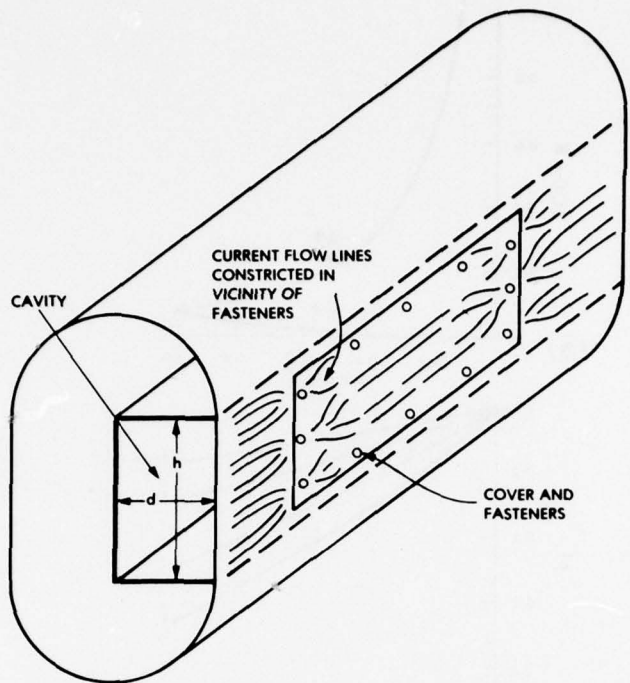


Figure 4.44 Effects of Covers and Fasteners

path. The resistance introduced by the fasteners is important because it is frequently much higher than the intrinsic resistance of the metal surface and because the resistance is not subjected to the skin effects that retard the build-up of current density on the inner surface.

An equivalent circuit of the cavity, including the effects of fasteners, is shown in Figure 4.45. R_f is the equivalent resistance of the fasteners. Circulated through this resistance is the undistorted current flowing in the exterior face of the fuselage. The sum of R_1 and R_2 is equal to the intrinsic resistance of the loop-defining cavity, the resistances given by the equations in Figure 4.42. The external current will develop a voltage across only a portion of this resistance, since it flows in only a portion of the loop. Letting R_1 be the resistance through which the external current flows, that resistance may be assumed to be subjected to the current as retarded by the pulse penetration time constant. The two voltages developed across these resistances then circulate current around the entire loop. The rate at which the current builds up will then be the rate at which the magnetic field inside the cavity builds up.

4.5.4 Diffusion Theory - A Summary

Diffusion is a low-frequency phenomenon tied in with the voltages produced by the flow of current through the resistance of the metallic surface. The voltages produced on conductors within a

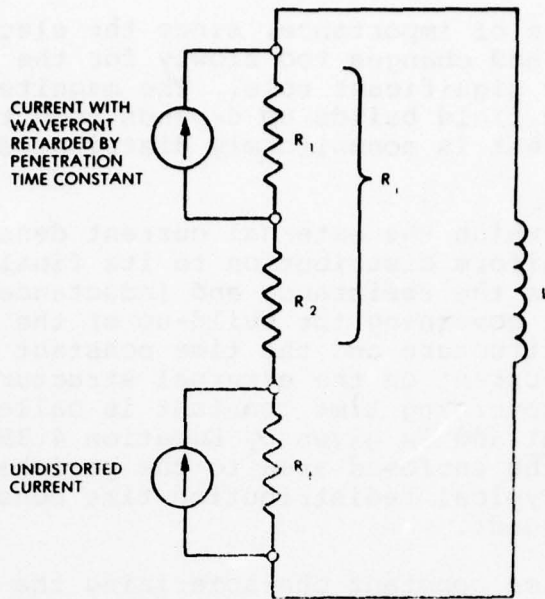


Figure 4.45 Possible Equivalent Circuit Governing Build-up of Magnetic Field Inside a Cavity

structure are the sum of those produced by the resistance drops and by the changing magnetic field passing between a conductor and the return path for that conductor, whether it is the metal surface through which the external current is flowing or whether it is a separate conductor. It is difficult, however, to separate the two components of voltage, since the magnetically induced component has, initially, the same waveshape as that of the resistively generated electric field along the inner surface. This somewhat puzzling phenomenon is merely a reflection of the fact that the internal current, and hence the internal magnetic field, build up at a rate proportional to the integral of the electric field on the inner surface. The magnetically induced voltage, responding as it does to the derivative of the magnetic field, of course has the same waveshape as that of the internal electric field.

In response to a step function of current on the outer surface of the structure, the electric field on the inner surface builds up according to a pattern characteristic of diffusion of energy through a distributed medium. The waveshape, given by Equation 4.36 and Figure 4.27, is characterized by a time constant called the pulse penetration time. The magnitude of the pulse penetration time is given by Equation 4.37 and is on the order of microseconds or tens of microseconds for the materials commonly used to form the metal surface of an aircraft.

The factors governing the rate at which the field builds up to its final value are the internal resistance and inductance of the structure or, more accurately, the internal impedance of the enclosure. Resistance and inductance form the only components of

impedance that are of importance, since the electric field is too low in amplitude and changes too slowly for the internal capacitance to play any significant role. The magnitude to which the internal magnetic field builds up depends upon the degree to which the external current is nonuniformly distributed over the surface of the structure.

The rate at which the external current density changes from its initial nonuniform distribution to its final uniform distribution also involves the resistance and inductance of the structure. The time constant governing the build-up of the magnetic field internal to the structure and the time constant governing the redistribution of current on the external structure are virtually identical. The governing time constant is called the redistribution time constant and is given by Equation 4.39. It is governed by the ratio of the enclosed area to the peripheral distance around the structure. Typical redistribution time constants are on the order of milliseconds.

Since the time constant characterizing the diffusion phenomena are longer (usually) than the waveforms associated with the return stroke of lightning, it follows that the internal magnetic fields will not reach their ultimate magnitude when an aircraft carries lightning current. It also follows that the duration of the magnetic fields in an aircraft, at least those where the dominant coupling mode is diffusion, will be of longer duration than the lightning current.

Diffusion effects also govern the fields within cavities, particularly those with tightly fastened doors or covers. The tools available to evaluate fields within cavities are not as well developed as those available to evaluate the fields within structures exposed to the field on all sides, such as wings and fuselages. The fasteners used to hold covers in place over cavities have an important effect on the fields within the cavities. Before these effects can be evaluated analytically, measurements of the effective resistance introduced into the current path by those fasteners must be supplied. At the present time there are no such measurements.

4.6 THE COMPUTER PROGRAM DIFFMAG

4.6.1 Introduction

DIFFMAG is a program that calculates the magnetic field in and around a group of current carrying conductors. Figure 4.4 showed how a group of conductors could be used to represent a continuous structure, and Section 4.2.2 discussed the degree to which such a group of conductors could allow one to calculate the magnetic field at the surface of a structure so defined. As presented in Sections 4.4.1 and 4.5.1, that surface magnetic field intensity is the starting point for a calculation of the fields internal to the structure. In Figure 4.4, the surface was defined by a group

of parallel conductors. DIFFMAG allows the conductors to be skewed with respect to each other. If they skewed, the field will be different at varying points along the length of the surface. In this respect, DIFFMAG differs from similar routines used in earlier works that could only deal with parallel conductors.

Section 4.5.1 discussed how the magnetic field changes from a pattern governed by the magnetically distributed currents on the surface to a pattern governed by the resistively distributed currents. DIFFMAG calculates the magnetic field under the two conditions. The transition between the two takes place with a time constant given by Equation 4.39. DIFFMAG provides some, but not all, of the terms that one needs to calculate that time constant.

Section 4.4 discussed the ways that the program APERTURE allows one to specify whether the fields were to be tabulated at discrete points or not, the range over which they should be calculated, and the type of format in which the output was to be presented. DIFFMAG provides the user the same type of options. To the degree possible, the format of the input data file was made similar to the format of the input data file used for APERTURE. DIFFMAG also allows one to calculate the total flux passing through loops within the structure, in a manner similar to APERTURE.

DIFFMAG is composed of a MAIN program and several subroutines. The theory, program listings, and flow charts of the various parts will be discussed separately.

4.6.2 MAIN

The MAIN portion of the program supplies the program steps necessary to read the required data, call upon the various subroutines, and print the necessary output data. In MAIN is also calculated the manner in which the current divides among the various conductors with which one defines the structure under study. A major task done in MAIN is to calculate the self- and mutual inductances of the various filaments, since it is those inductances that determine the manner in which the current distributes.

4.6.2.1 Theory Behind MAIN. In Figure 4.46, a surface defined by a group of conductors or filaments is shown. The conductors are joined at their ends by conducting sheets. The sheets are shown here as planes, but they could, in concept, be any surface. A current is shown entering one of the sheets and exiting from the other sheet. Each of the conductors has associated with it a self-inductance and between each pair of conductors there is mutual inductance. Let the self-inductances be $L_1, L_2 \dots L_n$ and the mutual inductances be $M_{12}, M_{13} \dots M_{ij}$ where i and j both extend from 1 to the total number of conductors n. Let these inductances be arranged as shown in Figure 4.47. One can then formulate the following set of equations that relate the voltage across, and the current through, each of the conductors to the various inductances.

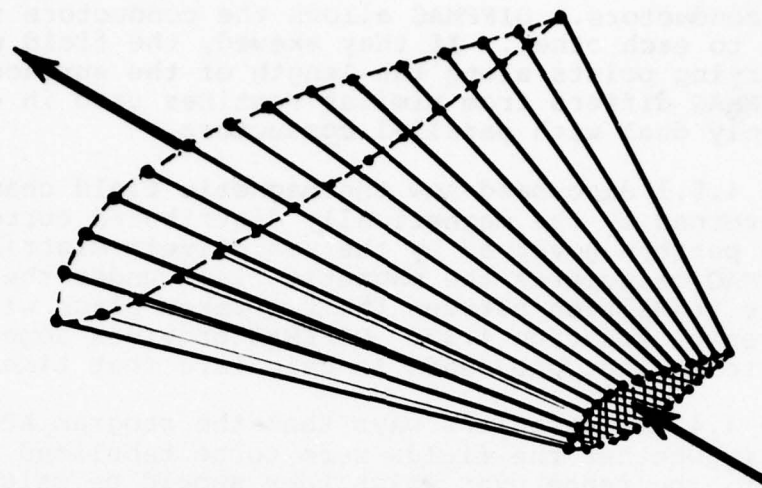


Figure 4.46 A Surface Defined by Filaments

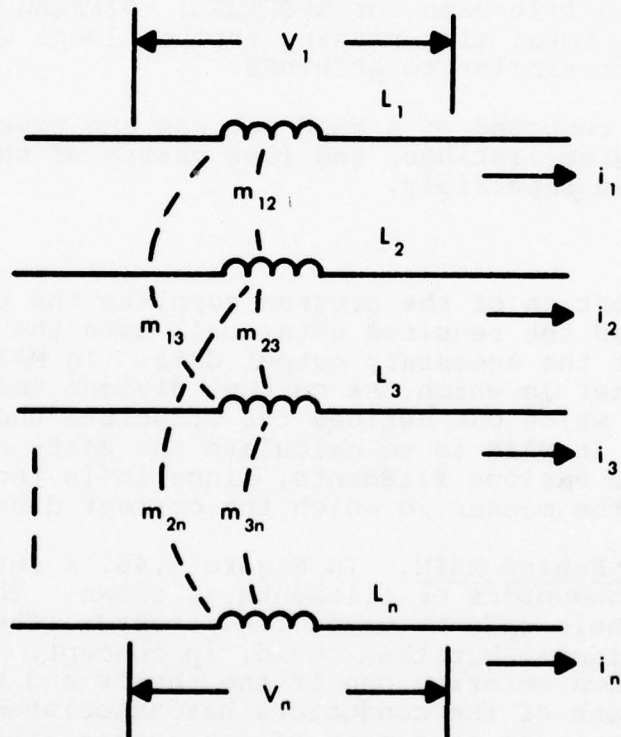


Figure 4.47 Mutually Coupled Inductances

$$v_1/\omega = L_1 i_1 - M_{12} i_2 - M_{13} i_3 \dots \dots \dots - M_{1n} i_n \quad (4.49)$$

$$v_2/\omega = -M_{21} i_1 + L_2 i_2 - M_{23} i_3 \dots \dots \dots - M_{2n} i_n \quad (4.50)$$

$$v_3/\omega = -M_{31} i_1 - M_{32} i_2 + L_3 i_3 \dots \dots \dots - M_{3n} i_n \quad (4.51)$$

$$V_n/\omega = -M_{n1}i_1 - M_{n2}i_2 - M_{n3}i_3 \dots + L_n i_n \quad (4.52)$$

If the angular frequency ω is suppressed, Equations 4.49 through 4.52 may be placed in matrix notation as follows:

$$\begin{bmatrix} V_1 \\ V_2 \\ V_3 \\ \vdots \\ V_n \end{bmatrix} = \begin{bmatrix} L_1 & -M_{12} & -M_{13} & \dots & -M_{1n} \\ -M_{21} & L_2 & -M_{23} & \dots & -M_{2n} \\ -M_{31} & -M_{32} & L_3 & \dots & -M_{3n} \\ \vdots & \vdots & \vdots & \ddots & \vdots \\ -M_{n1} & -M_{n2} & -M_{n3} & \dots & L_{nn} \end{bmatrix} \times \begin{bmatrix} i_1 \\ i_2 \\ i_3 \\ \vdots \\ i_n \end{bmatrix} \quad (4.53)$$

or, in more compact notation

$$| V | = | M | \times | i | \quad (4.54)$$

In Equations 4.53 and 4.54, the normalized angular frequency ω has been set equal to unity.

Multiplying by the inverse of the M matrix, $| M |^{-1}$ gives the following:

$$[M]^{-1} \times [V] = [M]^{-1} \times [M] \times [i] \quad (4.55)$$

or

$$[i] = [M]^{-1} \times [V] \quad (4.56)$$

$$\begin{bmatrix} i_1 \\ i_2 \\ i_3 \\ \vdots \\ i_n \end{bmatrix} = \begin{bmatrix} m_{11}m_{12}m_{13} \dots m_{1n} \\ m_{21}m_{22}m_{23} \dots m_{2n} \\ m_{31}m_{32}m_{33} \dots m_{3n} \\ \vdots \\ m_{n1}m_{n2}m_{n3} \dots m_{nn} \end{bmatrix} \times \begin{bmatrix} V_1 \\ V_2 \\ V_3 \\ \vdots \\ V_n \end{bmatrix} \quad (4.57)$$

where $m_{11}, m_{12} \dots m_{nn}$ are the elements of the inverse of M matrix.

If all of the voltages are the same and equal to V, as is the case if all of the inductances are connected in parallel, the absolute current in each element is

$$i_1 = (m_{11} + m_{12} + m_{13} \dots + m_{1n}) V \quad (4.58)$$

$$i_2 = (m_{12} + m_{21} + m_{23} \dots + m_{2n}) V \quad (4.59)$$

$$i_3 = (m_{31} + m_{32} + m_{33} \dots + m_{3n}) V \quad (4.60)$$

.

.

$$i_n = (m_{n1} + m_{n2} + m_{n3} \dots + m_{nn}) V \quad (4.61)$$

The total current that flows, which is proportional to the impressed voltage, is

$$i_r = (i_1 + i_2 + i_3 + \dots + i_n) V \quad (4.62)$$

The fraction of the total current that flows in each circuit is

$$I_1 = \frac{i_1}{i_r} \quad (4.63)$$

$$I_2 = \frac{i_2}{i_r} \quad (4.64)$$

$$I_3 = \frac{i_3}{i_r} \quad (4.65)$$

.

.

$$I_n = \frac{i_n}{i_r} \quad (4.66)$$

Under dc conditions, the current divides according to the dc resistance of the conductors. In DIFFMAG, the current is assumed to divide directly with the diameter of the conductors and inversely as their length. The program thus assumes all conductors to be made of the same material or to have all the same conductivity. Conductivity could be entered as an input quantity, but that refinement was not felt to be necessary.

Another refinement that could be made would allow one to determine the division of current as a function of frequency. In

Equations 4.53 through 4.66, the angular frequency ω was suppressed. If it were not suppressed and impedance terms were to be expressed as

$$Z = R + j\omega L \quad (4.67)$$

the matrix inversion and manipulation routines would give the division of current as a function of frequency. Drawbacks to doing this are that the matrices would have to be inverted at each frequency, and that the output of current division would have to be printed at each frequency. Those matrices are frequently rather large and the amount of output data would be sizable. Nevertheless, that is a refinement that might be worth making at some time.

The calculation of inductance of the conductors starts with a description of where the conductors are located in space. That description includes the location of the end points, the conductor length, and the diameter of the conductor, quantities that are illustrated in Figure 4.48. The various quantities, which must be entered as data by the user, are stored in a matrix D(i,j), the layout of which is illustrated in Figure 4.49. The length of the filament can be calculated from the locations of the end points as

$$l = \left[(x_s - x_f)^2 + (y_s - y_f)^2 + (z_s - z_f)^2 \right]^{1/2} \quad (4.68)$$

and is stored in location D(i,9).

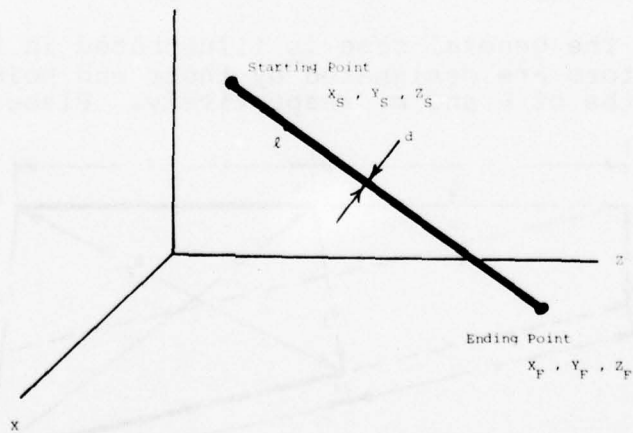


Figure 4.48 A General Conductor in Space

Conductor Number	COORDINATES OF STARTING POINT OF FILAMENT			COORDINATES OF ENDING POINT OF FILAMENT			DIAMETER OF CONDUCTOR	LENGTH OF CONDUCTOR
	x_s	y_s	z_s	x_f	y_f	z_f		
1	1							
2	2							
3	3							

128	128							
129	129							
130	130							

Figure 4.49 Layout of Matrix $D(i,j)$

4.6.2.2 Calculation of Mutual Inductance. As a general case there are two conductors oriented in space. The conductors neither intersect nor do their projections meet at a common point; thus, they do not lie in the same plane. If the filaments are parallel or lie in the same plane, they constitute special cases and are dealt with separately. The calculation of inductance follows the formulation given by Grover (Reference 4.12).

General Case. The general case is illustrated in Figure 4.50. The two conductors are designated by their end points AB and ab. They have lengths of ℓ and m , respectively. Planes are passed

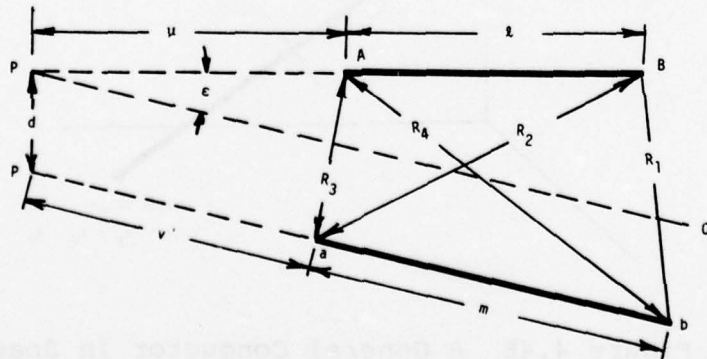


Figure 4.50 Two Filaments Placed in any Arbitrary Locations

through the filaments in such a way as to intersect at right angles. In Figure 4.50, PC represents the line of intersection. The angle formed by the line of intersection and the projection of conductor AB is designated ϵ . R_1 through R_4 represent the distances between the ends of the filaments. Other relevant quantities are given in Figure 4.50. Then

$$\alpha^2 = R_4^2 - R_3^2 + R_2^2 - R_1^2 \quad (4.69)$$

$$\cos \epsilon = \frac{\alpha^2}{2lm} \quad (4.70)$$

$$\mu = l \left[\frac{2m^2(R_2^2 - R_3^2 - l^2) + \alpha^2(R_4^2 - R_3^2 - m^2)}{4l^2m^2 - \alpha^4} \right] \quad (4.71)$$

$$v = m \left[\frac{2l^2(R_4^2 - R_3^2 - m^2) + \alpha^2(R_2^2 - R_3^2 - l^2)}{4l^2m^2 - \alpha^4} \right] \quad (4.72)$$

$$d^2 = R_3^2 - \mu^2 - v^2 + 2\mu v \cos \epsilon \quad (4.73)$$

let

$$\Omega = \tan^{-1} \left[\frac{d^2 \cos \epsilon + (\mu + l)(v + m) \sin^2 \epsilon}{d R_1 \sin \epsilon} \right]$$

$$- \tan^{-1} \left[\frac{d^2 \cos \epsilon + (\mu + l)v \sin^2 \epsilon}{d R_2 \sin \epsilon} \right]$$

$$+ \tan^{-1} \left[\frac{d^2 \cos \epsilon + \mu v \sin^2 \epsilon}{d R_3 \sin \epsilon} \right]$$

$$- \tan^{-1} \left[\frac{d^2 \cos \epsilon + \mu(v + m) \sin^2 \epsilon}{d R_4 \sin \epsilon} \right] \quad (4.74)$$

then

$$\begin{aligned}\frac{M}{0.2 \cos \epsilon} &= (\mu + \ell) \tanh^{-1} \frac{m}{R_1 + R_2} \\ &+ (v + m) \tanh^{-1} \frac{\ell}{R_1 + R_4} \\ &- \mu \tanh^{-1} \frac{m}{R_3 + R_4} \\ &- v \tanh^{-1} \frac{\ell}{R_2 + R_3} \\ &- \frac{\Omega d}{\sin \epsilon} \quad \mu H/m\end{aligned}\tag{4.75}$$

An alternative formulation of Equation 4.75 that avoids the use of inverse hyperbolic functions is possible by noting that

$$\tanh^{-1} x = \frac{1}{2} \log \epsilon \frac{1+x}{1-x} \tag{4.76}$$

or that

$$\tanh^{-1} \frac{m}{R_1 + R_2} = \frac{1}{2} \log \epsilon \frac{R_1 + R_2 + m}{R_1 + R_2 - m} \tag{4.77}$$

Then

$$\begin{aligned}\frac{M}{0.2 \cos \epsilon} &= \frac{(\mu + \ell)}{2} \log \epsilon \frac{R_1 + R_2 + m}{R_1 + R_2 - m} \\ &+ \frac{(v + m)}{2} \log \epsilon \frac{R_1 + R_4 + \ell}{R_1 + R_4 - \ell} \\ &- \frac{\mu}{2} \log \epsilon \frac{R_3 + R_4 + m}{R_3 + R_4 - m}\end{aligned}$$

$$-\frac{v}{2} \log \epsilon \frac{R_2 + R_3 + l}{R_2 + R_3 - l}$$

$$-\frac{\Omega d}{\sin \epsilon} \quad \mu\text{H/m} \quad (4.78)$$

Conductors in the Same Plane; Not Intersecting and Not Parallel. This case is illustrated in Figure 4.51. The expression for mutual inductance is the same as Equation 4.75 or Equation 4.78 except that

$$\Omega = 0 \quad (4.79)$$

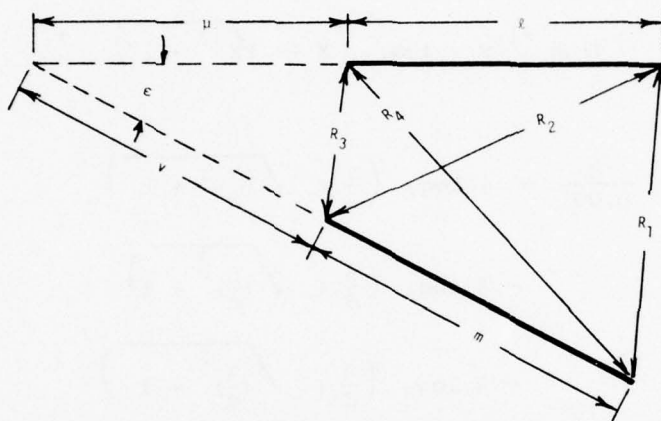


Figure 4.51 Two Filaments in the Same Plane but not Parallel

Parallel Conductors. This case is illustrated in Figure 4.52. If we let

$$\alpha = l + m + \delta \quad (4.80)$$

$$\beta = l + \delta \quad (4.81)$$

$$\delta = m + \delta \quad (4.82)$$

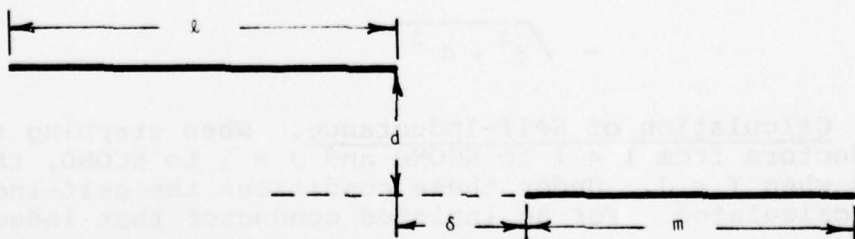


Figure 4.52 Parallel Filaments

then

$$\begin{aligned}
 \frac{M}{0.001} = & \alpha \sinh^{-1} \frac{\alpha}{d} - \beta \sinh^{-1} \frac{\beta}{d} - \delta \sinh^{-1} \frac{\delta}{d} \\
 & + \delta \sinh^{-1} \frac{\delta}{d} - \sqrt{\alpha^2 + d^2} + \sqrt{\beta^2 + d^2} \\
 & + \sqrt{\delta^2 + d^2} - \sqrt{\delta^2 + d^2} \quad \mu\text{H/m} \tag{4.83}
 \end{aligned}$$

The inverse hyperbolic sines may be eliminated by making use of the identity

$$\sinh^{-1} x = \log_e \left(x + \sqrt{x^2 + 1} \right) \tag{4.84}$$

Then

$$\begin{aligned}
 \frac{M}{0.001} = & \alpha \log_e \left(\frac{\alpha}{d} + \sqrt{\left(\frac{\alpha}{d}\right)^2 + 1} \right) \\
 & - \beta \log_e \left(\frac{\beta}{d} + \sqrt{\left(\frac{\beta}{d}\right)^2 + 1} \right) \\
 & - \delta \log_e \left(\frac{\delta}{d} + \sqrt{\left(\frac{\delta}{d}\right)^2 + 1} \right) \\
 & + \delta \log_e \left(\frac{\delta}{d} + \sqrt{\left(\frac{\delta}{d}\right)^2 + 1} \right) \\
 & - \sqrt{\alpha^2 + d^2} \\
 & + \sqrt{\beta^2 + d^2} \\
 & + \sqrt{\delta^2 + d^2} \\
 & - \sqrt{\delta^2 + d^2} \tag{4.85}
 \end{aligned}$$

4.6.2.3 Calculation of Self-Inductance. When stepping through the conductors from $I = 1$ to $NCOND$ and $J = 1$ to $NCOND$, there will be times when $I = J$. Under these conditions the self-inductance must be calculated. For an isolated conductor that inductance is

$$L = 0.2 l \left[\log_{\epsilon} \left(\frac{l}{d} \right) - 0.75 \right] \mu\text{H/m} \quad (4.86)$$

where

l = length

d = diameter

Equation 4.86 ignores the flux internal to the conductor.

4.6.2.4 Program Description - MAIN. The input data for DIFFMAG, shown in Figure 4.53, is controlled by the operation of MAIN. A program listing for MAIN is shown in Figure 4.54 and a flow chart shown in Figure 4.55. These components will be described in some detail.

Starting at line 5000, array sizes are set and certain quantities designated as real or integer. The program is presently dimensioned for a maximum of 80 conductors. If more conductors are required and can be accommodated, the dimensions must be increased accordingly.

In line 5120, the input file is opened. This file must be stored separately under the name INFILE.

In line 5260, the number of conductors is read. This number, referred to as NCOND, is entered in line 10 of the input data file. In this and all the other READ statements, the line number associated with that line of data is read as LINE. LINE is not used, but is read only to keep the data in correct sequence. If an input data file were constructed without line numbers, all of the READ statements would have to be changed.

Using lines 5320 and 5340, the number of conductors is printed on the output data sheet. Much more of the input data is printed out. From this point on in this discussion, the printing of data and headings will be treated only when it is not immediately clear how that printing is controlled.

In line 5500 a factor F is read. F indicates the units used to describe the location and size of the conductors. Those dimensions may be given in either English or metric units-inches, centimeters, or meters-but the calculations of DIFFMAG are made using metric units. If the input data is given as meters, F is designated as 1.0. If dimensions are given in centimeters, F is 0.01, and if the dimensions are given in inches, F is 0.0254.

In line 5640 a control character IOFLAG2 is read. IOFLAG2 controls whether or not data describing the conductors is to be printed. If IOFLAG2 = 1, that data is printed, and if IOFLAG2 = 0, it is not printed.

10 Number of conductors
 (NCOND)

 20 A factor relating to the dimensional units used
 to describe the filaments. If those dimensions
 are given in meters F=1. If they are given in
 centimeters F=.01. If they are given in inches
 F=.0254

 25 A control character. If IOFLAG2=1 the data describing
 the filaments is
 printed.
 If IOFLAG2=0 the data is not
 printed

 30 $\frac{1}{D(I,1)}, \frac{XS}{D(I,2)}, \frac{YS}{D(I,3)}, \frac{ZS}{D(I,4)}, \frac{XE}{D(I,5)}, \frac{YE}{D(I,6)}, \frac{ZE}{D(I,7)}, \frac{DIAM}{D(I,8)}$

 40 2, _____, _____, _____, _____, _____, _____, _____

 50 3, _____, _____, _____, _____, _____, _____, _____

 Starting ending conductor
 coordinates coordinates diameter

 Use additional lines as required to describe
 all the filaments

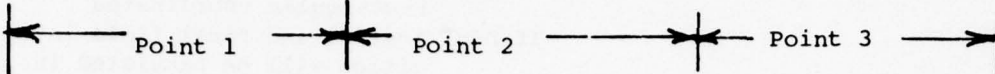
 1010 Total conductor current in Amperes
 (TOTALI)

 1020 A control character. If IOFLAG2=1 the distribution of
 current in the fil-
 aments is printed.
 If IOFLAG2=0 the distribution is
 not printed

Figure 4.53 Input Data for Program DIFFMAG

1030 _____ Number of intercept calculations to be made
(NINTER)

1040 $\frac{X_1}{(PLX1)}, \frac{Y_1}{(PLY1)}, \frac{Z_1}{(PLZ1)}, \dots, \frac{X_2}{(PLX2)}, \frac{Y_2}{(PLY2)}, \frac{Z_2}{(PLZ2)}, \dots, \frac{X_3}{(PLX3)}, \frac{Y_3}{(PLY3)}, \frac{Z_3}{(PLZ3)}$

1050 _____, _____, _____, _____, _____, _____, _____, _____, _____


Use additional lines as necessary to describe NINTER intercepting planes

2000 _____, _____ Control Characters
(ID3) (ID4)

If ID3=1 there should be made calculations of the field strength over a volume
If ID3=0 there should not be made such calculations
If ID4=1 initial and final field intensities will be tabulated in rectangular coordinates
If ID4=2 initial and final field intensities will be tabulated in polar coordinates
If ID4=3 only the magnitudes of the initial and final magnitudes will be tabulated

2010 _____, _____, _____
(ZPA) (ZPB) (ZPC)

ZPA is the starting point
ZPB is the ending point

2020 _____, _____, _____
(YPA) (YPB) (YPC)

ZPC is the increment between the starting and ending points

2030 _____, _____, _____
(XPA) (XPB) (XPC)

Ditto for X and Y

Figure 4.53 Input Data for Program DIFFMAG - Continued

2040 ,
 (D5) (D6)

Control characters

- If D5=1 there should be calculations made of the field strength at specific points
- If D5=0 there should not be made such calculations
- If D6=1 initial and final field intensities will be tabulated in rectangular coordinates
- If D6=2 initial and final field intensities will be tabulated in polar coordinates
- If D6=3 only the magnitudes of the initial and final field intensities will be tabulated

3000 (NPOINT) Number of specific points at which calculations
are to be made

3010 $\frac{X}{(XP)}, \frac{Y}{(YP)}, \frac{Z}{(ZP)}$ X, Y, and Z coordinates of point at which field intensity is to be calculated

3020 _____, _____, _____

Use additional lines as necessary to describe NPOINT points

3500 (D7) A control character

If D7=1 there will be made calculations
of the flux through a loop
If D7=0 there will not be made such
calculations

Figure 4.53 Input Data for Program DIFFMAG Continued

4010 $\frac{X_1}{(XP_1)}, \frac{Y_1}{(YP_1)}, \frac{Z_1}{(ZP_1)}, \frac{X_2}{(XP_2)}, \frac{Y_2}{(YP_2)}, \frac{Z_2}{(ZP_2)}$



Four points, all in the same plane, that describe the loop. The points should go in sequence around the loop.

4020 $\frac{X_3}{(XP_3)}, \frac{Y_3}{(YP_3)}, \frac{Z_3}{(ZP_3)}, \frac{X_4}{(XP_4)}, \frac{Y_4}{(YP_4)}, \frac{Z_4}{(ZP_4)}$



4030 _____, _____, _____, _____, _____, _____

4040 _____, _____, _____, _____, _____, _____

Use additional lines as necessary to describe NLOOP loops

ADDITIONAL NOTES ABOUT INPUT DATA

- 1 If there are no intercepting planes enter NINTER=0 and leave line 1040 blank. The next line should be line 2000.
- 2 If ID3=0 enter a dummy value (1,2 or 3) for ID4 and leave lines 2010,2020, and 2030 blank. The next line should be line 2040.
- 3 If D5=0 enter a dummy value (1,2,or 3) for D5 and leave line 3000 and 3010 blank. The next line should be 3500.
- 4 If D7=0 leave lines 4000,4010 and 4020 blank.
- 5 The program will stop automatically when it runs out of input data.
- 6 Error messages generated during the running of the program generally indicate an incorrect entry of input data.

Figure 4.53 Input Data for Program DIFFMAG Concluded

```

1000C DIFFMAG
1005C FOR DETAILED INFORMATION ON THIS PROGRAM CONTACT
1010C
1020C      F. A. FISHER
1025C      BLDG 9 ROOM 200
1030C      GENERAL ELECTRIC COMPANY
1040C      100 WOODLAWN AVE
1050C      PITTSFIELD, MASS 01201
1060C
1070C      PHONE (413) 494-4380
1080C
1100C IF A GROUP OF CONDUCTORS ARE CONNECTED AT THEIR ENDS AND
1110C CURRENT IS PASSED THROUGH THEM, THAT CURRENT WILL INITIALLY
1120C DIVIDE AMONG THE CONDUCTORS IN A MANNER PROPORTIONAL TO THE
1130C SELF AND MUTUAL INDUCTANCES OF THE CONDUCTORS. THE CURRENT
1140C WILL THEN REDISTRIBUTE ITSELF UNTIL FINALLY THE CURRENT WILL
1150C BE DIVIDED IN PROPORTION TO THE RESISTANCE OF THE CONDUCTORS.
1160C
1170C THE CURRENT IN THE CONDUCTORS WILL PRODUCE MAGNETIC FIELDS.
1180C THE FIELD AT ANY POINT WILL BE THE SUM OF THE PARTIAL FIELDS
1190C PRODUCED BY THE INDIVIDUAL CURRENTS IN THE INDIVIDUAL
1200C CONDUCTORS.
1210C
1220C THIS PROGRAM, "DIFFMAG", CALCULATES HOW THE CURRENT DIVIDES
1230C AND CALCULATES THE MAGNETIC FIELDS PRODUCED BY THE CURRENTS.
1240C
1250C THE USER MUST SUPPLY INFORMATION ON WHERE THE CONDUCTORS ARE LOC-
1260C ATED, WHERE HE WISHES THE FIELDS TO BE CALCULATED AND THE TYPE OF
1270C CALCULATIONS THAT HE WISHES TO HAVE MADE. THE NECESSARY INFOR-
1280C MATION MUST BE LOCATED IN A FILE NAMED "INFILE", THE CHARAC-
1290C TERISTICS OF WHICH ARE AS FOLLOWS. EACH LINE OF DATA MUST
1300C HAVE A LINE NUMBER, THOUGH THE LINE NUMBERS NEED NOT BE IDENTICAL
1310C TO THOSE GIVEN BELOW.
1320C
1330C ****
1340C -----NATURE OF INFILE-----
1345C
1350C
1360C LINE #      DATA
1370C
1380C 10      NUMBER OF CONDUCTORS (80 OR LESS, UNLESS PROGRAM
1390C           DIMENSIONS ARE INCREASED)
1395C
1400C 20      A FACTOR F.   F=1.0 IF DIMENSIONS ARE GIVEN IN METERS
1410C           F=.01 IF DIMENSIONS IN CENTIMETERS
1420C           F=.0254 IF DIMENSIONS IN INCHES
1425C
1430C 25      A CONTROL CHARACTER; 1 IF CONDUCTOR DESCRIPTIONS ARE
1440C           TO BE PRINTED AND 0 (ZERO) IF NOT PRINTED.
1445C
1450C 30      COND #, XS , YS , ZS , XF , YF , ZF , DIAM
1455C
1457C           COND # = SEQUENTIAL NUMBER OF CONDUCTOR.
1460C           XS = X COORDINATE OF STARTING POINT

```

Figure 4.54 Listing of Program DIFFMAG

1470C YS = Y COORDINATE OF STARTING POINT
 1480C ZS = Z COORDINATE OF STARTING POINT
 1490C XF , YF , ZF DITTO FOR ENDING POINT
 1495C
 1500C DIAM = DIAMETER OF CONDUCTOR
 1510C
 1520C USE ADDITIONAL LINES AS NECESSARY TO DESCRIBE ALL
 1525C CONDUCTORS.
 1527C
 1530C
 1540C 1010 TOTAL CURRENT IN AMPERES
 1545C
 1550C 1020 A CONTROL CHARACTER; 1 IF THE DISTRIBUTION OF CURRENT
 1560C IN THE FILAMENTS IS TO BE PRINTED AND 0 (ZERO) IF NOT.
 1565C
 1570C 1030 NUMBER OF INTERCEPT CALCULATIONS TO BE MADE.
 1575C
 1580C 1040 X1 , Y1 , Z1 , X2 , Y2 , Z2 , X3 , Y3 , Z3
 1585C
 1590C THESE ARE X , Y , AND Z COORDINATES THAT DEFINE PLANES.
 1600C USE ADDITIONAL LINES FOR ADDITIONAL PLANES.
 1605C
 1610C 2000 ID3, ID4 ID3 = 1 IF FIELD STRENGTH IS TO BE CALCULATED
 1620C OVER AN VOLUME AND 0 (ZERO) IF NOT.
 1630C ID4 = 1 IF RECTANGULAR COORDINATES ARE TO BE USED AND 2
 1640C IF POLAR COORDINATES ARE TO BE USED. IF ONLY MAGNITUDES
 1650C OF FIELD STRENGTH ARE NEEDED LET ID4 = 3.
 1655C
 1660C 2010 ZPA , ZPB , ZPC ZPA = STARTING POINT FOR CALCS
 1670C ZPB = ENDING POINT
 1680C ZPC = INCREMENT
 1690C
 1700C 2020 YPA , YPB , YPC DITTO FOR Y
 1710C 2030 XPA , XPB , XPC DITTO FOR X
 1715C
 1720C 2040 D5,D6 CONTROL CHARACTERS. D5=1 IF THERE ARE TO BE
 1730C CALCULATIONS OF FIELD STRENGTH AT SPECIFIC
 1740C POINTS AND D5=0 (ZERO) IF NOT. D6=1 IF RECTAN-
 1750C GULAR COORDINATES, D6=2 IF POLAR COORDINATES AND
 1760C D6=3 IF ONLY MAGNITUDES ARE NEEDED.
 1765C
 1770C 3000 NUMBER OF SPECIFIC POINTS AT WHICH CALCS ARE TO BE MADE.
 1775C
 1780C 3010 XP , YP , ZP THESE ARE THE X , Y , AND Z COORDINATES OF
 1790C THE POINT AT WHICH THE CALCULATION IS TO
 1795C BE MADE. USE ADDITIONAL LINES AS NECESS-
 1800C ARY TO DESCRIBE ALL POINTS.
 1805C
 1810C 3500 D7 A CONTROL CHARACTER. D7=1 IF CALCULATIONS ARE TO
 1820C BE MADE OF FLUX THROUGH A LOOP AND D7=0 IF NOT.
 1825C
 1830C 4000 NUMBER OF LOOPS FOR WHICH CALCULATIONS ARE TO BE MADE.
 1835C
 1840C 4010 X1 , Y1 , Z1 , X2 , Y2 , Z2 FOUR POINTS, ALL IN THE

Figure 4.54 Listing of Program DIFFMAG Continued

```

1850C 4020 X3 , Y3 , Z3 , X4 , Y4 , Z4      SAME PLANE, THAT DESCRIBE
1855C
1860C
1870C      THE POINTS
1880C      SHOULD GO IN SEQUENCE AROUND THE LOOP. USE ADDITIONAL
1885C      PAIRS OF LINES TO DESCRIBE ALL LOOPS.
1890C -----
1900C -----END OF INFILE-----
1910C -----NOTES ABOUT INFILE-----
1920C
1930C IF THERE ARE NO INTERCEPTING PLANES ENTER 0 ON LINE 1030 AND LEAVE
1940C LINE 1040 BLANK. THE NEXT LINE SHOULD BE 2000.
1945C
1950C IF ID3=0 ENTER A DUMMY VALUE (1,2, OR 3) FOR ID4 AND LEAVE LINES
1960C 2010,2020, AND 2030 BLANK. THE NEXT LINE SHOULD BE 2040.
1965C
1970C IF D5=0 ENTER A DUMMY VALUE (1,2 OR 3) FOR D6 AND LEAVE LINES
1975C 3000 AND 3010 BLANK. THE NEXT LINE SHOULD BE 3500.
1977C
1980C IF D7=0 LEAVE LINES 4000,4010, AND 4020 BLANK.
1990C
2000C THE PROGRAM WILL STOP AUTOMATICALLY WHEN IT RUNS OUT OF DATA.
2010C
2020C ERROR MESSAGES GENERATED DURING THE RUNNING OF THE PROGRAM GEN-
2030C     ERALLY INDICATE AN INCORRECT ENTRY OF INPUT DATA.
2035C
2040C -----END OF NOTES-----
2050C ****
2060C
5000 DIMENSION XM(80,80),V(80,1),CUR(80,1),D(80,9)
5020 DIMENSION CURDIS(80),RCURDIS(80),XNUMER(80),DENOM(80)
5040 DIMENSION THETA(80),DIST(80),HFLDT(80),HFLDR(80)
5060 INTEGER OUTFIL,CONNO
5080 INTEGER D5,D6,D7
5100 COMMON PX1,PY1,PZ1,PX2,PY2,PZ2,PX3,PY3,PZ3,PX4,PY4,PZ4,N1
5120 CALL OPENF(09,"INFILE?",ISTAT,1,0,1)
5140 WRITE(06,2431)ISTAT
5160 WRITE(06,5860)
5180 WRITE(06,1236)
5200C DATA IN INFILE IS SPECIFICALLY FOR THIS PROGRAM
5220 PI=3.1415926536
5240C NCOND IS THE NUMBER OF CONDUCTORS TO BE CONSIDERED
5260 READ(09,2431)LINE,NCOND
5280 N=NCOND
5300C---
5320 WRITE(06,1233)NCOND
5340 1233 FORMAT(" THIS ANALYSIS DEALS WITH",I5," CONDUCTORS")
5360C-----
5380 WRITE(06,1236)
5400 1236 FORMAT("   ")
5420 2431 FORMAT(V)
5440C F RELATES TO THE DIMENSIONS OF INPUT COORDINATES AND IS
5460C 1 IF DIMENSIONS ARE IN METERS, .01 IF IN CENTIMETERS AND
5480C IS .0254 IF IN INCHES

```

Figure 4.54 Listing of Program DIFFMAG Continued

```

5500 READ(09,2432)LINE,F
5520C---
5540 WRITE(06,1333)F
5560 1333 FORMAT(" THE FACTOR F RELATING TO DIMENSIONS IS",1E10.3)
5580C -----
5600C IF IOFLAG2=1 WE PRINT THE DATA DESCRIBING THE CONDUCTORS
5620C IF IOFLAG2=0 WE DO NOT PRINT THAT DATA
5640 READ(09,2432)LINE,IOFLAG2
5660 IF(IOFLAG2<0.5)GOTO 1334 →
5680 WRITE(06,1236)
5700C -----
5720 WRITE(06,5860)
5740 WRITE(06,1236)
5760 WRITE(06,1335)
5780 WRITE(06,1336)
5800 1334 CONTINUE ←
5820 1335 FORMAT(" THE FOLLOWING DATA GIVES THE COORDINATES THAT")
5840 1336 FORMAT(" DEFINE THE START AND END POINTS")
5860 WRITE(06,1236)
5880 WRITE(06,1236)
5900 2432 FORMAT(V)
5920C WE WILL NOW READ THE COORDINATES THAT DEFINE THE START AND
5940C END POINTS OF THE CONDUCTORS
5960 IF(IOFLAG2<0.5)GOTO 2334 →
5980 2333 WRITE(06,3900)
6000 WRITE(06,1236)
6020 2334 CONTINUE ←
6040 DO 2445 I=1,NCOND,1 ←
6060 READ(09,2432)LINE,D(I,1),D(I,2),D(I,3),D(I,4),D(I,5),
6080& D(I,6),D(I,7),D(I,8)
6100 IF(IOFLAG2<0.5)GOTO 4300 →
6110C WE WILL NOW START PRINTING THE START AND END POINTS
6120 WRITE(06,4100)I,D(I,2),D(I,3),D(I,4)
6140 WRITE(06,4200)I,D(I,5),D(I,6),D(I,7)
6160 WRITE(06,1236)
6180 4300 CONTINUE ←
6200C THIS ENDS THE READING OF COORDINATES THAT DEFINE CONDUCTORS
6220 2388 FORMAT(A7)
6240 DO 2444 J=2,8 ←
6260 D(I,J)=D(I,J)*F
6280 2444 CONTINUE →
6300 2445 CONTINUE →
6320 N1=NCOND
6340 I=N1
6360C IDUM,JDUM AND KDUM ARE USED IN A MATRIX INVERSION CALL
6380 IDUM=N1
6400 JDUM=N1
6420 KDUM=N1
6440 DO 3500 I=1,N1
6460 V(I,1)=1.
6480 3500 CONTINUE
6500 3900 FORMAT(" CONDUCTOR",7X,"X",11X,"Y",11X,"Z")
6540 DO 4400 I=1,N1
6560 INDX=I

```

Figure 4.54 Listing of Program DIFFMAG Continued

```

6580 4100 FORMAT(1X,I2,3X,"START",3E12.3)
6600 4200 FORMAT(1X,I2,3X,"END",2X,3E12.3)
6620 4400 CONTINUE
6640 4500 CONTINUE
6660 IF(IOFLAG2<0.5)GOTO 5910 →
6680 5850 WRITE(06,5860)
6700 WRITE(06,1236)
6720 5860 FORMAT("*****")
6740 WRITE(06,5870)
6760 WRITE(06,5871)
6780 WRITE(06,1236)
6800 WRITE(06,1236)
6820 WRITE(06,5860)
6840 WRITE(06,1236)
6860 25100 FORMAT(V)
6880 WRITE(06,5900)
6900 5870 FORMAT(" THE FOLLOWING DATA DESCRIBES THE LENGTH AND")
6920 5871 FORMAT(" DIAMETER OF THE CONDUCTORS")
6940 WRITE(06,1236)
6960 5900 FORMAT(1X,"CONDUCTOR",4X,"LENGTH",7X,"DIAMETER")
6980C THIS ENDS PRINTING OF CONDUCTOR COORDINATES
7000 5910 CONTINUE ←
7020 DO 6700 I=1,N1 ←
7040 ISAVE=IFIX(D(I,1))
7060 X=D(I,2)-D(I,5)
7080 Y=D(I,3)-D(I,6)
7100 Z=D(I,4)-D(I,7)
7120 D(I,9)=SQRT(X*X+Y*Y+Z*Z)
7140 D(I,9)=D(I,9)/F
7160 D(I,8) =D(I,8)/F
7180 IF(IOFLAG2<0.5)GOTO 5990 →
7200 WRITE(06,6600) ISAVE,D(I,9),D(I,8)
7220 5990 CONTINUE ←
7240 6600 FORMAT(3X,13,7X,1E12.5,1X,1E12.5)
7260 D(I,9)=D(I,9)*F
7280 D(I,8)=D(I,8)*F
7300 6700 CONTINUE ←
7320 IF(IOFLAG2<0.5)GOTO 6703 →
7340 WRITE(06,1236)
7360 WRITE(06,6720)
7380 WRITE(06,1236)
7400 6720 FORMAT("*****")
7420 6721 FORMAT( " THE FOLLOWING DATA GIVES THE DISTANCES BETWEEN")
7440 6722 FORMAT(" THE ENDS OF THE FILAMENTS")
7460 WRITE(06,1236)
7480 WRITE(06,6721)
7500 WRITE(06,6722)
7520 WRITE(06,1236)
7540 WRITE(06,6720)
7560 WRITE(06,1236)
7580 WRITE(06,6702)
7600 6702 FORMAT(" I TO J "," START      END")
7620 WRITE(06,1236)
7640 6703 CONTINUE ←

```

Figure 4.54 Listing of Program DIFFMAG - Continued

```

7650 IF(IOFLAG2<0.5)GOTO 6710 →
7660 DO 6706 I=2,NCOND,1 ←
7680 J=I-1
7700 X1=D(I,2)-D(J,2)
7720 Y1=D(I,3)-D(J,3)
7740 Z1=D(I,4)-D(J,4)
7760 DELS=SQRT(X1*X1+Y1*Y1+Z1*Z1)
7780 X2=D(I,5)-D(J,5)
7800 Y2=D(I,6)-D(J,6)
7820 Z2=D(I,7)-D(J,7)
7840 DELE=SQRT(X2*X2+Y2*Y2+Z2*Z2)
7860 II=IFIX(D(I,1))
7880 IJ=IFIX(D(J,1))
7920 WRITE(06,6704)II,IJ,DELS,DELE
7940 6704 FORMAT(14,14,2E12.5)
7960 6706 CONTINUE →
7980 WRITE(06,1236)
8000 WRITE(06,5860)
8020 WRITE(06,1236)
8040 6710 CONTINUE ←
8060 READ(09,25100)LINE,TOTALI
8080 WRITE(06,4753)TOTALI
8100 WRITE(06,1236)
8120 WRITE(06,5860)
8140 WRITE(06,1236)
8160 4753 FORMAT(" THE TOTAL CURRENT IS",1E12.3," AMPERES")
8180C HERE WE START CALCULATION OF L AND M
8200 6800 E4=2.71828182845
8220 DO 18700 I=1,N1 ← From Line 10500
8240 DO 18600 J=1,N1 ← From Line 10480
8260 IF(I .EQ. J) GO TO 13600 → To Line 9580
8280 X=D(I,5)-D(J,5)
8300 Y=D(I,6)-D(J,6)
8320 Z=D(I,7)-D(J,7)
8340 Q1=X*X+Y*Y+Z*Z
8360 R1=SQRT(Q1)
8380 X=D(I,5)-D(J,2)
8400 Y=D(I,6)-D(J,3)
8420 Z=D(I,7)-D(J,4)
8440 Q2=X*X+Y*Y+Z*Z
8460 R2=SQRT(Q2)
8480 X=D(I,2)-D(J,2)
8500 Y=D(I,3)-D(J,3)
8520 Z=D(I,4)-D(J,4)
8540 Q3=X*X+Y*Y+Z*Z
8560 R3=SQRT(Q3)
8580 X=D(I,2)-D(J,5)
8600 Y=D(I,3)-D(J,6)
8620 Z=D(I,4)-D(J,7)
8640 Q4=X*X+Y*Y+Z*Z
8660 R4=SQRT(Q4)
8680 A1=Q4-Q3+Q2-Q1
8700 A2=SQRT(ABS(A1))
8720 E1=A1/(2*D(I,9)*D(J,9))

```

Figure 4.54 Listing of Program DIFFMAG - Continued

```

8740 E2=1-E1*E1
8760 E3=SQRT(E2)
8780C-
8800 IF(ABS(E1).GT.0.9999)GOTO 14400 →
8820 XK1=2*D(J,9)*D(J,9)*(Q2-Q3-D(I,9)*D(I,9))
8840 XK2=A1*(Q4-Q3-D(J,9)*D(J,9))
8860 XK3=(2*D(I,9)*D(J,9))**2-A1*A1
8880 U1=D(I,9)*(XK1+XK2)/XK3
8900 XK1=2*D(I,9)*D(I,9)*(Q4-Q3-D(J,9)*D(J,9))
8920 XK2=A1*(Q2-Q3-D(I,9)*D(I,9))
8940 V1=D(J,9)*(XK1+XK2)/XK3
8960 D1=Q3-U1-V1*V1+2*U1*V1*E1
8980 D2=SQRT(ABS(D1))
9000C-
9020 IF(ABS(D2/SQRT(D(I,9)*D(J,9))).GT.0.002)GOTO 11200 →
9040C-
9060C THIS FORCES W=0 WHEN THE FILAMENTS LIE IN THE SAME PLANE
9080 W=0
9100 GOTO 12300 →
9120 11200 XK1=(D1*E1+(U1+D(I,9))*(V1+D(J,9))*E2)/(D2*R1*E3) ←
9140 XK1=ATAN(XK1)
9160 XK2=(D1*E1+(U1+D(I,9))*V1*E2)/(D2*R2*E3)
9180 XK2=ATAN(XK2)
9200 XK3=(D1*E1+U1*V1*E2)/(D2*R3*E3)
9220 XK3=ATAN(XK3)
9240 XK4=(D1*E1+U1*(V1+D(J,9))*E2)/(D2*R4*E3)
9260 XK4=ATAN(XK4)
9280 W=XK1-XK2+XK3-XK4
9300 12300 XK1=D(J,9)/(R1+R2) ←
9320 XK1=(ALOG(1+XK1)-ALOG(1-XK1))*(U1+D(I,9))
9340 XK2=D(I,9)/(R1+R4)
9360 XK2=(ALOG(1+XK2)-ALOG(1-XK2))*(V1+D(J,9))
9380 XK3=D(J,9)/(R3+R4)
9400 XK3=(ALOG(1+XK3)-ALOG(1-XK3))*U1 From line 8260
9420 XK4=D(I,9)/(R2+R3)
9440 XK4=(ALOG(1+XK4)-ALOG(1-XK4))*V1
9460 XM(I,J)=0.1*E1*(XK1+XK2-XK3-XK4-W*D2/E3)
9480C THIS ENDS THE GENERAL CASE FOR CALCULATION OF M
9500C-
9520 GOTO 18600
9540C-
9560C THIS STARTS CALCULATIONS FOR SELF INDUCTANCE
9580 13600 XM(I,J)=0.2*D(I,9)*(ALOG(4*D(I,9)/D(I,8))-0.75)
9600C THIS ENDS CALCULATIONS FOR SELF INDUCTANCE
9620C-
9640 GOTO 18600
9660C-
9680C THIS STARTS ROUTINE FOR CALCULATION OF M FOR PARALLEL FILAMENTS
9700 14400 CONTINUE ←
9720 ALPHA=D(J,9)*D(J,9)+Q3-Q2
9740 ALPHA=ALPHA/(2*D(J,9)*R3)
9760 ALPHA=ARCCOS(ALPHA)
9780 BETA=D(J,9)*D(J,9)+Q2-Q3
9800 BETA=BETA/(2*D(J,9)*R2) To line 10480

```

Figure 4.54 Listing of Program DIFFMAG - Continued

```

9820 BETA=ARCOS(BETA)
9840 PI=3.14159265
9860 BETA1=PI-BETA
9880 D2=D(I,9)*SIN(ALPHA)*SIN(BETA1)
9900 D2=D2/SIN(BETA1-ALPHA)
9910 D1=D2*D2
9920 D4=-SQRT(Q2-D2*D2)
9940 XK1=D(I,9)+D(J,9)+D4
9960 XK2=D(I,9)+D4
9980 XK3=D(J,9)+D4
10000 XK4=XK1/D2
10020 XK4=XK4+SQRT(XK4*XK4+1)
10040 XK4=XK1* ALOG(XK4)
10060 XK5=XK2/D2
10080 XK5=XK5+SQRT(XK5*XK5+1)
10100 XK5=XK2* ALOG(XK5)
10120 XK6=XK3/D2
10140 XK6=XK6+SQRT(XK6*XK6+1)
10160 XK6=XK3* ALOG(XK6)
10180 XK7=D4/D2
10200 XK7=XK7+SQRT(XK7*XK7+1)
10220 XK7=D4* ALOG(XK7)
10260 XL9=XK1*XK1+D1
10280 XL1=SQRT(ABS(XL9))
10300 XL8=XK2*XK2+D1
10320 XL2=SQRT(ABS(XL8))
10340 XL7=XK3*XK3+D1
10360 XL3=SQRT(ABS(XL7))
10380 XL6=D4*D4+D1
10400 XL4=SQRT(ABS(XL6))
10420 11415 CONTINUE
10440 XM(I,J)=0.1*(XK4-XK5-XK6+XK7-XL1+XL2+XL3-XL4)
10460C THIS ENDS ROUTINE FOR CALCULATION OF M FOR PARALLEL FILAMENTS
10480 18600 CONTINUE -----> To line 8240
10500 18700 CONTINUE -----> To line 8220
10520C -----
10540 WRITE(06,1236)
10546 WRITE(06,5860)
10560C -----
10580C BEGIN CALCULATIONS OF CURRENT DISTRIBUTION IN FILAMENTS
10600 CALL MATRIX(XM, IDUM, JDUM, KDUM)
10620 DO 19760 I=1,N1 <
10640 IROW=I
10660 ICOL=I
10680 TEMP=0.
10700 DO 19759 J=1,N1 <
10720 ICOL=J
10740 IRO=J
10760 TEMP=TEMP+(XM(IROW,ICOL)*V(IRO,1))
10780 19759 CONTINUE >
10800 CUR(IROW,1)=TEMP
10820 19760 CONTINUE >
10840 CUR1=0
10860 DO 20100 I=1,N1 <
10880 CUR1=CUR(I,1)+CUR1
10900 20100 CONTINUE >

```

Figure 4.54 Listing of Program DIFFMAG - Continued

```

10920 DO 20400 I=1,N1 ←
10940 CURDIS(I)=CUR(I,1)*TOTALI/CUR1
10960 20400 CONTINUE
10980 RCUR1=0
11000 DO 20502 I=1,N1 ←
11020 RCURDIS(I)=V(IRO,1)*D(I,8)/D(I,9)
11040 RCUR1=RCUR1+RCURDIS(I)
11060 20502 CONTINUE
11080 DO 20850 I=1,N1 ←
11100 RCURDIS(I)=RCURDIS(I)*TOTALI/RCUR1
11120 20850 CONTINUE
11140 5339 FORMAT(" LINE",I10)
11160 READ(09,2431)LINE,IOFLAG2
11180C --
11200C --
11220 IF(IOFLAG2)20950,20950,20800 ←
11240 20800 WRITE(06,20810) ←
11260 WRITE(06,1236)
11280 WRITE(06,20802)
11300 20802 FORMAT(1X,"CONDUCTOR",5X,"MAG I",7X,"RES I")
11320 WRITE(06,1236)
11340 DO 20900 I=1,N1 ←
11360 WRITE(06,20804)I,CURDIS(I),RCURDIS(I)
11380 20804 FORMAT(2X,I3,5X,2E12.3)
11400 20810 FORMAT(" THE FOLLOWING DATA TELLS HOW THE CURRENT DIVIDES")
11420 20900 CONTINUE →
11440 20950 CONTINUE ←
11460 WRITE(06,1236)
11480 WRITE(06,5860)
11500 WRITE(06,1236)
11520 READ(09,2431)LINE,NINTER
11540C --
11560 WRITE(06,5513)NINTER
11580 5513 FORMAT(" THERE ARE",I4," INTERCEPTING PLANES")
11600 WRITE(06,1236)
11620 WRITE(06,5860)
11640 WRITE(06,1236)
11660C THIS BEGINS THE CALCULATION OF INTERCEPT POINTS
11680 DO 32810 I9=1,NINTER,1 ←
11700C --
11720 2100 CONTINUE
11740 READ(09,21002)LINE,PLX1,PLY1,PLZ1,PLX2,PLY2,PLZ2,
11760C PLX3,PLY3,PLZ3
11780C --
11800 WRITE(06,21001)
11820 21001 FORMAT(" THE POINTS DEFINING A PLANE ARE")
11840 WRITE(06,1236)
11860 21002 FORMAT(V)
11880 WRITE(06,21004)
11900 WRITE(06,1236)
11920 21004 FORMAT(" PLANE NUMBER POINT NUMBER",10X,"X",11X,"Y",11X,"Z")
11940 I8=1
11960 WRITE(06,21006)I9,I8,PLX1,PLY1,PLZ1
11980 I8=2

```

From Line 13060

Figure 4.54 Listing of Program DIFFMAG - Continued

THIS PAGE IS BEST QUALITY PRACTICALLY
FROM COPY FURNISHED TO DDC

```

12000 WRITE(06,21006)I9,I8,PLX2,PLY2,PLZ2
12020 I8=3
12040 WRITE(06,21006)I9,I8,PLX3,PLY3,PLZ3
12060 21006 FORMAT(5X,I3,11X,I3,8X,3E12.3)
12080 WRITE(06,1236)
12100 WRITE(06,21007)
12120 21007 FORMAT(" THAT PLANE INTERCEPTS THE FILAMENTS AS FOLLOWS")
12140 A11=1;A12=1;A13=1
12160C --
12180 CALL PLAN1(PLX1,PLY1,PLZ1,PLX2,PLY2,PLZ2,PLX3,PLY3,PLZ3,
12200& A11,A12,A13)
12220 WRITE(06,1236)
12240 WRITE(06,1236)
12260 WRITE (06,30100)
12280 WRITE(06,1236)
12300 30100 FORMAT(1X,"CONDUCTOR",4X,"X INTER",5X,"Y INTER",
12320& 5X,"Z INTER",5X,"DELTA S",5X,"DELTA H")
12340 STOT=0
12360C --
12380 I=1
12400 CALL INCEPT(A11,A12,A13,I,D,XI,YI,ZI)
12420 X1=XI;Y1=YI;Z1=ZI
12440 D031600 I=2,NCOND,1 ←
12460C --
12480 CALL INCEPT(A11,A12,A13,I,D,XI,YI,ZI)
12500 DELX= XI-X1;DELY=YI-Y1;DELZ=ZI-Z1
12520 DELS=SQRT(DELX*DELX+DELY*DELY+DELZ*DELZ)
12540IAVE= (CURDIS(I)+CURDIS(I-1))/2
12560 DELH=IAVE/DELS
12580 WRITE(06,31300)I-1,X1,Y1,Z1,DELS,DELH
12600 31300 FORMAT(3X,I3,5X,5E12.3)
12620 STOT=STOT+DELS
12640 X1=XI;Y1=YI;Z1=ZI
12660 31600 CONTINUE →
12680 I=1
12700C --
12720 CALL INCEPT(A11,A12,A13,I,D,XI,YI,ZI)
12740 DELX=X1-XI;DELY=YI-YI;DELZ=Z1-ZI
12760 DELD=SQRT(DELX*DELX+DELY*DELY+DELZ*DELZ)
12780 DELH=IAVE/DELS
12800 WRITE(06,31300)NCOND,X1,Y1,Z1,DELS,DELH
12820 STOT=STOT+DELS
12840 WRITE(06,1236)
12860 WRITE(06,32500)STOT
12880 32500 FORMAT(" PERIPHERAL DISTANCE=      ",1E10.3," METERS")
12900 HAVE=TOTALI/STOT
12920 WRITE(06,1236)
12940 WRITE(06,32800) HAVE
12960 WRITE(06,1236)
12980 32800 FORMAT(1X,"AVERAGE FIELD INTENSITY= ",1E10.3,
13000& " AMPERES PER METER")
13020 WRITE(06,5860)
13040 WRITE(06,1236)
13060 32810 CONTINUE

```

Figure 4.54 Listing of Program DIFFMAG - Continued

THIS PAGE IS BEST QUALITY PRACTICABLE
FROM COPY FURNISHED TO DDG

```

13080C THIS ENDS THE CALCULATION OF INTERCEPT POINTS
13100 32910 FORMAT(V)
13120C --
13140 32915 CONTINUE
13160 READ(09,32910)LINE, ID3, ID4
13180 WRITE(06,6323) ID3, ID4
13200 6323 FORMAT(" ID3=", I3, " AND ID4=", I3)
13220 WRITE(06,1236)
13240 WRITE(06,5860)
13260 WRITE(06,1236)
13270 IF(ID3.LT.0.5)GOTO 33410
13280 READ(09,32910)LINE,ZPA,ZPB,ZPC
13300 READ(09,32910)LINE,YPA,YPB,YPC
13320 READ(09,32910)LINE,XPA,XPB,XPC
13340 WRITE(06,6404)ZPA,ZPB,ZPC
13360 WRITE(06,6406)YPA,YPB,YPC
13380 WRITE(06,6408)XPA,XPB,XPC
13400 WRITE(06,1236)
13420 WRITE(06,5860)
13440C --
13460 6404 FORMAT(" ZPA,ZPB AND ZPC ARE",3E12.3)
13480 6406 FORMAT(" YPA,YPB AND YPC ARE",3E12.3)
13500 6408 FORMAT("XPA,XPB AND XPC ARE",3E12.3)
13520 WRITE(06,1236)
13540 32920 CONTINUE
13560 J1=IFIX((ZFB-ZPA)/ZPC)+1
13580 J2=IFIX((YPB-YPA)/YPC)+1
13600 J3=IFIX((XPB-XPA)/XPC)+1
13640 GOTO(33100,33120,33125),ID4
13660 33070 FORMAT(5X,"X",11X,"Y",11X,"Z",9X,"H-X",9X,"H-Y",9X,"H-Z")
13680 33080 FORMAT(5X,"X",11X,"Y",11X,"Z",9X,"H-TOT",7X,"LAT-ANG",
13700& 6X,"LONG ANG")
13720 33085 FORMAT(5X,"X",11X,"Y",11X,"Z",9X,"H-MAGNETIC H-RESISTIVE")
13740 33180 FORMAT(6E12.3)
13760 33185 FORMAT(5E12.3)
13780 33100 WRITE(06,33070)
13800 WRITE(06,1236)
13820 GOTO 33130 →
13840 33120 WRITE(06,33080)
13860 WRITE(06,1236)
13880 GOTO 33130 →
13900 33125 WRITE(06,33085)
13920 WRITE(06,1236)
13940 33130 CONTINUE ←
13960 DO 33400 I3=1,J3,1 ←
13980 WRITE(06,1236)
14000 DO 33400 I2=1,J2,1 ←
14020 WRITE(06,1236)
14040 DO 33400 I1=1,J1,1 ←
14060 XP1=XPA+(I3-1)*XPC
14080 XP=XP1
14100 YP1=YPA+(I2-1)*YPC
14120 YP=YP1
14140 ZP1=ZPA+(I1-1)*ZPC

```

Figure 4.54 Listing of Program DIFFMAG - Continued

THIS PAGE IS BEST QUALITY PRACTICABLE
FROM COPY FURNISHED TO DDC

```

14160 ZP=ZP1
14180 GOTO (33200,33220,33310),ID4
14200 33200 FLAG1=1
14220 CALL FILSUM(FLAG1,N,XP,YP,ZP,D,RCURDIS,CURDIS,HX0,HY0,HZ0)
14240 WRITE(06,33180)XP1,YP1,ZP1,HX0,HY0,HZ0
14260 FLAG1=0
14280 CALL FILSUM(FLAG1,N,XP,YP,ZP,D,RCURDIS,CURDIS,HX0,HY0,HZ0)-
14300 WRITE(06,33180)XP1,YP1,ZP1,HX0,HY0,HZ0
14320 GOTO 33400
14340 33220 FLAG1=1
14360 CALL FILSUM(FLAG1,N,XP,YP,ZP,D,RCURDIS,CURDIS,HX0,HY0,HZ0)
14380 CALL VSUM(HX0,HY0,HZ0,HTOT,ANG1,ANG2)
14400 WRITE(06,33180)XP1,YP1,ZP1,HTOT,ANG1,ANG2
14420 FLAG1=0
14440 CALL FILSUM(FLAG1,N,XP,YP,ZP,D,RCURDIS,CURDIS,HX0,HY0,HZ0)
14460 CALL VSUM(HX0,HY0,HZ0,HTOT,ANG1,ANG2)
14480 WRITE(06,33180)XP1,YP1,ZP1,HTOT,ANG1,ANG2
14500 GOTO 33400
14520 33310 CONTINUE
14540 FLAG1=1
14560 CALL FILSUM(FLAG1,N,XP,YP,ZP,D,RCURDIS,CURDIS,HX0,HY0,HZ0)
14580 CALL VSUM(HX0,HY0,HZ0,HTOT,ANG1,ANG2)
14600 HTOTM=HTOT
14620 FLAG1=0
14640 CALL FILSUM(FLAG1,N,XP,YP,ZP,D,RCURDIS,CURDIS,HX0,HY0,HZ0)
14660 CALL VSUM(HX0,HY0,HZ0,HTOT,ANG1,ANG2)
14680 HTOTR=HTOT
14700 WRITE(06,33185)XP1,YP1,ZP1,HTOTM,HTOTR
14720C --
14740 33400 CONTINUE
14760 33410 CONTINUE
14780 WRITE(06,1236)
14800 WRITE(06,5860)
14820 WRITE(06,1236)
14840 READ(09,32910)LINE,D5,D6
14860 WRITE(06,7331)D5,D6
14880 7331 FORMAT(" D5=",I3," AND D6=",I3)
14900 WRITE(06,1236)
14920 WRITE(06,5860)
14940 WRITE(06,1236)
14950 IF(D5.LT.0.5)GOTO 35300 → To line 16140
14960 READ(09,32910)LINE,NPOINT
14980 WRITE(06,1236)
15000 WRITE(06,7503)NPOINT
15020 7503 FORMAT(" CALCULATIONS WILL BE MADE AT",I3," POINTS")
15040 WRITE(06,1236)
15080 GOTO(33600,33800,34000),D6 →
15100 33600 WRITE(06,33070) ←
15120 WRITE(06,1236)
15140 GOTO 34200
15160 33800 WRITE(06,33080) ←
15180 WRITE(06,1236)
15200 GOTO 34200
15220 34000 WRITE(06,33085) ←

```

Figure 4.54 Listing of Program DIFFMAG - Continued

**THIS PAGE IS BEST QUALITY PRACTICABLE
FROM COPY FURNISHED TO DDC**

```

15240 WRITE(06,1236)
152600 --
15280 34200 CONTINUE
153000 --
153200 WRITE(06,1236)
153400 --
153600 32900 CONTINUE
153800 THIS STARTS CALCULATION OF FIELDS AT DISCRETE POINTS
15400 DO 35299 I6=1,NPOINT+1
154400 --
154600 34400 READ(07,32910)LINE,XP,YP,ZP
154800 --
15500 GOTO(34600,34800,35000),06
15520 34600 FLAG1=1
155400 --
15560 CALL FILSUM(FLAG1,N,XP,YP,ZP,D,RCURDIS,CURDIS,HX0,HY0,HZ0)
15580 WRITE(06,33180)XP,YP,ZP,HX0,HY0,HZ0
15600 FLAG1=0
15620 CALL FILSUM(FLAG1,N,XP,YP,ZP,D,RCURDIS,CURDIS,HX0,HY0,HZ0)
15640 WRITE(06,33180)XP,YP,ZP,HX0,HY0,HZ0
15660 WRITE(06,1236)
15680 GOTO 35200
15700 34800 FLAG1=1
15720 CALL FILSUM(FLAG1,N,XP,YP,ZP,D,RCURDIS,CURDIS,HX0,HY0,HZ0)
15740 CALL VSUM(HX0,HY0,HZ0,HTOT,ANG1,ANG2)
15760 WRITE(06,33180)XP,YP,ZP,HTOT,ANG1,ANG2
15780 FLAG1=0
15800 CALL FILSUM(FLAG1,N,XP,YP,ZP,D,RCURDIS,CURDIS,HX0,HY0,HZ0)
15820 CALL VSUM(HX0,HY0,HZ0,HTOT,ANG1,ANG2)
15840 WRITE(06,33180)XP,YP,ZP,HTOT,ANG1,ANG2
15860 GOTO 35200
15880 35000 FLAG1=1
15900 CALL FILSUM(FLAG1,N,XP,YP,ZP,D,RCURDIS,CURDIS,HX0,HY0,HZ0)
15920 CALL VSUM(HX0,HY0,HZ0,HTOT,ANG1,ANG2)
15940 HTOTM=HTOT
15960 FLAG1=0
15980 CALL FILSUM(FLAG1,N,XP,YP,ZP,D,RCURDIS,CURDIS,HX0,HY0,HZ0)
16000 CALL VSUM(HX0,HY0,HZ0,HTOT,ANG1,ANG2)
16020 WRITE(06,33185)XP,YP,ZP,HTOTM,HTOT
16040 35200 CONTINUE
16060 WRITE(06,1236)
16080 --
16100 THIS ENDS CALCULATION OF FIELDS AT DISCRETE POINTS
16120 35299 CONTINUE
16140 35300 CONTINUE
16160 WRITE(06,5860)
16180 WRITE(06,1236)
16200 --
16220 READ(09,32910)LINE,07
16240 WRITE(06,8115)07
16260 8115 FORMAT("07 IS",I8)
16280 WRITE(06,1236)
16300 WRITE(06,5860)
16320 WRITE(06,1236)

```

From line 14950

Figure 4.54 Listing of Program DIFFMAG - Continued

**THIS PAGE IS BEST QUALITY PRACTICABLE
FROM COPY FURNISHED TO DDC**

```

16340C --
16360 IF(D7)36300,36300,35350 →
16380 35350 I5=1 ←
16400C --
16420 READ(07,35360)LINE,NLOOP
16440 35360 FORMAT(V)
16460 WRITE(06,35365)NLOOP
16480 WRITE(06,1236)
16500 35365 FORMAT(" THERE WILL BE CALCULATIONS MADE FOR",I3," LOOPS")
16520 WRITE(06,1236)
16540 DO 36200 I=1,NLOOP,1 ←
16560 35370 CONTINUE
16580C --
16600 READ(09,35360)LINE,PX1,FY1,PZ1,PX2,PY2,PZ2
16620 READ(09,35360)LINE,PX3,PY3,PZ3,PX4,PY4,PZ4
16640 WRITE(06,1236)
16660 WRITE(06,35380)
16680 35380 FORMAT(" LOOP POINT",6X,"X",11X,"Y",11X,"Z")
16700 WRITE(06,1236)
16720 I7=1
16740 WRITE(06,35390)I5,I7,PX1,PY1,PZ1
16760 I7=2
16780 WRITE(06,35390)I5,I7,PX2,PY2,PZ2
16800 I7=3
16820 WRITE(06,35390)I5,I7,PX3,PY3,PZ3
16840 I7=4
16860 WRITE(06,35390)I5,I7,PX4,←,←,←
16880 WRITE(06,1236)
16900 35390 FORMAT(1X,I3,3X,I3,3X,SE12.3)
16920 WRITE(06,1236)
16940C --
16960 35400 FORMAT(" LOOP NUMBER",I5," MAGNETIC DISTRIBUTION")
16980 35500 FORMAT(" LOOP NUMBER",I5," RESISTIVE DISTRIBUTION")
17000 WRITE(06,1236)
17020 FLAG1=1
17040 CALL LOOP(FLAG1,D,RCURDIS,CURDIS,AREA,BTOT)
17060C --
17080 WRITE(06,35800)AREA
17100 WRITE(06,1236)
17120 WRITE(06,35400)I5
17140 WRITE(06,36000)BTOT
17160 WRITE(06,1236)
17180 WRITE(06,1236)
17200 35800 FORMAT(" LOOP AREA=",1E12.3," SQUARE METERS")
17220 36000 FORMAT(" TOTAL FLUX=",1E12.3," WEBERS")
17240 FLAG1=0
17260C --
17280 CALL LOOP(FLAG1,D,RCURDIS,CURDIS,4REA,BTOT)
17300 WRITE(06,35500)I5
17320 WRITE(06,36000) BTOT
17340 WRITE(06,1236)
17360 WRITE(06,5360)
17380 WRITE(06,1236)
17400 I5=I5+1 →

```

↓

↓

17420 36190 CONTIN
17440 36080 CONTIN
17460 STOPPRINT

Figure 4.54 Listing of Program DIFFMAG - Concluded

**THIS PAGE IS BEST QUALITY PRACTICABLE
FROM COPY FURNISHED TO DDC**

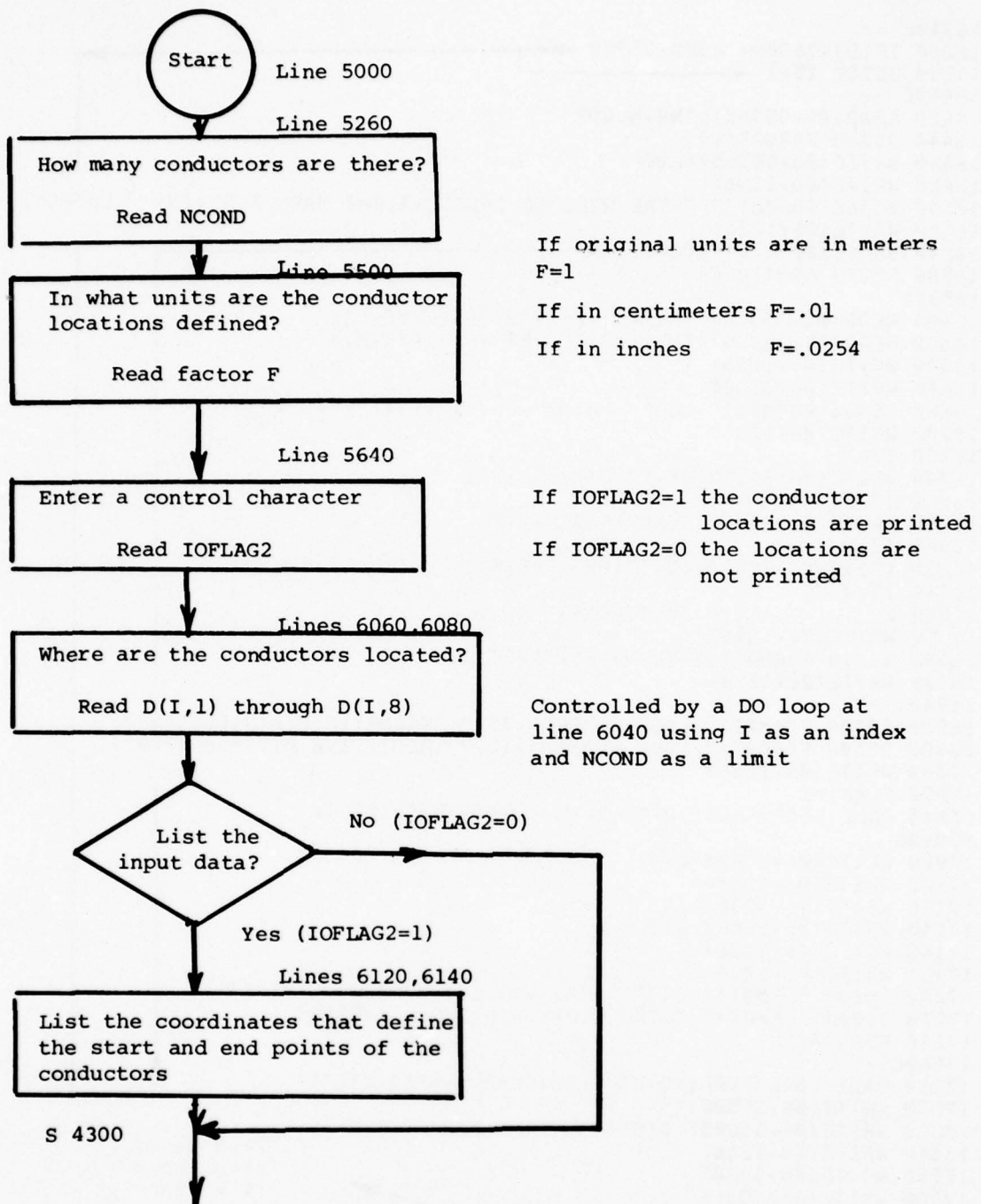


Figure 4.55 Program DIFFMAG - MAIN

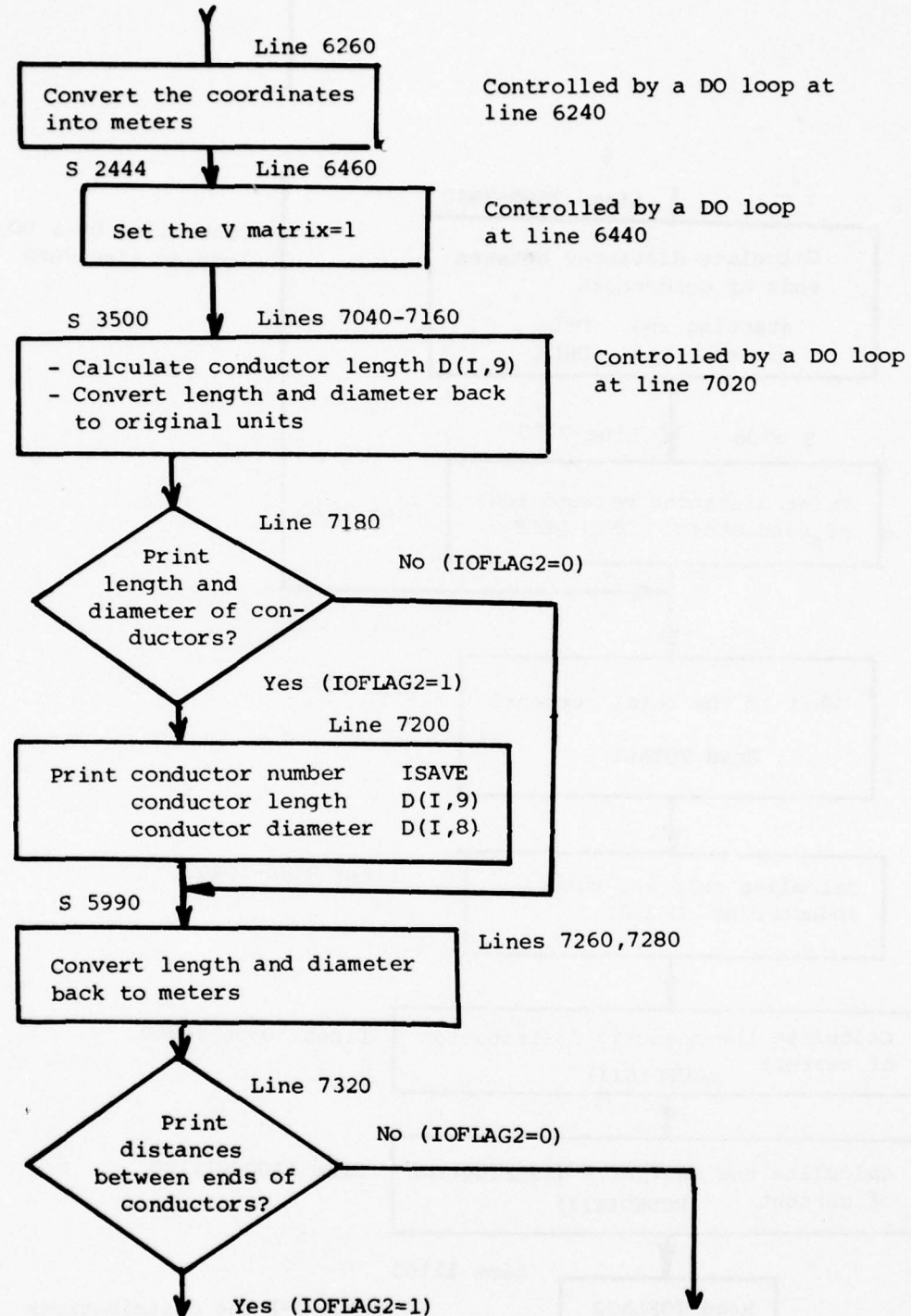


Figure 4.55 Program DIFFMAG - MAIN Continued

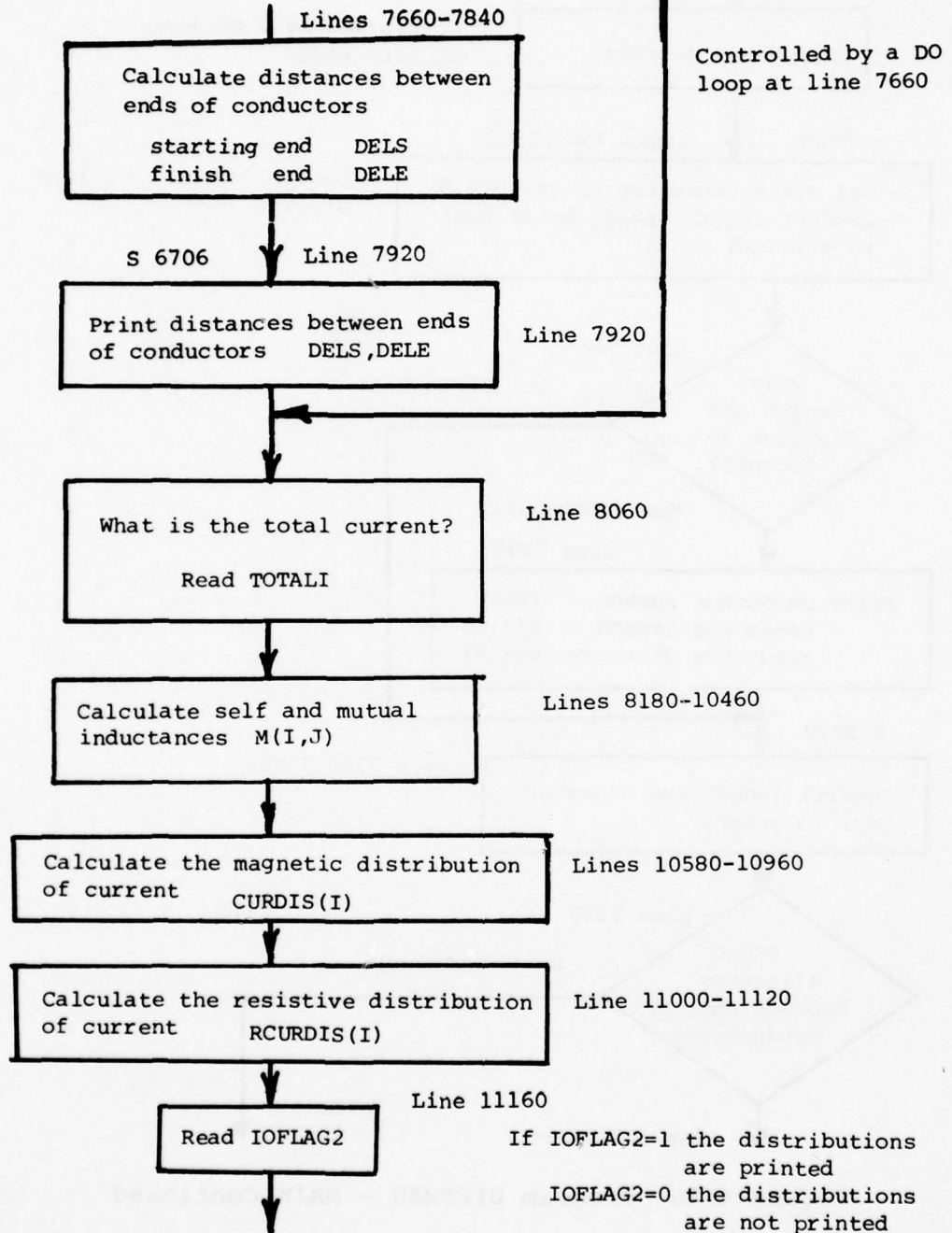


Figure 4.55 Program DIFFMAG - MAIN Continued

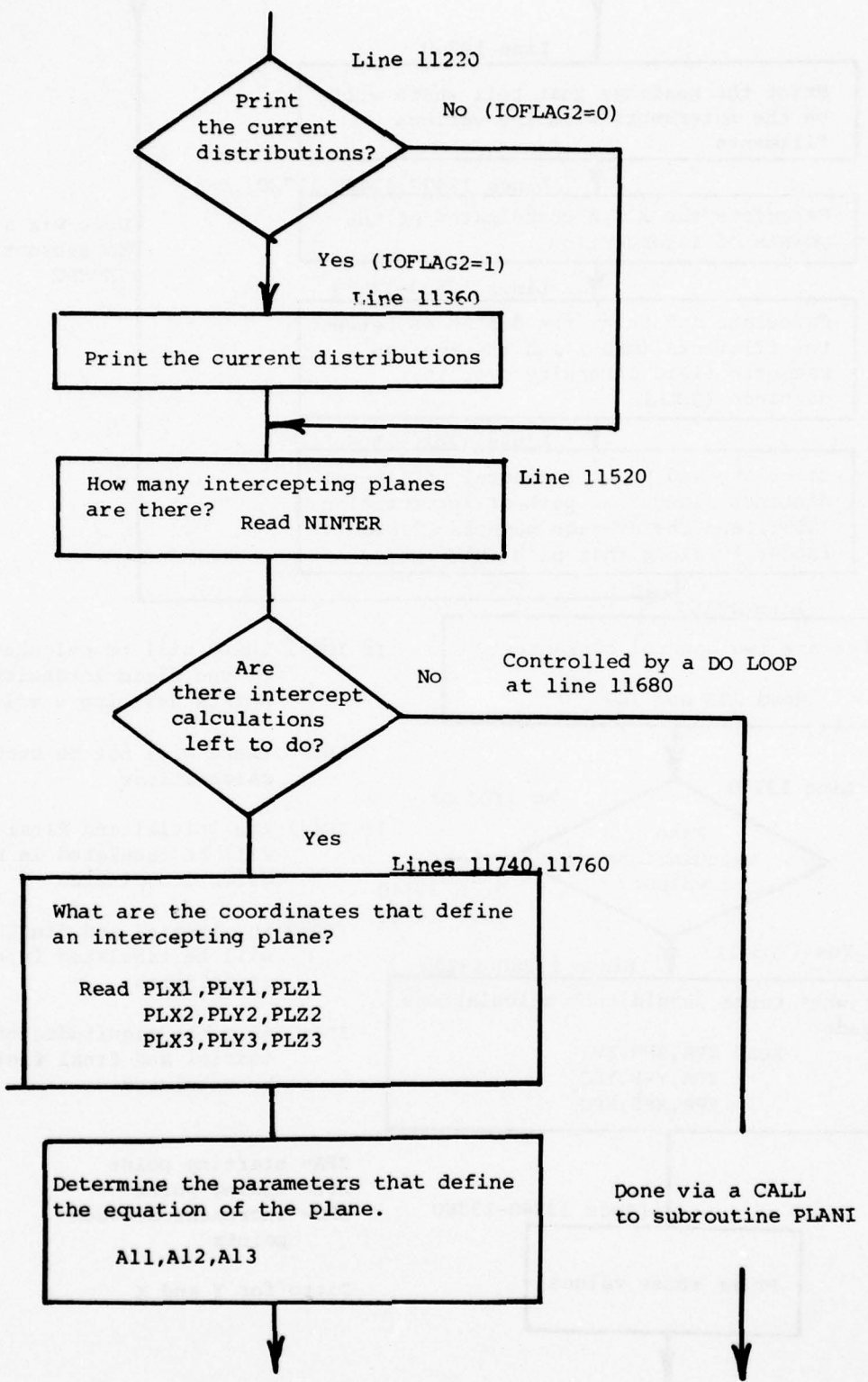


Figure 4.55 Program DIFFMAG - MAIN Continued

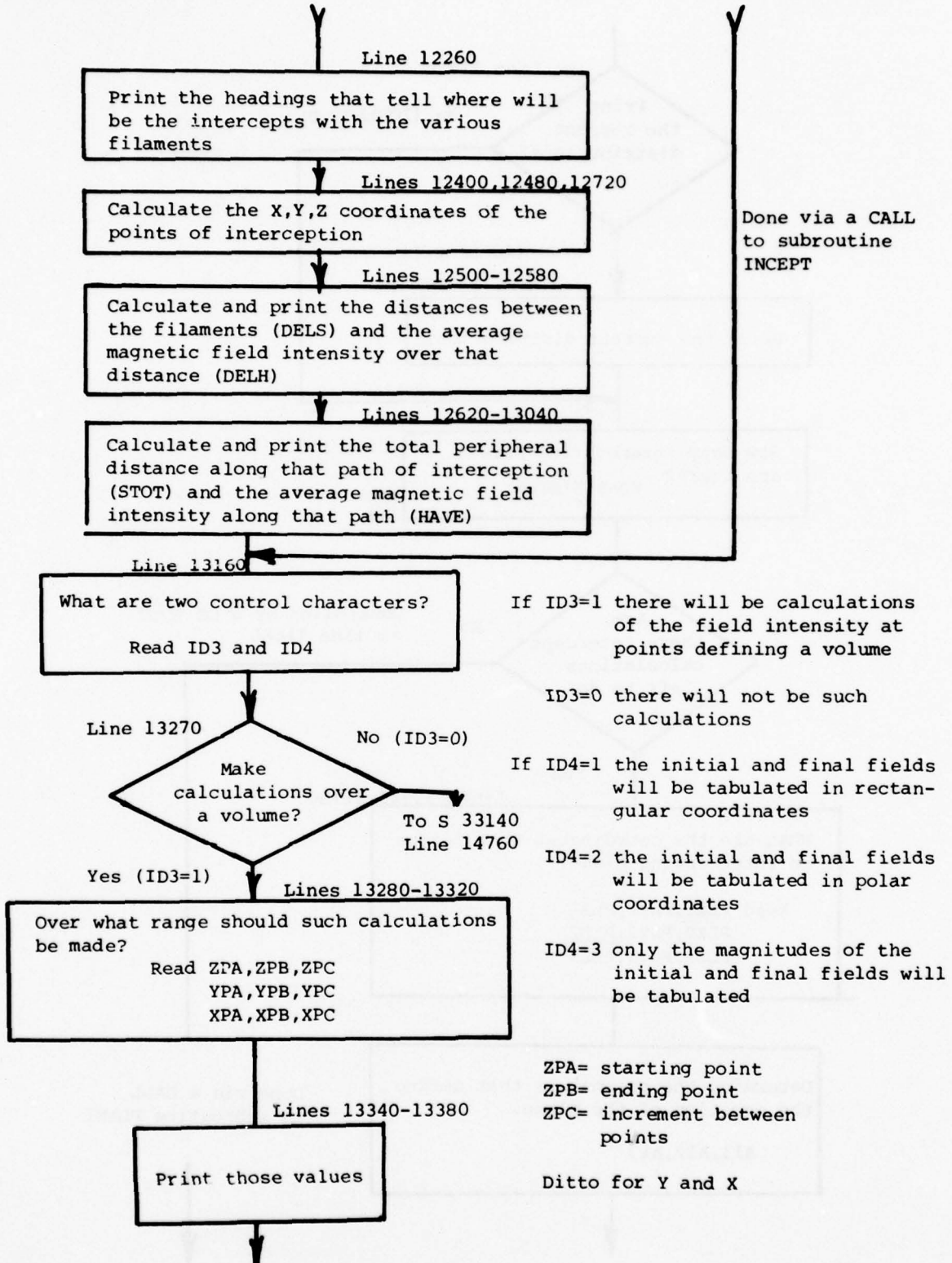


Figure 4.55 Program DIFFMAG - MAIN Continued

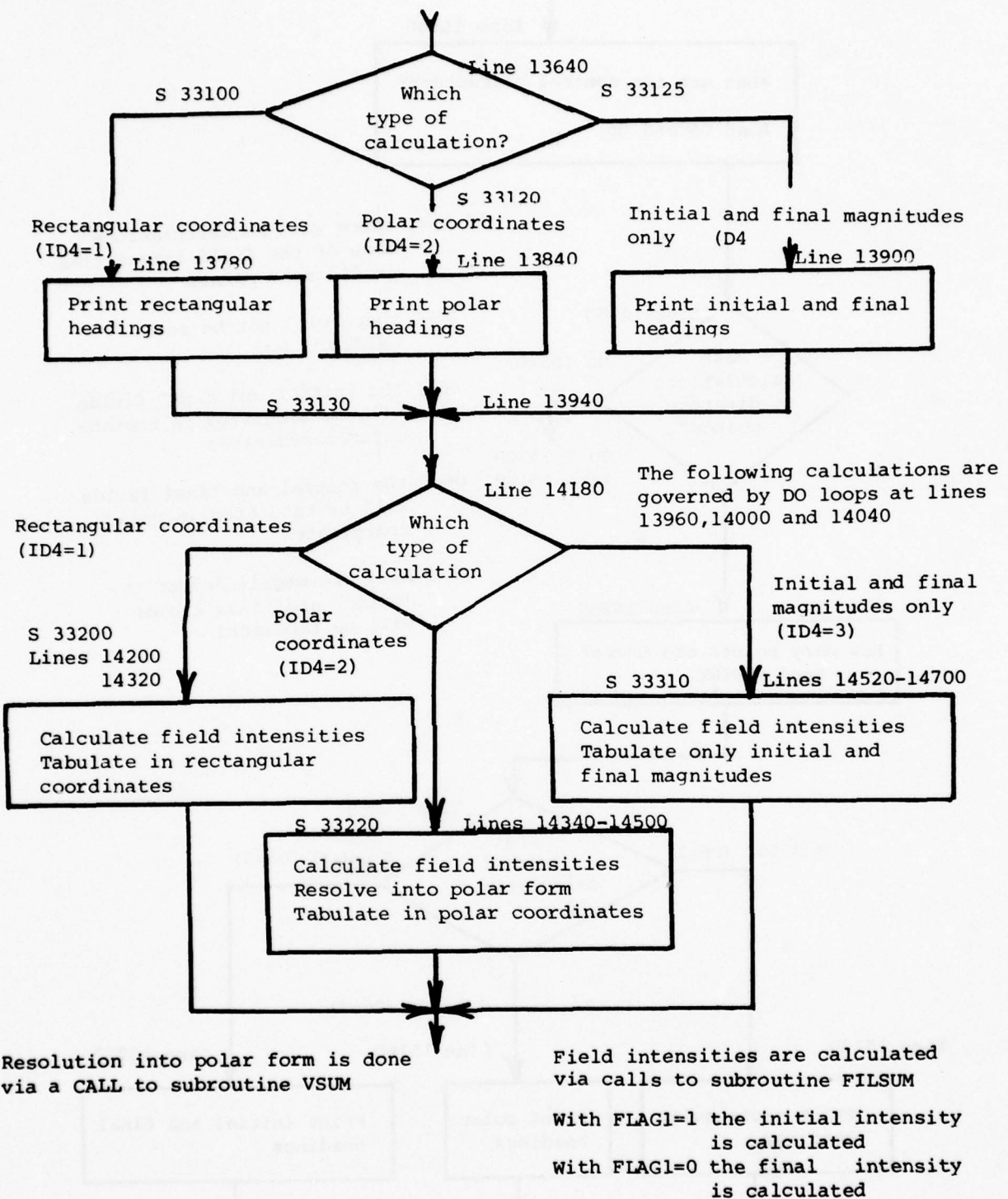


Figure 4.55 Program DIFFMAG - MAIN Continued

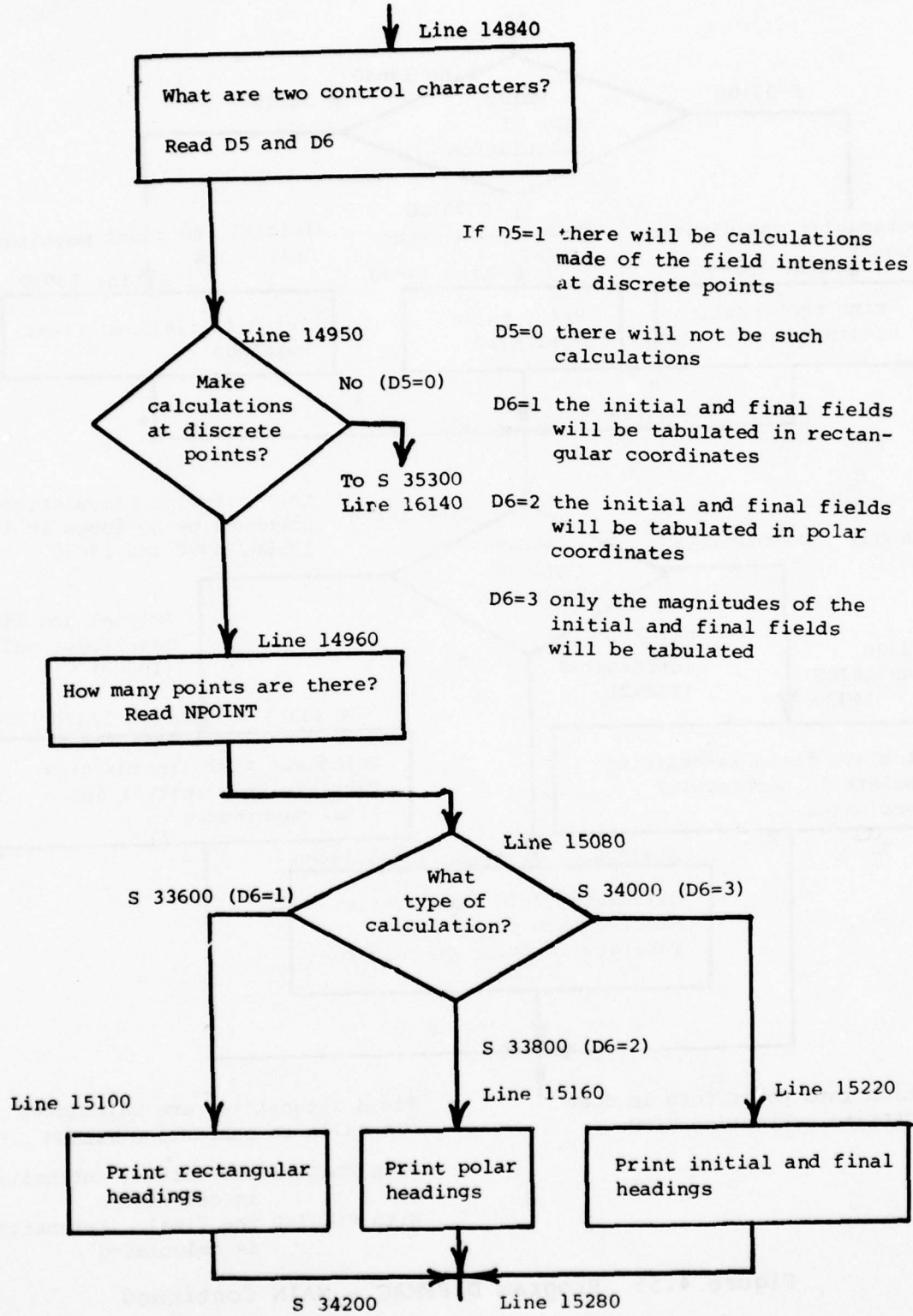


Figure 4.55 Program DIFFMAG - MAIN Continued

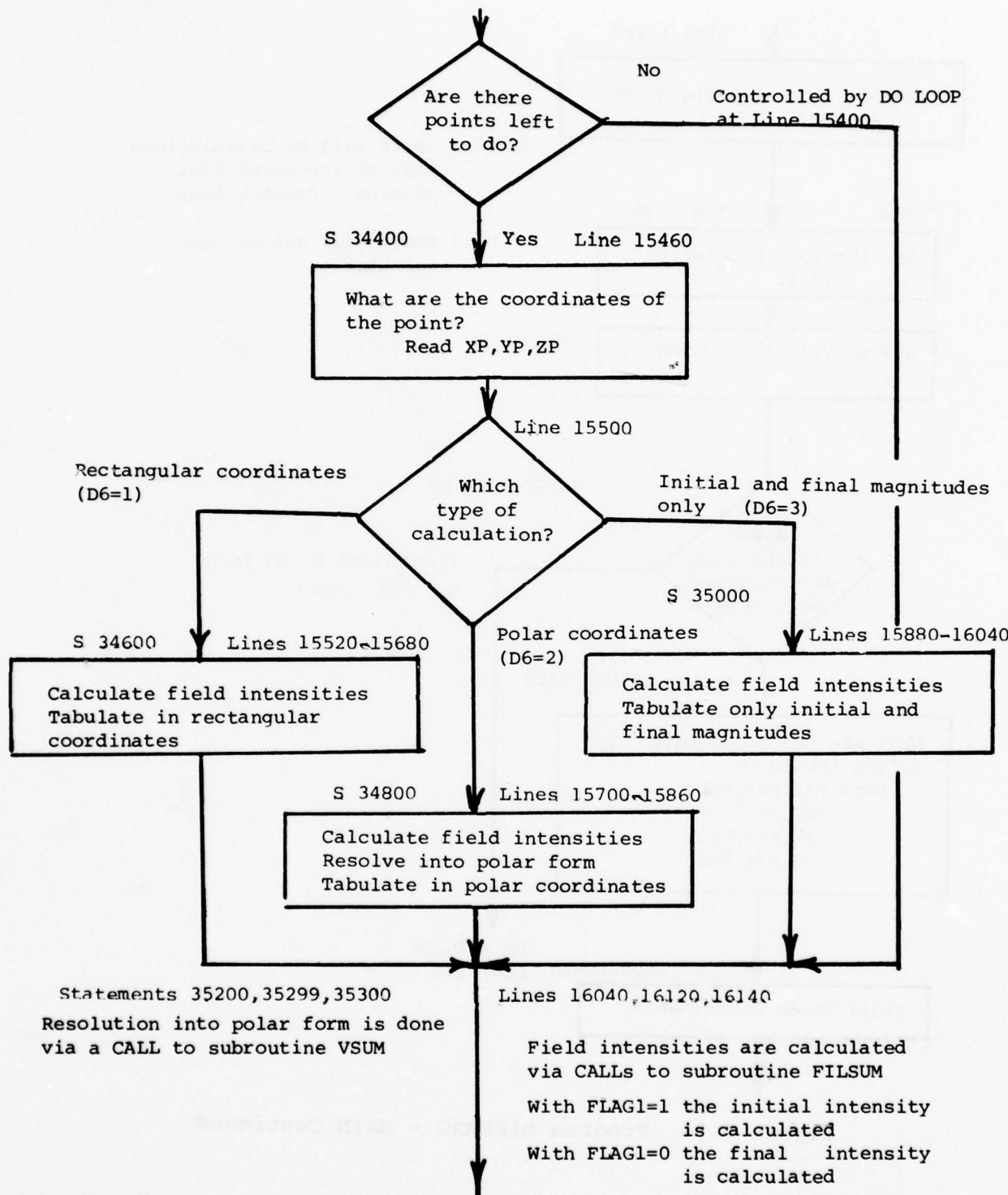


Figure 4.55 Program DIFFMAG - MAIN Continued

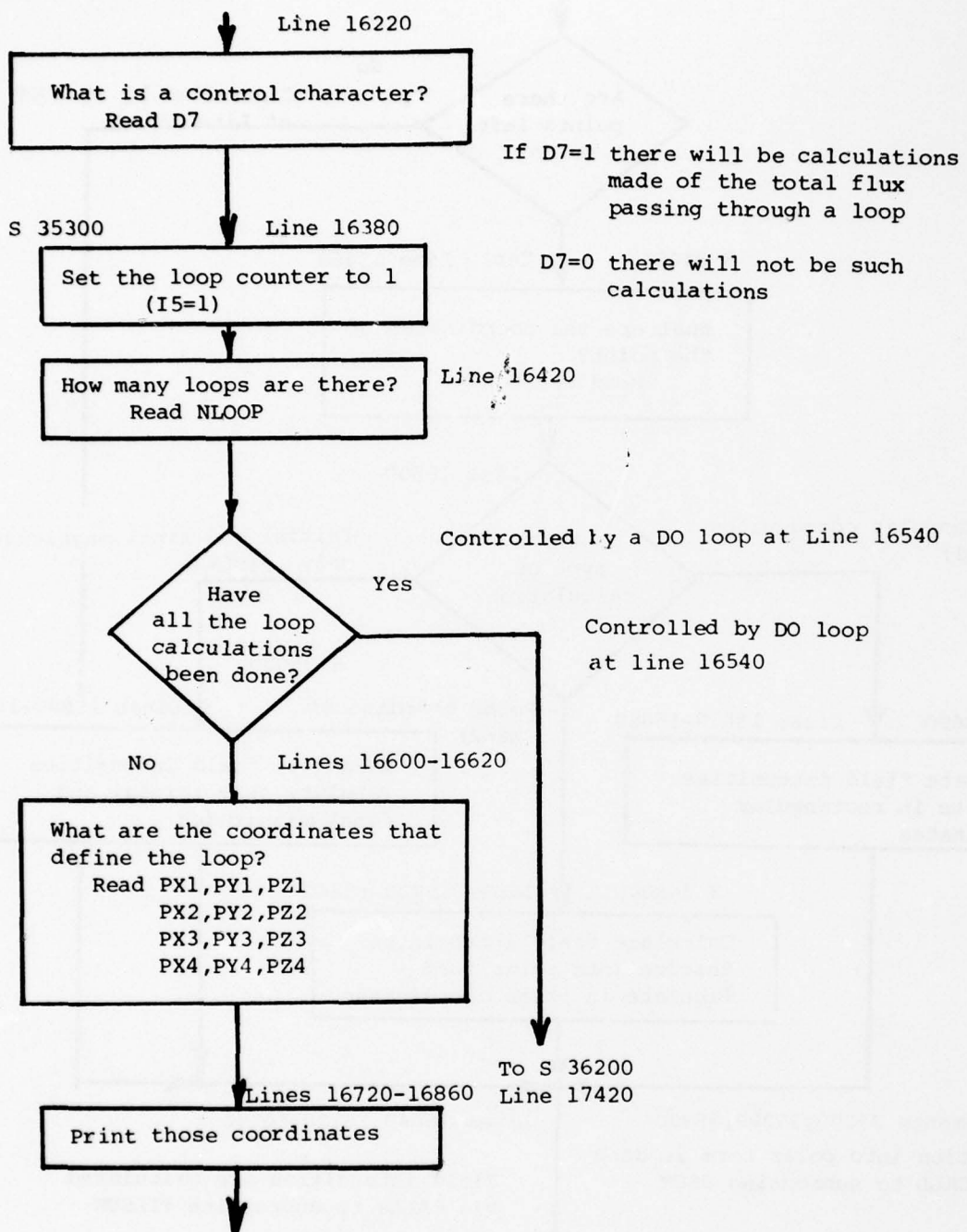


Figure 4.55 Program DIFFMAG - MAIN Continued

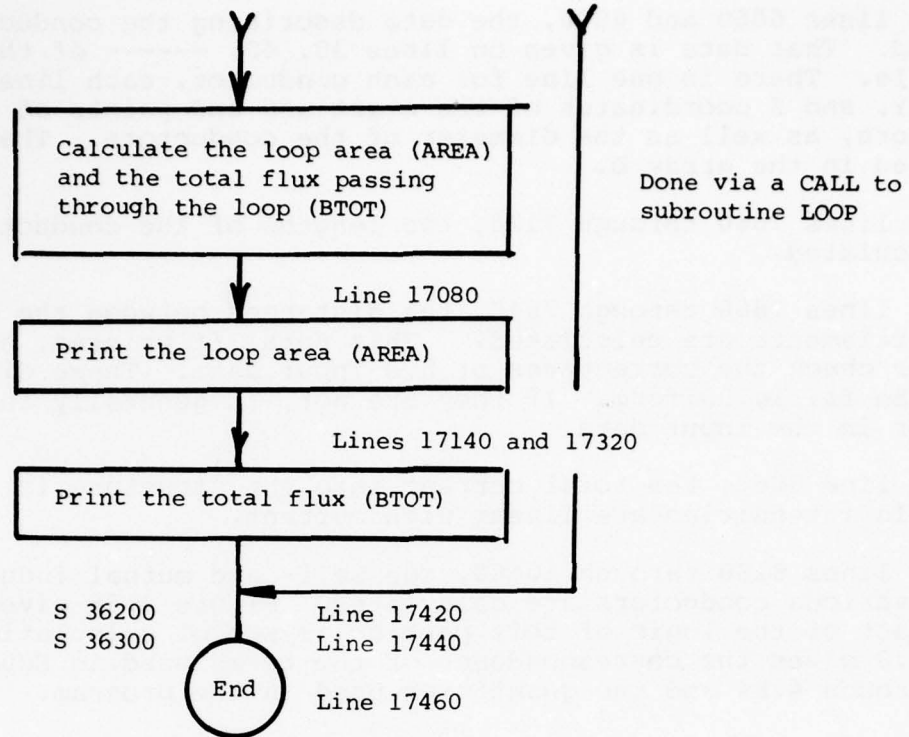


Figure 4.55 Program DIFFMAG - MAIN Concluded

In lines 6060 and 6080, the data describing the conductors are read. That data is given on lines 30, 40, ----- of the input data file. There is one line for each conductor, each line giving the X, Y, and Z coordinates of the start and end points of the conductors, as well as the diameter of the conductors. That data is stored in the array D.

In lines 7060 through 7120, the lengths of the conductors are calculated.

In lines 7660 through 7840, the distances between the ends of the filaments are calculated. This data, if printed, helps the user check the correctness of his input data. These distances should be fairly uniform. If they are not, it generally indicates an error in the input data.

In line 8060, the total current into the structure is read. The field intensities are linear with current.

In lines 8180 through 10460, the self- and mutual inductances of the various conductors are calculated. Figure 4.56 gives a flow chart of the logic of this particular set of calculations. Table 4.3 gives the correspondence of the terms used in Equations 4.68 through 4.84 and the quantities used in the program.

In lines 10580 through 10960, the magnetic distribution of current is calculated. The matrix inversion called for by Equations 4.55 through 4.57 is performed via a call to the subroutine MATRIX.

In lines 11000 through 11120, the resistive distribution of current is calculated. Allowance is made for the different diameters and lengths of the conductors, but all conductors are assumed to be made of the same material and hence to have the same conductivity.

In line 11160, another control character is read, this one controlling whether or not the distribution of currents is to be printed.

Starting at line 11520, calculations are made where the various conductors intercept planes that the user might desire to specify. The purpose of the plane, described in more detail in Section 4.6.5, is to determine the magnetic field intensity along the surface of the structure along a defined path. The number of planes is entered at line 11520 and the coordinates of three points that define the plane are read at line 11740. Subroutine PLANI is used to calculate the equation of the plane from those three points, and subroutine INCEPT is used to calculate the points at which the conductors intercept the plane. If those points are plotted by the user on a piece of graph paper, the user can determine the area enclosed by the structure at those points. That area is one of the factors governing the redistribution time constant. Another factor is the peripheral distance around the structure. This quantity is returned by the subroutine INCEPT.

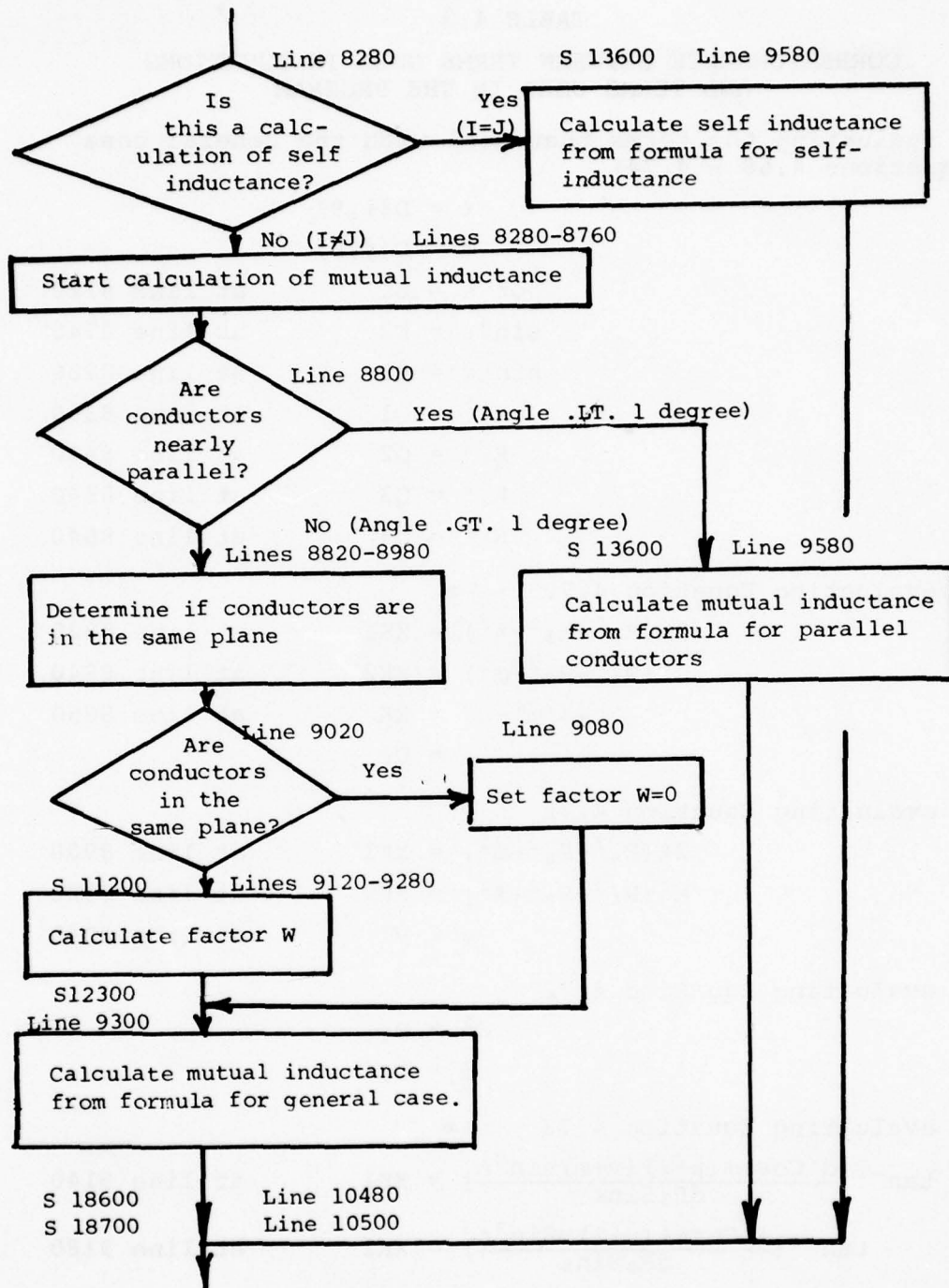


Figure 4.56 Calculation of Self and Mutual Inductance

TABLE 4.3
CORRESPONDENCE BETWEEN TERMS USED IN EQUATIONS
AND TERMS USED IN THE PROGRAM

When evaluating the terms that deal with the general case
(Equations 4.68 - 4.74)

$\ell = D(i, 9)$	
$m = D(j, 9)$	
$\cos \epsilon = E1$	at line 8720
$\sin^2 \epsilon = E2$	at line 8740
$\sin \epsilon = E3$	at line 8760
$R_1^2 = Q1$	at line 8360
$R_2^2 = Q2$	at line 8440
$R_3^2 = Q3$	at line 8540
$R_4^2 = Q4$	at line 8640

When evaluating Equation 4.70

$2m(R_2^2 - R_3^2 - \ell^2) = XK1$	at line 8820
$\alpha^2(R_4^2 - R_3^2 - m^2) = XK2$	at line 8840
$4\ell^2m^2 - \alpha^4 = XK$	at line 8860
$= UL$	

When evaluating Equation 4.71

$2\ell(R_4^2 - R_3^2 - m^2) = XK1$	at line 8900
$\alpha^2(R_2^2 - R_3^2 - \ell^2) = XK2$	at line 8920
$v = VL$	at line 8940

When evaluating Equation 4.72

$$\begin{aligned} d^2 &= D_1 \\ d &= D_2 \end{aligned}$$

When evaluating Equation 4.73

$\tan^{-1} \left[\frac{d^2 \cos \epsilon + (\mu + \ell)(v + m) \sin^2 \epsilon}{dR_1 \sin \epsilon} \right] = XK1$	at line 9140
$\tan^{-1} \left[\frac{d^2 \cos \epsilon + (\mu + \ell)v \sin^2 \epsilon}{dR_2 \sin \epsilon} \right] = XK2$	at line 9180
$\tan^{-1} \left[\frac{d^2 \cos \epsilon + \mu v \sin^2 \epsilon}{dR_3 \sin \epsilon} \right] = XK3$	at line 9220
$\tan^{-1} \left[\frac{d^2 \cos \epsilon + \mu(v + m) \sin^2 \epsilon}{dR_4 \sin \epsilon} \right] = XK4$	at line 9260
$\Omega = W$	at line 9280

TABLE 4.3 (Continued)

M is calculated from Equation 4.74 using the identity of
Equation 4.75 to evaluate the inverse hyperbolic tangents

$$(\mu+\lambda)\tanh^{-1}\frac{m}{R_1+R_2} = XK1 \quad \text{at line 9320}$$

$$(v+m)\tanh^{-1}\frac{\lambda}{R_1+R_4} = XK2 \quad \text{at line 9360}$$

$$\mu \tanh^{-1}\frac{m}{R_3+R_4} = XK3 \quad \text{at line 9400}$$

$$v \tanh^{-1}\frac{\lambda}{R_2+R_3} = XK4 \quad \text{at line 9440}$$

$$M = XM(i,j) \quad \text{at line 9460}$$

When evaluating the Equations 4.79 - 4.82 for parallel conductors

$$d = D2 \quad \text{at line 9900}$$

$$\delta = D4 \quad \text{at line 9920}$$

$$\alpha = XK1 \quad \text{at line 9940}$$

$$\beta = XK2 \quad \text{at line 9960}$$

$$\gamma = XK3 \quad \text{at line 9980}$$

$$\alpha \log_e \left[\frac{\alpha}{d} + \sqrt{\left(\frac{\alpha}{d} \right)^2 + 1} \right] = XK4 \quad \text{at line 10040}$$

$$\beta \log_e \left[\frac{\beta}{d} + \sqrt{\left(\frac{\beta}{d} \right)^2 + 1} \right] = XK5 \quad \text{at line 10100}$$

$$\gamma \log_e \left[\frac{\gamma}{d} + \sqrt{\left(\frac{\gamma}{d} \right)^2 + 1} \right] = XK6 \quad \text{at line 10160}$$

$$\delta \log_e \left[\frac{\delta}{d} + \sqrt{\left(\frac{\delta}{d} \right)^2 + 1} \right] = XK7 \quad \text{at line 10220}$$

$$\sqrt{\alpha^2 + d^2} = XL1 \quad \text{at line 10280}$$

$$\sqrt{\beta^2 + d^2} = XL2 \quad \text{at line 10320}$$

$$\sqrt{\gamma^2 + d^2} = XL3 \quad \text{at line 10360}$$

$$\sqrt{\delta^2 + d^2} = XL4 \quad \text{at line 10400}$$

$$M = XM(i,j) \quad \text{at line 10440}$$

Possibly there could be developed a computer routine that would calculate the enclosed area from the coordinates of the points of intersection. At the moment, such a routine is not available.

In line 13160 there are read two control characters. One of them, ID3, controls whether or not there are to be made calculations of the field intensity at points that define a volume. The other, ID4, determines whether the field intensities are to be printed out in rectangular or spherical coordinates. In lines 13270 through 13320 are read the quantities that define the volume over which the calculations are to be made. Those points are defined and entered in the same manner as they were in the program APERTURE.

In lines 13560 through 13600, the quantities J1 through J3 are used to index the X, Y, and Z coordinates of the points at which the calculations are to be made.

Assuming calculations are to be made at those points, lines 13640 through 13900 are used to print the appropriate types of headings for the tabulations of field strength.

The calculations of field strength are made by summing the magnetic fields produced by the current flowing in the various conductors. That calculation is made via a call to the subroutine FILSUM. FILSUM is entered with the coordinates of the point at which the calculation is to be made, XP, YP, and AP, along with the control character FLAG1. For each point calculations are made, first for the field as determined by the magnetic distribution of current and then for the field as determined by the resistive distribution of current. If FLAG1 is set equal to 1, the magnetic distribution of current is used; and if FLAG1 is set equal to 0, the resistive distribution is used. FILSUM returns the field strengths in rectangular coordinates. If a tabulation in polar coordinates is desired, the conversion is made via a call to the subroutine VSUM.

In line 14840, two more control characters, D5 and D6, are read. These control whether or not the user wishes the field strength to be calculated at discrete points and, if so, whether he wishes the field strength to be returned in rectangular or polar coordinates. The calculation of field strength at those points is done in the same manner as the calculation of field strength at points defining a volume.

In line 16220, a control character, D7, is read that controls whether or not there are to be made calculations of the total flux passing through a loop. If there are to be such calculations, the number of loops is read at line 16420 and the points defining the loop at lines 16600 and 16620. The calculation of total flux is made via a call to subroutine LOOP. LOOP returns two quantities, the area of the loop and the total flux passing through the loop. Two calls are made to LOOP, the first using the magnetically

determined distribution of current to calculate the initial value of flux, and the second using the resistively determined distribution of current to calculate the final value of flux.

The MAIN portion of the program ends at line 17480.

4.6.2.5 Subroutine MATRIX. The subroutine MATRIX is an adaptation of a standard matrix inversion program. It is used to invert the impedance matrix when calculating the manner in which current divides among the various conductors. A listing of MATRIX is given in Figure 4.57. It is entered with the impedance matrix M (i,j) and the three quantities IDUM, JDUM, and KDUM that give the order of the matrix. The inverted matrix is returned in the same array, M (i,j), with which it was entered.

4.6.3 Subroutine FILSUM

This subroutine calculates the magnetic field produced by each current-carrying filament and sums those fields to get the total field at a specific point.

It receives the following data:

FLAG1	which tells whether the routine is to calculate the initial or the final field intensity
FLAG1 = 1	initial field intensity using CURDIS (I)
FLAG1 = 0	final field intensity using RCURDIS (I)
CURDIS (I)	which is the array of currents determined magnetically
RCURDIS (I)	which is the array of currents determined resistively
N	which tells how many filaments there are
XP, YP, ZP	which are the points at which the field intensity is to be calculated
D(I,J)	which is the data defining the locations of the filaments

It returns the following data:

HXO,HYO,HZO which are the field strengths oriented along the reference X, Y, and Z axes.

The geometry under study is shown on Figure 4.58. The filament producing the magnetic field runs between P₁ and P₂. The point at which the field is to be calculated is designated P.

```

17490C -----
17500 SUBROUTINE MATRIX(M, IDUM, JDUM, KDUM)
17520 DIMENSION M(40,40)
17540 DIMENSION LABEL(40)
17560 REAL M, TEMP
17580***INVERT
17600***KDUM IS ROWS AND COLUMNS OF A-L AND M ARE ZERO
17620***NOTE::::::::::RESULTS ARE STORED IN M---NOT C!!!!
17640 NR=KDUM
17660 NC=KDUM
17680 DO 21 J1=1,NR
17700 21 LABEL(J1)=J1
17720 DO 291 J1=1,NR
17740**FIND REMAINING ROW CONTAINING LARGEST***
17760**ABSOLUTE VALUE I' PIVOTAL COLUMN*****
17780 TMP1=0.
17800 DO 121 J2=J1,NR
17820 TMP2=ABS(M(J2,J1))
17840 IF(TMP2-TMP1) 121,121,1210
17860 1210 TMP1=TMP2
17880 IBIG=J2
17900 121 CONTINUE
17920 IF(IBIG.EQ.J1)GO TO 201
17940**REARRANGE ROWS TO PLACE LARGEST ABSOLUTE
17960**VALUE IN PIVOT POSITION*****
17980 DO 141 J2=1,NC
18000 TEMP=M(J1,J2)
18020 M(J1,J2)=M(IBIG,J2)
18040 141 M(IBIG,J2)=TEMP
18060 N=LABEL(J1)
18080 LABEL(J1)=LABEL(IBIG)
18100 LABEL(IBIG)=N
18120*** ::::COMPUTED COEFFICIENTS IN PIVOTAL ROW::::
18140 201 TEMP=M(J1,J1)
18160 M(J1,J1)=1.0
18180 DO 221 J2=1,NC
18200 221 M(J1,J2)=M(J1,J2)/TEMP
18220**COMPUTE COEFFICIENT IN OTHER ROWS****

```

Figure 4.57 Program Listing of Subroutine MATRIX

```
18240 DO 281 J2=1,NR
18260 IF(J2.EQ.J1) GO TO 281
18280 TEMP=M(J2,J1)
18300 M(J2,J1)=0.
18320 DO 241 J3=1,NC
18340 241 M(J2,J3)=M(J2,J3)-TEMP*M(J1,J3)
18360 281 CONTINUE
18380 291 CONTINUE
18400**INTERCHANGE COLUMNS ACCORDING TO
18420**INTERCHANGES OF ROWS OF ORIGINAL MATRIX**
18440 301 N1=NR-1
18460 DO 391 J1=1,N1
18480 DO 321 J2=J1,NR
18500 IF(LABEL(J2).NE.J1) GO TO 321
18520 IF(J2.EQ.J1) GO TO 391
18540 GO TO 341
18560 321 CONTINUE
18580 341 DO 361 J3=1,NR
18600 TEMP=M(J3,J1)
18620 M(J3,J1)=M(J3,J2)
18640 361 M(J3,J2)=TEMP
18660 LABEL(J2)=LABEL(J1)
18680 391 CONTINUE
18700 500 RETURN; END
```

Figure 4.57 Program Listing of Subroutine Matrix-Concluded

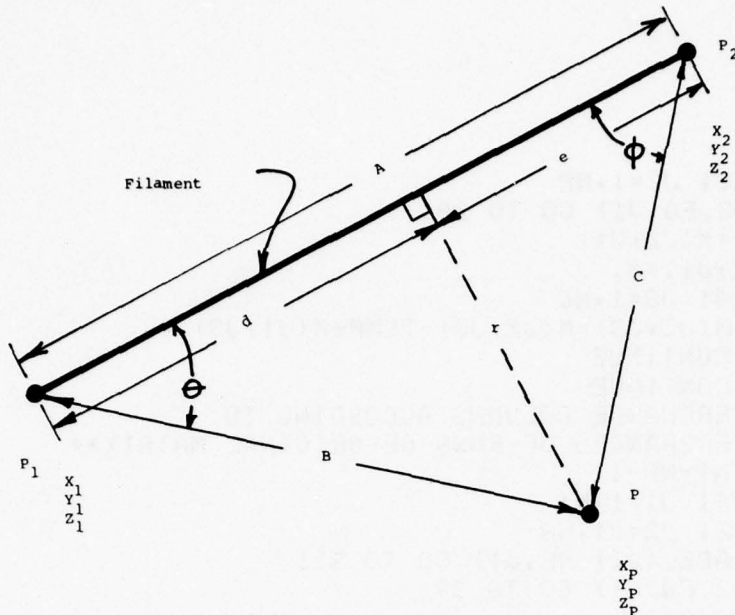


Figure 4.58 A Current Carrying Filament

Let i , j , and k be unit vectors parallel respectively to the X , Y , and Z axes.

The filament may be considered a vector \underline{A} whose magnitude is A . Likewise, the lines joining the ends of the filament to P may be considered as vectors \underline{B} and \underline{C} of magnitudes B and C .

$$\underline{A} = A_1 i + A_2 j + A_3 k \quad (4.87)$$

$$\underline{A} = (x_2 - x_1)i + (y_2 - y_1)j + (z_2 - z_1)k \quad (4.88)$$

$$A = \sqrt{(x_2 - x_1)^2 + (y_2 - y_1)^2 + (z_2 - z_1)^2} \quad (4.89)$$

$$\underline{B} = B_1 i + B_2 j + B_3 k \quad (4.90)$$

$$\underline{B} = (x_p - x_1)i + (y_p - y_1)j + (z_p - z_1)k \quad (4.91)$$

$$B = \sqrt{(x_p - x_1)^2 + (y_p - y_1)^2 + (z_p - z_1)^2} \quad (4.92)$$

$$\underline{C} = C_1 \mathbf{i} + C_2 \mathbf{j} + C_3 \mathbf{k} \quad (4.93)$$

$$\underline{C} = (x_p - x_2) \mathbf{i} + (y_p - y_2) \mathbf{i} + (z_p - z_2) \mathbf{k} \quad (4.94)$$

$$C = \sqrt{(x_p - x_2)^2 + (y_p - y_2)^2 + (z_p - z_2)^2} \quad (4.95)$$

$$\cos \theta = \frac{A^2 + B^2 - C^2}{2 AB} \quad (4.96)$$

$$\cos \phi = \frac{A^2 + C^2 - B^2}{2 AC} \quad (4.97)$$

$$d = B \cos \theta = \frac{A^2 + B^2 - C^2}{2 A} \quad (4.98)$$

$$e = C \cos \phi = \frac{A^2 + C^2 - B^2}{2 A} \quad (4.99)$$

$$r = \sqrt{B^2 - d^2} \quad (4.100)$$

The magnetic field intensity at P is

$$H_{\text{mag}} = \frac{I (\cos \theta + \cos \phi)}{2\pi r} \quad (4.101)$$

This field is oriented perpendicular to the plane defined by the vectors A, B, and C. The vector that is oriented perpendicular to that plane is N_U where

$$\underline{N_U} = N_{U1} \mathbf{i} + N_{U2} \mathbf{j} + N_{U3} \mathbf{k} \quad (4.102)$$

and where

$$NU1 = (A_2 B_3 - A_3 B_2) \quad (4.103)$$

$$NU2 = (A_1 B_3 - A_3 B_1) \quad (4.104)$$

$$NU3 = (A_1 B_2 - A_2 B_1) \quad (4.105)$$

The magnitude of this vector is

$$NU = \sqrt{(NU1)^2 + (NU2)^2 + (NU3)^2} \quad (4.106)$$

The magnitudes of the X, Y, and Z components of the unit vector normal to the plane are

$$NUX = NU1/NU \quad (4.107)$$

$$NUY = NU2/NU \quad (4.108)$$

$$NUZ = NU3/NU \quad (4.109)$$

The X, Y, and Z components of the field at P are then

$$HX = H MAG \times NUX \quad (4.110)$$

$$HY = H MAG \times NUY \quad (4.111)$$

$$HZ = H MAG \times NUZ \quad (4.112)$$

A listing of the subroutine is given on Figure 4.59.

A flow chart of the subroutines is shown on Figure 4.60. In the subroutine, which occupies lines 18720 through 19580, the sums of the individual field strengths are taken by a DO loop at line 18900. The DO loop uses I as an index with N, the number of conductors, as the limit. In the program, the following quantities are used:

$x_1 = D(I,2)$
 $x_2 = D(I,5)$
 $y_1 = D(I,3)$
 $y_2 = D(I,6)$
 $z_1 = D(I,4)$
 $z_2 = D(I,7)$
 $A = D(I,8)$
 $B = BLEN$
 $C = CLEN$
 $r = RAD$
 $\cos \phi = COSA$
 $\cos \theta = COSB$

The subroutine itself is fairly straightforward, following the order of Equations 4.87 through 4.102 fairly directly.

```

18720C -----
18740 SUBROUTINE FILSUM(FLAG,N,XP,YP,ZP,D,RCURDIS,CURDIS,HX0,HY0,HZ0)
18760 DIMENSION D(40,9),RCURDIS(40),CURDIS(40)
18780 REAL NU,NU1,NU2,NU3,NUX,NUY,NUZ
18800 TWOPI=6.28318531
18820 HX0=0
18840 HY0=0
18860 HZ0=0
18880 I=1
18900 DO 1000 I=1,N,1
18920 IF(FLAG>0.5) GO TO 1010
18940C FILI=RESISTIVE CURRENT DISTRIBUTION
18960 FILI=RCURDIS(I)
18980 GO TO 1020
19000 1010 CONTINUE
19020C FILI=MAGNETIC CURRENT DISTRIBUTION
19040 FILI=CURDIS(I)
19060 1020 CONTINUE
19080 A1=D(I,5)-D(I,2);A2=D(I,6)-D(I,3);A3=D(I,7)-D(I,4)
19100 B1=XP-D(I,2);B2=YP-D(I,3);B3=ZP-D(I,4)
19120 C1=XP-D(I,5);C2=YP-D(I,6);C3=ZP-D(I,7)
19140 BLEN=SQRT((B1*B1+B2*B2+B3*B3))
19160 CLEN=SQRT(C1*C1+C2*C2+C3*C3)
19180 COSA=(D(I,9)*D(I,9)+BLEN*BLEN-CLEN*CLEN)/(2.*D(I,9))
19200 COSA=COSA/BLEN
19220 COSB=(D(I,9)*D(I,9)+CLEN*CLEN-BLEN*BLEN)/(2.*D(I,9))
19240 COSB=COSB/CLEN
19260 RAD=BLEN*SQRT(1-COSA*COSA)
19280 HMAG=- (FILI*(COSA+COSB)/(TWOPI*RAD))
19300C THESE ARE THE COMPONENTS OF THE NORMAL VECTOR
19320 NU1=A2*B3-A3*B2
19340 NU2=A3*B1-A1*B3
19360 NU3=A1*B2-A2*B1
19380 NU=SQRT(NU1*NU1+NU2*NU2+NU3*NU3)
19400 NUX=NU1/NU;NUY=NU2/NU;NUZ=NU3/NU
19420 HXN=HMAG*NUX
19440 HYN=HMAG*NUY
19460 HZN=HMAG*NUZ
19480
19500 HX0=HX0+HXN
19520 HY0=HY0+HYN
19540 HZ0=HZ0+HZN
19560 1000 CONTINUE
19580 RETURNEND

```

Figure 4.59 Program Listing of Subroutine FILSUM

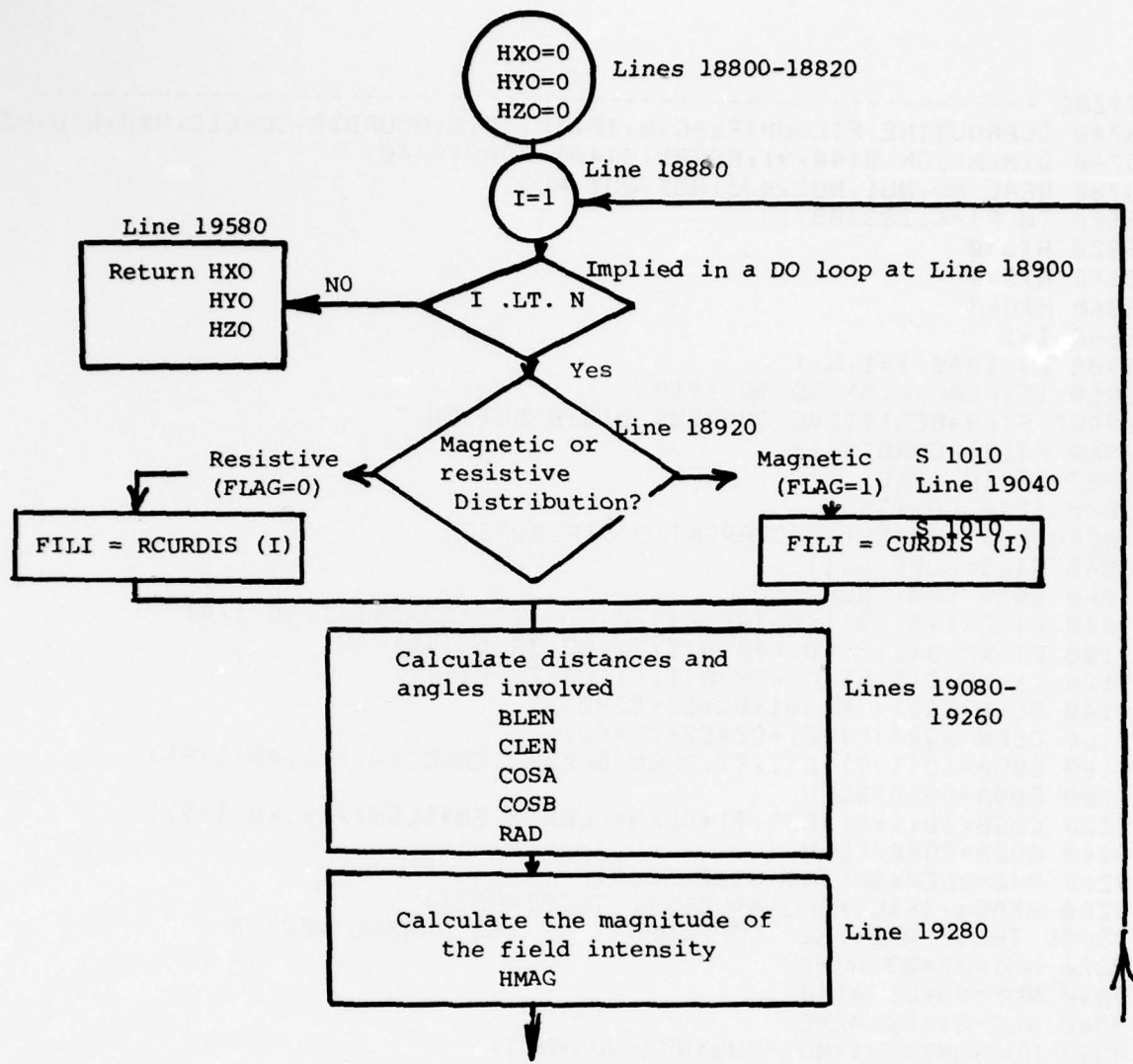


Figure 4.60 Flow Chart of Subroutine FILSUM

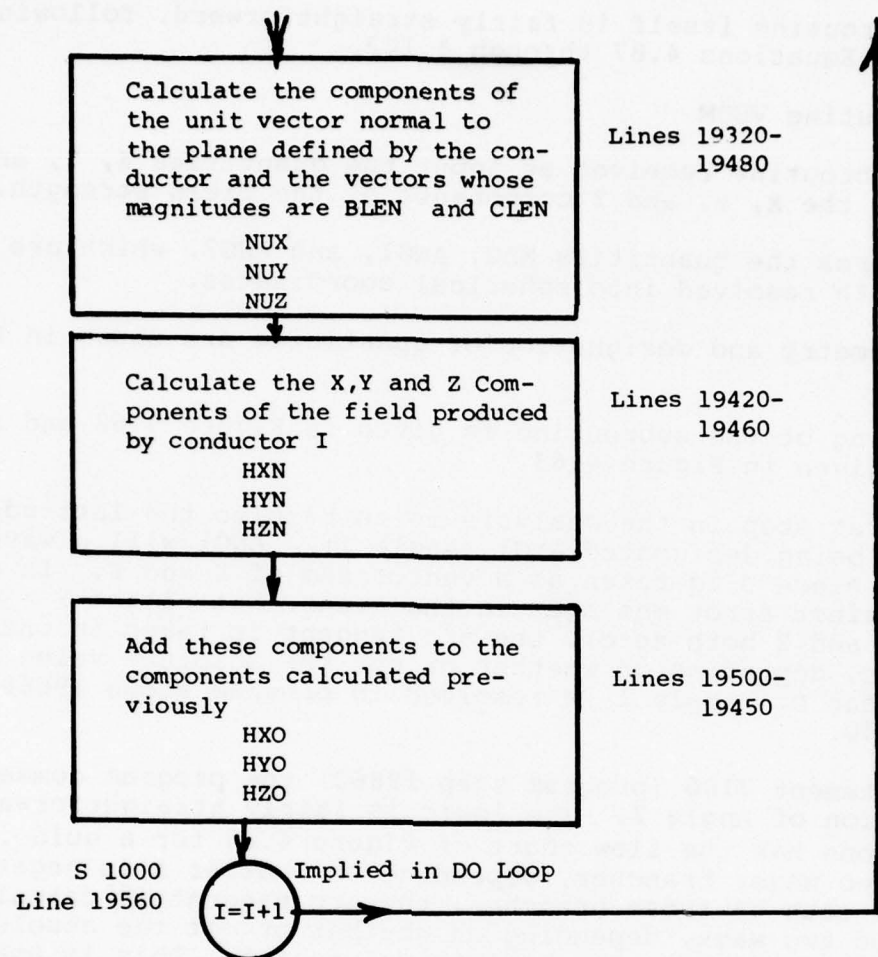


Figure 4.60 Flow Chart of Subroutine FILSUM - Concluded

The subroutine itself is fairly straightforward, following the order of Equations 4.87 through 4.102.

4.6.4 Subroutine VSUM

This subroutine receives as input the quantities X, Y, and Z, which are the X, Y, and Z components of the field strength.

It returns the quantities MAG, ANG1, and ANG2, which are the field strength resolved into spherical coordinates.

The geometry and designation of quantities are shown in Figure 4.61.

A listing of the subroutine is given in Figure 4.62 and a flow chart given in Figure 4.63.

The first step in the analysis is to resolve the latitude angle, this being designated ANG1 (Angle 1). ANG1 will always be positive since D is taken as a vector sum of X and Z. In order to guard against error messages in the event that either Y = 0 or D = 0 (X and Z both zero), the arc tangent is taken in one of two branches, depending on whether or not the absolute value of Y is less than D. Angle 1 is resolved in program steps 19660 through 19840.

At statement 7100 (program step 19860) the program commences the resolution of Angle 2. The logic is fairly straightforward as long as one has the flow chart of Figure 4.63 for a guide. There are two major branches, depending on whether Z is negative or not. In each of those branches, the arc tangent is calculated in either of two ways, depending on whether or not the absolute value of X is less than the absolute value of Z. This is again done in order to guard against division by zero in the event that either X or Z is zero.

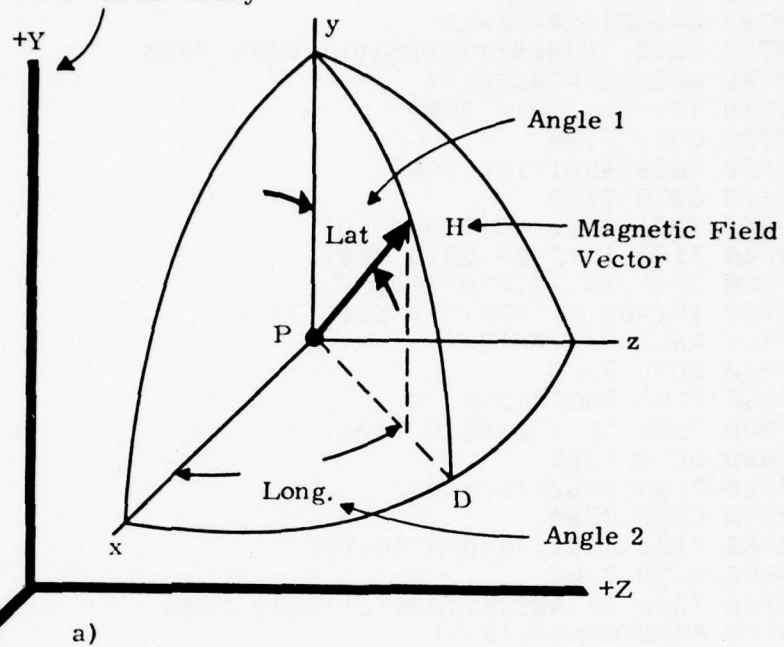
There is a possibility both X and Z could be zero, and in this case, Angle 2 is set to 45°.

The remaining statements are included to present Angle 2 in the range -180° to +130°.

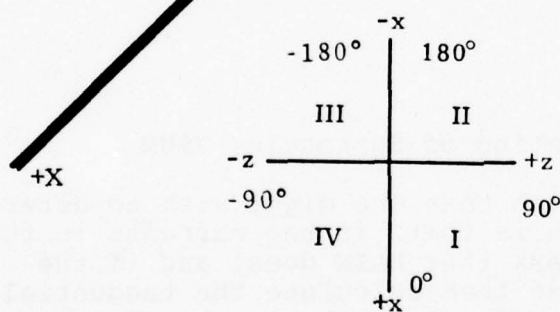
4.6.5 Subroutines PLANI and INCEPT

Figure 4.64 shows a surface defined by a group of filaments. If a plane is passed through these filaments, as in Figure 4.65, each of the filaments will intersect the plane at some specific

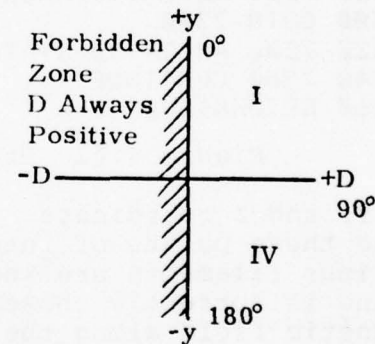
Axes Describing the Point Under Study



a)



b)



c)

Figure 4.61 Conventions Regarding Angles: (a) Latitude and Longitude Angles Defined; (b) Quadrant Designations for Longitude; (c) Quadrant Designations for Latitude

```

19600C -----
19620 SUBROUTINE VSUM(X,Y,Z,MAG,ANG1,ANG2)
19640 REAL MAG
19660 MAG=SQRT(X*X+Y*Y+Z*Z)
19680 Q=57.2957795
19700 D=SQRT(X*X+Z*Z)
19720 7000 IF(ABS(Y)<ABS(D)) GOTO 7006
19740 ANG1=Q*ATAN(D/Y)
19760 IF(Y<0) GOTO 7004
19780 GOTO 7100
19800 7004 ANG1=180 +ANG1
19820 GOTO 7100
19840 7006 ANG1=90-ATAN(Y/D)
19860 7100 IF(Z<0) GOTO 7200
19880 IF(X.EQ.Z)GOTO 7102
19900 IF(ABS(X)<ABS(Z)) GOTO 7106
19920 ANG2=Q*ATAN(Z/X)
19940 GOTO 7103
19960 7102 ANG2=45.0
19980 7103 IF(X<0)GOTO 7104
20000 GOTO 7300
20020 7104 ANG2=180+ANG2
20040 GOTO 7300
20060 7106 ANG2=90-Q*ATAN(X/Z)
20080 GOTO 7300
20100 7200 IF(ABS(X)<ABS(Z))GOTO 7206
20120 ANG2=Q*ATAN(Z/X)
20140 IF(X<0) GOTO 7204
20160 GOTO 7300
20180 7204 ANG2=180+ANG2
20200 GOTO 7300
20220 7206 ANG2=-90-Q*ATAN(X/Z)
20240 7300 CONTINUE
20260 RETURN;END

```

Figure 4.62 Program Listing of Subroutine VSUM

X, Y, and Z coordinate. The reason that one might wish to determine these points of intersection is that, if the currents in the various filaments are known (a task that MAIN does) and if the plane is correctly chosen, one can then calculate the tangential magnetic field along the path traced out by the points of intersection of the filaments with the plane. As shown in Figure 4.66, the tangential magnetic field at P is equal to the current density at P, and this current density can be approximated as

$$H_p = \frac{i_1 - i_2}{s} \quad (4.113)$$

The i_1 and i_2 , in Equation 4.113, are the currents in the two filaments on either side of the point under study, and S is the spacing between the filaments. The tangential field will be oriented at right angles to the streamlines of the current. The spacing

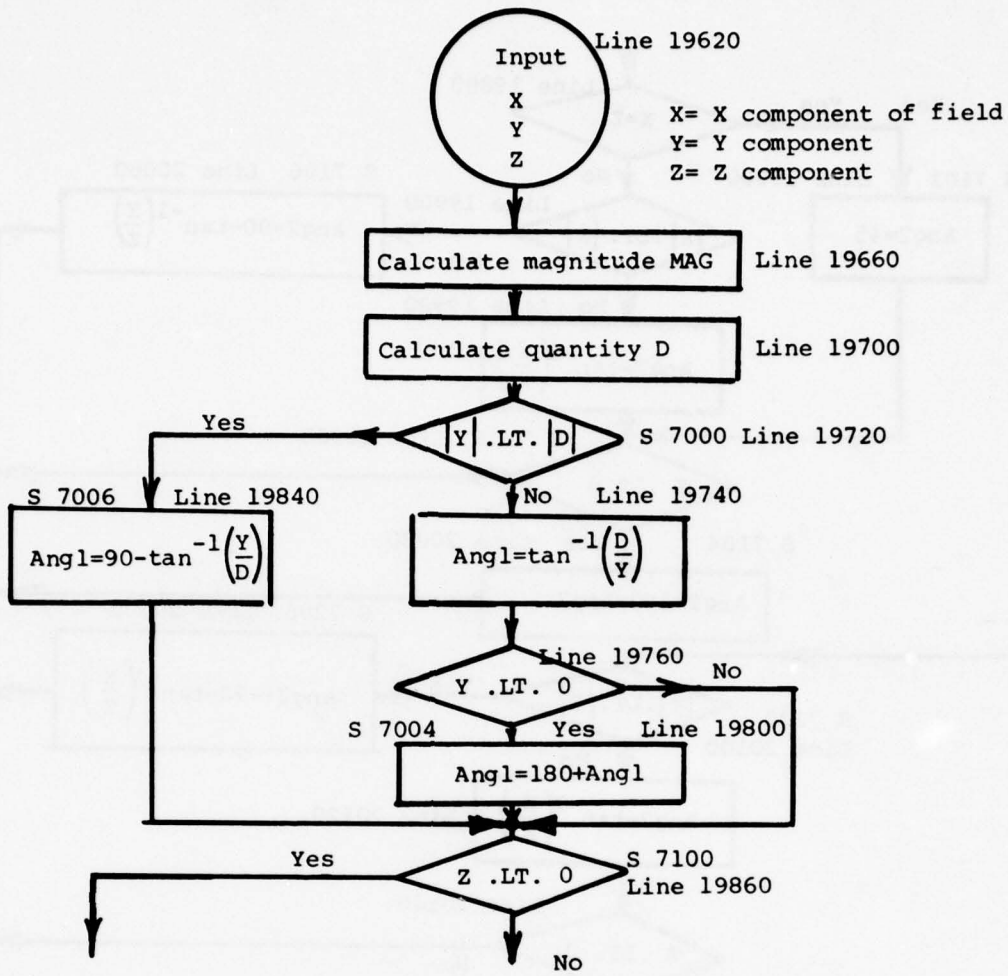


Figure 4.63 Flow Chart of Subroutine VSUM

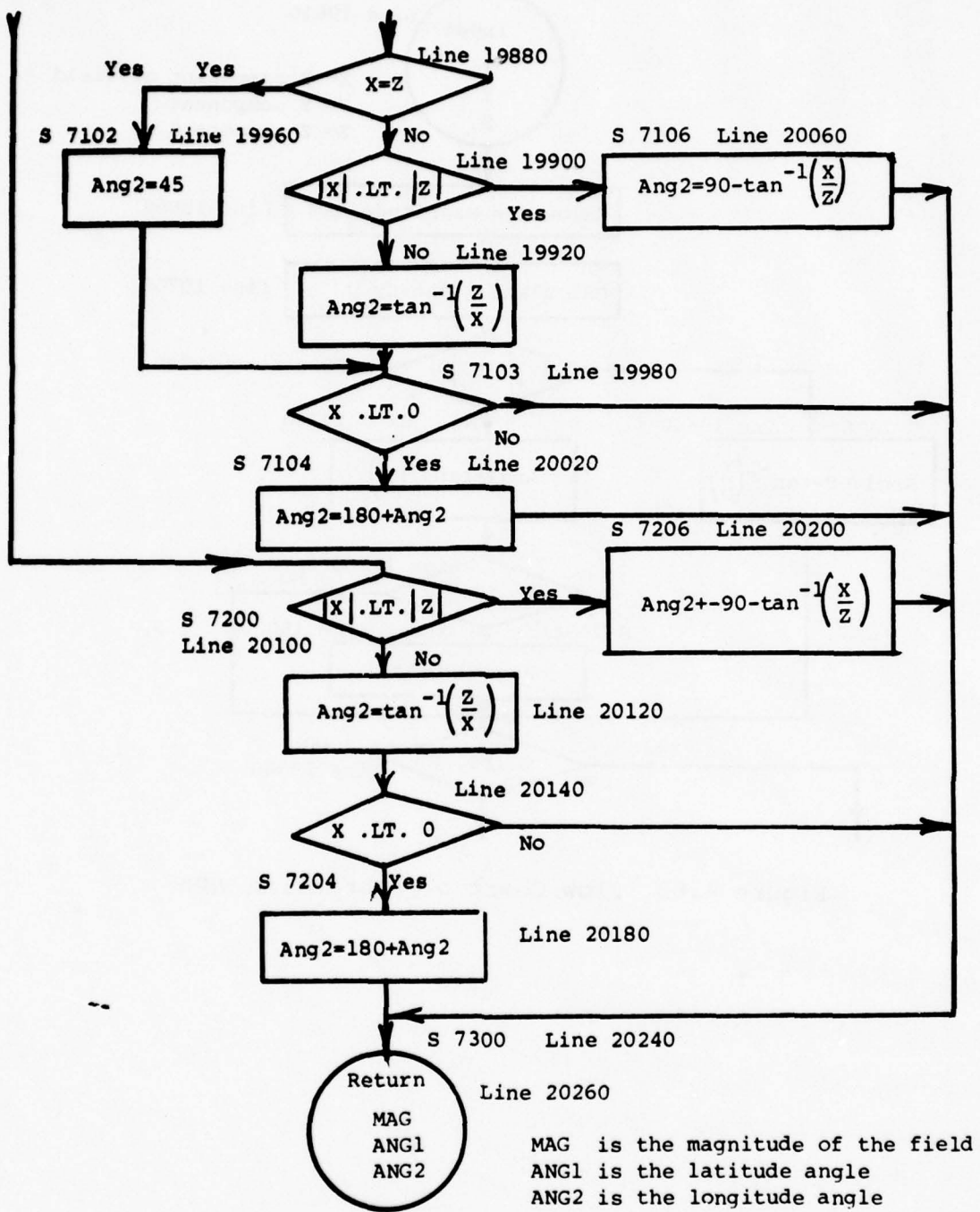


Figure 4.63 Flow Chart of Subroutine VSUM - Concluded

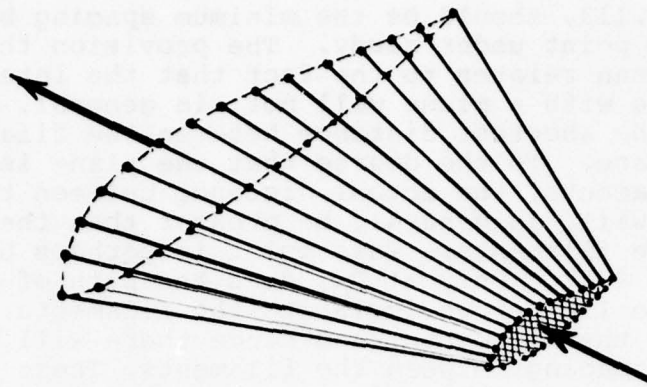


Figure 4.64 A Surface Defined by Filaments

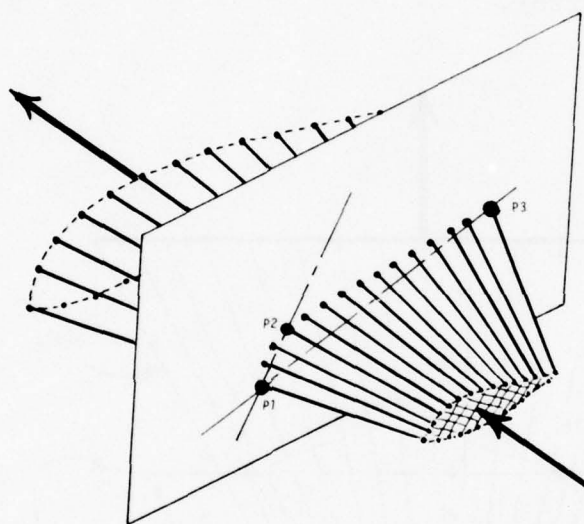


Figure 4.65 A Plane Intersecting the Filaments

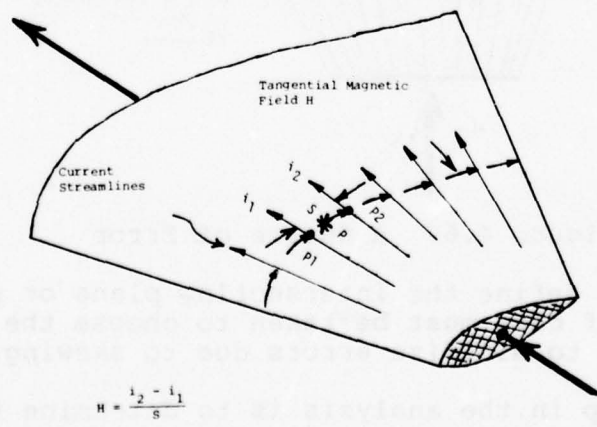


Figure 4.66 The Tangential Magnetic Field

S , in Equation 4.113, should be the minimum spacing between the filaments at the point under study. The provision that the plane be correctly chosen relates to the fact that the intersection of a current surface with a plane will not, in general, trace out a path that is the shortest distance between the filament which defines the surface. To the degree that the plane is skewed to the defining filaments, the actual distance between the points of intersection will, in general, be greater than the minimum distance between the filaments. This point is perhaps better illustrated in Figure 4.67. Only at P_C , does the path of the intersection of the plane lie perpendicular to the filaments. At P_A and P_B it lies askew the filaments, and hence there will be an error in the computed spacing between the filaments. These errors will be proportional to $\cos\alpha$ and $\cos\beta$, respectively. Generally, if the intersecting plane is well chosen, the error will be relatively small; since even for relatively large angular displacements, the cosine does not depart greatly from unity. For example, if $\alpha = 20^\circ$, $\cos\alpha = 0.94$, a 6% error.

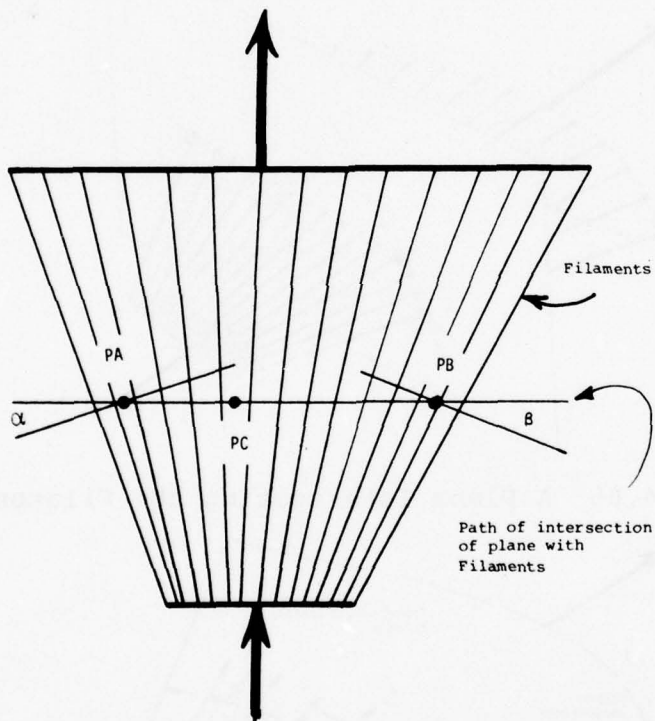


Figure 4.67 A Source of Error

The user must define the intersecting plane or planes, and a certain amount of care must be taken to choose the orientation of the plane so as to minimize errors due to skewing.

The first step in the analysis is to determine the three quantities that determine the coordinates of the intersecting plane. This is done in the subroutine PLANI.

4.6.5.1 PLANI

The equation of the plane is of the form

$$A_{11} X + A_{12} Y + A_{13} Z = 1 \quad (4.114)$$

If the three defining points P_1 , P_2 , and P_3 are respectively at (X_1, Y_1, Z_1) , (X_2, Y_2, Z_2) , and (X_3, Y_3, Z_3) , then the equation of the plane must satisfy those three locations simultaneously.

$$A_{11} X_1 + A_{12} Y_1 + A_{13} Z_1 = 1 \quad (4.115)$$

$$A_{11} X_2 + A_{12} Y_2 + A_{13} Z_2 = 1 \quad (4.116)$$

$$A_{11} X_3 + A_{12} Y_3 + A_{13} Z_3 = 1 \quad (4.117)$$

These may be put in matrix form as

$$\begin{bmatrix} A_{11} \\ A_{12} \\ A_{13} \end{bmatrix} \times \begin{bmatrix} X_1 & Y_1 & Z_1 \\ X_2 & Y_2 & Z_2 \\ X_3 & Y_3 & Z_3 \end{bmatrix} = \begin{bmatrix} 1 \\ 1 \\ 1 \end{bmatrix} \quad (4.118)$$

or

$$\begin{bmatrix} A_{11} \\ A_{12} \\ A_{13} \end{bmatrix} \times \begin{bmatrix} C \end{bmatrix} = \begin{bmatrix} 1 \\ 1 \\ 1 \end{bmatrix} \quad (4.119)$$

Multiplying by the inverse of the C matrix

$$\begin{bmatrix} A_{11} \\ A_{12} \\ A_{13} \end{bmatrix} \times \begin{bmatrix} C \end{bmatrix} \times \begin{bmatrix} C^{-1} \end{bmatrix} = \begin{bmatrix} 1 \\ 1 \\ 1 \end{bmatrix} \times \begin{bmatrix} C^{-1} \end{bmatrix} \quad (4.120)$$

from which

$$A_{11} = C_{11} + C_{12} + C_{13} \quad (4.121)$$

$$A12 = C21 + C22 + C23 \quad (4.122)$$

$$A13 = C31 + C32 + C33 \quad (4.123)$$

where

$$C11 = (Y2 \times Z3 - Y3 \times Z2)/D \quad (4.124)$$

$$C12 = - (Y1 \times Z3 - Y3 \times Z1)/D \quad (4.125)$$

$$C13 = (Y1 \times Z2 - Y2 \times Z1)/D \quad (4.126)$$

$$C21 = - (X2 \times Z3 - X3 \times Z2)/D \quad (4.127)$$

$$C22 = (X1 \times Z3 - X3 \times Z2)/D \quad (4.128)$$

$$C23 = - (X1 \times Z2 - X2 \times Z1)/D \quad (4.129)$$

$$C31 = (X2 \times Y3 - X3 \times Y2)/D \quad (4.130)$$

$$C32 = - (X1 \times Y3 - X3 \times Y1)/D \quad (4.131)$$

$$C33 = (X1 \times Y2 - X2 \times Y1)/D \quad (4.132)$$

and

$$\begin{aligned} D = & X1 Y2 Z3 + Y1 Z2 X3 + Z1 Y3 X2 \\ & - X3 Y2 Z1 - X2 Y1 Z3 - X1 Z2 Y3 \end{aligned} \quad (4.133)$$

The subroutine PLANI occupies lines 23400 through 23480 of the main program DIFFMAG. Since the logic is a straightforward solution of Equations 4.114 through 4.133, no flow chart is presented. The only thing not straightforward about the subroutine is lines 23460 and 23480. If the plane is passed through the origin, $X=Y=Z=0$, the denominator of the matrix is singular and error messages would be generated by the computer. To preclude these, the three factors of the equation of the plane are arbitrarily set equal to 1000 if the absolute value of the denominator is less than 10^{-4} .

4.6.5.2 INCEPT. After the factors defining the equation of the plane have been determined in PLANI, those factors are then used in the subroutine INCEPT, which determines where that plane intercepts the filament.

Let the starting and end points of a filament be given by (x_1, y_1, z_1) and (x_2, y_2, z_2) , respectively. The general equation of a line in space may be given as

$$\frac{(x - x_1)}{(x_2 - x_1)} = \frac{(y - y_1)}{(y_2 - y_1)} = \frac{(z - z_1)}{(z_2 - z_1)} \quad (4.134)$$

This may be put into the following three forms.

$$(x - x_1)(y_2 - y_1) = (y - y_1)(x_2 - x_1) \quad (4.135)$$

$$(y - y_1)(z_2 - z_1) = (z - z_1)(y_2 - y_1) \quad (4.136)$$

$$(x - x_1)(z_2 - z_1) = (z - z_1)(x_2 - x_1) \quad (4.137)$$

These may in turn be put into the form

$$A_{21}x + A_{22}y + A_{23}z = D_2 \quad (4.138)$$

$$A_{31}x + A_{32}y + A_{33}z = D_3 \quad (4.139)$$

$$A_{41}x + A_{42}y + A_{43}z = D_4 \quad (4.140)$$

where

$$A_{21} = (y_2 - y_1) \quad (4.141)$$

$$A_{22} = -(x_2 - x_1) \quad (4.142)$$

$$A_{23} = 0 \quad (4.143)$$

$$A_{31} = 0 \quad (4.144)$$

$$A_{32} = (z_2 - z_1) \quad (4.145)$$

$$A_{33} = -(y_2 - y_1) \quad (4.146)$$

$$A_{41} = (z_2 - z_1) \quad (4.147)$$

$$A_{42} = 0 \quad (4.148)$$

$$A_{43} = -(x_2 - x_1) \quad (4.149)$$

$$D_2 = x_1(y_2 - y_1) - y_1(x_2 - x_1) \quad (4.150)$$

$$D_3 = Y_1 (Z_2 - Z_1) - Z_1 (Y_2 - Y_1) \quad (4.151)$$

$$D_4 = X_1 (Z_2 - Z_1) - Z_1 (X_2 - X_1) \quad (4.152)$$

In general, any two of Equations 4.135 through 4.137, will define the line in space. In some cases the proper two must be selected, a point that will be touched upon later. At the point of intersection, the equations defining the plane and the line must be satisfied simultaneously.

Equation 4.114, defining the plane, and Equations 4.13 through 4.140, defining the line, may be put in the matrix form

$$\begin{bmatrix} A_{11} & A_{12} & A_{13} \\ A_{21} & A_{22} & A_{23} \\ A_{31} & A_{32} & A_{33} \end{bmatrix} \times \begin{bmatrix} X \\ Y \\ Z \end{bmatrix} = \begin{bmatrix} 1 \\ D_2 \\ D_3 \end{bmatrix} \quad (4.153)$$

or

$$\begin{bmatrix} A \\ \vdots \end{bmatrix} \times \begin{bmatrix} X \\ Y \\ Z \end{bmatrix} = \begin{bmatrix} 1 \\ D_2 \\ D_3 \end{bmatrix} \quad (4.154)$$

Multiplying by the inverse of the A matrix

$$\begin{bmatrix} X \\ Y \\ Z \end{bmatrix} = \begin{bmatrix} A^{-1} \\ \vdots \end{bmatrix} \times \begin{bmatrix} 1 \\ D_2 \\ D_3 \end{bmatrix} \quad (4.155)$$

Designating the elements of the inverse matrix as B₁₁, B₁₂, B₁₃, etc.

$$\begin{bmatrix} X \\ Y \\ Z \end{bmatrix} = \begin{bmatrix} B_{11} & B_{12} & B_{13} \\ B_{21} & B_{22} & B_{23} \\ B_{31} & B_{32} & B_{33} \end{bmatrix} \times \begin{bmatrix} 1 \\ D_2 \\ D_3 \end{bmatrix} \quad (4.156)$$

hence

$$X = B_{11} + B_{12} D_2 + B_{13} D_3 \quad (4.157)$$

$$Y = B_{21} + B_{22} D_2 + B_{23} D_3 \quad (4.158)$$

$$Z = B_{31} + B_{32} D_2 + B_{33} D_3 \quad (4.159)$$

The elements of the inverse matrix are

$$B_{11} = (A_{22} \times A_{23} - A_{32} \times A_{23})/D \quad (4.160)$$

$$B_{12} = - (A_{12} \times A_{33} - A_{32} \times A_{13})/D \quad (4.161)$$

$$B_{13} = (A_{12} \times A_{23} - A_{22} \times A_{13})/D \quad (4.162)$$

$$B_{21} = - (A_{21} \times A_{33} - A_{31} \times A_{23})/D \quad (4.163)$$

$$B_{22} = (A_{11} \times A_{33} - A_{31} \times A_{13})/D \quad (4.164)$$

$$B_{23} = - (A_{11} \times A_{23} - A_{21} \times A_{13})/D \quad (4.165)$$

$$B_{31} = (A_{21} \times A_{32} - A_{31} \times A_{22})/D \quad (4.166)$$

$$B_{32} = - (A_{11} \times A_{32} - A_{31} \times A_{12})/D \quad (4.167)$$

$$B_{33} = (A_{11} \times A_{22} - A_{21} \times A_{12})/D \quad (4.168)$$

where

$$D = A_{11} \times A_{22} \times A_{33} + A_{12} \times A_{23} \times A_{33} + A_{13} \times A_{32} \times A_{21} \\ - A_{31} \times A_{22} \times A_{13} - A_{21} \times A_{12} \times A_{33} - A_{11} \times A_{23} \times A_{32} \quad (4.169)$$

Equation 4.153 was based upon the use of Equations 4.138 and 4.139. It could also have been based upon a combination of Equations 4.137 and 4.140 or Equations 4.139 and 4.140. Under some conditions, such as the intercepting plane being parallel to one of the coordinate axes, one or the other combinations of the equations will give a denominator which is singular. This can be avoided by testing for singularities and using the combination of the equations that does not give a singularity.

Listings of the subroutines PLANI and INCEPT are shown in Figures 4.68 and 4.69. A flow chart of INCEPT is shown in Figure 4.70. No flow chart of PLANI is shown since PLANI consists of only a straightforward evaluation of Equations 4.134 through 4.169. The only thing that might be confusing about INCEPT is the selection of the appropriate equations with which to define the plane. In line 22620, the quantity TEST is defined as the sum of the absolute value of all the terms that make up the denominator function D in Equations 4.160 through 4.168. If TEST is very small, that fact is taken as signifying that the equations are poorly formulated and a new set of equations chosen such that TEST is a reasonable value. If no formulation of equations gives a good value for TEST, as would occur if a plane were passed through the origin of the coordinate axes, then the intercept value area will all return as 999. An intercept value of 999 has no physical significance other than as a warning and as a means of insuring that the program does not return unintelligible error messages.

```

23400C -----
23420 SUBROUTINE PLANI(X1,Y1,Z1,X2,Y2,Z2,X3,Y3,Z3,A11,A12,A13)
23440 DENOM=X1*Y2*Z3+Y1*Z2*X3+Z1*Y3*X2-X3*Y2*Z1-X2*Y1*Z3-X1*Z2*Y3
23460 DENO=ABS(DENOM)
23480 IF(DENO.GT.1E-4)GOTO 35659
23500 A11=1000;A12=1000;A13=1000
23520 GOTO 35890
23540 35659 CONTINUE
23560 C11=Y2*Z3-Y3*Z2
23580 C12=-(Y1*Z3-Y3*Z1)
23600 C13=Y1*Z2-Y2*Z1
23620 C21=-(X2*Z3-X3*Z2)
23640 C22=X1*Z3-X3*Z1
23660 C23=-(X1*Z2-X2*Z1)
23680 C31=X2*Y3-X3*Y2
23700 C32=-(X1*Y3-X3*Y1)
23720 C33=X1*Y2-X2*Y1
23740 A11=(C11+C12+C13)/DENOM
23760 A12=(C21+C22+C23)/DENOM
23780 A13=(C31+C32+C33)/DENOM
23800 35890 CONTINUE
23820 RETURN;END
23840 STOP;END

```

Figure 4.68 Program Listing of Subroutine PLANI

4.6.6 Subroutine LOOP

Figure 4.71 shows a loop defined by four points in space, P₁ through P₄, all of the points being assumed to lie in the indicated plane. At some point, PL, within this loop there will be a magnetic flux vector \bar{H} . The XYZ components of this vector may be determined from the previous equations. The component of \bar{H} that is normal to the plane is that part parallel to the normal vector, \bar{N} , at point PL, or

$$H_n = \bar{H} \cos \alpha \quad (4.170)$$

which is equivalent in vector notation to the dot product

$$H_n = \bar{H} \cdot \bar{N} \quad (4.171)$$

where \bar{N} is the unit vector normal to the plane defined by points P₁ through P₄.

Points P₁, P₂, and P₃ will be used to define the plane in which all of the points are assumed to lie. Two vectors that define the plane, $\overline{P_1P_2}$ and $\overline{P_2P_3}$, are then

```

22200C -----
22220 SUBROUTINE INCEPT(A11,A12,A13,I,D,XI,YI,ZI)
22240C
22260C IN THIS ROUTINE THERE MAY BE GENERATED ERROR MESSAGES WHEN
22280C THERE ARE ONLY TWO CONDUCTORS OR SOME OTHER COMBINATION OF
22300C PARAMETERS GIVES A SINGULAR MATRIX FOR THE A MATRIX
22320C
22340 DIMENSION D(40,9)
22360 D1=1
22380 AA21=D(I,6)-D(I,3)
22400 AA22=D(I,2)-D(I,5)
22420 AA23=0
22440 AA31=0
22460 AA32=D(I,7)-D(I,4)
22480 AA33=D(I,3)-D(I,6)
22500 AA41=D(I,7)-D(I,4)
22520 AA42=0
22540 AA43=D(I,2)-D(I,5)
22560 AD2=D(I,2)*AA21+D(I,3)*AA22
22580 AD3=D(I,3)*AA32-D(I,4)*AA21
22600 AD4=D(I,2)*AA41+D(I,4)*AA43
22620 TEST=ABS(A11)+ABS(A12)+ABS(A13)+ABS(AA21)+ABS(AA22)+ABS(AA32)+
22640& ABS(AA33)+ABS(AA41)+ABS(AA43)
22660 TEST1=ABS(TEST/1000)
22680 A21=AA21;A22=AA22;A23=AA23
22700 A31=AA31;A32=AA32;A33=AA33
22720 D2=AD2;D3=AD3
22740 DENOM=A11*A22*A33+A12*A23*A33+A13*A32*A21
22760 DENOM=DENOM-A31*A22*A13-A21*A12*A33-A11*A23*A32
22780 IF(ABS(DENOM)>TEST1)GOTO 100
22800 A31=AA41;A32=AA42;A33=AA43
22820 D3=AD4
22840 DENOM=A11*A22*A33+A12*A23*A33+A13*A32*A21-A31*A22*A13-
22860&A21*A12*A31-A11*A23*A32
22880 IF (ABS(DENOM)>TEST1)GOTO 100
22900 A21=AA31;A22=AA32;A23=AA33

```

Figure 4.69 Program Listing of Subroutine INCEPT

```
22920 D2=AD3
22940 DENOM=A11*A22*A33+A12*A23*A33+A13*A23*A32-
22960& A31*A22*A13-A21*A12*A33-A11*A23*A32
22980 IF(ABS(DENOM)<TEST1)GOTO 140
23000 100 CONTINUE
23020 B11=A22*A33-A32*A23
23040 B12=-(A12*A33-A32*A13)
23060 B13=A12*A23-A22*A13
23080 B21=-(A21*A33-A31*A23)
23100 B22=A11*A33-A31*A13
23120 B23=-(A11*A23-A21*A13)
23140 B31=A21*A32-A31*A22
23160 B32=-(A11*A32-A31*A12)
23180 B33=A11*A22-A21*A12
23200 XI=B11*D1+B12*D2+B13*D3
23220 XI=XI/DENOM
23240 YI=B21*D1+B22*D2+B23*D3
23260 YI=YI/DENOM
23280 ZI=B31*D1+B32*D2+B33*D3
23300 ZI=ZI/DENOM
23320 GOTO 130
23340 140 XI=999;YI=999;ZI=999
23360 130 CONTINUE
23380 RETURN;END
```

Figure 4.69 Program Listing of Subroutine Incept-Concluded

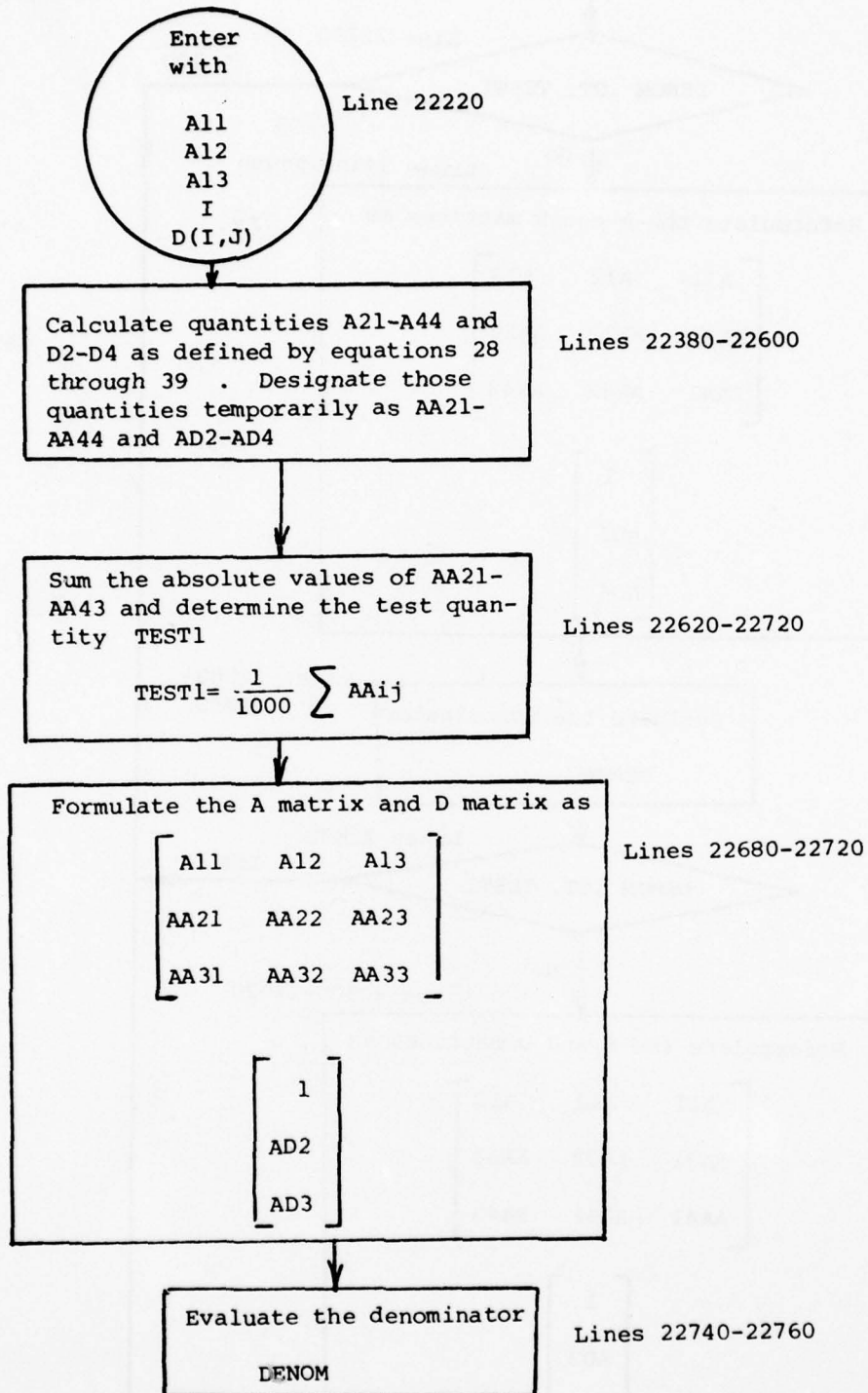


Figure 4.70 Flow Chart of Subroutine INCEPT

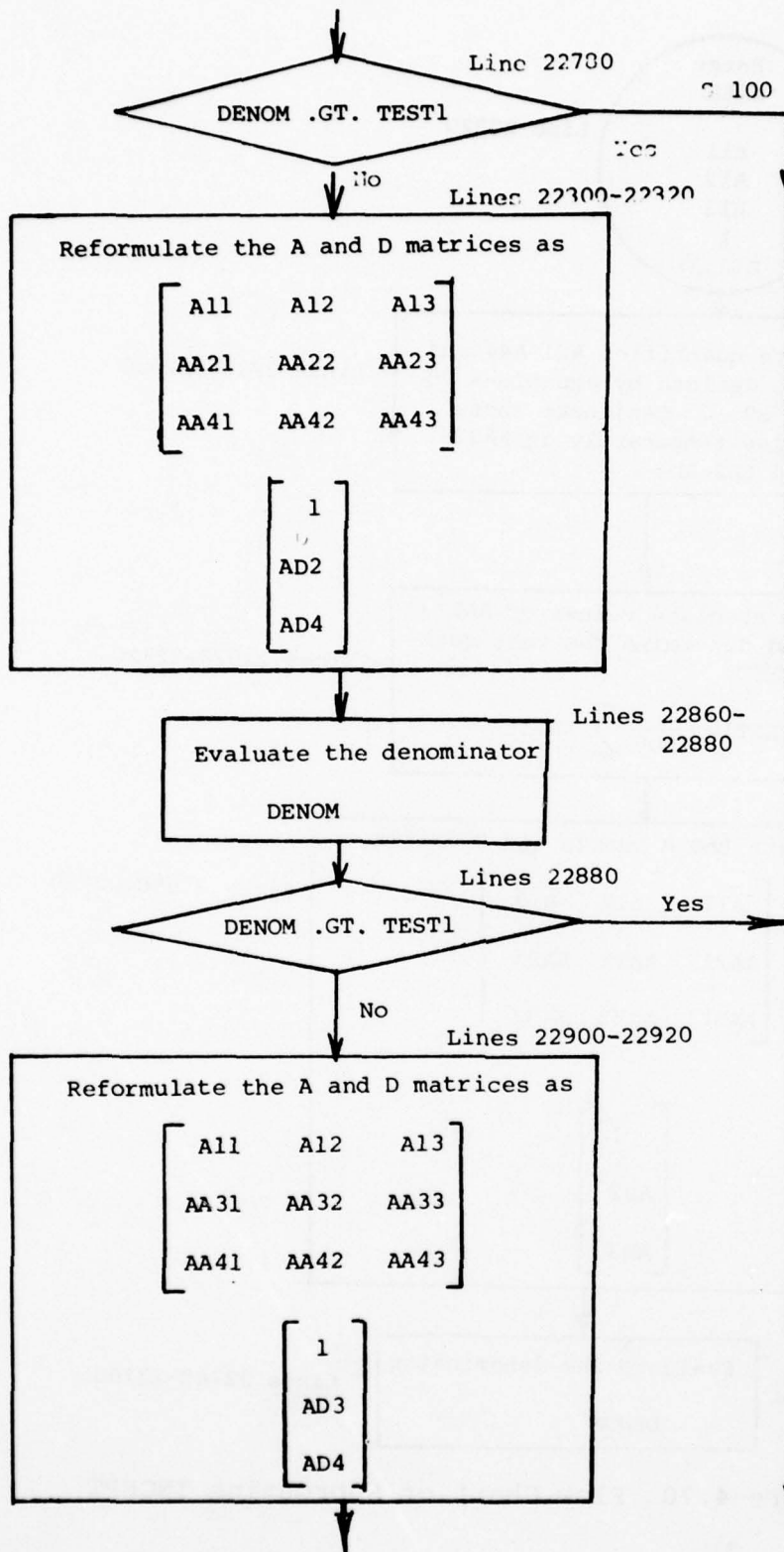


Figure 4.70 Flow Chart of Subroutine INCEPT - Continued

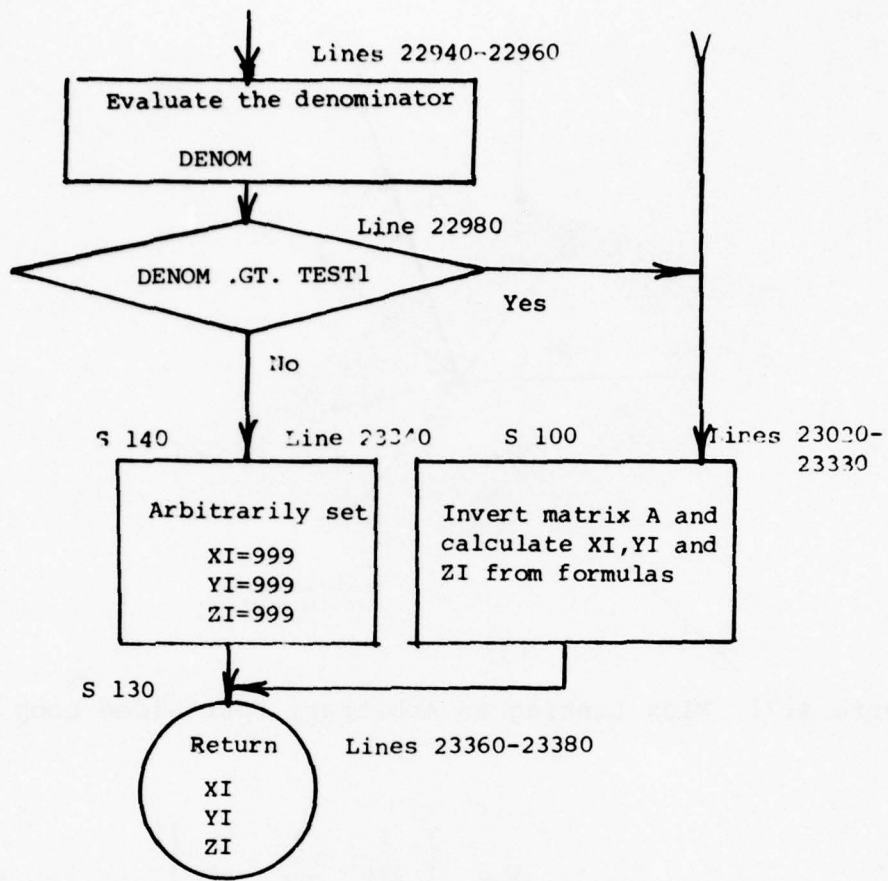


Figure 4.70 Flow Chart of Subroutine INCEPT - Concluded

$$\overline{P1P2} = (XP2 - XP1)i + (YP2 - YP1)j + (ZP2 - ZP1)k \quad (4.172)$$

$$\overline{P2P3} = (XP3 - XP2)i + (YP3 - YP2)j + (ZP3 - ZP2)k \quad (4.173)$$

The normal to the plane defined by these vectors is given by the cross product

$$\overline{N} = \overline{P1P2} \times \overline{P2P3} \quad (4.174)$$

which in matrix notation is

$$\overline{N} = \begin{vmatrix} i & j & k \\ (XP2 - XP1) & (YP2 - YP1) & (ZP2 - ZP1) \\ (XP3 - XP2) & (YP3 - YP2) & (ZP3 - ZP2) \end{vmatrix} \quad (4.175)$$

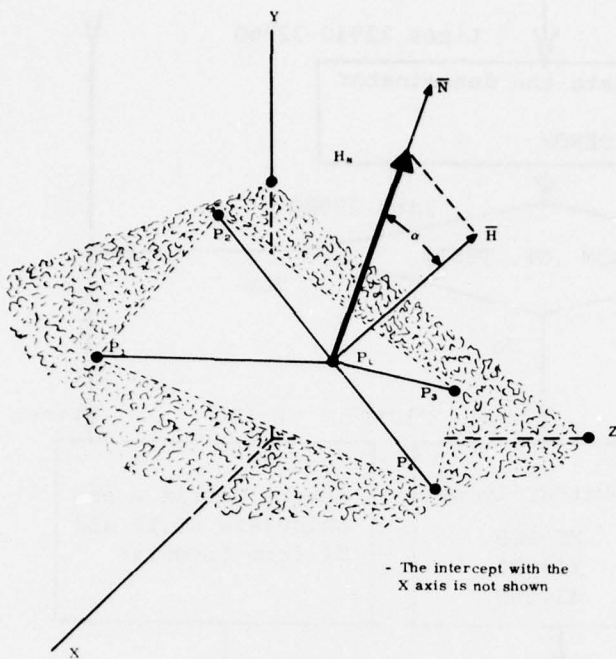


Figure 4.71 Flux Linking an Arbitrary Four Sided Loop

or

$$\bar{N} = \begin{vmatrix} i & j & k \\ X_{21} & Y_{21} & Z_{21} \\ X_{32} & Y_{32} & Z_{32} \end{vmatrix} \quad (4.176)$$

where $X_{21}, Y_{21} \dots Z_{32}$ are the corresponding quantities in Equation 4.175. Expanding the determinant in Equation 4.176 gives

$$\begin{aligned} \bar{N} = & (Y_{21} Z_{32} - Y_{32} Z_{21})i \\ & - (X_{21} Z_{32} - Y_{32} Z_{21})j \\ & + (X_{21} Y_{32} - X_{32} Y_{21})k \end{aligned} \quad (4.177)$$

The unit vector normal to the plane will be

$$\bar{N} = N_{UX} i + N_{UY} j + N_{UZ} k \quad (4.178)$$

where

$$NUX = (Y_{21} Z_{32} - Y_{32} Z_{21})/NU \quad (4.179)$$

$$NUY = (X_{21} Z_{32} - X_{32} Z_{21})/NU \quad (4.180)$$

$$NUZ = (X_{21} Y_{32} - X_{32} Y_{21})/NU \quad (4.181)$$

$$\begin{aligned} NU^2 = & (Y_{21} Z_{32} - Y_{32} Z_{21})^2 + (X_{21} Z_{32} - X_{32} Z_{21})^2 \\ & + (X_{21} Y_{32} - X_{32} Y_{21})^2 \end{aligned} \quad (4.182)$$

The total magnetic flux normal to the loop is determined by a numerical integration process. The process is shown in Figure 4.72. The plane is divided vertically and horizontally into six equally spaced strips. For this discussion, "vertical" will mean the direction of point 1 to point 2 or point 4 to point 3, and "horizontal" will mean the direction of point P1 to point P4 or Point P2 to point P3.

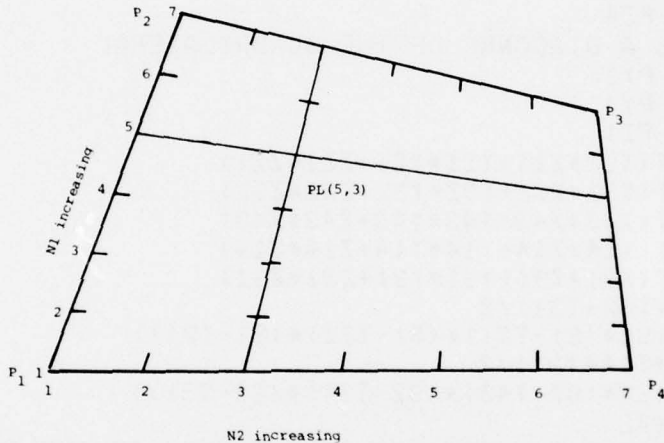


Figure 4.72 Integration Techniques for Flux in a Plane

The 6 strips define 7 lines vertically, the intersections of which define 49 points (7×7), of which point PL (5,3) is shown. The flux density at each point is evaluated and then integrated numerically along each of the vertical strips. The resultant 7 values are integrated horizontally to obtain the total magnetic flux linking the plane. The integration process used is called Weddle's rule (Reference 4.13) and is based on fitting a sixth order polynomial to the array of points and then integrating the resultant polynomial. The result is

$$\sum H \cdot \Delta X = \frac{3}{10} \Delta X (H_1 + 5H_2 + H_3 + 6H_4 + H_5 + 5H_6 + H_7) \quad (4.183)$$

A listing of subroutine LOOP is given on Figure 4.73, and a flow chart given on Figure 4.74.

```

20280C -----
20300 SUBROUTINE LOOP(FLAG1,D,RCURDIS,CURDIS,AREA,BTOT)
20320 COMMON PX1,PY1,PZ1,PX2,PY2,PZ2,PX3,PY3,PZ3,PX4,PY4,PZ4,N1
20340 DIMENSION HN(7,7)
20360 DIMENSION T86A(7)
20380 DIMENSION PATHA(7)
20400 REAL NU1,NU2,NU3,NU,NUX,NUY,NUZ
20420 REAL NU1,NU2,NU3,NU,NUX,NUY,NUZ
20440C THESE ARE THE SIDES OF THE QUADRILATERAL
20460 X21=PX2-PX1
20480 X32=PX3-PX2
20500 X43=PX4-PX3
20520 X14=PX1-PX4
20540 Y21=PY2-PY1
20560 Y32=PY3-PY2
20580 Y43=PY4-PY3
20600 Y14=PY1-PY4
20620 Z21=PZ2-PZ1
20640 Z32=PZ3-PZ2
20660 Z43=PZ4-PZ3
20680 Z14=PZ1-PZ4
20700C THIS IS A DIAGONAL OF THE QUADRILATERAL
20720 X31=PX3-PX1
20740 Y31=PY3-PY1
20760 Z31=PZ3-PZ1
20780 T21=SQRT(X21*X21+Y21*Y21+Z21*Z21)
20800 T32=SQRT(X32*X32+Y32*Y32+Z32*Z32)
20820 T43=SQRT(X43*X43+Y43*Y43+Z43*Z43)
20840 T14=SQRT(X14*X14+Y14*Y14+Z14*Z14)
20860 T31=SQRT(X31*X31+Y31*Y31+Z31*Z31)
20880 S1=(T21+T32+T31)/2
20900 A1=SQRT(S1*(S1-T21)*(S1-T32)*(S1-T31))
20920 S2=(T43+T14+T31)/2
20940 A2=SQRT(S2*(S2-T43)*(S2-T14)*(S2-T31))
20960 AREA=A1+A2
20980C THESE ARE THE MIDPOINTS OF THE ENDS OF THE QUADRILATERAL
21000 XPM1=PX1+X21/2
21020 YPM1=PY1+Y21/2
21040 ZPM1=PZ1+Z21/2
21060 XPM2=PX4-X43/2
21080 YPM2=PY4-Y43/2
21100 ZPM2=PZ4-Z43/2
21120 XPM21=XPM2-XPM1
21140 YPM21=YPM2-YPM1
21160 ZPM21=ZPM2-ZPM1
21180 TPM=SQRT(XPM21*XPM21+YPM21*YPM21+ZPM21*ZPM21)
21200C THESE ARE THE COMPONENTS OF THE NORMAL VECTOR
21220 NU1=Y21*Z32-Y32*Z21
21240 NU2=-X21*Z32+X32*Z21
21260 NU3=X21*Y32-X32*Y21
21280 NU=SQRT(NU1*NU1+NU2*NU2+NU3*NU3)
21300C THESE ARE THE COMONONENTS OF THE UNIT NORMAL VECTOR

```

Figure 4.73 Program Listing of Subroutine LOOP

```

21320 NUX=NU1/NU
21340 NUY=NU2/NU
21360 NUZ=NU3/NU
21380 3550 CONTINUE
21400 3560 DO 3880 N2=1,7,1
21420 3570 DO 3880 N4=1,7,1
21440 XP6=PX2+X32*(N2-1)/6
21460 YP6=PY2+Y32*(N2-1)/6
21480 ZP6=PZ2+Z32*(N2-1)/6
21500 XP8=PX1-X14*(N2-1)/6
21520 YP8=PY1-Y14*(N2-1)/6
21540 ZP8=PZ1-Z14*(N2-1)/6
21560 X86=XP8-XP6
21580 Y86=YP8-YP6
21600 Z86=ZP8-ZP6
21620 T86=SQRT(X86*X86+Y86*Y86+Z86*Z86)
21640 XP=XP8-X86*(N4-1)/6
21660 YP=YP8-Y86*(N4-1)/6
21680 ZP=ZP8-Z86*(N4-1)/6
21700 CALL FILSUM(FLAG1,N1,XP,YP,ZP,D,RCURDIS,CURDIS,HX0,HY0,HZ0)
21720 HNP=HX0*NUX+HY0*NUY+HZ0*NUZ
21740C THESE ARE THE HN'S AT THE VARIOUS POINTS OF THE QUADRILATERAL
21760 HN(N4,N2)=HNP
21780C THESE ARE THE DISTANCES TOP TO BOTTOM ALONG THE QUADRILATERAL
21800 T86A(N2)=T86
21820 3880 CONTINUE
21840 3890 D03950 N2=1,7,1
21860 DELTA1=T86A(N2)/6
21880C THIS EVALUATES FLUX ALONG THE LINES IN THE DIRECTION P1-->P2
21900C AND P4-->P3
21920 PATH=HN(1,N2)+5*HN(2,N2)+HN(3,N2)+6*HN(4,N2)+HN(5,N2)
21940& +5*HN(6,N2)+HN(7,N2)
21960 PATHA(N2)=0.3*DELTA1*PATH
21980 3950 CONTINUE
22000 DELTA2=TPM/6
22020C THIS EVALUATES THE RESULTANT FLUX IN THE DIRECTION P1-->P4
22040C AND P2-->P3
22060 120 FORMAT("-----LEAVING INCEPT-----")
22080 HTOT=PATHA(1)+5*PATHA(2)+PATHA(3)+6*PATHA(4)+PATHA(5)
22100& +5*PATHA(6)+PATHA(7)
22120 HTOT=0.3*DELTA2*HTOT
22140 BTOT=HTOT*1.25663706E-6
22160 JX=JX+1
22180 RETURN;END

```

Figure 4.73 Program Listing of Subroutine LOOP - Concluded

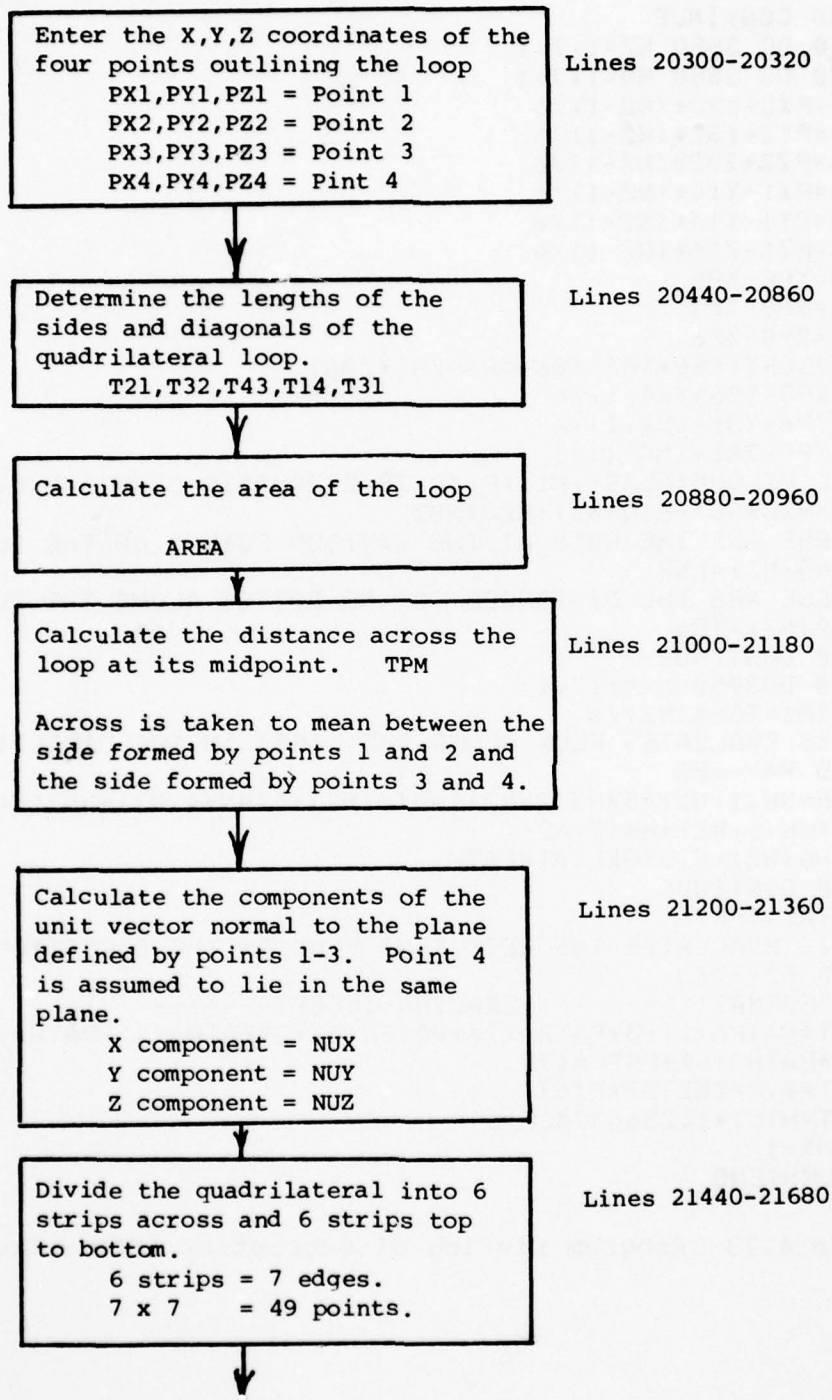


Figure 4.74 Flow Chart of Subroutine LOOP

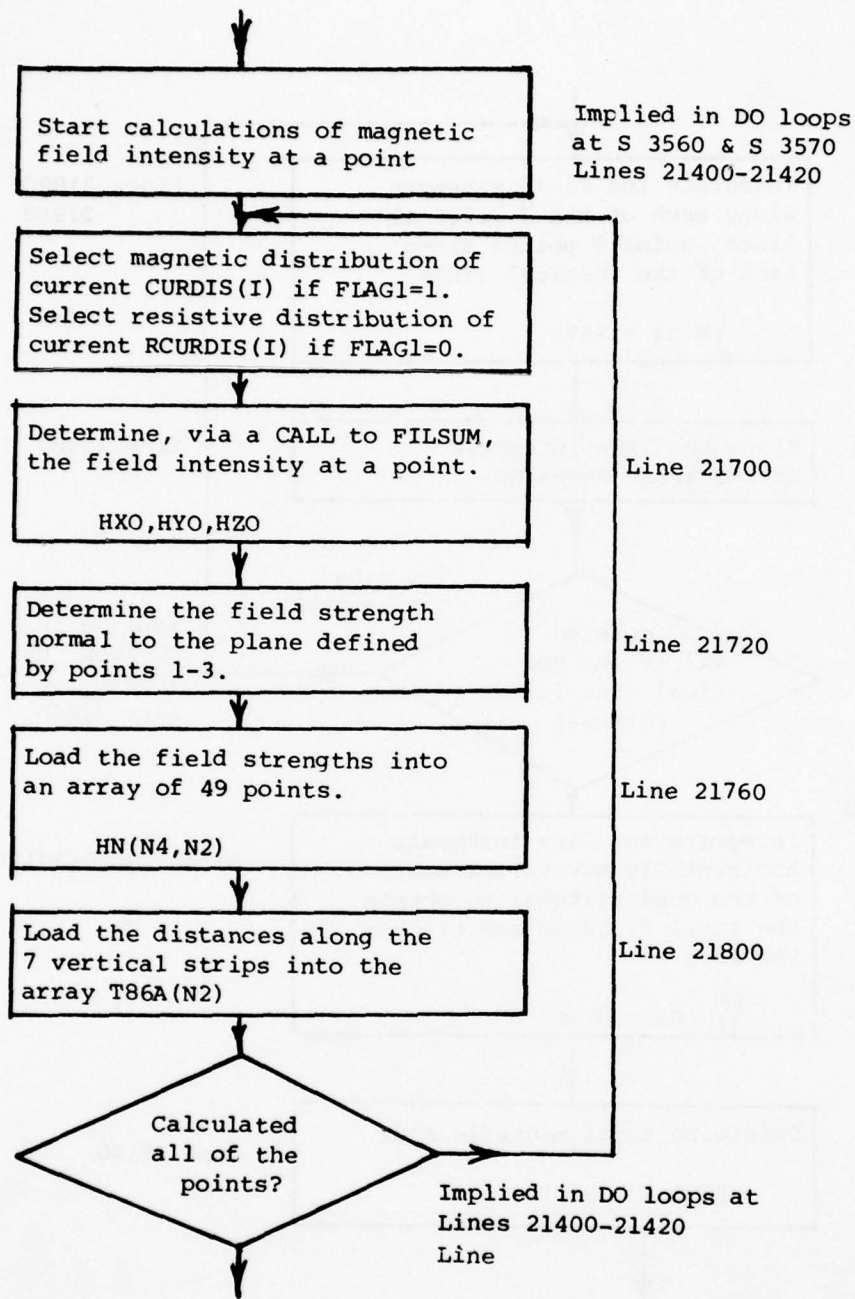


Figure 4.74 Flow Chart of Subroutine LOOP - Continued

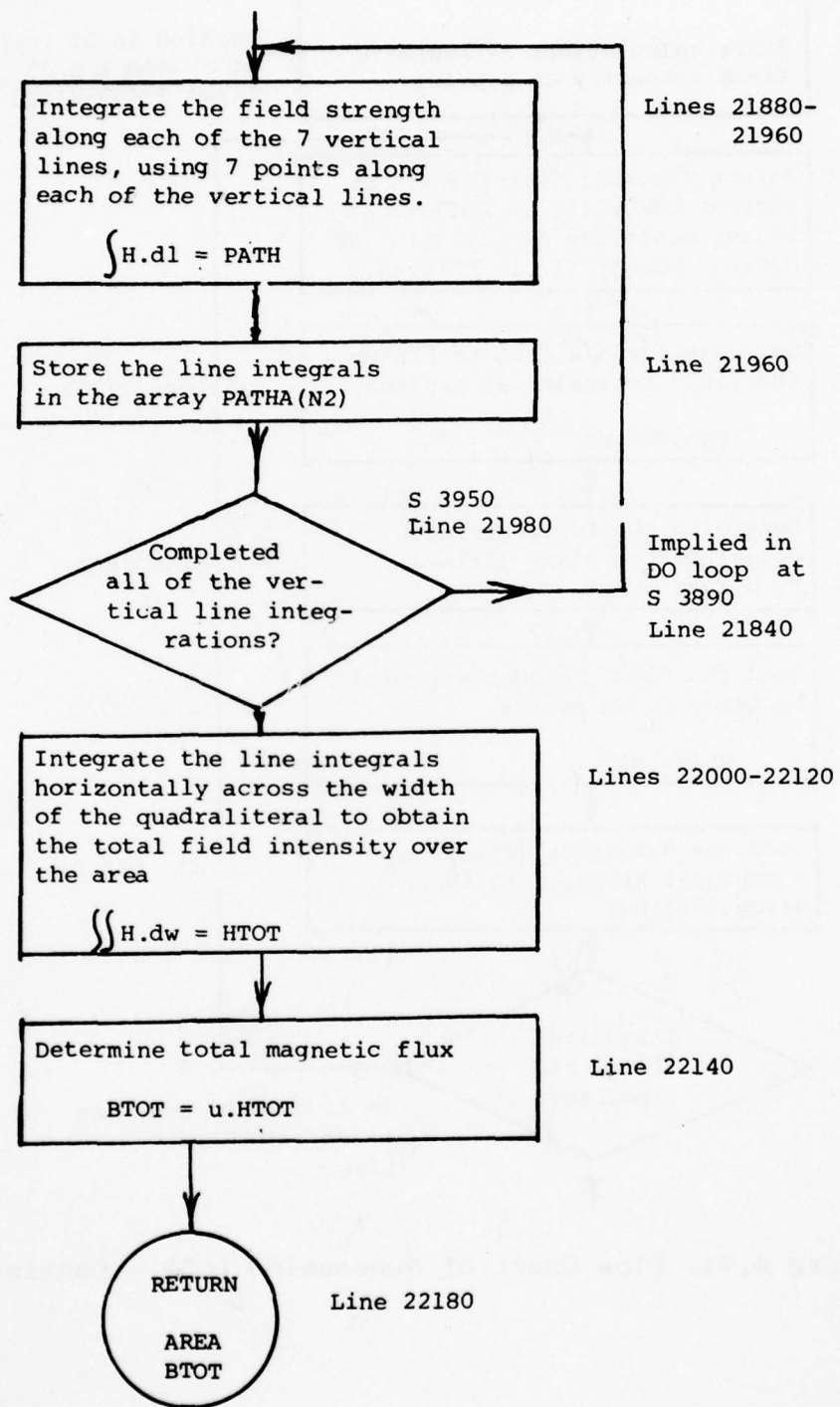


Figure 4.74 Flow Chart of Subroutine LOOP - Concluded

In lines 20300 through 20320, the X, Y, and Z coordinates of the points which define the loop are used.

In lines 20440 through 20960 the lengths of the sides and diagonals of the quadrilateral loop are calculated. From these dimensions the area of the loop is determined.

In lines 21000 through 21180, the distance horizontally across the loop at its midpoint is calculated. "Horizontally" is here taken to be the direction from point P2 to point P3 or from point P1 to point P4. The term "vertically" is taken to be in the direction from point P1 to point P2 or point P4 to point P3. In this sense these terms have no relation as to whether the loop itself is oriented horizontally or vertically with respect to the reference XYZ axes.

In lines 21200 through 21360, the components of the unit vector are calculated perpendicular to the plane defined by the loop under consideration. Mathematically, this operation consists of taking two vectors that line in the planes point 1 - point 2, and point 2 - point 3, and in taking the cross-product of these two vectors.

Next, the quadrilateral is divided into six strips vertically and six strips horizontally; the field strength is calculated at the intersection of each of the dividing lines. This makes a total of 49 points. This field strength is calculated by a call to the subroutine FILSUM. FILSUM returns the X, Y, and Z components of field strength with reference to the original reference axes.

In line 21720, a dot product of the field strength vector and the unit vector normal to the plane are performed in order to determine the component of the magnetic field perpendicular to the loop under consideration. The field strengths are loaded into an array, HN, at line 21760. The vertical distances along each of the thirteen strips are loaded into an array T86 at line 21800.

In lines 21920 and 21940, line integrals of the magnetic field strength are taken along each of the seven vertical paths. This integral is evaluated numerically by dividing the vertical strip into seven points. The integration routine used is Weddel's rule, which was described earlier. These line integrals are stored in the array PATHA. The seven line integrals are then integrated horizontally to obtain the total magnetic field linking the plane. The double integral of H is taken in line 22080 and then multiplied by the permeability of air to obtain the total magnetic flux in webers. This latter multiplication is taken at line 22140.

AD-A062 606

GENERAL ELECTRIC CORPORATE RESEARCH AND DEVELOPMENT --ETC F/G 1/13
ANALYSIS AND CALCULATIONS OF LIGHTNING INTERACTIONS WITH AIRCRAFT -- ETC (U)
AUG 78 F A FISHER F33615-76-C-3122

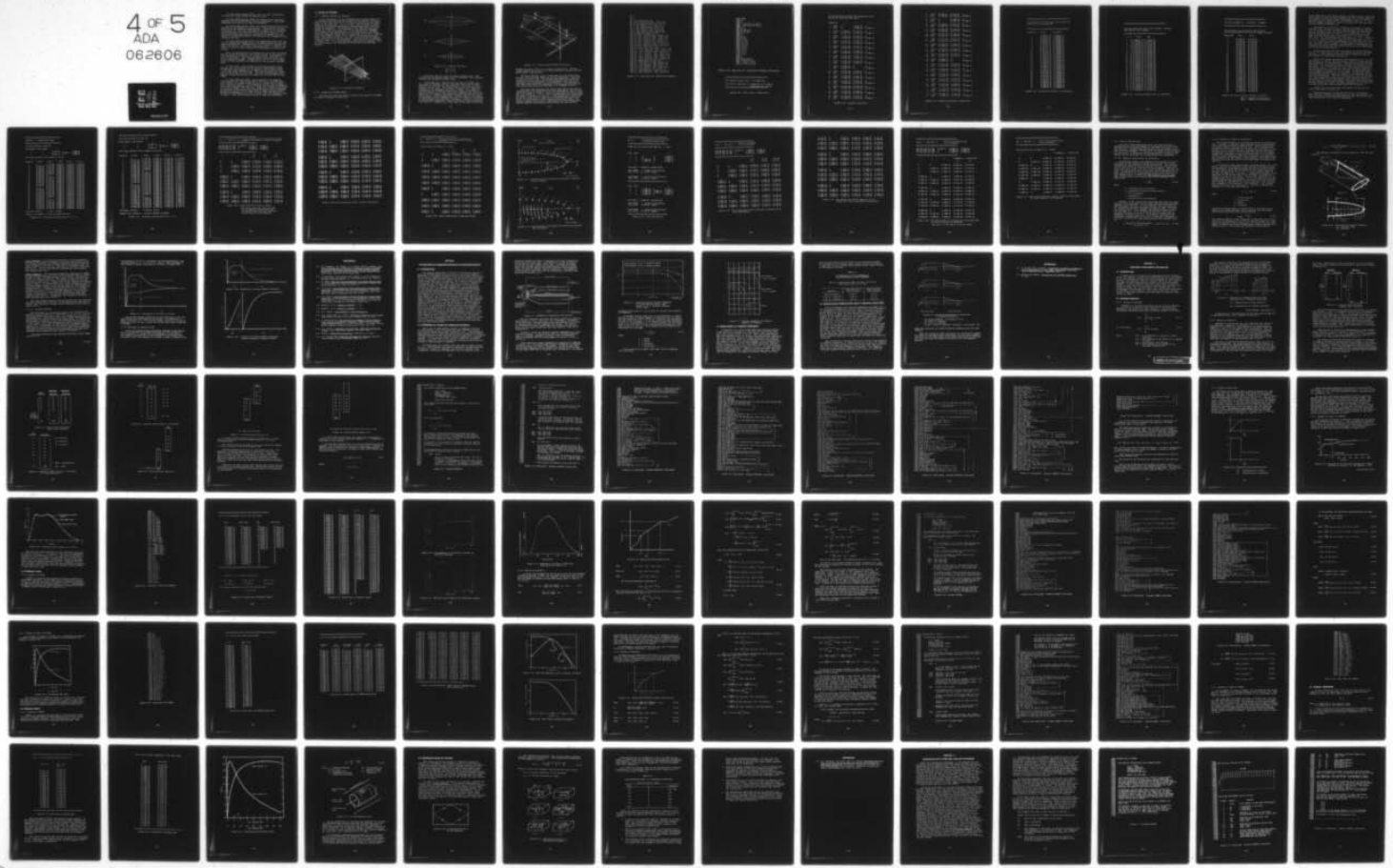
UNCLASSIFIED

SRD-78-044

AFFDL-TR-78-106

NL

4 OF 5
ADA
062606



In lines 20300 through 20320, the X, Y, and Z coordinates of the points which define the loop are used.

In lines 20440 through 20960 the lengths of the sides and diagonals of the quadrilateral loop are calculated. From these dimensions the area of the loop is determined.

In lines 21000 through 21180, the distance horizontally across the loop at its midpoint is calculated. "Horizontally" is here taken to be the direction from point P2 to point P3 or from point P1 to point P4. The term "vertically" is taken to be in the direction from point P1 to point P2 or point P4 to point P3. In this sense these terms have no relation as to whether the loop itself is oriented horizontally or vertically with respect to the reference XYZ axes.

In lines 21200 through 21360, the components of the unit vector are calculated perpendicular to the plane defined by the loop under consideration. Mathematically, this operation consists of taking two vectors that line in the planes point 1 - point 2, and point 2 - point 3, and in taking the cross-product of these two vectors.

Next, the quadrilateral is divided into six strips vertically and six strips horizontally; the field strength is calculated at the intersection of each of the dividing lines. This makes a total of 49 points. This field strength is calculated by a call to the subroutine FILSUM. FILSUM returns the X, Y, and Z components of field strength with reference to the original reference axes.

In line 21720, a dot product of the field strength vector and the unit vector normal to the plane are performed in order to determine the component of the magnetic field perpendicular to the loop under consideration. The field strengths are loaded into an array, HN, at line 21760. The vertical distances along each of the thirteen strips are loaded into an array T86 at line 21800.

In lines 21920 and 21940, line integrals of the magnetic field strength are taken along each of the seven vertical paths. This integral is evaluated numerically by dividing the vertical strip into seven points. The integration routine used is Weddel's rule, which was described earlier. These line integrals are stored in the array PATHA. The seven line integrals are then integrated horizontally to obtain the total magnetic field linking the plane. The double integral of H is taken in line 22080 and then multiplied by the permeability of air to obtain the total magnetic flux in webers. This latter multiplication is taken at line 22140.

4.7 USAGE OF DIFFMAG

4.7.1 Geometry Chosen for Analysis

As an illustration of what DIFFMAG does, consider Figure 4.75. A wing-shaped structure has an elliptical cross section of dimensions 1.0 m at one end by 0.2 m at the other end, and twice those dimensions at the other end. It is 6 m long. The structure is represented by 32 conductors arranged at approximately equal intervals around the periphery. The locations of the conductors are illustrated in Figure 4.76. The locations at the ends are described by the user. The locations at $Z = 2$ are calculated by DIFFMAG. Those locations are determined by the intersection of the conductors with imaginary planes that are specified by the user, a typical plane being shown in Figure 4.75. Within the structure are two loops, one horizontal and one vertical, through which the magnetic flux that passes is to be determined. These loops are illustrated in Figure 4.77. It is also desired to calculate the magnetic field at various points, the locations of which will be illustrated shortly.

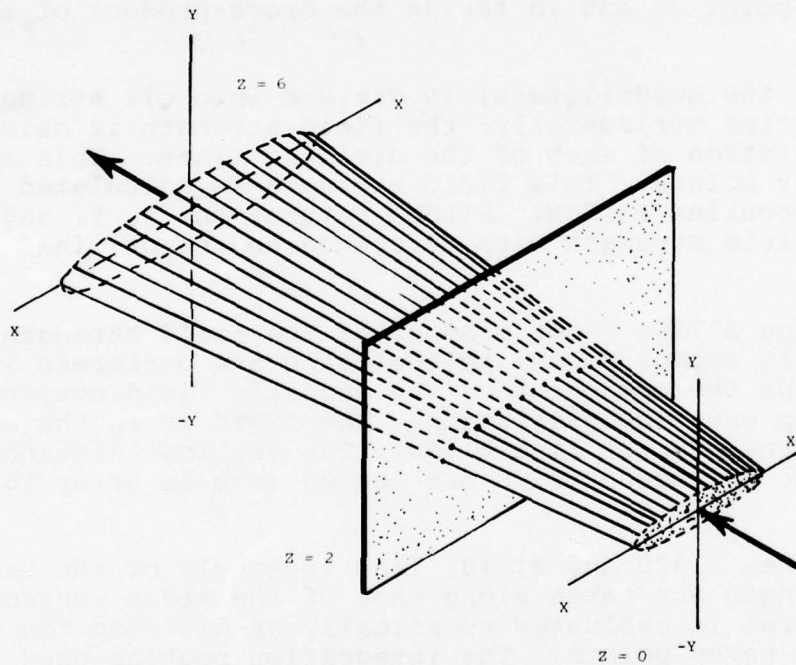


Figure 4.75 Illustrative Geometry

4.7.2 Example of DIFFMAG Output

The data file that was used to initiate the running of DIFFMAG is shown in Figures 4.78 and 4.79.

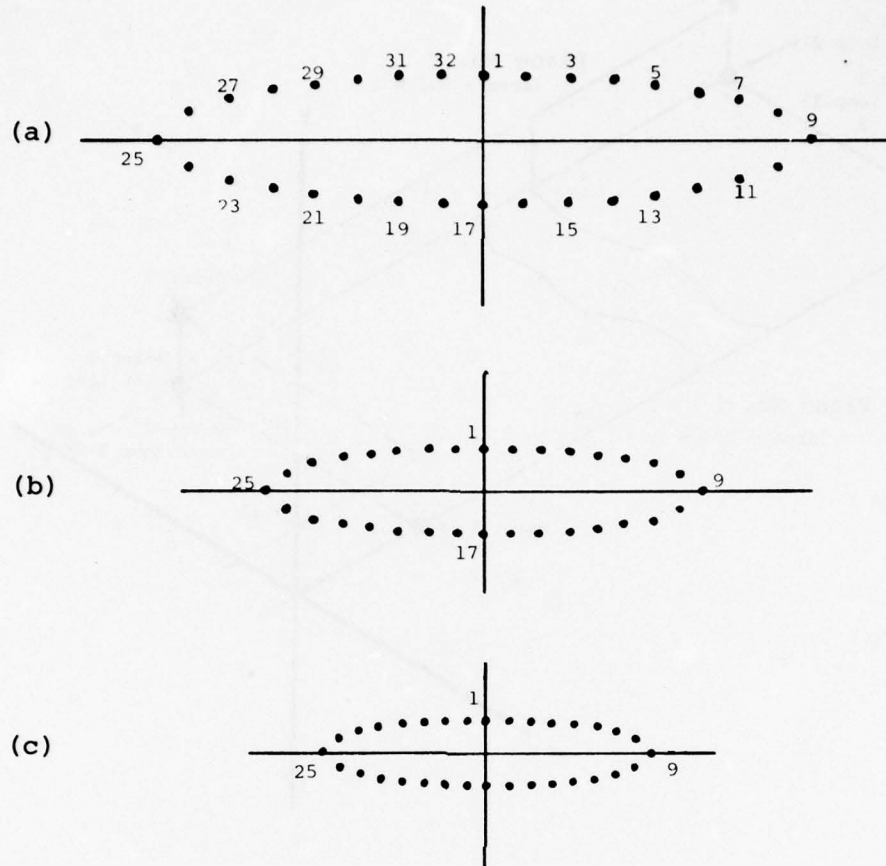


Figure 4.76 Conductor Locations

- (a) $Z = 6$
- (b) $Z = 2$
- (c) $Z = 0$

The first lines of output are shown in Figure 4.80. They confirm that the analysis deals with 32 conductors, the locations of which are described in meter units.

In the data file, line 25 gives the value of IOFLAG2 as 1. This control character initiates the printing of the data that describes the locations of the conductors. That data is shown in Figures 4.81 and 4.82. The program then prints the length and diameter of the conductors, as shown in Figure 4.83. These calculated data are valuable primarily as a means of checking on the correctness of the input data used to describe the conductors. Generally, the length of the conductors should be equal to, or at least follow, a smooth progression. Unusual jumps in the length of conductors usually indicate that one of the start or end points of the conductors was described incorrectly. This can be verified by checking the appropriate lines of input data given in Figures 4.78 and 4.79. Another set of data that can be used to help check

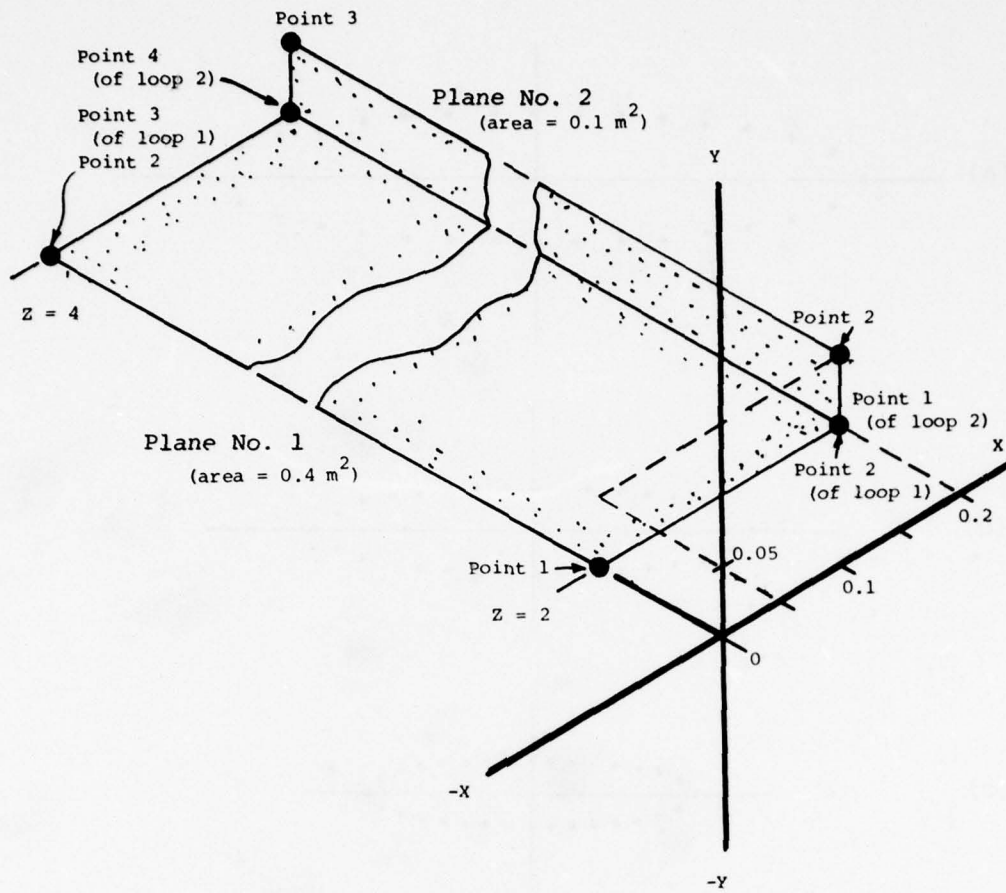


Figure 4.77 Loops Contained Within Structure

whether the data is correct is given in Figure 4.84. The distances between the conductors at their end points should also normally follow a smooth path.

The most important type of output data is that which tells how the current divides among the various conductors. That data is given in Figure 4.85. The program calculates the current as controlled by the inductances of the conductors and then as determined by the resistances of the conductors. The printing of that data would have been suppressed if the control character on line 1020 of the input file had been a "0" instead of a "1."

The input data describes two planes along which the path of intersection of the conductors was to be determined. One of those planes was shown in Figure 4.75 and the other was parallel to that one, but located at $Z = 4$ m. The calculated points of interception are shown in Figures 4.86 and 4.87. The program first prints the points that were used to describe the plane and then prints the points of intersection of the conductors with that plane. The distance between the points of intersection and the average tangential magnetic field between those points are also printed.

10 32
20 1
25 1
30 1,0,.1,0,0,.2,6,.01
40 2,.065,.09915,0,.130,.19830,6,.01
50 3,.130,.09656,0,.260,.1931,6,.01
60 4,.196,.092,0,.392,.184,6,.01
70 5,.261,.0853,0,.522,.1706,6,.01
80 6,.325,.0760,0,.650,.152,6,.01
90 7,.390,.0626,0,.780,.1252,6,.01
100 8,.451,.0432,0,.902,.0864,6,.01
110 9,.500,0,0,1.00,0,6,.01
120 10,.451,-.0432,0,.902,-.0864,6,.01
130 11,.390,-.0626,0,.780,-.1252,6,.01
140 12,.325,-.0760,0,.650,-.152,6,.01
150 13,.261,-.0853,0,.522,-.1706,6,.01
160 14,.196,-.092,0,.392,-.184,6,.01
170 15,.130,-.09656,0,.260,-.1931,6,.01
180 16,.065,-.09915,0,.130,-.1983,6,.01
190 17,0,-.10,0,0,-.20,6,.01
200 18,-.065,-.09915,0,-.130,-.1983,6,.01
210 19,-.130,-.09656,0,-.260,-.1931,6,.01
220 20,-.196,-.092,0,-.392,-.184,6,.01
230 21,-.261,-.0853,0,-.522,-.1706,6,.01
240 22,-.325,-.0760,0,-.650,-.152,6,.01
250 23,-.390,-.0626,0,-.780,-.1252,6,.01
260 24,-.451,-.0432,0,-.902,-.0864,6,.01
270 25,-.500,0,0,-1.00,0,6,.01
280 26,-.451,.0432,0,-.902,.0864,6,.01
290 27,-.390,.0626,0,-.780,.1252,6,.01
300 28,-.325,.0760,0,-.650,.152,6,.01
310 29,-.261,.0853,0,-.522,.1706,6,.01
320 30,-.196,.092,0,-.392,.184,6,.01
330 31,-.130,.09656,0,-.260,.1931,6,.01
340 32,-.065,.09915,0,-.130,.1983,6,.01

Figure 4.78 Input Data for Illustrative Example

```
1010 1000
1020 1
1030 2
1040 -.5,0,2,0,1,2,.5,0,2
1050 -.5,0,4,0,1,4,.5,0,4
2000 1,1
2010 2,2,2
2020 0,.05,.025
2030 0,.3,.05
2040 1,1
3000 11
3010 0,0,2
3020 0,.3,2
3030 .2,0,2
3040 .2,.3,2
3050 .4,.3,2
3060 .8,.3,2
3070 .8,0,2
3080 0,1,2
3090 .4,1,2
3100 1,1,2
3110 1,0,2
3500 1
4000 2
4010 0,0,2,0,0,0,4
4020 .2,0,4,.2,0,2
4030 .2,0,2,.2,.05,2
4040 .2,.05,4,.2,0,4
```

Figure 4.79 Input Data for Illustrative Example (Conclusion)

```
*****
THIS ANALYSIS DEALS WITH    32 CONDUCTORS
THE FACTOR F RELATING TO DIMENSIONS IS 0.100E 01
(Dimensions are in meters)
*****
```

Figure 4.80 First Lines of Output Data

THE FOLLOWING DATA GIVES THE COORDINATES THAT
DEFINE THE START AND END POINTS

CONDUCTOR		X	Y	Z
1	START	0.	0.100E 00	0.
1	END	0.	0.200E 00	0.600E 01
2	START	0.650E-01	0.992E-01	0.
2	END	0.130E 00	0.198E 00	0.600E 01
3	START	0.130E 00	0.966E-01	0.
3	END	0.260E 00	0.193E 00	0.600E 01
4	START	0.196E 00	0.920E-01	0.
4	END	0.392E 00	0.184E 00	0.600E 01
5	START	0.261E 00	0.853E-01	0.
5	END	0.522E 00	0.171E 00	0.600E 01
6	START	0.325E 00	0.760E-01	0.
6	END	0.650E 00	0.152E 00	0.600E 01
7	START	0.390E 00	0.626E-01	0.
7	END	0.780E 00	0.125E 00	0.600E 01
8	START	0.451E 00	0.432E-01	0.
8	END	0.902E 00	0.864E-01	0.600E 01
9	START	0.500E 00	0.	0.
9	END	0.100E 01	0.	0.600E 01
10	START	0.451E 00	-0.432E-01	0.
10	END	0.902E 00	-0.864E-01	0.600E 01
11	START	0.390E 00	-0.626E-01	0.
11	END	0.780E 00	-0.125E 00	0.600E 01
12	START	0.325E 00	-0.760E-01	0.
12	END	0.650E 00	-0.152E 00	0.600E 01
13	START	0.261E 00	-0.853E-01	0.
13	END	0.522E 00	-0.171E 00	0.600E 01
14	START	0.196E 00	-0.920E-01	0.
14	END	0.392E 00	-0.184E 00	0.600E 01
15	START	0.130E 00	-0.966E-01	0.
15	END	0.260E 00	-0.193E 00	0.600E 01

Figure 4.81 Conductor Locations

16	START	0.650E-01	-0.992E-01	0.
16	END	0.130E 00	-0.198E 00	0.600E 01
17	START	0.	-0.100E 00	0.
17	END	0.	-0.200E 00	0.600E 01
18	START	-0.650E-01	-0.992E-01	0.
18	END	-0.130E 00	-0.198E 00	0.600E 01
19	START	-0.130E 00	-0.966E-01	0.
19	END	-0.260E 00	-0.193E 00	0.600E 01
20	START	-0.196E 00	-0.920E-01	0.
20	END	-0.392E 00	-0.184E 00	0.600E 01
21	START	-0.261E 00	-0.853E-01	0.
21	END	-0.522E 00	-0.171E 00	0.600E 01
22	START	-0.325E 00	-0.760E-01	0.
22	END	-0.650E 00	-0.152E 00	0.600E 01
23	START	-0.390E 00	-0.626E-01	0.
23	END	-0.780E 00	-0.125E 00	0.600E 01
24	START	-0.451E 00	-0.432E-01	0.
24	END	-0.902E 00	-0.864E-01	0.600E 01
25	START	-0.500E 00	0.	0.
25	END	-0.100E 01	0.	0.600E 01
26	START	-0.451E 00	0.432E-01	0.
26	END	-0.902E 00	0.864E-01	0.600E 01
27	START	-0.390E 00	0.626E-01	0.
27	END	-0.780E 00	0.125E 00	0.600E 01
28	START	-0.325E 00	0.760E-01	0.
28	END	-0.650E 00	0.152E 00	0.600E 01
29	START	-0.261E 00	0.853E-01	0.
29	END	-0.522E 00	0.171E 00	0.600E 01
30	START	-0.196E 00	0.920E-01	0.
30	END	-0.392E 00	0.184E 00	0.600E 01
31	START	-0.130E 00	0.966E-01	0.
31	END	-0.260E 00	0.193E 00	0.600E 01
32	START	-0.650E-01	0.992E-01	0.
32	END	-0.130E 00	0.198E 00	0.600E 01

Figure 4.82 Conductor Locations (Conclusion)

THE FOLLOWING DATA DESCRIBES THE LENGTH AND
DIAMETER OF THE CONDUCTORS

CONDUCTOR	LENGTH	DIAMETER
1	0.60008E 01	0.10000E-01
2	0.60012E 01	0.10000E-01
3	0.60022E 01	0.10000E-01
4	0.60039E 01	0.10000E-01
5	0.60063E 01	0.10000E-01
6	0.60093E 01	0.10000E-01
7	0.60130E 01	0.10000E-01
8	0.60171E 01	0.10000E-01
9	0.60208E 01	0.10000E-01
10	0.60171E 01	0.10000E-01
11	0.60130E 01	0.10000E-01
12	0.60093E 01	0.10000E-01
13	0.60063E 01	0.10000E-01
14	0.60039E 01	0.10000E-01
15	0.60022E 01	0.10000E-01
16	0.60012E 01	0.10000E-01
17	0.60008E 01	0.10000E-01
18	0.60012E 01	0.10000E-01
19	0.60022E 01	0.10000E-01
20	0.60039E 01	0.10000E-01
21	0.60063E 01	0.10000E-01
22	0.60093E 01	0.10000E-01
23	0.60130E 01	0.10000E-01
24	0.60171E 01	0.10000E-01
25	0.60208E 01	0.10000E-01
26	0.60171E 01	0.10000E-01
27	0.60130E 01	0.10000E-01
28	0.60093E 01	0.10000E-01
29	0.60063E 01	0.10000E-01
30	0.60039E 01	0.10000E-01
31	0.60022E 01	0.10000E-01
32	0.60012E 01	0.10000E-01

Figure 4.83 Length and Diameter of Conductors

THE FOLLOWING DATA GIVES THE DISTANCES BETWEEN
THE ENDS OF THE FILAMENTS

I TO J	START	END
--------	-------	-----

2 1	0.65006E-01	0.13001E 00
3 2	0.65052E-01	0.13010E 00
4 3	0.66157E-01	0.13231E 00
5 4	0.65344E-01	0.13069E 00
6 5	0.64672E-01	0.12934E 00
7 6	0.66367E-01	0.13273E 00
8 7	0.64011E-01	0.12802E 00
9 8	0.65324E-01	0.13065E 00
10 9	0.65324E-01	0.13065E 00
11 10	0.64011E-01	0.12802E 00
12 11	0.66367E-01	0.13273E 00
13 12	0.64672E-01	0.12934E 00
14 13	0.65344E-01	0.13069E 00
15 14	0.66157E-01	0.13231E 00
16 15	0.65052E-01	0.13010E 00
17 16	0.65006E-01	0.13001E 00
18 17	0.65006E-01	0.13001E 00
19 18	0.65052E-01	0.13010E 00
20 19	0.66157E-01	0.13231E 00
21 20	0.65344E-01	0.13069E 00
22 21	0.64672E-01	0.12934E 00
23 22	0.66367E-01	0.13273E 00
24 23	0.64011E-01	0.12802E 00
25 24	0.65324E-01	0.13065E 00
26 25	0.65324E-01	0.13065E 00
27 26	0.64011E-01	0.12802E 00
28 27	0.66367E-01	0.13273E 00
29 28	0.64672E-01	0.12934E 00
30 29	0.65344E-01	0.13069E 00
31 30	0.66157E-01	0.13231E 00
32 31	0.65052E-01	0.13010E 00

Figure 4.84 Distances Between Ends of Conductors

THE TOTAL CURRENT IS 0.100E 04 AMPERES

THE FOLLOWING DATA TELLS HOW THE CURRENT DIVIDES

CONDUCTOR	MAG I	RES I
1	0.230E 02	0.313E 02
2	0.231E 02	0.313E 02
3	0.238E 02	0.313E 02
4	0.248E 02	0.313E 02
5	0.264E 02	0.313E 02
6	0.291E 02	0.312E 02
7	0.341E 02	0.312E 02
8	0.424E 02	0.312E 02
9	0.695E 02	0.312E 02
10	0.424E 02	0.312E 02
11	0.341E 02	0.312E 02
12	0.291E 02	0.312E 02
13	0.264E 02	0.313E 02
14	0.248E 02	0.313E 02
15	0.238E 02	0.313E 02
16	0.231E 02	0.313E 02
17	0.230E 02	0.313E 02
18	0.231E 02	0.313E 02
19	0.238E 02	0.313E 02
20	0.248E 02	0.313E 02
21	0.264E 02	0.313E 02
22	0.291E 02	0.312E 02
23	0.341E 02	0.312E 02
24	0.424E 02	0.312E 02
25	0.695E 02	0.312E 02
26	0.424E 02	0.312E 02
27	0.341E 02	0.312E 02
28	0.291E 02	0.312E 02
29	0.264E 02	0.313E 02
30	0.248E 02	0.313E 02
31	0.238E 02	0.313E 02
32	0.231E 02	0.313E 02

Figure 4.85 Total Current and How it Divides

MAG I = Magnetic distribution
RES I = Resistive distribution

On any given line, the spacing (DELTA S) and the average tangential field (DELTA H) refer to that conductor and the conductor below it. For example, the spacing between Conductors 3 and 4 is 0.882E-1 m, and that value is listed on the line opposite Conductor 3. The spacing between Conductors 32 and 1 is 0.867E-1 m, and that value is given opposite Conductor 32.

The magnetic fields over a volume are presented in Figures 4.88 and 4.89. The points used to define the volume are shown on the top of Figure 4.88. The data indicate that the field calculations should be made starting at $Z = 2$, ending at $Z = 2$, and made in increments of 2 m. This is the format with which one would call for calculations to be made at $Z = 2$ m only. Along the Y axis, the calculations are to be made at $Y = 0$, $Y = 0.25$ and $Y = 0.5$ m. Along the X axis, they are to be made from $X = 0$ to $X = 0.3$ m, and to be made in increments of 0.05 m over that interval. At each point in Figures 4.88 and 4.89, the first line of data gives the field intensity as determined by the magnetic distribution of current, and the second line gives it as determined by the resistive distribution.

Figure 4.90 gives the field intensities at several discrete points. For both sets of data, the control characters (ID4 and D6) were 1, which specifies that the field intensities were to be presented in rectangular coordinates.

Figure 4.91 shows, for half of the structure at $Z = 2$ m, the distribution of current and the magnetic fields as determined by the inductances of the conductors. The arrows show the direction and strength of the magnetic fields internal and external to the structure. The internal fields are too small to show clearly on this scale, and, in any case, are only the residual fields that are calculated when a distributed structure is approximated by a finite number of conductors. In all cases, the external fields are oriented tangentially to the structure. Figure 4.92 shows the corresponding data when the current in the conductors is controlled by resistance. While it is difficult to see on this figure, the orientation of the external field changes slightly so that some of the field lines penetrate the structure, giving rise to the internal field pattern shown. Since the structure is symmetrical around its center, the field vanishes at $X = 0$ and $Y = 0$. At other points the field is bowed away from the center.

Figure 4.93 gives the total flux passing through the two loops illustrated in Figure 4.77.

Figures 4.94 and 4.95 show the form of the calculations when the field intensity is calculated in polar coordinates. Figures 4.96 and 4.97 show the same data when only the initial and final magnitudes of the field are presented.

THERE ARE 2 INTERCEPTING PLANES

THE POINTS DEFINING A PLANE ARE

PLANE NUMBER	POINT NUMBER	X	Y	Z
1	1	-0.500E 00	0.	0.200E 01
1	2	0.	0.100E 01	0.200E 01
1	3	0.500E 00	0.	0.200E 01

THAT PLANE INTERCEPTS THE FILAMENTS AS FOLLOWS

CONDUCTOR	X INTER	Y INTER	Z INTER	DELTA S	DELTA H
1	0.	0.133E 00	0.200E 01	0.867E-01	0.265E 03
2	0.867E-01	0.132E 00	0.200E 01	0.867E-01	0.265E 03
3	0.173E 00	0.129E 00	0.200E 01	0.882E-01	0.272E 03
4	0.261E 00	0.123E 00	0.200E 01	0.871E-01	0.287E 03
5	0.348E 00	0.114E 00	0.200E 01	0.862E-01	0.313E 03
6	0.433E 00	0.101E 00	0.200E 01	0.885E-01	0.350E 03
7	0.520E 00	0.835E-01	0.200E 01	0.853E-01	0.445E 03
8	0.601E 00	0.576E-01	0.200E 01	0.871E-01	0.631E 03
9	0.667E 00	0.	0.200E 01	0.871E-01	0.631E 03
10	0.601E 00	-0.576E-01	0.200E 01	0.853E-01	0.445E 03
11	0.520E 00	-0.835E-01	0.200E 01	0.885E-01	0.350E 03
12	0.433E 00	-0.101E 00	0.200E 01	0.862E-01	0.313E 03
13	0.348E 00	-0.114E 00	0.200E 01	0.871E-01	0.287E 03
14	0.261E 00	-0.123E 00	0.200E 01	0.882E-01	0.272E 03
15	0.173E 00	-0.129E 00	0.200E 01	0.867E-01	0.265E 03
16	0.867E-01	-0.132E 00	0.200E 01	0.867E-01	0.265E 03
17	0.	-0.133E 00	0.200E 01	0.867E-01	0.265E 03
18	-0.867E-01	-0.132E 00	0.200E 01	0.867E-01	0.265E 03
19	-0.173E 00	-0.129E 00	0.200E 01	0.882E-01	0.272E 03
20	-0.261E 00	-0.123E 00	0.200E 01	0.871E-01	0.287E 03
21	-0.348E 00	-0.114E 00	0.200E 01	0.862E-01	0.313E 03
22	-0.433E 00	-0.101E 00	0.200E 01	0.885E-01	0.350E 03
23	-0.520E 00	-0.835E-01	0.200E 01	0.853E-01	0.445E 03
24	-0.601E 00	-0.576E-01	0.200E 01	0.871E-01	0.631E 03
25	-0.667E 00	0.	0.200E 01	0.871E-01	0.631E 03
26	-0.601E 00	0.576E-01	0.200E 01	0.853E-01	0.445E 03
27	-0.520E 00	0.835E-01	0.200E 01	0.885E-01	0.350E 03
28	-0.433E 00	0.101E 00	0.200E 01	0.862E-01	0.313E 03
29	-0.348E 00	0.114E 00	0.200E 01	0.871E-01	0.287E 03
30	-0.261E 00	0.123E 00	0.200E 01	0.882E-01	0.272E 03
31	-0.173E 00	0.129E 00	0.200E 01	0.867E-01	0.265E 03
32	-0.867E-01	0.132E 00	0.200E 01	0.867E-01	0.265E 03

PERIPHERAL DISTANCE= 0.278E 01 METERS

AVERAGE FIELD INTENSITY= 0.359E 03 AMPERES PER METER

Figure 4.86 Intercept Calculations for Z = 2 m

THE POINTS DEFINING A PLANE ARE

PLANE NUMBER	POINT NUMBER	X	Y	Z
2	1	-0.500E 00	0.	0.400E 01
2	2	0.	0.100E 01	0.400E 01
2	3	0.500E 00	0.	0.400E 01

THAT PLANE INTERCEPTS THE FILAMENTS AS FOLLOWS

CONDUCTOR	X INTER	Y INTER	Z INTER	DELTA S	DELTA H
1	0.	0.167E 00	0.400E 01	0.100E 00	0.212E 03
2	0.108E 00	0.165E 00	0.400E 01	0.108E 00	0.212E 03
3	0.217E 00	0.161E 00	0.400E 01	0.110E 00	0.218E 03
4	0.327E 00	0.153E 00	0.400E 01	0.109E 00	0.230E 03
5	0.435E 00	0.142E 00	0.400E 01	0.108E 00	0.250E 03
6	0.542E 00	0.127E 00	0.400E 01	0.111E 00	0.280E 03
7	0.650E 00	0.104E 00	0.400E 01	0.107E 00	0.356E 03
8	0.752E 00	0.720E-01	0.400E 01	0.109E 00	0.505E 03
9	0.833E 00	0.	0.400E 01	0.109E 00	0.505E 03
10	0.752E 00	-0.720E-01	0.400E 01	0.107E 00	0.356E 03
11	0.650E 00	-0.104E 00	0.400E 01	0.111E 00	0.280E 03
12	0.542E 00	-0.127E 00	0.400E 01	0.108E 00	0.250E 03
13	0.435E 00	-0.142E 00	0.400E 01	0.109E 00	0.230E 03
14	0.327E 00	-0.153E 00	0.400E 01	0.110E 00	0.218E 03
15	0.217E 00	-0.161E 00	0.400E 01	0.108E 00	0.212E 03
16	0.108E 00	-0.165E 00	0.400E 01	0.108E 00	0.212E 03
17	0.	-0.167E 00	0.400E 01	0.108E 00	0.212E 03
18	-0.108E 00	-0.165E 00	0.400E 01	0.108E 00	0.212E 03
19	-0.217E 00	-0.161E 00	0.400E 01	0.110E 00	0.218E 03
20	-0.327E 00	-0.153E 00	0.400E 01	0.109E 00	0.230E 03
21	-0.435E 00	-0.142E 00	0.400E 01	0.108E 00	0.250E 03
22	-0.542E 00	-0.127E 00	0.400E 01	0.111E 00	0.280E 03
23	-0.650E 00	-0.104E 00	0.400E 01	0.107E 00	0.356E 03
24	-0.752E 00	-0.720E-01	0.400E 01	0.109E 00	0.505E 03
25	-0.833E 00	0.	0.400E 01	0.109E 00	0.505E 03
26	-0.752E 00	0.720E-01	0.400E 01	0.107E 00	0.356E 03
27	-0.650E 00	0.104E 00	0.400E 01	0.111E 00	0.280E 03
28	-0.542E 00	0.127E 00	0.400E 01	0.108E 00	0.250E 03
29	-0.435E 00	0.142E 00	0.400E 01	0.109E 00	0.230E 03
30	-0.327E 00	0.153E 00	0.400E 01	0.110E 00	0.218E 03
31	-0.217E 00	0.161E 00	0.400E 01	0.108E 00	0.212E 03
32	-0.108E 00	0.165E 00	0.400E 01	0.108E 00	0.212E 03

PERIPHERAL DISTANCE= 0.348E 01 METERS

AVERAGE FIELD INTENSITY= 0.287E 03 AMPERES PER METER

Figure 4.87 Intercept Calculations for Z = 4 m

 ID3= 1 AND ID4= 1 (Field intensities will be calculated over a volume)
 (Data will be presented in rectangular coordinates)

 ZPA,ZPB AND ZPC ARE 0.200E 01 0.200E 01 0.200E 01
 YPA,YPB AND YPC ARE 0. 0.500E-01 0.250E-01
 XPA,XPB AND XPC ARE 0. 0.300E 00 0.500E-01

X	Y	Z	H-X A/m	H-Y A/m	H-Z A/m
0.	0.	0.200E 01	-0.411E-02	0.128E-01	-0.947E-03
0.	0.	0.200E 01	-0.160E-01	0.363E-01	-0.128E-02
0.	0.250E-01	0.200E 01	-0.312E 01	0.182E-01	-0.130E-02
0.	0.250E-01	0.200E 01	-0.131E 02	0.510E-01	-0.185E-02
0.	0.500E-01	0.200E 01	-0.705E 01	0.237E-01	-0.181E-02
0.	0.500E-01	0.200E 01	-0.273E 02	0.693E-01	-0.268E-02
0.500E-01	0.	0.200E 01	-0.161E-01	-0.347E 01	-0.432E-03
0.500E-01	0.	0.200E 01	-0.455E-01	-0.232E 02	-0.436E-03
0.500E-01	0.250E-01	0.200E 01	-0.283E 01	-0.338E 01	0.275E-01
0.500E-01	0.250E-01	0.200E 01	-0.127E 02	-0.231E 02	0.151E 00
0.500E-01	0.500E-01	0.200E 01	-0.491E 01	-0.277E 01	0.468E-01
0.500E-01	0.500E-01	0.200E 01	-0.244E 02	-0.223E 02	0.290E 00
0.100E 00	0.	0.200E 01	-0.202E-01	-0.721E 01	0.459E-03
0.100E 00	0.	0.200E 01	-0.554E-01	-0.469E 02	0.971E-03
0.100E 00	0.250E-01	0.200E 01	-0.314E 01	-0.733E 01	0.625E-01
0.100E 00	0.250E-01	0.200E 01	-0.132E 02	-0.470E 02	0.312E 00
0.100E 00	0.500E-01	0.200E 01	-0.669E 01	-0.830E 01	0.136E 00
0.100E 00	0.500E-01	0.200E 01	-0.269E 02	-0.484E 02	0.639E 00

Figure 4.88 Field Intensities Over a Volume

(The first line gives the field due
 to the magnetic distribution and
 the second line gives the field due
 to the resistive distribution)

$0.150E\ 00$	$0.$	$0.200E\ 01$	$-0.859E-02$	$-0.109E\ 02$	$0.966E-03$
$0.150E\ 00$	$0.$	$0.200E\ 01$	$-0.291E-01$	$-0.703E\ 02$	$0.163E-02$
$0.150E\ 00$	$0.250E-01$	$0.200E\ 01$	$-0.316E\ 01$	$-0.107E\ 02$	$0.938E-01$
$0.150E\ 00$	$0.250E-01$	$0.200E\ 01$	$-0.131E\ 02$	$-0.701E\ 02$	$0.467E\ 00$
$0.150E\ 00$	$0.500E-01$	$0.200E\ 01$	$-0.644E\ 01$	$-0.936E\ 01$	$0.181E\ 00$
$0.150E\ 00$	$0.500E-01$	$0.200E\ 01$	$-0.263E\ 02$	$-0.683E\ 02$	$0.923E\ 00$
$0.200E\ 00$	$0.$	$0.200E\ 01$	$0.641E-03$	$-0.148E\ 02$	$0.100E-02$
$0.200E\ 00$	$0.$	$0.200E\ 01$	$-0.505E-02$	$-0.942E\ 02$	$0.151E-02$
$0.200E\ 00$	$0.250E-01$	$0.200E\ 01$	$-0.287E\ 01$	$-0.150E\ 02$	$0.120E\ 00$
$0.200E\ 00$	$0.250E-01$	$0.200E\ 01$	$-0.128E\ 02$	$-0.943E\ 02$	$0.615E\ 00$
$0.200E\ 00$	$0.500E-01$	$0.200E\ 01$	$-0.481E\ 01$	$-0.163E\ 02$	$0.223E\ 00$
$0.200E\ 00$	$0.500E-01$	$0.200E\ 01$	$-0.243E\ 02$	$-0.961E\ 02$	$0.121E\ 01$
$0.250E\ 00$	$0.$	$0.200E\ 01$	$0.391E-02$	$-0.190E\ 02$	$0.886E-03$
$0.250E\ 00$	$0.$	$0.200E\ 01$	$0.462E-02$	$-0.118E\ 03$	$0.122E-02$
$0.250E\ 00$	$0.250E-01$	$0.200E\ 01$	$-0.394E\ 01$	$-0.187E\ 02$	$0.183E\ 00$
$0.250E\ 00$	$0.250E-01$	$0.200E\ 01$	$-0.142E\ 02$	$-0.118E\ 03$	$0.813E\ 00$
$0.250E\ 00$	$0.500E-01$	$0.200E\ 01$	$-0.952E\ 01$	$-0.172E\ 02$	$0.406E\ 00$
$0.250E\ 00$	$0.500E-01$	$0.200E\ 01$	$-0.304E\ 02$	$-0.116E\ 03$	$0.167E\ 01$
$0.300E\ 00$	$0.$	$0.200E\ 01$	$0.418E-02$	$-0.244E\ 02$	$0.764E-03$
$0.300E\ 00$	$0.$	$0.200E\ 01$	$0.690E-02$	$-0.144E\ 03$	$0.988E-03$
$0.300E\ 00$	$0.250E-01$	$0.200E\ 01$	$-0.372E\ 01$	$-0.241E\ 02$	$0.216E\ 00$
$0.300E\ 00$	$0.250E-01$	$0.200E\ 01$	$-0.140E\ 02$	$-0.144E\ 03$	$0.978E\ 00$
$0.300E\ 00$	$0.500E-01$	$0.200E\ 01$	$-0.466E\ 01$	$-0.232E\ 02$	$0.321E\ 00$
$0.300E\ 00$	$0.500E-01$	$0.200E\ 01$	$-0.247E\ 02$	$-0.143E\ 03$	$0.182E\ 01$

Figure 4.89 Field Intensities Over a Volume (Conclusion)

D5= 1 AND D6= 1 (Calculations will be made at discrete points)
(Data will be given in rectangular coordinates)

CALCULATIONS WILL BE MADE AT 11 POINTS

X	Y	Z	H-X	H-Y	H-Z
			A/m	A/m	A/m
0.	0.	0.200E 01	-0.411E-02	0.128E-01	-0.947E-03
0.	0.	0.200E 01	-0.160E-01	0.363E-01	-0.128E-02
0.	0.300E 01	0.200E 01	0.698E 02	-0.137E-04	0.317E-05
0.	0.300E 01	0.200E 01	0.703E 02	-0.570E-05	-0.537E-06
0.200E 00	0.	0.200E 01	0.641E-03	-0.148E 02	0.100E-02
0.200E 00	0.	0.200E 01	-0.505E-02	-0.942E 02	0.151E-02
0.200E 00	0.300E 00	0.200E 01	0.465E 03	-0.657E 02	-0.916E 01
0.200E 00	0.300E 00	0.200E 01	0.527E 03	-0.115E 03	-0.885E 01
0.400E 00	0.300E 00	0.200E 01	0.465E 03	-0.159E 03	-0.173E 02
0.400E 00	0.300E 00	0.200E 01	0.477E 03	-0.234E 03	-0.151E 02
0.800E 00	0.300E 00	0.200E 01	0.256E 03	-0.342E 03	-0.128E 02
0.800E 00	0.300E 00	0.200E 01	0.219E 03	-0.346E 03	-0.896E 01
0.800E 00	0.	0.200E 01	0.130E-02	-0.644E 03	0.227E-03
0.800E 00	0.	0.200E 01	0.168E-02	-0.554E 03	0.314E-03
0.	0.100E 01	0.200E 01	0.249E 03	-0.371E-03	0.171E-04
0.	0.100E 01	0.200E 01	0.260E 03	-0.254E-03	-0.818E-05
0.400E 00	0.100E 01	0.200E 01	0.231E 03	-0.670E 02	-0.317E 01
0.400E 00	0.100E 01	0.200E 01	0.237E 03	-0.745E 06	-0.251E 01
0.100E 01	0.100E 01	0.200E 01	0.153E 03	-0.123E 03	-0.370E 01
0.100E 01	0.100E 01	0.200E 01	0.150E 03	-0.128E 03	-0.280E 01
0.100E 01	0.	0.200E 01	0.861E-03	-0.390E 03	0.168E-03
0.100E 01	0.	0.200E 01	0.104E-02	-0.363E 03	0.243E-03

Figure 4.90 Field Intensities at Discrete Points

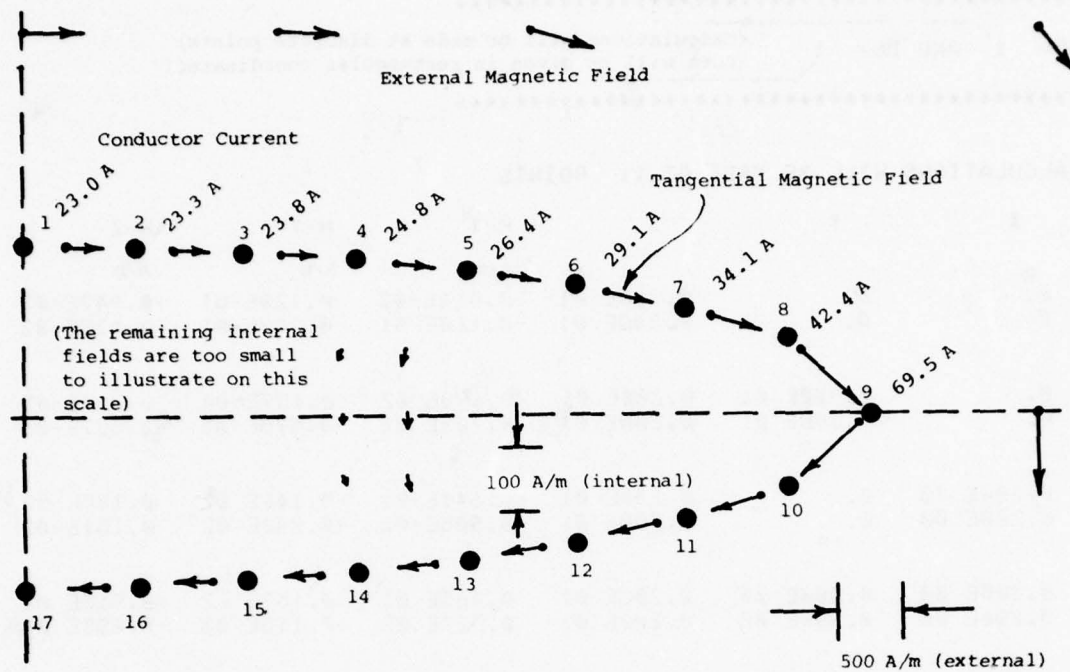


Figure 4.91 Field Patterns as Determined by Magnetic Distribution of Current

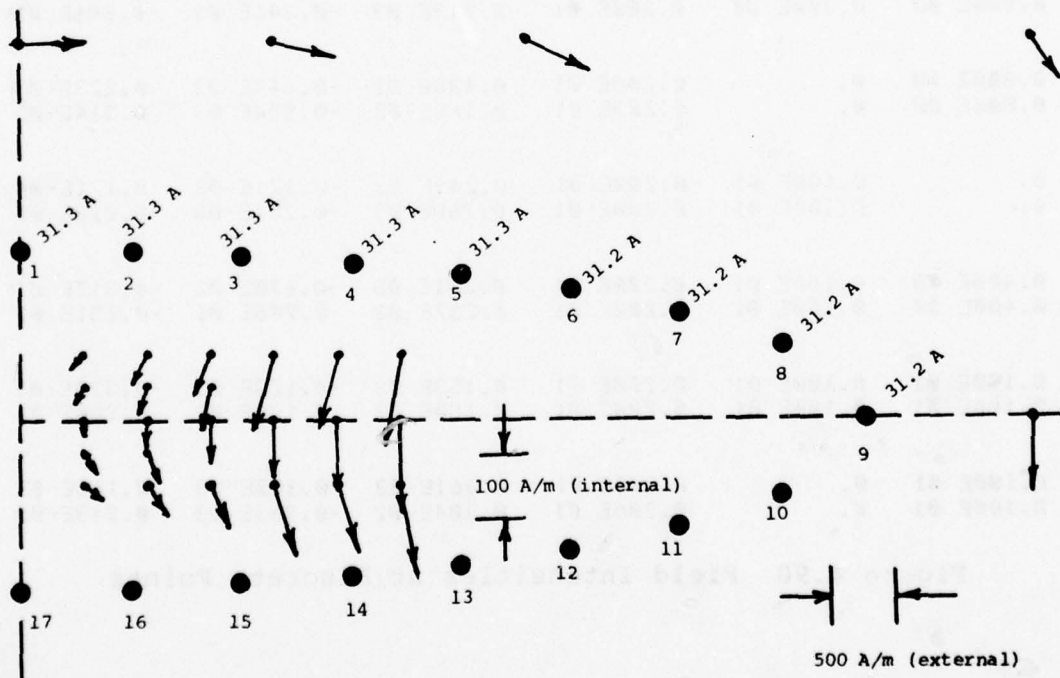


Figure 4.92 Field Patterns as Determined by Resistive Distribution of Current

D7 IS 1 (Calculations will be made of total
 flux passing through a loop)

THERE WILL BE CALCULATIONS MADE FOR 2 LOOPS

LOOP	POINT	X	Y	Z
1	1	0.	0.	0.200E 01
1	2	0.	0.	0.400E 01
1	3	0.200E 00	0.	0.400E 01
1	4	0.200E 00	0.	0.200E 01

LOOP AREA= 0.400E 00 SQUARE METERS

LOOP NUMBER 1 MAGNETIC DISTRIBUTION
TOTAL FLUX= -0.292E-05 WEBERS

LOOP NUMBER 1 RESISTIVE DISTRIBUTION
TOTAL FLUX= -0.188E-04 WEBERS

LOOP	POINT	X	Y	Z
2	1	0.200E 00	0.	0.200E 01
2	2	0.200E 00	0.500E-01	0.200E 01
2	3	0.200E 00	0.500E-01	0.400E 01
2	4	0.200E 00	0.	0.400E 01

LOOP AREA= 0.100E 00 SQUARE METERS

LOOP NUMBER 2 MAGNETIC DISTRIBUTION
TOTAL FLUX= -0.324E-06 WEBERS

LOOP NUMBER 2 RESISTIVE DISTRIBUTION
TOTAL FLUX= -0.133E-05 WEBERS

Figure 4.93 Loop Calculations

 ID3= 1 AND ID4= 2 (Data will be presented
 in polar coordinates)

ZPA,ZPB AND ZPC ARE 0.200E 01 0.200E 01 0.200E 01
 YPA,YPB AND YPC ARE 0. 0.500E-01 0.250E-01
 XPA,XPB AND XPC ARE 0. 0.300E 00 0.500E-01

X	Y	Z	H-TOT (A/m)	LAT-ANG (Degrees)	LONG ANG (Degrees)
0.	0.	0.200E 01	0.505E-04	0.160E 03	0.180E 03
0.	0.	0.200E 01	0.769E-05	0.297E 02	0.137E-06
0.	0.250E-01	0.200E 01	0.312E 01	0.900E 02	0.180E 03
0.	0.250E-01	0.200E 01	0.131E 02	0.900E 02	0.180E 03
0.	0.500E-01	0.200E 01	0.705E 01	0.900E 02	0.180E 03
0.	0.500E-01	0.200E 01	0.273E 02	0.900E 02	0.180E 03
0.500E-01	0.	0.200E 01	0.348E 01	0.180E 03	0.180E 03
0.500E-01	0.	0.200E 01	0.233E 02	0.180E 03	0.261E 00
0.500E-01	0.250E-01	0.200E 01	0.441E 01	0.140E 03	0.179E 03
0.500E-01	0.250E-01	0.200E 01	0.264E 02	0.151E 03	0.179E 03
0.500E-01	0.500E-01	0.200E 01	0.563E 01	0.120E 03	0.179E 03
0.500E-01	0.500E-01	0.200E 01	0.330E 02	0.133E 03	0.179E 03
0.100E 00	0.	0.200E 01	0.720E 01	0.180E 03	0.179E 03
0.100E 00	0.	0.200E 01	0.469E 02	0.180E 03	0.560E 00
0.100E 00	0.250E-01	0.200E 01	0.795E 01	0.157E 03	0.179E 03
0.100E 00	0.250E-01	0.200E 01	0.488E 02	0.164E 03	0.179E 03
0.100E 00	0.500E-01	0.200E 01	0.106E 02	0.141E 03	0.179E 03
0.100E 00	0.500E-01	0.200E 01	0.552E 02	0.151E 03	0.179E 03

Figure 4.94 Data Format When Field Intensity is Resolved Into Polar Coordinates

$0.150E\ 00$	$0.$	$0.200E\ 01$	$0.108E\ 02$	$0.180E\ 03$	$0.179E\ 03$
$0.150E\ 00$	$0.$	$0.200E\ 01$	$0.703E\ 02$	$0.180E\ 03$	$0.450E\ 02$
$0.150E\ 00$	$0.250E-01$	$0.200E\ 01$	$0.111E\ 02$	$0.164E\ 03$	$0.178E\ 03$
$0.150E\ 00$	$0.250E-01$	$0.200E\ 01$	$0.713E\ 02$	$0.169E\ 03$	$0.178E\ 03$
$0.150E\ 00$	$0.500E-01$	$0.200E\ 01$	$0.113E\ 02$	$0.145E\ 03$	$0.178E\ 03$
$0.150E\ 00$	$0.500E-01$	$0.200E\ 01$	$0.732E\ 02$	$0.159E\ 03$	$0.178E\ 03$
$0.200E\ 00$	$0.$	$0.200E\ 01$	$0.148E\ 02$	$0.180E\ 03$	$0.178E\ 03$
$0.200E\ 00$	$0.$	$0.200E\ 01$	$0.941E\ 02$	$0.180E\ 03$	$0.708E\ 00$
$0.200E\ 00$	$0.250E-01$	$0.200E\ 01$	$0.152E\ 02$	$0.169E\ 03$	$0.178E\ 03$
$0.200E\ 00$	$0.250E-01$	$0.200E\ 01$	$0.952E\ 02$	$0.172E\ 03$	$0.177E\ 03$
$0.200E\ 00$	$0.500E-01$	$0.200E\ 01$	$0.170E\ 02$	$0.163E\ 03$	$0.177E\ 03$
$0.200E\ 00$	$0.500E-01$	$0.200E\ 01$	$0.991E\ 02$	$0.166E\ 03$	$0.177E\ 03$
$0.250E\ 00$	$0.$	$0.200E\ 01$	$0.190E\ 02$	$0.180E\ 03$	$0.178E\ 03$
$0.250E\ 00$	$0.$	$0.200E\ 01$	$0.118E\ 03$	$0.180E\ 03$	$0.278E\ 01$
$0.250E\ 00$	$0.250E-01$	$0.200E\ 01$	$0.191E\ 02$	$0.168E\ 03$	$0.177E\ 03$
$0.250E\ 00$	$0.250E-01$	$0.200E\ 01$	$0.119E\ 03$	$0.173E\ 03$	$0.177E\ 03$
$0.250E\ 00$	$0.500E-01$	$0.200E\ 01$	$0.196E\ 02$	$0.151E\ 03$	$0.178E\ 03$
$0.250E\ 00$	$0.500E-01$	$0.200E\ 01$	$0.120E\ 03$	$0.165E\ 03$	$0.177E\ 03$
$0.300E\ 00$	$0.$	$0.200E\ 01$	$0.244E\ 02$	$0.180E\ 03$	$0.178E\ 03$
$0.300E\ 00$	$0.$	$0.200E\ 01$	$0.144E\ 03$	$0.180E\ 03$	$0.191E\ 02$
$0.300E\ 00$	$0.250E-01$	$0.200E\ 01$	$0.244E\ 02$	$0.171E\ 03$	$0.177E\ 03$
$0.300E\ 00$	$0.250E-01$	$0.200E\ 01$	$0.145E\ 03$	$0.174E\ 03$	$0.176E\ 03$
$0.300E\ 00$	$0.500E-01$	$0.200E\ 01$	$0.237E\ 02$	$0.169E\ 03$	$0.176E\ 03$
$0.300E\ 00$	$0.500E-01$	$0.200E\ 01$	$0.145E\ 03$	$0.170E\ 03$	$0.176E\ 03$

Figure 4.95 Data Format When Field Intensity is Resolved Into Polar Coordinates (Conclusion)

 ID3= 1 AND ID4= 3 (Initial and final magnitudes
 will be presented)

ZPA,ZPB AND ZPC ARE 0.200E 01 0.200E 01 0.200E 01
 YPA,YPB AND YPC ARE 0. 0.500E-01 0.250E-01
 XPA,XPB AND XPC ARE 0. 0.300E 00 0.500E-01

X	Y	Z	H-MAGNETIC	H-RESISTIVE
			A/m	A/m
0.	0.	0.200E 01	0.505E-04	0.769E-05
0.	0.250E-01	0.200E 01	0.312E 01	0.131E 02
0.	0.500E-01	0.200E 01	0.705E 01	0.273E 02
0.500E-01	0.	0.200E 01	0.348E 01	0.233E 02
0.500E-01	0.250E-01	0.200E 01	0.441E 01	0.264E 02
0.500E-01	0.500E-01	0.200E 01	0.563E 01	0.330E 02
0.100E 00	0.	0.200E 01	0.720E 01	0.469E 02
0.100E 00	0.250E-01	0.200E 01	0.795E 01	0.488E 02
0.100E 00	0.500E-01	0.200E 01	0.106E 02	0.552E 02
0.150E 00	0.	0.200E 01	0.108E 02	0.703E 02
0.150E 00	0.250E-01	0.200E 01	0.111E 02	0.713E 02
0.150E 00	0.500E-01	0.200E 01	0.113E 02	0.732E 02
0.200E 00	0.	0.200E 01	0.148E 02	0.941E 02
0.200E 00	0.250E-01	0.200E 01	0.152E 02	0.952E 02
0.200E 00	0.500E-01	0.200E 01	0.170E 02	0.991E 02

Figure 4.96 Data Format When Only Initial and Final Magnitudes
 of Field Intensity are Presented
 (Data for X = 0.25 and X = 0.30 not shown)

D5= 1 AND D6= 3 (Initial and final magnitudes
will be presented)

CALCULATIONS WILL BE MADE AT 11 POINTS

X	Y	Z	H-MAGNETIC	H-RESISTIVE
0.	0.	0.200E 01	0.505E-04	0.668E-05
0.	0.300E 01	0.200E 01	0.698E 02	0.589E-07
0.200E 00	0.	0.200E 01	0.148E 02	0.941E 02
0.200E 00	0.300E 00	0.200E 01	0.470E 03	0.116E 03
0.400E 00	0.300E 00	0.200E 01	0.492E 03	0.234E 03
0.800E 00	0.300E 00	0.200E 01	0.428E 03	0.346E 03
0.800E 00	0.	0.200E 01	0.644E 03	0.554E 03
0.	0.100E 01	0.200E 01	0.249E 03	0.224E-06
0.400E 00	0.100E 01	0.200E 01	0.240E 03	0.746E 02
0.100E 01	0.100E 01	0.200E 01	0.196E 03	0.128E 03
0.100E 01	0.	0.200E 01	0.390E 03	0.363E 03

Figure 4.97 Data Format When Only Initial and Final Magnitudes
of Field Intensity are Presented

4.7.3 How to Use the Data

Like most computer-generated data, the data generated by DIFFMAG requires a certain amount of interpretation to be of use. The amount of interpretation depends upon what one wishes to do with the data. Broadly speaking, there are three things one might wish to do with DIFFMAG: (1) determine the magnetic field within the structure, (2) determine the voltage between a conductor and ground, and (3) determine the voltage between two conductors.

4.7.3.1 Magnetic Field Within the Structure

As explained earlier, the magnetic fields within the structure start at zero amplitude and build up to some final value determined by the resistive current distribution. The magnitude of that final field is given by the data of which Figures 4.88, 4.89, 4.90, 4.94, 4.95, 4.96 and 4.97 are examples. The rate at which the field builds up to that value must be determined by the user. As explained in earlier sections, the fields build up to their final value in an approximately exponential manner with a time constant that is called the redistribution time constant. That redistribution time constant was earlier (Equation 4.39) shown to be

$$\tau = \frac{\mu Aa}{\rho P} \quad (4.184)$$

where

A = enclosed area of structure

P = peripheral distance around structure

a = skin thickness

μ = permeability

ρ = resistivity of the material

DIFFMAG, in the routine that calculates the points of interception of the conductors with a plane, determines the peripheral distance along that path. It also supplies the coordinates of the intersection points from which the user can plot the points of intersection and then, perhaps by graphical means, calculate the enclosed area. As an example, the structure shown in Figure 4.75 has, at $Z = 2$ m, an enclosed area of 0.279 m^2 and a peripheral distance of 2.78 m. If we were to assume that the structure, of which Figure 4.75 is an outline, was made from aluminum of conductivity $2.69 \times 10^{-8} \Omega \cdot \text{m}$ and had a thickness of 0.050 in. (1.27×10^{-3}), the redistribution time constant would be

$$\tau = \frac{4\pi \times 10^{-7} \times .279 \times 1.27 \times 10^{-3}}{2.69 \times 10^{-8} \times 2.78} = 5.954 \times 10^{-3} \text{ sec} \quad (4.185)$$

4.7.3.2 Voltage to Ground on Conductors

The initial build-up of flux does not follow an exponential path. Instead, it follows a path governed by the pulse-penetration time constant given by Equation 4.37. When one discusses the initial rate of increase of the flux, one is generally concerned with the voltage that the changing flux can induce in conductors, and it is more fruitful to discuss the rate of change of magnetic flux than it is to discuss the magnetic flux itself. Indeed, when discussing voltages on conductors, it is possible to skirt almost completely the issue of magnetic flux and confine one's attention to the surface current density calculated by the routine that gives the output of the type shown in Figures 4.86 and 4.91.

To illustrate this point further, consider Figure 4.98, which shows a cylinder of elliptical cross section and parallel sides. For purposes of illustration, assume the major and minor axes to be 1.33 m and 0.266 m, the dimensions of the flared elliptical cylinder (Figure 4.75) at $Z = 2$ m. In this cylinder there are located two conductors: Conductor 1, immediately adjacent to the inner wall at the narrow edge of the cylinder, and Conductor 2, towards, but not at, the center. Each of the conductors is connected to the end of the cylinder. If we are concerned with the voltage between the conductors and the other end of the cylinder, that voltage is governed by the current density in the cylinder wall adjacent to the conductor. For Conductor 1, the relevant current density is that along Path A. The total voltage from Conductor 1 to the wall then would be

$$V = \int_0^l j \frac{\rho}{a} dx \quad (4.186)$$

where

j = current density

ρ = resistivity

l = length

a = thickness

Since the structure shown in Figure 4.98 is of uniform cross section, the current density will be uniform over the length. Under those conditions, the voltage would be

$$V_{1-gnd} = \frac{j \rho l}{a} \quad (4.187)$$

As a numeric example, again assume the conductivity to be $2.69 \times 10^{-8} \Omega \cdot m$, the thickness $1.27 \times 10^{-3} m$, and the length 6 m. Also assume the current density along path A to be 631 A/m, the value shown in Figure 4.86 as the average current density between conductors 8 and 9. The voltage on Conductor 1 would then be

$$v_{1-g} = \frac{2.69 \times 10^{-8} \times 631 \times 6}{1.27 \times 10^{-3}} = 8.02 \times 10^{-2} \text{ volts} \quad (4.188)$$

The voltage on Conductor 2 can be looked at from two view points.

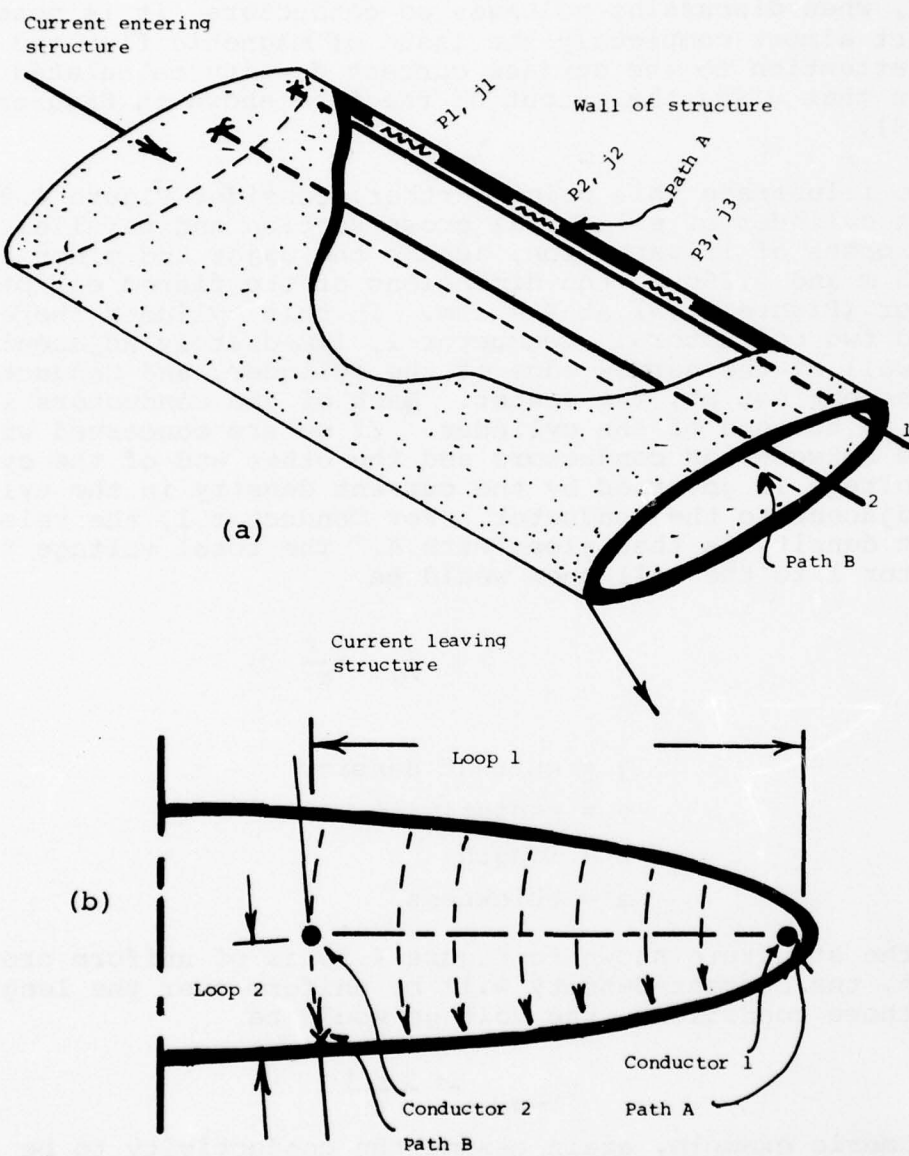


Figure 4.98 Structure with Parallel Geometry
 (a) Isometric View
 (b) End View

First Viewpoint. The voltage on Conductor 2 can be regarded as the sum of the resistive component of voltage along Path A minus the voltage induced by the changing magnetic flux that passes between Conductor 1 and Path A. That loop is designated Loop 1 in Figure 4.98. This is the most difficult way to look at the problem, since it is not clear from the analyses how that magnetic flux changes with time.

Second Viewpoint. The voltage on Conductor 2 may also be viewed as the resistive drop along Path B minus the magnetically induced voltage in Loop 2 between Conductor 2 and Path B. The question, though, is "where is Path B?" The answer is that Path B is that path which orients Loop 2 along the direction taken by the magnetic flux lines in such a manner that no net magnetic flux passes through Loop 2. The orientation of the lines of magnetic flux is given by DIFFMAG, either in the routine where the flux density is calculated over a volume or the routine where it is calculated at discrete points. Fitting the orientation of Loop 2 is seldom critical; an eyeball fit is generally adequate. As a practical matter, Path B can be taken along the path that is physically closest to Conductor 1. The current density along that path would be about 270 A/m. Accordingly, the voltage on Conductor 2 would then be about 3.43×10^{-2} V.

The final current density would be uniform over the structure and have a magnitude of 359 A/m, as indicated by the last line in Figure 4.86. The final voltage on both conductors would then be 4.56×10^{-2} V.

4.7.3.3 Voltage Waveshape

The waveshapes of the voltages between the conductors and ground will be the same as the waveshapes of the current densities along the appropriate paths: Path A for Conductor 1 and Path B for Conductor 2. Since along Path A the current density will decrease from its initial value to its final value, it follows that the voltage on Conductor 1 will also decrease from an initial to a final value. The current density and, hence, voltage will rise to its initial value with the characteristic waveshape shown in Figure 4.26. On Conductor 2, the initial value will be somewhat less than the final value, but the rise to the initial value and the decay to the final value will be governed by the same time constants that characterize the voltage on Conductor 1.

The pulse penetration time constant was earlier given (Equation 4.37) as

$$\tau = \frac{ua^2}{\pi^2 \rho} \quad (4.189)$$

For aluminum of 0.050 in. thickness, the pulse-penetration time constant would be $\tau = 7.73 \times 10^{-6} = 7.63 \mu\text{s}$. The waveshapes of the voltage to ground would then be as shown in Figure 4.99.

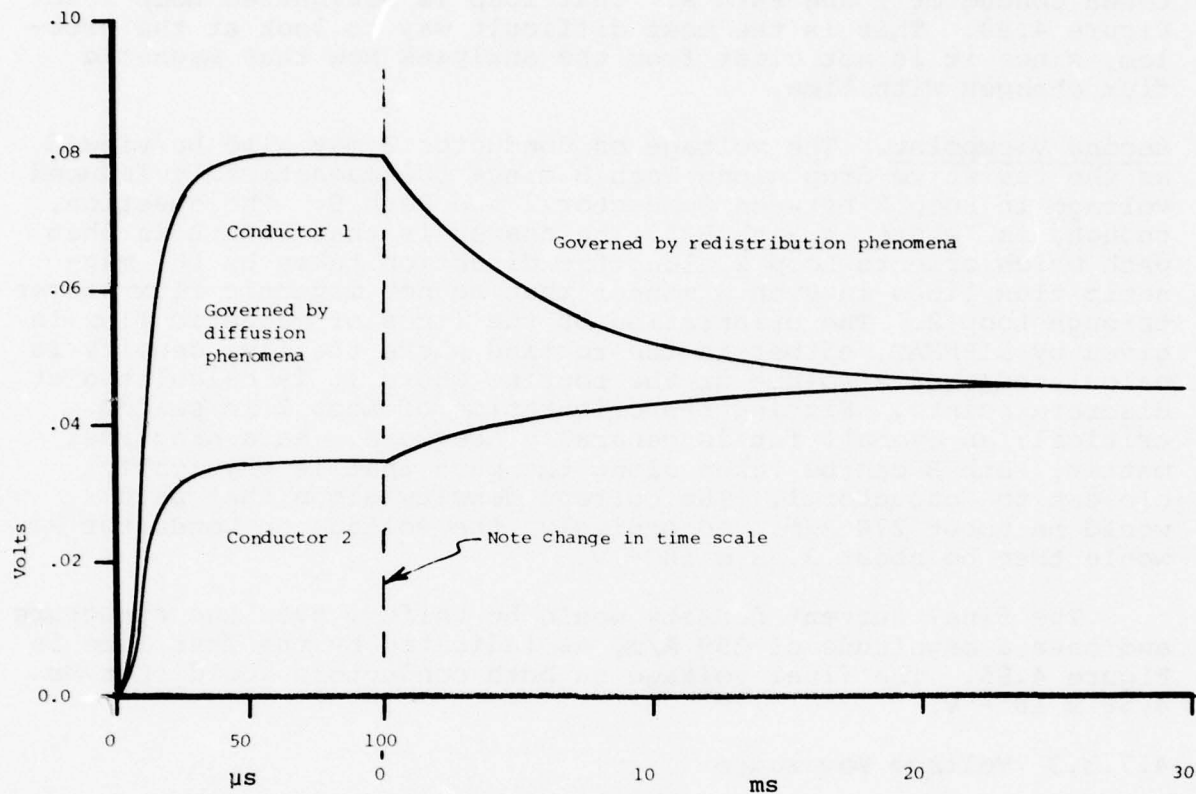


Figure 4.99 Waveshapes of Voltages to Ground

The voltage between conductors is the difference in the voltages between the two conductors and ground. Its waveshape is shown in Figure 4.100. The voltage between conductors, of course, eventually falls to zero, unlike the voltage from either conductor to ground.

4.7.4 Waveshape of Magnetic Field

Since the voltage between conductors responds to the derivative of the magnetic flux passing through the loop between the two conductors, it follows that the waveshape of the magnetic flux would be proportional to the integral of the voltage given in Figure 4.100. The integral of voltage is shown in Figure 4.101.

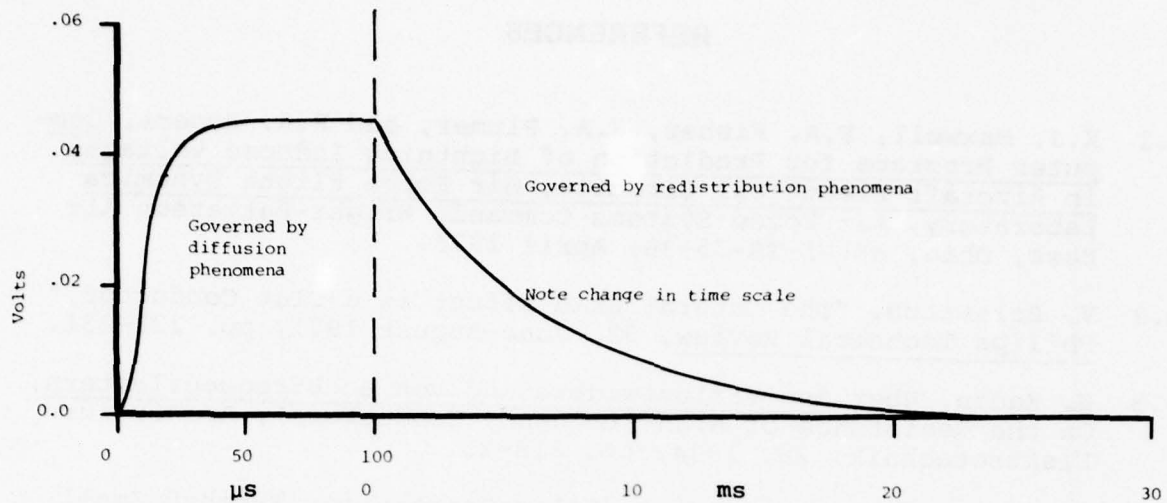
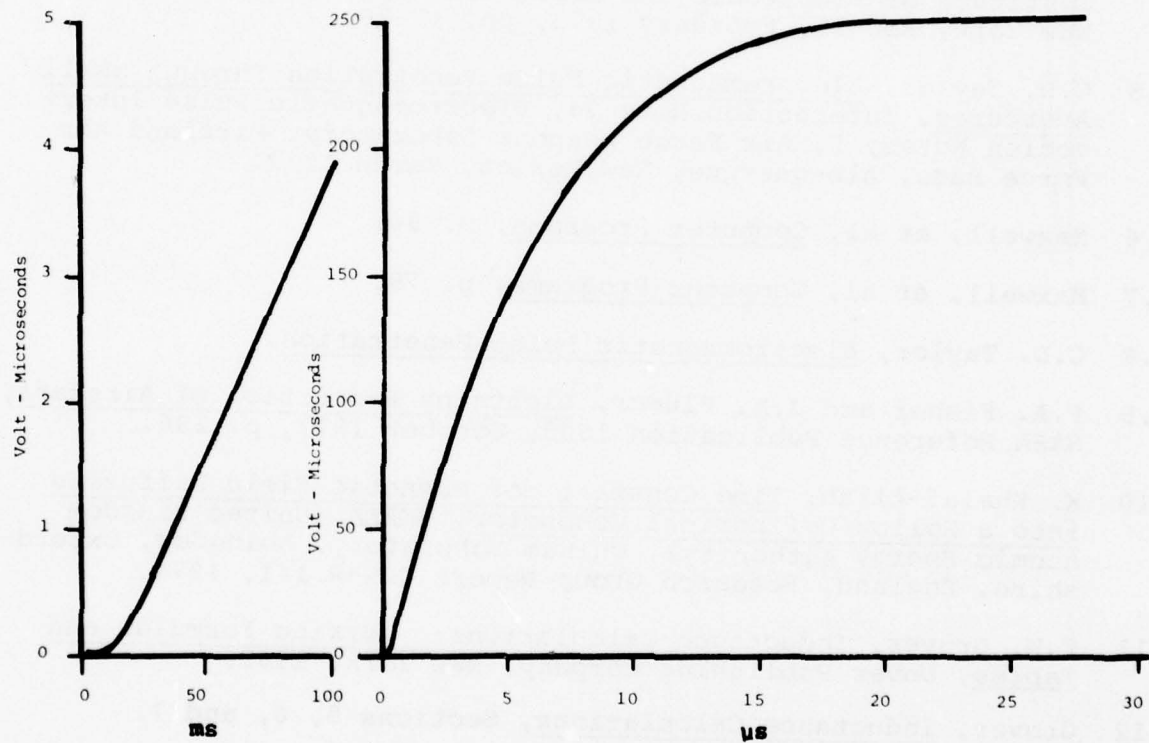


Figure 4.100 Waveshape of Voltage Between Conductors



**Figure 4.101 Integral of Voltage Between Conductors
(Hence waveshape of magnetic field)**

REFERENCES

- 4.1 K.J. Maxwell, F.A. Fisher, J.A. Plumer, and P.R. Rogers, Computer Programs for Prediction of Lightning Induced Voltages in Aircraft Electrical Circuits, Air Force Flight Dynamics Laboratory, Air Force Systems Command, Wright-Patterson Air Base, Ohio, AFFDL-TR-75-36; April 1975.
- 4.2 V. Belevitch, "The Lateral Skin Effect in a Flat Conductor," Philips Technical Review, 32, June-August 1971, pp. 221-231.
- 4.3 H. Kaden, Über den Verlustwiderstand von Hochfrequenzleitern, On the Resistance of High-Frequency Conductors), Archiv für Elektrotechnik, 28, 1934, pp. 818-25.
- 4.4 C.D. Taylor, Electromagnetic Pulse Penetration Through Small Apertures, IEEE Transactions on Electromagnetic Capability, 1, Institute of Electronic and Electrical Engineers, New York, New York, EMC-15, February 1973, pp. 17-26.
- 4.5 C.D. Taylor, Electromagnetic Pulse Penetration Through Small Apertures, Interaction Note 74, Electromagnetic Pulse Interaction Notes, 5, Air Force Weapons Laboratory, Kirtland Air Force Base, Albuquerque, New Mexico, March 1973.
- 4.6 Maxwell, et al, Computer Programs, p. 84.
- 4.7 Maxwell, et al, Computer Programs, p. 79.
- 4.8 C.D. Taylor, Electromagnetic Pulse Penetration.
- 4.9 F.A. Fisher and J.A. Plumer, Lightning Protection of Aircraft, NASA Reference Publication 1008, October 1977, p. 296.
- 4.10 K. Khalaf-Allah, Time Constant for Magnetic Field Diffusion into a Hollow Cylindrical Conductor, UKAEA (United Kingdom Atomic Energy Authority), Culham Laboratory, Abingdon, Oxfordshire, England, Research Group Report CLM-R 141, 1974.
- 4.11 F.W. Grover, Inductance Calculations: Working Formulas and Tables, Dover Publishing Company, New York, 1962.
- 4.12 Grover, Inductance Calculations, Sections 5, 6, and 7.
- 4.13 J.B. Scarborough, Numerical Mathematical Analysis (4th Ed.), Johns Hopkins Press, Baltimore, 1958, p. 133.

SECTION V

THE INFLUENCE OF COMPOSITE MATERIALS ON DIFFUSION EFFECTS

5.1 INTRODUCTION

The analyses presented in Section 4 of diffusion effects in metal structures apply equally as well to the usual composite materials, if allowance is made for their much higher resistivity. Of the normal composite materials, the one with the lowest resistivity is graphite, and its resistivity is on the order of 3000 times higher than that of aluminum. As a result, the pulse-penetration time and redistribution time of a structure composed of graphite would be about 3000 times faster than that of an aluminum structure of the same dimensions. To a large extent, one can say that the retarding effects on waveshape produced by the diffusion process in an aluminum structure would reduce to calculating the corresponding dc resistance voltages or to calculating the final distribution of magnetic field. If one were dealing with a boron structure, dc resistances would be much higher yet, and if one were dealing with some type of fiber-glass structure, the calculations would not apply. The question, "What is the effect of composite materials on lightning electromagnetic compatibility?" can be answered in a summary form by stating that, in an aircraft making extensive use of composite materials, the protection previously given by the structural skin is no longer available. The lightning-electromagnetic compatibility problems must now be solved without the benefit of the aircraft metallic skin. Systems engineers will have to provide their own shielding against electromagnetic fields or else they will have to be prepared to deal with much higher currents and voltages on their circuits than they are used to dealing with. The cost of providing that shielding or protection, either in weight or in development costs, will be more highly visible than in the past, and program managers should not be taken unaware by those higher costs.

5.2 EXPERIMENTAL STUDIES ON COMPOSITE MATERIALS

There were no experimental studies of composite materials in this program, since the subject has been studied by others, particularly Straw and Piszker (Reference 5.1). The data which they present that are most descriptive of the comparison between composite materials and metals are the data they took, in a quadraxial test fixture, of the surface transfer impedance of graphite samples. In a quadraxial test fixture, current is circulated through a cylinder, and the voltage drop produced along the inner surface of that cylinder is measured.

The quadraxial test fixture that they used is shown in Figure 5.1. The outermost electrode is basically a ground electrode. In service, current is injected into the drive cylinder from a generator (oscillator and amplifier) and is returned to the

generator through two paths in parallel, the outer cylinder and on the cylinder under test. A transformer is used to measure the current in the cylinder under test. A sensing electrode, inside the cylinder under test, measures the internal voltage drop. The various tapered transition sections and termination resistors serve to prevent internal resonances. The geometry of the cylinder under test will be recognized as basically that described in Section 4.5.1.

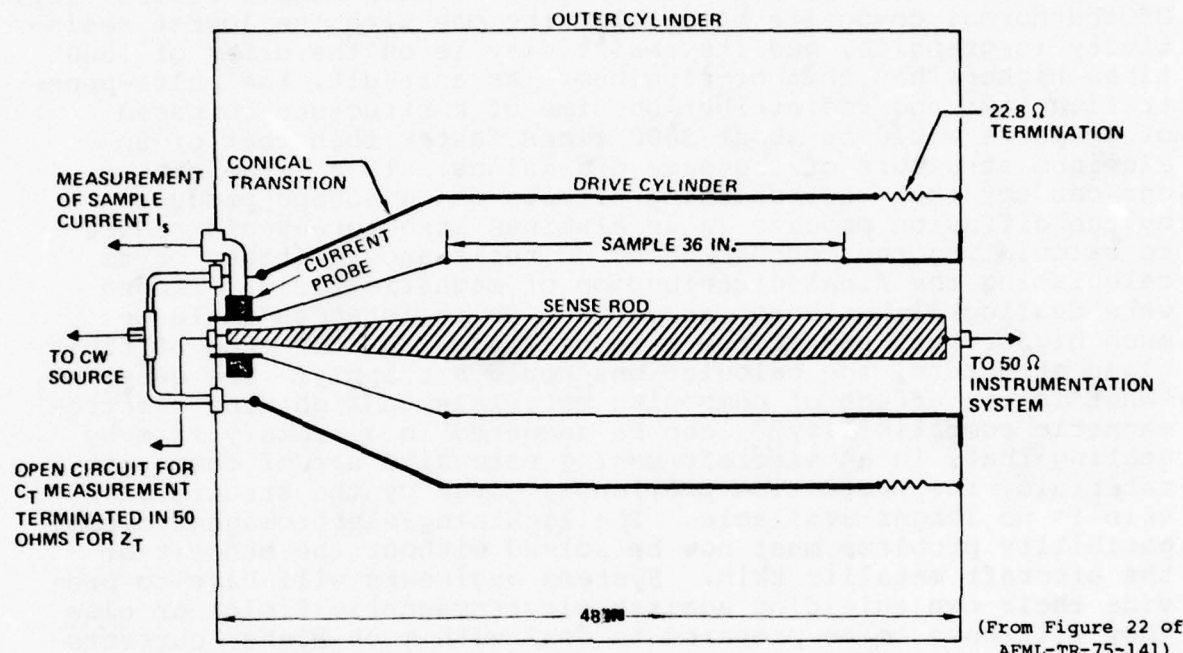
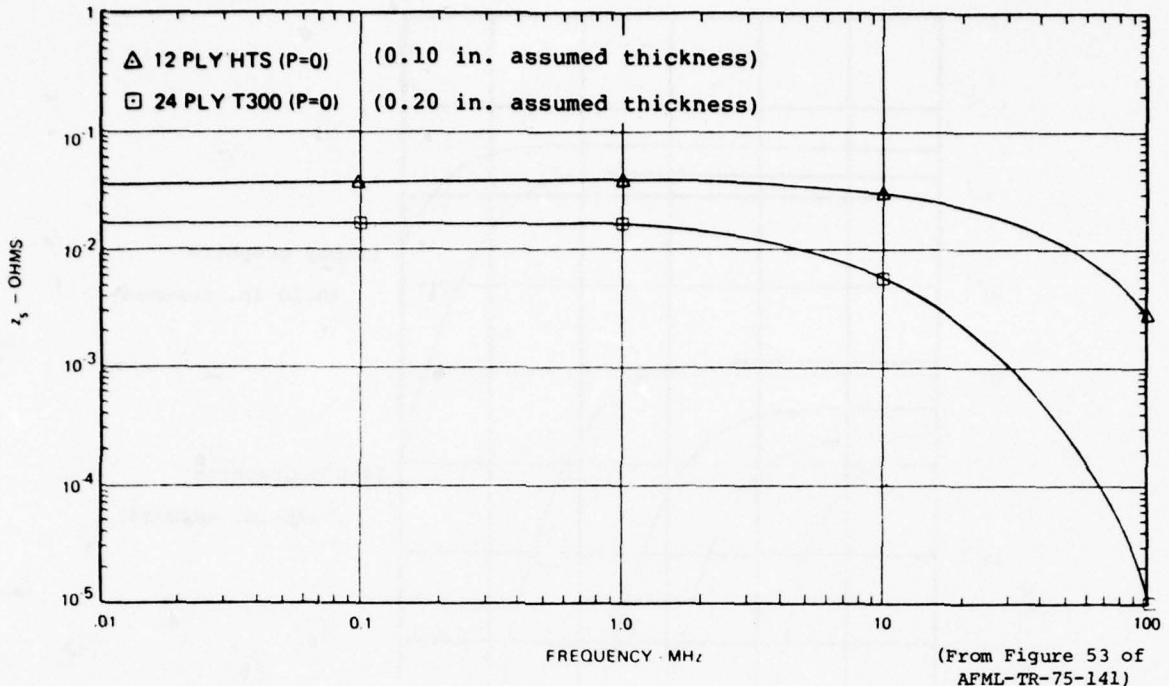


Figure 5.1 Schematic of Quadraxial Test Fixture

The test specimens that they used were cylinders of graphite-epoxy material, 36 in. long and 6 in. in diameter. Cylinders of two different thicknesses were used; one composed of 12 plies of graphite-epoxy and one composed of 24 plies. The authors do not mention in their report what the thickness of the walls were, but one might assume that they were about 0.1 and 0.2 in., respectively.

Figure 5.2 shows the measured transfer impedances as a function of frequency. It can be seen that over a broad frequency range the transfer impedance is equal to the dc resistance. That dc resistance for the 24-ply sample is 0.017Ω or $4.72 \times 10^{-4} \Omega / \text{in.}$

These measured transfer impedances of graphite are compared, in Figure 5.3, to the calculated transfer impedances of aluminum having the same, or thinner, thicknesses. It can be seen that the transfer impedance of the graphite is several orders of magnitude higher than that of aluminum, and, furthermore, the transfer



(From Figure 53 of
AFML-TR-75-141)

Figure 5.2 Measured Surface Transfer Impedance of 12-Ply HTS and 24-Ply T300 Graphite (6 in. diameter cylinder, 36 in. long)

impedance stays equal to its dc value for several more decades of frequency.

In another section (page 102) of the Reference 5.1 report, mention is made of another sample of 24-ply material for which the resistance was $9.08 \times 10^{-4} \Omega/\text{in}$. Possibly, the discrepancy was due to joint effects. If we assume the cylinder dimensions to be 6 in. in diameter, 0.2 in. wall thickness, and the resistance to be $9.08 \times 10^{-4} \Omega/\text{in}$., the material resistivity is then seen to be $8.7 \times 10^{-5} \Omega\text{-m}$. This follows from the equation for resistance of a cylinder:

$$R = \frac{\ell \rho}{2\pi a t} \quad (5.1)$$

where

- ℓ = length
- a = radius
- t = thickness
- ρ = resistivity

This resistivity is about 3200 times that of aluminum, $2.69 \times 10^{-8} \Omega\text{-m}$.

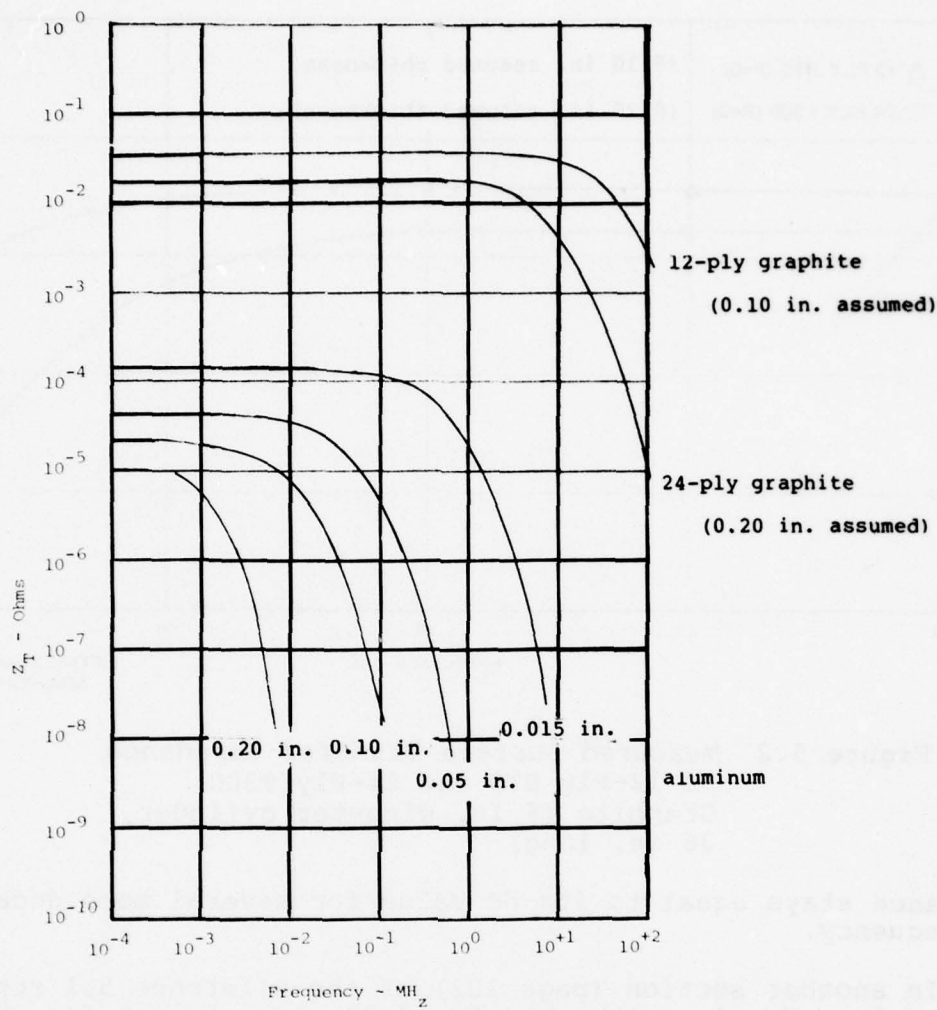


Figure 5.3 Transfer Impedance of Graphite Compared to Aluminum

5.3 SIGNIFICANCE OF TRANSFER IMPEDANCE

In Section 4.5.2, data illustrating the diffusion effects in an elliptical cylinder 2 m long with major and minor axes of 47 and 9.4 cm, respectively, was shown. That cylinder was made from aluminum 0.015 in. thick. The oscilloscopes clearly show the characteristics of the pulse penetration and redistribution time constants. Table 5.1 shows calculated time constants for three such cylinders; two of aluminum and one of graphite. The graphite cylinder is of 24-ply graphite of a thickness estimated to be 0.20 in. Of the two aluminum cylinders, one has a wall thickness of 0.015 in., the value used in the experiment, and the other has wall thickness of 0.20 in., the same thickness as the graphite cylinder. Figure 5.4 shows how those three cylinders would respond to a step function current wave. The fact that the response of the graphite cylinder reaches its final

value so much faster than do either of the aluminum cylinders is a reflection of the much higher resistivity of the graphite. In addition, a given current would produce a much higher voltage in the graphite cylinder.

TABLE 5.1

A COMPARISON OF PULSE PENETRATION
AND REDISTRIBUTION TIME CONSTANTS

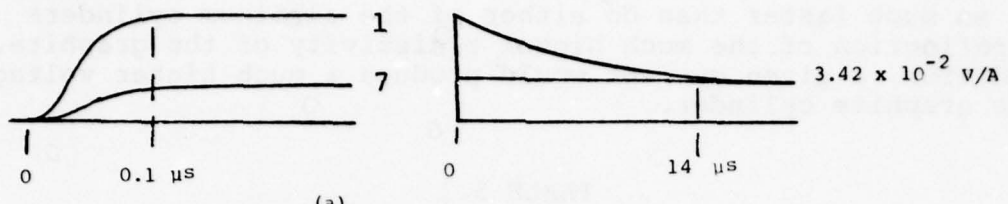
(For an elliptical cylinder of major axis 47 cm
and a minor axis of 9.4 cm)

Material	Pulse Penetration Time Constant	Redistribution Time Constant
24-ply graphite	0.038 μ s	4.8 μ s
0.015 in. aluminum	0.69 μ s	1.2 ms
0.20 in. aluminum	122 μ s	15.5 ms

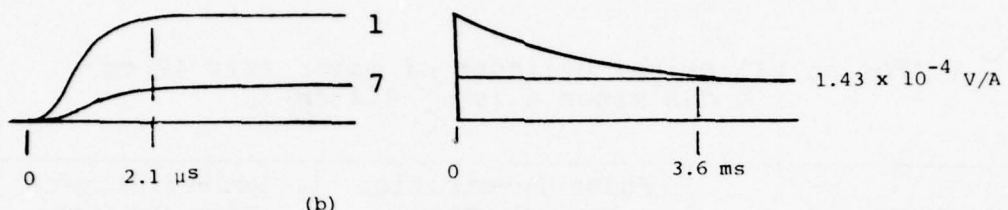
5.4 MISCELLANEOUS OBSERVATIONS ABOUT COMPOSITE STRUCTURES

Strictly speaking, the diffusion phenomena will apply only for a structure composed of isotropic materials, whose resistivity is independent of the current flow. There is concern that composite materials might not have such properties, either because of the layers of epoxy (or other binder) used between plies or because of the general nature of the composite materials. An example of the latter would be boron that is deposited on a tungsten filament. The conductivity of the tungsten is much higher than that of the boron, giving a preferred current path along the tungsten. For graphite, the problem is more theoretical than real; since the plies of carbon are laminated together under pressure, the filaments of the different plies come into contact at enough points that the material does behave like an isotropic material. For boron materials, the concerns may be more valid, but in the real lightning environment, where a structure would be carrying large lightning currents, there would probably be internal sparking between plies that were isolated from each other, sparking sufficient to again make the material essentially isotropic.

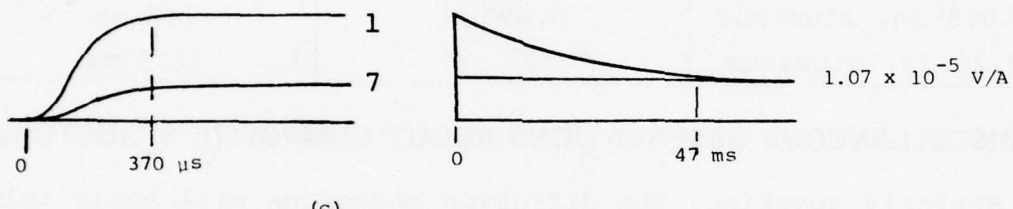
When attempting to pursue theoretical studies of the behavior of composite materials, it would be well not to push the analysis too far, since most actual structures would either have a graphite skin over an aluminum framework or would have thin composite skins over a more massive composite framework. The elementary diffusion phenomena described here and in Section 4 would not



(a)



(b)



(c)

Fast Time Scale

Slow Time Scale

Figure 5.4 Predicted Waveshapes in Structures of Different Materials

- (a) 24-ply graphite - thickness 0.20 in.
- (b) 0.015 in. aluminum
- (c) 0.20 in. aluminum
- (1 and 7 refer to conductor locations - see Figure 4.36)

apply when materials of widely different conductivities are used together.

When the structures under evaluation are sufficiently elementary that the diffusion theory does apply, one can treat composite structures in the same manner as one would treat metal structures. One need only know the effective resistivity of the composite material.

REFERENCES

- 5.1 D. Straw and L. Piszker, Interaction of Advanced Composites with Electromagnetic Pulse (EMP) Environment, Technical Report AFML-TR-75-141, (September 1975).
- 5.2 Straw and Piszker, Interaction of Advanced Composites, p. 102.

SECTION VI

ADDITIONAL TOOLS USEFUL FOR ANALYSIS

6.1 INTRODUCTION

In this section, several other computer tools and formulas useful for analysis of lightning induced effects will be presented. All of the computer routines have been presented as "stand alone" routines, and therefore require a certain amount of user input to use them in conjunction with one another, and with the program DIFFMAG. It was originally hoped that they could be linked together so that data from one routine could be used directly with another routine, but, as explained in the introduction, the bookkeeping tasks required to effect such linking were too complex to implement in this program. The various tools are, however, useful to those who wish to pursue the study of lightning interactions in depth.

6.2 PROGRAM CONVOLUT

6.2.1 Purpose of CONVOLUT

CONVOLUT is a program with which one may find the response of a system to an arbitrary input function if one knows the response of the system to a step function or impulse function. The program evaluates convolution integrals, either of the form

$$Y(t) = \int_0^t B(t) \frac{d}{dt} P(t-u) du \quad (6.1)$$

or of the form

$$Y(t) = \int_0^t B(t) M(t-u) du \quad (6.2)$$

where

- $P(t)$ = the response of a system to a step function
- $M(t)$ = the response of the system to an impulse function
- $B(t)$ = an arbitrary time function
- $Y(t)$ = the response of the system to the arbitrary function $B(t)$

The program is based on the observation that an arbitrary function, $B(t)$, can be approximated numerically, as shown in Figure 6.1, as either the sum of a series of step functions or as a series of impulse functions properly shifted in time. It follows, therefore, that the response of a system to the input $B(t)$ can be obtained by making an appropriate summation of the response of the system to a step function or impulse function.

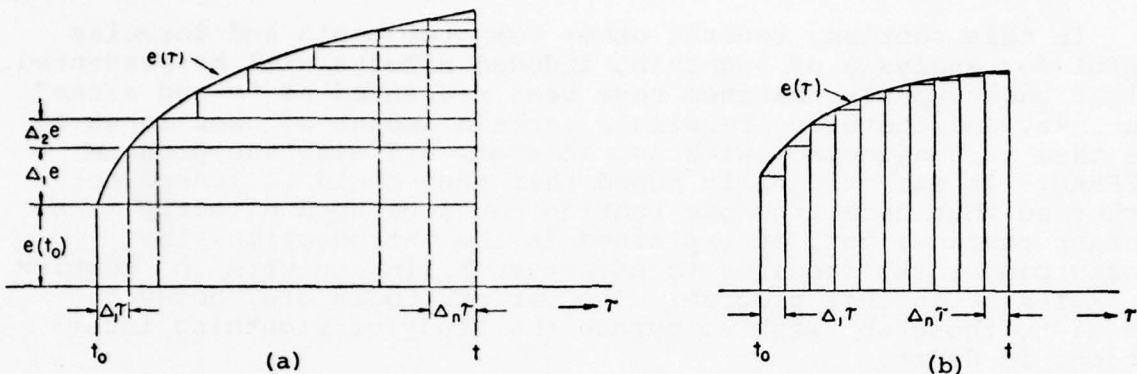


Figure 6.1 Analysis of a General Function as the Superposition of Elementary Functions

- (a) Superposition of step functions
- (b) Superposition of impulse functions

(From Goldman, Reference 6.1)

In Equation 6.1, the derivative of the step function, $\frac{d}{dt} P(t)$, is numerically equal to the impulse function $M(t)$.

6.2.2 Method of Operation

CONVOLUT is entered with two time functions, $P(t)$ and $B(t)$. By convention, though not by necessity, $P(t)$ is taken as the response of the system to a step function, one whose amplitude jumps to 1.0 at $t = 0$ and remains there indefinitely. $B(t)$ is an arbitrary function of time. If the user wishes to evaluate Equation 6.2, the input function $P(t)$ is used to designate the function $M(t)$ of Equation 6.2. $M(t)$ is the response of the system to a unit-impulse function, one whose duration is short compared to the response of the system, and whose amplitude is such that the product of amplitude and time is unity.

The data are entered as numerical pairs, time, and the corresponding amplitude. The spacing between the sample points, or the times at which the amplitude samples are taken, need not be equal. The user may therefore take samples frequently in a region where the amplitude changes rapidly with time, and take them only infrequently in regions where the amplitude changes only slowly.

with time. These sets of data are referred to as the original input functions, Function 1 and Function 2, and are illustrated in Figure 6.2.

FUNCTION 1		FUNCTION 2	
Time	Amplitude	Time	Amplitude
t_a	Y_a	t_1	B_1
t_b	Y_b	t_2	B_2
t_c	Y_c	t_3	B_3
t_d	Y_d	t_4	B_4
		t_s	B_5
t_{nn}	Y_{nn}	t_{mm}	B_{mm}

Figure 6.2 Original Input Functions
(unequal time intervals)

From these functions, two additional functions, $C(t)$ and $D(t)$, are derived. C and D , illustrated in Figure 6.3, are spaced at equal time intervals, $\Delta t = \text{TIME 1}$, and are derived from the original input functions by linear interpolation between the time points at which the user has defined the input data. The amplitudes of C and D are accurate representations of the original input data to the extent that the user sampled the original input functions at points between which the functions could be approximated by straight lines. Functions C and D are stored in the program as arrays. The times corresponding to the amplitudes are not stored explicitly.

From function C , which is a representation of the original input function P , there is derived a fifth function, E . E is either the derivative of C (or P) or equal to C (or P) depending on whether the user is evaluating Equation 6.1 or Equation 6.2. Function E is illustrated in Figures 6.4 and 6.5.

The process by which the convolution integral is evaluated is shown in Figures 6.6 through 6.8 for the times t_1 , t_2 , and t_5 . Basically, the process involves constructing a time-reversed table of function D and then multiplying the tabular values of D and E together. At t_1 , only one pair of values are multiplied together. At t_{200} , there would be 200 values multiplied together, and, consequently, the execution of the program takes much longer as the number of time steps increases.

Time (implied)	<u>FUNCTION 1</u>		<u>FUNCTION 2</u>
	Amplitude	Amplitude	Amplitude
t1	C1	D1	
t2	C2	D2	
t3	C3	D3	
t4	C4	D4	
t5	C5	D5	
t6	C6	D6	
	⋮	⋮	⋮
tN3	CN3	DN3	

T is uniform and equal to Time 2

Figure 6.3 Derived Input Functions (equal time intervals)

Time (implied)	<u>Amplitude</u>	
t1	E1	$E1 = (C2-C1)/\Delta t$
t2	E2	$E2 = (C3-C2)/\Delta t$
t3	E3	$E3 = (C4-C3)/\Delta t$
t4	E4	
t5	E5	
t6	E6	
⋮	⋮	
⋮	⋮	
⋮	⋮	
tN	EN3	$EN3-1 = (CN3-2CN3-1)/\Delta t$ $EN3 = EN3-1$

Figure 6.4 Function E When Option 1 is Selected (E = derivative of C)

Time (implied)	Amplitude	
t1	E1	E1 = C1
t2	E2	E2 = C2
t3	E3	E3 = C3
t4	E4	E4 = C4
t5	E5	E5 = C5
t6	E6	E6 = C6
tN3	EN3	EN3 = CN3

Figure 6.5 Function E When Option 2 is Selected

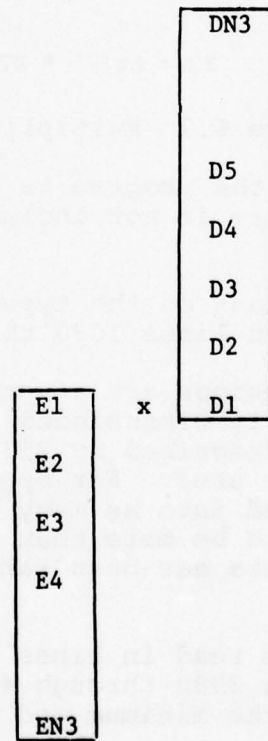
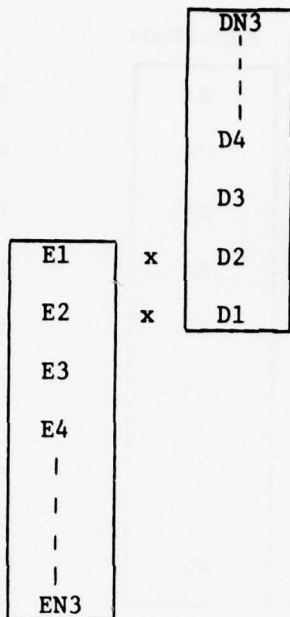


Figure 6.6 Multiplication Steps at t_1



$$Y2 = \Delta t(E1 * D2 + E2 * D1)$$

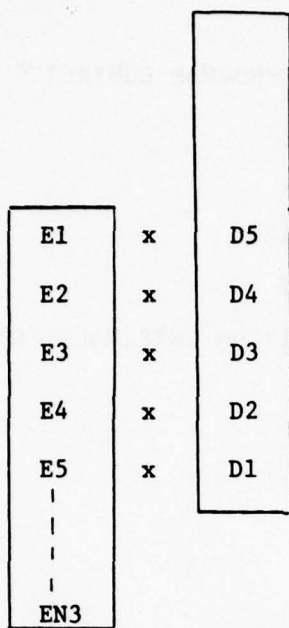
Figure 6.7 Multiplication Steps at t_2

A listing of the program is given in Figure 6.9. A flow chart of the program is not included because it is fairly straightforward.

The instructions on the type of data with which the program is run are given in lines 1020 through 3280.

Program dimensions are given in lines 3300 and 3320. The program is presently dimensioned so that each of the input functions can be described by 250 pairs of data. Fewer pairs can, of course, be used. For operation of the program, this data may be divided into as many as 250 increments, a number which has seemed to be more than adequate for all functions for which the input data has been taken from measurements on physical systems.

Function 1 is read in lines 3520 through 3960, while function 2 is read in lines 3980 through 4460. During the reading of each of the functions the minimum and maximum values of the functions are determined.



$$Y5 = \Delta t(E1 * D5 + E2 * D4 + E3 * D3 + E4 * D2 + E1 * D5)$$

Figure 6.8 Multiplication Steps at t_5

In lines 4480 through 4900, the input data is printed for inspection if the control character IOFLAG4 = 1. If IOFLAG4 = 0, that data is not printed.

In lines 4940 through 5220, the data as originally given is expanded, and the functions C and D are constructed. Subroutine QUACK is used to perform the necessary linear interpolations. The derivative of function C is taken in lines 5300 through 5360 using the relation

$$P'_{tn} = \frac{1}{t} (P_n - P_{n-1}) \quad (6.3)$$

where

$$t = t_n - t_{n-1}$$

```

1020C PROGRAM NAME IS CONVOLUT
1040C
1060C FOR FURTHER INFORMATION ON THIS PROGRAM CONTACT
1080C
1100C F.A. FISHER
1120C BLDG 9 - ROOM 200
1140C GENERAL ELECTRIC CO.
1160C 100 WOODLAWN AVE.
1180C PITTSFIELD, MASS 01201
1200C
1220C PHONE (413)-494-4380
1240C
1260C THIS PROGRAM EVALUATES SUPERPOSITION INTEGRALS, EITHER OF THE
1280C FIRST KIND
1300C
1320C      /--
1340C      /
1360C Y(T) = / B(T) D/DT [P(T-U)DU]
1380C      /
1400C      --/ 0
1420C
1440C
1460C OR OF THE SECOND KIND
1480C
1500C
1520C      /--
1540C      /
1560C Y(T) = / B(T) P(T-U)DU
1580C      /
1600C      --/ 0
1620C
1640C
1660C IF FUNCTION P IS THE TIME RESPONSE OF A SYSTEM TO A STEP
1680C FUNCTION INPUT AND FUNCTION B IS AN ARBITRARY TIME FUNCTION
1700C INPUT, THEN FUNCTION Y WILL BE THE RESPONSE FO THE SYSTEM TO
1720C THE ARBITRARY INPUT FUNCTION B. FOR A STEP FUNCTION INPUT ONE
1740C WOULD USE AN INTEGRAL OF THE FIRST KIND
1760C
1780C IF FUNCTION P IS THE RESPONSE TO AN IMPULSE FUNCTION, THEN THE
1800C RESPONSE OF THE SYSTEM COULD BE EVALUATED BY USING AN INTEGRAL
1820C OF THE SECOND KIND.
1840C
1860C
1880C THE PROGRAM REQUIRES DATA INPUT FROM A FILE NAMED INCOFIL, THE
1900C CHARACTERISTICS OF WHICH ARE AS FOLLOWS:
1920C
1940C 1000 IOFLAG3
1960C
1980C THIS IS A CONTROL CHARACTER THAT SELECTS THE TYPE OF
2000C INTEGRAL TO BE USED.
2020C IF IOFLAG3 = 1 AN INTEGRAL OF THE FIRST KIND IS USED
2040C TO EVALUATE THE RESPONSE IN TERMS OF A STEP FUNCTION
2060C RESPONSE. IF IOFLAG3 = 2 AN INTEGRAL OF THE SECOND
2080C KIND IS USED TO EVALUATE THE RESPONSE IN TERMS OF THE

```

Figure 6.9 Program CONVOLUT

2100C RESPONSE TO AN IMPULSE FUNCTION.
 2120C
 2140C 2000 IOFLAG4,IOFLAGS
 2160C
 2180C THESE ARE CONTROL CHARACTERS, 1 (ONE) OR 0 (ZERO)
 2200C THAT CONTROL WHETHER OR NOT THE INPUT AND OUTPUT
 2220C DATA ARE TO BE PRINTED AND PLOTTED.
 2240C IF IOFLAG4 = 1 THE INPUT DATA WILL BE LISTED, BUT
 2260C WILL NOT BE SO LISTED IF IOFLAG4 = 0
 2280C IF IOFLAG5= 1 THE INPUT AND OUTPUT DATA WILL BE
 2300C PLOTTED, BUT WILL NOT BE IF IOFLAGS = 0.
 2320C
 2340C 3000 NN
 2360C
 2380C NN IS A NUMBER THAT TELLS HOW MANY PAIRS OF DATA,
 2400C TIME AND AMPLITUDE, WILL BE USED TO DESCRIBE
 2420C THE FIRST FUNCTION.
 2440C
 2460C 3010 TIME, AMPLITUDE
 2480C 3020 TIME, AMPLITUDE
 2500C 3030 TIME, AMPLITUDE
 2520C
 2540C THESE ARE PAIRED VALUES OF TIME AND AMPLITUDE THAT
 2560C DEFINE THE FIRST FUNCTION. USE AS MANY LINES OF
 2580C DATA AS NECESSARY TO DEFINE THE FUNCTION. THE DATA
 2600C DOES NOT HAVE TO BE DEFINED AT EQUAL TIME INTERVALS.
 2620C
 2640C 4000 MM
 2660C
 2680C MM IS A NUMBER THAT TELLS HOW MANY PAIRS OF DATA
 2700C THAT WILL BE USED TO DESCRIBE THE SECOND FUNCTION.
 2720C
 2740C 4010 TIME, AMPLITUDE
 2760C 4020 TIME, AMPLITUDE
 2780C 4030 TIME, AMPLITUDE
 2800C
 2820C THESE ARE PAIRED VALUES THAT DESCRIBE THE SECOND
 2840C FUNCTION.
 2860C
 2880C 5000 N3,TIME1,TIME2
 2900C
 2920C N3 IS THE NUMBER OF SHORT SEGMENTS INTO WHICH THE
 2940C PROGRAM SHOULD DIVIDE THE DATA DESCRIBING THE INPUT
 2960C FUNCTIONS IN ORDER TO PERFORM THE CALCULATIONS WITH
 2980C THE DESIRED ACCURACY. A REASONABLE NUMBER IS BETWEEN
 3000C 100 AND 200. THE LIMIT ON N3 IS 250 UNLESS THE PROG-
 3020C RAM DIMENSIONS ARE CHANGED.
 3040C
 3060C TIME 1 IS THE SIZE OF THE TIME INTERVAL WITH WHICH
 3080C THE CALCULATIONS ARE MADE. IF N3 = 100 AND TIME1 = 0.1
 3100C MICROSECONDS THE CALCULATIONS WILL COVER THE RANGE
 3120C 0 TO 10 MICROSECONDS.
 3140C
 3160C TIME2 CONTROLS THE AMOUNT OF OUTPUT DATA THAT IS

Figure 6.9 (Continued) Program CONVOLUT (Continued)

```

3180C PRINTED OR PLOTTED. IF TIME 2 = 5 EVERY FIFTH LINE OF
3200C DATA WILL BE PRINTED OR PLOTTED. THUS OUTPUT DATA
3220C WOULD BE GIVEN AT INTERVALS OF 0.5 MICROSECONDS.
3240C IF TIME2 = 1 EVERY LINE WILL BE PRINTED OR PLOTTED.
3260C
3280C -----
3300 DIMENSION B(2,250),C(1,250),D(1,250),P(2,250),Y(1,250)
3320 DIMENSION E(1,250)
3340 INTEGER INCOFIL
3360 CALL OPENF(09,"INCOFIL;",ISTAT,1,0,1)
3380 3001 FORMAT(" ****")
3400 WRITE(06,3001)
3420 WRITE(06,3000)
3440 3000 FORMAT(" ")
3460 READ(09,110)LINE,IOFLAG3
3480 READ(09,110)LINE,IOFLAG4,IOFLAG5
3500 READ(09,110)LINE,NN
3520C INPUT OF FUNCTION #1 BEGINS
3540 3035 FORMAT(I3)
3560 PMAX=0.0
3580 PMIN=0.0
3600 DO 112 J=1,NN
3620 N1=J
3640 READ(09,110)LINE,P(1,J),P(2,J)
3660 110 FORMAT(V)
3680 IF(PMAX .GE. P(2,J)) GO TO 3076
3700 PMAX=P(2,J)
3720 GO TO 3077
3740 3076 PMAX=PMAX
3760 3077 IF(PMIN .LE. P(2,J)) GO TO 3080
3780 PMIN=P(2,J)
3800 GO TO 111
3820 3080 PMIN=PMIN
3840 IF(J .GT. 1) GO TO 3166
3860 GO TO 111
3880 3166 IF(P(1,J)) 3200,3200,111
3900 111 CONTINUE
3920 112 CONTINUE
3940C THE MINIMUM AND MAXIMUM VALUES OF FUNCTION P ARE PMIN AND PMAX
3960C END OF INPUT OF FUNCTION #1
3980 3200 CONTINUE
4000C INPUT OF FUNCTION #2 BEGINS
4020 READ(09,110)LINE,MM
4040 3205 FORMAT(I3)
4060 BMAX=0.0
4080 BMIN=0.0
4100 DO 120 J=1,MM
4120 N2=J
4140 READ(09,110)LINE,B(1,J),B(2,J)
4160 118 FORMAT(V)
4180 IF(BMAX .GE. B(2,J)) GO TO 3156
4200 BMAX=B(2,J)
4220 GO TO 3157
4240 3156 BMAX=BMAX

```

The flowchart illustrates the execution flow of the program. It starts with reading data for Function #1 (lines 3600-3920). After reading each row, it calculates the maximum (PMAX) and minimum (PMIN) values of the second column (lines 3640-3780). If PMAX is greater than or equal to PMIN, it proceeds to line 3076; otherwise, it goes to line 3080. Both paths eventually lead to line 111, which continues the loop until all rows are processed. Following this, the program moves to the input of Function #2 (lines 4020-4240), where it reads data and calculates the maximum (BMAX) and minimum (BMIN) values of the second column. Similar to Function #1, it checks if BMAX is greater than or equal to BMIN, leading to line 3156 if true, or line 3157 if false. Both paths eventually lead to line 3156, which continues the loop until all rows are processed.

Figure 6.9 (Continued) Program CONVOLUT (Continued)

```

4260 3157 IF(BMIN .LE. B(2,J)) GO TO 3160 ←
4280 BMIN=B(2,J)
4300 GO TO 119 ━━━━━━
4320 3160 BMIN=BMIN ←
4340 IF(J .GT. 1) GO TO 3354 ━━━━
4360 GO TO 119 ━━━━
4380 3354 IF(B(1,J)) 3380,3380,119 ←
4400 119 CONTINUE
4420 120 CONTINUE
4440C THE MINIMUM AND MAXIMUM VALUES OF FUNCTION B ARE BMIN AND BMAX
4460C END OF INPUT OF FUNCTION #2
4480 3380 IF(N1 .GE. N2) GO TO 124
4500 INDEX=N2
4520 GO TO 126 ━━━━
4540 124 INDEX=N1 ←
4560 125 CONTINUE
4580 126 CONTINUE ←
4600 IF(IOFLAG4) 301,301,129 ━━━━
4620 129 WRITE(06,131) ←
4640 131 FORMAT(" THIS IS THE ORIGINAL FORM OF THE INPUT DATA")
4660 WRITE(06,3000)
4680 130 FORMAT(7X,"FUNCTION NUMBER ONE",9X,"FUNCTION NUMBER TWO")
4700 WRITE(06,136)
4720 WRITE(06,3000)
4740 136 FORMAT(//6X,"TIME",11X,"AMPLITUDE",8X,"TIME",11X,"AMPLITUDE")
4760 138 FORMAT(//,10X,"X",13X,"F(X)",15X,"X",15X,"F(X)")
4780 DO 300 I=1,INDEX
4800 WRITE(06,165) P(1,I),P(2,I),B(1,I),B(2,I)
4820 165 FORMAT(3X,1E14.4,2X,1E14.4,3X,1E14.4,2X,1E14.4)
4840 300 CONTINUE ←
4860 WRITE(06,3000)
4880 WRITE(06,3001)
4900 WRITE(06,3000)
4920 301 CONTINUE ←
4940 WRITE(06,315)
4960 315 FORMAT(//,5X,"SUPERPOSITION INTEGRAL CALCULATION")
4980 WRITE(06,330)
5000 330 FORMAT(//,4X,"COMP INTVL",10X,"TOTAL INTVL",10X,"PRNTG INTVL")
5020 WRITE(06,3000)
5040 READ(09,3572)LINE,N3,TIME1,TIME2
5060 3572 FORMAT(V)
5080 WRITE(06,350) TIME1,N3*TIME1,TIME1*TIME2
5100 350 FORMAT(2X,1E14.4,5X,1E14.4,6X,1E14.4)
5120 TIME=0.
5140 DO 390 K=1,N3+1
5160 NINE=K
5180 CALL QUACK(P,B,C,D,I,NINE,N1,N2,TIME)
5200 TIME =TIME+TIME1
5220 390 CONTINUE ←
5240C NOW WE START TO TAKE THE DERIVATIVE OF FUNCTION C
5260 N=1
5280 IF(IOFLAG3>1.5)GOTO 450
5300 DO 430 N=1,N3 ←
5320 E(1,N)=(C(1,N+1)-C(1,N))/TIME2

```

Figure 6.9 (Continued) Program CONVOLUT (Continued)

```

5340 430 CONTINUE
5360 E(1,N3)=E(1,N3-1)
5380C NOW WE HAVE FINISHED TAKING THE DERIVATIVE
5400 GOTO 465
5420 450 DO 460 N=1,N3
5440 E(I,N)=C(1,N) ←
5460 460 CONTINUE ←
5480 465 CONTINUE ←
5500 TIME=0.
5520 Q=1.
5540 Y(1,Q)=0.
5560 DO 600 J=1,N3 ←
5580 YS=0
5600C HERE WE START THE HEART OF THE CONVOLUTION ROUTINE BY MULTIPLYING
5620C TOGETHER THE FUNCTION E AND THE TIME REVERSED FUNCTION DERIVED
5640C FROM FUNCTION D
5660 DO 540 I=1,0 ←
5680 YS1=E(1,I)*D(1,1+Q-I)*TIME1
5700 YS=YS1+YS
5720 Y(1,Q)=YS
5740 540 CONTINUE ←
5760C THIS ENDS THE MULTIPLICATION
5780 590 Q=Q+1.
5800 600 CONTINUE ←
5820 U=0.
5840 XL=0.
5860 DO 660 I=1,N3 ←
5880 IF(Y(1,I) .LT. U) GO TO 650
5900 U=Y(1,I)
5920 650 IF(Y(1,I) .GT. XL) GO TO 660 ←
5940 XL=Y(1,I)
5960 660 CONTINUE ←
5980C THE MINIMUM AND MAXIMUM VALUES OF THE RESPONSE FUNCTION Y
6000C ARE XL AND U
6020 WRITE(06,675)
6040 675 FORMAT(//,1X,"MINIMUM AND MAXIMUM VALUES OF THE RESPONSE ARE")
6060 WRITE(06,3000)
6080 WRITE(06,685) XL,U
6100 685 FORMAT(3X,1E14.4,5X,1E14.4)
6120 WRITE(06,730)
6140 WRITE(06,3000)
6160 730 FORMAT(//,10X,"T",13X,"F1(T)",11X,"F2(T)",11X,"F1*F2")
6180 TIME=0.
6200 XN5=TIME2
6220 DO 820 I=1,N3+1 ←
6240 IF(XN5 .LT. TIME2) GO TO 800 ←
6260 WRITE(06,780)TIME,C(1,I),D(1,I),Y(1,I)
6280 780 FORMAT(4X,1E14.4,2X,1E14.4,2X,1E14.4,2X,1E14.4)
6300 786 FORMAT(2E14.4)
6320 XN5=0.
6340 800 TIME=TIME+TIME1 ←
6360 XN5=XN5+1.
6380 820 CONTINUE ←
6400 WRITE(06,3000)

```

Figure 6.9 (Continued) Program CONVOLUT (Continued)

```

6420 WRITE(06,3001)
6440 WRITE(06,3000)
6460 IF(IOFLAG5) 2060,2060,1170
6480C BEGIN PLOTTING ROUTINE
6500 1170 TIME =0
6520 XN5=TIME2
6540 ICOUNT=0
6560 R0=PMIN
6580 R1=PMAX
6600 WRITE(06,1180)
6620 1180 FORMAT(" THIS IS A PLOT OF FUNCTION 1 OR FUNCTION C")
6640 GO TO 1222
6660 1200 R0=BMIN <----- From Line 8100
6680 R1=BMAX
6700 WRITE(06,1202)
6720 1202 FORMAT(" THIS IS A PLOT OF FUNCTION 2 OR FUNCTION D")
6740 GO TO 1222
6760 1210 R0=XL <----- To Line 8140
6780 WRITE(06,1212)
6800 1212 FORMAT(" THIS IS A PLOT OF THE RESPONSE FUNCTION")
6820 R1=U
6840 1222 WRITE(06,1223) TIME <----- To Line 8140
6860 1223 FORMAT(//1X,"T-MIN=",1E14.4)
6880 WRITE(06,1227) R0,R1
6900 1227 FORMAT(5X,1E10.3,47X,1E10.3)
6920 WRITE(06,1241)
6940 1241 FORMAT(5X,"I.....I.....I.....I.....I.....I.....")
6960 WRITE(06,1246)
6980 1246 FORMAT(V)
7000 XN6=10.
7020 NCNT=ICOUNT+1
7040 DO 1650 J=1,N3+1
7060 GO TO (4340,4355,1350),NCNT
7080 4340 R=C(1,J)
7100 GO TO 1360
7120 4355 R=D(1,J) <----- To Line 8140
7140 GO TO 1360
7160 1350 R=Y(1,J) <----- To Line 8140
7180 1360 IF(XN5 .LT. TIME2) GO TO 1630
7200 1420 IF(R .GT. R1) GO TO 1600
7220 IF(R .LT. R0) GO TO 1600
7240 XN5=0.
7260 CHARACTER FORM*8//"/
7280 CHARACTER A*1
7300 DATA A/1H+/
7320 RANGE=R1-R0
7340 PCRANGE=R/(R1-R0)
7360 SHIFT=PCRANGE*60.
7380 KSHIFT=SHIFT+5.
7400 RESHIFT=SHIFT-KSHIFT
7420 IF(RESHIFT .GT. 0.5) GO TO 1455
7440 GO TO 1456
7460 1455 KSHIFT=KSHIFT+1 <----- To Line 8140
7480 1456 ENCODE(FORM,1457)KSHIFT,"X,A1"

```

Figure 6.9 (Continued) Program CONVOLUT (Continued)

```

7500 1457 FORMAT("(",I2,A4,")")
7520 WRITE(06,FORMA)
7540 IF(XN6 .EQ. 10.) GOTO 1400
7560 WRITE(06,1381)
7580 1381 FORMAT(1H+"   ")
7600 GOTO 1605
7620 1400 WRITE(06,1401) ←
7640 1401 FORMAT(1H+," ---")
7660 XN6=0
7680 GO TO 1605
7700 1600 WRITE(06,1601) R ←
7720 1601 FORMAT(1H+,"OFF SCALE: R=",1E14.8)
7740 1605 CONTINUE ←
7760 XN5=0.
7780 XN6=XN6+1
7800 1630 XN5=XN5+1.
7820 TIME=TIME+TIME1
7840 1650 CONTINUE ←
7860 WRITE(06,1661)
7880 1661 FORMAT(5X,"I.....I.....I.....I.....I.....I.....")
7900 TIME=TIME-TIME1
7920 WRITE(06,1681) TIME
7940 1681 FORMAT(/,1X,"TMAX=",1E14.4)
7960 WRITE(06,3000)
7980 WRITE(06,3000)
8000 WRITE(06,3000)
8020 1700 ICOUNT=ICOUNT+1
8040 TIME=0.0
8060 IF(ICOUNT .GT. 2) GO TO 2060
8080 IF(ICOUNT .GT. 1) GO TO 1210
8100 GO TO 1200 → To Line 6660
8120C END OF PLOTTING ROUTINE ← From Line 6460
8140 2060 CONTINUE
8160 STOP;END
8180 SUBROUTINE QUACK(P,B,C,D,I,K,N1,N2,TIME)
8200C THIS SUBROUTINE EXPANDS THE ORIGINAL INPUT FUNCTIONS P AND B AND
8220C GENERATES TWO NEW FUNCTIONS C AND D AT EQUAL TIME INTERVALS
8240 DIMENSION P(2,50), B(2,50),C(1,250),D(1,250)
8260 IF(P(1,1) .GE. TIME) GO TO 3100 .
8280 IF(P(1,N1) .LE. TIME) GO TO 3120
8300 DO 3060 J=1,N1
8320 IF(P(1,J) .GT. TIME) GO TO 3070
8340 3060 CONTINUE
8360 3070 Q3=(P(2,J)-P(2,J-1))/(P(1,J)-P(1,J-1)) ←
8380 C(1,K)=P(2,J-1)+Q3*(TIME-P(1,J-1))
8400 GO TO 3170
8420 3100 C(1,K)=P(2,1) ←
8440 GO TO 3170 ←
8460 3120 C(1,K)=P(2,N1) ←
8480 3170 IF(B(1,1) .GT. TIME) GO TO 3250
8500 IF(B(1,N2) .LE. TIME) GO TO 3270
8520 DO 3210 J=1,N2
8540 IF(B(1,J) .GT. TIME) GO TO 3220
8560 3210 CONTINUE

```

The flowchart illustrates the execution flow of the program. It starts with a main loop from line 7500 through 8560. Inside this loop, there are several output statements (e.g., 7520, 7620, 7700, 7920) and control statements (e.g., 8060, 8080). A call to subroutine QUACK is made at line 8180. The subroutine QUACK handles the expansion of input functions P and B into C and D. It uses a DO loop from 3060 to 3120 to calculate values for C(1,K) based on P(2,J) and P(1,J). It also includes logic to handle boundary conditions (lines 8420, 8440, 8460) and to skip calculations if the current time is greater than the function value (lines 8480, 8500). The main loop resumes at line 8560 after the subroutine returns.

Figure 6.9 (Continued) Program CONVOLUT (Continued)

```

8580 3220 Q3=(B(2,J)-B(2,J-1))/(B(1,J)-B(1,J-1)) ←
8600 D(1,K)=B(2,J-1)+Q3*(TIME-B(1,J-1))
8620 GO TO 3280
8640 3250 D(1,K)=B(2,1) ←
8660 GO TO 3280
8680 3270 D(1,K)=B(2,N2)
8700 3280 RETURN;END
8720 STOP;END

```

Figure 6.9 (Conclusion) Program CONVOLUT (Conclusion)

If, in the running of the program, Option 2 (Equation 6.2) is selected, this step is bypassed, and function E is made numerically equal to function C.

The multiplications by which the integral is evaluated are done in lines 5660 through 5800. The multiplication process is done N3 times, with the number of multiplications increasing from 1 at time 1, to N3 times for time N3. Over the interval t , (TIME1), the two functions are assumed to have constant amplitude. A more accurate integration routine could be based on Simpson's rule

$$y \, dx = \frac{h}{3} (y_0 + 4y_1 + 2y_2 + 4y_3 + 2y_4 + \dots + 2y_{n-2} + 4y_{n-1} + y_n) \quad (6.4)$$

but, so far, this has not seemed necessary. One minor complication in using Simpson's rule is that the number of terms to be used would vary from step to step.

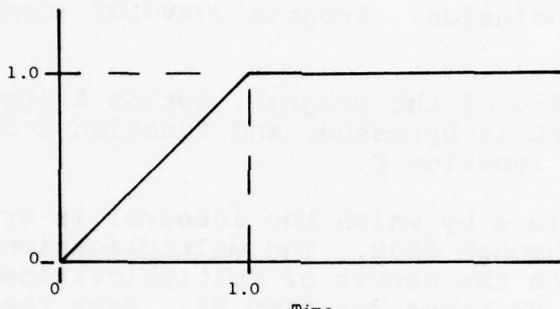
The minimum and maximum values of the response are found in lines 5850 through 5960.

The values of the functions are tabulated in lines 6020 and 6300.

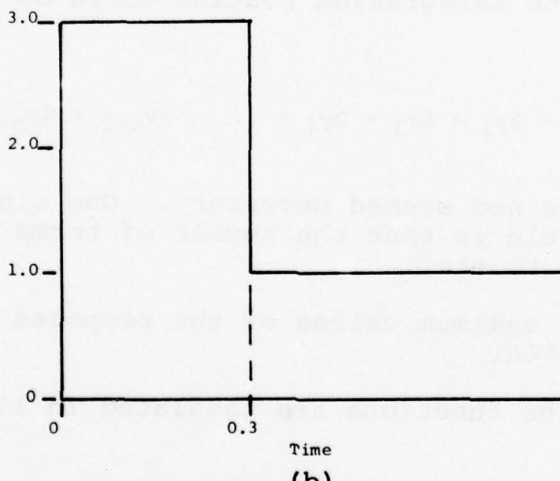
Most of the remainder of the program is taken up with a routine that plots the input and response functions. The function to be plotted is selected in lines 7020 through 7160. The plotting routine can be bypassed entirely by making IOFLAG5 = 0 in the input data.

6.2.3 Notes on Input Data

The format of the input data is shown in Figure 6.9. The user must use care in representing some functions by straight-line segments. The simplest type of function to represent is the elementary ramp function shown in Figure 6.10a. This function need be represented by only two points, one at $t = 0$ and one at $t = 1$. Points after $t = 1$ need not be entered, since the program takes the coordinates of the last entry to pertain to all subsequent times, as well. A function with discontinuities, such as Figure 6.10b, requires a bit more care, in that the function should be represented at times just before and just after the discontinuity. Just before or just after means at some time before or after the next increment of time entered as TIME1. Accordingly, the first discontinuity of Figure 6.10b is defined by the points ($t = 0$, $A = 0$) and ($t = .001$, $A = 3$).



(a)



(b)

Figure 6.10 Functions With Discontinuities

- (a) Discontinuity of slope
- (b) Discontinuity of amplitude

These two points define the function until the second discontinuity, this being defined by the points ($t = 0.3$, $A = 3$) and ($t = 0.301$, $A = 1$). The last coordinate defines the waveform for all subsequent times.

The accuracy with which the program treats the functions depends upon the size of the computation interval TIME1. The shorter the time interval, the more accurate the results, but the greater the computation time will be. While the program does not use much computation time as computer routines go, great accuracy is seldom justified for the type of use to which the program is apt to be put. If the input functions are to be derived from oscillographic measurements, and if the functions are not of very complex waveshape, then representing the function at 100 - 200 points will give an accuracy similar to that with which the original functions are known.

6.2.4 Example of Usage of CONVOLUT

To illustrate the usage of CONVOLUT, consider the elliptical cylinder described in Section 4.7. For the conductor located at the center, the voltage produced by a step-function current of 1000 A would be as shown in Figure 6.11. The object of the calculation is to determine how that conductor would respond to a different current wave having the shape of Figure 6.12.

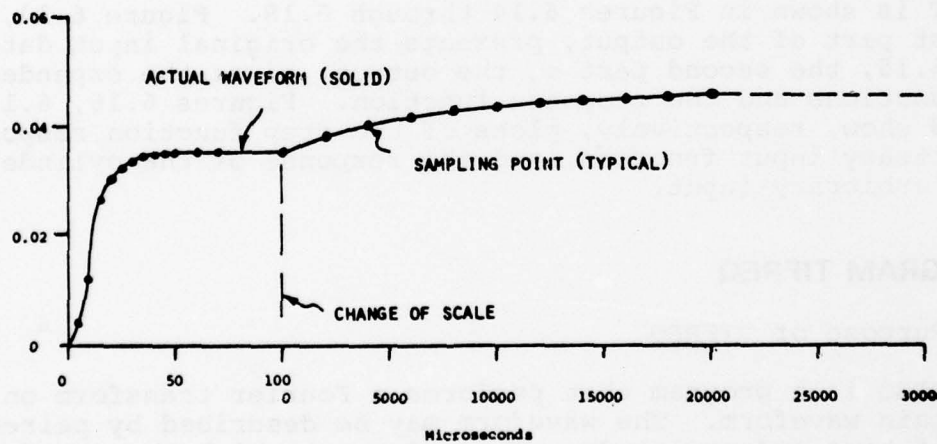


Figure 6.11 Response of an Elliptical Cylinder to a Step Function of Current ($I = 1000$ Amperes = 1 kA)

(From Figure 4.99)

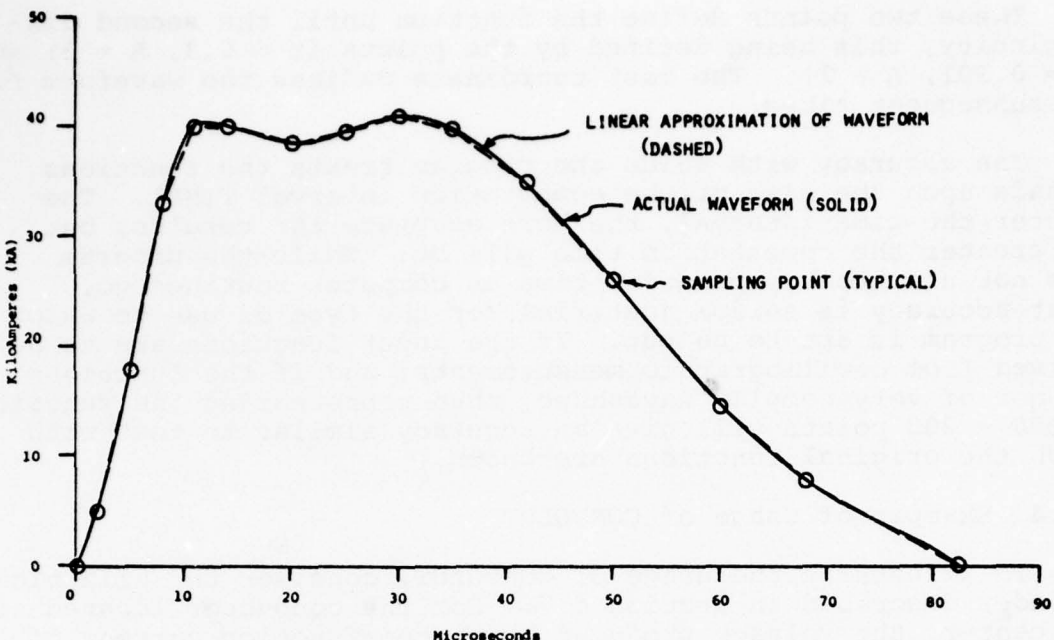


Figure 6.12 Arbitrary Input Current ($I = 41$ kA)

The data file that describes the two time-domain functions is shown in Figure 6.13. The data in this file is represented by the dots in Figures 6.11 and 6.12. The material produced by CONVOLUT is shown in Figures 6.14 through 6.18. Figure 6.14, the first part of the output, presents the original input data. Figure 6.15, the second part of the output, gives the expanded input functions and the response function. Figures 6.16, 6.17, and 6.18 show, respectively, plots of the step function response, the arbitrary input function, and the response of the cylinder to that arbitrary input.

6.3 PROGRAM TIFREQ

6.3.1 Purpose of TIFREQ

TIFREQ is a program that performs a Fourier transform on a time-domain waveform. The waveform may be described by paired values of time and amplitude. The points at which the waveform is sampled need not be uniformly spaced in time. A complementary program that performs the inverse transform, frequency-to-time, is FREQTI, which is described in Section 6.4.

1000 1
2000 1,1
3000 24
3010 0,0
3020 5,.004
3030 10,.013
3040 15,.0265
3050 20,.0300
3060 25,.0313
3070 30,.0340
3080 35,.0345
3090 40,.0347
3100 45,.0349
3110 50,.0350
3120 60,.0353
3130 70,.0355
3140 100,.0355
3150 2000,.0380
3160 4000,.0402
3170 6000,.0418
3180 8000,.0430
3190 10000,.0436
3200 12000,.0440
3210 14000,.0455
3220 16000,.0450
3230 18000,.0455
3240 20000,.0460
4000 15
4015 0,0
4020 2,5
4030 5,16
4040 8,33
4050 11,40
4060 14,40
4070 20,38.5
4080 25,39.5
4090 30,41
4100 35,40
4110 42,35
4120 50,26
4130 60,14.5
4140 68,7.8
4150 80,0
5000 100,1,2

Figure 6.13 Listing of Data File INCOFIL

THIS IS THE ORIGINAL FORM OF THE INPUT DATA

TIME	AMPLITUDE	TIME	AMPLITUDE
0.	0.	0.	0.
0.5000E 01	0.4000E-02	0.2000E 01	0.5000E 01
0.1000E 02	0.1300E-01	0.5000E 01	0.1600E 02
0.1500E 02	0.2650E-01	0.8000E 01	0.3300E 02
0.2000E 02	0.3000E-01	0.1100E 02	0.4000E 02
0.2500E 02	0.3130E-01	0.1400E 02	0.4000E 02
0.3000E 02	0.3400E-01	0.2000E 02	0.3850E 02
0.3500E 02	0.3450E-01	0.2500E 02	0.3950E 02
0.4000E 02	0.3470E-01	0.3000E 02	0.4100E 02
0.4500E 02	0.3490E-01	0.3500E 02	0.4000E 02
0.5000E 02	0.3500E-01	0.4200E 02	0.3500E 02
0.6000E 02	0.3530E-01	0.5000E 02	0.2600E 02
0.7000E 02	0.3550E-01	0.6000E 02	0.1450E 02
0.1000E 03	0.3550E-01	0.6800E 02	0.7800E 01
0.2000E 04	0.3800E-01	0.8300E 02	0.
0.4000E 04	0.4020E-01	0.	0.
0.6000E 04	0.4180E-01	0.	0.
0.8000E 04	0.4300E-01	0.	0.
0.1000E 05	0.4360E-01	0.	0.
0.1200E 05	0.4400E-01	0.	0.
0.1400E 05	0.4550E-01	0.	0.
0.1600E 05	0.4500E-01	0.	0.
0.1800E 05	0.4550E-01	0.	0.
0.2000E 05	0.4600E-01	0.	0.

SUPERPOSITION INTEGRAL CALCULATION

COMP INTVL	TOTAL INTVL	PRNTG INTVL
0.1000E 01	0.1000E 00	0.2000E 01

MINIMUM AND MAXIMUM VALUES OF THE RESPONSE ARE

0. 0.6866E 00

Figure 6.14 First Part of Tabular Output

T	F1(T)	F2(T)	F1*F2
0.	0.	0.	0.
0.2000E 01	0.1600E-02	0.5000E 01	0.3000E-02
0.4000E 01	0.3200E-02	0.1233E 02	0.1140E-01
0.6000E 01	0.5800E-02	0.2167E 02	0.2772E-01
0.8000E 01	0.9400E-02	0.3300E 02	0.5868E-01
0.1000E 02	0.1300E-01	0.3767E 02	0.1021E 00
0.1200E 02	0.1840E-01	0.4000E 02	0.1619E 00
0.1400E 02	0.2380E-01	0.4000E 02	0.2375E 00
0.1600E 02	0.2720E-01	0.3950E 02	0.3225E 00
0.1800E 02	0.2860E-01	0.3900E 02	0.4073E 00
0.2000E 02	0.3000E-01	0.3850E 02	0.4826E 00
0.2200E 02	0.3052E-01	0.3890E 02	0.5384E 00
0.2400E 02	0.3104E-01	0.3930E 02	0.5716E 00
0.2600E 02	0.3184E-01	0.3980E 02	0.5920E 00
0.2800E 02	0.3292E-01	0.4040E 02	0.6071E 00
0.3000E 02	0.3400E-01	0.4100E 02	0.6221E 00
0.3200E 02	0.3420E-01	0.4060E 02	0.6384E 00
0.3400E 02	0.3440E-01	0.4020E 02	0.6560E 00
0.3600E 02	0.3454E-01	0.3929E 02	0.6722E 00
0.3800E 02	0.3462E-01	0.3786E 02	0.6818E 00
0.4000E 02	0.3470E-01	0.3643E 02	0.6866E 00
0.4200E 02	0.3478E-01	0.3500E 02	0.6854E 00
0.4400E 02	0.3486E-01	0.3275E 02	0.6787E 00
0.4600E 02	0.3492E-01	0.3050E 02	0.6671E 00
0.4800E 02	0.3496E-01	0.2825E 02	0.6514E 00
0.5000E 02	0.3500E-01	0.2600E 02	0.6311E 00
0.5200E 02	0.3506E-01	0.2370E 02	0.6079E 00
0.5400E 02	0.3512E-01	0.2140E 02	0.5816E 00
0.5600E 02	0.3518E-01	0.1910E 02	0.5522E 00
0.5800E 02	0.3524E-01	0.1680E 02	0.5203E 00
0.6000E 02	0.3530E-01	0.1450E 02	0.4869E 00
0.6200E 02	0.3534E-01	0.1283E 02	0.4527E 00
0.6400E 02	0.3538E-01	0.1115E 02	0.4177E 00
0.6600E 02	0.3542E-01	0.9475E 01	0.3826E 00
0.6800E 02	0.3546E-01	0.7800E 01	0.3480E 00
0.7000E 02	0.3550E-01	0.6760E 01	0.3142E 00
0.7200E 02	0.3550E-01	0.5720E 01	0.2818E 00
0.7400E 02	0.3550E-01	0.4680E 01	0.2514E 00
0.7600E 02	0.3550E-01	0.3640E 01	0.2232E 00
0.7800E 02	0.3550E-01	0.2600E 01	0.1962E 00
0.8000E 02	0.3550E-01	0.1560E 01	0.1710E 00
0.8200E 02	0.3550E-01	0.5200E 00	0.1476E 00
0.8400E 02	0.3550E-01	0.	0.1259E 00
0.8600E 02	0.3550E-01	0.	0.1056E 00
0.8800E 02	0.3550E-01	0.	0.8687E-01
0.9000E 02	0.3550E-01	0.	0.7024E-01
0.9200E 02	0.3550E-01	0.	0.5572E-01
0.9400E 02	0.3550E-01	0.	0.4351E-01
0.9600E 02	0.3550E-01	0.	0.3443E-01
0.9800E 02	0.3550E-01	0.	0.2846E-01
0.1000E 03	0.3550E-01	0.	0.

Figure 6.15 Second Part of Tabular Output

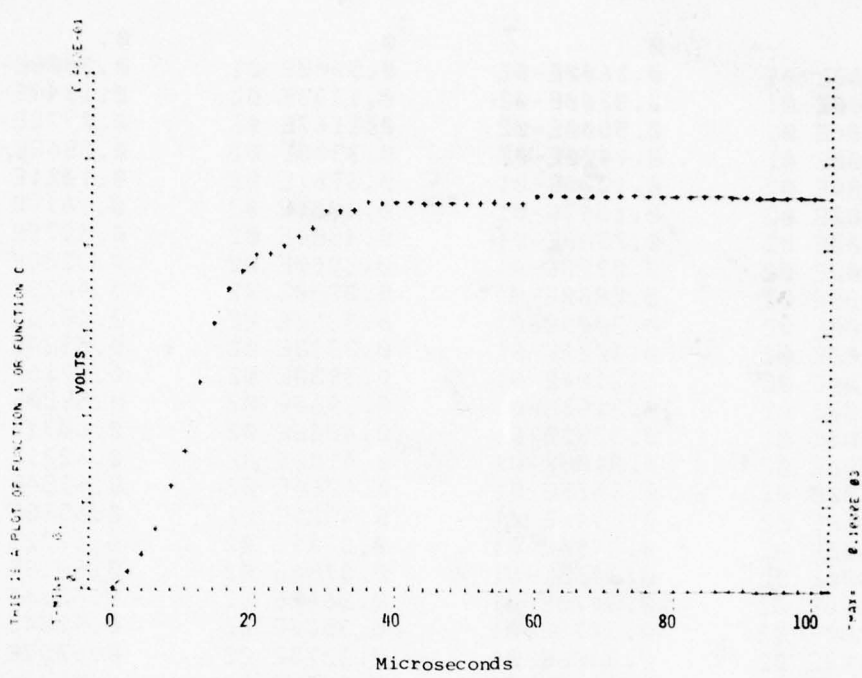


Figure 6.16 Step Response of Elliptical Cylinder as Plotted by Program

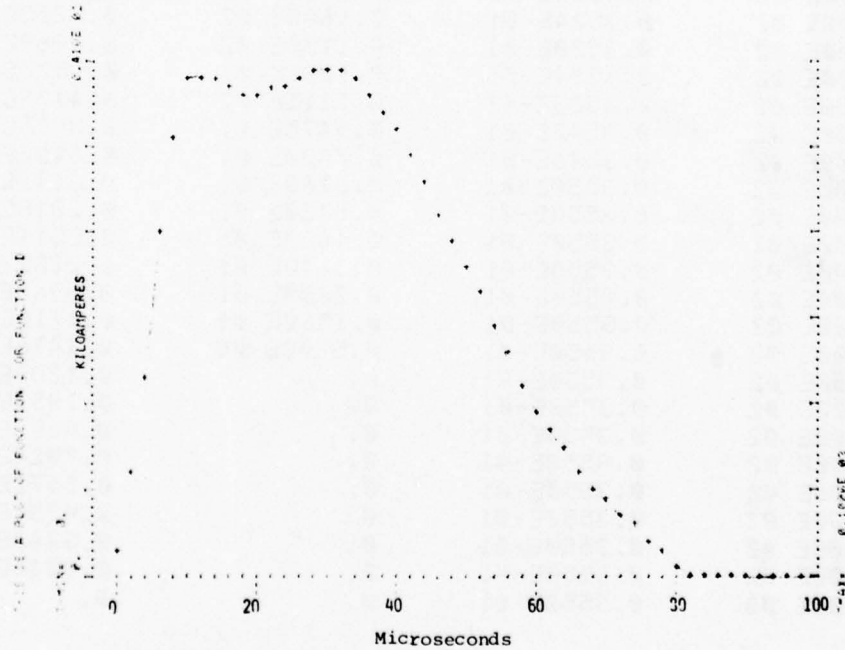


Figure 6.17 Arbitrary Input Function as Plotted by Program

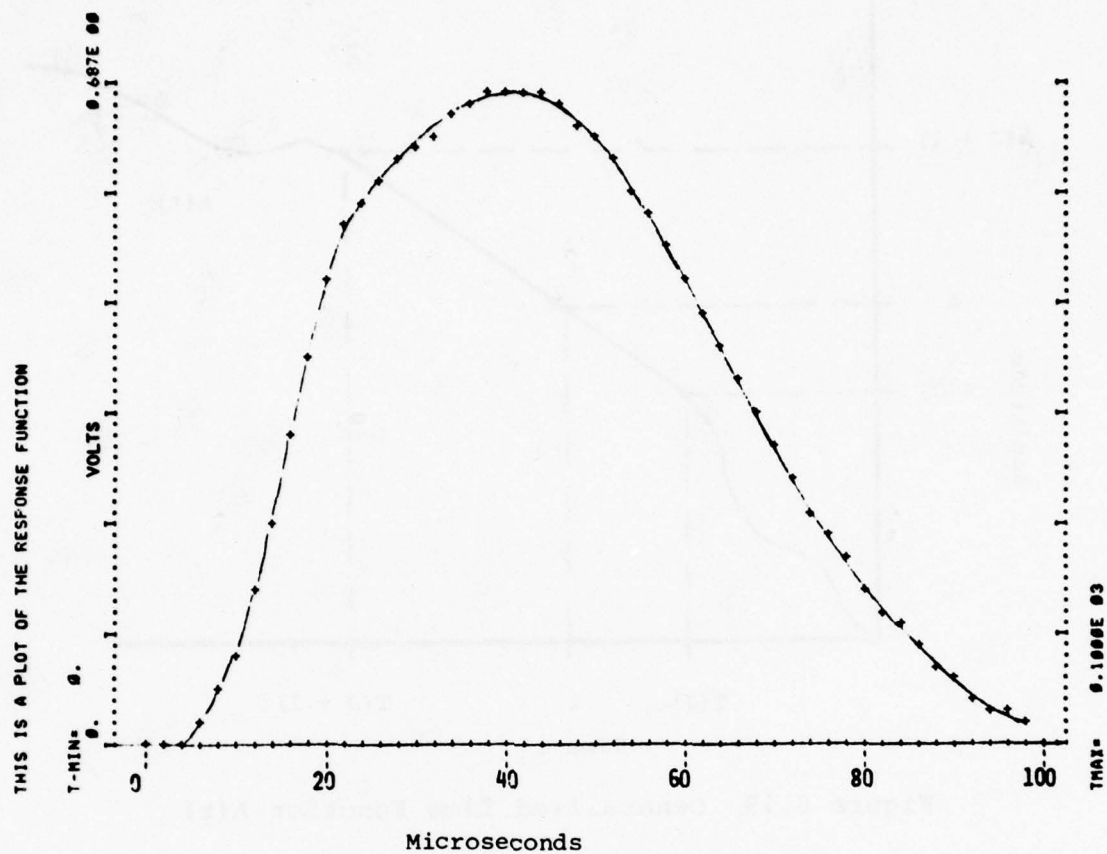


Figure 6.18 Response of Cylinder to Arbitrary Input Shown on Figure 6.17

6.3.2 Method of Operation

To obtain the mathematical derivation of the time-to-frequency conversion program, TIFREQ, let the generalized time function $A(t)$ be represented by straight-line segments, of which a typical segment is shown in Figure 6.19 over the region from $t = T(J)$ to $t = T(J+1)$.

Thus
$$A(t) = A(J) + \frac{[A(J+1) - A(J)]}{[T(J+1) - T(J)]} \times [t - T(J)] \quad (6.5)$$

Let
$$\frac{A(J+1) - A(J)}{T(J+1) - T(J)} = M(J) \quad (6.6)$$

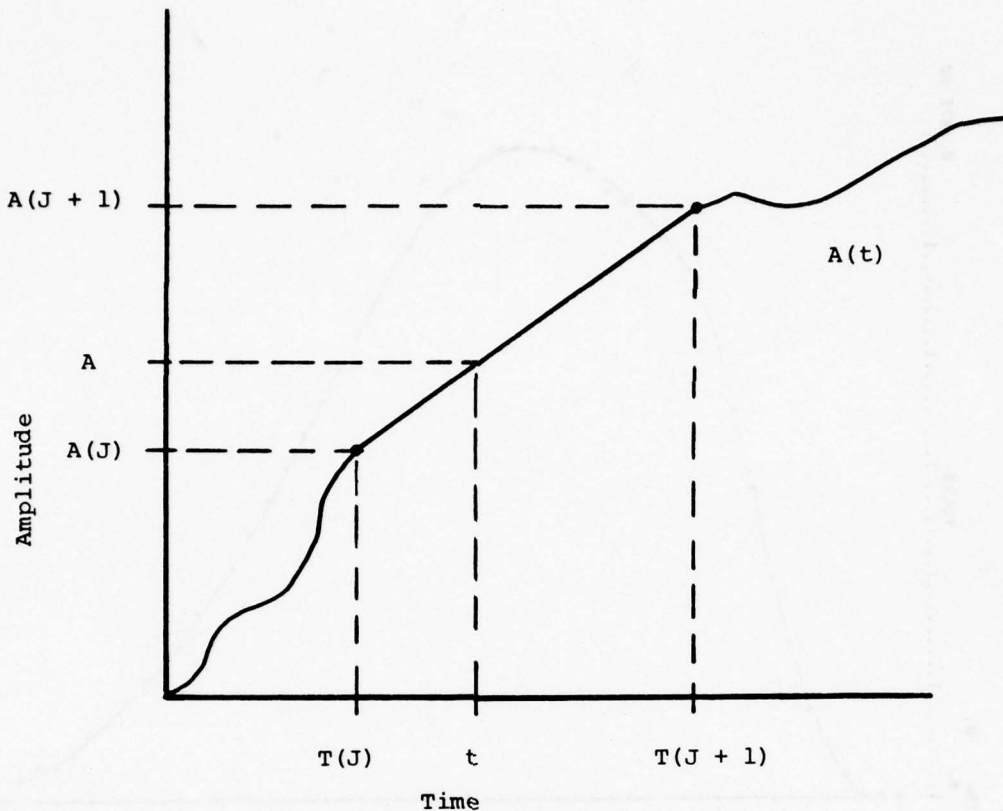


Figure 6.19 Generalized Time Function $A(t)$

Then
$$A(t) = A(J) - M(J) \times T(J) + M(J) \times t \quad (6.7)$$

Also let
$$A(J) - M(J) \times T(J) = B(J) \quad (6.8)$$

Then
$$A(t) = B(J) + M(J) \times t \quad (6.9)$$

The Fourier Transform is defined as

$$A(\omega) = \int_{-\infty}^{\infty} A(t) e^{-i\omega t} dt \quad (6.10)$$

The contribution towards $A(\omega)$ of the portion of the $A(t)$ waveform from $T(J)$ to $T(J+1)$ is, for $\omega > 0$,

$$A(\omega) = \int_{T(J)}^{T(J+1)} A(t) e^{-i\omega t} dt \quad (6.11)$$

$$A(\omega) = \int_{T(J)}^{T(J+1)} B(J) e^{-i\omega t} dt + \int_{T(J)}^{T(J+1)} M(J) te^{-i\omega t} dt \quad (6.12)$$

$$A(\omega) = \left[\frac{jB(J)}{\omega} e^{-i\omega t} + \frac{(-i\omega t - 1)M(J)}{(-i\omega)^2} e^{-i\omega t} \right]_{T(J)}^{T(J+1)} \quad (6.13)$$

$$A(\omega) = \left[\frac{jB(J)}{\omega} e^{-i\omega t} + \frac{jtM(J)}{\omega} e^{-i\omega t} + \frac{M(J)}{\omega^2} e^{-j\omega t} \right]_{T(J)}^{T(J+1)} \quad (6.14)$$

$$\begin{aligned} A(\omega) &= \frac{iB(J)}{\omega} (\cos \omega t - i \sin \omega t) \\ &+ \frac{jtM(J)}{\omega} (\cos \omega t - i \sin \omega t) \\ &+ \frac{M(J)}{\omega^2} (\cos \omega t - i \sin \omega t) \end{aligned} \Bigg]_{T(J)}^{T(J+1)} \quad (6.15)$$

Real and imaginary parts are separated in the form

$$A(\omega) = \alpha(\omega) + i \beta(\omega) \quad (6.16)$$

Thus

$$\begin{aligned} \alpha &= \frac{B(J)}{\omega} (\sin [\omega \times T(J+1)] - \sin [\omega \times T(J)]) \\ &+ \frac{M(J)}{\omega} (T(J+1) \sin [\omega \times T(J+1)] - T(J) \sin [\omega \times T(J)]) \\ &+ \frac{M(J)}{\omega^2} (\cos [\omega \times T(J+1)] - \cos [\omega \times T(J)]) \end{aligned} \quad (6.17)$$

$$\begin{aligned} \beta &= \frac{B(J)}{\omega} (\cos [\omega \times T(J+1)] - \cos [\omega \times T(J)]) \\ &+ \frac{M(J)}{\omega} (T(J+1) \cos [\omega \times T(J+1)] - T(J) \cos [\omega \times T(J)]) \\ &- \frac{M(J)}{\omega^2} (\sin [\omega \times T(J+1)] - \sin [\omega \times T(J)]) \end{aligned} \quad (6.18)$$

In polar form

$$A(\omega) = r \angle \theta \quad (6.19)$$

where $\gamma = \sqrt{\alpha^2 + \beta^2}$ (6.20)

and $\delta = \tan^{-1}\left(\frac{\alpha}{\beta}\right)$ (6.21)

When $\omega = 0$

$$A(\omega) = \int_{T(J)}^{T(J+1)} A(t) e^{\omega t} dt = \int_{T(J)}^{T(J+1)} A(t) dt \quad (6.22)$$

$$A(\omega) = \int_{T_1}^{T_2} (B(J) + M(J) \times t) dt \quad (6.23)$$

$$A(\omega) = \left[B(J) \times t + \frac{M(J)}{2} \times t^2 \right] \Big|_{T(J)}^{T(J+1)} \quad (6.24)$$

$$A(\omega) = B(J) [T(J+1) - T(J)] + \frac{M(J)}{2} [(T(J+1))^2 - (T(J))^2] \quad (6.25)$$

This is the real part. The imaginary part at $\omega = 0$ is zero.

A listing of the program TIFREQ is shown in Figure 6.20. The data required to operate the program are shown in the early comments of the listing.

The program is fairly well documented in the listing. The input data is read into arrays F (for frequency) and A (for amplitude). After it is read, it is printed out for inspection and for the record. The printing is under the control of character IOFLAG6. In this version of the program, IOFLAG6 is set internally to 1, the value that signifies that the input data is to be printed. If the user were to desire the option of printing or not printing the data, a value of IOFLAG6 could be read in as data. A value of 0 for IOFLAG6 would suppress the printing.

After the data is read and printed, the auxiliary arrays M and B are then formed according to equations 6.6 and 6.8. Equation 6.15 is then evaluated over each of the time intervals given by the input data, and the results are summed to give the integral over the total time interval covered by the input data. The evaluations are done in the subroutine FOURIER.

When F=0, a separate evaluation of equation 6.25 is done in lines 3660 through 3960.

10200 PROGRAM NAME IS TIFREQ
10400
10600 FOR COMPLETE INFORMATION ON THIS PROGRAM CONTACT
10800
11000 F.A. FISHER
11200 BLDG 9 ROOM 200
11400 GENERAL ELECTRIC CO.
11600 100 WOODLAWN AVE.
11800 PITTSFIELD, MASS 01201
12000
12200 PHONE (413)-494-4380
12400
12600 THIS PROGRAM ACCEPTS AN ARBITRARY FUNCTION OF TIME AND PROVIDES A
12800 FOURIER TRANSFORM OF THAT TIME FUNCTION.
13000
13200 THE PROGRAM REQUIRES DATA FROM AN INPUT FILE "TIFRFIL", THE
13400 CHARACTERISTICS OF WHICH FOLLOW;
13600
13800 1000 . KK
14000
14200 KK IS THE NUMBER OF PAIRS OF DATA, TIME AND AMPLITUDE
14400 THAT WILL BE USED TO DESCRIBE THE TIME FUNCTION
14600
14800 1010 FSTART,DECades
15000
15200 FSTART IS THE FIRST FREQUENCY (OTHER THAN ZERO) AT
15400 WHICH A CALCULATION WILL BE MADE.
15600
15800 DECADES IS THE NUMBER OF DECADES FOR WHICH THE
16000 CALCULATIONS WILL BE MADE.
16200
16400 2000 TIME, AMPLITUDE
16600 2010 TIME, AMPLITUDE
16800 2020 TIME, AMPLITUDE
17000
17200 THESE ARE PAIRED VALUES OF TIME AND AMPLITUDE THAT
17400 DESCRIBE THE TIME FUNCTION. THE TIME INTERVALS DO
17600 NOT HAVE TO BE OF EQUAL WIDTH. USE AS MANY LINES
17800 OF DATA AS NECESSARY.
18000
18200 THE PROGRAM AS HERE PRESENTED REQUIRES THE DATA FILE
18400 TO HAVE LINE NUMBERS. IT ALSO RESTRICTS THE INDIVIDUAL
18600 LINES OF DATA TO HAVE ONLY ONE PAIR OF DATA PER LINE.
18800
19000 THE PROGRAM ASSUMES THAT THE TIME FUNCTION IS DESCRIBED
19200 IN UNITS OF SECONDS. THE OUTPUT FREQUENCIES ARE THEN
19400 PRESENTED IN HERTZ (HZ) AND THE SPECTRAL DENSITIES
19600 PRESENTED IN UNITS OF VOLT-SECONDS PER CYCLE
19800 BANDWIDTH.
20000
20200 IF TIME IS PRESENTED IN MILLISECONDS THE FREQUENCIES
20400 WILL BE PRESENTED IN KILOHERTZ (KHZ) AND SPECTRAL
20600 DENSITIES IN VOLT-MILLISECONDS, REGARDLESS OF WHAT
20800 THE HEADINGS SAY. IF TIME IS IN MICROSECONDS THE

Figure 6.20 Program TIFREQ

```

2100C CORRESPONDING DATA WILL BE IN MEGAHERTZ (MHZ) AND
2120C VOLT-MICROSECONDS.
2140C -----
2160C DIMENSION T(110),B(110),M(110),F(110),A(110)
2200 DOUBLE PRECISION A,T,M,B,REAL4,OMEGA,REAL1,REAL2,XIMAG4,TOTAL
2220 DOUBLE PRECISION PHASE,POWER,OMEGINV,OMEGSQ,REAL3,XIMAG1
2240 DOUBLE PRECISION XIMAG2,XIMAG3
2260 INTEGER OUTFILE
2280 INTEGER DECADES
2300 INFILE=8
2320 OUTFILE=10
2340 IOFLAG6=1
2360 CALL OPENF(09,"TIFRFIL;",ISTAT,1,0,1)
2380 100 FORMAT(" ****")
2400 110 FORMAT(" ")
2420 WRITE(06,110)
2440 WRITE(06,110)
2460 WRITE(06,100)
2480 WRITE(06,110)
2500 WRITE(06,120)
2520 WRITE(06,110)
2540 120 FORMAT(" THIS IS THE TIME DOMAIN INPUT DATA")
2560 WRITE(06,110)
2580 PI=3.1415926536
2600 TWOP1=2.*PI
2620C -----
2640C THESE ARE THE BASIC FREQUENCIES AT WHICH THE OUTPUT WILL BE PRESENTED
2660 DATA F(1)/1./,F(2)/1.5/,F(3)/2./,F(4)/3./,F(5)/4./,F(6)/5./,F(7)/6./
2680 DATA F(8)/7./,F(9)/8./,F(10)/9./
2700C -----
2720C IN THE FOLLOWING SECTIONS THE INPUT DATA IS READ AND PRINTED
2740C INPUT OF TABULATED DATA FROM DATA FILE
2760 READ(09,6096)LINE,KK
2780 6096 FORMAT(V)
2800 READ(09,6096)LINE,FSTART,DECADES
2820 DO 150 I=1,10 ←
2840 F(I)=F(I)*FSTART ←
2860 150 CONTINUE ←
2880 DO 170 K=1,KK ←
2900 160 READ(09,6096,END=6150)LINE,T(K),A(K)
2920 KSAVE=K
2940 IF(K .GT. 1) GO TO 6136
2950 GO TO 170
2980 6136 IF(T(K)) 6150,6150,170
3000 170 CONTINUE ←
3020 6150 IF(IOFLAG6 .EQ. 0) GO TO 250 ←
3040 WRITE(06,220)
3060 220 FORMAT(//,3X,"TIME",11X,"AMPLITUDE")
3080 WRITE(06,240) (T(K),A(K),K=1,KK)
3100 240 FORMAT(1X,1E9.3,8X,1E9.3)
3120 250 CONTINUE ←
3140C THIS ENDS THE READING AND PRINTING OF INPUT DATA
3160C -----

```

Figure 6.20 (Continued) Program TIFREQ (Continued)

```

3180C THE FOLLOWING LINES PRINT THE OUTPUT HEADINGS
3200 WRITE(06,110)
3220 WRITE(06,100)
3240 WRITE(06,110)
3260 WRITE(06,130)
3280 130 FORMAT(" THIS IS THE FOURIER TRANSFORM OF THE ABOVE DATA")
3300 WRITE(06,110)
3320 WRITE(06,290)
3340 290 FORMAT(//,"FREQUENCY",7X,"REAL",6X,"IMAGINARY",5X,"TOTAL",6X,
3360 "PHASE",8X,"POWER")
3380 WRITE(06,310)
3400 310 FORMAT(3X,"HZ",10X,"VOLT-SEC",4X,"VOLT-SEC",4X,"VOLT-SEC",
3420 4X,"DEG",6X,"(VOLT-SEC**2")
3440C THIS ENDS THE PRINTING OF HEADINGS
3460C -----
3520 WRITE(06,110)
3540 DO 350 J=1,KSAVE <
3560 M(J)=(A(J+1)-A(J))/(T(J+1)-T(J))
3580 B(J)=A(J)-M(J)*T(J)
3600 350 CONTINUE
3640C -----
3660C THE FOLLOWING ROUTINE CALCULATES THE DC COMPONENT OF THE
3680C TRANSFORM; REAL4
3700 REAL4=0.
3720 FREQ=0.
3740 OMEGA=0.
3760 DO 430 J=1,KSAVE+1 <
3780 REAL1=B(J)*(T(J+1)-T(J))
3800 REAL2=M(J)*(.5)*(T(J+1)*T(J+1)-T(J)*T(J))
3820 REAL4=REAL1+REAL2+REAL4
3840 430 CONTINUE
3860 XIMAG4=0.
3880 TOTAL=REAL4
3900 PHASE=0.
3920 POWER=TOTAL**2.
3940 WRITE(06,480) FREQ,REAL4,XIMAG4,TOTAL,PHASE,POWER
3960 480 FORMAT(1X,1E9.3,4X,1E9.3,2X,1E10.3,3X,1E9.3,2X,1E10.3,4X,1E9.3)
3980C THIS ENDS THE ROUTINE THAT CALCULATES THE DC COMPONENT
4000C -----
4020C WE WILL NOW START THE ROUTINE FOR CALCULATING THE TRANSFORM
4040C AT FREQUENCIES GREATER THAN ZERO.
4060 AFREQ=FREQ
4080 AREAL4=REAL4
4100 DO 590 I=1,DECades <
4120 DO 580 L=1,10 <
4140 FREQ=F(L)*(10.***(I-1))
4160 CALL FOURIER(FREQ,KSAVE,REAL4,XIMAG4,TOTAL,POWER,PHASE,T,B,M)
4180 WRITE(06,576) FREQ,REAL4,XIMAG4,TOTAL,PHASE,POWER
4200 576 FORMAT(1X,1E9.3,4X,1E9.3,2X,1E10.3,3X,1E9.3,2X,1E10.3,4X,1E9.3)
4220 578 FORMAT(2E14.8)
4240 580 CONTINUE

```

Figure 6.20 (Continued) Program TIFREQ (Continued)

```

4260 590 CONTINUE
4280 WRITE(06,110)
4300 WRITE(06,100)
4320 WRITE(06,110)
4340 9999 CONTINUE
4360 STOP;END
4380C -----
4400C THE FOLLOWING SUBROUTINE EVALUATES THE EXPRESSIONS BY WHICH
4420C INTEGRALS ARE TAKEN
4440 SUBROUTINE FOURIER(FREQ,IKSAVE,REAL4,XIMAG4,TOTAL,POWER,PHASE,T,B,M)
4460 DOUBLE PRECISION REAL4,XIMAG4,TOTAL,POWER,PHASE,T,B,M
4480 DIMENSION T(110),B(110),M(110)
4500 PI=3.14159265367
4520 TWOPI=2.*PI
4540 OMEGA=TWOPI*FREQ
4560 OMEGINV=1./OMEGA
4580 OMEGSQ=OMEGINV**2
4600 REAL4=0.
4620 XIMAG4=0.
4640 DO 10280 INDEX=1,IKSAVE+1
4660 SIN1=DSIN(OMEGA*T(INDEX))
4680 SIN2=DSIN(OMEGA*T(INDEX+1))
4700 COS1=DCOS(OMEGA*T(INDEX))
4720 COS2=DCOS(OMEGA*T(INDEX+1))
4740 REAL1=B(INDEX)*OMEGINV*(SIN2-SIN1)
4760 REAL2=M(INDEX)*OMEGINV*(T(INDEX+1)*SIN2-T(INDEX)*SIN1)
4780 REAL3=M(INDEX)*OMEGSQ*(COS2-COS1)
4800 REAL4=REAL1+REAL2+REAL3+REAL4
4820 XIMAG1=B(INDEX)*OMEGINV*(COS2-COS1)
4840 XIMAG2=M(INDEX)*OMEGINV*(T(INDEX+1)*COS2-T(INDEX)*COS1)
4860 XIMAG3=M(INDEX)*OMEGSQ*(SIN2-SIN1)
4880 XIMAG4=XIMAG1+XIMAG2-XIMAG3+XIMAG4
4900 POWER=REAL4**2+XIMAG4**2
4920 TOTAL=DSQRT(POWER)
4940 PHASE=180.*(1/PI)*DATAN(XIMAG4/REAL4)
4960 IF(REAL4 .LT. 0.) GO TO 10240
4980 GO TO 10280
5000 10240 IF(XIMAG4 .LT. 0.) GO TO 10270
5020 PHASE=180.+PHASE
5040 GO TO 10280
5060 10270 PHASE=-180.-PHASE
5080 10280 CONTINUE
5100 RETURN;END
5120 STOP;END

```

Figure 6.20 (Conclusion) Program TIFREQ (Conclusion)

In the program, the following representations are used:

$$\begin{aligned} \text{REAL4} &= \text{Real part of transform} \\ &= \text{REAL1} + \text{REAL2} + \text{REAL3} \end{aligned} \quad (6.26)$$

where

$$\text{REAL1} = \frac{B(J)}{\omega} (\sin [\omega \times T(J+1)] - \sin [\omega \times T(J)]) \quad (6.27)$$

$$\text{REAL2} = \frac{M(J)}{\omega} (T(J+1) \sin [\omega \times T(J+1)] - T(J) \sin [\omega \times T(J)]) \quad (6.28)$$

$$\text{REAL3} = \frac{M(J)}{\omega^2} (\cos [\omega \times T(J+1)] - \cos [\omega \times T(J)]) \quad (6.29)$$

and where

$$\text{SIN1} = \sin [\omega \times T(J+1)] \quad (6.30)$$

$$\text{SIN2} = \sin [\omega \times T(J)] \quad (6.31)$$

$$\text{COS1} = \cos [\omega \times T(J+1)] \quad (6.32)$$

$$\text{COS2} = \cos [\omega \times T(J)] \quad (6.33)$$

Also

$$\begin{aligned} \text{XIMAG4} &= \text{Imaginary part of transform} \\ &= \text{XIMAG1} + \text{XIMAG2} - \text{XIMAG3} \end{aligned} \quad (6.34)$$

where

$$\text{XIMAG1} = \frac{B(J)}{\omega} (\cos [\omega \times T(J+1)] - \cos [\omega \times T(J)]) \quad (6.35)$$

$$\text{XIMAG2} = \frac{M(J)}{\omega} (T(J+1) \cos [\omega \times T(J+1)] - T(J) \cos [\omega \times T(J)]) \quad (6.36)$$

$$\text{XIMAG3} = \frac{M(J)}{\omega^2} (\sin [\omega \times T(J+1)] - \sin [\omega \times T(J)]) \quad (6.37)$$

6.3.3 Example of Usage of TIFREQ

As an example of usage of TIFREQ, let us determine the Fourier transform of the time-domain pulse shown (on two different time scales) in Figure 6.21.

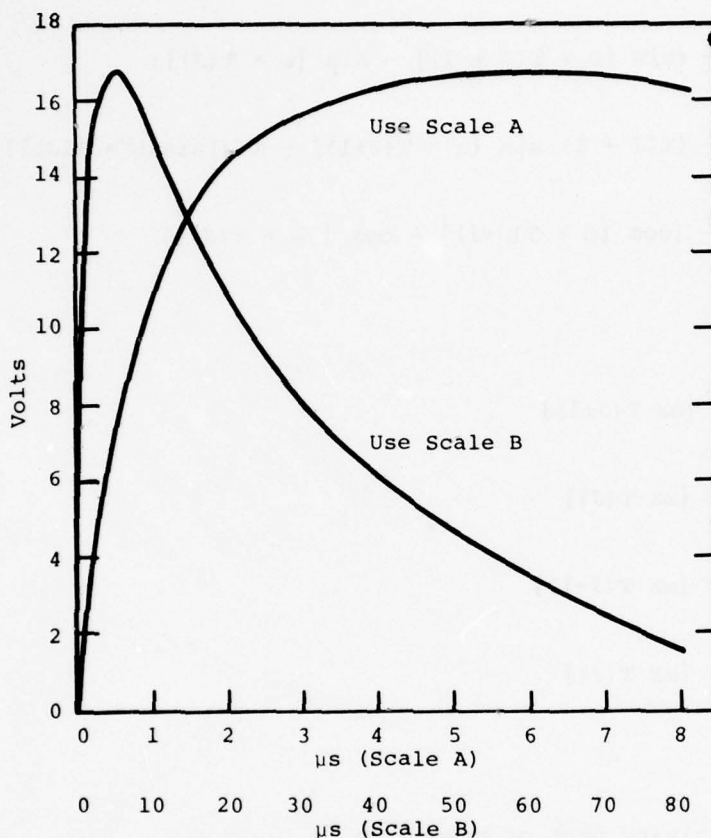


Figure 6.21 Time-Domain Test Wave

The input data for TIFREQ are shown in Figure 6.22. The output data is shown in Figures 6.23 and 6.24. A plot of the real and imaginary portions of the transform is shown in Figure 6.25. A plot of the total response (which would normally be obtained by measurement with a spectrum analyzer) is shown in Figure 6.26.

6.4 PROGRAM FREQTI

6.4.1 Purpose of FREQTI

FREQTI is a program that performs an inverse Fourier transform of a frequency-domain system response and gives the corresponding time-domain response. The frequency-domain data are described by paired values of frequency and amplitude. The

1000 39
1010 10,6
2000 0,0
2010 1E-7,1.5
2020 2E-7,3.1
2030 3E-7,4.6
2040 4E-7,6.2
2050 5E-7,7.2
2060 6E-7,8.1
2080 8E-7,9.5
2100 1E-6,10.5
2120 1.2E-6,11.5
2140 1.4E-6,12.3
2160 1.6E-6,13
2180 1.8E-6,13.6
2200 2.0E-6,14.0
2250 2.5E-6,14.8
2300 3E-6,15.40
2350 3.5E-6,15.7
2400 4.0E-6,16.1
2405 4.5E-6,16.3
2410 5E-6,16.4
2415 5.5E-6,16.5
2420 6E-6,16.6
2425 6.5E-6,16.62
2430 7E-6,16.6
2435 7.5E-6,16.50
2440 8E-6,16.4
2450 9E-6,16.0
2460 1E-5,15.5
2465 1.5E-5,13.0
2470 2E-5,11.2
2475 2.5E-5,9.7
2480 3E-5,8.5
2490 4E-5,6.5
2500 5E-5,5
2510 6E-5,3.7
2520 7E-5,2.7
2525 8E-5,1.6
2530 9E-5,0.6
2540 1E-4,0

Figure 6.22 Input Data for TIFREQ

THIS IS THE TIME DOMAIN INPUT DATA

TIME	AMPLITUDE
0.	0.
0.100E-06	0.150E 01
0.200E-06	0.310E 01
0.300E-06	0.460E 01
0.400E-06	0.620E 01
0.500E-06	0.720E 01
0.600E-06	0.810E 01
0.800E-06	0.950E 01
0.100E-05	0.105E 02
0.120E-05	0.115E 02
0.140E-05	0.123E 02
0.160E-05	0.130E 02
0.180E-05	0.136E 02
0.200E-05	0.140E 02
0.250E-05	0.148E 02
0.300E-05	0.154E 02
0.350E-05	0.157E 02
0.400E-05	0.161E 02
0.450E-05	0.163E 02
0.500E-05	0.164E 02
0.550E-05	0.165E 02
0.600E-05	0.166E 02
0.650E-05	0.166E 02
0.700E-05	0.166E 02
0.750E-05	0.165E 02
0.800E-05	0.164E 02
0.900E-05	0.160E 02
0.100E-04	0.155E 02
0.150E-04	0.130E 02
0.200E-04	0.112E 02
0.250E-04	0.970E 01
0.300E-04	0.850E 01
0.400E-04	0.650E 01
0.500E-04	0.500E 01
0.600E-04	0.370E 01
0.700E-04	0.270E 01
0.800E-04	0.160E 01
0.900E-04	0.600E 00
0.100E-03	0.

Figure 6.23 First Part of TIFREQ Output Data

THIS IS THE FOURIER TRANSFORM OF THE ABOVE DATA

FREQUENCY HZ	REAL VOLT-SEC	IMAGINARY VOLT-SEC	TOTAL VOLT-SEC	PHASE DEG	POWER (VOLT-SEC ²)
0.	0.620E-03	0.	0.620E-03	0.	0.385E-06
0.100E 02	0.622E-03	-0.111E-05	0.622E-03	-0.102E 00	0.387E-06
0.150E 02	0.622E-03	-0.166E-05	0.622E-03	-0.153E 00	0.386E-06
0.200E 02	0.621E-03	-0.221E-05	0.621E-03	-0.204E 00	0.385E-06
0.300E 02	0.620E-03	-0.332E-05	0.620E-03	-0.307E 00	0.385E-06
0.400E 02	0.620E-03	-0.442E-05	0.620E-03	-0.409E 00	0.384E-06
0.500E 02	0.620E-03	-0.553E-05	0.620E-03	-0.511E 00	0.385E-06
0.600E 02	0.620E-03	-0.664E-05	0.620E-03	-0.613E 00	0.385E-06
0.700E 02	0.620E-03	-0.774E-05	0.620E-03	-0.715E 00	0.385E-06
0.800E 02	0.620E-03	-0.885E-05	0.620E-03	-0.818E 00	0.385E-06
0.900E 02	0.620E-03	-0.995E-05	0.620E-03	-0.920E 00	0.385E-06
0.100E 03	0.620E-03	-0.111E-04	0.620E-03	-0.102E 01	0.385E-06
0.150E 03	0.620E-03	-0.166E-04	0.620E-03	-0.153E 01	0.385E-06
0.200E 03	0.620E-03	-0.221E-04	0.620E-03	-0.204E 01	0.384E-06
0.300E 03	0.619E-03	-0.331E-04	0.620E-03	-0.307E 01	0.384E-06
0.400E 03	0.618E-03	-0.441E-04	0.619E-03	-0.409E 01	0.384E-06
0.500E 03	0.616E-03	-0.551E-04	0.619E-03	-0.511E 01	0.383E-06
0.600E 03	0.615E-03	-0.660E-04	0.618E-03	-0.613E 01	0.382E-06
0.700E 03	0.613E-03	-0.768E-04	0.617E-03	-0.715E 01	0.381E-06
0.800E 03	0.610E-03	-0.876E-04	0.617E-03	-0.816E 01	0.380E-06
0.900E 03	0.608E-03	-0.982E-04	0.616E-03	-0.918E 01	0.379E-06
0.100E 04	0.605E-03	-0.109E-03	0.615E-03	-0.102E 02	0.378E-06
0.150E 04	0.586E-03	-0.160E-03	0.607E-03	-0.153E 02	0.369E-06
0.200E 04	0.561E-03	-0.207E-03	0.598E-03	-0.203E 02	0.357E-06
0.300E 04	0.494E-03	-0.286E-03	0.570E-03	-0.301E 02	0.325E-06
0.400E 04	0.412E-03	-0.340E-03	0.534E-03	-0.395E 02	0.286E-06
0.500E 04	0.327E-03	-0.367E-03	0.492E-03	-0.483E 02	0.242E-06
0.600E 04	0.246E-03	-0.370E-03	0.444E-03	-0.563E 02	0.197E-06
0.700E 04	0.178E-03	-0.353E-03	0.395E-03	-0.633E 02	0.156E-06

Figure 6.24 Second Part of TIFREQ Output Data

0.800E 04	0.125E-03	-0.324E-03	0.347E-03	-0.689E 02	0.121E-06
0.900E 04	0.893E-04	-0.290E-03	0.304E-03	-0.729E 02	0.922E-07
0.100E 05	0.684E-04	-0.258E-03	0.266E-03	-0.751E 02	0.710E-07
0.150E 05	0.451E-04	-0.187E-03	0.192E-03	-0.764E 02	0.370E-07
0.200E 05	0.474E-05	-0.151E-03	0.151E-03	-0.882E 02	0.228E-07
0.300E 05	-0.121E-04	-0.101E-03	0.102E-03	-0.263E 03	0.104E-07
0.400E 05	-0.185E-04	-0.705E-04	0.729E-04	-0.255E 03	0.531E-08
0.500E 05	-0.205E-04	-0.513E-04	0.552E-04	-0.248E 03	0.305E-08
0.600E 05	-0.185E-04	-0.387E-04	0.429E-04	-0.244E 03	0.184E-08
0.700E 05	-0.171E-04	-0.297E-04	0.343E-04	-0.240E 03	0.117E-08
0.800E 05	-0.150E-04	-0.234E-04	0.278E-04	-0.237E 03	0.771E-09
0.900E 05	-0.125E-04	-0.197E-04	0.233E-04	-0.238E 03	0.543E-09
0.100E 06	-0.114E-04	-0.170E-04	0.205E-04	-0.236E 03	0.419E-09
0.150E 06	-0.771E-05	-0.946E-05	0.122E-04	-0.231E 03	0.149E-09
0.200E 06	-0.623E-05	-0.550E-05	0.831E-05	-0.221E 03	0.691E-10
0.300E 06	-0.353E-05	-0.243E-05	0.429E-05	-0.214E 03	0.184E-10
0.400E 06	-0.238E-05	-0.121E-05	0.267E-05	-0.207E 03	0.713E-11
0.500E 06	-0.161E-05	-0.811E-06	0.180E-05	-0.207E 03	0.326E-11
0.600E 06	-0.131E-05	-0.472E-06	0.139E-05	-0.200E 03	0.193E-11
0.700E 06	-0.988E-06	-0.344E-06	0.105E-05	-0.199E 03	0.109E-11
0.800E 06	-0.907E-06	-0.224E-06	0.934E-06	-0.194E 03	0.872E-12
0.900E 06	-0.723E-06	-0.585E-07	0.726E-06	-0.185E 03	0.527E-12
0.100E 07	-0.537E-06	0.351E-08	0.537E-06	0.180E 03	0.288E-12
0.150E 07	-0.195E-06	0.694E-07	0.207E-06	0.160E 03	0.430E-13
0.200E 07	-0.808E-07	0.301E-07	0.863E-07	0.160E 03	0.744E-14
0.300E 07	-0.471E-07	-0.113E-07	0.484E-07	-0.194E 03	0.234E-14
0.400E 07	-0.273E-07	0.465E-08	0.277E-07	0.170E 03	0.766E-15
0.500E 07	0.105E-08	0.896E-16	0.105E-08	0.487E-05	0.111E-17
0.600E 07	-0.121E-07	-0.207E-08	0.123E-07	-0.190E 03	0.151E-15
0.700E 07	-0.865E-08	0.208E-08	0.889E-08	0.166E 03	0.791E-16
0.800E 07	-0.505E-08	-0.188E-08	0.539E-08	-0.200E 03	0.291E-16
0.900E 07	-0.663E-08	-0.434E-10	0.663E-08	-0.180E 03	0.439E-16

Figure 6.24 (Conclusion) Second Part of TIFREQ Output Data (Conclusion)

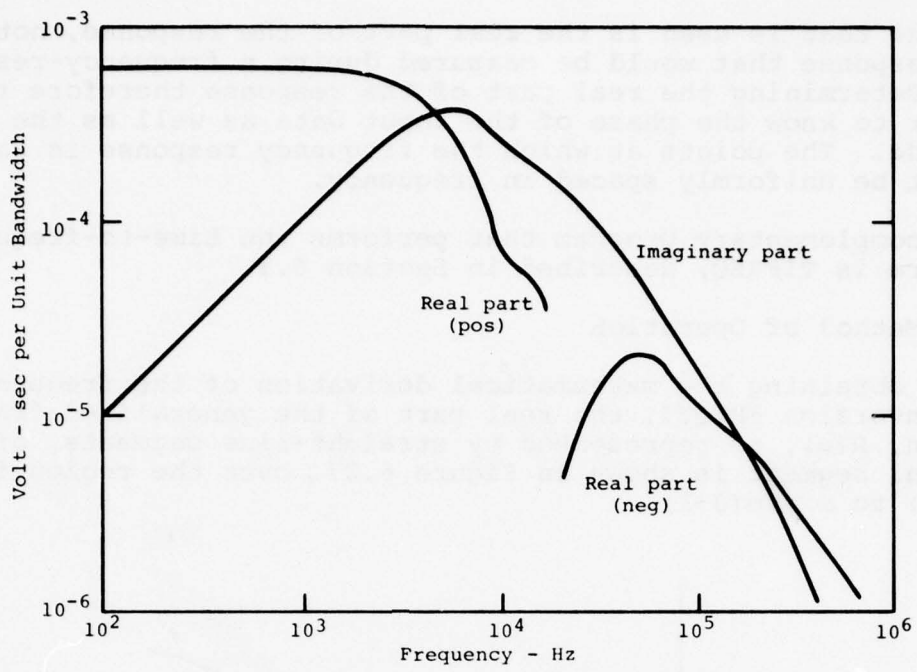


Figure 6.25 Real and Imaginary Parts of Fourier Transform

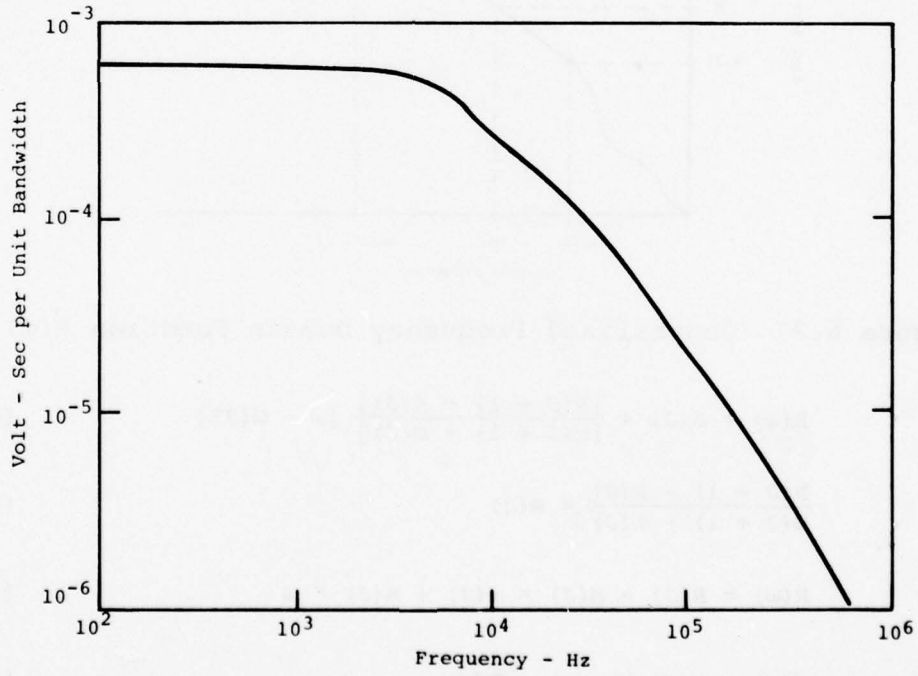


Figure 6.26 Total Part of Fourier Transform

amplitude that is used is the real part of the response, not the total response that would be measured during a frequency-response test. Determining the real part of the response therefore requires the user to know the phase of the input data as well as the total amplitude. The points at which the frequency response is sampled need not be uniformly spaced in frequency.

A complementary program that performs the time-to-frequency transform is TIFREQ, described in Section 6.3.

6.4.2 Method of Operation

In obtaining the mathematical derivation of the frequency-to-time conversion FREQT1, the real part of the generalized frequency function, $R(\omega)$, is represented by straight-line segments, of which a typical segment is shown in Figure 6.27, over the region from $\omega = \omega(J)$ to $\omega = \omega(J+1)$.

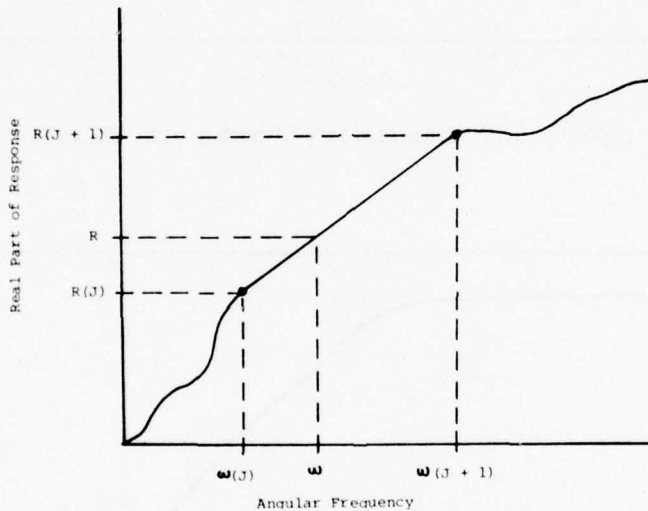


Figure 6.27 Generalized Frequency Domain Function $R(\omega)$

$$\text{Thus } R(\omega) = R(J) + \frac{[R(J+1) - R(J)]}{[\omega(J+1) - \omega(J)]} [\omega - \omega(J)] \quad (6.38)$$

$$\text{If } \frac{R(J+1) - R(J)}{\omega(J+1) - \omega(J)} = M(J) \quad (6.39)$$

$$\text{then } R(\omega) = R(J) - M(J) \times \omega(J) + M(J) \times \omega \quad (6.40)$$

$$\text{Also, if } R(\omega) - M(J) \times \omega(J) = B(J) \quad (6.41)$$

$$\text{then } R(\omega) = B(J) + M(J) \times \omega \quad (6.42)$$

If $R(\omega)$ is the real part of the Fourier Transform of $A(t)$, then

$$A(t) = 0 \text{ if } t < 0$$

$$A(t) = \frac{1}{\pi} \int_0^{\infty} R(\omega) d\omega \text{ if } t = 0 \quad (6.43)$$

$$A(t) = \frac{2}{\pi} \int_0^{\infty} R(\omega) \cos \omega t d\omega \text{ if } t > 0$$

For $t > 0$, the contribution toward $A(t)$ of the portion of the $R(\omega)$ spectrum from $\omega(J)$ to $\omega(J + 1)$ is

$$A(t) = \frac{2}{\pi} \int_{\omega(J)}^{\omega(J + 1)} R(\omega) \cos \omega t d\omega \quad (6.44)$$

$$A(t) = \frac{2}{\pi} \int_{\omega(J)}^{\omega(J + 1)} [B(J) + M(J)\omega] \cos (\omega t) d\omega \quad (6.45)$$

$$\begin{aligned} A(t) &= \frac{2}{\pi} \int_{\omega(J)}^{\omega(J + 1)} B(J) \cos (\omega t) d\omega \\ &\quad + \frac{2}{\pi} \int_{\omega(J)}^{\omega(J + 1)} M(J) \omega \cos (\omega t) d\omega \end{aligned} \quad (6.46)$$

$$\begin{aligned} A(t) &= \left[\frac{2 B(J)}{\pi t} \sin (\omega t) + \frac{2 M(J)}{\pi t^2} \cos (\omega t) \right. \\ &\quad \left. + \frac{2 M(J) \omega}{t} \sin (\omega t) \right] \Big|_{\omega(J)}^{\omega(J + 1)} \end{aligned} \quad (6.47)$$

$$\begin{aligned} A(t) &= \frac{2 B(J)}{\pi} \times \frac{1}{t} \times [\sin (\omega(J + 1)t) - \sin (\omega(J)t)] \\ &\quad + \frac{2 M(J)}{\pi} \times \frac{1}{t} \times \frac{1}{t} \times [\cos (\omega(J + 1)t) - \cos (\omega(J)t)] \end{aligned} \quad (6.48)$$

$$+ \frac{2 M(J)}{\pi} \times \frac{1}{t} \times [\omega(J + 1) \sin (\omega(J + 1)t) - \omega(J) \sin (\omega(J)t)]$$

$$\text{For } t = 0, A(t) = \frac{1}{\pi} \int_0^{\infty} R(\omega) d\omega \quad (6.49)$$

and the contribution from $\omega(J)$ to $\omega(J + 1)$ is

$$A(t) = \frac{1}{\pi} \int_{\omega(J)}^{\omega(J + 1)} (B(J) + M(J)\omega) d\omega \quad (6.50)$$

$$A(t) = \frac{1}{\pi} \int_{\omega(J)}^{\omega(J + 1)} B(J) \omega + \frac{1}{\pi} \int_{\omega(J)}^{\omega(J + 1)} M(J)\omega d\omega \quad (6.51)$$

$$A(t) = \frac{B(J)}{\pi} [\omega]_{\omega(J)}^{\omega(J + 1)} + \frac{M(J)}{2\pi} [\omega^2]_{\omega(J)}^{\omega(J + 1)} \quad (6.52)$$

$$A(t) = \frac{B(J)}{\pi} [\omega(J + 1) - \omega(J)] + \frac{M(J)}{2\pi} [(\omega(J + 1))^2 - (\omega(J))^2] \quad (6.53)$$

A listing of the program FREQTI is shown in Figure 6.28. The data required to operate the program are shown in the early comments of the listing.

The program is documented in the listing. The input data is read into arrays FREQ and XREAL. After it is read, it is printed out for inspection and for the record. The printing is under the control of a control character, IOFLAG8. In this version of the program, IOFLAG8 is set internally to 1, the value that signifies that the input data is to be printed. If the user were to desire the option of printing or not printing the data, a value of IOFLAG8 could be read in as data. A value of 0 for IOFLAG8 would suppress the printing.

After the data are read and printed, the auxiliary arrays XM and B are then formed according to Equations 6.39 and 6.41. Equation 6.48 is then evaluated over each of the frequency intervals given by the input data, and the results are summed to give the integral over the total frequency interval covered by the input data.

When $t = 0$, a separate evaluation of Equation 6.53 is done in lines 3600 through 3780.

In the program, the following representations are used:

VECTOR = amplitude of time function

= V1 + V2 + V3

where

$$V1 = \frac{2 B(J)}{\pi} \times \frac{1}{t} \times [\sin(\omega(J + 1)t) - \sin(\omega(J)t)] \quad (6.54)$$

1020C PROGRAM NAME IS FREQTI
1040C
1060C FOR DETAILED INFORMATION ON THIS PROGRAM CONTACT
1080C
1100C F. A. FISHER
1120C BLDG 9 ROOM 200
1140C GENERAL ELECTRIC COMPANY
1160C 100 WOODLAWN AVE
1180C PITTSFIELD, MASS 01201
1200C
1220C PHONE (413)-494-4380
1240C
1260C THIS PROGRAM ACCEPTS THE REAL PART OF A FUNCTION OF FREQUENCY
1280C AND PROVIDES AN INVERSE FOURIER TRANSFORM TO GIVE THE TIME
1300C DOMAIN FUNCTION.
1320C
1340C THE PROGRAM REQUIRES DATA FROM AN INPUT FILE "FRTIFIL", THE
1360C CHARACTERISTICS OF WHICH FOLLOW;
1380C
1400C 1000 LL
1420C
1440C LL IS THE NUMBER OF PAIRS OF DATA, FREQUENCY AND
1460C AMPLITUDE (REAL PART ONLY) THAT DESCRIBE THE
1480C FREQUENCY FUNCTION.
1500C
1520C 2000 FREQUENCY, AMPLITUDE OF REAL PART
1540C 2010 FREQUENCY, AMPLITUDE
1560C 2020 FREQUENCY, AMPLITUDE
1580C
1600C THESE ARE PAIRED VALUES OF FREQUENCY AND AMPLITUDE
1620C THAT DESCRIBE THE FREQUENCY FUNCTION. THE
1640C FREQUENCIES DO NOT HAVE TO BE EVENLY SPACED. USE
1660C AS MANY LINES OF DATA AS NECESSARY.
1680C
1700C 3000 TSTART1,TSTOP1,TSTEP1
1720C
1740C THE PROGRAM ALLOWS YOU TO CALCULATE THE INVERSE
1760C TRANSFORM OVER TWO DIFFERENT TIME RANGES.
1780C
1800C TSTART1 IS THE TIME AT WHICH YOU WANT THE FIRST
1820C INTERVAL TO START. MOST COMMONLY TSTART1 WILL
1840C BE ZERO.
1860C
1880C TSTOP1 IS THE TIME AT WHICH YOU WANT THE FIRST
1900C INTERVAL TO END.
1920C
1940C BETWEEN TSTART1 AND TSTOP1 THE OUTPUT WILL BE
1960C PRESENTED AT TIMES THAT ARE TSTEP1 APART.
1980C
2000C
2020C 3010 TSTOP2,TSTEP2
2040C
2060C THESE VALUES DESCRIBE THE SECOND TIME INTERVAL.
2080C THAT INTERVAL WILL START AT TSTOP1, END AT STOP2

Figure 6.28 Program FREQTI 82.3 script

```

2100C AND WILL BE COVERED IN INCREMENTS OF TSTEP2.
2120C
2140C THE PROGRAM ASSUMES THAT THE FREQUENCIES ARE
2160C DESCRIBED IN UNITS OF HERTZ AND THAT TIME IS
2180C DESCRIBED IN UNITS OF SECONDS.
2200C
2220C IF FREQUENCY IS IN KILOHERTZ TIME SHOULD BE IN
2240C MILLISECONDS. IF FREQUENCY IS IN MEGAHERTZ
2260C TIME SHOULD BE IN MICROSECONDS.
2280C
2300C -----
2320 DIMENSION B(110),FREQ(110),XM(110),OMEGA(110),XREAL(110)
2340 DOUBLE PRECISION B,FREQ,XM,OMEGA,XREAL
2360 CALL OPENF(09,"FRTIFIL;",ISTAT,1,0,1)
2380 100 FORMAT(" ****")
2400 110 FORMAT(" ")
2420 WRITE(06,110)
2440 WRITE(06,100)
2460 WRITE(06,110)
2480 115 FORMAT(" THIS IS THE FREQUENCY DOMAIN INPUT DATA")
2500 120 FORMAT(" THIS IS THE INVERSE TRANSFORM OF THE ABOVE DATA")
2520 WRITE(06,115)
2540 IOFLAG8=1
2560 PI=3.1415926536
2580 PINV=1./PI
2600 TOPINV=2.*PINV
2620C -----
2640C THE FOLLOWING SECTIONS READ AND PRINT THE INPUT DATA
2660C THE INPUT DATA IS STORED IN ARRAYS FREQ AND XREAL
2680 READ(09,161,END=180)LINE,LL
2700 DO 170 I=1,LL
2720 READ(09,161,END=180)LINE,FREQ(I),XREAL(I)
2740 ISAVE=I
2760 161 FORMAT(V)
2780 170 CONTINUE
2800 180 CONTINUE
2820 7170 IF(IOFLAG8) 250,250,210
2840 210 WRITE(06,220)
2860 220 FORMAT(//,8X,"FREQUENCY",8X,"AMPLITUDE")
2880 WRITE(06,222)
2900 WRITE(06,110)
2920 222 FORMAT(25X,"REAL")
2940 DO 245 J=1,ISAVE
2960 WRITE(06,240) FREQ(J),XREAL(J)
2980 240 FORMAT(3X,1E14.3,3X,1E14.3)
3000 245 CONTINUE
3020 250 NFILE=1
3040C THIS ENDS THE READING OF INPUT FREQUENCY DATA
3060C -----
3080C WE NOW START READING THE TIME VALUES THAT CONTROL THE RANGE
3100C OVER WHICH CALCULATIONS ARE MADE
3120 READ(09,161,END=180)LINE,TSTART1,TSTOP1,TSTEP1
3140 READ(09,161,END=180)LINE,TSTOP2,TSTEP2
3160C -----

```

Figure 6.28 (Continued) Program FREQTI (Continued)

```

3180 265 FORMAT(V)
3200C WE WILL NOW START THE CALCULATIONS OF THE INVERSE TRANSFORM
3220 WRITE(06,110)
3240 WRITE(06,100)
3260 WRITE(06,110)
3280 WRITE(06,120)
3300 WRITE(06,110)
3320 WRITE(06,290)
3340 WRITE(06,110)
3360 290 FORMAT(//,9X,"TIME",12X,"AMPLITUDE")
3380 DO 320 K=1,ISAVE ←
3400 OMEGA(K)=2.*PI*FREQ(K)
3420 320 CONTINUE
3440C -----
3460 DO 360 L=1,ISAVE ←
3480 XM(L)=(XREAL(L+1)-XREAL(L))/(OMEGA(L+1)-OMEGA(L))
3500 B(L)=XREAL(L)-(XM(L)*OMEGA(L))
3520 360 CONTINUE
3540 TIME=TSTART1
3560 IF(TIME .GT. 0.) GO TO 480
3580C -----
3600C THIS IS THE ROUTINE THAT PERFORMS THE CALCULATIONS IF T=0
3620 VECTOR=0.
3640 TIME=0.
3660 DO 440 N=1,ISAVE ←
3680 V1=PINV*B(N)*(OMEGA(N+1)-OMEGA(N))
3700 V2=XM(N)*PINV*((OMEGA(N+1)**2)-(OMEGA(N)**2))*(.5)
3720 VECTOR=V1+V2+VECTOR
3740 440 CONTINUE
3760 WRITE(06,460) TIME,VECTOR
3780 460 FORMAT(3X,1E14.3,3X,1E14.3)
3800C -----
3820C THIS IS THE ROUTINE THAT PERFORMS THE CALCULATIONS IF T>0
3840 7500 TIME=TIME+TSTEP1 ←
3860 GO TO 480
3880 477 TIME=TIME+TSTEP2 ↓
3900 480 VECTOR=0. ←
3920 TINV=1./TIME
3940 TINVSQ=TINV**2
3960 DO 600 NDX=1,ISAVE+1 ←
3980 SIN1=DSIN(OMEGA(NDX)*TIME)
4000 SIN2=DSIN(OMEGA(NDX+1)*TIME)
4020 COS1=DCOS(OMEGA(NDX)*TIME)
4040 COS2=DCOS(OMEGA(NDX+1)*TIME)
4060 V1=TOPINV*(B(NDX)*TINV*(SIN2-SIN1))
4080 V2=TOPINV*XM(NDX)*TINV*(COS2-COS1)
4100 V3=TOPINV*XM(NDX)*TINV*(OMEGA(NDX+1)*SIN2-OMEGA(NDX)*SIN1)
4120 VECTOR=V1+V2+V3+VECTOR
4140 600 CONTINUE
4160 WRITE(06,606) TIME,VECTOR
4180 606 FORMAT(3X,1E14.3,3X,1E14.3)
4200 IF(TIME .GE. TSTOP1) GO TO 7710
4220 GO TO 7500
4240 7710 IF(TIME .GE. TSTOP2) GO TO 999 ←

```

Figure 6.28 (Continued) Program FREQTI (Continued)

```

4260 GO TO 477
4280 999 CONTINUE
4300 WRITE(06,110)
4320 WRITE(06,100)
4340 WRITE(06,110)
4360 STOP;END

```

Figure 6.28 (Conclusion) Program FREQTI (Conclusion)

$$v_2 = \frac{2 M(J)}{\pi} \times \frac{1}{t} \times \frac{1}{t} \times [\cos(\omega(J+1)t) - \cos(\omega(J)t)] \quad (6.55)$$

$$v_3 = \frac{2 M(J)}{\pi} \times \frac{1}{t} \times \frac{1}{t} \times [\omega(J+1)\sin(\omega(J+1)t) - \omega(J)\sin(\omega(J)t)] \quad (6.56)$$

and where

$$\text{SIN1} = \sin(\omega(J)t) \quad (6.57)$$

$$\text{SIN2} = \sin(\omega(J+1)t) \quad (6.58)$$

$$\text{COS1} = \cos(\omega(J)t) \quad (6.59)$$

$$\text{COS2} = \cos(\omega(J+1)t) \quad (6.60)$$

6.4.3 Example of Usage of FREQTI

As an example of usage of FREQTI, let us determine the inverse Fourier transform of the frequency-domain data 6.24 and 6.25. That data is, of course, the Fourier transform of the time-domain pulse shown in Figure 6.21.

The input data for FREQTI are shown in Figure 6.29. The output data are shown in Figures 6.30 and 6.31. A plot of the output data is shown in Figure 6.32. The waveform of the reconstructed pulse is very similar to the original pulse used as input to TIFREQ, as indeed it should be. The data from which the time domain output was constructed for times greater than 10 microseconds were obtained by running FREQTI again with different values for TSTART1, TSTOP1, TSTEP1, TSTOP2 and TSTEP2. That data is not shown in tabular form.

```

1000 24
2000 0,.620E-3
2010 10,.622E-3
2030 30,.620E-3
2090 200,.620E-3
2200 800,.610E-3
2400 4000,.412E-3
2450 7000,.178E-3
2480 9000,.893E-4
2500 15000,.451E-4
2510 .2E5,.474E-5
2520 .3E5,-.121E-4
2530 .5E5,-.205E-4
2540 .7E5,-.171E-4
2570 .9E5,-.125E-4
2590 .150E6,-.771E-5
2610 .3E6,-.353E-5
2630 .5E6,-.161E-5
2650 .7E6,-.988E-6
2670 .9E6,-.723E-6
2690 .150E7,-.195E-6
2720 .3E7,-.471E-7
2740 .5E7,.105E-8
2760 .7E7,-.865E-8
2780 .9E8,-.663E-8
3000 0,2E-6,1E-7
3010 10E-6,.5E-6

```

Figure 6.29 Input Data for FREQTI

6.5 INTERNAL IMPEDANCE

Inside a conducting shell there will be both electric and magnetic fields, the magnitudes of which are related by the impedance of the air space within the shell.

$$\frac{E}{H} = Z \quad (6.61)$$

where E = magnitude of the electric field
 H = magnitude of the magnetic field

A wave travelling in free space encounters an impedance of 377 Ω . Inside closed structures the impedance is less, at least at frequencies below the self-resonant frequencies of the enclosed volume.

THIS IS THE FREQUENCY DOMAIN INPUT DATA

FREQUENCY	AMPLITUDE REAL
0.	0.620E-03
0.100E 02	0.622E-03
0.300E 02	0.620E-03
0.200E 03	0.620E-03
0.800E 03	0.610E-03
0.400E 04	0.412E-03
0.700E 04	0.178E-03
0.900E 04	0.893E-04
0.150E 05	0.451E-04
0.200E 05	0.474E-05
0.300E 05	-0.121E-04
0.500E 05	-0.205E-04
0.700E 05	-0.171E-04
0.900E 05	-0.125E-04
0.150E 06	-0.771E-05
0.300E 06	-0.353E-05
0.500E 06	-0.161E-05
0.700E 06	-0.988E-06
0.900E 06	-0.723E-06
0.150E 07	-0.195E-06
0.300E 07	-0.471E-07
0.500E 07	0.105E-08
0.700E 07	-0.865E-08
0.900E 08	-0.663E-08

Figure 6.30 First Part of Output Data

The field pattern within enclosures is quite complex. At the surface of the enclosure, the electric field tangential to the surface must be zero (for perfect conductors), whereas the magnetic field is zero normal to the surface. Magnetic fields can exist only tangential to the surface, and electric fields can exist only normal to the surface. At all other points, the electric- and magnetic-field vectors will be oriented at right angles to each other, and will have amplitudes related to the physical characteristics of the enclosure and the frequency involved.

One type of structure that is easy to visualize is the open-ended, infinitely long cylinder shown in Figure 6.33. Kozakoff, et al, (Reference 6.1) show that the internal impedance that characterizes such a structure is

THIS IS THE INVERSE TRANSFORM OF THE ABOVE DATA

TIME	AMPLITUDE
0.	-0.934E 00
0.100E-06	0.857E 00
0.200E-06	0.297E 01
0.300E-06	0.448E 01
0.400E-06	0.587E 01
0.500E-06	0.702E 01
0.600E-06	0.803E 01
0.700E-06	0.876E 01
0.800E-06	0.936E 01
0.900E-06	0.996E 01
0.100E-05	0.106E 02
0.110E-05	0.112E 02
0.120E-05	0.118E 02
0.130E-05	0.123E 02
0.140E-05	0.127E 02
0.150E-05	0.130E 02
0.160E-05	0.133E 02
0.170E-05	0.135E 02
0.180E-05	0.138E 02
0.190E-05	0.141E 02
0.200E-05	0.143E 02
0.210E-05	0.145E 02
0.260E-05	0.152E 02
0.310E-05	0.157E 02
0.360E-05	0.161E 02
0.410E-05	0.164E 02
0.460E-05	0.165E 02
0.510E-05	0.166E 02
0.560E-05	0.168E 02
0.610E-05	0.168E 02
0.660E-05	0.168E 02
0.710E-05	0.166E 02
0.760E-05	0.165E 02
0.810E-05	0.163E 02
0.860E-05	0.161E 02
0.910E-05	0.159E 02
0.960E-05	0.157E 02
0.101E-04	0.155E 02

Figure 6.31 Second Part of Output Data

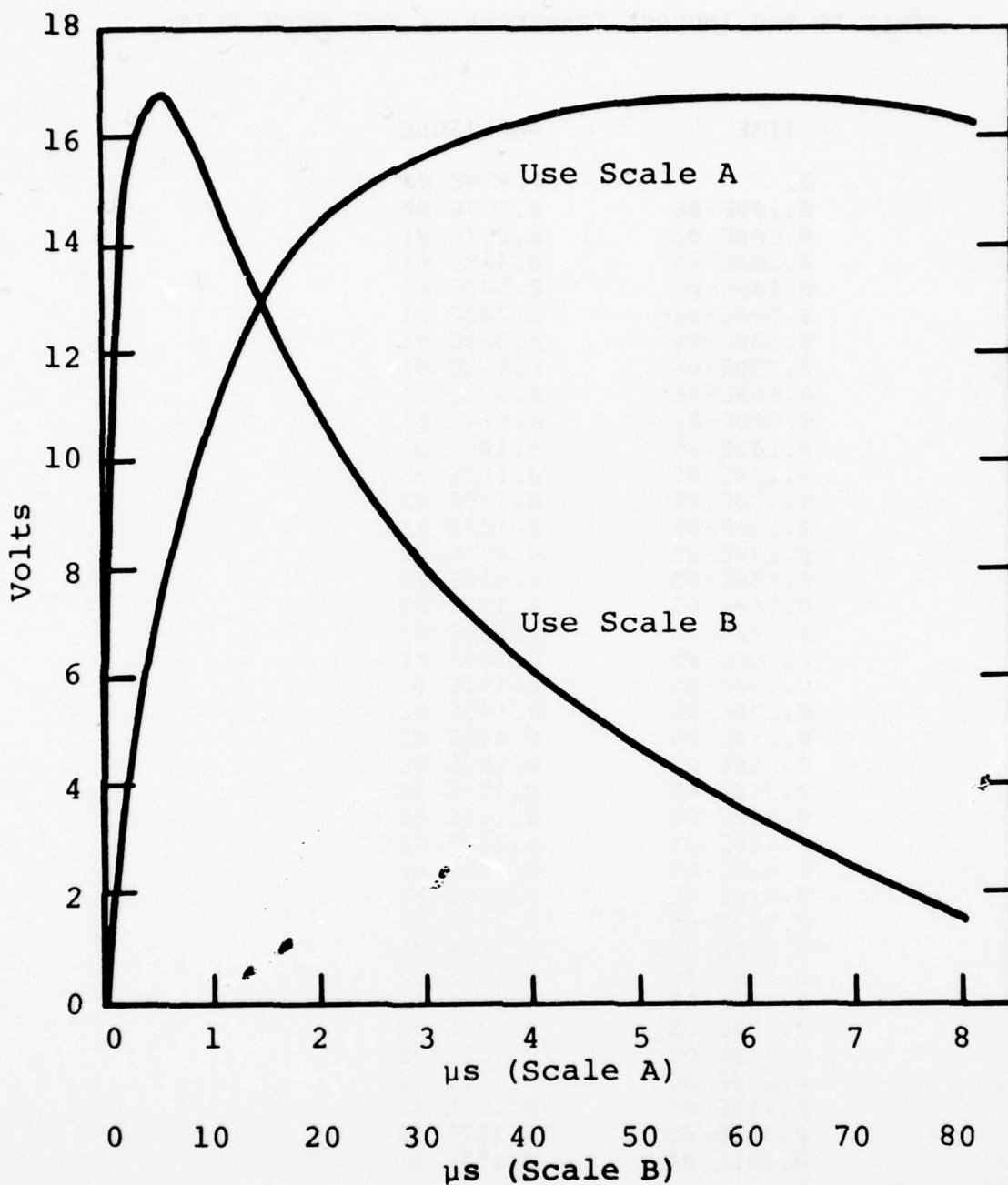


Figure 6.32 Reconstructed Time Domain Wave

$$Z_W = \frac{E_0}{H_z} = \frac{j\omega\mu_0 A}{L} \quad (6.62)$$

where ω = angular frequency
 $\mu_0 = 4 \times 10^{-7}$
 A = enclosed area
 L = peripheral distance around the enclosure

E_0 = circumferential electric field
 H_z = magnetic field along axis

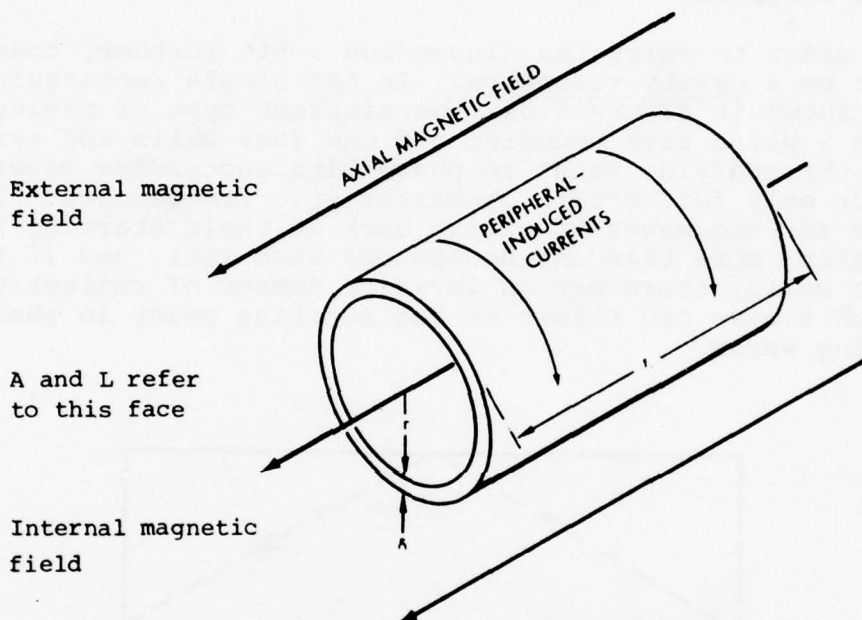


Figure 6.33 An Open-Ended Cylinder

As the dimensions of a structure are decreased the enclosed area decreases more rapidly than does the distance around the structure; it follows, then, that the internal impedance of small structures will be smaller than the internal impedance of large structures. As a numerical example, consider a cylinder of 1 m radius. Such a structure will have an internal impedance of $3.95 \times 10^{-3} \Omega$ at 1 kHz and 3.95Ω at 1 MHz.

At frequencies approaching and beyond the self-resonance points of an enclosure, the impedance can change drastically. The procedures for calculating the electric fields and magnetic fields within enclosures at or near the resonance points are sufficiently complicated that the concept of internal impedance is of dubious utility when studying lightning interactions.

6.6 RESONANCE MODES OF CAVITIES

When making analytical studies of lightning interaction effects, it is tempting (and probably correct) to say that, at frequencies approaching the natural resonance modes of enclosures in which electronic equipment may be located, all bets are off. While cavity resonance effects are noted in EMP studies, there have been no comparable studies made during lightning effects testing to let one say that there are not cavity resonance effects with which one must deal. The various Lightning Transient Analysis tests with which this author has been associated have not shown evidence of such effects, but that is not to say that such effects have not occurred.

In order to carry the discussion a bit further, consider what is meant by a cavity resonance. In the simple rectangular enclosure shown in Figure 6.34, the simplest type of cavity resonance involves a plane wave bouncing off the four walls and arriving back at the starting point in phase with succeeding waves. This can occur only for certain characteristic frequencies. It is possible for the waves to arrive back at their starting point after making more than one bounce off each wall, and if there are more walls, there are an infinite number of reflection patterns for which a wave can return to the starting point in phase with succeeding waves.

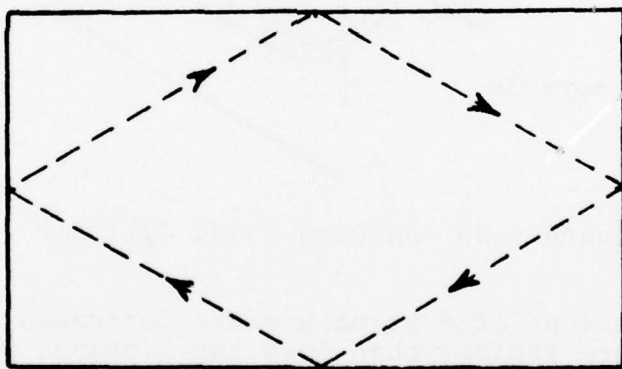


Figure 6.34 An Elementary Mode of Cavity Resonance

For rectangular enclosures, some of the simpler resonance modes are shown in Figure 6.35. The frequencies corresponding to such modes are given by

$$f(m,n,p) = \frac{c_0}{2} \sqrt{\frac{m^2}{a} + \frac{n^2}{b} + \frac{p^2}{c}} \quad (6.63)$$

where m, n and p are integers identifying the resonance modes

a, b, c are the dimensions of the enclosure

$$c_0 = 3 \times 10^8 \text{ m/s (velocity of light)}$$

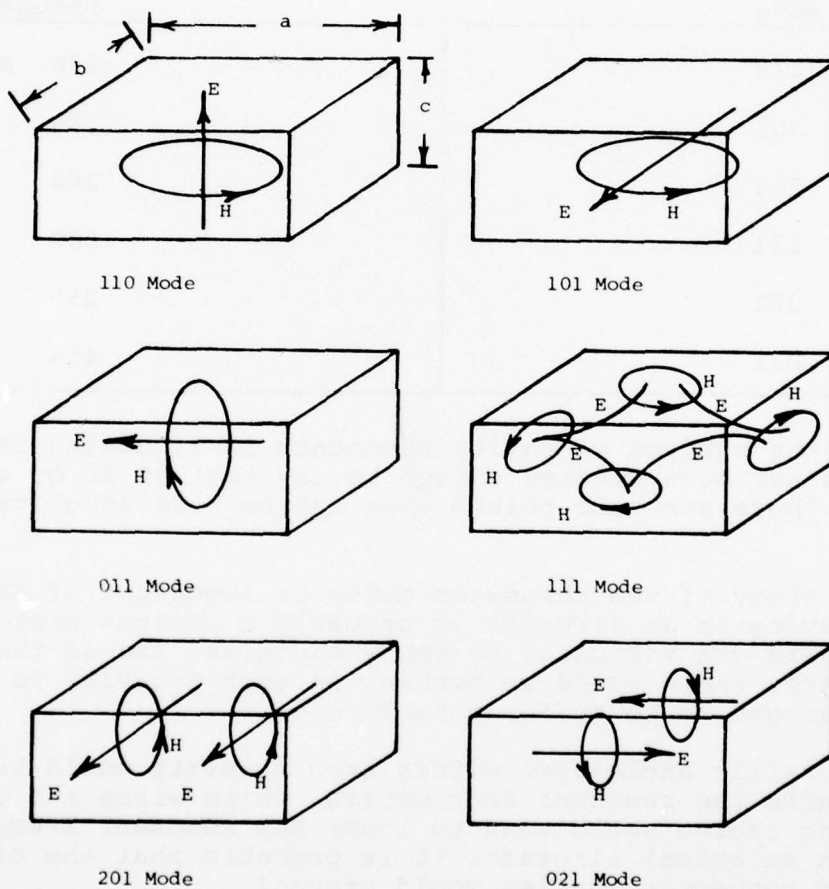


Figure 6.35 Some Resonance Modes in a Rectangular Enclosure

The magnitude of the integers m , n , or p is equal to the number of repetitions of the magnetic field along the corresponding dimension. Thus, the 110 mode has one wavelength of magnetic field along each of the a and b dimensions, and no wavelengths along the c dimension.

As a numerical example, some of the characteristic resonance frequencies of a rectangular enclosure having dimensions $0.7 \times 1 \times 1.5$ m are given in Table 6.1.

TABLE 6.1
SOME RESONANCE MODES IN A RECTANGULAR ENCLOSURE

Mode	Frequency
110	236 MHz
101	180
011	262
111	280
201	250
021	454

While the subject of cavity resonance in lightning interactions has not been studied enough to say that it is or is not a problem, there are some points that can be made about the subject:

1. A study of the resonance modes or impedance of an empty cavity in an aircraft is probably a useless exercise. There are virtually no empty cavities, and if there were, there would be nothing in such a cavity to be damaged or to suffer interference.
2. Metallic enclosures within such a cavity would tend to raise the resonant frequencies, while wires and connecting cables would tend to lower the resonant frequencies. In an actual aircraft, it is probable that the effects of connecting cables would prevail.
3. The principal value of knowing the resonance frequencies of an enclosure is in knowing the frequency above which one should not even attempt to make an interaction study

using simple methods of analysis. As such, only the lowest frequency resonance mode is of interest. Note that this is not to say that the higher order resonance modes are not of importance.

4. Electrical energy oscillating in a cavity-resonance mode will only appear if there is a source to excite that oscillation. Whether a lightning flash contains frequency components high enough to excite the resonance modes of cavities in which electrical equipment is located is a subject on which we have no real knowledge, only speculation.
5. Enclosures that act as cavity resonators frequently have quite high Q factors. That is to say, they have only small losses. If some transient electromagnetic condition excites a cavity oscillation, that oscillation may persist for a time much longer than the transient that excited the oscillation.
6. The frequencies associated with cavity resonances are apt to be in the same order as the frequencies associated with digital equipment located in the enclosures. Thus, one can speculate that a cavity resonance, if it occurs, might be more of a problem for digital electronics than it would for analog electronics.

REFERENCES

6.1 D.J. Kozakoff, A.T. Bolt, and F.D. Howard, Shielding Effectiveness of Various Shaped Geometrical Enclosures in Terms of Normalized Parameters (San Antonio, Texas, 6-8 October 1970), 1970 IEEE Regional Electromagnetic Compatibility Symposium Record 70C64-REGENC, pp. V-A-1 to V-A-11.

SECTION VII

INTERACTION WITH OTHER EMC ANALYSIS TECHNIQUES

When this program was undertaken, it was expected that the "Lightning Analysis Computer Program" would eventually become a subroutine of the IEMCAP program. This goal has not been reached, partly because the physical understanding of lightning interactions is not yet far enough along, and partly because the computer bookkeeping to do all this under machine control was too involved for this program. We have, however, attempted to present a format in which the results of lightning interactions can be incorporated so that, at some future time, machine analysis of lightning interactions might become possible. In this section, we will discuss that format, discuss its present state, and discuss what is still lacking in that format; the concepts have not reached maturity; others in the EMC community may expand them to a point where they will be truly usable.

During the development of the Space Shuttle Lightning Criteria Document (Reference 7.1), the concept of dividing a structure into magnetic field zones and characterizing the magnetic field in each of those zones by a rapid component (the aperture-coupled component) and a slow component (the diffusion-coupled component) was formulated. Each of these components was characterized by a peak amplitude and two times: a time to crest of an equivalent triangular wave and a decay time (to half value) of the triangular wave. Lightning transient-analysis tests on aircraft (Reference 7.2) showed that the magnetic fields were distinctly different in the various regions of an aircraft. The tests demonstrated, as had previously been known, that the magnetic field would have different times to crest and different decay times in the various zones, whereas in the Shuttle analyses it was assumed, for simplicity, that all aperture-coupled components would have one waveshape, and all diffusion-coupled components would have a different waveshape. Other investigators (Reference 7.3) have supported the division of magnetic-field phenomena into two distinctly different time regimes, one characterized by rapid penetration of fields, and one characterized by slow penetration of fields. Tests have also shown, however, that there are magnetic-field components that are characterized by more rapid variations than those of the aperture-coupled fields. Loosely speaking, these fields are produced by the flow of current on internal wiring and structural members. In Reference 7.2, Fisher proposed that these components be called the reradiated component of magnetic field. The title is unimportant, but the physical presence of these higher frequency fields is unmistakable. There have been no studies of how to calculate the magnitude of these fields, but any analysis procedure should at least recognize the existence of such fields.

The procedure that we recommend for analysis of the data from any lightning analysis program is to construct a "map", or, more accurately, a data file, in which a summary of the factors that define the electromagnetic field environment at a number of points within the aircraft can be stored. From this file, a user can determine, either by machine or by hand calculation, the approximate magnitude of signals likely to be induced on typical wiring by those fields. Note that the emphasis is on approximate magnitudes and typical wiring. It appears unreasonable to expect that one will be able to calculate the exact magnitude of signals induced on any particular circuit, given the complexity of the wiring to be found in actual aircraft.

As previously discussed, the task of defining the electromagnetic field environment and constructing such a data file or "map" is a complex job that should be done only once, using whatever tools are available for the purpose, whether those tools be analytical or experimental in nature. Saying that the task should be done once and correctly, of course, does not mean that the data in the file cannot be updated and corrected during the evolution of a particular aircraft. It merely says that the task should not be done anew each time a different engineering group wishes to perform a lightning compatibility analysis.

Since such a task will require a great deal of human interaction, it is appropriate to develop a computer routine with which one can put data into a file, examine or retrieve the data, and change or update the data, if necessary. That routine is called CHANGER and is shown in Figure 7.1. The routine allows one to define a point in space by a point number and by the X, Y, and Z coordinates of the point. It then provides a number of factors that characterize the electromagnetic field at that point.

The elements that make up the file are as follows:

POINT This is the point number, an arbitrary designation.

XP This is the X coordinate of the point.

YP The Y coordinate.

ZP The Z coordinate.

Z The impedance of the point, as defined by Equation 6.62. This impedance is calculated at 1 MHz. The impedance at other frequencies would be in proportion to the frequency.

FMAX This would be the maximum frequency at which one would be justified at assuming the impedance to be as given by Equation 6.62.

1000C PROGRAM NAME IS CHANGER
1020C
1040C
1060C FOR COMPLETE INFORMATION ON THIS PROGRAM CONTACT
1080C
1100C F. A. FISHER
1120C BLDG 9 - ROOM 200
1140C GENERAL ELECTRIC CO.
1160C 100 WOODLAWN AVE.
1180C PITTSFIELD, MASS 0120
1200C
1220C PHONE (413)-494-4380
1240C
1260C THIS PROGRAM ALLOWS ONE TO DEFINE A POINT BY A POINT NUMBER
1280C AND BY ITS LOCATIONS IN SPACE, ITS X,Y AND Z COORDINATES.
1300C IN A FILE ADJACENT TO THE COORDINATES DEFINING THIS POINT ONE
1320C CAN THEN STORE CERTAIN QUANTITIES THAT DEFINE THE CHARACTERISTICS
1340C OF THE MAGNETIC FIELD AT THAT POINT. BY SO DOING ONE MAY CON-
1360C STRUCT A "MAP", OR MORE ACCURATELY AN ACCESSIBLE FILE, THAT
1380C DESCRIBES THE MAGNETIC FIELD WITHIN AN AIRCRAFT.
1400C
1420C IN PRINCIPLE, ONE CAN STORE DATA IN THIS FILE IN TWO WAYS,
1440C EITHER UNDER MACHINE CONTROL FROM A PROGRAM THAT CALCULATES
1460C THE MAGNETIC FIELD AT THE POINT, OR , MORE LIKELY, BY HAND.
1480C IF DATA IS STORED BY HAND IT MAY COME EITHER FROM EXPERIMENTAL
1500C MEASUREMENTS OR BY CALCULATIONS THE RESULTS OF WHICH MAY NEED
1520C FURTHER INSPECTION BY HUMAN INTELLECT BEFORE BEING PLACED IN
1540C A DATA FILE FOR USE BY OTHERS.
1560C
1580C THE FILE IN WHICH THE DATA TO BE STORED IS A "RANDOM" FILE
1600C NAMED "MAP".
1620C
1640C THIS PROGRAM, "CHANGER", ALLOWS ONE TO INSPECT THE CONTENTS
1660C OF THE FILE, TO ENTER DATA INTO THE FILE, OR TO CHANGE
1680C THE CONTENTS OF THE FILE. ONE IS ABLE TO INSERT NEW POINTS
1700C INTO THE FILE AND THEN TO ORDER THOSE POINTS IN SEQUENCE
1720C ACCORDING TO THEIR X , Y , OR Z COORDINATES.
1740C -----
1760C

Figure 7.1 Program CHANGER

1780C
 1800C THE LAYOUT OF THE MAP IS AS FOLLOWS
 1820C
 1840C
 1860C
 1880C COLUMN
 1900C
 1920C 1 2 3 4 5 6 7 8 9 10 11 12 13 14 15 16 17 18 19 20 21 22
 1940C 1 *
 1960C 2 *
 1980C 3 *
 2000C 4 * *
 2020C R . *
 2040C O . *
 2060C W . *
 2080C . *
 2100C . *
 2120C . *
 2140C N *
 2160C
 2180C
 2200C
 2220C THE COLUMN ASSIGNMENTS ARE AS FOLLOWS
 2240C
 2260C
 2280C COLUMN QUANTITY REMARKS
 2300C
 2320C 1 POINT POINT NUMBER, AN ARBITRARY DESIGNATION
 2340C
 2360C 2 XP X COORDINATE OF THE POINT
 2380C 3 YP Y COORDINATE
 2400C 4 ZP Z COORDINATE
 2420C
 2440C 5 Z IMPEDANCE, AT 1 MHZ, AT THE POINT
 2460C 6 FMAX MAXIMUM FREQUENCY AT WHICH Z MIGHT APPLY
 2480C
 2500C 7 HRT MAGNITUDE OF RE-READIATED FIELD
 2520C 8 TR1 TIME TO PEAK
 2540C 9 TR2 DECAY TIME
 2560C
 2580C 10 HAT MAGNITUDE OF APERTURE COUPLED FIELD
 2600C 11 TA1 TIME TO PEAK
 2620C 12 TA2 DECAY TIME
 2640C
 2660C 13 J1 INITIAL MAGNITUDE OF DIFFUSION COUPLED
 2680C ELECTRIC FIELD ALONG INNER SURFACE
 2700C 14 T1 PULSE PENETRATION TIME CONSTANT
 2720C 15 J2 FINAL MAGNITUDE OF ELECTRIC FIELD
 2740C 16 T2 REDISTRIBUTION TIME CONSTANT
 2760C

Figure 7.1 (Continued) Program CHANGER (Continued)

```

2780C   17    HDT      MAGNITUDE OF DIFFUSION COUPLED FIELD
2800C   18    TD1      TIME TO PEAK
2820C   19    TD2      TIME
2840C
2860C   20    F1       FIRST BREAK FREQUENCY
2880C   21    A1       AMPLITUDE AT F1
2900C   22    F2       SECOND BREAK FREQUENCY
2920C   23    A2       AMPLITUDE AT F2
2940C   24    F3       THIRD BREAK FREQUENCY
2960C   25    A3       AMPLITUDE AT F3
2980C
3000C
3020C THIS IS AN INTERACTIVE PROGRAM TO BE USED AT TELETYPE TERMINAL
3040C WHEN THE PROGRAM RUNS IT WILL ASK QUESTIONS AND THE USER WILL REPLY
3060C
3080C THE PROGRAM WILL FIRST ASK WHETHER THE USER WANTS TO CHANGE
3100C DATA, SORT DATA, LIST DATA OR STOP. THE USER MAKES HIS REPLY
3120C
3140C
3160C IF THE REPLY IS "CHANGE", THE PROGRAM WILL ASK FOR THE ROW IN
3180C WHICH THE CHANGES ARE TO BE MADE. THE USER TYPES THE ROW NUMBER.
3200C THE PROGRAM WILL THEN ASK FOR THE NAME OF THE VARIABLE TO BE
3220C CHANGED AND FOR THE NEW VALUE OF THAT VARIABLE. THIS PROCESS
3240C CONTINUES UNTIL THE USER REPLIES "DONE".
3260C THE PROGRAM THEN ASKS FOR ANOTHER ROW NUMBER AND THE PROCESS
3280C CONTINUES UNTIL THE USER REPLIES WITH "-1" TO THE REQUEST
3300C FOR ROW NUMBER.
3320C
3340C IF THE REPLY TO THE INITIAL REQUEST IS "SORT", THE PROGRAM
3360C WILL ASK FOR THE ROWS WITH WHICH TO START AND STOP.
3380C THE USER MUST THEN TYPE IN THE THREE PRIORITIES BY WHICH THE
3400C DATA IS TO BE SORTED. THESE MAY BE:
3420C
3440C   X,Y,Z
3460C   X,Z,Y
3480C   Y,X,Z
3500C   Y,Z,X
3520C   Z,X,Y
3540C   Z,Y,X
3560C IF THE REPLY TO THE INITIAL REQUEST IS "LIST", THE PROGRAM
3580C WILL ASK FOR THE ROW NUMBERS WITH WHICH TO START AND STOP.
3600C
3620C IF THE REPLY IS "STOP", THE PROGRAM JUST STOPS.
3640C
3660C
3680C -----

```

Figure 7.1 (Continued) Program CHANGER (Continued)

AD-A062 606

GENERAL ELECTRIC CORPORATE RESEARCH AND DEVELOPMENT --ETC F/G 1/3
ANALYSIS AND CALCULATIONS OF LIGHTNING INTERACTIONS WITH AIRCRA--ETC(U)

AUG 78 F A FISHER

F33615-76-C-3122

UNCLASSIFIED

SRD-78-044

AFFDL-TR-78-106

NL

5 OF 5
ADA
062606



END
DATE
FILMED
3 -79
DDC

```

3700C
3720C
3740 DIMENSION ALPHA(50,25),BETA(50),B(25),TEMP(50,25),VALUE(25)
3760 CHARACTER A*5(26),COMMAND*6(4),CMMND,C*5(26),SORT*4(3),SORTS*4(3)
3780 INTEGER ROW1,ROW2
3800 DATA A/"POINT","XP","YP","ZP","Z","FMAX","HRT",
3820& "TR1","TR2","HAT","TA1","TA2","J1","T1","J2","T2",
3840& "HDT","TD1","TD2","F1","A1","F2","A2","F3","A3","DONE"/
3860 CALL ATTACH(01,"/MAP:",3,1,ISTAT,)
3880 DATA COMMAND//CHANGE//,SORT//,LIST//,STOP///
3900 DATA SORT//X//,Y//,Z///
3920 CALL RANSIZ(01,25)
3940 151 WRITE(06,5)
3960 5 FORMAT(/4X,"DO YOU WANT TO CHANGE,SORT,LIST DATA OR STOP?")
3980 READ(05,7) CMMND
4000 7 FORMAT(V)
4020 DO 8 JX=1,4
4040 IF(COMMAND(JX) .EQ. CMMND) GO TO 158
4060C
4080C
4100 GO TO 8
4120C
4140C
4160C
4180C
4200 158 GOTO (160,410,410,999),JX
4220C
4240 8 CONTINUE
4260C
4280 160 CONTINUE
4300C
4320C YOU WIND UP HERE IF YOU WANT TO CHANGE A ROW
4340 WRITE(06,20)
4360 20 FORMAT(/,4X,"CHANGES TO BE MADE IN WHICH ROW?")
4380 READ(05,30) I
4400 30 FORMAT(V)
4420C
4440 IF(I .EQ. -1) GO TO 999
4460 IF(I .EQ. 0) GO TO 997
4480C
4500 READ(01,I)B
4520 WRITE(06,40)
4540 40 FORMAT(/,4X,"NAMES OF VARIABLES AND ASSOCIATED VALUES TO GO")
4560 WRITE(06,41)
4580 41 FORMAT(4X,"INTO MAP.ONE PAIR AT A TIME")
4600C
4620 DO 50 J=1,26

```

Figure 7.1 (Continued) Program CHANGER (Continued)

```

4640C
4660 IF(C(J).EQ.A(26))GOTO 70
4680C
4700 READ(05,60) C(J),VALUE(J)
4720 60 FORMAT(V)
4740C
4760 IF(C(J).EQ.A(26))GOTO 70
4780C
4800 50 CONTINUE
4820 70 CONTINUE
4840C
4860 DO 80 K=1,22
4880 DO 90 L=1,22
4900C
4920 IF(C(J).EQ.A(26))GOTO 85
4940C
4960 IF(C(K) .EQ. A(L)) GO TO 10
4980C
5000 90 CONTINUE
5020 10 WRITE(06,110) A(L),B(L),A(L),VALUE(K)
5040 110 FORMAT(4X,"OLD ",A5,"=",1E10.3,4X,"NEW ",A5,"=",1E10.3)
5060 B(L)=VALUE(K)
5080C
5100 80 CONTINUE
5120C
5140 85 CONTINUE
5160 WRITE(01'I) B
5180C
5200 GO TO 160
5220C
5240 410 CONTINUE
5260C YOU WIND UP HERE IF YOU WANT TO SORT OUT THE LOCATIONS
5280C OR IF YOU WANT TO LIST THE DATA
5300C
5320 WRITE(06,22)
5340 22 FORMAT(/,4X,"WHAT ARE START AND STOP ROW NUMBERS?")
5360 READ(05,210) ROW1,ROW2
5380 210 FORMAT(V)
5400C
5420C
5440 GOTO (211,500),JX-1
5460C
5480C
5500 211 WRITE(06,220)
5520 220 FORMAT(/,4X,"WHAT ARE THE PRIORITIES ON WHICH DATA IS TO BE SORTED?")
5540 READ(05,230) SORTS
5560 230 FORMAT(3A4)
5580C

```

Figure 7.1 (Continued) Program CHANGER (Continued)

```
5600 500 DO 250 J=ROW1,ROW2
5620 READ(01'J) (ALPHA(J,K),K=1,22)
5640 250 CONTINUE
5660C
5680C
5700 GOTO (251,510),JX-1
5720C
5740C
5760 251 DO 260 L=1,3
5780C
5800 DO 270 M=1,3
5820 IF(SORT(M) .EQ. SORTS(L)) GO TO 280
5840C
5860 270 CONTINUE
5880C
5900 280 CONTINUE
5920 DO 290 N=ROW1,ROW2
5940 IF(ALPHA(N,M+1) .GE. ALPHA(N+1,M+1)) GO TO 300
5960C
5980 DO 310 NDX=1,25
6000 TEMP(N,NDX)=ALPHA(N+1,NDX)
6020 310 CONTINUE
6040C
6060 GO TO 315
6080C
6100 300 DO 320 NDX=1,25
6120 TEMP(N,NDX)=ALPHA(N,NDX)
6140 320 CONTINUE
6160C
6180 315 CONTINUE
6200 290 CONTINUE
6220 260 CONTINUE
6240C
6260 DO 330 II=ROW1,ROW2
6280 DO 340 IJ=1,25
6300 ALPHA(II,IJ)=TEMP(II,IJ)
6320 340 CONTINUE
6340 330 CONTINUE
6360C
6380 DO 350 IK=ROW1,ROW2
6400 WRITE(01'IK) (ALPHA(IK,IL),IL=1,25)
6420 350 CONTINUE
```

Figure 7.1 (Continued) Program CHANGER (Continued)

```

6440C
6460 GOTO 355
6480C
6500 530 FORMAT(/,7X,A5,4(7X,A5))
6520 532 FORMAT(/,2X,A5,6(7X,A5))
6540 510 CONTINUE
6560 WRITE(06,530) A(1),A(2),A(3),A(4)
6580 WRITE(06,30)
6600 DO 600 II=ROW1,ROW2
6620 WRITE(06,550) ALPHA(II,1),ALPHA(II,2),ALPHA(II,3),ALPHA(II,4)
6640 600 CONTINUE
6660 WRITE(06,30)
6680 WRITE(06,30)
6700 WRITE(06,530) A(1),A(5),A(6)
6720 WRITE(06,30)
6740 DO 610 II=ROW1,ROW2
6760 WRITE(06,550) ALPHA(II,1),ALPHA(II,5),ALPHA(II,6)
6780 610 CONTINUE
6800 WRITE(06,30)
6820 WRITE(06,30)
6840 WRITE(06,530) A(1),A(7),A(8),A(9)
6860 WRITE(06,30)
6880 DO 620 II=ROW1,ROW2
6900 WRITE(06,550) ALPHA(II,1),ALPHA(II,7),ALPHA(II,8),ALPHA(II,9)
6920 620 CONTINUE
6940 WRITE(06,30)
6960 WRITE(06,30)
6980 WRITE(06,530) A(1),A(10),A(11),A(12)
7000 WRITE(06,30)
7020 DO 630 II=ROW1,ROW2
7040 WRITE(06,550) ALPHA(II,1),ALPHA(II,10),ALPHA(II,11),ALPHA(II,12)
7060 630 CONTINUE
7080 WRITE(06,30)
7100 WRITE(06,30)
7120 WRITE(06,530) A(1),A(13),A(14),A(15),A(16)
7140 WRITE(06,30)
7160 DO 640 II=ROW1,ROW2
7180 WRITE(06,550) ALPHA(II,1),ALPHA(II,13),ALPHA(II,14),
7200& ALPHA(II,15),ALPHA(II,16)
7220 640 CONTINUE
7240 WRITE(06,30)
7260 WRITE(06,30)

```

Figure 7.1 (Continued) Program CHANGER (Continued)

```
7280 WRITE(06,530) A(1),A(17),A(18),A(19)
7300 WRITE(06,30)
7320 DO 650 II=ROW1,ROW2
7340 WRITE(06,550) ALPHA(II,1),ALPHA(II,17),ALPHA(II,18),ALPHA(II,19)
7360 650 CONTINUE
7380 WRITE(06,30)
7400 WRITE(06,30)
7420 WRITE(06,530) A(1),A(20),A(21),A(22),A(23)
7440 WRITE(06,30)
7460 DO 660 II=ROW1,ROW2
7480 WRITE(06,550) ALPHA(II,1),ALPHA(II,20),ALPHA(II,21),ALPHA(II,22),
7500& ALPHA(II,23)
7520 660 CONTINUE
7540 WRITE(06,30)
7560 WRITE(06,30)
7580 WRITE(06,530) A(1),A(24),A(25)
7600 WRITE(06,30)
7620 DO 670 II=ROW1,ROW2
7640 WRITE(06,550) ALPHA(II,1),ALPHA(II,24),ALPHA(II,25)
7660 670 CONTINUE
7680 550 FORMAT(2X,1E10.3,4(2X,1E10.3))
7700 560 FORMAT(4X,I6,6(2X,1E10.3))
7720 540 CONTINUE
7740 520 CONTINUE
7760C
7780 355 GOTO 151
7800C
7820 997 WRITE(06,998)
7840 998 FORMAT(/,4X,"ILLEGAL ROW NUMBER!--ZERO NOT ALLOWED!")
7860C
7880 GO TO 151
7900C
7920 999 CONTINUE
7940C YOU WIND UP HERE IF YOU WANT TO STOP
7960 STOP;END
```

Figure 7.1 (Conclusion) Program CHANGER (Conclusion)

The following data would describe the magnetic field in the time domain. For designation of quantities refer to Figure 7.2.

HRT The total amplitude of the reradiated component of magnetic field. Since neither this report nor any other seems to offer any guidance as to how this quantity can be calculated, this quantity primarily reserves a space for the entry of experimentally determined data, if available.

TR1 The time to crest of the reradiated component of magnetic field.

TR2 The decay time of the reradiated component.

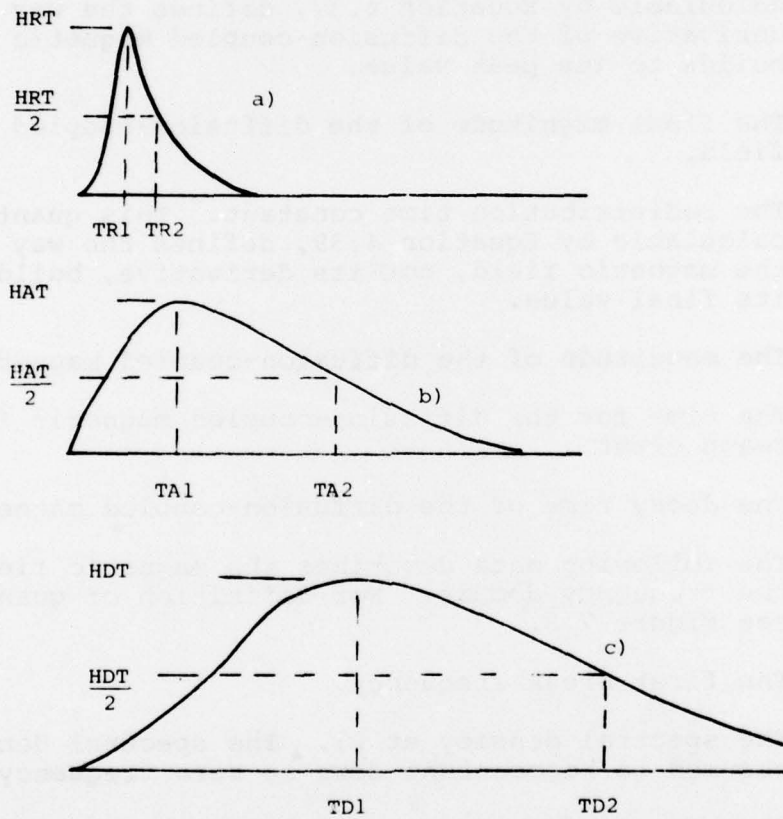


Figure 7.2 Quantities Describing, in the Time Domain, the Magnetic Field

- (a) The reradiation field component
- (b) The aperture coupled field component
- (c) The diffusion coupled field component

HAT The total amplitude of the aperture-coupled magnetic field. Aperture-coupled fields can be determined with the aid of, among other tools, the program APERTURE.

TAL The time to crest of the aperture-coupled field.

TA2 The decay time of the aperture-coupled field.

J1 The initial magnitude of the diffusion-coupled electric field on the interior surface of the structure. As explained in Section 4, this quantity also defines the magnitude of the derivative of the diffusion-coupled magnetic field, and so defines the voltages induced by the diffusion-coupled field.

T1 The pulse penetration time constant. This quantity, calculable by Equation 4.37, defines the way that the derivative of the diffusion-coupled magnetic field builds to its peak value.

J2 The final magnitude of the diffusion-coupled electric field.

T2 The redistribution time constant. This quantity, calculable by Equation 4.39, defines the way that the magnetic field, not its derivative, builds to its final value.

HDT The magnitude of the diffusion-coupled magnetic field.

TD1 The time for the diffusion-coupled magnetic field to reach crest.

TD2 The decay time of the diffusion-coupled magnetic field.

The following data describes the magnetic fields in the frequency domain. For definition of quantities, see Figure 7.3.

F1 The first break frequency.

A1 The spectral density at F1. The spectral density is assumed to be constant down to zero frequency.

F2 The second break frequency.

A2 The spectral density at F2. The amplitude of the spectral density would be assumed to vary linearly according to the logarithm of the frequency between F1 and F2.

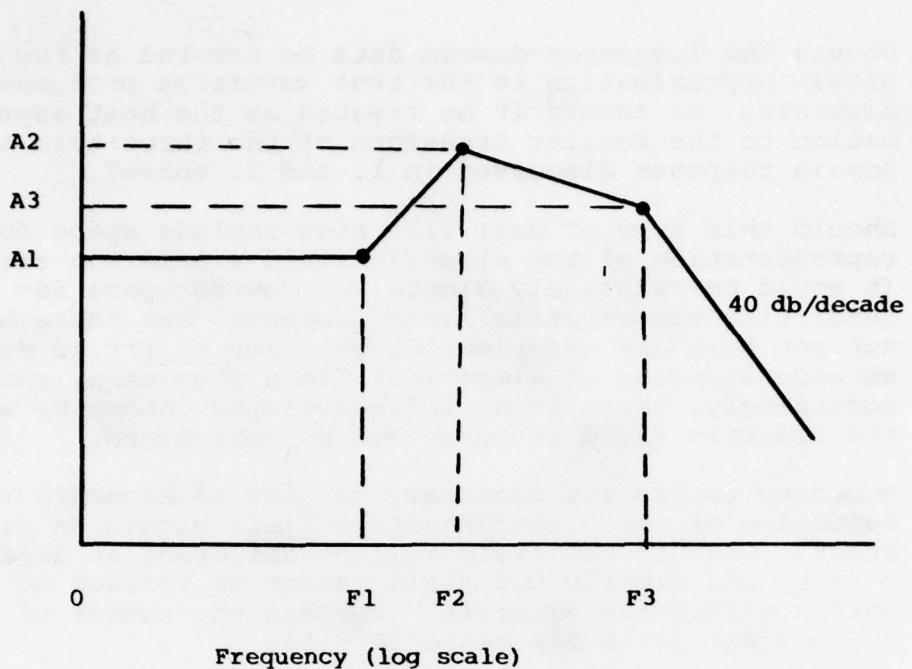


Figure 7.3 Quantities That Define, in the Frequency Domain, the Magnetic Field

F3 The third break frequency.

A3 The spectral density at F_3 . The amplitude of the spectral density would be assumed to vary uniformly with the logarithm of frequency between F_2 and F_3 . Above F_3 , the amplitude of the spectral density would be assumed to fall at the rate of 40 db/decade from its value at F_3 .

At this stage, it is appropriate to say that these quantities are put forward as suggestions for the quantities that define the magnetic field. Some unanswered questions are as follows:

1. Can the magnetic field be characterized adequately, in the time domain, as the sum of three independently determined terms?
2. Should the various terms be treated as triangular waves or as double exponential waves? Triangular waves are easier to treat by hand analysis, but exponential terms are more nearly representative of the physical response. Given the limitations of lightning compatibility theory, perhaps one cannot really distinguish the difference in the two representations.
3. In the frequency domain, can the total environment be specified adequately by three break points?

4. Should the frequency-domain data be treated as the best simple approximation to the true waveforms produced by lightning, or should it be treated as the best approximation to the Fourier transform of the three-term time-domain response discussed in 1. and 2. above?
5. Should this type of data file also include space for a representation of the electric field within the aircraft? It would be relatively simple to provide space for data describing the electric field response, but there have not yet been any experimental programs to try to develop an understanding of electrical field phenomena, and, accordingly, there is no well-developed theory by which the electric field response can be determined.
6. How many points are necessary to give an accurate representation of the electromagnetic field within an aircraft? Clearly the field will be different at different points, and clearly the field cannot be defined at all points within the aircraft. Perhaps the number of points to consider is in the range 20 - 50.

The question of just how the data stored in such a map would be used is not addressed here. If an analysis is to be performed with the aid of IEMCAP, the relevant quantities to be used would be the frequency domain data at the point or points nearest the equipment or wiring under analysis. CHANGER provides the capability of organizing the points at which the data is presented in order, according to the X, Y and Z coordinates of the point. It does not provide a way of checking to see if a certain physical location in the aircraft has been characterized by more than one set of data, perhaps at coordinates that are very close to each other, but not identical. Neither does it provide the capability of selecting the set of data that is closest to a particular point at which the user (including another computer program in the definition of user) may wish to make an analysis. The user would have to provide his own routines for searching out and reading the appropriate data from the file.

The IEMCAP routines use the electric-field intensity as the quantity with which analyses are made. Analyses of the response of an aircraft structure to lightning seem to be made more naturally in terms of the magnetic field intensity. For an analysis using IEMCAP, one would determine, through the use of the impedance at the point in question, the electric-field intensity that corresponds to the magnetic-field intensity. The programs presented in this report do not provide the capability for making such transformations under machine control.

Since this section of the report is concerned more with concepts than with working computer programs, it should be noted that

the slots used for storage of magnetic-field data in the frequency domain could also be used for storage of the equivalent information after it was converted to the equivalent electric-field intensity.

If analysis is not to be done using the IEMCAP routines, references 7.4 and 7.5 present methods for determining open-circuit voltages and short-circuit currents on cables from the magnetic-field data stored in the map of magnetic fields. More elaborate methods of treating the interactions were, of course, given in Section 3.

REFERENCES

- 7.1 Space Shuttle Program Lightning Protection Criteria Document, JSC-07636, Revision A, National Aeronautics and Space Administration, Lyndon B. Johnson Space Center, Houston, Texas, November 4, 1975.
- 7.2 J.A. Plumer, F.A. Fisher, and L.C. Walko, Lightning Effects on the NASA F-8 Digital-Fly-By-Wire Airplane, NASA CR-2524, prepared by the High Voltage Laboratory, Environmental Electromagnetics Unit, Corporate Research and Development, General Electric Company, Pittsfield, Massachusetts, for the National Aeronautics and Space Administration, Lewis Research Center, Cleveland, Ohio, March 1975.
- 7.3 B.J.C. Burrows, Induced Voltages - Measurement Techniques and Typical Values, Proceedings of the 1975 Conference on Lightning and Static Electricity, Culham Laboratory, England, 14-17 April 1975; also various informal communications.
- 7.4 Space Shuttle Program Lightning Protection Criteria Document, Revision A, pp. F-2 through F-10.
- 7.5 F.A. Fisher and J.A. Plumer, Lightning Protection of Aircraft, NASA Reference Publication 1008, Chapter 12.

SECTION VIII

CONCLUSIONS AND RECOMMENDATIONS

This section summarizes several points made earlier and expanded upon in Section 2. It also includes recommendations for future research into better lightning compatibility.

The state of knowledge about lightning interactions is still such that it would be better described as an art than as a science. There is much about the art that is still imperfectly understood. The art is sufficiently complex that it does not yet seem possible to summarize that art in a "Lightning Transient Analysis Computer Program" that is both self-contained and capable of being used productively by non-specialists.

This report is based on the premise that it is possible to determine the electromagnetic field within an aircraft, and then, from knowledge about that field, to estimate, roughly at least, the currents and voltages induced on simple wiring structures. The phrase "simple wiring structures" needs to be emphasized. It is not now possible, nor is it likely to be possible in the foreseeable future, to calculate the actual induced voltages on all circuits of an actual aircraft.

The task of determining those electromagnetic fields is sufficiently complex and time consuming that it should be done by specialists, should be done as a well-defined engineering task, and should be done early in the design phase of a particular aircraft. The person determining those fields should call upon any tools that are appropriate. There is room for a mixture of analytical and experimental effort. There is even a place for well-informed guesswork. Determining those fields does not seem to be a task for non-specialists.

Determining those fields internal to the aircraft involves first determining the field intensities external to the aircraft. For magnetic fields, this is equivalent to determining the external-current density. The present report provides one tool, DIFFMAG, to aid in the determination of that current density. A variety of other tools are available, both analytical and experimental. A task that might profitably be sponsored would be to explain the various techniques in "how-to-do-it" style. Possibly a seminar or short course would be appropriate.

The dominant modes of coupling of magnetic fields into the interior of an aircraft are through apertures and by diffusion through the structural skin of the aircraft. The most important mode of coupling is through apertures. Aperture coupling has been extensively studied, and a well-developed theory exists. One place where the state of knowledge is deficient is in how to treat

poorly defined apertures. Most real apertures in an aircraft are poorly defined, an example being the seams around doors or covers to the compartments where electronic equipment is apt to be located on aircraft. A program aimed at providing engineering guidance for treating poorly defined apertures might be profitably undertaken.

Virtually nothing is known about the electric-field intensity that might exist at the surface of an aircraft when the aircraft is struck by lightning. That electric field is probably a highly non-linear function of the lightning current or of the charge contained in the leader of the lightning channel. This report provides some speculation as to what that electric field might be, but is only speculation. Experimental studies using high voltages, possibly on scale models of aircraft, might provide useful guidance for the working engineer and help clarify the importance of electric fields vis-a-vis magnetic fields.

Aperture coupling provides magnetic fields having basically the same waveshape as the external magnetic field. Diffusion coupling provides magnetic fields having rise and fall times much slower than the external fields. Magnetic fields having faster rise and fall times than the external fields also exist in the aircraft. Frequently, these fields are oscillatory in nature. In this report, we suggest the designation reradiated fields, since they seem to be produced by the flow of current on wiring harnesses and structural members. The character and reason for existence of such fields has never been studied, nor are there any methods by which the magnitude and time history of such fields may be calculated. Research into the nature of such fields might profitably be made.

This report provides a discussion, supported by much detailed explanation, on how one can use a network-analysis program like ECAP to calculate the response of a distributed wiring harness to the internal electromagnetic fields. This report discusses what can and cannot be done, and gives a good illustration of the magnitude of the task if a detailed analysis is to be done.

When this program was undertaken, there was an expectation that the computer routines to be developed could be incorporated into the IEMCAP program. During the conduct of this study, it became apparent that the state of the art does not yet permit this to be done. Any "Lightning" routines that could be put into IEMCAP at this time would have to make such brutal compromises with physical reality that they would be of dubious worth. They certainly would not give answers from which one could make a yes/no decision on whether any particular piece of equipment would survive the effects of lightning.

In this report, we do present an outline of an approach on how the electromagnetic field environment may be described in a data file that may be used in future generations of lightning

interaction programs. One part of this approach provides, in the frequency domain, data on the electromagnetic fields at selected points. Such data are what would be used by IEMCAP. We also present a computer program by which a user can, in an interactive mode of operation, put data into such a file. This program allows one to incorporate experimentally-determined data into a file usable by machine computation routines. The material we present here is still in a rather embryonic state of development. It has not yet been used in a machine-oriented effort to try to determine whether an aircraft electronic system would or would not have lightning compatibility.

This report discusses the degree to which experimental measurements of diffusion phenomena agree with analytical predictions. It also emphasizes the point that close agreement between currents or voltages predicted by theory and currents, or voltages measured on an actual aircraft would be largely fortuitous. One of the things sorely lacking in the lightning interaction art is a set of measurements of the response of a well-defined aircraft-like structure to simulated lightning. Virtually all measurements on aircraft have been performed with the Lightning Transient Analysis (LTA) technique and have mostly been concerned with determining whether or not a given aircraft is reasonably protected against lightning. In all such programs, the collection of data on simplified, well-defined circuits has been of secondary importance. Some organizations have made measurements on simplified structures, but those measurements have practically never been either attempted or confirmed by a different organization or researcher. As a result, there is little commonality of test data in the various organizations.

A research program that might profitably be undertaken would be to define a reasonably simple test structure, or set of structures, upon which different organizations could make similar tests, and with which theoretical predictions could be checked against experimental measurements.